The background of the book cover features a stunning aerial photograph of the Burj Khalifa in Dubai, United Arab Emirates. The tower stands tall and slender, its unique profile reaching towards the top of the frame. In the foreground, the city's dense urban sprawl is visible, with numerous other skyscrapers and modern buildings. The sky above is a clear, pale blue, suggesting a bright day. The overall scene conveys a sense of architectural achievement and urban development.

Fourteenth Edition

Design of
**Concrete
Structures**

Arthur H. Nilson

David Darwin

Charles W. Dolan

DESIGN_{of} CONCRETE STRUCTURES

DESIGN of CONCRETE STRUCTURES

Fourteenth Edition

Arthur H. Nilson

*Professor Emeritus
College of Engineering
Cornell University*

David Darwin

*Deane E. Ackers Distinguished Professor
of Civil, Environmental & Architectural Engineering
University of Kansas*

Charles W. Dolan

*H. T. Person Professor of Engineering
University of Wyoming*



Higher Education

Boston Burr Ridge, IL Dubuque, IA New York San Francisco St. Louis
Bangkok Bogotá Caracas Kuala Lumpur Lisbon London Madrid Mexico City
Milan Montreal New Delhi Santiago Seoul Singapore Sydney Taipei Toronto



DESIGN OF CONCRETE STRUCTURES, FOURTEENTH EDITION

Published by McGraw-Hill, a business unit of The McGraw-Hill Companies, Inc., 1221 Avenue of the Americas, New York, NY 10020. Copyright © 2010 by The McGraw-Hill Companies, Inc. All rights reserved. Previous editions © 2004, 1997, and 1991. No part of this publication may be reproduced or distributed in any form or by any means, or stored in a database or retrieval system, without the prior written consent of The McGraw-Hill Companies, Inc., including, but not limited to, in any network or other electronic storage or transmission, or broadcast for distance learning.

Some ancillaries, including electronic and print components, may not be available to customers outside the United States.

This book is printed on recycled, acid-free paper containing 10% postconsumer waste.

1 2 3 4 5 6 7 8 9 0 QPD/QPD 0 9

ISBN 978-0-07-329349-3

MHID 0-07-329349-0

Global Publisher: *Raghothaman Srinivasan*

Sponsoring Editor: *Debra B. Hash*

Director of Development: *Kristine Tibbetts*

Developmental Editor: *Lorraine K. Buczek*

Senior Marketing Manager: *Curt Reynolds*

Project Manager: *Melissa M. Leick*

Lead Production Supervisor: *Sandy Ludovissy*

Associate Design Coordinator: *Brenda A. Rolwes*

Cover Designer: *Studio Montage, St. Louis, Missouri*

(USE) Cover Image: *Getty Images*

Lead Photo Research Coordinator: *Carrie K. Burger*

Compositor: *Laserwords Private Limited*

Typeface: *10.5/12 Times Roman*

Printer: *Quebecor World Dubuque, IA*

All credits appearing on page or at the end of the book are considered to be an extension of the copyright page.

Library of Congress Cataloging-in-Publication Data

Nilson, Arthur H.

Design of concrete structures / Arthur H. Nilson, David Darwin, Charles W. Dolan.—14th ed.

p. cm.

Includes index.

ISBN 978-0-07-329349-3—ISBN 0-07-329349-0 (hard copy : alk. paper) 1. Reinforced concrete construction. 2. Prestressed concrete construction. I. Darwin, David.

II. Dolan, Charles W. (Charles William), 1943- III. Title.

TA683.2.N55 2010

624.1'834—dc22

2009006344

About the Authors

Arthur H. Nilson was engaged in research, teaching, and consulting relating to structural concrete for over 40 years. He has been a member of the faculty of the College of Engineering at Cornell University since 1956, in charge of undergraduate and graduate courses in the design of reinforced concrete and prestressed concrete structures until his retirement in 1991. He served as Chairman of the Department of Structural Engineering from 1978 to 1985. Dr. Nilson has served on many professional committees, including Building Code Subcommittee 318-D of the American Concrete Institute (ACI). His pioneering work on high-strength concrete has been widely recognized. He was awarded the ACI Wason Medal for materials research in 1974, the ACI Wason Medal for best technical paper in 1986 and 1987, and the ACI Structural Research Award in 1993. Professor Nilson is an Honorary Member of ACI and a Fellow in the American Society of Civil Engineers (ASCE). He has been honored by the civil engineering student body at Cornell for outstanding teaching. He was elected Professor Emeritus in 1991. He has held research appointments or lectureships at the University of Manchester, Salford University, and the Technical University of Milan. He is a registered professional engineer in several states and, prior to entering teaching, was engaged in full-time professional practice. He received the B.S. degree from Stanford University in 1948, the M.S. from Cornell in 1956, and the Ph.D. from the University of California at Berkeley in 1967.

David Darwin has been a member of the faculty at the University of Kansas since 1974 and has been director of the Structural Engineering and Materials Laboratory since 1982. He was appointed the Deane E. Ackers Distinguished Professor of Civil Engineering in 1990. Dr. Darwin served as President of the American Concrete Institute in 2007–2008 and is a member and past chair of ACI Committees 224 on Cracking and 408 on Bond and Development of Reinforcement. He is also a member of ACI Building Code Subcommittee 318-B on Reinforcement and Development and of ACI-ASCE Committee 445 on Shear and Torsion. Dr. Darwin is an acknowledged expert on concrete crack control and bond between steel reinforcement and concrete. He received the ACI Arthur R. Anderson Award in 1992 for his research efforts in plain and reinforced concrete, the ACI Structural Research Award in 1996, and the ACI Joe W. Kelly Award in 2005 for his contributions to teaching and design. He has also received a number of awards from the American Society of Civil Engineers, including the Walter L. Huber Civil Engineering Research Prize in 1985; the Moisseiff Award in 1991; the State-of-the-Art of Civil Engineering Award in 1996 and 2000; the Richard R. Torrens Award in 1997; and the Dennis L. Tewksbury Award in 2008. He has been honored for his teaching by the civil engineering students at the University

of Kansas. He is past editor of the ASCE *Journal of Structural Engineering*. Professor Darwin is a Fellow of ACI and ASCE. He is a licensed professional engineer and serves as a consultant in the fields of concrete materials and structures. He was honored with the Distinguished Alumnus Award from the University of Illinois Civil and Environmental Engineering Alumni Association in 2003. Between his M.S. and Ph.D. degrees, he served four years with the U.S. Army Corps of Engineers. He received the B.S. and M.S. degrees from Cornell University in 1967 and 1968 and the Ph.D. from the University of Illinois at Urbana-Champaign in 1974.

Charles W. Dolan has been on the faculty at the University of Wyoming since 1991, serving as Department Head from 1998 to 2001. He was appointed the H. T. Person Professor of Engineering in 2002. He is currently chair of Building Code Subcommittee 318-R of the American Concrete Institute. He has served as chair of the Technical Activities Committee, of ACI Committee 358 on Transit Guideways, and of ACI-ASCE Committee 423 on Prestressed Concrete. In private design practice for nearly 20 years, he was the project engineer on the Walt Disney World Monorail, the Detroit Downtown Peoplemover guideway, and the Dallas–Fort Worth Airport transit system guideway and is responsible for the conceptual design of the Dubai Palm Island monorail. He received the T. Y. Lin Award from ASCE in 1973 for outstanding contributions to the field of prestressed concrete and the Arthur R. Anderson award from ACI in 2005 for advancements in the design of reinforced and prestressed concrete structures. A Fellow in ACI and the Prestressed Concrete Institute (PCI), he is an internationally recognized leader in the development of fiber reinforced polymers for concrete reinforcement. He is a registered professional engineer and a consultant in the design of structural concrete. He received the B.S. from the University of Massachusetts in 1965 and the M.S. and Ph.D. from Cornell University in 1967 and 1989.

Contents

About the Authors	v
Preface	xiv
Chapter 1 Introduction	1
1.1 Concrete, Reinforced Concrete, and Prestressed Concrete	1
1.2 Structural Forms	2
1.3 Loads	8
1.4 Serviceability, Strength, and Structural Safety	12
1.5 Design Basis	15
1.6 Design Codes and Specifications	16
1.7 Safety Provisions of the ACI Code	17
1.8 Fundamental Assumptions for Reinforced Concrete Behavior	19
1.9 Behavior of Members Subject to Axial Loads	20
References	26
Problems	27
Chapter 2 Materials	28
2.1 Introduction	28
2.2 Cement	28
2.3 Aggregates	29
2.4 Proportioning and Mixing Concrete	31
2.5 Conveying, Placing, Compacting, and Curing	33
2.6 Quality Control	34
2.7 Admixtures	38
2.8 Properties in Compression	40
2.9 Properties in Tension	46
2.10 Strength under Combined Stress	48
2.11 Shrinkage and Temperature Effects	49
2.12 High-Strength Concrete	52
2.13 Reinforcing Steels for Concrete	54
2.14 Reinforcing Bars	55
2.15 Welded Wire Reinforcement	61
2.16 Prestressing Steels	61
References	63
Problems	65

Chapter 3	Flexural Analysis and Design of Beams	67
3.1	Introduction	67
3.2	Bending of Homogeneous Beams	67
3.3	Reinforced Concrete Beam Behavior	69
3.4	Design of Tension-Reinforced Rectangular Beams	80
3.5	Design Aids	94
3.6	Practical Considerations in the Design of Beams	97
3.7	Rectangular Beams with Tension and Compression Reinforcement	99
3.8	T Beams	108
	References	115
	Problems	116
Chapter 4	Shear and Diagonal Tension in Beams	120
4.1	Introduction	120
4.2	Diagonal Tension in Homogeneous Elastic Beams	121
4.3	Reinforced Concrete Beams without Shear Reinforcement	124
4.4	Reinforced Concrete Beams with Web Reinforcement	131
4.5	ACI Code Provisions for Shear Design	136
4.6	Effect of Axial Forces	145
4.7	Beams with Varying Depth	150
4.8	Alternative Models for Shear Analysis and Design	151
4.9	Shear-Friction Design Method	160
	References	164
	Problems	166
Chapter 5	Bond, Anchorage, and Development Length	168
5.1	Fundamentals of Flexural Bond	168
5.2	Bond Strength and Development Length	172
5.3	ACI Code Provisions for Development of Tension Reinforcement	177
5.4	Anchorage of Tension Bars by Hooks	181
5.5	Anchorage in Tension Using Headed Bars	185
5.6	Anchorage Requirements for Web Reinforcement	189
5.7	Welded Wire Reinforcement	190
5.8	Development of Bars in Compression	191
5.9	Bundled Bars	191
5.10	Bar Cutoff and Bend Points in Beams	192
5.11	Structural Integrity Provisions	199
5.12	Integrated Beam Design Example	200
5.13	Bar Splices	204
	References	207
	Problems	208
Chapter 6	Serviceability	213
6.1	Introduction	213
6.2	Cracking in Flexural Members	213

		216
6.3	ACI Code Provisions for Crack Control	219
6.4	Control of Deflections	220
6.5	Immediate Deflections	223
6.6	Deflections Due to Long-Term Loads	223
6.7	ACI Code Provisions For Control of Deflections	226
6.8	Deflections Due to Shrinkage and Temperature Changes	232
6.9	Moment vs. Curvature for Reinforced Concrete Sections	234
	References	238
	Problems	238
Chapter 7	Analysis and Design for Torsion	241
7.1	Introduction	241
7.2	Torsion in Plain Concrete Members	242
7.3	Torsion in Reinforced Concrete Members	245
7.4	Torsion Plus Shear	249
7.5	ACI Code Provisions for Torsion Design	250
	References	258
	Problems	259
Chapter 8	Short Columns	262
8.1	Introduction: Axial Compression	262
8.2	Lateral Ties and Spirals	265
8.3	Compression Plus Bending of Rectangular Columns	269
8.4	Strain Compatibility Analysis and Interaction Diagrams	270
8.5	Balanced Failure	273
8.6	Distributed Reinforcement	276
8.7	Unsymmetrical Reinforcement	278
8.8	Circular Columns	279
8.9	ACI Code Provisions for Column Design	281
8.10	Design Aids	282
8.11	Biaxial Bending	285
8.12	Load Contour Method	287
8.13	Reciprocal Load Method	288
8.14	Computer Analysis for Biaxial Bending of Columns	291
8.15	Bar Splicing in Columns	292
8.16	Transmission of Column Loads Through Floor Systems	293
	References	294
	Problems	295
Chapter 9	Slender Columns	299
9.1	Introduction	299
9.2	Concentrically Loaded Columns	300
9.3	Compression Plus Bending	303
9.4	ACI Criteria for Slenderness Effects in Columns	309
9.5	ACI Criteria for Nonsway vs. Sway Structures	310

9.6	ACI Moment Magnifier Method for Nonsway Frames	312
9.7	ACI Moment Magnifier Method for Sway Frames	320
9.8	Second-Order Analysis for Slenderness Effects	325
	References	327
	Problems	328
Chapter 10	Strut-and-Tie Models	332
10.1	Introduction	332
10.2	Development of Strut-and-Tie Models	332
10.3	Strut-and-Tie Design Methodology	336
10.4	ACI Provisions for Strut-and-Tie Models	342
10.5	Applications	347
	References	356
	Problems	356
Chapter 11	Design of Reinforcement at Joints	358
11.1	Introduction	358
11.2	Beam-Column Joints	359
11.3	Strut-and-Tie Model for Joint Behavior	371
11.4	Beam-to-Girder Joints	373
11.5	Ledge Girders	374
11.6	Corners and T Joints	377
11.7	Brackets and Corbels	380
	References	384
	Problems	385
Chapter 12	Analysis of Indeterminate Beams and Frames	387
12.1	Continuity	387
12.2	Loading	389
12.3	Simplifications in Frame Analysis	391
12.4	Methods for Elastic Analysis	393
12.5	Idealization of the Structure	394
12.6	Preliminary Design and Guidelines for Proportioning Members	399
12.7	Approximate Analysis	401
12.8	ACI Moment Coefficients	406
12.9	Limit Analysis	409
12.10	Conclusion	420
	References	421
	Problems	421
Chapter 13	Analysis and Design of Slabs	424
13.1	Types of Slabs	424
13.2	Design of One-Way Slabs	426
13.3	Temperature and Shrinkage Reinforcement	429
13.4	Behavior of Two-Way Edge-Supported Slabs	432
13.5	Two-Way Column-Supported Slabs	436

13.6	Direct Design Method for Column-Supported Slabs	439
13.7	Flexural Reinforcement for Column-Supported Slabs	445
13.8	Depth Limitations of the ACI Code	447
13.9	Equivalent Frame Method	454
13.10	Shear Design in Flat Plates and Flat Slabs	462
13.11	Transfer of Moments at Columns	477
13.12	Openings in Slabs	480
13.13	Deflection Calculations	482
13.14	Analysis for Horizontal Loads	489
	References	490
	Problems	492
Chapter 14	Yield Line Analysis for Slabs	497
14.1	Introduction	497
14.2	Upper and Lower Bound Theorems	500
14.3	Rules for Yield Lines	500
14.4	Analysis by Segment Equilibrium	504
14.5	Analysis by Virtual Work	506
14.6	Orthotropic Reinforcement and Skewed Yield Lines	511
14.7	Special Conditions at Edges and Corners	513
14.8	Fan Patterns at Concentrated Loads	515
14.9	Limitations of Yield Line Theory	516
	References	517
	Problems	517
Chapter 15	Strip Method for Slabs	522
15.1	Introduction	522
15.2	Basic Principles	523
15.3	Choice of Load Distribution	524
15.4	Rectangular Slabs	527
15.5	Fixed Edges and Continuity	529
15.6	Unsupported Edges	534
15.7	Slabs with Holes	542
15.8	Advanced Strip Method	546
15.9	Comparisons of Methods for Slab Analysis and Design	554
	References	555
	Problems	555
Chapter 16	Footings and Foundations	559
16.1	Types and Functions	559
16.2	Spread Footings	559
16.3	Design Factors	560
16.4	Loads, Bearing Pressures, and Footing Size	561
16.5	Wall Footings	563
16.6	Column Footings	565
16.7	Combined Footings	574
16.8	Two-Column Footings	575
16.9	Strip, Grid, and Mat Foundations	582

16.10	Pile Caps	584
	References	587
	Problems	587
Chapter 17	Retaining Walls	589
17.1	Function and Types of Retaining Walls	589
17.2	Earth Pressure	589
17.3	Earth Pressure for Common Conditions of Loading	593
17.4	External Stability	594
17.5	Basis of Structural Design	597
17.6	Drainage and Other Details	598
17.7	Example: Design of a Gravity Retaining Wall	599
17.8	Example: Design of a Cantilever Retaining Wall	601
17.9	Counterfort Retaining Walls	608
17.10	Precast Retaining Walls	610
	References	611
	Problems	611
Chapter 18	Concrete Building Systems	613
18.1	Introduction	613
18.2	Floor and Roof Systems	614
18.3	Panel, Curtain, and Bearing Walls	627
18.4	Shear Walls	628
18.5	Precast Concrete for Buildings	631
18.6	Engineering Drawings for Buildings	646
	References	646
Chapter 19	Prestressed Concrete	648
19.1	Introduction	648
19.2	Effects of Prestressing	649
19.3	Sources of Prestress Force	653
19.4	Prestressing Steels	656
19.5	Concrete for Prestressed Construction	658
19.6	Elastic Flexural Analysis	660
19.7	Flexural Strength	666
19.8	Partial Prestressing	670
19.9	Flexural Design Based on Concrete Stress Limits	672
19.10	Shape Selection	682
19.11	Tendon Profiles	683
19.12	Flexural Design Based on Load Balancing	685
19.13	Loss of Prestress	690
19.14	Shear, Diagonal Tension, and Web Reinforcement	694
19.15	Bond Stress, Transfer Length, and Development Length	701
19.16	Anchorage Zone Design	702
19.17	Deflection	706
19.18	Crack Control for Class C Flexural Members	710
	References	710
	Problems	711

Chapter 20	Seismic Design	714
20.1	Introduction	714
20.2	Structural Response	716
20.3	Seismic Loading Criteria	721
20.4	ACI Provisions for Earthquake-Resistant Structures	726
20.5	ACI Provisions for Special Moment Frames	727
20.6	ACI Provisions for Special Structural Walls, Coupling Beams, Diaphragms, and Trusses	739
20.7	ACI Provisions for Shear Strength	742
20.8	ACI Provisions for Intermediate Moment Frames References Problems	747 749 749
Appendix A	Design Aids	751
Appendix B	SI Conversion Factors: Inch-Pound Units to SI Units	785
Index		787

Preface

The fourteenth edition of *Design of Concrete Structures* has the same dual objectives as the previous work: first to establish a firm understanding of the behavior of structural concrete, then to develop proficiency in the methods used in current design practice. It has been updated in accordance with the provisions of the 2008 American Concrete Institute (ACI) Building Code.

It is generally recognized that mere training in special design skills and codified procedures is inadequate for successful professional practice. As new research becomes available and new design methods are continually introduced, these procedures are subject to frequent changes. To understand and keep abreast of these rapid developments and to engage safely in innovative design, the engineer needs a thorough grounding in the basic performance of concrete and steel as structural materials, and in the behavior of reinforced concrete members and structures. On the other hand, the main business of the structural engineer is to design structures safely, economically, and efficiently. Consequently, with this basic understanding as a firm foundation, familiarity with current design procedures is essential. This edition, like the preceding ones, addresses both needs.

The text not only presents the basic mechanics of structural concrete and methods for the design of individual members for bending, shear, torsion, and axial forces, but also provides much detail pertaining to applications in the various types of structural systems, including an extensive presentation of slabs, footings, foundations, and retaining walls. The important topic of joint design is included. The chapter on flexural design has been expanded to improve the presentation of both the basic material and the example problems, coverage of seismic design is updated, and an introduction to prestressed concrete is included, as in previous editions.

There have been a number of significant changes in the 2008 ACI Building Code, which governs design practice in most of the United States and serves as a model code in many other countries as well. Among these are a reorganization of the provisions for both slender column and earthquake design, the former with some simplification compared to earlier Codes and the latter with some important additions; and the addition of headed studs for use as shear reinforcement in two-way slabs and headed deformed bars as another option for use in anchoring reinforcement.

In addition to changes in the ACI Code, the text includes the modified compression field theory method of shear design as updated in the 2008 Interim Revisions to the American Association of State Highway and Transportation Officials (AASHTO) *LRFD Bridge Design Specifications*.

A feature of the text is the comprehensive presentation of all aspects of slab design. A chapter covering one-way and two-way edge-supported and column-supported slabs, including the new Code material on headed studs, is followed by chapters on slab analysis and design based on the theory of plasticity covering, respectively, the yield

line method for analysis and the strip method for design of slabs, both particularly useful for innovative structures.

A special strength of the text is the analysis chapter, which includes load combinations for use in design, a description of envelope curves for moment and shear, guidelines for proportioning members under both gravity and lateral loads, and procedures for developing preliminary designs of reinforced concrete structures.

Most present-day design is carried out using computer programs, either general-purpose, commercially available software or individual programs written for special needs. Step-by-step procedures are given throughout the book to guide the student and engineer through the increasingly complex methodology of current design, with the emphasis on understanding the design process. Once mastered, these procedures are easily converted into flowcharts to aid in programming. References are given, where appropriate, to the more widely used commercial programs.

The text will be found suitable for either a one or two-semester course in the design of concrete structures. If the curriculum permits only a single course (probably taught in the fourth undergraduate year), the following will provide a good basis: the introduction and treatment of materials found in Chapters 1 and 2, respectively; the material on flexure, shear, and anchorage in Chapters 3, 4, and 5; Chapter 6 on serviceability; Chapter 8 on short columns; and the introduction to one and two-way slabs found in the first four sections of Chapter 13. Time may or may not permit classroom coverage of frame analysis or building systems, Chapters 12 and 18, but these could well be assigned as independent reading, concurrent with the earlier work of the course. In the authors' experience, such complementary outside reading tends to enhance student motivation.

The text is more than adequate for a second course, most likely taught in the first year of graduate study. The authors have found that this is an excellent opportunity to provide students with a more general understanding of reinforced concrete structural design, often beginning with Chapters 12 and 18 and followed by the increasingly important topics of torsion, Chapter 7; slender columns, Chapter 9; the strut-and-tie method, Chapter 10; and the design and detailing of joints, Chapter 11. It should also offer an opportunity for a much expanded study of slabs, including the remaining sections of Chapter 13, plus the methods for slab analysis and design based on plasticity theory found in Chapters 14 and 15, yield line analysis and the strip method of design. Other topics appropriate to a second course include foundations and retaining walls, Chapters 16 and 17, and the introduction to seismic design in Chapter 20. Prestressed concrete is sufficiently important to justify a separate course. If time constraints do not permit this, Chapter 19 provides an introduction and can be used as the text for a one-credit-hour course.

At the end of each chapter, the user will find extensive reference lists, which provide an entry into the literature for those wishing to increase their knowledge through independent study. For professors, the instructor's solution manual is available online at www.mhhe.com/concrete.

A word must be said about units. In the United States, regrettably, the transition from U.S. Customary System units to the metric system has proceeded very slowly, and in many quarters not at all. This is in part because of the expense to the construction industry of the conversion, but perhaps also because of perceived shortcomings in the SI metric system (use of derived units such as the pascal, elimination of the convenient centimeter, etc.) compared with the traditional European metric system. Although most basic science courses are taught using SI units, in most upper-class and graduate design courses, inch-pound units are customarily used, reflecting conditions of practice here. Accordingly, inch-pound units are used throughout the text, although

graphs and basic data in Chapter 2 are given in dual units. Appendix B gives the SI equivalents of inch-pound units. An SI version of the ACI Building Code is available.

A brief historical note may be of interest. This book is the fourteenth edition of a textbook originated in 1923 by Leonard C. Urquhart and Charles E. O'Rourke, both professors of structural engineering at Cornell University at that time. Over its remarkable 86-year history, new editions have kept pace with research, improved materials, and new methods of analysis and design. The second, third, and fourth editions firmly established the work as a leading text for elementary courses in the subject area. Professor George Winter, also of Cornell, collaborated with Urquhart in preparing the fifth and sixth editions. Winter and the present senior author were responsible for the seventh, eighth, and ninth editions, which substantially expanded both the scope and the depth of the presentation. The tenth, eleventh, and twelfth editions were prepared by Professor Nilson subsequent to Professor Winter's passing in 1982, the latter with Professor David Darwin of the University of Kansas serving as a contributor.

Professors Nilson and Darwin were joined by Professor Charles Dolan of the University of Wyoming beginning with the thirteenth edition. All three have been deeply involved in research and teaching in the fields of reinforced and prestressed concrete, as well as professional Code-writing committees, and have spent significant time in professional practice, invaluable in developing the perspective and structural judgement that sets this book apart.

Special thanks are due to reviewers and former students for their many helpful comments and suggestions for this and previous editions. In particular, the authors would like to thank the following reviewers: Paul Barr, Utah State University; Robert N. Emerson, Oklahoma State University; A. Fafitis, Arizona State University; R. Craig Henderson, Tennessee Technological University; Max Porter, Iowa State University; Pizhong Qiao, The University of Akron; Aziz Saber, Louisiana Tech University; and Eric Steinberg, Ohio University. Thanks are also due to the McGraw-Hill project team, notably Debra Hash, Sponsoring Editor; Lorraine Buczak, Developmental Editor; and Melissa Leick, Project Manager.

We gladly acknowledge our indebtedness to the original authors. Although it is safe to say that neither Urquhart nor O'Rourke would recognize very much of the detail, the approach to the subject and the educational philosophy that did so much to account for the success of the early editions would be familiar. We acknowledge with particular gratitude the influence of Professor George Winter in developing a point of view that has shaped the work in the chapters that follow.

*Arthur H. Nilson
David Darwin
Charles W. Dolan*

ELECTRONIC TEXTBOOK OPTIONS

Ebooks are an innovative way for students to save money and create a greener environment at the same time. An ebook can save students about half the cost of a traditional textbook and offers unique features like a powerful search engine, highlighting, and the ability to share notes with classmates using ebooks.

McGraw-Hill offers two ebook options: purchasing a downloadable book from VitalSource or a subscription to the book from CourseSmart. To talk about the ebook options, contact your McGraw-Hill Sales Representative or visit the sites directly at www.vitalsource.com and www.coursesmart.com.

1

Introduction

1.1

CONCRETE, REINFORCED CONCRETE, AND PRESTRESSED CONCRETE

Concrete is a stonelike material obtained by permitting a carefully proportioned mixture of cement, sand and gravel or other aggregate, and water to harden in forms of the shape and dimensions of the desired structure. The bulk of the material consists of fine and coarse aggregate. Cement and water interact chemically to bind the aggregate particles into a solid mass. Additional water, over and above that needed for this chemical reaction, is necessary to give the mixture the workability that enables it to fill the forms and surround the embedded reinforcing steel prior to hardening. Concretes with a wide range of properties can be obtained by appropriate adjustment of the proportions of the constituent materials. Special cements (such as high early strength cements), special aggregates (such as various lightweight or heavyweight aggregates), admixtures (such as plasticizers, air-entraining agents, silica fume, and fly ash), and special curing methods (such as steam-curing) permit an even wider variety of properties to be obtained.

These properties depend to a very substantial degree on the proportions of the mix, on the thoroughness with which the various constituents are intermixed, and on the conditions of humidity and temperature in which the mix is maintained from the moment it is placed in the forms until it is fully hardened. The process of controlling conditions after placement is known as *curing*. To protect against the unintentional production of substandard concrete, a high degree of skillful control and supervision is necessary throughout the process, from the proportioning by weight of the individual components, through mixing and placing, until the completion of curing.

The factors that make concrete a universal building material are so pronounced that it has been used, in more primitive kinds and ways than at present, for thousands of years, starting with lime mortars from 12,000 to 6000 BCE in Crete, Cyprus, Greece, and the Middle East. The facility with which, while plastic, it can be deposited and made to fill forms or molds of almost any practical shape is one of these factors. Its high fire and weather resistance is an evident advantage. Most of the constituent materials, with the exception of cement and additives, are usually available at low cost locally or at small distances from the construction site. Its compressive strength, like that of natural stones, is high, which makes it suitable for members primarily subject to compression, such as columns and arches. On the other hand, again as in natural stones, it is a relatively brittle material whose tensile strength is small compared with its compressive strength. This prevents its economical use in structural members that are subject to tension either entirely (such as in tie-rods) or over part of their cross sections (such as in beams or other flexural members).

To offset this limitation, it was found possible, in the second half of the nineteenth century, to use steel with its high tensile strength to reinforce concrete, chiefly in those places where its low tensile strength would limit the carrying capacity of the member. The reinforcement, usually round steel rods with appropriate surface deformations to provide interlocking, is placed in the forms in advance of the concrete. When completely surrounded by the hardened concrete mass, it forms an integral part of the member. The resulting combination of two materials, known as *reinforced concrete*, combines many of the advantages of each: the relatively low cost, good weather and fire resistance, good compressive strength, and excellent formability of concrete and the high tensile strength and much greater ductility and toughness of steel. It is this combination that allows the almost unlimited range of uses and possibilities of reinforced concrete in the construction of buildings, bridges, dams, tanks, reservoirs, and a host of other structures.

In more recent times, it has been found possible to produce steels, at relatively low cost, whose yield strength is 3 to 4 times and more than that of ordinary reinforcing steels. Likewise, it is possible to produce concrete 4 to 5 times as strong in compression as the more ordinary concretes. These high-strength materials offer many advantages, including smaller member cross sections, reduced dead load, and longer spans. However, there are limits to the strengths of the constituent materials beyond which certain problems arise. To be sure, the strength of such a member would increase roughly in proportion to those of the materials. However, the high strains that result from the high stresses that would otherwise be permissible would lead to large deformations and consequently large deflections of such members under ordinary loading conditions. Equally important, the large strains in such high-strength reinforcing steel would induce large cracks in the surrounding low tensile strength concrete, cracks that not only would be unsightly but also could significantly reduce the durability of the structure. This limits the useful yield strength of high-strength reinforcing steel to 80 ksi[†] according to many codes and specifications; 60 ksi steel is most commonly used.

A special way has been found, however, to use steels and concretes of very high strength in combination. This type of construction is known as *prestressed concrete*. The steel, in the form of wires, strands, or bars, is embedded in the concrete under high tension that is held in equilibrium by compressive stresses in the concrete after hardening. Because of this precompression, the concrete in a flexural member will crack on the tension side at a much larger load than when not so precompressed. Prestressing greatly reduces both the deflections and the tensile cracks at ordinary loads in such structures, and thereby enables these high-strength materials to be used effectively. Prestressed concrete has extended, to a very significant extent, the range of spans of structural concrete and the types of structures for which it is suited.

1.2 STRUCTURAL FORMS

The figures that follow show some of the principal structural forms of reinforced concrete. Pertinent design methods for many of them are discussed later in this volume.

Floor support systems for buildings include the monolithic slab-and-beam floor shown in Fig. 1.1, the one-way joist system of Fig. 1.2, and the flat plate floor, without beams or girders, shown in Fig. 1.3. The flat slab floor of Fig. 1.4, frequently used for more heavily loaded buildings such as warehouses, is similar to the flat plate floor, but makes use of increased slab thickness in the vicinity of the columns, as well

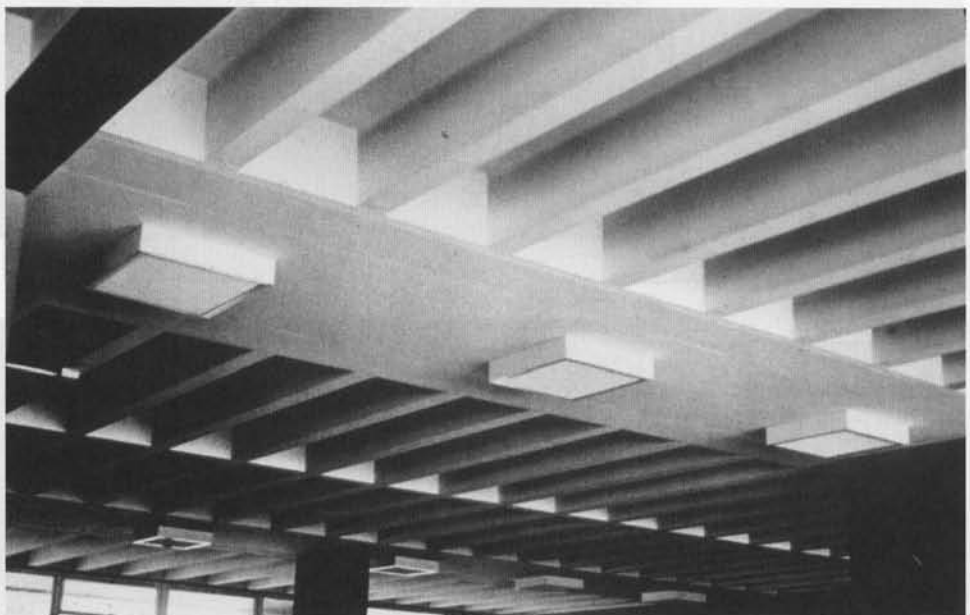
[†] Abbreviation for kips per square inch, or thousands of pounds per square inch.

FIGURE 1.1

One-way reinforced concrete floor slab with monolithic supporting beams. (*Portland Cement Association*.)

**FIGURE 1.2**

One-way joist floor system, with closely spaced ribs supported by monolithic concrete beams; transverse ribs provide for lateral distribution of localized loads. (*Portland Cement Association*.)



as flared column tops, to reduce stresses and increase strength in the support region. The choice among these and other systems for floors and roofs depends upon functional requirements, loads, spans, and permissible member depths, as well as on cost and esthetic factors.

Where long clear spans are required for roofs, concrete shells permit use of extremely thin surfaces, often thinner, relatively, than an eggshell. The folded plate roof of Fig. 1.5 is simple to form because it is composed of flat surfaces; such roofs have been employed for spans of 200 ft and more. The cylindrical shell of Fig. 1.6 is also relatively easy to form because it has only a single curvature; it is similar to the folded plate in its structural behavior and range of spans and loads. Shells of this type were once quite popular in the United States and remain popular in other parts of the world.

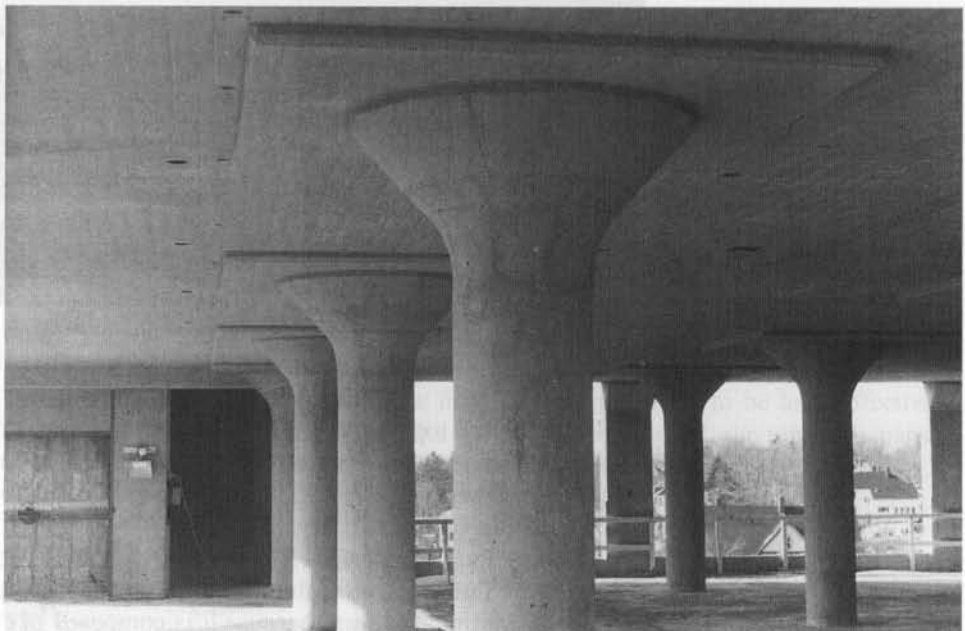
Doubly curved shell surfaces may be generated by simple mathematical curves such as circular arcs, parabolas, and hyperbolas, or they may be composed of complex combinations of shapes. The hyperbolic paraboloid shape, defined by a concave downward parabola moving along a concave upward parabolic path, has been widely

FIGURE 1.3

Flat plate floor slab, carried directly by columns without beams or girders. (*Portland Cement Association*.)

**FIGURE 1.4**

Flat slab floor, without beams but with slab thickness increased at the columns and with flared column tops to provide for local concentration of forces. (*University of Southern Maine*.)



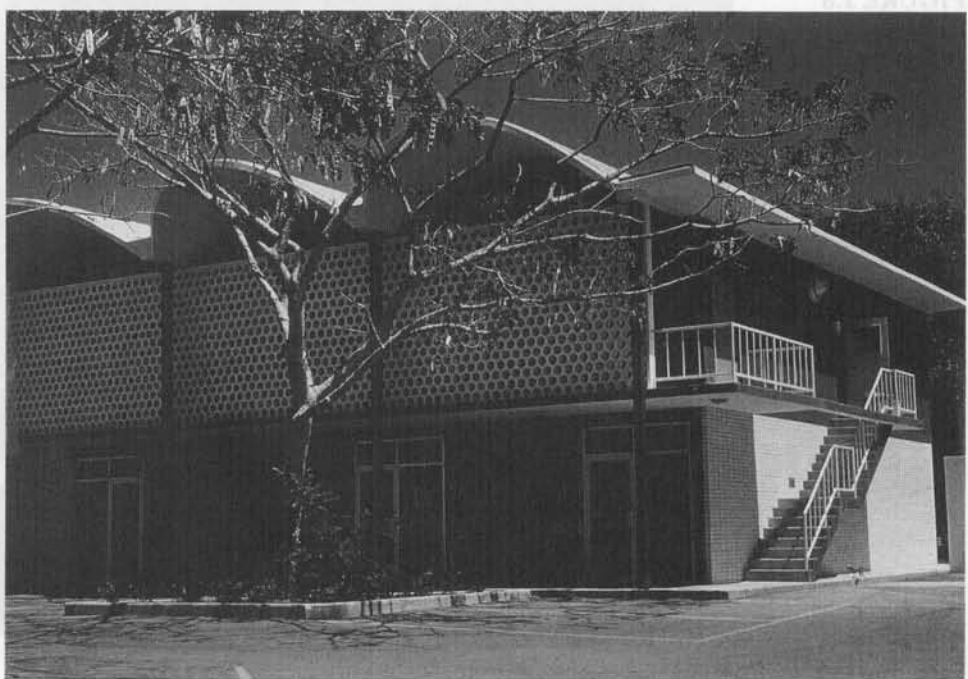
used. It has the interesting property that the doubly curved surface contains two systems of straight-line generators, permitting straight-form lumber to be used. The complex dome of Fig. 1.7, which provides shelter for performing arts events, consists essentially of a circular dome but includes monolithic, upwardly curved edge surfaces to provide stiffening and strengthening in that critical region.

FIGURE 1.5

Folded plate roof of 125 ft span that, in addition to carrying ordinary roof loads, carries the second floor as well from a system of cable hangers; the ground floor is kept free of columns.

**FIGURE 1.6**

Cylindrical shell roof providing column-free interior space.



Napoleon Bonaparte Broward Bridge, shown in Fig. 1.8, is a six-lane, cable-stayed structure that spans St. John's River at Dame Point, Jacksonville, Florida. Its 1300 ft center span is the

Bridge design has provided the opportunity for some of the most challenging and creative applications of structural engineering. The award-winning Napoleon Bonaparte Broward Bridge, shown in Fig. 1.8, is a six-lane, cable-stayed structure that spans St. John's River at Dame Point, Jacksonville, Florida. Its 1300 ft center span is the

FIGURE 1.7

Spherical shell in Lausanne, Switzerland. Upwardly curved edges provide stiffening for the central dome.

**FIGURE 1.8**

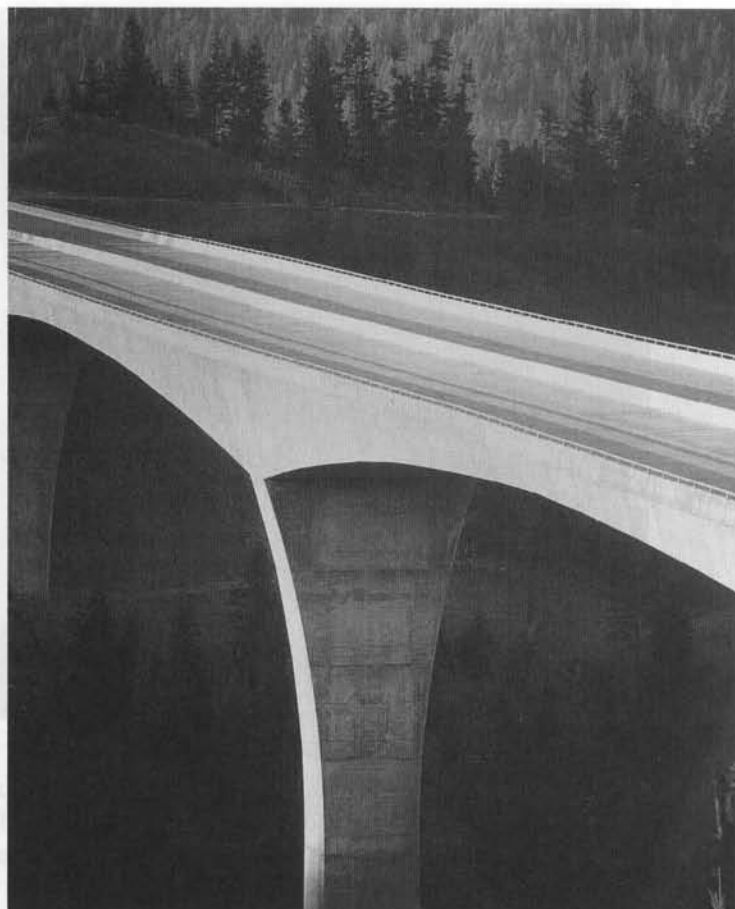
Napoleon Bonaparte Broward Bridge, with a 1300 ft center span at Dame Point, Jacksonville, Florida.
(HNTB Corporation, Kansas City, Missouri.)



second longest of its type in the western hemisphere. Figure 1.9 shows the Bennett Bay Centennial Bridge, a four-span continuous, segmentally cast-in-place box girder structure. Special attention was given to esthetics in this award-winning design. The spectacular Natchez Trace Parkway Bridge in Fig. 1.10, a two-span arch structure using hollow precast concrete elements, carries a two-lane highway 155 ft above the valley

FIGURE 1.9

Bennett Bay Centennial Bridge, Coeur d'Alene, Idaho, a four-span continuous concrete box girder structure of length 1730 ft. (HNTB Corporation, Kansas City, Missouri.)

**FIGURE 1.10**

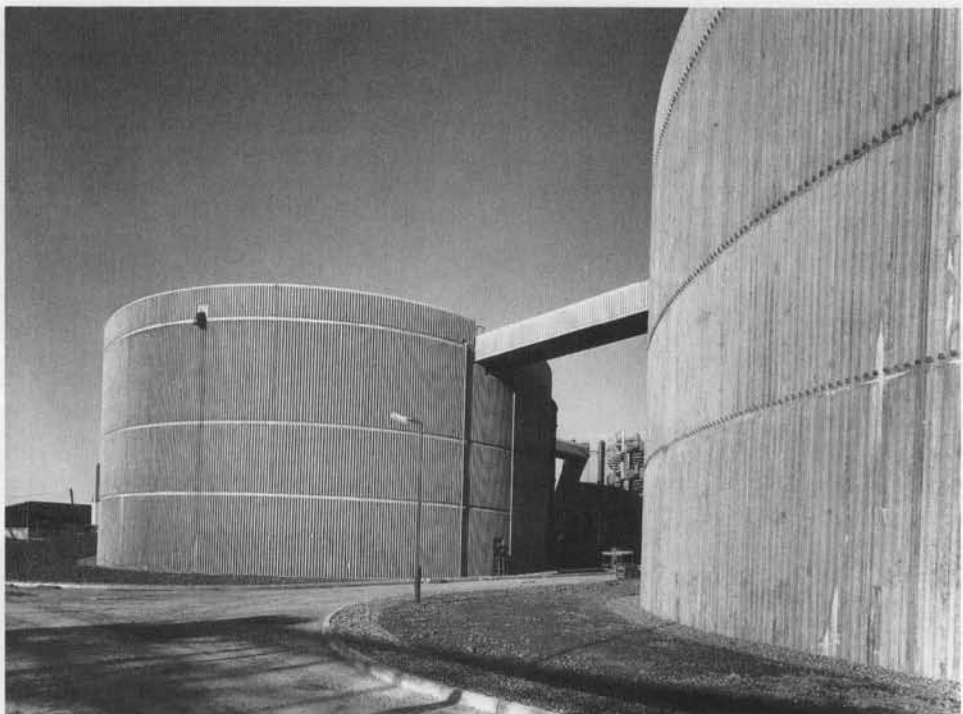
Natchez Trace Parkway Bridge near Franklin, Tennessee, an award-winning two-span concrete arch structure rising 155 ft above the valley floor. (Figg Engineering Group, Tallahassee, Florida.)



FIGURE 1.11

Circular concrete tanks used as a part of the wastewater purification facility at Howden, England.

(Northumbrian Water Authority with Luder and Jones, Architects.)



floor. This structure has won many honors, including awards from the American Society of Civil Engineers and the National Endowment for the Arts.

Cylindrical concrete tanks are widely used for storage of water or in waste purification plants. The design shown in Fig. 1.11 is proof that a sanitary engineering facility can be esthetically pleasing as well as functional. Cylindrical tanks are often prestressed circumferentially to maintain compression in the concrete and eliminate the cracking that would otherwise result from internal pressure.

Concrete structures may be designed to provide a wide array of surface textures, colors, and structural forms. Figure 1.12 shows a precast concrete building containing both color changes and architectural finishes.

The forms shown in Figs. 1.1 to 1.12 hardly constitute a complete inventory but are illustrative of the shapes appropriate to the properties of reinforced or prestressed concrete. They illustrate the adaptability of the material to a great variety of one-dimensional (beams, girders, columns), two-dimensional (slabs, arches, rigid frames), and three-dimensional (shells, tanks) structures and structural components. This variability allows the shape of the structure to be adapted to its function in an economical manner, and furnishes the architect and design engineer with a wide variety of possibilities for esthetically satisfying structural solutions.

1.3 LOADS

Loads that act on structures can be divided into three broad categories: dead loads, live loads, and environmental loads.

Dead loads are those that are constant in magnitude and fixed in location throughout the lifetime of the structure. Usually the major part of the dead load is the weight of the structure itself. This can be calculated with good accuracy from the design configuration, dimensions of the structure, and density of the material. For buildings, floor

FIGURE 1.12

Concrete structures can be produced in a wide range of colors, finishes, and architectural detailing.

(Courtesy of Rocky Mountain Prestress Corp.)



fill, finish floors, and plastered ceilings are usually included as dead loads, and an allowance is made for suspended loads such as piping and lighting fixtures. For bridges, dead loads may include wearing surfaces, sidewalks, and curbs, and an allowance is made for piping and other suspended loads.

Live loads consist chiefly of occupancy loads in buildings and traffic loads on bridges. They may be either fully or partially in place or not present at all, and may also change in location. Their magnitude and distribution at any given time are uncertain, and even their maximum intensities throughout the lifetime of the structure are not known with precision. The minimum live loads for which the floors and roof of a building should be designed are usually specified in the building code that governs at the site of construction. Representative values of minimum live loads to be used in a wide variety of buildings are found in *Minimum Design Loads for Buildings and Other Structures* (Ref. 1.1), a portion of which is reprinted in Table 1.1. The table gives uniformly distributed live loads for various types of occupancies; these include impact provisions where necessary. These loads are expected maxima and considerably exceed average values.

In addition to these uniformly distributed loads, it is recommended that, as an alternative to the uniform load, floors be designed to support safely certain concentrated loads if these produce a greater stress. For example, according to Ref. 1.1, office floors are to be designed to carry a load of 2000 lb distributed over an area 2.5 ft square (6.25 ft^2), to allow for the weight of a safe or other heavy equipment, and stair treads must safely support a 300 lb load applied on the center of the tread. Certain reductions are often permitted in live loads for members supporting large areas, on the premise that it is not likely that the entire area would be fully loaded at one time (Refs. 1.1 and 1.2).

TABLE 1.1
Minimum uniformly distributed live loads

Occupancy or Use	Live Load, psf ^a	Occupancy or Use	Live Load, psf ^a
Apartments (see residential)		Dining rooms and restaurants	100
Access floor systems		Dwellings (see residential)	
Office use	50	Fire escapes	100
Computer use	100	On single-family dwellings only	40
Armories and drill rooms	150	Garages (passenger cars only)	40
Assembly areas and theaters		Trucks and buses ^b	
Fixed seats (fastened to floor)	60	Grandstands (see stadium and arena bleachers)	
Lobbies	100	Gymnasiums, main floors and balconies ^c	100
Movable seats	100	Hospitals	
Platforms (assembly)	100	Operating rooms, laboratories	60
Stage floors	150	Patient rooms	40
Balconies (exterior)	100	Corridors above first floor	80
On one and two-family residences only, and not exceeding 100 ft ²	60	Hotels (see residential)	
Bowling alleys, poolrooms, and similar recreational areas	75	Libraries	
Catwalks for maintenance access	40	Reading rooms	60
Corridors		Stack rooms ^d	150
First floor	100	Corridors above first floor	80
Other floors, same as occupancy served except as indicated		Manufacturing	
Dance halls and ballrooms	100	Light	125
Decks (patio and roof)		Heavy	250
Same as area served, or for the type of occupancy accommodated		Marquees and canopies	75
		Office buildings	
		File and computer rooms shall be designed for heavier loads based on anticipated occupancy	
		Lobbies and first-floor corridors	100

(continued)

Tabulated live loads cannot always be used. The type of occupancy should be considered and the probable loads computed as accurately as possible. Warehouses for heavy storage may be designed for loads as high as 500 psf or more; unusually heavy operations in manufacturing buildings may require an increase in the 250 psf value specified in Table 1.1; special provisions must be made for all definitely located heavy concentrated loads.

Live loads for highway bridges are specified by the American Association of State Highway and Transportation Officials (AASHTO) in its *LRFD Bridge Design Specifications* (Ref. 1.3). For railway bridges, the American Railway Engineering and Maintenance-of-Way Association (AREMA) has published the *Manual of Railway Engineering* (Ref. 1.4), which specifies traffic loads.

Environmental loads consist mainly of snow loads, wind pressure and suction, earthquake loads (i.e., inertia forces caused by earthquake motions), soil pressures on subsurface portions of structures, loads from possible ponding of rainwater on flat surfaces, and forces caused by temperature differentials. Like live loads, environmental loads at any given time are uncertain in both magnitude and distribution. Reference 1.1 contains much information on environmental loads, which is often modified locally depending, for instance, on local climatic or seismic conditions.

Figure 1.13, from the 1972 edition of Ref. 1.1, gives snow loads for the continental United States and is included here for illustration only. The 2005 edition

TABLE 1.1
(Continued)

Occupancy or Use	Live Load, psf ^a	Occupancy or Use	Live Load, psf ^a
Offices	50	Schools	
Corridors above first floor	80	Classrooms	40
Penal institutions		Corridors above first floor	80
Cell blocks	40	First-floor corridors	100
Corridors	100	Sidewalks, vehicular driveways, and yards subject to trucking ^e	250
Residential		Stadiums and arenas	
Dwellings (one and two-family)		Bleachers ^c	100
Uninhabitable attics without storage	10	Fixed seats (fastened to floor) ^c	60
Uninhabitable attics with storage	20	Stairs and exit ways	100
Habitable attics and sleeping areas	30	One and two-family residences only	40
All other areas except stairs and balconies	40	Storage areas above ceilings	20
Hotels and multifamily houses		Storage warehouses (shall be designed for heavier loads if required for anticipated storage)	
Private rooms and corridors serving them	40	Light	125
Public rooms and corridors serving them	100	Heavy	250
Reviewing stands, grandstands, and bleachers ^c		Stores	
Roofs		Retail	
Ordinary flat, pitched, and curved roofs	20	First floor	100
Roofs used for promenade purposes	60	Upper floors	73
Roofs used for roof gardens or assembly purpose	100	Wholesale, all floors	125
Roofs used for other special purposes ^f		Walkways and elevated platforms (other than exitways)	60
Awnings and canopies		Yards and terraces, pedestrians	100
Fabric construction supported by a lightweight rigid skeleton structure ^g	5		
All other construction	20		

^a Pounds per square foot.

^b Garages accommodating trucks and buses shall be designed in accordance with an approved method that contains provisions for truck and bus loadings.

^c In addition to the vertical live loads, the design shall include horizontal swaying forces applied to each row of seats as follows: 24 lb per linear seat applied in the direction parallel to each row of seats and 10 lb per linear ft of seat applied in the direction perpendicular to each row of seats. The parallel and perpendicular horizontal swaying forces need not be applied simultaneously.

^d The loading applies to stack room floors that support nonmobile, double-faced library bookstacks subject to the following limitations: (a) The nominal bookstack unit height shall not exceed 90 in.; (b) the nominal shelf depth shall not exceed 12 in. for each face; and (c) parallel rows of double-faced bookstacks shall be separated by aisles not less than 36 in. wide.

^e Other uniform loads in accordance with an approved method that contains provisions for truck loadings shall also be considered where appropriate.

^f Roofs used for other special purposes shall be designed for appropriate loads as approved by the authority having jurisdiction.

^g Nonreducible.

Source: From Ref. 1.1. Used by permission of the American Society of Civil Engineers.

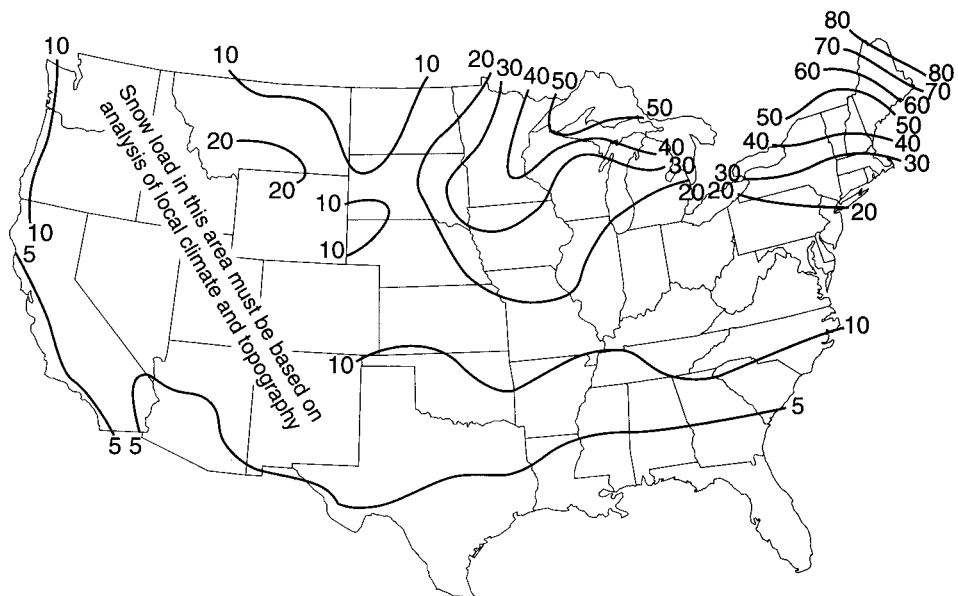
of Ref. 1.1 gives much more detailed information. In either case, specified values represent not average values, but expected upper limits. A minimum roof load of 20 psf is often specified to provide for construction and repair loads and to ensure reasonable stiffness.

Much progress has been made in developing rational methods for predicting horizontal forces on structures due to wind and seismic action. Reference 1.1 summarizes current thinking regarding wind forces and has much information pertaining to earthquake loads as well. Reference 1.5 presents detailed recommendations for lateral forces from earthquakes.

Reference 1.1 specifies design wind pressures per square foot of vertical wall surface. Depending upon locality, these equivalent static forces vary from about 10 to 50 psf.

FIGURE 1.13

Snow load in pounds per square foot (psf) on the ground, 50-year mean recurrence interval. (From Minimum Design Loads for Buildings and Other Structures, ANSI A58.1-1972, American National Standards Institute, New York, NY, 1972.)



Factors include basic wind speed, exposure (urban vs. open terrain, for example), height of the structure, the importance of the structure (i.e., consequences of failure), and gust effect factors to account for the fluctuating nature of the wind and its interaction with the structure.

Seismic forces may be found for a particular structure by elastic or inelastic dynamic analysis, considering expected ground accelerations and the mass, stiffness, and damping characteristics of the construction. However, often the design is based on equivalent static forces calculated from provisions such as those of Refs. 1.1 and 1.5. The base shear is found by considering such factors as location, type of structure and its occupancy, total dead load, and the particular soil condition. The total lateral force is distributed to floors over the entire height of the structure in such a way as to approximate the distribution of forces obtained from a dynamic analysis.

1.4 SERVICEABILITY, STRENGTH, AND STRUCTURAL SAFETY

To serve its purpose, a structure must be safe against collapse and serviceable in use. Serviceability requires that deflections be adequately small; that cracks, if any, be kept to tolerable limits; that vibrations be minimized; etc. Safety requires that the strength of the structure be adequate for all loads that may foreseeably act on it. If the strength of a structure, built as designed, could be predicted accurately, and if the loads and their internal effects (moments, shears, axial forces) were known accurately, safety could be ensured by providing a carrying capacity just barely in excess of the known loads. However, there are a number of sources of uncertainty in the analysis, design, and construction of reinforced concrete structures. These sources of uncertainty, which require a definite margin of safety, may be listed as follows:

1. Actual loads may differ from those assumed.
2. Actual loads may be distributed in a manner different from that assumed.

3. The assumptions and simplifications inherent in any analysis may result in calculated load effects—moments, shears, etc.—different from those that, in fact, act in the structure.
4. The actual structural behavior may differ from that assumed, owing to imperfect knowledge.
5. Actual member dimensions may differ from those specified.
6. Reinforcement may not be in its proper position.
7. Actual material strength may be different from that specified.

In addition, in the establishment of a safety specification, consideration must be given to the consequences of failure. In some cases, a failure would be merely an inconvenience. In other cases, loss of life and significant loss of property may be involved. A further consideration should be the nature of the failure, should it occur. A gradual failure with ample warning permitting remedial measures is preferable to a sudden, unexpected collapse.

It is evident that the selection of an appropriate margin of safety is not a simple matter. However, progress has been made toward rational safety provisions in design codes (Refs. 1.6 to 1.11).

a. Variability of Loads

Since the maximum load that will occur during the life of a structure is uncertain, it can be considered a random variable. In spite of this uncertainty, the engineer must provide an adequate structure. A probability model for the maximum load can be devised by means of a probability density function for loads, as represented by the frequency curve of Fig. 1.14a. The exact form of this distribution curve, for any particular type of loading such as office loads, can be determined only on the basis of statistical data obtained from large-scale load surveys. A number of such surveys have been completed. For types of loads for which such data are scarce, fairly reliable information can be obtained from experience, observation, and judgment.

In such a frequency curve (Fig. 1.14a), the area under the curve between two abscissas, such as loads Q_1 and Q_2 , represents the probability of occurrence of loads Q of magnitude $Q_1 < Q < Q_2$. A specified service load Q_d for design is selected conservatively in the upper region of Q in the distribution curve, as shown. The probability of occurrence of loads larger than Q_d is then given by the shaded area to the right of Q_d . It is seen that this specified service load is considerably larger than the mean load \bar{Q} acting on the structure. This mean load is much more typical of average load conditions than the design load Q_d .

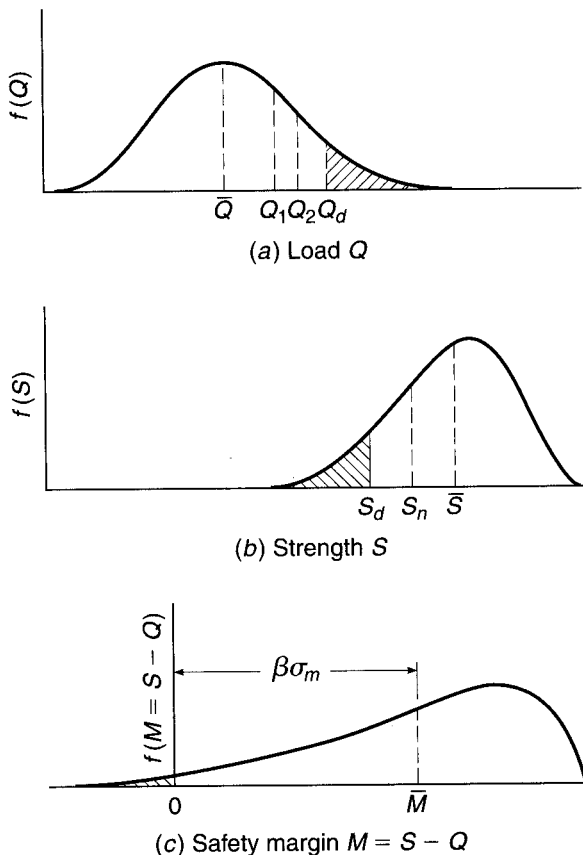
b. Strength

The strength of a structure depends on the strength of the materials from which it is made. For this purpose, minimum material strengths are specified in standardized ways. Actual material strengths cannot be known precisely and therefore also constitute random variables (see Section 2.6). Structural strength depends, furthermore, on the care with which a structure is built, which in turn reflects the quality of supervision and inspection. Member sizes may differ from specified dimensions, reinforcement may be out of position, poorly placed concrete may show voids, etc.

Strength of the entire structure or of a population of repetitive structures, e.g., highway overpasses, can also be considered a random variable with a probability density function of the type shown in Fig. 1.14b. As in the case of loads, the exact form

FIGURE 1.14

Frequency curves for
(a) loads Q , (b) strengths S ,
and (c) safety margin M .



of this function cannot be known but can be approximated from known data, such as statistics of actual, measured materials and member strengths and similar information. Considerable information of this type has been, or is being, developed and used.

c. Structural Safety

A given structure has a *safety margin* M if

$$M = S - Q > 0 \quad (1.1)$$

i.e., if the strength of the structure is larger than the load acting on it. Since S and Q are random variables, the safety margin $M = S - Q$ is also a random variable. A plot of the probability function of M may appear as in Fig. 1.14c. Failure occurs when M is less than zero. Thus, the probability of failure is represented by the shaded area in the figure.

Even though the precise form of the probability density functions for S and Q , and therefore for M , is not known, much can be achieved in the way of a rational approach to structural safety. One such approach is to require that the mean safety margin M be a specified number β of standard deviations σ_m above zero. It can be demonstrated that this results in the requirement that

$$\psi_s \bar{S} \geq \psi_L \bar{Q} \quad (1.2)$$

where ψ_s is a partial safety coefficient smaller than one applied to the mean strength \bar{S} and ψ_L is a partial safety coefficient larger than one applied to the mean load \bar{Q} .

The magnitude of each partial safety coefficient depends on the variance of the quantity to which it applies, S or Q , and on the chosen value of β , the reliability index of the structure. As a general guide, a value of the safety index β between 3 and 4 corresponds to a probability of failure of the order of 1:100,000 (Ref. 1.8). The value of β is often established by calibration against well-proved and established designs.

In practice, it is more convenient to introduce partial safety coefficients with respect to code-specified loads which, as already noted, considerably exceed average values, rather than with respect to mean loads as in Eq. (1.2); similarly, the partial safety coefficient for strength is applied to nominal strength generally computed somewhat conservatively, rather than to mean strengths as in Eq. (1.2). A restatement of the safety requirement in these terms is

$$\phi S_n \geq \gamma Q_d \quad (1.3a)$$

in which ϕ is a strength reduction factor applied to nominal strength S_n and γ is a load factor applied to calculated or code-specified design loads Q_d . Furthermore, recognizing the differences in variability between, say, dead loads D and live loads L , it is both reasonable and easy to introduce different load factors for different types of loads. The preceding equation can thus be written

$$\phi S_n \geq \gamma_d D + \gamma_l L \quad (1.3b)$$

in which γ_d is a load factor somewhat greater than 1.0 applied to the calculated dead load D and γ_l is a larger load factor applied to the code-specified live load L . When additional loads, such as the wind load W , are to be considered, the reduced probability that maximum dead, live, and wind or other loads will act simultaneously can be incorporated by using modified load factors such that

$$\phi S_n \geq \gamma_{d_i} D + \gamma_{l_i} L + \gamma_{w_i} W + \dots \quad (1.3c)$$

Present U.S. design specifications follow the format of Eqs. (1.3b) and (1.3c).

1.5 DESIGN BASIS

The single most important characteristic of any structural member is its actual strength, which must be large enough to resist, with some margin to spare, all foreseeable loads that may act on it during the life of the structure, without failure or other distress. It is logical, therefore, to proportion members, i.e., to select concrete dimensions and reinforcement, so that member strengths are adequate to resist forces resulting from certain hypothetical overload stages, significantly above loads expected actually to occur in service. This design concept is known as *strength design*.

For reinforced concrete structures at loads close to and at failure, one or both of the materials, concrete and steel, are invariably in their nonlinear inelastic range. That is, concrete in a structural member reaches its maximum strength and subsequent fracture at stresses and strains far beyond the initial elastic range in which stresses and strains are fairly proportional. Similarly, steel close to and at failure of the member is usually stressed beyond its elastic domain into and even beyond the yield region. Consequently, the nominal strength of a member must be calculated on the basis of this inelastic behavior of the materials.

A member designed by the strength method must also perform in a satisfactory way under normal service loading. For example, beam deflections must be limited to acceptable values, and the number and width of flexural cracks at service loads must

be controlled. Serviceability limit conditions are an important part of the total design, although attention is focused initially on strength.

Historically, members were proportioned so that stresses in the steel and concrete resulting from normal service loads were within specified limits. These limits, known as *allowable stresses*, were only fractions of the failure stresses of the materials. For members proportioned on such a service load basis, the margin of safety was provided by stipulating allowable stresses under service loads that were appropriately small fractions of the compressive concrete strength and the steel yield stress. We now refer to this basis for design as *service load design*. Allowable stresses, in practice, were set at about one-half the concrete compressive strength and one-half the yield stress of the steel.

Because of the difference in realism and reliability, the strength design method has displaced the older service load design method. However, the older method provides the basis for some serviceability checks and is the design basis for many older structures. Throughout this text, strength design is presented almost exclusively.

1.6 DESIGN CODES AND SPECIFICATIONS

The design of concrete structures such as those of Figs. 1.1 to 1.12 is generally done within the framework of codes giving specific requirements for materials, structural analysis, member proportioning, etc. The International Building Code (Ref. 1.2) is an example of a consensus code governing structural design and is often adopted by local municipalities. The responsibility of preparing material-specific portions of the codes rests with various professional groups, trade associations, and technical institutes. In contrast with many other industrialized nations, the United States does not have an official, government-sanctioned, national code.

The American Concrete Institute (ACI) has long been a leader in such efforts. As one part of its activity, the American Concrete Institute has published the widely recognized *Building Code Requirements for Structural Concrete and Commentary* (Ref. 1.12), which serves as a guide in the design and construction of reinforced concrete buildings. The ACI Code has no official status in itself. However, it is generally regarded as an authoritative statement of current good practice in the field of reinforced concrete. As a result, it has been incorporated into the International Building Code and similar codes, which in turn are adopted by law into municipal and regional building codes that do have legal status. Its provisions thereby attain, in effect, legal standing. Most reinforced concrete buildings and related construction in the United States are designed in accordance with the current ACI Code. It has also served as a model document for many other countries. The commentary incorporated in Ref. 1.12 provides background material and rationale for the Code provisions. The American Concrete Institute also publishes important journals and standards, as well as recommendations for the analysis and design of special types of concrete structures such as the tanks shown in Fig. 1.11.

Most highway bridges in the United States are designed according to the requirements of the AASHTO bridge specifications (Ref. 1.3) which not only contain the provisions relating to loads and load distributions mentioned earlier, but also include detailed provisions for the design and construction of concrete bridges. Many of the provisions follow ACI Code provisions closely, although a number of significant differences will be found.

The design of railway bridges is done according to the specifications of the AREMA *Manual of Railway Engineering* (Ref. 1.4). It, too, is patterned after the ACI

Code in most respects, but it contains much additional material pertaining to railway structures of all types.

No code or design specification can be construed as a substitute for sound engineering judgment in the design of concrete structures. In structural practice, special circumstances are frequently encountered where code provisions can serve only as a guide, and the engineer must rely upon a firm understanding of the basic principles of structural mechanics applied to reinforced or prestressed concrete, and an intimate knowledge of the nature of the materials.

1.7 SAFETY PROVISIONS OF THE ACI CODE

The safety provisions of the ACI Code are given in the form of Eqs. (1.3b) and (1.3c) using strength reduction factors and load factors. These factors are based to some extent on statistical information but to a larger degree on experience, engineering judgment, and compromise. In words, the design strength ϕS_n of a structure or member must be at least equal to the required strength U calculated from the factored loads, i.e.,

$$\text{Design strength} \geq \text{required strength}$$

or

$$\phi S_n \geq U \quad (1.4)$$

The nominal strength S_n is computed (usually somewhat conservatively) by accepted methods. The required strength U is calculated by applying appropriate load factors to the respective service loads: dead load D , live load L , wind load W , earthquake load E , earth pressure H , fluid pressure F , snow load S , rain load R , and environmental effects T that may include settlement, creep, shrinkage, and temperature change. Loads are defined in a general sense, to include either loads or the related internal effects such as moments, shears, and thrusts. Thus, in specific terms for a member subjected, say, to moment, shear, and axial load

$$\phi M_n \geq M_u \quad (1.5a)$$

$$\phi V_n \geq V_u \quad (1.5b)$$

$$\phi P_n \geq P_u \quad (1.5c)$$

where the subscripts n denote the nominal strengths in flexure, shear, and axial load, respectively, and the subscripts u denote the factored load moment, shear, and axial load. In computing the factored load effects on the right, load factors may be applied either to the service loads themselves or to the internal load effects calculated from the service loads.

The load factors specified in the ACI Code, to be applied to calculated dead loads and those live and environmental loads specified in the appropriate codes or standards, are summarized in Table 1.2. These are consistent with the concepts introduced in Section 1.4 and with SEI/ASCE 7, *Minimum Design Loads for Buildings and Other Structures* (Ref. 1.1), and allow design of composite structures using combinations of structural steel and reinforced concrete. For individual loads, lower factors are used for loads known with greater certainty, e.g., dead load, compared with loads of greater variability, e.g., live loads. Further, for load combinations such as dead plus live loads plus wind forces, reductions are applied to one load or the other that reflect the improbability that an excessively large live load coincides with an unusually high windstorm. The

TABLE 1.2
Factored load combinations for determining required strength U in the ACI Code

Condition ^a	Factored Load or Load Effect U
Basic ^b	$U = 1.2D + 1.6L$
Dead plus fluid ^b	$U = 1.4(D + F)$
Snow, rain, temperature, and wind	$U = 1.2(D + F + T) + 1.6(L + H) + 0.5(L, \text{ or } S \text{ or } R)$ $U = 1.2D + 1.6(L, \text{ or } S \text{ or } R) + (1.0L \text{ or } 0.8W)$ $U = 1.2D + 1.6W + 1.0L + 0.5(L, \text{ or } S \text{ or } R)$ $U = 0.9D + 1.6W + 1.6H$
Earthquake	$U = 1.2D + 1.0E + 1.0L + 0.2S$ $U = 0.9D + 1.0E + 1.6H$

^a Where the following represent the loads or related internal moments or forces resulting from the listed factors: D = dead load; E = earthquake; F = fluids; H = weight or pressure from soil; L = live load; L_r = roof live load; R = rain; S = snow; T = cumulative effects of temperature, creep, shrinkage, and differential settlement; W = wind.

^b The ACI Code includes F or H loads in the load combinations. The “basic” load condition of $1.2D + 1.6L$ reflects the fact that most buildings have neither F nor H loads present and that $1.4D$ rarely governs design.

factors also reflect, in a general way, uncertainties with which internal load effects are calculated from external loads in systems as complex as highly indeterminate, inelastic reinforced concrete structures which, in addition, consist of variable-section members (because of tension cracking, discontinuous reinforcement, etc.). Finally, the load factors also distinguish between two situations, particularly when horizontal forces are present in addition to gravity, i.e., the situation where the effects of all simultaneous loads are additive, as distinct from that in which various load effects counteract one another. For example, in a retaining wall the soil pressure produces an overturning moment, and the gravity forces produce a counteracting stabilizing moment.

In all cases in Table 1.2, the controlling equation is the one that gives the largest factored load effect U .

The strength reduction factors ϕ in the ACI Code are given different values depending on the state of knowledge, i.e., the accuracy with which various strengths can be calculated. Thus, the value for bending is higher than that for shear or bearing. Also, ϕ values reflect the probable importance, for the survival of the structure, of the particular member and of the probable quality control achievable. For both these reasons, a lower value is used for columns than for beams. Table 1.3 gives the ϕ values specified in the ACI Code.

The joint application of strength reduction factors (Table 1.3) and load factors (Table 1.2) is aimed at producing approximate probabilities of understrength of the order of 1/100 and of overloads of 1/1000. This results in a probability of structural failure of the order of 1/100,000.

In addition to the values given in Table 1.3, ACI Code Appendix B, “Alternative Provisions for Reinforced and Prestressed Concrete Flexural and Compression Members,” allows the use of load factors and strength reduction factors from previous editions of the ACI Code. The load factors and strength reduction factors of ACI Code Appendix B are calibrated in conjunction with the detailed requirements of that appendix. Consequently, they may not be interchanged with the provisions of the main body of the Code.

TABLE 1.3
Strength reduction factors in the ACI Code

Strength Condition	Strength Reduction Factor ϕ
Tension-controlled sections ^a	0.90
Compression-controlled sections ^b	
Members with spiral reinforcement	0.75
Other reinforced members	0.65
Shear and torsion	0.75
Bearing on concrete	0.65
Post-tensioned anchorage zones	0.85
Strut-and-tie models ^c	0.75

^a Chapter 19 discusses reductions in ϕ for pretensioned members where strand embedment is less than the development length.

^b Chapter 3 contains a discussion of the linear variation of ϕ between tension and compression-controlled sections. Chapter 8 discusses the conditions that allow an increase in ϕ for spirally reinforced columns.

^c Strut-and-tie models are described in Chapter 10.

1.8 FUNDAMENTAL ASSUMPTIONS FOR REINFORCED CONCRETE BEHAVIOR

The chief task of the structural engineer is the design of structures. *Design* is the determination of the general shape and all specific dimensions of a particular structure so that it will perform the function for which it is created and will safely withstand the influences that will act on it throughout its useful life. These influences are primarily the loads and other forces to which it will be subjected, as well as other detrimental agents, such as temperature fluctuations, foundation settlements, and corrosive influences. *Structural mechanics* is one of the main tools in this process of design. As here understood, it is the body of knowledge that permits one to predict with a good degree of certainty how a structure of given shape and dimensions will behave when acted upon by known forces or other mechanical influences. The chief items of behavior that are of practical interest are (1) the strength of the structure, i.e., that magnitude of loads of a given distribution which will cause the structure to fail, and (2) the deformations, such as deflections and extent of cracking, that the structure will undergo when loaded under service conditions.

The fundamental propositions on which the mechanics of reinforced concrete is based are as follows:

1. The internal forces, such as bending moments, shear forces, and normal and shear stresses, at any section of a member are in equilibrium with the effects of the external loads at that section. This proposition is not an assumption but a fact, because any body or any portion thereof can be at rest only if all forces acting on it are in equilibrium.
2. The strain in an embedded reinforcing bar (unit extension or compression) is the same as that of the surrounding concrete. Expressed differently, it is assumed that perfect bonding exists between concrete and steel at the interface, so that no slip can occur between the two materials. Hence, as the one deforms, so must the other. With modern deformed bars (see Section 2.14), a high degree of mechanical

- interlocking is provided in addition to the natural surface adhesion, so this assumption is very close to correct.
3. Cross sections that were plane prior to loading continue to be plane in the member under load. Accurate measurements have shown that when a reinforced concrete member is loaded close to failure, this assumption is not absolutely accurate. However, the deviations are usually minor, and the results of theory based on this assumption check well with extensive test information.
 4. In view of the fact that the tensile strength of concrete is only a small fraction of its compressive strength (see Section 2.9), the concrete in that part of a member which is in tension is usually cracked. While these cracks, in well-designed members, are generally so narrow as to be hardly visible (they are known as *hairline* cracks), they evidently render the cracked concrete incapable of resisting tension stress. Correspondingly, it is assumed that concrete is not capable of resisting any tension stress whatever. This assumption is evidently a simplification of the actual situation because, in fact, concrete prior to cracking, as well as the concrete located between cracks, does resist tension stresses of small magnitude. Later in discussions of the resistance of reinforced concrete beams to shear, it will become apparent that under certain conditions this particular assumption is dispensed with and advantage is taken of the modest tensile strength that concrete can develop.
 5. The theory is based on the actual stress-strain relationships and strength properties of the two constituent materials (see Sections 2.8 and 2.14) or some reasonable equivalent simplifications thereof. The fact that nonelastic behavior is reflected in modern theory, that concrete is assumed to be ineffective in tension, and that the joint action of the two materials is taken into consideration results in analytical methods which are considerably more complex, and also more challenging, than those that are adequate for members made of a single, substantially elastic material.

These five assumptions permit one to predict by calculation the performance of reinforced concrete members only for some simple situations. Actually, the joint action of two materials as dissimilar and complicated as concrete and steel is so complex that it has not yet lent itself to purely analytical treatment. For this reason, methods of design and analysis, while using these assumptions, are very largely based on the results of extensive and continuing experimental research. They are modified and improved as additional test evidence becomes available.

1.9 BEHAVIOR OF MEMBERS SUBJECT TO AXIAL LOADS

Many of the fundamentals of the behavior of reinforced concrete, through the full range of loading from zero to ultimate, can be illustrated clearly in the context of members subject to simple axial compression or tension. The basic concepts illustrated here will be recognized in later chapters in the analysis and design of beams, slabs, eccentrically loaded columns, and other members subject to more complex loadings.

a. Axial Compression

In members that sustain chiefly or exclusively axial compression loads, such as building columns, it is economical to make the concrete carry most of the load. Still, some steel reinforcement is always provided for various reasons. For one, very few members

are truly axially loaded; steel is essential for resisting any bending that may exist. For another, if part of the total load is carried by steel with its much greater strength, the cross-sectional dimensions of the member can be reduced—the more so, the larger the amount of reinforcement.

The two chief forms of reinforced concrete columns are shown in Fig. 1.15. In the square column, the four longitudinal bars serve as main reinforcement. They are held in place by transverse small-diameter steel ties that prevent displacement of the main bars during construction operations and counteract any tendency of the compression-loaded bars to buckle out of the concrete by bursting the thin outer cover. On the left is shown a round column with eight main reinforcing bars. These are surrounded by a closely spaced spiral that serves the same purpose as the more widely spaced ties but also acts to confine the concrete within it, thereby increasing its resistance to axial compression. The discussion that follows applies to tied columns.

When axial load is applied, the compression strain is the same over the entire cross section and, in view of the bonding between concrete and steel, is the same in the two materials (see propositions 2 and 3 in Section 1.8). To illustrate the action of such a member as load is applied, Fig. 1.16 shows two typical stress-strain curves, one for a concrete with compressive strength $f'_c = 4000$ psi and the other for a steel with yield stress $f_y = 60,000$ psi. The curves for the two materials are drawn on the same graph using different vertical stress scales. Curve *b* has the shape that would be obtained in a concrete cylinder test. The rate of loading in most structures is considerably slower than that in a cylinder test, and this affects the shape of the curve. Curve *c*, therefore, is drawn as being characteristic of the performance of concrete under slow loading. Under these conditions, tests have shown that the maximum reliable compressive strength of reinforced concrete is about $0.85f'_c$, as shown.

FIGURE 1.15
Reinforced concrete
columns.

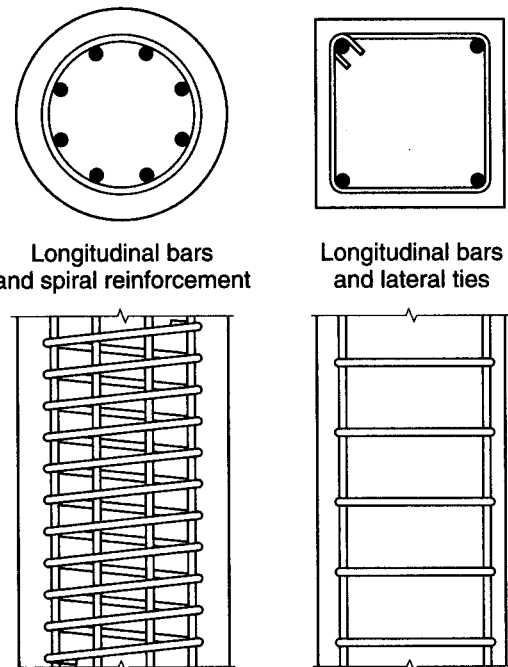
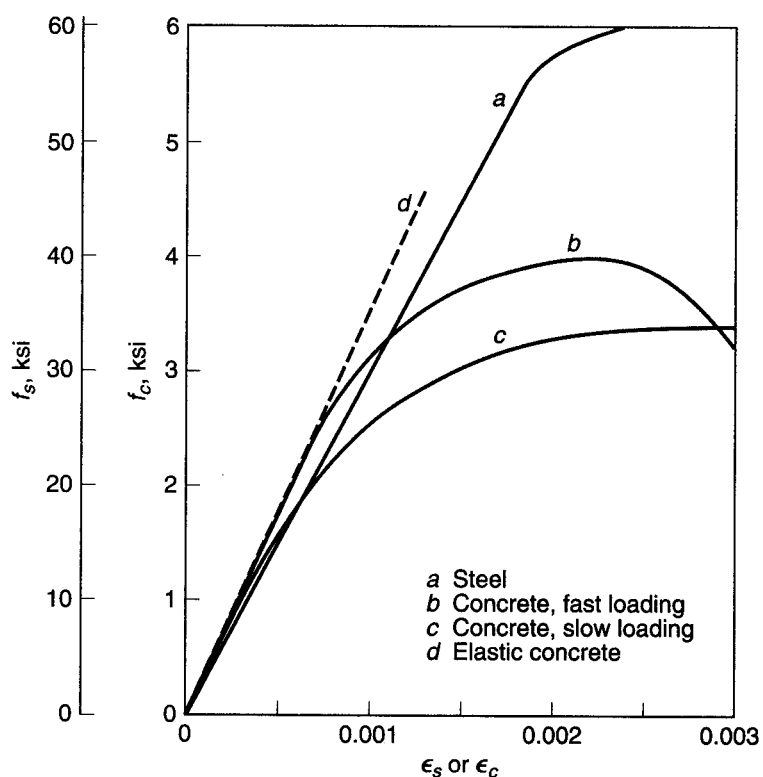


FIGURE 1.16
Concrete and steel stress-strain curves.



ELASTIC BEHAVIOR At low stresses, up to about $f'_c/2$, the concrete is seen to behave nearly elastically, i.e., stresses and strains are quite closely proportional; the straight line d represents this range of behavior with little error for both rates of loading. For the given concrete, the range extends to a strain of about 0.0005. The steel, on the other hand, is seen to be elastic nearly to its yield point of 60 ksi, or to the much greater strain of about 0.002.

Because the compression strain in the concrete, at any given load, is equal to the compression strain in the steel,

$$\epsilon_c = \frac{f_c}{E_c} = \epsilon_s = \frac{f_s}{E_s}$$

from which the relation between the steel stress f_s and the concrete stress f_c is obtained as

$$f_s = \frac{E_s}{E_c} f_c = n f_c \quad (1.6)$$

where $n = E_s/E_c$ is known as the *modular ratio*.

Let

A_c = net area of concrete, i.e., gross area minus area occupied by reinforcing bars

A_g = gross area

A_{st} = total area of reinforcing bars

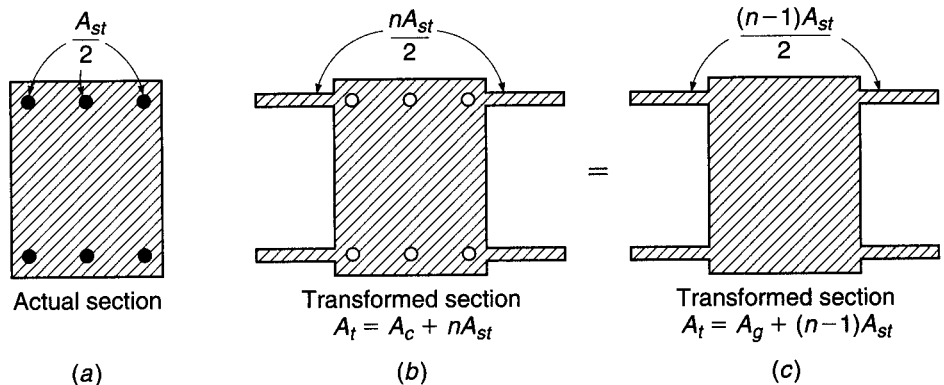
P = axial load

Then

$$P = f_c A_c + f_s A_{st} = f_c A_c + n f_c A_{st}$$

FIGURE 1.17

Transformed section in axial compression.



or

$$P = f_c(A_c + nA_{st}) \quad (1.7)$$

The term $A_c + nA_{st}$ can be interpreted as the area of a fictitious concrete cross section, the *transformed area*, which when subjected to the particular concrete stress f_c results in the same axial load P as the actual section composed of both steel and concrete. This transformed concrete area is seen to consist of the actual concrete area plus n times the area of the reinforcement. It can be visualized as shown in Fig. 1.17. That is, in Fig. 1.17b the three bars along each of the two faces are thought of as being removed and replaced, at the same distance from the axis of the section, with added areas of fictitious concrete of total amount nA_{st} . Alternatively, as shown in Fig. 1.17c, one can think of the area of the steel bars as replaced with concrete, in which case one has to add to the gross concrete area A_g so obtained only $(n - 1)A_{st}$ to obtain the same total transformed area. Therefore, alternatively,

$$P = f_c[A_g + (n - 1)A_{st}] \quad (1.8)$$

If load and cross-sectional dimensions are known, the concrete stress can be found by solving Eq. (1.7) or (1.8) for f_c , and the steel stress can be calculated from Eq. (1.6). These relations hold in the range in which the concrete behaves nearly elastically, i.e., up to about 50 to 60 percent of f'_c . For reasons of safety and serviceability, concrete stresses in structures under normal conditions are kept within this range. Therefore, these relations permit one to calculate *service load stresses*.

EXAMPLE 1.1

A column made of the materials defined in Fig. 1.16 has a cross section of 16 × 20 in. and is reinforced by six No. 9 (No. 29) bars, disposed as shown in Fig. 1.17. (See Tables A.1 and A.2 of Appendix A for bar diameters and areas and Section 2.14 for a description of bar size designations.) Determine the axial load that will stress the concrete to 1200 psi. The modular ratio n may be assumed equal to 8. (In view of the scatter inherent in E_c , it is customary and satisfactory to round off the value of n to the nearest integer.)

SOLUTION. One finds $A_g = 16 \times 20 = 320 \text{ in}^2$, and from Appendix A, Table A.2, two No. 9 (No. 29) bars provide steel area $A_{st} = 6.00 \text{ in}^2$ or 1.88 percent of the gross area. The load on the column, from Eq. (1.8), is $P = 1200[320 + (8 - 1)6.00] = 434,000 \text{ lb}$. Of this total load, the concrete is seen to carry $P_c = f_c A_c = f_c(A_g - A_{st}) = 1200(320 - 6) = 377,000 \text{ lb}$, and the steel $P_s = f_s A_{st} = (nf_c)A_{st} = 9600 \times 6 = 57,600 \text{ lb}$, which is 13.3 percent of the total axial load.

INELASTIC RANGE Inspection of Fig. 1.16 shows that the elastic relationships that have been used so far cannot be applied beyond a strain of about 0.0005 for the given concrete. To obtain information on the behavior of the member at larger strains and, correspondingly, at larger loads, it is therefore necessary to make direct use of the information in Fig. 1.16.

EXAMPLE 1.2

One may want to calculate the magnitude of the axial load that will produce a strain or unit shortening $\epsilon_c = \epsilon_s = 0.0010$ in the column of Example 1.1. At this strain the steel is seen to be still elastic, so that the steel stress $f_s = \epsilon_s E_s = 0.001 \times 29,000,000 = 29,000$ psi. The concrete is in the inelastic range, so that its stress cannot be directly calculated, but it can be read from the stress-strain curve for the given value of strain.

1. If the member has been loaded at a fast rate, curve *b* holds at the instant when the entire load is applied. The stress for $\epsilon = 0.001$ can be read as $f_c = 3200$ psi. Consequently, the total load can be obtained from

$$P = f_c A_c + f_s A_{st} \quad (1.9)$$

which applies in the inelastic as well as in the elastic range. Hence, $P = 3200(320 - 6) + 29,000 \times 6 = 1,005,000 + 174,000 = 1,179,000$ lb. Of this total load, the steel is seen to carry 174,000 lb, or 14.7 percent.

2. For slowly applied or sustained loading, curve *c* represents the behavior of the concrete. Its stress at a strain of 0.001 can be read as $f_c = 2400$ psi. Then $P = 2400 \times 314 + 29,000 \times 6 = 754,000 + 174,000 = 928,000$ lb. Of this total load, the steel is seen to carry 18.8 percent.

Comparison of the results for fast and slow loading shows the following. Owing to creep of concrete, a given shortening of the column is produced by a smaller load when slowly applied or sustained over some length of time than when quickly applied. More important, the farther the stress is beyond the proportional limit of the concrete, and the more slowly the load is applied or the longer it is sustained, the smaller the share of the total load carried by the concrete and the larger the share carried by the steel. In the sample column, the steel was seen to carry 13.3 percent of the load in the elastic range, 14.7 percent for a strain of 0.001 under fast loading, and 18.8 percent at the same strain under slow or sustained loading.

STRENGTH The one quantity of chief interest to the structural designer is *strength*, i.e., the maximum load that the structure or member will carry. Information on stresses, strains, and similar quantities serves chiefly as a tool for determining carrying capacity. The performance of the column discussed so far indicates two things: (1) in the range of large stresses and strains that precede attainment of the maximum load and subsequent failure, elastic relationships cannot be used; (2) the member behaves differently under fast and under slow or sustained loading and shows less resistance to the latter than to the former. In usual construction, many types of loads, such as the weight of the structure and any permanent equipment housed therein, are sustained, and others are applied at slow rates. For this reason, to calculate a reliable magnitude of compressive strength, curve *c* of Fig. 1.16 must be used as far as the concrete is concerned.

The steel reaches its tensile strength (peak of the curve) at strains on the order of 0.08 (see Fig. 2.15). Concrete, on the other hand, fails by crushing at the much smaller strain of about 0.003 and, as seen from Fig. 1.16 (curve *c*), reaches its maximum stress in the strain range of 0.002 to 0.003. Because the strains in steel and concrete are equal in axial compression, the load at which the steel begins to yield can be calculated from the information in Fig. 1.16.

If the small knee prior to yielding of the steel is disregarded, i.e., if the steel is assumed to be sharp-yielding, the strain at which it yields is

$$\epsilon_y = \frac{f_y}{E_s} \quad (1.10)$$

or

$$\epsilon_y = \frac{60,000}{29,000,000} = 0.00207$$

At this strain, curve *c* of Fig. 1.16 indicates a stress of 3200 psi in the concrete; therefore, by Eq. (1.9), the load in the member when the steel starts yielding is $P_y = 3200 \times 314 + 60,000 \times 6 = 1,365,000$ lb. At this load the concrete has not yet reached its full strength, which, as mentioned before, can be assumed as $0.85f'_c = 3400$ psi for slow or sustained loading, and therefore the load on the member can be further increased. During this stage of loading, the steel keeps yielding at constant stress. Finally, the nominal capacity[†] of the member is reached when the concrete crushes while the steel yields, i.e.,

$$P_n = 0.85f'_c A_c + f_y A_{st} \quad (1.11)$$

Numerous careful tests have shown the reliability of Eq. (1.11) in predicting the ultimate strength of a concentrically loaded reinforced concrete column, provided its slenderness ratio is small so that buckling will not reduce its strength.

For the particular numerical example, $P_n = 3400 \times 314 + 60,000 \times 6 = 1,068,000 + 360,000 = 1,428,000$ lb. At this stage the steel carries 25.2 percent of the load.

SUMMARY In the elastic range, the steel carries a relatively small portion of the total load of an axially compressed member. As member strength is approached, there occurs a redistribution of the relative shares of the load resisted by concrete and steel, the latter taking an increasing amount. The nominal capacity, at which the member is on the point of failure, consists of the contribution of the steel when it is stressed to the yield point plus that of the concrete when its stress has attained a value of $0.85f'_c$, as reflected in Eq. (1.11).

b. Axial Tension

The tension strength of concrete is only a small fraction of its compressive strength. It follows that reinforced concrete is not well suited for use in tension members because the concrete will contribute little, if anything, to their strength. Still, there are situations in which reinforced concrete is stressed in tension, chiefly in tie-rods in structures such as arches. Such members consist of one or more bars embedded in concrete in a symmetric arrangement similar to compression members (see Figs. 1.15 and 1.17).

When the tension force in the member is small enough for the stress in the concrete to be considerably below its tensile strength, both steel and concrete behave elastically. In this situation, all the expressions derived for elastic behavior in compression in Section 1.9a are identically valid for tension. In particular, Eq. (1.7) becomes

$$P = f_{ct}(A_c + nA_{st}) \quad (1.12)$$

where f_{ct} is the tensile stress in the concrete.

[†] Throughout this book quantities that refer to the strength of members, calculated by accepted analysis methods, are furnished with the subscript *n*, which stands for "nominal." This notation is in agreement with the ACI Code. It is intended to convey that the actual strength of any member is bound to deviate to some extent from its calculated, nominal value because of inevitable variations of dimensions, materials properties, and other parameters. Design in all cases is based on this nominal strength, which represents the best available estimate of the actual member strength.

However, when the load is further increased, the concrete reaches its tensile strength at a stress and strain on the order of one-tenth of what it could sustain in compression. At this stage, the concrete cracks across the entire cross section. When this happens, it ceases to resist any part of the applied tension force, since, evidently, no force can be transmitted across the air gap in the crack. At any load larger than that which caused the concrete to crack, the steel is called upon to resist the entire tension force. Correspondingly, at this stage,

$$P = f_s A_{st} \quad (1.13)$$

With further increased load, the tensile stress f_s in the steel reaches the yield point f_y . When this occurs, the tension members cease to exhibit small, elastic deformations but instead stretch a sizable and permanent amount at substantially constant load. This does not impair the strength of the member. Its elongation, however, becomes so large (on the order of 1 percent or more of its length) as to render it useless. Therefore, the maximum useful strength P_{nt} of a tension member is the force that will just cause the steel stress to reach the yield point. That is,

$$P_{nt} = f_y A_{st} \quad (1.14)$$

To provide adequate safety, the force permitted in a tension member under normal service loads should be limited to about $\frac{1}{2}P_{nt}$. Because the concrete has cracked at loads considerably smaller than this, concrete does not contribute to the carrying capacity of the member in service. It does serve, however, as fire and corrosion protection and often improves the appearance of the structure.

There are situations, though, in which reinforced concrete is used in axial tension under conditions in which the occurrence of tension cracks must be prevented. A case in point is a circular tank (see Fig. 1.11). To provide watertightness, the hoop tension caused by the fluid pressure must be prevented from causing the concrete to crack. In this case, Eq. (1.12) can be used to determine a safe value for the axial tension force P by using, for the concrete tension stress f_{ct} , an appropriate fraction of the tensile strength of the concrete, i.e., of the stress that would cause the concrete to crack.

REFERENCES

- 1.1. *Minimum Design Loads for Buildings and Other Structures*, ASCE/SEI 7-05, American Society of Civil Engineers, Reston, VA, 2005.
- 1.2. *International Building Code*, International Code Council, Washington, DC, 2006.
- 1.3. *AASHTO LRFD Bridge Design Specifications*, 4th ed., American Association of State Highway and Transportation Officials (AASHTO), Washington, DC, 2008.
- 1.4. *Manual of Railway Engineering*, American Railway Engineering and Maintenance-of-Way Association (AREMA), Landover, MD, 2008.
- 1.5. *Building Seismic Safety Council NEHRP Recommended Provisions for Seismic Regulations for New Buildings and Other Structures*, 2000 edition, Part 1, "Provisions," FEMA 368, Part 2, "Commentary," FEMA 369, Federal Emergency Management Agency, Washington, DC, March 2001.
- 1.6. J. G. MacGregor, S. A. Mirza, and B. Ellingwood, "Statistical Analysis of Resistance of Reinforced and Prestressed Concrete Members," *J. ACI*, vol. 80, no. 3, 1983, pp. 167-176.
- 1.7. J. G. MacGregor, "Load and Resistance Factors for Concrete Design," *J. ACI*, vol. 80, no. 4, 1983, pp. 279-287.
- 1.8. J. G. MacGregor, "Safety and Limit States Design for Reinforced Concrete," *Can. J. Civ. Eng.*, vol. 3, no. 4, 1976, pp. 484-513.
- 1.9. G. Winter, "Safety and Serviceability Provisions of the ACI Building Code," ACI-CEB-FIP-PCI Symposium, *ACI Special Publication SP-59*, 1979.
- 1.10. A. S. Nowak and M. M. Szerszen, "Calibration of Design Code for Buildings (ACI 318): Part 1—Statistical Models for Resistance," *ACI Struct. J.*, vol. 100, no. 3, 2003, pp. 377-382.

- 1.11 M. M. Szerszen and A. S. Nowak, "Calibration of Design Code for Buildings (ACI 318): Part 2—Reliability Analysis and Resistance Factors," *ACI Struct. J.*, vol. 100, no. 3, 2003, pp. 383–391.
- 1.12. *Building Code Requirements for Structural Concrete and Commentary* (ACI 318-08), American Concrete Institute, Farmington Hills, MI, 2008.

PROBLEMS

- 1.1. A 16×20 in. column is made of the same concrete and reinforced with the same six No. 9 (No. 29) bars as the column in Examples 1.1 and 1.2, except that a steel with yield strength $f_y = 40$ ksi is used. The stress-strain diagram of this reinforcing steel is shown in Fig. 2.15 for $f_y = 40$ ksi. For this column determine (a) the axial load that will stress the concrete to 1200 psi; (b) the load at which the steel starts yielding; (c) the maximum load; and (d) the share of the total load carried by the reinforcement at these three stages of loading. Compare results with those calculated in the examples for $f_y = 60$ ksi, keeping in mind, in regard to relative economy, that the price per pound for reinforcing steels with 40 and 60 ksi yield points is about the same.
- 1.2. The area of steel, expressed as a percentage of gross concrete area, for the column of Problem 1.1 is lower than would often be used in practice. Recalculate the comparisons of Problem 1.1, using f_y of 40 ksi and 60 ksi as before, but for a 16×20 in. column reinforced with eight No. 11 (No. 36) bars. Compare your results with those of Problem 1.1.
- 1.3. A square concrete column with dimensions 22×22 in. is reinforced with a total of eight No. 10 (No. 32) bars arranged uniformly around the column perimeter. Material strengths are $f_y = 60$ ksi and $f'_c = 4000$ psi, with stress-strain curves as given by curves *a* and *c* of Fig. 1.16. Calculate the percentages of total load carried by the concrete and by the steel as load is gradually increased from 0 to failure, which is assumed to occur when the concrete strain reaches a limit value of 0.0030. Determine the loads at strain increments of 0.0005 up to the failure strain, and graph your results, plotting load percentages vs. strain. The modular ratio may be assumed at $n = 8$ for these materials.
- 1.4. A 20×24 in. column is made of the same concrete as used in Examples 1.1 and 1.2. It is reinforced with six No. 11 (No. 36) bars with $f_y = 60$ ksi. For this column section, determine (a) the axial load that the section will carry at a concrete stress of 1400 psi; (b) the load on the section when the steel begins to yield; (c) the maximum load if the section is loaded slowly; and (d) the maximum load if the section is loaded rapidly. The area of one No. 11 (No. 36) bar is 1.56 in^2 . Determine the percent of the load carried by the steel and the concrete for each combination.
- 1.5. A 24 in. diameter column is made of the same concrete as used in Examples 1.1 and 1.2. The area of reinforcement equals 2.1 percent of the gross cross section (that is, $A_s = 0.021A_g$) and $f_y = 60$ ksi. For this column section, determine (a) the axial load the section will carry at a concrete stress of 1200 psi; (b) the load on the section when the steel begins to yield; (c) the maximum load if the section is loaded slowly; (d) the maximum load if the section is loaded rapidly; and (e) the maximum load if the reinforcement in the column is raised to 6.5 percent of the gross cross section and the column is loaded slowly. Comment on your answer, especially the percent of the load carried by the steel and the concrete for each combination.

2

Materials

2.1 INTRODUCTION

The structures and component members treated in this text are composed of concrete reinforced with steel bars, and in some cases prestressed with steel wire, strand, or alloy bars. An understanding of the materials characteristics and behavior under load is fundamental to understanding the performance of structural concrete, and to safe, economical, and serviceable design of concrete structures. Although prior exposure to the fundamentals of material behavior is assumed, a brief review is presented in this chapter, as well as a description of the types of bar reinforcement and prestressing steels in common use. Numerous references are given as a guide for those seeking more information on any of the topics discussed.

2.2 CEMENT

A cementitious material is one that has the adhesive and cohesive properties necessary to bond inert aggregates into a solid mass of adequate strength and durability. This technologically important category of materials includes not only cements proper but also limes, asphalts, and tars as they are used in road building, and others. For making structural concrete, *hydraulic cements* are used exclusively. Water is needed for the chemical process (hydration) in which the cement powder sets and hardens into one solid mass. Of the various hydraulic cements that have been developed, *portland cement*, which was first patented in England in 1824, is by far the most common.

Portland cement is a finely powdered, grayish material that consists chiefly of calcium and aluminum silicates.[†] The common raw materials from which it is made are limestones, which provide CaO, and clays or shales, which furnish SiO₂ and Al₂O₃. These are ground, blended, fused to clinkers in a kiln, and cooled. Gypsum is added and the mixture is ground to the required fineness. The material is shipped in bulk or in bags containing 94 lb of cement.

Over the years, five standard types of portland cement have been developed. Type I, *normal* portland cement, is used for over 90 percent of construction in the United States. Concretes made with Type I portland cement generally need one to two weeks to reach sufficient strength so that forms of beams and slabs can be removed and

[†] See ASTM C150, "Standard Specification for Portland Cement." This and other ASTM references are published and periodically updated by ASTM International (formerly the American Society for Testing and Materials), West Conshohoken, PA.

reasonable loads applied; they reach their design strength after 28 days and continue to gain strength thereafter at a decreasing rate. To speed construction when needed, *high early strength cements* such as Type III have been developed. They are costlier than ordinary portland cement, but within 7 to 14 days they reach the strength achieved using Type I at 28 days. Type III portland cement contains the same basic compounds as Type I, but the relative proportions differ and it is ground more finely.

When cement is mixed with water to form a soft paste, it gradually stiffens until it becomes a solid. This process is known as *setting* and *hardening*. The cement is said to have set when it has gained sufficient rigidity to support an arbitrarily defined pressure, after which it continues for a long time to harden, i.e., to gain further strength. The water in the paste dissolves material at the surfaces of the cement grains and forms a gel that gradually increases in volume and stiffness. This leads to a rapid stiffening of the paste 2 to 4 hours after water has been added to the cement. *Hydration* continues to proceed deeper into the cement grains, at decreasing speed, with continued stiffening and hardening of the mass. The principal products of hydration are calcium silicate hydrate, which is insoluble, and calcium hydroxide, which is soluble.

In ordinary concrete, the cement is probably never completely hydrated. The gel structure of the hardened paste seems to be the chief reason for the volume changes that are caused in concrete by variations in moisture, such as the shrinkage of concrete as it dries.

For complete hydration of a given amount of cement, an amount of water equal to about 25 percent of that of cement, by weight—i.e., a *water-cement ratio* of 0.25—is needed chemically. An additional amount must be present, however, to provide mobility for the water in the cement paste during the hydration process so that it can reach the cement particles and to provide the necessary workability of the concrete mix. For normal concretes, the water-cement ratio is generally in the range of about 0.40 to 0.60, although for high-strength concretes, ratios as low as 0.21 have been used. In this case, the needed workability is obtained through the use of admixtures.

Any amount of water above that consumed in the chemical reaction produces pores in the cement paste. The strength of the hardened paste decreases in inverse proportion to the fraction of the total volume occupied by pores. Put differently, since only the solids, and not the voids, resist stress, strength increases directly as the fraction of the total volume occupied by the solids. That is why the strength of the cement paste depends primarily on, and decreases directly with, an increasing water-cement ratio.

The chemical process involved in the setting and hardening liberates heat, known as *heat of hydration*. In large concrete masses, such as dams, this heat is dissipated very slowly and results in a temperature rise and volume expansion of the concrete during hydration, with subsequent cooling and contraction. To avoid the serious cracking and weakening that may result from this process, special measures must be taken for its control.

2.3 AGGREGATES

In ordinary structural concretes the aggregates occupy 65 to 75 percent of the volume of the hardened mass. The remainder consists of hardened cement paste, uncombined water (i.e., water not involved in the hydration of the cement), and air voids. The latter two do not contribute to the strength of the concrete. In general, the more densely the

aggregate can be packed, the better the durability and economy of the concrete. For this reason the gradation of the particle sizes in the aggregate, to produce close packing, is of considerable importance. It is also important that the aggregate have good strength, durability, and weather resistance; that its surface be free from impurities such as loam, clay, silt, and organic matter that may weaken the bond with cement paste; and that no unfavorable chemical reaction take place between it and the cement.

Natural aggregates are generally classified as fine and coarse. *Fine aggregate* (typically natural sand) is any material that will pass a No. 4 sieve, i.e., a sieve with four openings per linear inch. Material coarser than this is classified as *coarse aggregate*. When favorable gradation is desired, aggregates are separated by sieving into two or three size groups of sand and several size groups of coarse aggregate. These can then be combined according to grading charts to result in a densely packed aggregate. The *maximum size of coarse aggregate* in reinforced concrete is governed by the requirement that it shall easily fit into the forms and between the reinforcing bars. For this purpose it should not be larger than one-fifth of the narrowest dimension of the forms or one-third of the depth of slabs, nor three-quarters of the minimum distance between reinforcing bars. Requirements for satisfactory aggregates are found in ASTM C33, "Standard Specification for Concrete Aggregates," and authoritative information on aggregate properties and their influence on concrete properties, as well as guidance in selection, preparation, and handling of aggregate, is found in Ref. 2.1.

The unit weight of *stone concrete*, i.e., concrete with natural stone aggregate, varies from about 140 to 152 pounds per cubic foot (pcf) and can generally be assumed to be 145 pcf. For special purposes, lightweight concretes, on one hand, and heavy concretes, on the other, are used.

A variety of *lightweight* aggregates are available. Some unprocessed aggregates, such as pumice or cinders, are suitable for insulating concretes, but for structural lightweight concrete, *processed aggregates* are used because of better control. These consist of expanded shales, clays, slates, slags, or pelletized fly ash. They are light in weight because of the porous, cellular structure of the individual aggregate particle, which is achieved by gas or steam formation in processing the aggregates in rotary kilns at high temperatures (generally in excess of 2000°F). Requirements for satisfactory lightweight aggregates are found in ASTM C330, "Standard Specification for Lightweight Aggregates for Structural Concrete."

Three classes of lightweight concrete are distinguished in Ref. 2.2: low-density concretes, which are chiefly employed for insulation and whose unit weight rarely exceeds 50 pcf; moderate strength concretes, with unit weights from about 60 to 85 pcf and compressive strengths of 1000 to 2500 psi, which are chiefly used as fill, e.g., over light-gage steel floor panels; and structural concretes, with unit weights from 90 to 120 pcf and compressive strengths comparable to those of stone concretes. Similarities and differences in structural characteristics of lightweight and stone concretes are discussed in Sections 2.8 and 2.9.

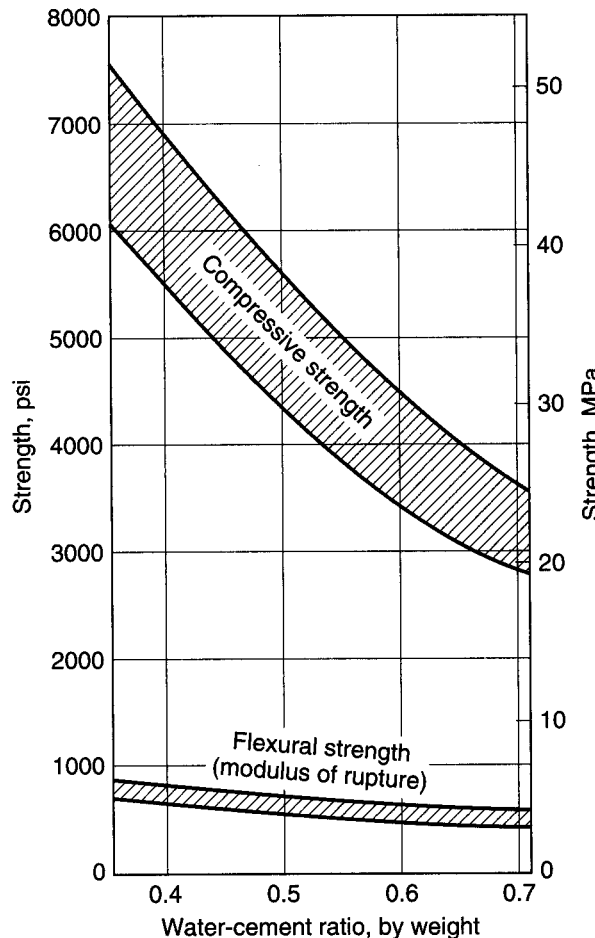
Heavyweight concrete is sometimes required for shielding against gamma and X-radiation in nuclear reactors and similar installations, for protective structures, and for special purposes, such as counterweights of lift bridges. Heavy aggregates are used for such concretes. These consist of heavy iron ores or barite (barium sulfate) rock crushed to suitable sizes. Steel in the form of scrap, punchings, or shot (as fines) is also used. Unit weights of heavyweight concretes with natural heavy rock aggregates range from about 200 to 230 pcf; if iron punchings are added to high-density ores, weights as high as 270 pcf are achieved. The weight may be as high as 330 pcf if ores are used for the fines only and steel for the coarse aggregate.

2.4 PROPORTIONING AND MIXING CONCRETE

The various components of a mix are proportioned so that the resulting concrete has adequate strength, proper workability for placing, and low cost. The third calls for use of the minimum amount of cement (the most costly of the components) that will achieve adequate properties. The better the gradation of aggregates, i.e., the smaller the volume of voids, the less cement paste is needed to fill these voids. In addition to the water required for hydration, water is needed for wetting the surface of the aggregate. As water is added, the plasticity and fluidity of the mix increase (i.e., its workability improves), but the strength decreases because of the larger volume of voids created by the free water. To reduce the free water while retaining the workability, cement must be added. Therefore, as for the cement paste, the *water-cement ratio* is the chief factor that controls the strength of the concrete. For a given water-cement ratio, one selects the minimum amount of cement that will secure the desired workability.

Figure 2.1 shows the decisive influence of the water-cement ratio on the compressive strength of concrete. Its influence on the tensile strength, as measured by the nominal flexural strength or modulus of rupture, is seen to be pronounced but much

FIGURE 2.1
Effect of water-cement ratio
on 28-day compressive and
flexural tensile strength.
(Adapted from Ref. 2.3.)



smaller than its effect on the compressive strength. This seems to be so because, in addition to the void ratio, the tensile strength depends strongly on the strength of bond between coarse aggregate and cement mortar (i.e., cement paste plus fine aggregate). According to tests at Cornell University, this bond strength is only slightly affected by the water-cement ratio (Ref. 2.4).

It is customary to define the *proportions* of a concrete mix in terms of the total weight of each component needed to make up 1 yd³ of wet concrete, such as 517 lb of cement, 300 lb of water, 1270 lb of sand, and 1940 lb of coarse aggregate, plus the total volume of air, in percent, when air is deliberately *entrained* in the mix (typically 4 to 7 percent). The weights of the fine and coarse aggregates are based on material in the *saturated surface dry condition*, in which, as the description implies, the aggregates are fully saturated but have no water on the exterior of the particles.

Various methods of proportioning are used to obtain mixes of the desired properties from the cements and aggregates at hand. One is the *trial-batch method*. Selecting a water-cement ratio from information such as that in Fig. 2.1, one produces several small trial batches with varying amounts of aggregate to obtain the required strength, consistency, and other properties with a minimum amount of paste. Concrete *consistency* is most frequently measured by the *slump test*. A metal mold in the shape of a truncated cone 12 in. high is filled with fresh concrete in a carefully specified manner. Immediately upon being filled, the mold is lifted off, and the slump of the concrete is measured as the difference in height between the mold and the pile of concrete. The slump is a good measure of the total water content in the mix and should be kept as low as is compatible with workability. Slumps for concretes in building construction generally range from 2 to 5 in., although higher slumps are used with the aid of chemical admixtures.

The so-called ACI method of proportioning makes use of the slump test in connection with a set of tables that, for a variety of conditions (types of structures, dimensions of members, degree of exposure to weathering, etc.), permit one to estimate proportions that will result in the desired properties (Ref. 2.5). These preliminary selected proportions are checked and adjusted by means of trial batches to result in concrete of the desired quality. Inevitably, strength properties of a concrete of given proportions scatter from batch to batch. It is therefore necessary to select proportions that will furnish an average strength sufficiently greater than the specified design strength for even the accidentally weaker batches to be of adequate quality (for details, see Section 2.6). Discussion in detail of practices for proportioning concrete is beyond the scope of this volume; this topic is treated fully in Refs. 2.5 and 2.6, both for stone concrete and for lightweight aggregate concrete.

If the results of trial batches or field experience are not available, the ACI Code allows concrete to be proportioned based on other experience or information, if approved by the registered design professional overseeing the project. This alternative may not be applied for specified compressive strengths greater than 5000 psi.

On all but the smallest jobs, *batching* is carried out in special batching plants. Separate hoppers contain cement and the various fractions of aggregate. Proportions are controlled, by weight, by means of manually operated or automatic scales connected to the hoppers. The mixing water is batched either by measuring tanks or by water meters.

The principal purpose of *mixing* is to produce an intimate mixture of cement, water, fine and coarse aggregate, and possible admixtures of uniform consistency throughout each batch. This is achieved in machine mixers of the revolving-drum type. Minimum mixing time is 1 min for mixers of not more than 1 yd³ capacity, with an additional 15 sec for each additional 1 yd³. Mixing can be continued for a considerable

time without adverse effect. This fact is particularly important in connection with ready mixed concrete.

On large projects, particularly in the open country where ample space is available, movable mixing plants are installed and operated at the site. On the other hand, in construction under congested city conditions, on smaller jobs, and frequently in highway construction, *ready mixed concrete* is used. Such concrete is batched in a stationary plant and then hauled to the site in trucks in one of three ways: (1) mixed completely at the stationary plant and hauled in a truck agitator, (2) transit-mixed, i.e., batched at the plant but mixed in a truck mixer, or (3) partially mixed at the plant with mixing completed in a truck mixer. Concrete should be discharged from the mixer or agitator within a limited time after the water is added to the batch. Although specifications often provide a single value for all conditions, the maximum mixing time should be based on the concrete temperature because higher temperatures lead to increased rates of *slump loss* and rapid setting. Conversely, lower temperatures increase the period during which the concrete remains workable. A good guide for maximum mixing time is to allow 1 hour at a temperature of 70°F, plus (or minus) 15 min for each 5°F drop (or rise) in concrete temperature for concrete temperatures between 40 and 90°F. Ten minutes may be used at 95°F, the practical upper limit for normal mixing and placing.

Much information on proportioning and other aspects of design and control of concrete mixtures will be found in Refs. 2.7 and 2.8.

2.5 CONVEYING, PLACING, COMPACTING, AND CURING

Conveying of most building concrete from the mixer or truck to the form is done in bottom-dump buckets or by pumping through steel pipelines. The chief danger during conveying is that of *segregation*. The individual components of concrete tend to segregate because of their dissimilarity. In overly wet concrete standing in containers or forms, the heavier coarse aggregate particles tend to settle, and the lighter materials, particularly water, tend to rise. Lateral movement, such as flow within the forms, tends to separate the coarse gravel from the finer components of the mix.

Placing is the process of transferring the fresh concrete from the conveying device to its final place in the forms. Prior to placing, loose rust must be removed from reinforcement, forms must be cleaned, and hardened surfaces of previous concrete lifts must be cleaned and treated appropriately. Placing and consolidating are critical in their effect on the final quality of the concrete. Proper placement must avoid segregation, displacement of forms or of reinforcement in the forms, and poor bond between successive layers of concrete. Immediately upon placing, the concrete should be *consolidated*, usually by means of vibrators. Consolidation prevents honeycombing, ensures close contact with forms and reinforcement, and serves as a partial remedy to possible prior segregation. Consolidation is achieved by high-frequency, power-driven *vibrators*. These are of the *internal* type, immersed in the concrete, or of the *external* type, attached to the forms. The former are preferable but must be supplemented by the latter where narrow forms or other obstacles make immersion impossible (Ref. 2.9).

Fresh concrete gains strength most rapidly during the first few days and weeks. Structural design is generally based on the *28-day strength*, about 70 percent of which is reached at the end of the first week after placing. The final concrete strength depends greatly on the conditions of moisture and temperature during this initial period. The maintenance of proper conditions during this time is known as *curing*. Thirty percent of the strength or more can be lost by premature drying out of the concrete; similar

amounts may be lost by permitting the concrete temperature to drop to 40°F or lower during the first few days unless the concrete is kept continuously moist for a long time thereafter. Freezing of fresh concrete may reduce its strength by 50 percent or more.

To prevent such damage, concrete should be protected from loss of moisture for at least 7 days and, in more sensitive work, up to 14 days. When high early strength cements are used, curing periods can be cut in half. Curing can be achieved by keeping exposed surfaces continually wet through sprinkling, ponding, or covering with plastic film or by the use of sealing compounds, which, when properly used, form evaporation-retarding membranes. In addition to improving strength, proper moist-curing provides better shrinkage control. To protect the concrete against low temperatures during cold weather, the mixing water, and occasionally the aggregates, is heated; temperature insulation is used where possible; and special admixtures are employed. When air temperatures are very low, external heat may have to be supplied in addition to insulation (Refs. 2.7, 2.8, 2.10, and 2.11).

2.6 QUALITY CONTROL

The quality of mill-produced materials, such as structural or reinforcing steel, is ensured by the producer, who must exercise systematic quality controls, usually specified by pertinent ASTM standards. Concrete, in contrast, is produced at or close to the site, and its final qualities are affected by a number of factors, which have been discussed briefly. Thus, systematic quality control must be instituted at the construction site.

The main measure of the structural quality of concrete is its *compressive strength*. Tests for this property are made on cylindrical specimens of height equal to twice the diameter, usually 6×12 in. or 4×8 in. Impervious molds of this shape are filled with concrete during the operation of placement as specified by ASTM C172, "Standard Method of Sampling Freshly Mixed Concrete," and ASTM C31, "Standard Practice for Making and Curing Concrete Test Specimens in the Field." The cylinders are moist-cured at about 70°F, generally for 28 days, and then tested in the laboratory at a specified rate of loading. The compressive strength obtained from such tests is known as the *cylinder strength* f'_c and is the main property specified for design purposes.

To provide structural safety, continuous control is necessary to ensure that the strength of the concrete as furnished is in satisfactory agreement with the value called for by the designer. The ACI Code specifies that two 6×12 in. or three 4×8 in. cylinders must be tested for each 150 yd^3 of concrete or for each 5000 ft^2 of surface area actually placed, but not less than once a day. As mentioned in Section 2.4, the results of strength tests of different batches mixed to identical proportions show inevitable scatter. The scatter can be reduced by closer control, but occasional tests below the cylinder strength specified in the design cannot be avoided.

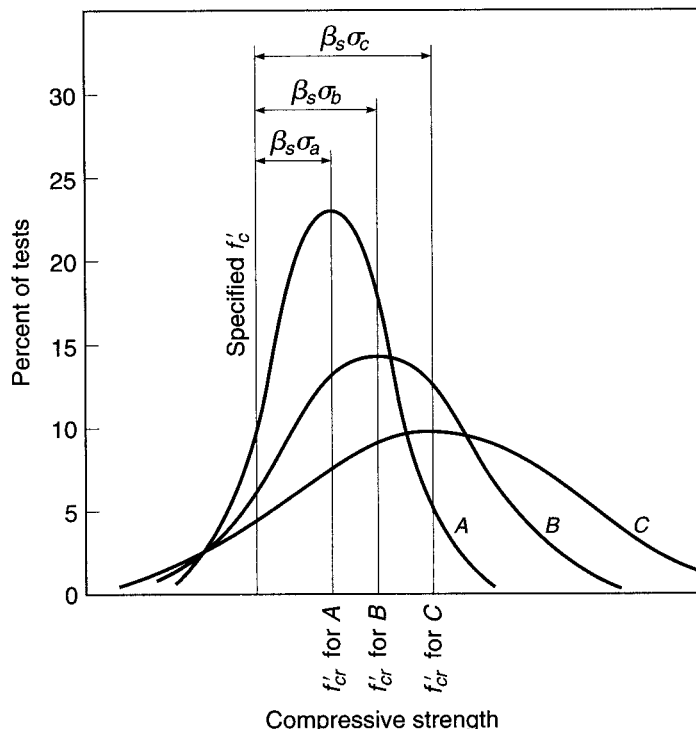
To ensure adequate concrete strength in spite of such scatter, the ACI Code stipulates that concrete quality is satisfactory if

1. No individual strength test result (the average of two or three cylinder tests depending on cylinder size) falls below the required f'_c by more than 500 psi when f'_c is 5000 psi or less or by more than $0.10f'_c$ when f'_c is more than 5000 psi, and
2. Every arithmetic average of any three consecutive strength tests equals or exceeds f'_c .

It is evident that if concrete were proportioned so that its mean strength were just equal to the required strength f'_c , it would not pass these quality requirements, because about one-half of its strength test results would fall below the required f'_c . It is

FIGURE 2.2

Frequency curves and average strengths for various degrees of control of concretes with specified design strength f'_c . (Adapted from Ref. 2.12.)



therefore necessary to proportion the concrete so that its mean strength f'_{cr} , used as the basis for selection of suitable proportions, exceeds the required design strength f'_c by an amount sufficient to ensure that the two quoted requirements are met. The minimum amount by which the required mean strength must exceed f'_c can be determined only by statistical methods because of the random nature of test scatter. Requirements have been derived, based on statistical analysis, to be used as a guide to proper proportioning of the concrete at the plant so that the probability of strength deficiency at the construction site is acceptably low.

The basis for these requirements is illustrated in Fig. 2.2, which shows three normal frequency curves giving the distribution of strength test results. The specified design strength is f'_c . The curves correspond to three different degrees of quality control, curve A representing the best control, i.e., the least scatter, and curve C the worst control, with the most scatter. The degree of control is measured statistically by the standard deviation σ (σ_a for curve A, σ_b for curve B, and σ_c for curve C), which is relatively small for producer A and relatively large for producer C. All three distributions have the same probability of strength less than the specified value f'_c ; i.e., each has the same fractional part of the total area under the curve to the left of f'_c . For any normal distribution curve, that fractional part is defined by the index β_s , a multiplier applied to the standard deviation σ ; β_s is the same for all three distributions of Fig. 2.2. It is seen that, to satisfy the requirement that, say, 1 test in 100 will fall below f'_c (with the value of β_s thus determined), for producer A with the best quality control the mean strength f'_{cr} can be much closer to the specified f'_c than for producer C with the most poorly controlled operation.

On the basis of such studies, the ACI Code requires that concrete production facilities maintain records from which the standard deviation achieved in the particular facility can be determined. It then stipulates the minimum amount by which the required

average compressive strength f'_{cr} , aimed at when selecting concrete proportions, must exceed the specified compressive strength f'_c . In accordance with ACI Code 5.3.1, the value of f'_{cr} is equal to the larger of the values in Eqs. (2.1) and (2.2).

$$f'_{cr} = f'_c + 1.34s_s \quad (2.1)$$

or

$$f'_{cr} = \begin{cases} f'_c + 2.33s_s - 500 & \text{for } f'_c \leq 5000 \text{ psi} \\ 0.9f'_c + 2.33s_s & \text{for } f'_c > 5000 \text{ psi} \end{cases} \quad (2.2a)$$

$$(2.2b)$$

where s_s is the standard deviation of the test sample.

Equation (2.1) provides a probability of 1 in 100 that averages of three consecutive tests will be below the specified strength f'_c . Equations (2.2a) and (2.2b) provide a probability of 1 in 100 that an individual strength test will be more than 500 psi below the specified f'_c for f'_c up to 5000 psi or below $0.9f'_c$ for f'_c over 5000 psi.

To use Eqs. (2.1) and (2.2), ACI Code 5.3.1 requires that a minimum of 30 consecutive test results be available. The tests must represent concrete with (1) a specified compressive strength within 1000 psi of f'_c for the project and (2) materials, quality control, and conditions similar to those expected for the building in question. If fewer than 30 but at least 15 tests are available, the equations may still be used, but s_s must be multiplied by a factor from Table 2.1. If fewer than 15 tests have been made, the average strength must exceed f'_c by at least 1000 psi for f'_c less than or equal to 3000 psi, by at least 1200 psi for f'_c between 3000 and 5000 psi, and by $0.10f'_c + 700$ psi for f'_c over 5000 psi, according to the ACI Code.

It is seen that this method of control recognizes the fact that occasional deficient batches are inevitable. The requirements for f'_{cr} ensure (1) a small probability that such strength deficiencies as are bound to occur will be large enough to represent a serious danger and (2) an equally small probability that a sizable portion of the structure, as represented by three consecutive strength tests, will be made of below-par concrete.

Both the requirements described earlier in this section for determining if concrete, as produced, is of satisfactory quality and the process just described of selecting f'_{cr} are based on the same basic considerations but are applied independently, as demonstrated in Examples 2.1 and 2.2.

TABLE 2.1
Modification factors for sample standard deviation s_s when less than 30 tests are available

No. of Tests [†]	Modification Factor for Sample Standard Deviation [‡]
Less than 15	See paragraph following Eqs. (2.1) and (2.2)
15	1.16
20	1.08
25	1.03
30 or more	1.00

[†]Interpolate for intermediate values.

[‡]The sample standard deviation s_s must be multiplied by the modification factor prior to use in Eqs. (2.1) and (2.2).

EXAMPLE 2.1 A building design calls for specified concrete strength f'_c of 4000 psi. Calculate the average required strength f'_{cr} if (a) 30 consecutive tests for concrete with similar strength and materials produce a sample standard deviation s_s of 535 psi, (b) 15 consecutive tests for concrete with similar strength and materials produce a sample standard deviation s_s of 510 psi, and (c) less than 15 tests are available.

SOLUTION. (a) 30 tests available. Using $s_s = 535$ psi, Eq. (2.1) gives

$$f'_{cr} = f'_c + 1.34s_s = 4000 + 1.34 \times 535 = 4720 \text{ psi}^{\dagger}$$

Because the specified strength f'_c is less than 4000 psi, Eq. (2.2a) must be used.

$$f'_{cr} = f'_c + 2.33s_s - 500 = 4000 + 2.33 \times 535 - 500 = 4750 \text{ psi}$$

The required average strength f'_{cr} is equal to the larger value, 4750 psi.

(b) 15 tests available. Because only 15 tests are available, s_s , given as 510 psi, must be multiplied by 1.16, the factor from Table 2.1.

$$1.16 \times s_s = 1.16 \times 510 = 590 \text{ psi}$$

Again, using Eqs. (2.1) and (2.2a),

$$f'_{cr} = 4000 + 1.34 \times 590 = 4790 \text{ psi}$$

$$f'_{cr} = 4000 + 2.33 \times 590 - 500 = 4870 \text{ psi}$$

The larger value, 4870 psi, is selected as the required average strength f'_{cr} .

(c) Less than 15 tests available. Because f'_c is between 3000 and 5000 psi, the required average strength is

$$f'_{cr} = f'_c + 1200 = 4000 + 1200 = 5200 \text{ psi}$$

This example demonstrates that in cases where test data are available, good quality control, represented by a low sample standard deviation s_s , can be used to reduce the required average strength f'_{cr} . The example also demonstrates that a lack of certainty in the value of the standard deviation due to the limited availability of data results in higher values for f'_{cr} , as shown in parts (b) and (c). As additional test results become available, the higher safety margins can be reduced.

EXAMPLE 2.2 The first eight compressive strength test results for the building described in Example 2.1c are 4730, 4280, 3940, 4370, 5180, 4870, 4930, and 4850 psi.

(a) Are the test results satisfactory, and (b) in what fashion, if any, should the mixture proportions of the concrete be altered?

SOLUTION.

(a) For concrete to be considered satisfactory, no individual test may fall below $f'_c - 500$ psi and every arithmetic average of any three consecutive tests must equal f'_c . The eight tests meet these criteria. No test is less than $f'_c - 500$ psi = 4000 - 500 = 3500 psi, and the average of all sets of three consecutive tests exceeds f'_c [for example, $(4730 + 4280 + 3940)/3 = 4320$, $(4280 + 3940 + 4370)/3 = 4200$, etc.].

(b) To determine if the mixture proportions must be altered, we note that the solution to Example 2.1c requires that f'_{cr} equal or exceed 5200 psi. The average of the first eight tests is 4640 psi, well below the value of f'_{cr} . Thus, the mixture proportions should be modified by decreasing the water-cement ratio to increase the concrete strength. Once at least 15 tests are available, the value of f'_{cr} can be recalculated using Eqs. (2.1) and (2.2) with the

[†] ASTM International specifies that concrete cylinder strengths be recorded to the nearest 10 psi. Hence the values used for test results and f'_{cr} are rounded accordingly.

appropriate factor for S_s from Table 2.1. The mixture proportions can then be adjusted based on the new value of f'_{cr} , the strength of the concrete being produced, and the level of quality control, as represented by the sample standard deviation s_s .

In spite of scientific advances, building in general and concrete making in particular retain some elements of an art; they depend on many skills and imponderables. It is the task of systematic *inspection* to ensure close correspondence between plans and specifications and the finished structure. Inspection during construction should be carried out by a competent engineer, preferably the one who produced the design or one who is responsible to the design engineer. The inspector's main functions in regard to materials quality control are sampling, examination, and field testing of materials; control of concrete proportioning; inspection of batching, mixing, conveying, placing, compacting, and curing; and supervision of the preparation of specimens for laboratory tests. In addition, the inspector must inspect foundations, formwork, placing of reinforcing steel, and other pertinent features of the general progress of work; keep records of all the inspected items; and prepare periodic reports. The importance of thorough inspection to the correctness and adequate quality of the finished structure cannot be emphasized too strongly.

This brief account of concrete technology represents the merest outline of an important subject. Anyone in practice who is actually responsible for any of the phases of producing and placing concrete must be familiar with the details in much greater depth.

2.7 ADMIXTURES

In addition to the main components of concretes, *admixtures* are often used to improve concrete performance. There are admixtures to accelerate or retard setting and hardening, to improve workability, to increase strength, to improve durability, to decrease permeability, and to impart other properties (Ref. 2.13). The beneficial effects of particular admixtures are well established. Chemical admixtures should meet the requirements of ASTM C494, "Standard Specification for Chemical Admixtures for Concrete."

Air-entraining agents are probably the most commonly used admixtures. They cause the entrainment of air in the form of small dispersed bubbles in the concrete. These improve workability and durability (chiefly resistance to freezing and thawing) and reduce segregation during placing. They decrease concrete density because of the increased void ratio and thereby decrease strength; however, this decrease can be partially offset by a reduction of mixing water without loss of workability. The chief use of air-entrained concretes is in pavements, but they are also used for structures, particularly for exposed elements (Ref. 2.14).

Accelerating admixtures are used to reduce setting time and accelerate early strength development. Calcium chloride is the most widely used accelerator because of its cost effectiveness, but it should not be used in prestressed concrete and should be used with caution in reinforced concrete in a moist environment, because of its tendency to promote corrosion of steel. Nonchloride, noncorrosive accelerating admixtures are available, the principal one being calcium nitrite (Ref. 2.13).

Set-retarding admixtures are used primarily to offset the accelerating effect of high ambient temperature and to keep the concrete workable during the entire placing period. This helps to eliminate cracking due to form deflection and also keeps concrete workable long enough that succeeding lifts can be placed without the development of "cold" joints.

Certain organic compounds are used to reduce the water requirement of a concrete mix for a given slump. Such compounds are termed *plasticizers*. Reduction in water demand may result in either a reduction in the water-cement ratio for a given slump and cement content or an increase in slump for the same water-cement ratio and cement content. Plasticizers work by reducing the interparticle forces that exist between cement grains in the fresh paste, thereby increasing the paste fluidity. High-range water-reducing admixtures, or *superplasticizers*, are used to produce high-strength concrete (see Section 2.12) with a very low water-cement ratio while maintaining the higher slumps needed for proper placement and compaction of the concrete. They are also used to produce flowable concrete at conventional water-cement ratios. Superplasticizers differ from conventional water-reducing admixtures in that they do not act as retarders at high dosages; therefore, they can be used at higher dosage rates without severely slowing hydration (Refs. 2.13, 2.15, and 2.16). The specific effects of water-reducing admixtures vary with different cements, changes in water-cement ratio, mixing temperature, ambient temperature, and other job conditions, and trial batches are generally required.

When superplasticizers are combined with *viscosity-modifying admixtures*, they can be used to produce *self-consolidating concrete* (SCC). Self-consolidating concrete is highly fluid and does not require vibration to remove entrapped air. The viscosity modifying agents allow the concrete to remain cohesive even with a very high degree of fluidity. As a result, SCC can be used for members with congested reinforcement, such as beam-column joints in earthquake-resistant structures, and is widely used for precast concrete, especially precast prestressed concrete, a manufactured product (prestressed concrete is discussed in Chapter 19). The high fluidity of the mix, however, has been shown to have a negative impact on the bond strength between the concrete and prestressing steel located in the upper portions of a member, a shortcoming that should be considered in design (Ref. 2.17) but is not currently addressed in the ACI Code, and the composition of SCC mixtures may result in moduli of elasticity, creep, and shrinkage properties that differ from those of more traditional mixtures.

Fly ash and *silica fume* are pozzolans, highly active silicas, that combine with calcium hydroxide, the soluble product of cement hydration (Section 2.2), to form more calcium silicate hydrate, the insoluble product of cement hydration (Refs. 2.18 and 2.19). Pozzolans qualify as *supplementary cementitious materials*, also referred to as *mineral admixtures*, which are used to replace a part of the portland cement in concrete mixes. Fly ash, which is specified under ASTM C618, "Standard Specification for Coal Fly Ash and Raw or Calcified Natural Pozzolan for Use in Concrete," is precipitated electrostatically as a by-product of the exhaust fumes of coal-fired power stations. It is very finely divided and reacts with calcium hydroxide in the presence of moisture to form a cementitious material. It tends to increase the strength of concrete at ages over 28 days. Silica fume, which is specified under ASTM C1240, "Standard Specification for Silica Fume Used in Cementitious Mixtures," is a by-product resulting from the manufacture, in electric-arc furnaces, of ferro-silicon alloys and silicon metal. It is extremely finely divided and is highly cementitious when combined with portland cement. In contrast to fly ash, silica fume contributes mainly to strength gain at early ages, from 3 to 28 days. Both fly ash and silica fume, particularly the latter, have been important in the production of high-strength concrete (see Section 2.12).

Ground granulated blast-furnace slag (GGBFS), which is specified under ASTM C989, "Standard Specification for Ground Granulated Blast-Furnace Slag for Use in Concrete and Mortar," is another supplementary cementitious material. It is

produced by water quenching and grinding slag from the production of pig iron, the key ingredient used to make steel (Ref. 2.20). GGBFS consists primarily of calcium silicates, making it very similar to portland cement. As a result of the similarity, slag can be used in higher quantities than fly ash or silica fume, and the resulting material generally has similar or improved properties to those exhibited by concrete made with 100 percent portland cement.

When blast furnace slag, silica fume, fly ash, or a combination is used, it is customary to refer to the *water-cementitious material ratio* rather than the water-cement ratio. This typically may be as low as 0.25 for high-strength concrete, and ratios as low as 0.21 have been used (Refs. 2.21 and 2.22).

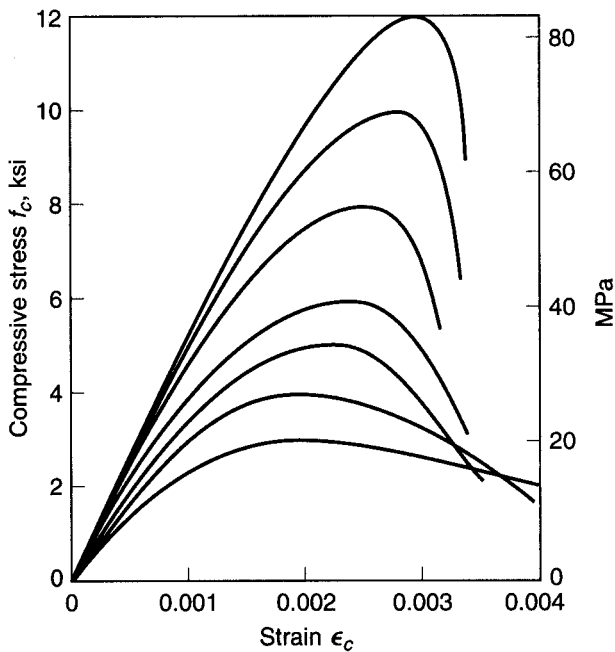
Historically, the high durability and high thermal mass of concrete structures have played a key role in *sustainable development*, that is, development that minimizes both its impact on the environment and the resources used both during and after construction. In sustainable development, the “cost” of concrete lies primarily in the manufacture of portland cement. The production of a ton of portland cement requires roughly the energy needed to operate a typical U.S. household for two weeks and generates approximately 0.9 ton of CO₂ (a greenhouse gas). The latter translates to about 250 lb of CO₂ for every cubic yard of concrete that is placed. The energy and greenhouse gases involved in the production of concrete, however, can be viewed as investments because properly designed reinforced concrete structures that take advantage of concrete’s thermal mass provide significant reductions in the energy and CO₂ needed for heating and cooling, and concrete’s inherent durability results in structures with long service lives. Because by-products, such as the mineral admixtures fly ash and blast furnace slag, involve minimal energy usage or greenhouse gas production, they have the potential to further improve the sustainability of concrete construction when used as a partial replacement for portland cement.

2.8 PROPERTIES IN COMPRESSION

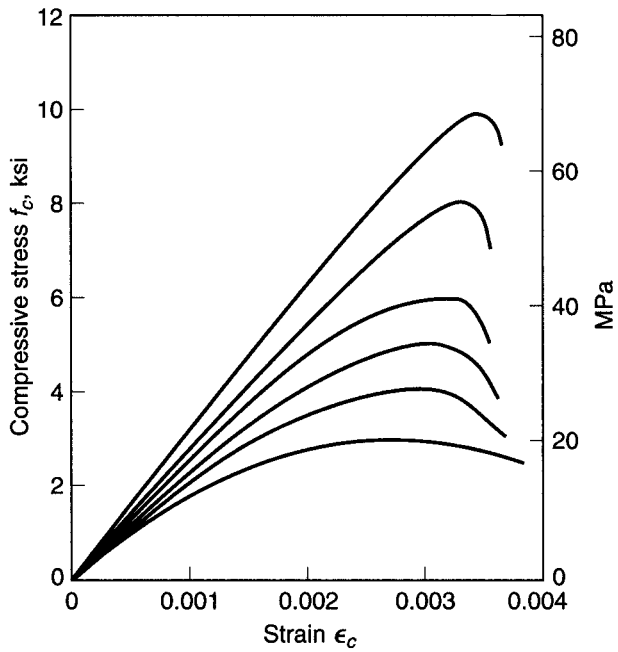
a. Short-Term Loading

Performance of a structure under load depends to a large degree on the stress-strain relationship of the material from which it is made, under the type of stress to which the material is subjected in the structure. Since concrete is used mostly in compression, its compressive stress-strain curve is of primary interest. Such a curve is obtained by appropriate strain measurements in cylinder tests (Section 2.6) or on the compression side in beams. Figure 2.3 shows a typical set of such curves for normal-density concrete, obtained from uniaxial compressive tests performed at normal, moderate testing speeds on concretes that are 28 days old. Figure 2.4 shows corresponding curves for lightweight concretes having a density of 100pcf.

All of the curves have somewhat similar character. They consist of an initial relatively straight elastic portion in which stress and strain are closely proportional, then begin to curve to the horizontal, reaching the maximum stress, i.e., the compressive strength, at a strain that ranges from about 0.002 to 0.003 for normal-density concretes, and from about 0.003 to 0.0035 for lightweight concretes (Refs. 2.23 and 2.24), the larger values in each case corresponding to the higher strengths. All curves show a descending branch after the peak stress is reached; however, the characteristics of the curves after peak stress are highly dependent upon the method of testing. If special procedures are followed in testing to ensure a constant strain rate while cylinder resistance is decreasing, long stable descending branches can be obtained (Ref. 2.25). In the absence of special devices, unloading past the point of peak stress

**FIGURE 2.3**

Typical compressive stress-strain curves for normal-density concrete with $w_c = 145$ pcf. (Adapted from Refs. 2.23 and 2.24.)

**FIGURE 2.4**

Typical compressive stress-strain curves for lightweight concrete with $w_c = 100$ pcf. (Adapted from Refs. 2.23 and 2.24.)

may be rapid, particularly for the higher-strength concretes, which are generally more brittle than low-strength concrete.

In present practice, the specified compressive strength f'_c is commonly in the range from 3000 to 5000 psi for normal-density cast-in-place concrete, and up to about 8000 psi for precast prestressed concrete members. Lightweight concrete strengths are somewhat below these values generally. The high-strength concretes, with f'_c to 15,000 psi or more, are used with increasing frequency, particularly for heavily loaded columns in high-rise concrete buildings and for long-span bridges (mostly prestressed) where a significant reduction in dead load may be realized by minimizing member cross section dimensions. (See Section 2.12.)

The *modulus of elasticity* E_c (in psi units), i.e., the slope of the initial straight portion of the stress-strain curve, is seen to be larger as the strength of the concrete increases. For concretes in the strength range to about 6000 psi, it can be computed with reasonable accuracy from the empirical equation found in the ACI Code

$$E_c = 33w_c^{1.5} \sqrt{f'_c} \quad (2.3)$$

where w_c is the unit weight of the hardened concrete in pcf and f'_c is its strength in psi. Equation (2.3) was obtained by testing structural concretes with values of w_c from 90 to 155 pcf. For normal sand-and-stone concretes, with $w_c = 145$ pcf, E_c may be taken as

$$E_c = 57,000 \sqrt{f'_c} \quad (2.4)$$

For compressive strengths in the range from 6000 to 12,000 psi, the ACI Code equation may overestimate E_c for both normalweight and lightweight material by as much as 20 percent. Based on research at Cornell University (Refs. 2.23 and 2.24), the

following equation is recommended for normal-density concretes with f'_c in the range of 3000 to 12,000 psi, and for lightweight concretes from 3000 to 9000 psi:

$$E_c = (40,000\sqrt{f'_c} + 1,000,000) \left(\frac{w_c}{145} \right)^{1.5} \quad (2.5)$$

where terms and units are as defined above for the ACI Code equations. When coarse aggregates with high moduli of elasticity are used, however, Eq. (2.4) may *underestimate* E_c . Thus, in cases where E_c is a key design criterion, it should be measured, rather than estimated, using Eq. (2.3), (2.4), or (2.5).

Information on concrete strength properties such as those discussed is usually obtained through tests made 28 days after placing. However, cement continues to hydrate, and consequently concrete continues to harden, long after this age, at a decreasing rate. Figure 2.5 shows a typical curve of the gain of concrete strength with age for concrete made using Type I (normal) cement and also Type III (high early strength) cement, each curve normalized with respect to the 28-day compressive strength. High early strength cements produce more rapid strength gain at early ages, although the rate of strength gain at later ages is generally less. Concretes using Type III cement are often used in precasting plants, and often the strength f'_c is specified at 7 days, rather than 28 days.

Note that the shape of the stress-strain curve for various concretes of the same cylinder strength, and even for the same concrete under various conditions of loading, varies considerably. An example of this is shown in Fig. 2.6, where different specimens of the same concrete are loaded at different rates of strain, from one corresponding to a relatively fast loading (0.001 per minute) to one corresponding to an extremely slow application of load (0.001 per 100 days). It is seen that the descending branch of the curve, indicative of internal disintegration of the material, is much more pronounced at fast than at slow rates of loading. It is also seen that the peaks of the curves, i.e., the maximum strengths reached, are somewhat smaller at slower rates of strain.

When compressed in one direction, concrete, like other materials, expands in the direction transverse to that of the applied stress. The ratio of the transverse to the longitudinal strain is known as *Poisson's ratio* and depends somewhat on strength, composition, and other factors. At stresses lower than about $0.7f'_c$, Poisson's ratio for concrete falls within the limits of 0.15 to 0.20.

FIGURE 2.5

Effect of age on compressive strength f'_c for moist-cured concrete. (Adapted from Ref. 2.26.)

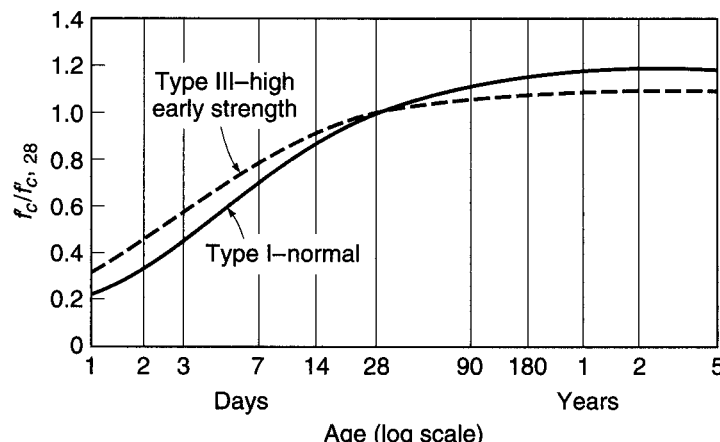
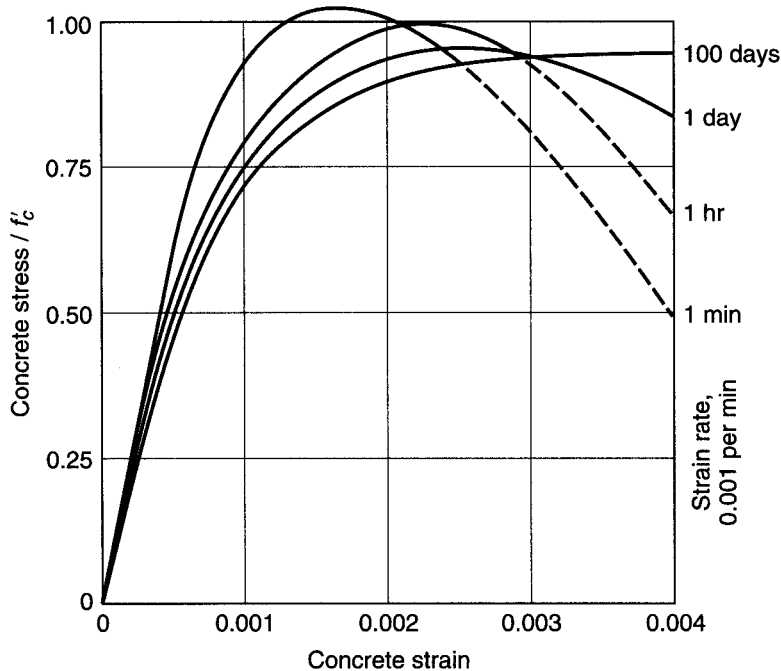


FIGURE 2.6

Stress-strain curves at various strain rates, concentric compression.
(Adapted from Ref. 2.27.)



b. Long-Term Loading

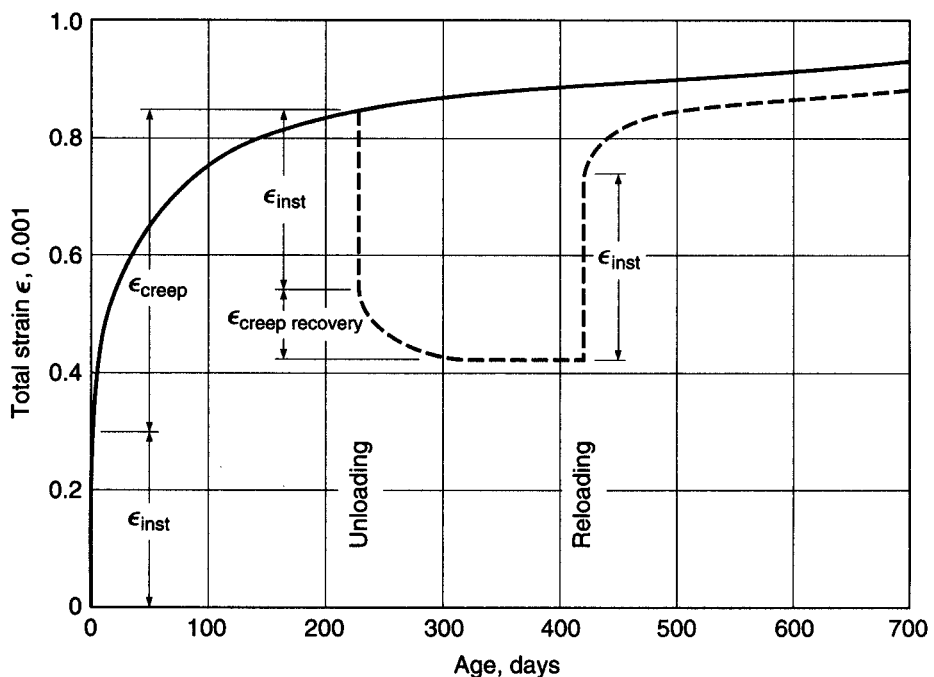
In some engineering materials, such as steel, strength and the stress-strain relationships are independent of rate and duration of loading, at least within the usual ranges of rate of stress, temperature, and other variables. In contrast, Fig. 2.6 illustrates the fact that the influence of time, in this case of rate of loading, on the behavior of concrete under load is pronounced. The main reason is that concrete creeps under load, while steel does not exhibit creep under conditions prevailing in buildings, bridges, and similar structures.

Creep is the slow deformation of a material over considerable lengths of time at constant stress or load. The nature of the creep process is shown schematically in Fig. 2.7. This particular concrete was loaded after 28 days with resulting instantaneous strain ϵ_{inst} . The load was then maintained for 230 days, during which time creep was seen to have increased the total deformation to almost 3 times its instantaneous value. If the load were maintained, the deformation would follow the solid curve. If the load is removed, as shown by the dashed curve, most of the elastic instantaneous strain ϵ_{inst} is recovered, and some creep recovery is seen to occur. If the concrete is reloaded at some later date, instantaneous and creep deformations develop again, as shown.

Creep deformations for a given concrete are practically proportional to the magnitude of the applied stress; at any given stress, and even at the same ratio of stress to compressive strength, high-strength concretes show less creep than lower-strength concretes (Ref. 2.28). As seen in Fig. 2.7, with elapsing time, creep proceeds at a decreasing rate and ceases after 2 to 5 years at a final value which, depending on concrete strength and other factors, is about 1.2 to 3 times the magnitude of the instantaneous strain. If, instead of being applied quickly and thereafter kept constant, the load is increased slowly and gradually, as is the case in many structures during and after construction, then instantaneous and creep deformations proceed simultaneously.

FIGURE 2.7

Typical creep curve (concrete loaded to 600 psi at age 28 days).



The effect is shown in Fig. 2.6; i.e., the previously discussed difference in the shape of the stress-strain curve for various rates of loading is chiefly the result of the creep deformation of concrete.

For stresses not exceeding about one-half the cylinder strength, creep strains are approximately proportional to stress. Because initial elastic strains are also proportional to stress in this range, this permits definition of the *creep coefficient*

$$C_{cu} = \frac{\epsilon_{cu}}{\epsilon_{ci}} \quad (2.6)$$

where ϵ_{cu} is the final asymptotic value of the additional creep strain and ϵ_{ci} is the initial, instantaneous strain when the load is first applied. Creep may also be expressed in terms of the *specific creep* δ_{cu} , defined as the additional time-dependent strain per psi stress. It can easily be shown that

$$C_{cu} = E_c \delta_{cu} \quad (2.7)$$

In addition to the stress level, creep depends on the average ambient relative humidity, being more than twice as large for 50 percent as for 100 percent humidity (Ref. 2.8). This is so because part of the reduction in volume under sustained load is caused by outward migration of free pore water, which evaporates into the surrounding atmosphere. Other factors of importance include the type of cement and aggregate, age of the concrete when first loaded, and concrete strength (Ref. 2.8). The creep coefficient for high-strength concrete is much less than that for low-strength concrete. However, sustained load stresses are apt to be higher so that the creep *deformation* may be as great for high-strength concrete, even though the creep coefficient is less.

The values of Table 2.2, quoted from Ref. 2.29 and extended for high-strength concrete based on research at Cornell University, are typical values for average humidity conditions, for concretes loaded at the age of 7 days.

TABLE 2.2
Typical creep parameters

Compressive Strength		Specific Creep δ_{cu}		Creep coefficient C_{cu}
psi	MPa	10^{-6} per psi	10^{-6} per MPa	
3,000	21	1.00	145	3.1
4,000	28	0.80	116	2.9
6,000	41	0.55	80	2.4
8,000	55	0.40	58	2.0
10,000	69	0.28	41	1.6
12,000	83	0.22	33	1.4

To illustrate, if the concrete in a column with $f'_c = 4000$ psi is subject to a long-time load that causes sustained stress of 1200 psi, then after several years under load the final value of the creep strain will be about $1200 \times 0.80 \times 10^{-6} = 0.00096$. Thus, if the column were 20 ft long, creep would shorten it by about $\frac{1}{4}$ in.

The creep coefficient at any time C_{ct} can be related to the ultimate creep coefficient C_{cu} . In Ref. 2.26, Branson suggests the equation

$$C_{ct} = \frac{t^{0.60}}{10 + t^{0.60}} C_{cu} \quad (2.8)$$

where t = time in days after loading.

In many special situations, e.g., slender members or frames, or in prestressed construction, the designer must take account of the combined effects of creep and shrinkage (Section 2.11). In such cases, rather than rely on the sample values of Table 2.2, more accurate information on creep parameters should be obtained, such as from Ref. 2.26 or 2.29.

Sustained loads affect not only the deformation but also the strength of concrete. The cylinder strength f'_c is determined at normal rates of test loading (about 35 psi/sec). Tests by Rüsch (Ref. 2.27) and at Cornell University (Refs. 2.30 and 2.31) have shown that, for concentrically loaded unreinforced concrete prisms and cylinders, the *strength under sustained load* is significantly smaller than f'_c , on the order of 75 percent of f'_c for loads maintained for a year or more. Thus, a member subjected to a sustained overload causing compressive stress of over 75 percent of f'_c may fail after a period of time, even though the load is not increased.

c. Fatigue

When concrete is subject to fluctuating rather than sustained loading, its *fatigue strength*, as for all other materials, is considerably smaller than its static strength. When plain concrete in compression is stressed cyclically from zero to maximum stress, its fatigue limit is from 50 to 60 percent of the static compressive strength, for 2,000,000 cycles. A reasonable estimate can be made for other stress ranges using the modified Goodman diagram (see Ref. 2.29). For other types of applied stress, such as flexural compressive stress in reinforced concrete beams or flexural tension in unreinforced beams or on the tension side of reinforced beams, the fatigue limit likewise

appears to be about 55 percent of the corresponding static strength. These figures, however, are for general guidance only. It is known that the fatigue strength of concrete depends not only on its static strength but also on moisture condition, age, and rate of loading (see Ref. 2.32).

2.9 PROPERTIES IN TENSION

While concrete is best employed in a manner that uses its favorable compressive strength, its behavior in tension is also important. The conditions under which cracks form and propagate on the tension side of reinforced concrete flexural members depend strongly on both the tensile strength and the fracture properties of the concrete, the latter dealing with the ease with which a crack progresses once it has formed. Concrete tensile stresses also occur as a result of shear, torsion, and other actions, and in most cases member behavior changes upon cracking. Thus, it is important to be able to predict, with reasonable accuracy, the tensile strength of concrete and to understand the factors that control crack propagation.

a. Tensile Strength

There are considerable experimental difficulties in determining the true tensile strength of concrete. In *direct tension* tests, minor misalignments and stress concentrations in the gripping devices are apt to mar the results. For many years, tensile strength has been measured in terms of the *modulus of rupture* f_r , the computed flexural tensile stress at which a test beam of plain concrete fractures. Because this nominal stress is computed on the assumption that concrete is an elastic material, and because this bending stress is localized at the outermost surface, it is apt to be larger than the strength of concrete in uniform axial tension. It is thus a measure of, but not identical with, the real axial tensile strength.

More recently the result of the *split-cylinder test* has established itself as a measure of the tensile strength of concrete. A concrete cylinder, the same as is used for compressive tests, is inserted in a compression testing machine in the horizontal position, so that compression is applied uniformly along two opposite generators. Pads are inserted between the compression platens of the machine and the cylinder to equalize and distribute the pressure. It can be shown that in an elastic cylinder so loaded, a nearly uniform tensile stress of magnitude $2P/(\pi dL)$ exists at right angles to the plane of load application. Correspondingly, such cylinders, when tested, split into two halves along that plane, at a stress f_{ct} that can be computed from the above expression. P is the applied compressive load at failure, and d and L are the diameter and length of the cylinder, respectively. Because of local stress conditions at the load lines and the presence of stresses at right angles to the aforementioned tension stresses, the results of the split-cylinder tests likewise are not identical with (but are believed to be a good measure of) the true axial tensile strength. The results of all types of tensile tests show considerably more scatter than those of compression tests.

Tensile strength, however determined, does not correlate well with the compressive strength f'_c . It appears that for sand-and-gravel concrete, the tensile strength depends primarily on the strength of bond between hardened cement paste and aggregate, whereas for lightweight concretes it depends largely on the tensile strength of the porous aggregate. The compressive strength, on the other hand, is much less determined by these particular characteristics.

Better correlation is found between the various measures of tensile strength and the square root of the compressive strength. The direct tensile strength, for example, ranges from about 3 to $5\sqrt{f'_c}$ for normal-density concretes, and from about 2 to $3\sqrt{f'_c}$ for all-lightweight concrete. Typical ranges of values for direct tensile strength, split-cylinder strength, and modulus of rupture are summarized in Table 2.3. In these expressions, f'_c is expressed in psi units, and the resulting tensile strengths are obtained in psi.

These approximate expressions show that tensile and compressive strengths are by no means proportional, and that any increase in compressive strength, such as that achieved by lowering the water-cement ratio, is accompanied by a much smaller percentage increase in tensile strength.

The ACI Code recommends that the modulus of rupture f_r be taken to equal $7.5\sqrt{f'_c}$ for normalweight concrete, and that this value be multiplied by 0.85 for "sand-lightweight" and 0.75 for "all-lightweight" concretes, giving values of $6.4\sqrt{f'_c}$ and $5.6\sqrt{f'_c}$, respectively, for those materials.

b. Tensile Fracture

The failure of concrete in tension involves both the formation and the propagation of cracks. The field of fracture mechanics deals with the latter. While reinforced concrete structures have been successfully designed and built for over 150 years without the use of fracture mechanics, the brittle response of high-strength concretes (Section 2.12), in tension as well as compression, increases the importance of the fracture properties of the material as distinct from tensile strength. Research dealing with the shear strength of high-strength concrete beams and the bond between reinforcing steel and high-strength concrete indicates relatively low increases in these structural properties with increases in concrete compressive strength (Refs. 2.33 and 2.34). While shear and bond strength are associated with the $\sqrt{f'_c}$ for normal-strength concrete, tests of high-strength concrete indicate that increases in shear and bond strengths are well below values predicted using $\sqrt{f'_c}$, indicating that concrete tensile strength alone is not the governing factor. An explanation for this behavior is provided by research at the University of Kansas and elsewhere (Refs. 2.35 and 2.36) that demonstrates that the energy required to fully open a crack (i.e., after the crack has started to grow) is largely independent of compressive strength, water-cement ratio, and age. Design expressions reflecting this research are not yet available. The behavior is, however, recognized in the ACI Code by limitations on the maximum value of $\sqrt{f'_c}$ that may be used to calculate shear and bond strength, as will be discussed in Chapters 4 and 5.

TABLE 2.3
Approximate range of tensile strengths of concrete

	Normalweight Concrete, psi	Lightweight Concrete, psi
Direct tensile strength f'_t	3 to $5\sqrt{f'_c}$	2 to $3\sqrt{f'_c}$
Split-cylinder strength f_{ct}	6 to $8\sqrt{f'_c}$	4 to $6\sqrt{f'_c}$
Modulus of rupture f_r	8 to $12\sqrt{f'_c}$	6 to $8\sqrt{f'_c}$

2.10 STRENGTH UNDER COMBINED STRESS

In many structural situations, concrete is subjected simultaneously to various stresses acting in various directions. For instance, in beams much of the concrete is subject simultaneously to compression and shear stresses, and in slabs and footings to compression in two perpendicular directions plus shear. By methods well known from the study of engineering mechanics, any state of combined stress, no matter how complex, can be reduced to three principal stresses acting at right angles to one another on an appropriately oriented elementary cube in the material. Any or all of the principal stresses can be either tension or compression. If any one of them is zero, a state of *biaxial* stress is said to exist; if two of them are zero, the state of stress is *uniaxial*, either simple compression or simple tension. In most cases, only the uniaxial strength properties of a material are known from simple tests, such as the cylinder strength f'_c and the tensile strength f'_t . For predicting the strengths of structures in which concrete is subject to biaxial or triaxial stress, it would be desirable to be able to calculate the strength of concrete in such states of stress, knowing from tests only either f'_c or f'_t and f'_t .

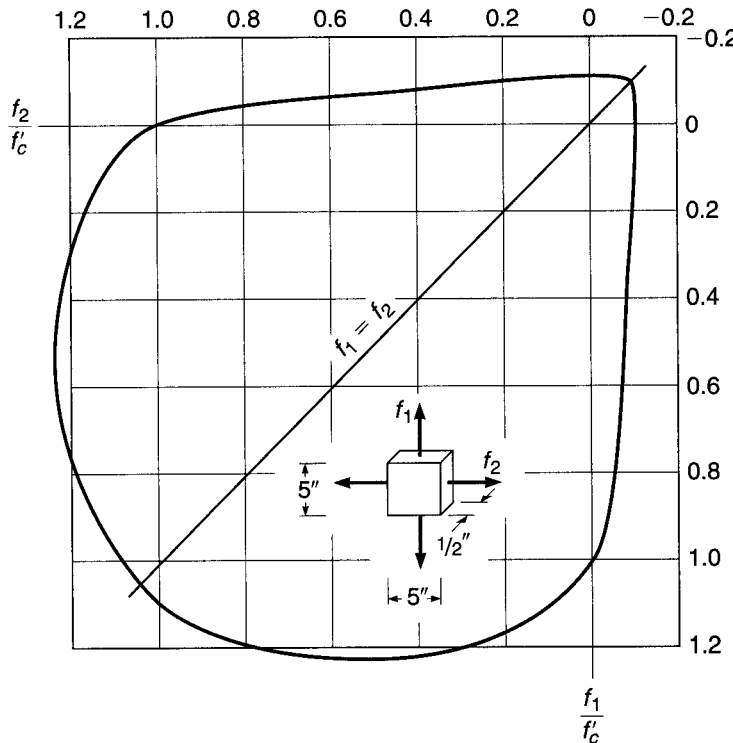
In spite of extensive and continuing research, no general theory of the strength of concrete under combined stress has yet emerged. Modifications of various strength theories, such as maximum stress, maximum strain, the Mohr-Coulomb, and the octahedral shear stress theories, all of which are discussed in structural mechanics texts, have been adapted with varying partial success to concrete. At present, none of these theories has been generally accepted, and many have obvious internal contradictions. The main difficulty in developing an adequate general strength theory lies in the highly nonhomogeneous nature of concrete, and in the degree to which its behavior at high stresses and at fracture is influenced by microcracking and other discontinuity phenomena (Refs. 2.8 and 2.37).

However, the strength of concrete has been well established by tests, at least for the biaxial stress state (Refs. 2.38 and 2.39). Results may be presented in the form of an interaction diagram such as Fig. 2.8, which shows the strength in direction 1 as a function of the stress applied in direction 2. All stresses are normalized in terms of the uniaxial compressive strength f'_c . It is seen that in the quadrant representing biaxial compression a strength increase as great as about 20 percent over the uniaxial compressive strength is attained, the amount of increase depending upon the ratio of f_2 to f_1 . In the biaxial tension quadrant, the strength in direction 1 is almost independent of stress in direction 2. When tension in direction 2 is combined with compression in direction 1, the compressive strength is reduced almost linearly, and vice versa. For example, lateral compression of about one-half the uniaxial compressive strength will reduce the tensile strength by almost one-half compared with its uniaxial value. This fact is of great importance in predicting diagonal tension cracking in deep beams or shear walls, for example.

Experimental investigations into the triaxial strength of concrete have been few, due mainly to the practical difficulty of applying load in three directions simultaneously without introducing significant restraint from the loading equipment (Ref. 2.40). From information now available, the following conclusions can be drawn relative to the triaxial strength of concrete: (1) in a state of equal triaxial compression, concrete strength may be an order of magnitude larger than the uniaxial compressive strength; (2) for equal biaxial compression combined with a smaller value of compression in the third direction, a strength increase greater than 20 percent can be expected; and (3) for stress states including compression combined with tension in at least one other direction, the intermediate principal stress is of little consequence, and the compressive strength can be predicted safely based on Fig. 2.8.

FIGURE 2.8

Strength of concrete in biaxial stress. (Adapted from Ref. 2.39.)



In fact, the strength of concrete under combined stress cannot yet be calculated rationally, and, equally important, in many situations in concrete structures it is nearly impossible to calculate all of the acting stresses and their directions; these are two of the main reasons for continued reliance on tests. Because of this, the design of reinforced concrete structures continues to be based more on extensive experimental information than on consistent analytical theory, particularly in the many situations where combined stresses occur.

2.11 SHRINKAGE AND TEMPERATURE EFFECTS

The deformations discussed in Section 2.8 were induced by stresses caused by external loads. Influences of a different nature cause concrete, even when free of any external loading, to undergo deformations and volume changes. The most important of these are shrinkage and the effects of temperature variations.

a. Shrinkage

As discussed in Sections 2.2 and 2.4, any workable concrete mix contains more water than is needed for hydration. If the concrete is exposed to air, the larger part of this free water evaporates in time, the rate and completeness of drying depending on ambient temperature and humidity conditions. As the concrete dries, it shrinks in volume, due initially to the capillary tension that develops in the water remaining in the concrete (Ref. 2.8). Conversely, if dry concrete is immersed in water, it expands, regaining much of the volume loss from prior shrinkage. Shrinkage, which continues at a decreasing rate for several months, depending on the configuration of the member,

is a detrimental property of concrete in several respects. When not adequately controlled, it will cause unsightly and often deleterious cracks, as in slabs, walls, etc. In structures that are statically indeterminate (and most concrete structures are), it can cause large and harmful stresses. In prestressed concrete it leads to partial loss of initial prestress. For these reasons it is essential that shrinkage be minimized and controlled.

As is clear from the nature of the process, a key factor in determining the amount of final shrinkage is the unit water content of the fresh concrete. This is illustrated in Fig. 2.9, which shows the amount of shrinkage for varying amounts of mixing water. The same aggregates were used for all tests, but in addition to and independently of the water content, the amount of cement was also varied from 376 to 1034 lb/yd³ of concrete. This very large variation of cement content causes a 20 to 30 percent variation in shrinkage strain for water contents between 250 to 350 lb/yd³, the range used for most structural concretes. Increasing the cement content increases the cement paste constituent of the concrete, where the shrinkage actually takes place, while reducing the aggregate content. Since most aggregates do not contribute to shrinkage, an increase in aggregate content can significantly decrease shrinkage. This is shown in Fig. 2.10, which compares the shrinkage of concretes with various aggregate contents with the shrinkage obtained for neat cement paste (cement and water alone). For example, increasing the aggregate content from 71 to 74 percent (at the same water-cement ratio) results in a 20 percent reduction in shrinkage (Ref. 2.29). Increased aggregate content may be obtained through the use of (1) a larger maximum size coarse aggregate (which also reduces the water content required for a given workability), (2) a concrete with lower workability, and (3) chemical admixtures to increase

FIGURE 2.9

Effect of water content on drying shrinkage. (From Ref. 2.3.)

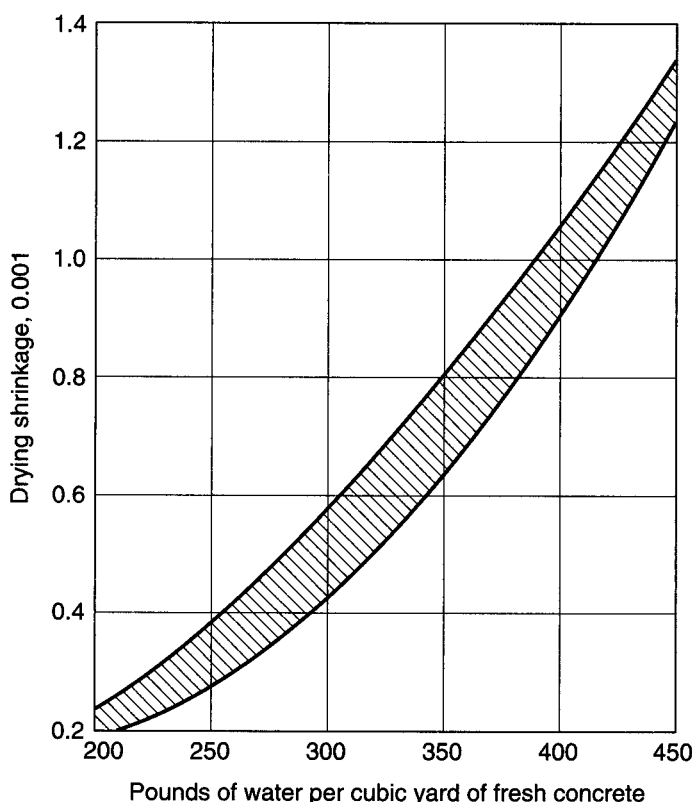
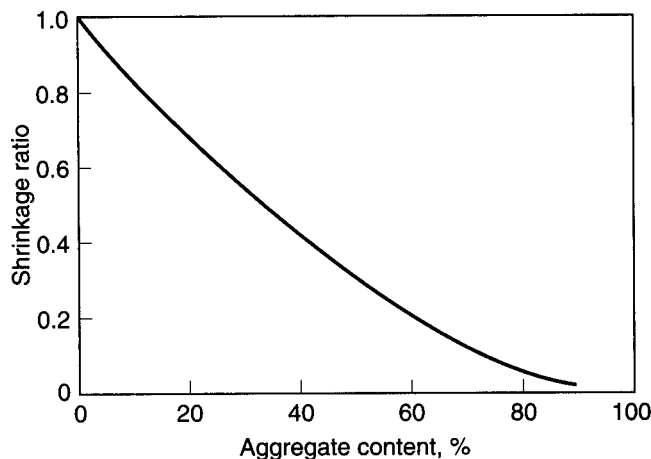


FIGURE 2.10

Influence of aggregate content in concrete (by volume) on the ratio of the shrinkage of concrete to the shrinkage of neat cement paste. (Adapted from Ref. 2.29, based on data in Ref. 2.41.)



workability at lower water contents. It is evident that an effective means of reducing shrinkage involves both a reduction in water content and an increase in aggregate content. In addition, prolonged and careful curing is beneficial for shrinkage control.

Values of final shrinkage for ordinary concretes are generally on the order of 400×10^{-6} to 800×10^{-6} , depending on the initial water content, ambient temperature and humidity conditions, and the nature of the aggregate. Highly absorptive aggregates with low moduli of elasticity, such as some sandstones and slates, result in shrinkage values 2 or more times those obtained with less absorptive materials, such as granites and some limestones. Some lightweight aggregates, in view of their great porosity, easily result in much larger shrinkage values than ordinary concretes.

For some purposes, such as predicting the time-dependent loss of force in prestressed concrete beams, it is important to estimate the amount of shrinkage as a function of time. Long-term studies (Ref. 2.26) show that, for moist-cured concrete at any time t after the initial 7 days, shrinkage can be predicted satisfactorily by the equation

$$\epsilon_{sh,t} = \frac{t}{35 + t} \epsilon_{sh,u} \quad (2.9)$$

where $\epsilon_{sh,t}$ is the unit shrinkage strain at time t in days and $\epsilon_{sh,u}$ is the ultimate value after a long period of time. Equation (2.9) pertains to "standard" conditions, defined in Ref. 2.26 to exist for humidity not in excess of 40 percent and for an average thickness of member of 6 in., and it applies both for normalweight and lightweight concretes. Modification factors are applied for nonstandard conditions, and separate equations are given for steam-cured members.

For structures in which a reduction in cracking is of particular importance, such as bridge decks, pavement slabs, and liquid storage tanks, the use of *expansive cement concrete* is appropriate. Shrinkage-compensating cement is constituted and proportioned such that the concrete will increase in volume after setting and during hardening. When the concrete is restrained by reinforcement or other means, the tendency to expand will result in compression. With subsequent drying, the shrinkage so produced, instead of causing a tension stress in the concrete that would result in cracking, merely reduces or relieves the expansive strains caused by the initial expansion (Ref. 2.42). Expansive cement is produced by adding a source of reactive aluminate to ordinary portland cement; approximately 90 percent of shrinkage-compensating cement is made up of the constituents of conventional portland cement.

Of the three main types of expansive cements produced, only type K is commercially available in the United States; it is about 20 percent more expensive than ordinary portland cement (Ref. 2.43). Requirements for expansive cement are given in ASTM C845, "Standard Specification for Expansive Hydraulic Cement." The usual admixtures can be used in shrinkage-compensating concrete, but trial mixes are necessary because some admixtures, particularly air-entraining agents, are not compatible with certain expansive cements.

b. Effect of Temperature Change

Like most other materials, concrete expands with increasing temperature and contracts with decreasing temperature. The effects of such volume changes are similar to those caused by shrinkage; i.e., temperature contraction can lead to objectionable cracking, particularly when superimposed on shrinkage. In indeterminate structures, deformations due to temperature changes can cause large and occasionally harmful stresses.

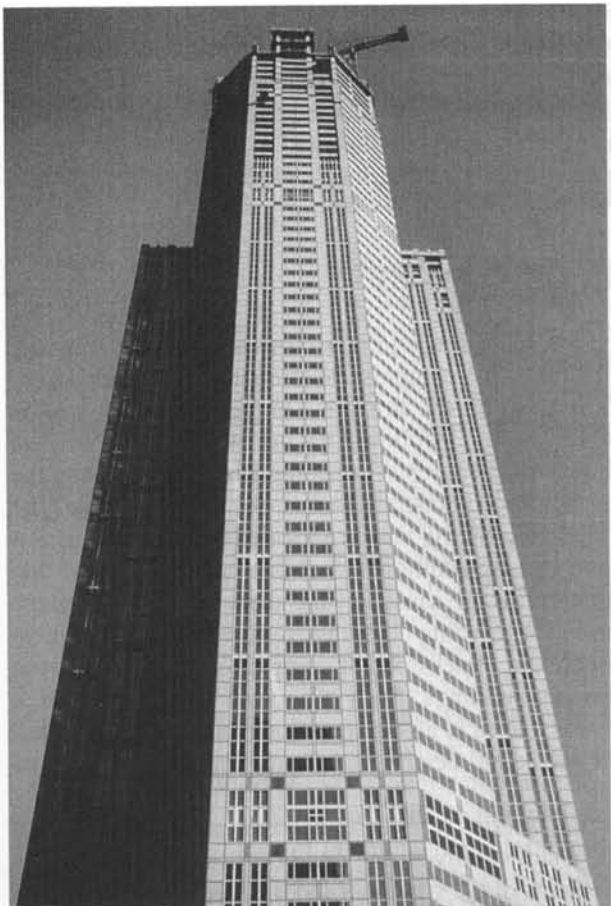
The coefficient of thermal expansion and contraction varies somewhat, depending upon the type of aggregate and richness of the mix. It is generally within the range of 4×10^{-6} to 7×10^{-6} per °F. A value of 5.5×10^{-6} is generally accepted as satisfactory for calculating stresses and deformations caused by temperature changes (Ref. 2.8).

2.12 HIGH-STRENGTH CONCRETE

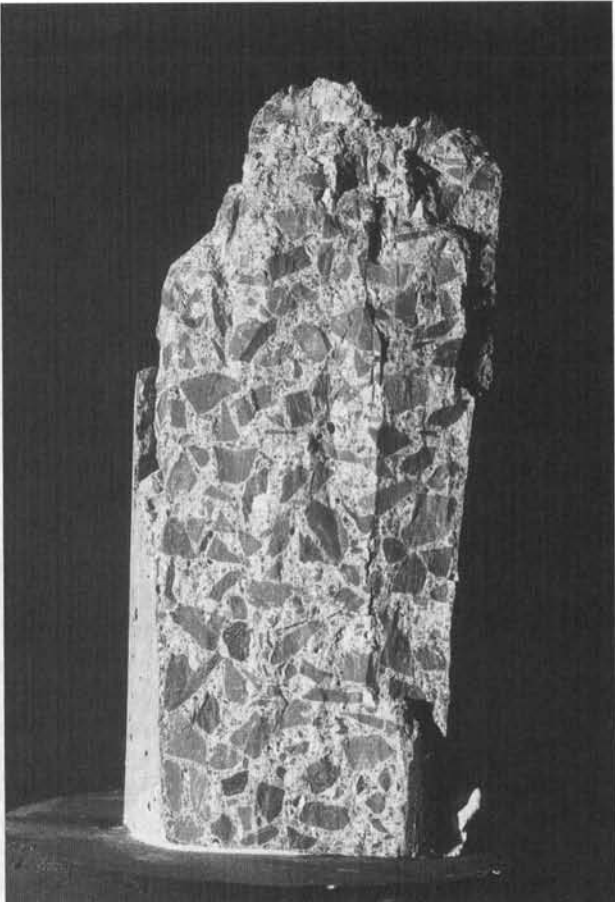
There are a number of applications in which *high-strength concrete* will provide improved structural performance. Although the exact definition is arbitrary, the term generally refers to concrete having uniaxial compressive strength in the range of about 8000 to 20,000 psi or higher. Such concretes can be made using carefully selected but widely available cements, sands, and stone; certain admixtures including high-range water-reducing superplasticizers, fly ash, and silica fume; plus very careful quality control during production (Refs. 2.44 and 2.45). In addition to higher strength in compression, most other engineering properties are improved, leading to use of the alternative term *high-performance concrete*.

The most common application of high-strength concretes has been in the columns of tall concrete buildings, where normal concrete would result in unacceptably large cross sections, with loss of valuable floor space. It has been shown that the use of the more expensive high-strength concrete mixes in columns not only saves floor area but also is more economical than increasing the amount of steel reinforcement. Concrete of up to 12,000 psi was specified for the lower-story columns of 311 South Wacker Drive in Chicago (see Fig. 2.11), a pioneering structure with a total height of 946 ft. Formerly holding the height record, it has been superseded by taller buildings; the present record is held by the tallest building and the tallest structure of any type in the world, the Burj Dubai in Dubai, United Arab Emirates, shown in Fig. 18.2, which has a total height in excess of 2100 ft.

For bridges, too, smaller cross sections bring significant advantages, and the resulting reduction in dead load permits longer spans. The higher elastic modulus and lower creep coefficient result in reduced initial and long-term deflections, and in the case of prestressed concrete bridges, initial and time-dependent losses of prestress force are less. Other recent applications of high-strength concrete include offshore oil structures, parking garages, bridge deck overlays, dam spillways, warehouses, and heavy industrial slabs (Ref. 2.46).

**FIGURE 2.11**

311 South Wacker Drive, Chicago, which is among the world's tallest buildings. High-strength concrete with $f'_c = 12,000$ psi was used in the lower stories. (*Courtesy of Portland Cement Association.*)

**FIGURE 2.12**

High-strength concrete test cylinder after uniaxial loading to failure; note the typically smooth fracture surface, with little aggregate interlock.

An essential requirement for high-strength concrete is a low water–cementitious material ratio. For normal concretes, this usually falls in the range from about 0.40 to 0.60 by weight, but for high-strength mixes it may be 0.25 or even lower. To permit proper placement of what would otherwise be a zero slump mix, high-range water-reducing admixtures, or superplasticizers, are essential and may increase slumps to as much as 6 or 8 in. Other additives include fly ash and, most notably, silica fume (see Section 2.7).

Much research in recent years has been devoted to establishing the fundamental and engineering properties of high-strength concretes, as well as the engineering characteristics of structural members made with the material (Refs. 2.33, 2.34, and 2.47 to 2.53). A large body of information is now available, permitting the engineer to use high-strength concrete with confidence when its advantages justify the higher cost. The compressive strength curves in Figs. 2.3 and 2.4 illustrate important differences compared with normal concrete, including a higher elastic modulus and an extended range of linear elastic response. Creep coefficients are reduced, as indicated in Table 2.2. Disadvantages include brittle behavior in compression (see Fig. 2.12), somewhat reduced ultimate strain capacity, and an increased tendency to crack when drying

shrinkage is restrained (Ref. 2.54), the latter resulting from the lower creep exhibited by the material. Strength under sustained load is a higher fraction of standard cylinder strength (Refs. 2.30 and 2.31), and high-strength concrete exhibits improved durability and abrasion resistance (Refs. 2.51 and 2.55). As broader experience is gained in practical applications, and as design codes are gradually updated to recognize the special properties of higher-strength concretes now available, much wider use can be expected.

2.13 REINFORCING STEELS FOR CONCRETE

The useful strength of ordinary reinforcing steels in tension as well as compression, i.e., the yield strength, is about 15 times the compressive strength of common structural concrete and well over 100 times its tensile strength. On the other hand, steel is a high-cost material compared with concrete. It follows that the two materials are best used in combination if the concrete is made to resist the compressive stresses and the steel the tensile stresses. Thus, in reinforced concrete beams, the concrete resists the compressive force, longitudinal steel reinforcing bars are located close to the tension face to resist the tension force, and usually additional steel bars are so disposed that they resist the inclined tension stresses that are caused by the shear force in the beams. However, reinforcement is also used for resisting compressive forces primarily where it is desired to reduce the cross-sectional dimensions of compression members, as in the lower-floor columns of multistory buildings. Even if no such necessity exists, a minimum amount of reinforcement is placed in all compression members to safeguard them against the effects of small accidental bending moments that might crack and even fail an unreinforced member.

For most effective reinforcing action, it is essential that steel and concrete deform together, i.e., that there be a sufficiently strong *bond* between the two materials to ensure that no relative movements of the steel bars and the surrounding concrete occur. This bond is provided by the relatively large *chemical adhesion* that develops at the steel-concrete interface, by the *natural roughness* of the mill scale of hot-rolled reinforcing bars and by the closely spaced rib-shaped *surface deformations* with which reinforcing bars are furnished to provide a high degree of interlocking of the two materials.

Additional features that make for the satisfactory joint performance of steel and concrete are the following:

1. The *thermal expansion coefficients* of the two materials, about 6.5×10^{-6} for steel vs. an average of 5.5×10^{-6} for concrete, are sufficiently close to forestall cracking and other undesirable effects of differential thermal deformations.
2. While the *corrosion resistance* of bare steel is poor, the concrete that surrounds the steel reinforcement provides excellent corrosion protection, minimizing corrosion problems and corresponding maintenance costs.
3. The *fire resistance* of unprotected steel is impaired by its high thermal conductivity and by the fact that its strength decreases sizably at high temperatures. Conversely, the thermal conductivity of concrete is relatively low. Thus, damage caused by even prolonged fire exposure, if any, is generally limited to the outer layer of concrete, and a moderate amount of concrete cover provides sufficient thermal insulation for the embedded reinforcement.

Steel is used in two different ways in concrete structures: as reinforcing steel and as prestressing steel. Reinforcing steel is placed in the forms prior to casting of the concrete. Stresses in the steel, as in the hardened concrete, are caused only by the loads

on the structure, except for possible parasitic stresses from shrinkage or similar causes. In contrast, in prestressed concrete structures, large tension forces are applied to the reinforcement prior to letting it act jointly with the concrete in resisting external loads. The steels for these two uses are very different and will be discussed separately.

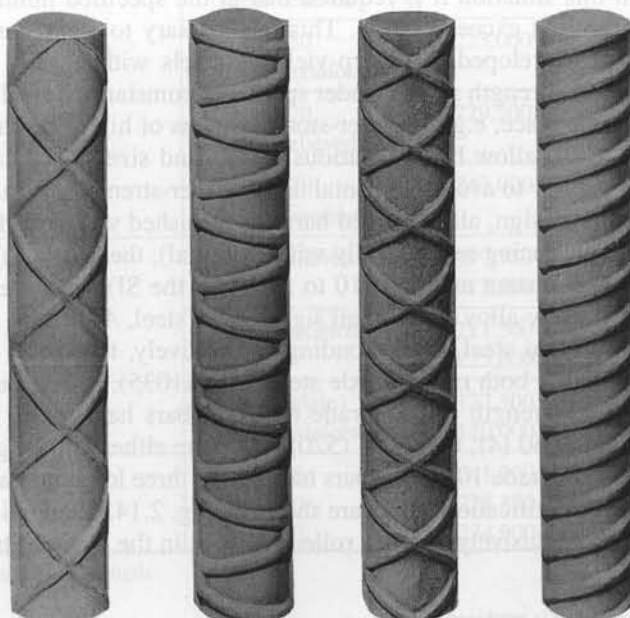
2.14 REINFORCING BARS

The most common type of reinforcing steel (as distinct from prestressing steel) is in the form of round bars, often called *rebars*, available in a large range of diameters from about $\frac{3}{8}$ to $1\frac{3}{8}$ in. for ordinary applications and in two heavy bar sizes of about $1\frac{3}{4}$ and $2\frac{1}{4}$ in. These bars are furnished with surface deformations for the purpose of increasing resistance to slip between steel and concrete. Minimum requirements for these deformations (spacing, projection, etc.) have been developed in experimental research. Different bar producers use different patterns, all of which satisfy these requirements. Figure 2.13 shows a variety of current types of deformations.

For many years, bar sizes have been designated by numbers, Nos. 3 to 11 being commonly used and Nos. 14 and 18 representing the two special large-sized bars previously mentioned. Designation by number, instead of by diameter, was introduced because the surface deformations make it impossible to define a single easily measured value of the diameter. The numbers are so arranged that the unit in the number designation corresponds closely to the number of $\frac{1}{8}$ in. of diameter size. A No. 5 bar, for example, has a nominal diameter of $\frac{5}{8}$ in. Bar sizes are rolled into the surface of the bars for easy identification.

For a number of years, ASTM standards have included a second designation for bar size, the International System of Units (SI), with the size being identified using the nominal diameter in millimeters. To limit the number of bar designations, reinforcing bar producers in the United States have converted to SI for marking the bars. Thus, Nos. 3 to 11 bars are marked with Nos. 10 to 36, and Nos. 14 and 18 bars with Nos. 43 and 57. Both systems are still used in the ASTM standards, and the older, customary

FIGURE 2.13
Types of deformed
reinforcing bars.



system is used in the 2008 ACI Code. To recognize the dual system of identifying and marking the bars, the customary bar designation system is retained throughout this text, followed by the SI bar designations in parentheses, such as No. 6 (No. 19). Table A.1 of Appendix A gives areas and weights of standard bars. Tables A.2 and A.3 give similar information for groups of bars.

a. **Grades and Strengths**

In reinforced concrete, a long-term trend is evident toward the use of higher-strength materials, both steel and concrete. Reinforcing bars with 40 ksi yield stress, once standard, have largely been replaced by bars with 60 ksi yield stress, both because they are more economical and because their use tends to reduce steel congestion in the forms. Bars with a yield stress of 75 ksi are often used in columns, and bars with a yield stress of 100 ksi are allowed to be used as confining reinforcement. Table 2.4 lists all presently available reinforcing steels, their grade designations, the ASTM specifications that define their properties (including deformations) in detail, and their two main minimum specified strength values. Grade 40 bars are no longer available in sizes larger than No. 6 (No. 19) and Grade 50 bars are available in sizes up to No. 8 (No. 25).[†]

The conversion to SI units described above also applies to the strength grades. Thus, Grade 40 is also designated as Grade 280 (for a yield strength of 280 MPa), Grade 60 is designated Grade 420, Grade 75 is designated Grade 520, and Grade 100 is designated Grade 690. The values 280, 420, 520, and 690 result in minimum yield strengths of 40.6, 60.9, 75.4, and 100.1 ksi; i.e., reinforcing steel is slightly stronger than implied by the grade in ksi. Grades based on inch-pound units will be used in this text.

Welding of reinforcing bars in making splices, or for convenience in fabricating reinforcing cages for placement in the forms, may result in metallurgical changes that reduce both strength and ductility, and special restrictions must be placed both on the type of steel used and the welding procedures. The provisions of ASTM A706 relate specifically to welding.

The ACI Code permits reinforcing steels up to $f_y = 80$ ksi for most applications. Such high-strength steels usually yield gradually but have no yield plateau (see Fig. 2.15). In this situation it is required that at the specified minimum yield strength the total strain not exceed 0.0035. This is necessary to make current design methods, which were developed for sharp-yielding steels with a yield plateau, applicable to such higher-strength steels. Under special circumstances, steel in this higher-strength range has its place, e.g., in lower-story columns of high-rise buildings.

To allow bars of various grades and sizes to be easily distinguished, which is necessary to avoid accidental use of lower-strength or smaller-size bars than called for in the design, all deformed bars are furnished with rolled-in markings. These identify the producing mill (usually with an initial), the bar size (Nos. 3 to 18 under the inch-pound system and Nos. 10 to 57 under the SI), the type of steel (*S* for carbon steel, *W* for low-alloy steel, a rail sign for rail steel, *A* for axle steel, and *CS* for low-carbon chromium steel, corresponding, respectively, to ASTM Specifications A615, A706, A996 for both rail and axle steel, and A1035), and an additional marking to identify higher-strength steels. Grade 60 (420) bars have either one longitudinal line or the number 60 (4); Grade 75 (520) bars have either two longitudinal lines or the number 75 (5); Grade 100 (690) bars have either three longitudinal bars or the number 100 (6). The identification marks are shown in Fig. 2.14. As mentioned earlier, SI markings are used exclusively for bars rolled by mills in the United States.

[†] In practice, very little Grade 50 reinforcement is produced.

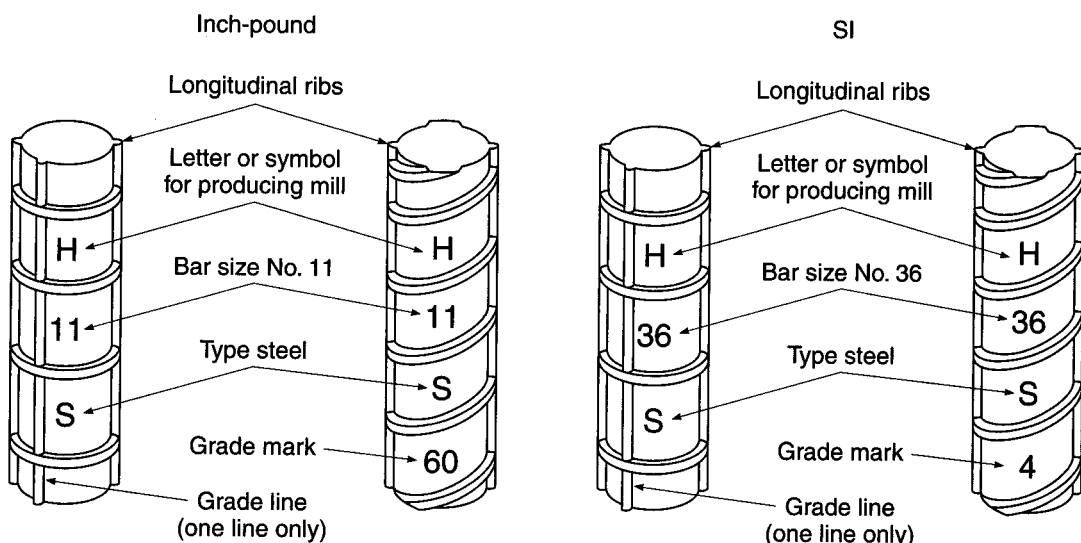
TABLE 2.4
Summary of minimum ASTM strength requirements

Product	ASTM Specification	Designation	Minimum Yield Strength, psi (MPa)	Minimum Tensile Strength, psi (MPa)
Reinforcing bars	A615	Grade 40	40,000 (280)	60,000 (420)
		Grade 60	60,000 (420)	90,000 (620)
		Grade 75	75,000 (520)	100,000 (690)
	A706	Grade 60	60,000 (420) [78,000 (540) maximum]	80,000 (550) ^a
		Grade 40	40,000 (280)	60,000 (420)
		Grade 50	50,000 (350)	80,000 (550)
	A996	Grade 60	60,000 (420)	90,000 (620)
		Grade 100	100,000 (690)	150,000 (1030)
	A1035			
	A184		Same as reinforcing bars	
Deformed bar mats	A767		Same as reinforcing bars	
Zinc-coated bars				
Epoxy-coated bars	A775, A934		Same as reinforcing bars	
Stainless-steel bars ^b	A955		Same as reinforcing bars	
Wire	A82		70,000 (480)	80,000 (550)
			75,000 (515)	85,000 (585)
Welded wire reinforcement	A185			
			65,000 (450)	75,000 (515)
			56,000 (385)	70,000 (485)
	A497		70,000 (480)	80,000 (550)
Prestressing tendons	A416	Grade 250 (stress-relieved)	212,500 (1465)	250,000 (1725)
		Grade 250 (low-relaxation)	225,000 (1555)	250,000 (1725)
		Grade 270 (stress-relieved)	229,500 (1580)	270,000 (1860)
		Grade 270 (low-relaxation)	243,000 (1675)	270,000 (1860)
	A421	Stress-relieved	199,750 (1375) to 212,500 (1465) ^c	235,000 (1620) to 250,000 (1725) ^c
Wire		Low-relaxation	211,500 (1455) to 225,000 (1550) ^c	235,000 (1620) to 250,000 (1725) ^c
A722	Type I (plain)	127,500 (800)	150,000 (1035)	
	Type II (deformed)	120,000 (825)	150,000 (1035)	
Bars	A779	Type 245	241,900 (1480)	247,000 (1700)
		Type 260	228,800 (1575)	263,000 (1810)
Compacted strand ^b		Type 270	234,900 (1620)	270,000 (1860)

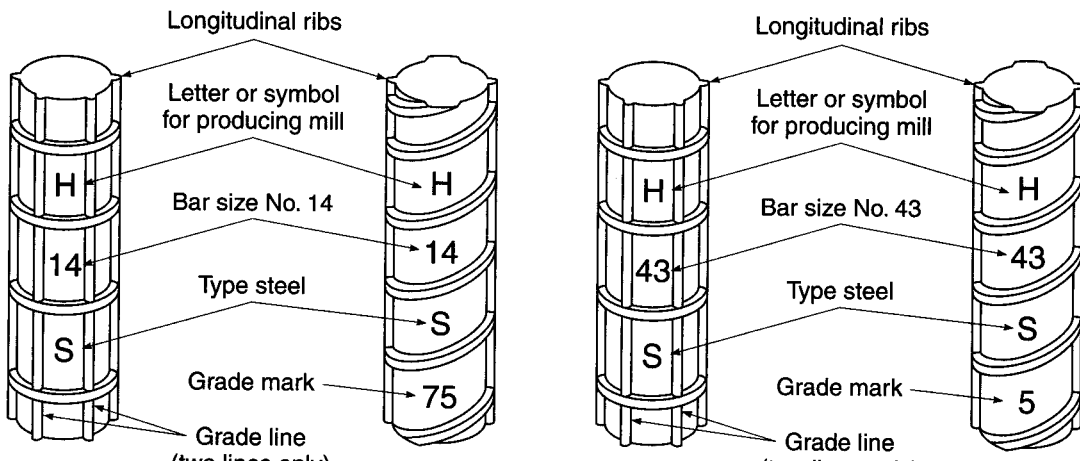
^a But not less than 1.25 times the actual yield strength.

^b Not listed in ACI 318.

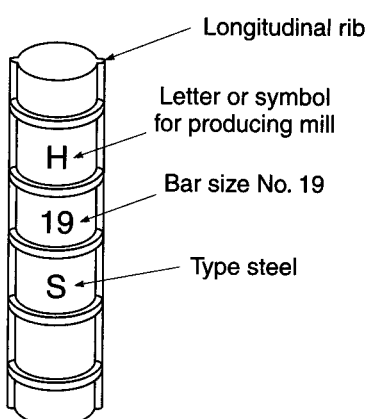
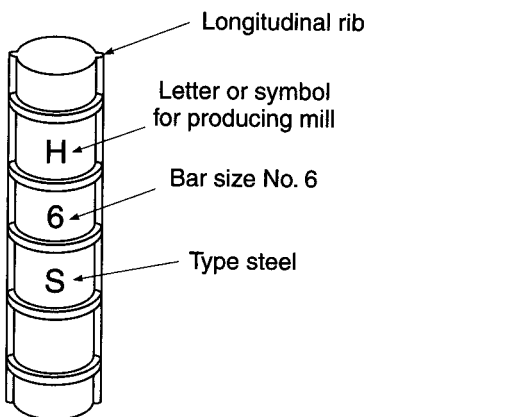
^c Minimum strength depends on wire size.



(a)



(b)



(c)

FIGURE 2.14

Marking system for reinforcing bars meeting ASTM Specifications A615, A706, and A996: (a) Grades 60 and 420; (b) Grades 75 and 520; (c) Grades 40, 50, 280, and 350. (Adapted from Ref. 2.56.) (Facing page.)

b. Stress-Strain Curves

The two chief numerical characteristics that determine the character of bar reinforcement are its *yield point* (generally identical in tension and compression) and its *modulus of elasticity* E_s . The latter is practically the same for all reinforcing steels (but not for prestressing steels) and is taken as $E_s = 29,000,000$ psi.

In addition, however, the shape of the stress-strain curve, and particularly of its initial portion, has significant influence on the performance of reinforced concrete members. Typical stress-strain curves for U.S. reinforcing steels are shown in Fig. 2.15. The complete stress-strain curves are shown in the left part of the figure; the right part gives the initial portions of the curves magnified 10 times.

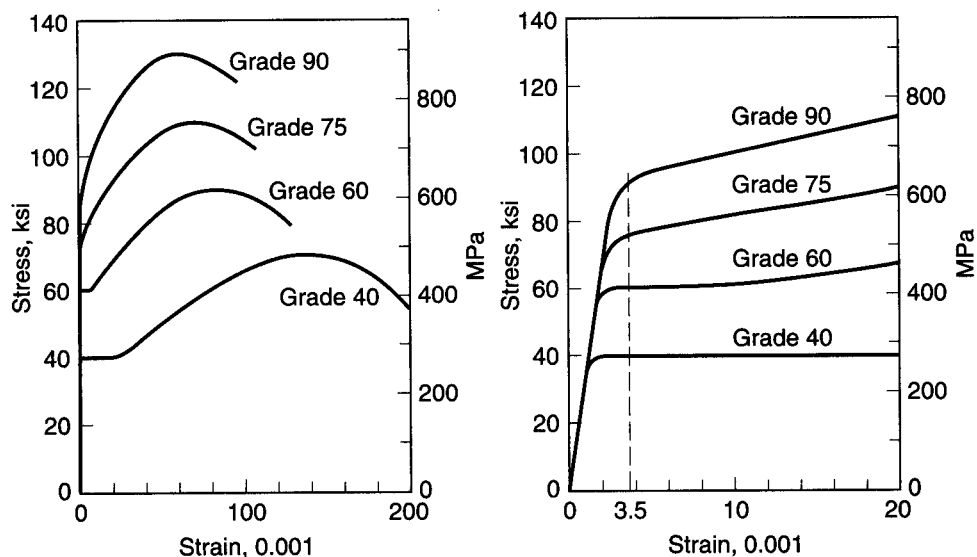
Low-carbon steels, typified by the Grade 40 curve, show an elastic portion followed by a *yield plateau*, i.e., a horizontal portion of the curve where strain continues to increase at constant stress. For such steels, the yield point is that stress at which the yield plateau establishes itself. With further strains, the stress begins to increase again, though at a slower rate, a process that is known as *strain-hardening*. The curve flattens out when the *tensile strength* is reached; it then turns down until fracture occurs. Higher-strength carbon steels, e.g., those with 60 ksi yield stress or higher, either have a yield plateau of much shorter length or enter strain-hardening immediately without any continued yielding at constant stress. In the latter case, the ACI Code specifies that the yield stress f_y be the stress corresponding to a strain of 0.0035, as shown in Fig. 2.15. Low-alloy, high-strength steels rarely show any yield plateau and usually enter strain-hardening immediately upon beginning to yield.

c. Fatigue Strength

In highway bridges and some other situations, both steel and concrete are subject to large numbers of stress fluctuations. Under such conditions, steel, just like concrete (Section 2.8c), is subject to *fatigue*. In metal fatigue, one or more microscopic cracks form after cyclic stress has been applied a significant number of times. These fatigue

FIGURE 2.15

Typical stress-strain curves for reinforcing bars.



cracks occur at points of stress concentrations or other discontinuities and gradually increase with increasing numbers of stress fluctuations. This reduces the remaining uncracked cross-sectional area of the bar until it becomes too small to resist the applied force. At this point the bar fails in a sudden, brittle manner.

For reinforcing bars it has been found (Refs. 2.32 and 2.57) that the fatigue strength, i.e., the stress at which a given stress fluctuation between f_{\max} and f_{\min} can be applied 2 million times or more without causing failure, is practically independent of the grade of steel. It has also been found that the stress range, i.e., the algebraic difference between maximum and minimum stress, $f_1 = f_{\max} - f_{\min}$, that can be sustained without fatigue failure depends on f_{\min} . Further, in deformed bars the degree of stress concentration at the location where the deformation joins the main cylindrical body of the bar tends to reduce the safe stress range. This stress concentration depends on the ratio r/h , where r is the base radius of the deformation and h its height. The radius r is the transition radius from the surface of the bar to that of the deformation; it is a fairly uncertain quantity that changes with roll wear as bars are being rolled.

On the basis of extensive tests (Ref. 2.57), the following formula has been developed for design:

$$f_r = 21 - 0.33f_{\min} + 8 \frac{r}{h} \quad (2.10)$$

where f_r = safe stress range, ksi

f_{\min} = minimum stress; positive if tension, negative if compression

r/h = ratio of base radius to height of rolled-on deformation (in the common situation where r/h is not known, a value of 0.3 may be used)

Where bars are exposed to fatigue regimes, stress concentrations such as welds or sharp bends should be avoided since they may impair fatigue strength.

d. Coated Reinforcing Bars

Galvanized or epoxy-coated reinforcing bars are often specified to minimize corrosion of reinforcement and consequent spalling of concrete under severe environmental conditions, such as in bridge decks or parking garages subject to deicing chemicals, port and marine structures, and wastewater treatment plants.

ASTM A767, "Standard Specification for Zinc-Coated (Galvanized) Steel Bars for Concrete Reinforcement," includes requirements for the zinc coating material, the galvanizing process, the class or weight of coating, finish and adherence of coating, and the method of fabrication. Bars are usually galvanized after cutting and bending. Supplementary requirements pertain to coating of sheared ends and repair of damaged coating if bars are fabricated after galvanizing.

Epoxy-coated bars, presently more widely used than galvanized bars, are governed by ASTM A775, "Standard Specification for Epoxy-Coated Reinforcing Steel Bars," which includes requirements for the coating material, surface preparation prior to coating, method of application, and limits on coating thickness, and by ASTM A934, "Standard Specification for Epoxy-Coated Prefabricated Steel Reinforcing Bars." Under ASTM A775, the coating is applied to straight bars in a production-line operation, and the bars are cut and bent after coating. Under ASTM A934, bars are bent to final shape prior to coating. Cut ends and small spots of damaged coating are suitably repaired after fabrication. Extra care is required in the field to ensure that the coating is not damaged during shipment and placing and that repairs are made if necessary.

2.15 WELDED WIRE REINFORCEMENT

Apart from single reinforcing bars, *welded wire reinforcement* (also described as *welded wire fabric*) is often used for reinforcing slabs and other surfaces, such as shells, and for shear reinforcement in thin beam webs, particularly in prestressed beams. Welded wire reinforcement consists of sets of longitudinal and transverse cold-drawn steel wires at right angles to each other and welded together at all points of intersection. The size and spacing of wires may be the same in both directions or may be different, depending on the requirements of the design.

The notation used to describe the type and size of welded wire fabric involves a letter-number combination. ASTM uses the letter "W" to designate smooth wire and letter "D" to describe deformed wire. The number following the letter gives the cross-sectional area of the wire in hundredths of a square inch. For example, a W5.0 wire is a smooth wire with a cross-sectional area of 0.05 in². A W5.5 wire has a cross-sectional area of 0.055 in². D6.0 indicates a deformed wire with a cross-sectional area of 0.06 in². Welded wire fabric having a designation 4 × 4 – W5.0 × W5.0 has wire spacings 4 in. in each way with smooth wire of cross-sectional area 0.05 in² in each direction. Sizes and spacings for common types of welded wire fabric and cross-sectional areas of steel per foot, as well as weight per 100 ft², are shown in Table A.12 of Appendix A.

ASTM Specifications A185 and A497 pertain to smooth and deformed welded wire fabric, respectively, as shown in Table 2.4. Because the yield stresses shown are specified at a strain of 0.005, the ACI Code requires that f_y be taken equal to 60 ksi unless the stress at a strain of 0.0035 is used.

2.16 PRESTRESSING STEELS

Prestressing steel is used in three forms: round wires, stranded cable, and alloy steel bars. Prestressing wire ranges in diameter from 0.192 to 0.276 in. It is made by cold-drawing high-carbon steel after which the wire is stress-relieved by heat treatment to produce the prescribed mechanical properties. Wires are normally bundled in groups of up to about 50 individual wires to produce prestressing tendons of the required strength. Stranded cable, more common than wire in U.S. practice, is fabricated with six wires wound around a seventh of slightly larger diameter. The pitch of the spiral winding is between 12 and 16 times the nominal diameter of the strand. Strand diameters range from 0.250 to 0.700 in. Alloy steel bars for prestressing are available in diameters from 0.750 to 1.375 in. as plain round bars and from 0.625 to 2.50 in. as deformed bars. Specific requirements for prestressing steels are found in ASTM A421, "Standard Specification for Uncoated Stress-Relieved Steel Wire for Prestressed Concrete"; ASTM A416, "Standard Specification for Steel Strand, Uncoated Seven-Wire Stress-Relieved for Prestressed Concrete"; and ASTM A722, "Standard Specification for Uncoated High-Strength Steel Bar for Prestressing Concrete." Table A.15 of Appendix A provides design information for U.S. prestressing steels.

a. Grades and Strengths

The tensile strengths of prestressing steels range from about 2.5 to 6 times the yield strengths of commonly used reinforcing bars. The grade designations correspond to the minimum specified tensile strength in ksi. For the widely used seven-wire strand,

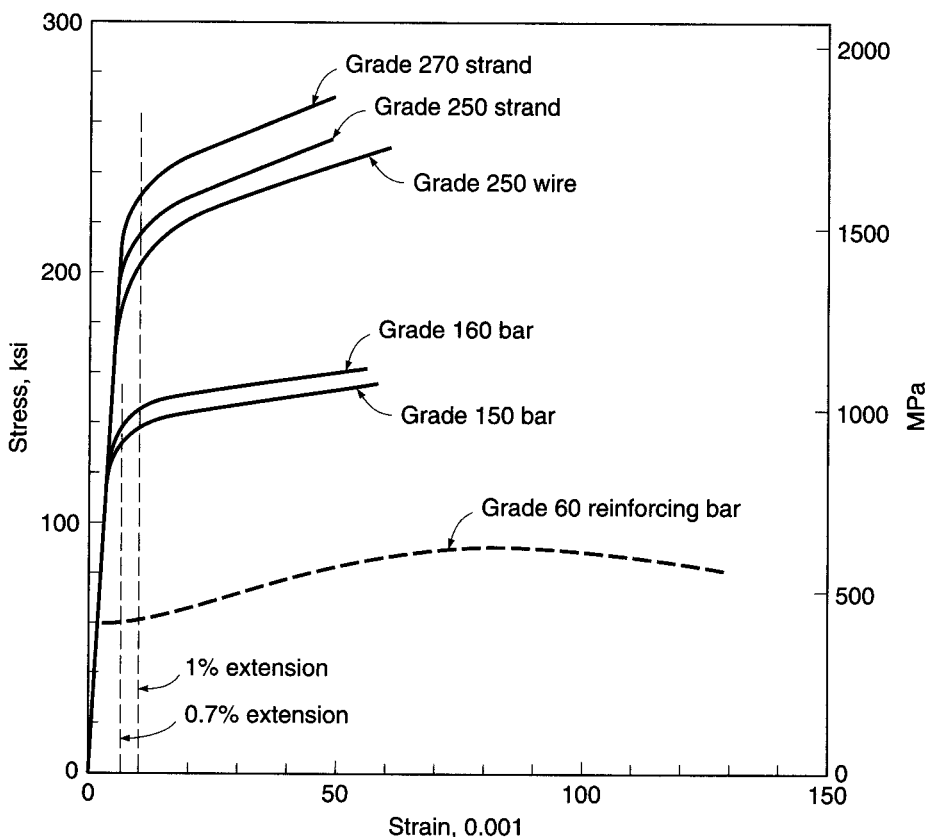
three grades are available: Grade 250 ($f_{pu} = 250$ ksi), Grade 270, and Grade 300, although the last is not yet recognized in ASTM A421. Grade 270 strand is used most often. For alloy steel bars, two grades are used: the regular Grade 150 is most common, but special Grade 160 bars may be ordered. Round wires may be obtained in Grades 235, 240, and 250, depending on diameter.

b. Stress-Strain Curves

Figure 2.16 shows stress-strain curves for prestressing wires, strand, and alloy bars of various grades. For comparison, the stress-strain curve for a Grade 60 reinforcing bar is also shown. It is seen that, in contrast to reinforcing bars, prestressing steels do not show a sharp yield point or yield plateau; i.e., they do not yield at constant or nearly constant stress. Yielding develops gradually, and in the inelastic range the curve continues to rise smoothly until the tensile strength is reached. Because well-defined yielding is not observed in these steels, the yield strength is somewhat arbitrarily defined as the stress at a total elongation of 1 percent for strand and wire and at 0.7 percent for alloy steel bars. Figure 2.16 shows that the yield strengths so defined represent a good limit below which stress and strain are fairly proportional, and above which strain increases much more rapidly with increasing stress. It is also seen that the spread between tensile strength and yield strength is smaller in prestressing steels than in reinforcing steels. It may further be noted that prestressing steels have significantly less ductility.

FIGURE 2.16

Typical stress-strain curves for prestressing steels.



While the modulus of elasticity E_s for bar reinforcement is taken as 29,000,000 psi, the effective modulus of prestressing steel varies, depending on the type of steel (e.g., strand vs. wire or bars) and type of use, and is best determined by test or supplied by the manufacturer. For unbonded strand (i.e., strand not embedded in concrete), the modulus may be as low as 26,000,000 psi. For bonded strand, E_s is usually about 27,000,000 psi, while for smooth round wires E_s is about 29,000,000 psi, the same as for reinforcing bars. The elastic modulus of alloy steel bars is usually taken as $E_s = 27,000,000$ psi.

c. Relaxation

When prestressing steel is stressed to the levels that are customary during initial tensioning and at service loads, it exhibits a property known as *relaxation*. Relaxation is defined as the loss of stress in stressed material held at constant length. (The same basic phenomenon is known as creep when defined in terms of change in strain of a material under constant stress.) To be specific, if a length of prestressing steel is stressed to a sizable fraction of its yield strength f_{py} (say, 80 to 90 percent) and held at a constant strain between fixed points such as the ends of a beam, the steel stress f_p will gradually decrease from its initial value f_{pi} . In prestressed concrete members this stress relaxation is important because it modifies the internal stresses in the concrete and changes the deflections of the beam some time after initial prestress was applied.

The amount of relaxation varies, depending on the type and grade of steel, the time under load, and the initial stress level. A satisfactory estimate for ordinary stress-relieved strand and wires can be obtained from Eq. (2.11), which was derived from more than 400 relaxation tests of up to 9 years' duration:

$$\frac{f_p}{f_{pi}} = 1 - \frac{\log t}{10} \left(\frac{f_{pi}}{f_{py}} - 0.55 \right) \quad (2.11)$$

where f_p is the final stress after t hours, f_{pi} is the initial stress, and f_{py} is the nominal yield stress (Ref. 2.58). In Eq. (2.11), $\log t$ is to the base 10, and f_{pi}/f_{py} not less than 0.55; below that value essentially no relaxation occurs.

The tests on which Eq. (2.11) is based were carried out on round, stress-relieved wires and are equally applicable to stress-relieved strand. In the absence of other information, results may be applied to alloy steel bars as well.

Low-relaxation strand has replaced stress-relieved strand as the industry standard. According to ASTM A416, such steel must exhibit relaxation after 1000 hours of not more than 2.5 percent when initially stressed to 70 percent of specified tensile strength and not more than 3.5 percent when loaded to 80 percent of tensile strength. For low-relaxation strand, Eq. (2.11) is replaced by

$$\frac{f_p}{f_{pi}} = 1 - \frac{\log t}{45} \left(\frac{f_{pi}}{f_{py}} - 0.55 \right) \quad (2.12)$$

REFERENCES

- 2.1. "Guide for Use of Normal Weight and Heavyweight Aggregate in Concrete," ACI Committee 221, *ACI Manual of Concrete Practice*, Part 1, 2009.
- 2.2. "Guide for Structural Lightweight Aggregate Concrete," ACI Committee 213, *ACI Manual of Concrete Practice*, Part 1, 2009.

- 2.3. G. E. Troxell, H. E. Davis, and J. W. Kelly, *Composition and Properties of Concrete*, 2nd ed., McGraw-Hill, New York, 1968.
- 2.4. T. T. C. Hsu and F. O. Slate, "Tensile Bond Strength between Aggregate and Cement Paste or Mortar," *J. ACI*, vol. 60, no. 4, 1963, pp. 465–486.
- 2.5. "Standard Practice for Selecting Proportions for Normal, Heavyweight, and Mass Concrete," ACI Committee 211, *ACI Manual of Concrete Practice*, Part 1, 2009.
- 2.6. "Standard Practice for Selecting Proportions for Structural Lightweight Concrete," ACI Committee 211, *ACI Manual of Concrete Practice*, Part 1, 2009.
- 2.7. S. A. Kosmatka, B. Kerkhoff, and W. C. Panarese, *Design and Control of Concrete Mixtures*, 14th ed., Portland Cement Association, Skokie, IL, 2003.
- 2.8. S. Mindess, J. F. Young, and D. Darwin, *Concrete*, 2nd ed., Prentice-Hall, Upper Saddle River, NJ, 2003.
- 2.9. "Guide for Consolidation of Concrete," ACI Committee 309, *ACI Manual of Concrete Practice*, Part 2, 2009.
- 2.10. "Guide for Measuring, Transporting, and Placing Concrete," ACI Committee 304, *ACI Manual of Concrete Practice*, Part 2, 2009.
- 2.11. "Cold Weather Concreting," ACI Committee 306, *ACI Manual of Concrete Practice*, Part 2, 2009.
- 2.12. "Recommended Practice for Evaluation of Strength Test Results of Concrete," ACI Committee 214, *ACI Manual of Concrete Practice*, Part 1, 2009.
- 2.13. "Chemical Admixtures for Concrete," ACI Committee 212, *ACI Manual of Concrete Practice*, Part 1, 2009.
- 2.14. K. C. Hover, "Why Is There Air in Concrete?" *Concr. Construction*, vol. 38, no. 1, 1993, pp. 11–15.
- 2.15. "Guide for the Use of High-Range Water-Reducing Admixtures (Superplasticizers) in Concrete," ACI Committee 212, *ACI Manual of Concrete Practice*, Part 1, 2009.
- 2.16. A. A. Ramezanianpour, V. Sivasundaram, and V. M. Malhotra, "Superplasticizers: Their Effect on the Strength Properties of Concrete," *Concr. Intl.*, vol. 17, no. 4, 1995, pp. 30–35.
- 2.17. R. J. Peterman, "The Effects of As-Cast Depth and Concrete Fluidity on Strand Bond," *PCI J.*, vol. 52, no. 3, 2007, pp. 72–101.
- 2.18. "Use of Fly Ash in Concrete," ACI Committee 232, *ACI Manual of Concrete Practice*, Part 1, 2009.
- 2.19. "Guide for the Use of Silica Fume in Concrete," ACI Committee 234, *ACI Manual of Concrete Practice*, Part 1, 2009.
- 2.20. "Guide to Use of Slag Cement in Concrete and Mortar," ACI Committee 233, *ACI Manual of Concrete Practice*, Part 1, 2009.
- 2.21. V. M. Malhotra, "Fly Ash, Silica Fume, and Rice-Husk Ash in Concrete: A Review," *Concr. Intl.*, vol. 15, no. 4, 1993, pp. 23–28.
- 2.22. G. Detwiler, "High-Strength Silica Fume Concrete—Chicago Style," *Concr. Intl.*, vol. 14, no. 10, 1992, pp. 32–36.
- 2.23. R. L. Carrasquillo, A. H. Nilson, and F. O. Slate, "Properties of High Strength Concrete Subject to Short Term Loads," *J. ACI*, vol. 78, no. 3, 1981, pp. 171–178.
- 2.24. F. O. Slate, A. H. Nilson, and S. Martinez, "Mechanical Properties of High-Strength Lightweight Concrete," *J. ACI*, vol. 83, no. 4, 1986, pp. 606–613.
- 2.25. P. T. Wang, S. P. Shah, and A. E. Naaman, "Stress-Strain Curves of Normal and Lightweight Concrete in Compression," *J. ACI*, vol. 75, no. 11, 1978, pp. 603–611.
- 2.26. D. E. Branson, *Deformation of Concrete Structures*, McGraw-Hill, New York, 1977.
- 2.27. H. Rüsch, "Researches toward a General Flexural Theory for Structural Concrete," *J. ACI*, vol. 32, no. 1, 1960, pp. 1–28.
- 2.28. A. S. Ngab, A. H. Nilson, and F. O. Slate, "Shrinkage and Creep of High-Strength Concrete," *J. ACI*, vol. 78, no. 4, 1981, pp. 255–261.
- 2.29. A. M. Neville, *Properties of Concrete*, 4th ed., John Wiley & Sons, Inc., New York, 1996.
- 2.30. M. M. Smadi, F. O. Slate, and A. H. Nilson, "High, Medium, and Low-Strength Concretes Subject to Sustained Overloads," *J. ACI*, vol. 82, no. 5, 1985, pp. 657–664.
- 2.31. M. M. Smadi, F. O. Slate, and A. H. Nilson, "Shrinkage and Creep of High, Medium, and Low-Strength Concretes, Including Overloads," *ACI Mater. J.*, vol. 84, no. 3, 1987, pp. 224–234.
- 2.32. "Fatigue of Concrete Structures," Special Publication SP-75, American Concrete Institute, Detroit, MI, 1982.
- 2.33. M. P. Collins and D. Kuchma, "How Safe Are Our Large, Lightly Reinforced Concrete Beams, Slabs, and Footings?" *ACI Struct. J.*, vol. 96, no. 4, 1999, pp. 482–490.
- 2.34. J. Zuo and D. Darwin, "Splice Strength of Conventional and High Relative Rib Area Bars in Normal and High Strength Concrete," *ACI Struct. J.*, vol. 97, no. 4, 2000, pp. 630–641.
- 2.35. D. Darwin, S. Barham, R. Kozul, and S. Luan, "Fracture Energy of High-Strength Concrete," *ACI Mater. J.*, vol. 98, no. 5, 2001, pp. 410–417.

- 2.36. E. A. Jensen and W. Hansen, "Fracture Energy Test for Highway Concrete—Determining the Effect of Coarse Aggregate on Crack Propagation Resistance," *Transp. Res. Rec.* 1730, 2001, pp. 10–16.
- 2.37. T. T. C. Hsu, F. O. Slate, G. M. Sturman, and G. Winter, "Microcracking of Plain Concrete and the Shape of the Stress-Strain Curve," *J. ACI*, vol. 60, no. 2, 1963, pp. 209–224.
- 2.38. H. Kupfer, H. K. Hilsdorf, and H. Rüsch, "Behavior of Concrete under Biaxial Stresses," *J. ACI*, vol. 66, no. 8, 1969, pp. 656–666.
- 2.39. M. E. Tasuij, F. O. Slate, and A. H. Nilson, "Stress-Strain Response and Fracture of Concrete in Biaxial Loading," *J. ACI*, vol. 75, no. 7, 1978, pp. 306–312.
- 2.40. K. H. Gerstle et al., "Strength of Concrete under Multiaxial Stress States," *Proc. Douglas McHenry International Symposium on Concrete and Concrete Structures*, ACI Special Publication SP-55, American Concrete Institute, 1978, pp. 103–131.
- 2.41. G. Pickett, "Effect of Aggregate on Shrinkage of Concrete and Hypothesis Concerning Shrinkage," *J. ACI*, vol. 52, no. 6, 1956, pp. 581–589.
- 2.42. "Standard Practice for the Use of Shrinkage-Compensating Cements," ACI Committee 223, *ACI Manual of Concrete Practice*, Part 1, 2009.
- 2.43. A. Neville, "Whither Expansive Cement," *Concr. Intl.*, vol. 16, no. 9, 1994, pp. 34–35.
- 2.44. "State-of-the-Art Report on High-Strength Concrete," ACI Committee 363, *ACI Manual of Concrete Practice*, Part 5, 2002.
- 2.45. S. P. Shah and S. H. Ahmad (eds.), *High-Performance Concrete: Properties and Applications*, McGraw-Hill, New York, 1994.
- 2.46. H. G. Russell, S. H. Gebler, and D. Whiting, "High-Strength Concrete: Weighing the Benefits," *Civ. Eng.*, vol. 59, no. 11, 1989, pp. 59–61.
- 2.47. A. H. Nilson, "High-Strength Concrete—An Overview of Cornell Research," *Proc. of Symposium on Utilization of High-Strength Concrete*, Stavanger, Norway, 1987, pp. 27–38.
- 2.48. A. H. Nilson, "Properties and Performance of High-Strength Concrete," *Proc. of IABSE Symposium on Concrete Structures for the Future*, Paris-Versailles, 1987, pp. 389–394.
- 2.49. A. H. Nilson, "Design Implications of Current Research on High-Strength Concrete," *High-Strength Concrete*, Special Publication SP-87, American Concrete Institute, Detroit, MI, 1985, pp. 85–118.
- 2.50. K. A. Paulson, A. H. Nilson, and K. C. Hover, "Long-Term Deflection of High-Strength Concrete Beams," *ACI Mater. J.*, vol. 88, no. 2, 1991, pp. 197–206.
- 2.51. A. E. Fiorato, "PCA Research on High-Strength Concrete," *Concr. Intl.*, vol. 11, no. 4, 1989, pp. 44–50.
- 2.52. N. J. Carino and J. R. Clifton, "High-Performance Concrete: Research Needs to Enhance Its Use," *Concr. Intl.*, vol. 13, no. 9, 1991, pp. 70–76.
- 2.53. A. Azizinamini, R. Pavel, E. Hatfield, and S. K. Ghosh, "Behavior of Spliced Reinforcing Bars Embedded in High-Strength Concrete," *ACI Struct. J.*, vol. 96, no. 5, 1999, pp. 826–835.
- 2.54. D. Darwin, J. Browning, and W. D. Lindquist, "Control of Cracking in Bridge Decks: Observations from the Field," *Cement, Concrete and Aggregates*, ASTM International, vol. 26, no. 2, 2004, pp. 148–154.
- 2.55. D. Whiting, "Durability of High-Strength Concrete," *Proc. of Katharine and Bryant Mather International Conference*, Special Publication SP-100, American Concrete Institute, Detroit, MI, 1987, pp. 169–186.
- 2.56. *Manual of Standard Practice*, 28th ed., Concrete Reinforcing Steel Institute, Schaumburg, IL, 2009.
- 2.57. W. G. Corley, J. M. Hanson, and T. Helgason, "Design of Reinforced Concrete for Fatigue," *J. Struct. Div., ASCE*, vol. 104, no. ST6, 1978, pp. 921–932.
- 2.58. W. G. Corley, M. A. Sozen, and C. P. Siess, "Time-Dependent Deflections of Prestressed Concrete Beams," *Highway Res. Board Bull.* No. 307, 1961, pp. 1–25.

PROBLEMS

- 2.1. The specified concrete strength f'_c for a new building is 6000 psi. Calculate the required average strength f'_c for the concrete (*a*) if there are no prior test results for concrete with a compressive strength within 1000 psi of f'_c made with similar materials, (*b*) if 20 test results for concrete with $f'_c = 5000$ psi made with similar materials produce a sample standard deviation s_s of 580 psi, and (*c*) if 30 tests with $f'_c = 5500$ psi made with similar materials produce a sample standard deviation s_s of 590 psi.
- 2.2. Ten consecutive strength tests are available for a new concrete mixture with $f'_c = 4000$ psi: 4590, 4750, 5280, 4210, 4460, 4170, 3750, 5110, 4640, and 4170 psi.

- (a) Do the strength results represent concrete of satisfactory quality? Explain your reasoning.
- (b) If f'_{cr} has been selected based on 30 consecutive test results from an earlier project with a sample standard deviation s_s of 510 psi, must the mixture proportions be adjusted? Explain.

3

Flexural Analysis and Design of Beams

3.1 INTRODUCTION

The fundamental assumptions upon which the analysis and design of reinforced concrete members are based were introduced in Section 1.8, and the application of those assumptions to the simple case of axial loading was developed in Section 1.9. The student should review Sections 1.8 and 1.9 at this time. In developing methods for the analysis and design of beams in this chapter, the same assumptions apply, and identical concepts will be used. This chapter will include analysis and design for flexure, including the dimensioning of the concrete cross section and the selection and placement of reinforcing steel. Other important aspects of beam design including shear reinforcement, bond, and anchorage of reinforcing bars, and the important questions of serviceability (e.g., limiting deflections and controlling concrete cracking) will be treated in Chapters 4, 5, and 6.

3.2 BENDING OF HOMOGENEOUS BEAMS

Reinforced concrete beams are nonhomogeneous in that they are made of two entirely different materials. The methods used in the analysis of reinforced concrete beams are therefore different from those used in the design or investigation of beams composed entirely of steel, wood, or any other structural material. The fundamental principles involved are, however, essentially the same. Briefly, these principles are as follows.

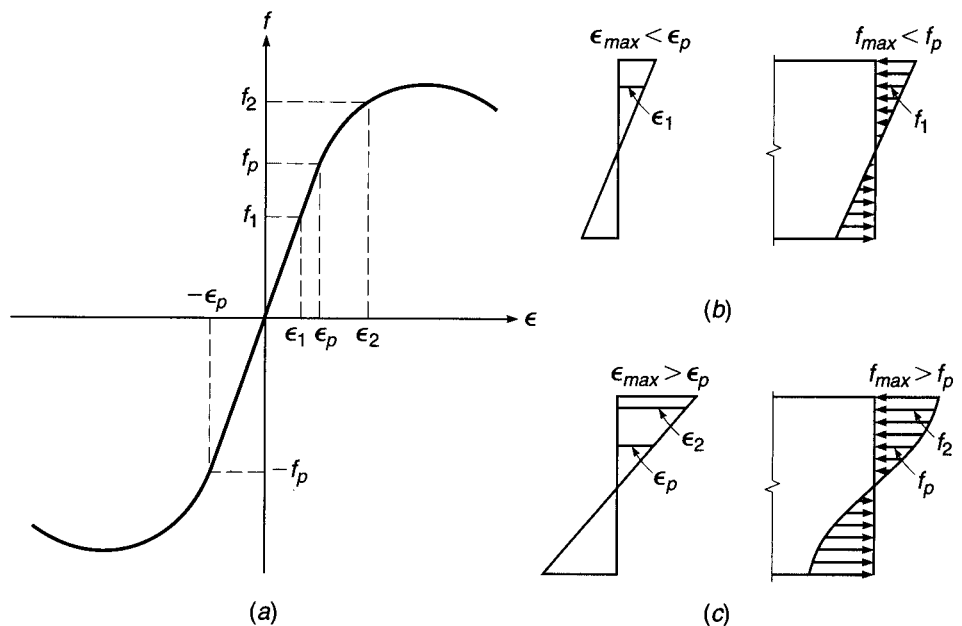
At any cross section there exist internal forces that can be resolved into components normal and tangential to the section. Those components that are normal to the section are the *bending* stresses (tension on one side of the neutral axis and compression on the other). Their function is to resist the bending moment at the section. The tangential components are known as the *shear* stresses, and they resist the transverse or shear forces.

Fundamental assumptions relating to flexure and flexural shear are as follows:

1. A cross section that was plane before loading remains plane under load. This means that the unit strains in a beam above and below the neutral axis are proportional to the distance from that axis.
2. The bending stress f at any point depends on the strain at that point in a manner given by the stress-strain diagram of the material. If the beam is made of a homogeneous material whose stress-strain diagram in tension and compression is that of Fig. 3.1a, the following holds. If the maximum strain at the outer fibers is smaller than the strain ϵ_p up to which stress and strain are proportional for the

FIGURE 3.1

Elastic and inelastic stress distributions in homogeneous beams.



given material, then the compression and tension stresses on either side of the axis are proportional to the distance from the axis, as shown in Fig. 3.1b. However, if the maximum strain at the outer fibers is larger than ϵ_p , this is no longer true. The situation that then occurs is shown in Fig. 3.1c; i.e., in the outer portions of the beam, where $\epsilon > \epsilon_p$, stresses and strains are no longer proportional. In these regions, the magnitude of stress at any level, such as f_2 in Fig. 3.1c, depends on the strain ϵ_2 at that level in the manner given by the stress-strain diagram of the material. In other words, for a given strain in the beam, the stress at a point is the same as that given by the stress-strain diagram for the same strain.

3. The distribution of the shear stresses ν over the depth of the section depends on the shape of the cross section and of the stress-strain diagram. These shear stresses are largest at the neutral axis and equal to zero at the outer fibers. The shear stresses on horizontal and vertical planes through any point are equal.
4. Owing to the combined action of shear stresses (horizontal and vertical) and flexure stresses, at any point in a beam there are inclined stresses of tension and compression, the largest of which form an angle of 90° with each other. The intensity of the inclined maximum or principal stress at any point is given by

$$t = \frac{f}{2} \pm \sqrt{\frac{f^2}{4} + \nu^2} \quad (3.1)$$

where f = intensity of normal fiber stress

ν = intensity of tangential shearing stress

The inclined stress makes an angle α with the horizontal such that $\tan 2\alpha = 2\nu/f$.

5. Since the horizontal and vertical shearing stresses are equal and the flexural stresses are zero at the neutral plane, the inclined tensile and compressive stresses at any point in that plane form an angle of 45° with the horizontal, the intensity of each being equal to the unit shear at the point.

6. When the stresses in the outer fibers are smaller than the proportional limit f_p , the beam behaves *elastically*, as shown in Fig. 3.1b. In this case the following pertains:
- The neutral axis passes through the center of gravity of the cross section.
 - The intensity of the bending stress normal to the section increases directly with the distance from the neutral axis and is a maximum at the extreme fibers. The stress at any given point in the cross section is represented by the equation

$$f = \frac{My}{I} \quad (3.2)$$

where f = bending stress at a distance y from neutral axis

M = external bending moment at section

I = moment of inertia of cross section about neutral axis

The maximum bending stress occurs at the outer fibers and is equal to

$$f_{\max} = \frac{Mc}{I} = \frac{M}{S} \quad (3.3)$$

where c = distance from neutral axis to outer fiber

$S = I/c$ = section modulus of cross section

- The shear stress (horizontal equals vertical) ν at any point in the cross section is given by

$$\nu = \frac{VQ}{Ib} \quad (3.4)$$

where V = total shear at section

Q = statical moment about neutral axis of that portion of cross section lying between a line through point in question parallel to neutral axis and nearest face (upper or lower) of beam

I = moment of inertia of cross section about neutral axis

b = width of beam at a given point

- The intensity of shear along a vertical cross section in a rectangular beam varies as the ordinates of a parabola, the intensity being zero at the outer fibers of the beam and a maximum at the neutral axis. For a total depth h , the maximum is $\frac{3}{2}V/bh$, since at the neutral axis $Q = bh^2/8$ and $I = bh^3/12$ in Eq. (3.4).

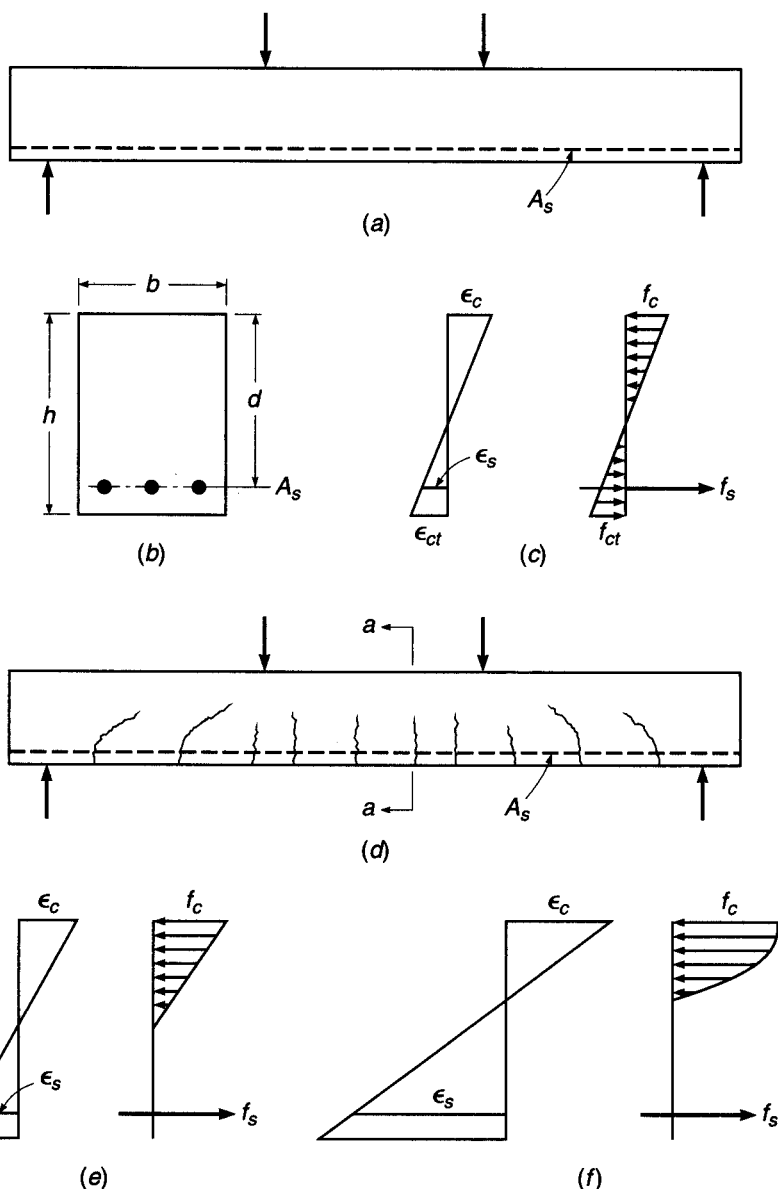
The remainder of this chapter deals only with bending stresses and their effects on reinforced concrete beams. Shear stresses and their effects are discussed separately in Chapter 4.

3.3 REINFORCED CONCRETE BEAM BEHAVIOR

Plain concrete beams are inefficient as flexural members because the tensile strength in bending (modulus of rupture, see Section 2.9) is a small fraction of the compressive strength. As a consequence, such beams fail on the tension side at low loads long before the strength of the concrete on the compression side has been fully utilized. For this reason, steel reinforcing bars are placed on the tension side as close to the extreme tension fiber as is compatible with proper fire and corrosion protection of the steel. In such a reinforced concrete beam, the tension caused by the bending moments is chiefly

FIGURE 3.2

Behavior of reinforced concrete beam under increasing load.



resisted by the steel reinforcement, while the concrete alone is usually capable of resisting the corresponding compression. Such joint action of the two materials is ensured if relative slip is prevented. This is achieved by using deformed bars with their high bond strength at the steel-concrete interface (see Section 2.14) and, if necessary, by special anchorage of the ends of the bars. A simple example of such a beam, with the customary designations for the cross-sectional dimensions, is shown in Fig. 3.2. For simplicity, the discussion that follows will deal with beams of rectangular cross section, even though members of other shapes are very common in most concrete structures.

When the load on such a beam is gradually increased from zero to the magnitude that will cause the beam to fail, several different stages of behavior can be clearly

distinguished. At low loads, as long as the maximum tensile stress in the concrete is smaller than the modulus of rupture, the entire concrete is effective in resisting stress, in compression on one side and in tension on the other side of the neutral axis. In addition, the reinforcement, deforming the same amount as the adjacent concrete, is also subject to tensile stresses. At this stage, all stresses in the concrete are of small magnitude and are proportional to strains. The distribution of strains and stresses in concrete and steel over the depth of the section is shown in Fig. 3.2c.

When the load is further increased, the tensile strength of the concrete is soon reached, and at this stage tension cracks develop. These propagate quickly upward to or close to the level of the neutral plane, which in turn shifts upward with progressive cracking. The general shape and distribution of these tension cracks is shown in Fig. 3.2d. In well-designed beams, the width of these cracks is so small (hairline cracks) that they are not objectionable from the viewpoint of either corrosion protection or appearance. Their presence, however, profoundly affects the behavior of the beam under load. Evidently, in a cracked section, i.e., in a cross section located at a crack such as *a-a* in Fig. 3.2d, the concrete does not transmit any tensile stresses. Hence, just as in tension members (Section 1.9b), the steel is called upon to resist the entire tension. At moderate loads, if the concrete stresses do not exceed approximately $f'_c/2$, stresses and strains continue to be closely proportional (see Fig. 1.16). The distribution of strains and stresses at or near a cracked section is then that shown in Fig. 3.2e. When the load is still further increased, stresses and strains rise correspondingly and are no longer proportional. The ensuing nonlinear relation between stresses and strains is that given by the concrete stress-strain curve. Therefore, just as in homogeneous beams (see Fig. 3.1), the distribution of concrete stresses on the compression side of the beam is of the same shape as the stress-strain curve. Figure 3.2f shows the distribution of strains and stresses close to the ultimate load.

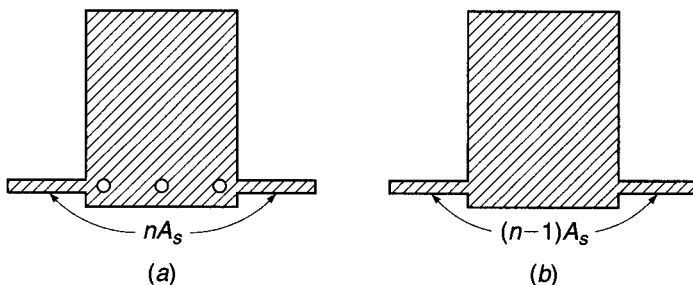
Eventually, the carrying capacity of the beam is reached. Failure can be caused in one of two ways. When relatively moderate amounts of reinforcement are employed, at some value of the load the steel will reach its yield point. At that stress, the reinforcement yields suddenly and stretches a large amount (see Fig. 2.15), and the tension cracks in the concrete widen visibly and propagate upward, with simultaneous significant deflection of the beam. When this happens, the strains in the remaining compression zone of the concrete increase to such a degree that crushing of the concrete, the *secondary compression failure*, ensues at a load only slightly larger than that which caused the steel to yield. Effectively, therefore, attainment of the yield point in the steel determines the carrying capacity of moderately reinforced beams. Such yield failure is gradual and is preceded by visible signs of distress, such as the widening and lengthening of cracks and the marked increase in deflection.

On the other hand, if large amounts of reinforcement or normal amounts of steel of very high strength are employed, the compressive strength of the concrete may be exhausted before the steel starts yielding. Concrete fails by crushing when strains become so large that they disrupt the integrity of the concrete. Exact criteria for this occurrence have yet to be established, but it has been observed that rectangular beams fail in compression when the concrete strains reach values of about 0.003 to 0.004. Compression failure through crushing of the concrete is sudden, of an almost explosive nature, and occurs without warning. For this reason it is good practice to dimension beams in such a manner that should they be overloaded, failure would be initiated by yielding of the steel rather than by crushing of the concrete.

The analysis of stresses and strength in the different stages just described will be discussed in the next several sections.

FIGURE 3.3

Uncracked transformed beam section.



a. Stresses Elastic and Section Uncracked

As long as the tensile stress in the concrete is smaller than the modulus of rupture, so that no tension cracks develop, the strain and stress distribution as shown in Fig. 3.2c is essentially the same as in an elastic, homogeneous beam (Fig. 3.1b). The only difference is the presence of another material, the steel reinforcement. As shown in Section 1.9a, in the elastic range, for any given value of strain, the stress in the steel is n times that of the concrete [Eq. (1.6)]. In the same section, it was shown that one can take account of this fact in calculations by replacing the actual steel-and-concrete cross section with a fictitious section thought of as consisting of concrete only. In this "transformed section," the actual area of the reinforcement is replaced with an equivalent concrete area equal to nA_s , located at the level of the steel. The transformed, uncracked section pertaining to the beam of Fig. 3.2b is shown in Fig. 3.3.

Once the transformed section has been obtained, the usual methods of analysis of elastic homogeneous beams apply. That is, the section properties (location of neutral axis, moment of inertia, section modulus, etc.) are calculated in the usual manner, and, in particular, stresses are computed with Eqs. (3.2) to (3.4).

EXAMPLE 3.1

A rectangular beam has the dimensions (see Fig. 3.2b) $b = 10$ in., $h = 25$ in., and $d = 23$ in. and is reinforced with three No. 8 (No. 25) bars so that $A_s = 2.37$ in.². The concrete cylinder strength f'_c is 4000 psi, and the tensile strength in bending (modulus of rupture) is 475 psi. The yield point of the steel f_y is 60,000 psi, the stress-strain curves of the materials being those of Fig. 1.16. Determine the stresses caused by a bending moment $M = 45$ ft-kips.

SOLUTION. With a value $n = E_s/E_c = 29,000,000/3,600,000 = 8$, one has to add to the rectangular outline an area $(n - 1)A_s = 7 \times 2.37 = 16.59$ in.², disposed as shown on Fig. 3.4, to obtain the uncracked, transformed section. Conventional calculations show that the location of the neutral axis of this section is given by $\bar{y} = 13.2$ in. from the top of the section, and its moment of inertia about this axis is 14,740 in.⁴. For $M = 45$ ft-kips = 540,000 in-lb, the concrete compression stress at the top fiber is, from Eq. (3.3),

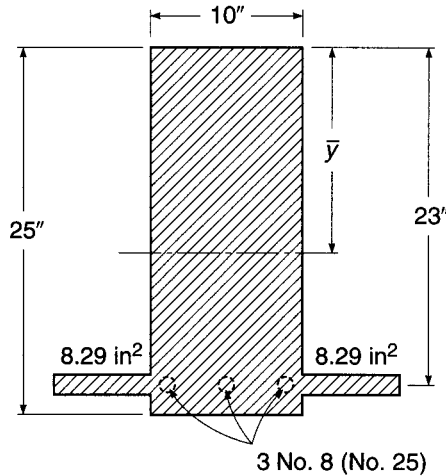
$$f_c = \frac{M\bar{y}}{I} = \frac{540,000 \times 13.2}{14,740} = 484 \text{ psi}$$

and, similarly, the concrete tension stress at the bottom fiber, 11.8 in. from the neutral axis, is

$$f_{ct} = \frac{540,000 \times 11.8}{14,740} = 432 \text{ psi}$$

FIGURE 3.4

Transformed beam section of Example 3.1.



Since this value is below the given tensile bending strength of the concrete, 475 psi, no tension cracks will form, and calculation by the uncracked, transformed section is justified. The stress in the steel, from Eqs. (1.6) and (3.2), is

$$f_s = n \frac{My}{I} = 8 \left(\frac{540,000 \times 9.8}{14,740} \right) = 2870 \text{ psi}$$

By comparing f_c and f_s with the concrete cylinder strength and the yield point, respectively, it is seen that at this stage the actual stresses are quite small compared with the available strengths of the two materials.

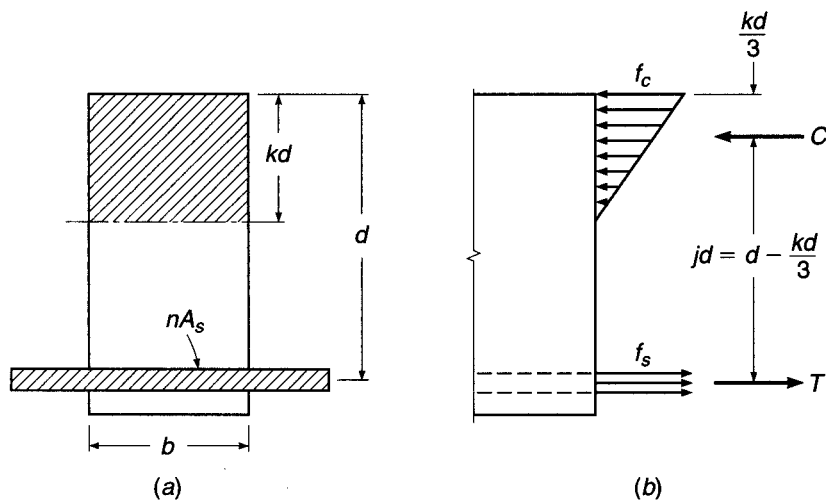
b. Stresses Elastic and Section Cracked

When the tensile stress f_{ct} exceeds the modulus of rupture, cracks form, as shown in Fig. 3.2d. If the concrete compressive stress is less than approximately $\frac{1}{2}f'_c$ and the steel stress has not reached the yield point, both materials continue to behave elastically, or very nearly so. This situation generally occurs in structures under normal service conditions and loads, since at these loads the stresses are generally of the order of magnitude just discussed. At this stage, for simplicity and with little if any error, it is assumed that tension cracks have progressed all the way to the neutral axis and that sections plane before bending are plane in the deformed member. The situation with regard to strain and stress distribution is that shown in Fig. 3.2e.

To compute stresses, and strains if desired, the device of the transformed section can still be used. One need only take account of the fact that all of the concrete that is stressed in tension is assumed cracked, and therefore effectively absent. As shown in Fig. 3.5a, the transformed section then consists of the concrete in compression on one side of the axis and n times the steel area on the other. The distance to the neutral axis, in this stage, is conventionally expressed as a fraction kd of the effective depth d . (Once the concrete is cracked, any material located below the steel is ineffective, which is why d is the effective depth of the beam.) To determine the location of the

FIGURE 3.5

Cracked transformed section.



neutral axis, the moment of the tension area about the axis is set equal to the moment of the compression area, which gives

$$b \frac{(kd)^2}{2} - nA_s(d - kd) = 0 \quad (3.5)$$

Having obtained kd by solving this quadratic equation, one can determine the moment of inertia and other properties of the transformed section as in the preceding case. Alternatively, one can proceed from basic principles by accounting directly for the forces that act on the cross section. These are shown in Fig. 3.5b. The concrete stress, with maximum value f_c at the outer edge, is distributed linearly as shown. The entire steel area A_s is subject to the stress f_s . Correspondingly, the total compression force C and the total tension force T are

$$C = \frac{f_c}{2} bkd \quad \text{and} \quad T = A_s f_s \quad (3.6)$$

The requirement that these two forces be equal numerically has been taken care of by the manner in which the location of the neutral axis has been determined.

Equilibrium requires that the couple constituted by the two forces C and T be equal numerically to the external bending moment M . Hence, taking moments about C gives

$$M = Tjd = A_s f_s jd \quad (3.7)$$

where jd is the internal lever arm between C and T . From Eq. (3.7), the steel stress is

$$f_s = \frac{M}{A_s jd} \quad (3.8)$$

Conversely, taking moments about T gives

$$M = Cjd = \frac{f_c}{2} bkdjd = \frac{f_c}{2} kbd^2 \quad (3.9)$$

from which the concrete stress is

$$f_c = \frac{2M}{kjb^2} \quad (3.10)$$

In using Eqs. (3.6) through (3.10), it is convenient to have equations by which k and j may be found directly, to establish the neutral axis distance kd and the internal lever arm jd . First defining the *reinforcement ratio* as

$$\rho = \frac{A_s}{bd} \quad (3.11)$$

then substituting $A_s = \rho bd$ into Eq. (3.5) and solving for k , one obtains

$$k = \sqrt{(\rho n)^2 + 2\rho n} - \rho n \quad (3.12)$$

From Fig. 3.5b it is seen that $jd = d - kd/3$, or

$$j = 1 - \frac{k}{3} \quad (3.13)$$

Values of k and j for elastic cracked section analysis, for common reinforcement ratios and modular ratios, are found in Table A.6 of Appendix A.

EXAMPLE 3.2

The beam of Example 3.1 is subject to a bending moment $M = 90$ ft-kips (rather than 45 ft-kips as previously). Calculate the relevant properties and stresses.

SOLUTION. If the section were to remain uncracked, the tensile stress in the concrete would now be twice its previous value, that is, 864 psi. Since this exceeds by far the modulus of rupture of the given concrete (475 psi), cracks will have formed and the analysis must be adapted consistent with Fig. 3.5. Equation (3.5), with the known quantities b , n , and A_s inserted, gives the distance to the neutral axis $kd = 7.6$ in., or $k = 7.6/23 = 0.33$. From Eq. (3.13), $j = 1 - 0.33/3 = 0.89$. With these values the steel stress is obtained from Eq. (3.8) as $f_s = 22,300$ psi, and the maximum concrete stress from Eq. (3.10) as $f_c = 1390$ psi.

Comparing the results with the pertinent values for the same beam when subject to one-half the moment, as previously calculated, one notices that (1) the neutral plane has migrated upward so that its distance from the top fiber has changed from 13.2 to 7.6 in.; (2) even though the bending moment has only been doubled, the steel stress has increased from 2870 to 22,300 psi, or about 7.8 times, and the concrete compression stress has increased from 484 to 1390 psi, or 2.9 times; (3) the moment of inertia of the cracked transformed section is easily computed to be 5910 in⁴, compared with 14,740 in⁴ for the uncracked section. This affects the magnitude of the deflection, as discussed in Chapter 6. Thus, it is seen how radical is the influence of the formation of tension cracks on the behavior of reinforced concrete beams.

c. Flexural Strength

It is of interest in structural practice to calculate those stresses and deformations that occur in a structure in service under design load. For reinforced concrete beams, this can be done by the methods just presented, which assume elastic behavior of both materials. It is equally, if not more, important that the structural engineer be able to predict with satisfactory accuracy the strength of a structure or structural member. By

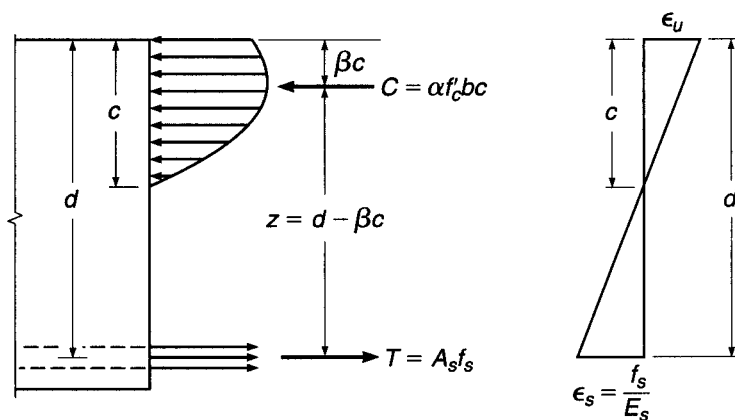
making this strength larger by an appropriate amount than the largest loads that can be expected during the lifetime of the structure, an adequate margin of safety is ensured. In the past, methods based on elastic analysis, like those just presented or variations thereof, have been used for this purpose. It is clear, however, that at or near the ultimate load, stresses are no longer proportional to strains. In regard to axial compression, this has been discussed in detail in Section 1.9, and in regard to bending, it has been pointed out that at high loads, close to failure, the distribution of stresses and strains is that of Fig. 3.2f rather than the elastic distribution of Fig. 3.2e. More realistic methods of analysis, based on actual inelastic rather than assumed elastic behavior of the materials and on results of extremely extensive experimental research, have been developed to predict the member strength. They are now used almost exclusively in structural design practice.

If the distribution of concrete compressive stresses at or near ultimate load (Fig. 3.2f) had a well-defined and invariable shape—parabolic, trapezoidal, or otherwise—it would be possible to derive a completely rational theory of bending strength, just as the theory of elastic bending with its known triangular shape of stress distribution (Figs. 3.1b and 3.2c and e) is straightforward and rational. Actually, inspection of Figs. 2.3, 2.4, and 2.6, and of many more concrete stress-strain curves that have been published, shows that the geometric shape of the stress distribution is quite varied and depends on a number of factors, such as the cylinder strength and the rate and duration of loading. For this and other reasons, a wholly rational flexural theory for reinforced concrete has not yet been developed (Refs. 3.1 to 3.3). Present methods of analysis, therefore, are based in part on known laws of mechanics and are supplemented, where needed, by extensive test information.

Let Fig. 3.6 represent the distribution of internal stresses and strains when the beam is about to fail. One desires a method to calculate that moment M_n (nominal moment) at which the beam will fail either by tension yielding of the steel or by crushing of the concrete in the outer compression fiber. For the first mode of failure, the criterion is that the steel stress equal the yield point, $f_s = f_y$. It has been mentioned before that an exact criterion for concrete compression failure is not yet known, but that for rectangular beams, strains of 0.003 to 0.004 have been measured immediately preceding failure. If one assumes, usually slightly conservatively, that the concrete is about to crush when the maximum strain reaches $\epsilon_u = 0.003$, comparison with a great many tests of beams and columns of a considerable variety of shapes and conditions of loading shows that a satisfactorily accurate and safe strength prediction can be

FIGURE 3.6

Stress distribution at ultimate load.



made (Ref. 3.4). In addition to these two criteria (yielding of the steel at a stress of f_y and crushing of the concrete at a strain of 0.003), it is not really necessary to know the exact shape of the concrete stress distribution in Fig. 3.6. What is necessary is to know, for a given distance c of the neutral axis, (1) the total resultant compression force C in the concrete and (2) its vertical location, i.e., its distance from the outer compression fiber.

In a rectangular beam, the area that is in compression is bc , and the total compression force on this area can be expressed as $C = f_{av}bc$, where f_{av} is the average compression stress on the area bc . Evidently, the average compressive stress that can be developed before failure occurs becomes larger, the higher the cylinder strength f'_c of the particular concrete. Let

$$\alpha = \frac{f_{av}}{f'_c} \quad (3.14)$$

Then

$$C = \alpha f'_c bc \quad (3.15)$$

For a given distance c to the neutral axis, the location of C can be defined as some fraction β of this distance. Thus, as indicated in Fig. 3.6, for a concrete of given strength it is necessary to know only α and β to completely define the effect of the concrete compressive stresses.

Extensive direct measurements, as well as indirect evaluations of numerous beam tests, have shown that the following values for α and β are satisfactorily accurate (see Ref. 3.5, where α is designated as $k_1 k_3$ and β as k_2):

α equals 0.72 for $f'_c \leq 4000$ psi and decreases by 0.04 for every 1000 psi above 4000 up to 8000 psi. For $f'_c > 8000$ psi, $\alpha = 0.56$.

β equals 0.425 for $f'_c \leq 4000$ psi and decreases by 0.025 for every 1000 psi above 4000 up to 8000 psi. For $f'_c > 8000$ psi, $\beta = 0.325$.

The decrease in α and β for high-strength concretes is related to the fact that such concretes are more brittle; i.e., they show a more sharply curved stress-strain plot with a smaller near-horizontal portion (see Figs. 2.3 and 2.4). Figure 3.7 shows these simple relations.

If this experimental information is accepted, the maximum moment can be calculated from the laws of equilibrium and from the assumption that plane cross sections remain plane. Equilibrium requires that

$$C = T \quad \text{or} \quad \alpha f'_c bc = A_s f_s \quad (3.16)$$

Also, the bending moment, being the couple of the forces C and T , can be written as either

$$M = Tz = A_s f_s (d - \beta c) \quad (3.17)$$

or

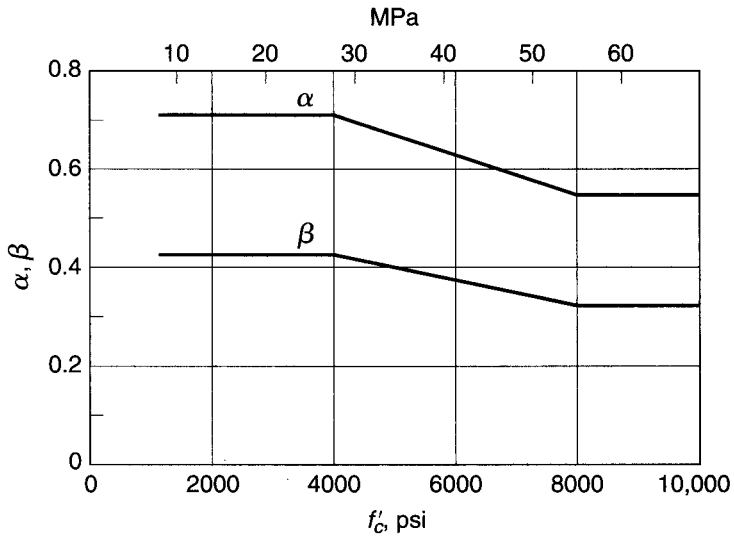
$$M = Cz = \alpha f'_c bc (d - \beta c) \quad (3.18)$$

For failure initiated by yielding of the tension steel, $f_s = f_y$. Substituting this value in Eq. (3.16), one obtains the distance to the neutral axis

$$c = \frac{A_s f_y}{\alpha f'_c b} \quad (3.19a)$$

FIGURE 3.7

Variation of α and β with concrete strength f'_c .



Alternatively, using $A_s = \rho bd$, the neutral axis distance is

$$c = \frac{\rho f_y d}{\alpha f'_c} \quad (3.19b)$$

giving the distance to the neutral axis when tension failure occurs. The nominal moment M_n is then obtained from Eq. (3.17) with the value for c just determined, and $f_s = f_y$; that is,

$$M_n = \rho f_y b d^2 \left(1 - \frac{\beta f_y \rho}{\alpha f'_c} \right) \quad (3.20a)$$

With the specific, experimentally obtained values for α and β given previously, this becomes

$$M_n = \rho f_y b d^2 \left(1 - 0.59 \frac{\rho f_y}{f'_c} \right) \quad (3.20b)$$

If, for larger reinforcement ratios, the steel does not reach yield at failure, then the strain in the concrete becomes $\epsilon_u = 0.003$, as previously discussed. The steel stress f_s , not having reached the yield point, is proportional to the steel strain ϵ_s ; i.e., according to Hooke's law,

$$f_s = \epsilon_s E_s$$

From the strain distribution of Fig. 3.6, the steel strain ϵ_s can be expressed in terms of the distance c by evaluating similar triangles, after which it is seen that

$$f_s = \epsilon_u E_s \frac{d - c}{c} \quad (3.21)$$

Then, from Eq. (3.16),

$$\alpha f'_c bc = A_s \epsilon_u E_s \frac{d - c}{c} \quad (3.22)$$

and this quadratic may be solved for c , the only unknown for the given beam. With both c and f_s known, the nominal moment of the beam, so heavily reinforced that failure occurs by crushing of the concrete, may be found from either Eq. (3.17) or Eq. (3.18).

Whether or not the steel has yielded at failure can be determined by comparing the actual reinforcement ratio with the *balanced reinforcement ratio* ρ_b , representing that amount of reinforcement necessary for the beam to fail by crushing of the concrete at the same load that causes the steel to yield. This means that the neutral axis must be so located that at the load at which the steel starts yielding, the concrete reaches its compressive strain limit ϵ_u . Correspondingly, setting $f_s = f_y$ in Eq. (3.21) and substituting the yield strain ϵ_y for f_y/E_s , one obtains the value of c defining the unique position of the neutral axis corresponding to simultaneous crushing of the concrete and initiation of yielding in the steel

$$c = \frac{\epsilon_u}{\epsilon_u + \epsilon_y} d \quad (3.23)$$

Substituting that value of c into Eq. (3.16), with $A_s f_s = \rho b d f_y$, one obtains for the balanced reinforcement ratio

$$\rho_b = \frac{\alpha f'_c}{f_y} \frac{\epsilon_u}{\epsilon_u + \epsilon_y} \quad (3.24)$$

EXAMPLE 3.3 Determine the nominal moment M_n at which the beam of Examples 3.1 and 3.2 will fail.

SOLUTION. For this beam the reinforcement ratio $\rho = A_s/(bd) = 2.37/(10 \times 23) = 0.0103$. The balanced reinforcement ratio is found from Eq. (3.24) to be 0.0284. Since the amount of steel in the beam is less than that which would cause failure by crushing of the concrete, the beam will fail in tension by yielding of the steel. Its nominal moment, from Eq. (3.20b), is

$$M_n = 0.0103 \times 60,000 \times 10 \times 23^2 \left(1 - 0.59 \frac{0.0103 \times 60,000}{4000} \right) \\ = 2,970,000 \text{ in-lb} = 248 \text{ ft-kips}$$

When the beam reaches M_n , the distance to its neutral axis, from Eq. (3.19b), is

$$c = \frac{0.0103 \times 60,000 \times 23}{0.72 \times 4000} = 4.94$$

It is informative to compare this result with those of Examples 3.1 and 3.2. In the previous calculations, it was found that at low loads, when the concrete had not yet cracked in tension, the neutral axis was located at a distance of 13.2 in. from the compression edge; at higher loads, when the tension concrete was cracked but stresses were still sufficiently small to be elastic, this distance was 7.6 in. Immediately before the beam fails, as has just been shown, this distance has further decreased to 4.9 in. For these same stages of loading, the stress in the steel increased from 2870 psi in the uncracked section, to 22,300 psi in the cracked elastic section, and to 60,000 psi at the nominal moment capacity. This migration of the neutral axis toward the compression edge and the increase in steel stress as load is increased is a graphic illustration of the differences between the various stages of behavior through which a reinforced concrete beam passes as its load is increased from zero to the value that causes it to fail. The examples also illustrate the fact that nominal moments cannot be determined accurately by elastic calculations.

3.4 DESIGN OF TENSION-REINFORCED RECTANGULAR BEAMS

For reasons that were explained in Chapter 1, the present design of reinforced concrete structures is based on the concept of providing sufficient strength to resist hypothetical overloads. The *nominal strength* of a proposed member is calculated based on the best current knowledge of member and material behavior. That nominal strength is modified by a *strength reduction factor* ϕ , less than unity, to obtain the *design strength*. The *required strength*, should the hypothetical overload stage actually be realized, is found by applying *load factors* γ , greater than unity, to the loads actually expected. These expected *service loads* include the calculated dead load, the calculated or legally specified live load, and environmental loads such as those due to wind, seismic action, or temperature. Thus reinforced concrete members are proportioned so that, as shown in Eq. (1.5),

$$\begin{aligned} M_u &\leq \phi M_n \\ P_u &\leq \phi P_n \\ V_u &\leq \phi V_n \end{aligned}$$

where the subscripts n denote the nominal strengths in flexure, thrust, and shear, respectively, and the subscripts u denote the factored load moment, thrust, and shear. The strength reduction factors ϕ normally differ, depending upon the type of strength to be calculated, the importance of the member in the structure, and other considerations discussed in detail in Chapter 1.

A member proportioned on the basis of adequate strength at a hypothetical overload stage must also perform in a satisfactory way under normal service load conditions. In specific terms, the deflection must be limited to an acceptable value, and concrete tensile cracks, which inevitably occur, must be of narrow width and well distributed throughout the tensile zone. Therefore, after proportioning for adequate strength, deflections are calculated and compared against limiting values (or otherwise controlled), and crack widths limited by specific means. This approach to design, referred to in Europe, and to some extent in U.S. practice, as *limit states design*, is the basis of the 2008 ACI Code, and it is the approach that will be followed in this and later chapters.

a. Equivalent Rectangular Stress Distribution

The method presented in Section 3.3c for calculating the flexural strength of reinforced concrete beams, derived from basic concepts of structural mechanics and pertinent experimental research information, also applies to situations other than the case of rectangular beams reinforced on the tension side. It can be used and gives valid answers for beams of other cross-sectional shapes, reinforced in other manners, and for members subject not only to simple bending but also to the simultaneous action of bending and axial force (compression or tension). However, the pertinent equations for these more complex cases become increasingly cumbersome and lengthy. What is more important, it becomes increasingly difficult for the designer to visualize the physical basis for the design methods and formulas; this could lead to a blind reliance on formulas, with a resulting lack of actual understanding. This is not only undesirable on general grounds but also, practically, is more likely to lead to numerical errors in design work than when the designer at all times has a clear picture of the physical situation in the member being dimensioned or analyzed. Fortunately, it is possible, essentially by a

conceptual trick, to formulate the strength analysis of reinforced concrete members in a different manner, which gives the same answers as the general analysis just developed but which is much more easily visualized and much more easily applied to cases of greater complexity than that of the simple rectangular beam. Its consistency is shown, and its application to more complex cases has been checked against the results of a vast number of tests on a great variety of types of members and conditions of loading (Ref. 3.4).

It was noted in the preceding section that the actual geometric shape of the concrete compressive stress distribution varies considerably and that, in fact, one need not know this shape exactly, provided one does know two things: (1) the magnitude C of the resultant of the concrete compressive stresses and (2) the location of this resultant. Information on these two quantities was obtained from the results of experimental research and expressed in the two parameters α and β .

Evidently, then, one can think of the actual complex stress distribution as replaced by a fictitious one of some simple geometric shape, provided that this fictitious distribution results in the same total compression force C applied at the same location as in the actual member when it is on the point of failure. Historically, a number of simplified, fictitious equivalent stress distributions have been proposed by investigators in various countries. The one generally accepted in this country, and increasingly abroad, was first proposed by C. S. Whitney (Ref. 3.4) and was subsequently elaborated and checked experimentally by others (see, for example, Refs. 3.5 and 3.6). The actual stress distribution immediately before failure and the fictitious equivalent distribution are shown in Fig. 3.8.

It is seen that the actual stress distribution is replaced by an equivalent one of simple rectangular outline. The intensity $\gamma f'_c$ of this equivalent constant stress and its depth $a = \beta_1 c$ are easily calculated from the two conditions that (1) the total compression force C and (2) its location, i.e., distance from the top fiber, must be the same in the equivalent rectangular as in the actual stress distribution. From Fig. 3.8a and b the first condition gives

$$C = \alpha f'_c c b = \gamma f'_c a b \quad \text{from which} \quad \gamma = \alpha \frac{c}{a}$$

FIGURE 3.8

Actual and equivalent rectangular stress distributions at ultimate load.

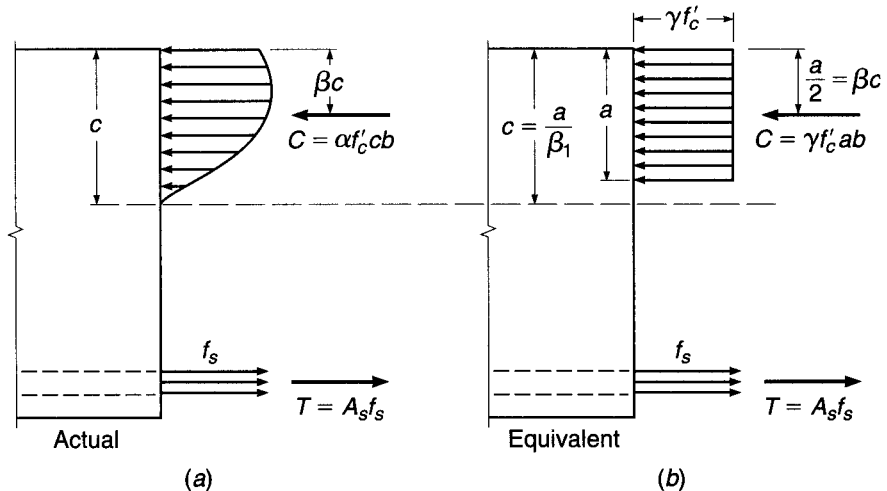


TABLE 3.1
Concrete stress block parameters

	f'_c , psi				
	≤ 4000	5000	6000	7000	≥ 8000
α	0.72	0.68	0.64	0.60	0.56
β	0.425	0.400	0.375	0.350	0.325
$\beta_1 = 2\beta$	0.85	0.80	0.75	0.70	0.65
$\gamma = \alpha/\beta_1$	0.85	0.85	0.85	0.86	0.86

With $a = \beta_1 c$, this gives $\gamma = \alpha/\beta_1$. The second condition simply requires that in the equivalent rectangular stress block, the force C be located at the same distance βc from the top fiber as in the actual distribution. It follows that $\beta_1 = 2\beta$.

To supply the details, the upper two lines of Table 3.1 present the experimental evidence of Fig. 3.7 in tabular form. The lower two lines give the just-derived parameters β_1 and γ for the rectangular stress block. It is seen that the stress intensity factor γ is essentially independent of f'_c and can be taken as 0.85 throughout. Hence, regardless of f'_c , the concrete compression force at failure in a rectangular beam of width b is

$$C = 0.85f'_c ab \quad (3.25)$$

Also, for the common concretes with $f'_c \leq 4000$ psi, the depth of the rectangular stress block is $a = 0.85c$, with c being the distance to the neutral axis. For higher-strength concretes, this distance is $a = \beta_1 c$, with the β_1 values shown in Table 3.1. This is expressed in ACI Code 10.2.7.3 as follows: For f'_c between 2500 and 4000 psi, β_1 shall be taken as 0.85; for f'_c above 4000 psi, β_1 shall be reduced linearly at a rate of 0.05 for each 1000 psi of strength in excess of 4000 psi, but β_1 shall not be taken as less than 0.65. In mathematical terms, the relationship between β_1 and f'_c can be expressed as

$$\beta_1 = 0.85 - 0.05 \frac{f'_c - 4000}{1000} \quad \text{and} \quad 0.65 \leq \beta_1 \leq 0.85 \quad (3.26)$$

The equivalent rectangular stress distribution can be used for deriving the equations that have been developed in Section 3.3c. The failure criteria, of course, are the same as before: yielding of the steel at $f_s = f_y$ or crushing of the concrete at $\epsilon_u = 0.003$. Because the rectangular stress block is easily visualized and its geometric properties are extremely simple, many calculations are carried out directly without reference to formally derived equations, as will be seen in the following sections.

b. Balanced Strain Condition

A reinforcement ratio ρ_b producing balanced strain conditions can be established based on the condition that, at balanced failure, the steel strain is exactly equal to ϵ_y when the strain in the concrete simultaneously reaches the crushing strain of $\epsilon_u = 0.003$. Referring to Fig. 3.6,

$$c = \frac{\epsilon_u}{\epsilon_u + \epsilon_y} d \quad (3.27)$$

which is seen to be identical to Eq. (3.23). Then from the equilibrium requirement that $C = T$

$$\rho_b f_y bd = 0.85 f'_c ab = 0.85 \beta_1 f'_c bc$$

from which

$$\rho_b = 0.85 \beta_1 \frac{f'_c}{f_y} \frac{\epsilon_u}{\epsilon_u + \epsilon_y} \quad (3.28)$$

This is easily shown to be equivalent to Eq. (3.24).

c. Underreinforced Beams

A compression failure in flexure, should it occur, gives little if any warning of distress, while a tension failure, initiated by yielding of the steel, typically is gradual. Distress is obvious from observing the large deflections and widening of concrete cracks associated with yielding of the steel reinforcement, and measures can be taken to avoid total collapse. In addition, most beams for which failure initiates by yielding possess substantial strength based on strain-hardening of the reinforcing steel, which is not accounted for in the calculations of M_n .

Because of these differences in behavior, it is prudent to require that beams be designed such that failure, if it occurs, will be by yielding of the steel, not by crushing of the concrete. This can be done, theoretically, by requiring that the reinforcement ratio ρ be less than the balance ratio ρ_b , given by Eq. (3.28).

In actual practice, the upper limit on ρ should be below ρ_b for the following reasons: (1) for a beam with ρ exactly equal to ρ_b , the compressive strain limit of the concrete would be reached, theoretically, at precisely the same moment that the steel reaches its yield stress, without significant yielding before failure; (2) material properties are never known precisely; (3) strain-hardening of the reinforcing steel, not accounted for in design, may lead to a brittle concrete compression failure even though ρ may be somewhat less than ρ_b ; (4) the actual steel area provided, considering standard reinforcing bar sizes, will always be equal to or larger than required, based on selected reinforcement ratio ρ , tending toward overreinforcement; and (5) the extra ductility provided by beams with lower values of ρ increases the deflection capability substantially and thus provides warning prior to failure.

d. ACI Code Provisions for Underreinforced Beams

While the nominal strength of a member may be computed based on principles of mechanics, the mechanics alone cannot establish safe limits for maximum reinforcement ratios. These limits are defined by the ACI Code. The limitations take two forms. First, the Code addresses the minimum tensile reinforcement strain allowed at nominal strength in the design of beams. Second, the Code defines strength reduction factors that may depend on the tensile strain at nominal strength. Both limitations are based on the *net tensile strain* ϵ_t of the reinforcement farthest from the compression face of the concrete at the depth d_r . The net tensile strain is exclusive of prestress, temperature, and shrinkage effects. For beams with a single layer of reinforcement, the depth to the centroid of the steel d is the same as d_r . For beams with multiple layers of reinforcement, d_r is greater than the depth to the centroid of

the reinforcement d_t . Substituting d_t for d and ϵ_t for ϵ_y in Eq. (3.27), the net tensile strain may be represented as

$$\epsilon_t = \epsilon_u \frac{d_t - c}{c} \quad (3.29)$$

Then based on Eq. (3.28), the reinforcement ratio to produce a selected value of net tensile strain is

$$\rho = 0.85\beta_1 \frac{f'_c}{f_y} \frac{d_t}{d} \frac{\epsilon_u}{\epsilon_u + \epsilon_t} \quad (3.30a)$$

or somewhat conservatively

$$\rho = 0.85\beta_1 \frac{f'_c}{f_y} \frac{\epsilon_u}{\epsilon_u + \epsilon_t} \quad (3.30b)$$

To ensure underreinforced behavior, ACI Code 10.3.5 establishes a minimum net tensile strain ϵ_t at the nominal member strength of 0.004 for members subjected to axial loads less than $0.10f'_c A_g$, where A_g is the gross area of the cross section. By way of comparison ϵ_y , the steel strain at the balanced condition, is 0.00207 for $f_y = 60,000$ psi and 0.00259 for $f_y = 75,000$ psi.

Using $\epsilon_t = 0.004$ in Eq. (3.30b) provides the maximum reinforcement ratio allowed by the ACI Code for beams

$$\rho_{\max} = 0.85\beta_1 \frac{f'_c}{f_y} \frac{\epsilon_u}{\epsilon_u + 0.004} \quad (3.30c)$$

The ACI Code further encourages the use of lower reinforcement ratios by allowing higher strength reduction factors in such beams. The Code defines a *tension-controlled member* as one with a net tensile strain greater than or equal to 0.005. The corresponding strength reduction factor is $\phi = 0.9$.[†] The Code additionally defines a *compression-controlled member* as having a net tensile strain of less than 0.002. The strength reduction factor for compression-controlled members is 0.65. A value of 0.75 may be used if the members are spirally reinforced. A value of $\epsilon_t = 0.002$ corresponds approximately to the yield strain for steel with $f_y = 60,000$ psi yield strength. Between net tensile strains of 0.002 and 0.005, the strength reduction factor varies linearly, and the ACI Code allows a linear interpolation of ϕ based on ϵ_t , as shown in Fig. 3.9. Based on Eq. (3.30b), the maximum reinforcement ratio for a tension-controlled beam is

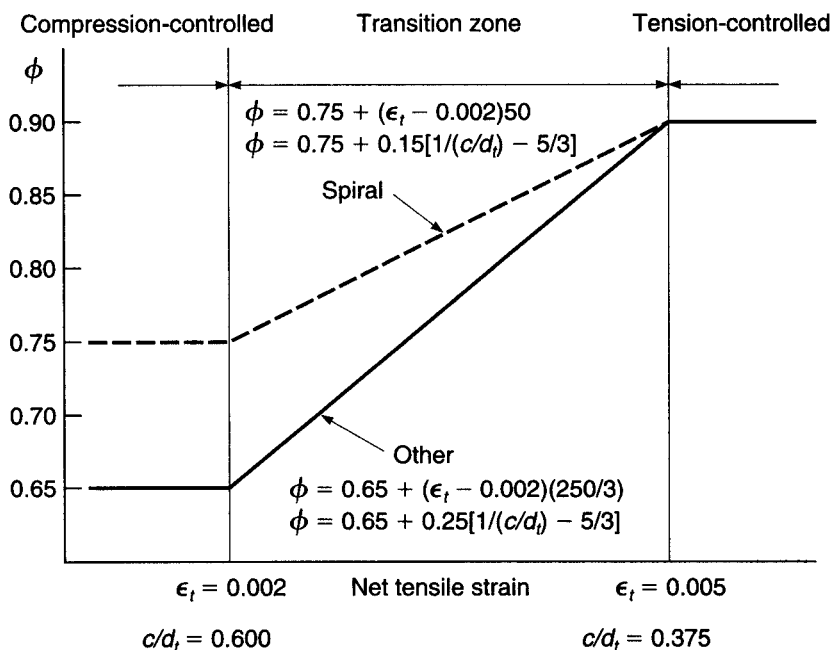
$$\rho_{0.005} = 0.85\beta_1 \frac{f'_c}{f_y} \frac{\epsilon_u}{\epsilon_u + 0.005} \quad (3.30d)$$

A comparison of Eqs. (3.30c) and (3.30d) shows that, for a given concrete cross section, using $\epsilon_t = 0.004$ will result in a higher reinforcement ratio, and thus a higher nominal flexural strength, than using $\epsilon_t = 0.005$. This higher strength, however, cannot be used to full advantage in design because the increase in flexural strength is canceled by the drop in ϕ as ϵ_t decreases from 0.005 to 0.004. As a result, the maximum practical reinforcement ratio for beams is attained at a net tensile strain of 0.005. Values of ϵ_t below 0.005 are not recommended for the design of members with low axial loads.

[†] The selection of a net tensile strain of 0.005 is intended to encompass the yield strain of all reinforcing steel including high-strength bars and prestressing tendons.

FIGURE 3.9

Variation of strength reduction factor with net tensile strain in the steel.



Calculation of the nominal moment capacity frequently involves determination of the depth of the equivalent rectangular stress block a . Since $c = a/\beta_1$, it is sometimes more convenient to compute c/d_t ratios than either ρ or the net tensile strain. The assumption that plane sections remain plane ensures a direct correlation between net tensile strain and the c/d_t ratio, as shown in Fig. 3.10. The maximum value of c/d_t for $\epsilon_t \geq 0.005$ is 0.375.

Comparing Eqs. (3.30a) and (3.30b), it can be seen that the maximum reinforcement ratios in Eqs. (3.30c) and (3.30d) are exact for beams with a single layer of reinforcement and slightly conservative for beams with multiple layers of reinforcement, where d_t is greater than d . Because $\epsilon_t \geq 0.004$ (better yet $\epsilon_t \geq 0.005$) ensures

FIGURE 3.10

Net tensile strain and c/d_t ratios.

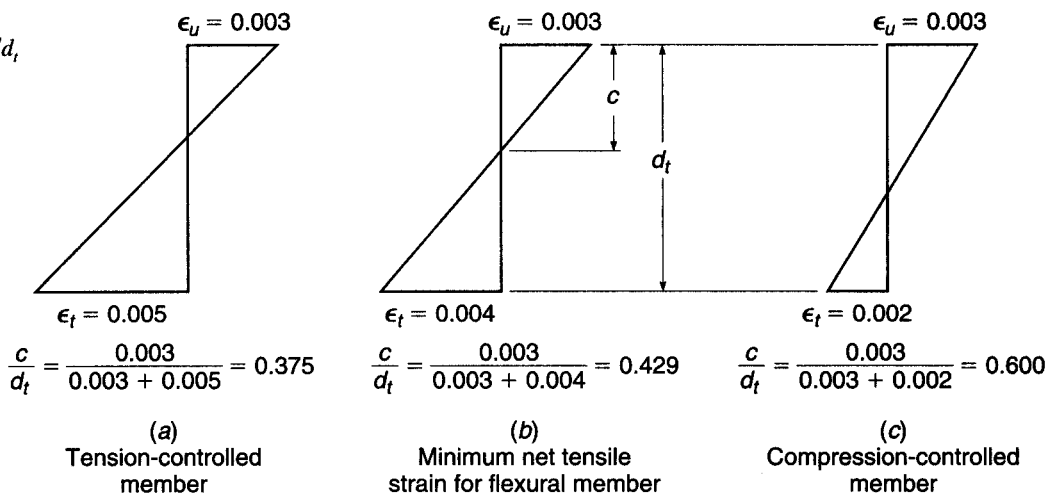
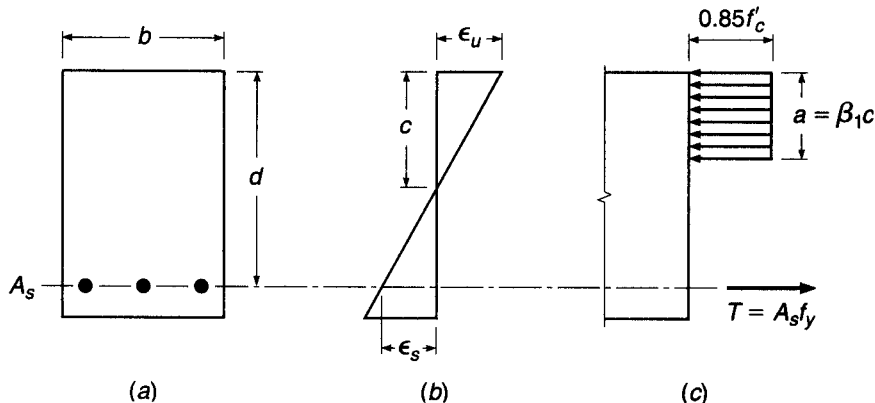


FIGURE 3.11

Singly reinforced rectangular beam.



that steel is yielding in tension, $f_s = f_y$ at failure, and the nominal flexural strength (referring to Fig. 3.11) is given by

$$M_n = A_s f_y \left(d - \frac{a}{2} \right) \quad (3.31)$$

where

$$a = \frac{A_s f_y}{0.85 f'_c b} \quad (3.32)$$

EXAMPLE 3.4 Using the equivalent rectangular stress distribution, directly calculate the nominal strength of the beam previously analyzed in Example 3.3. Recall that $b = 10$ in., $d = 23$ in., $A_s = 2.37 \text{ in}^2$, $f'_c = 4000$ psi, $f_y = 60,000$ psi, and $\beta_1 = 0.85$.

SOLUTION. The distribution of stresses, internal forces, and strains is shown in Fig. 3.11. The maximum practical reinforcement ratio is calculated from Eq. (3.30d) as

$$\rho_{0.005} = 0.85 \times 0.85 \frac{4000}{60,000} \frac{0.003}{0.003 + 0.005} = 0.0181$$

and comparison with the actual reinforcement ratio of 0.0103 confirms that the member is underreinforced and will fail by yielding of the steel. Alternatively, recalling that $c = 4.94$ in.,

$$\frac{c}{d_t} = \frac{c}{d} = \frac{4.94}{23} = 0.215$$

which is less than 0.375, the value of c/d , corresponding to $\epsilon_i = 0.005$, also confirming that the member is underreinforced. The depth of the equivalent stress block is found from the equilibrium condition that $C = T$. Hence $0.85f'_c ab = A_s f_y$, or $a = 2.37 \times 60,000 / (0.85 \times 4000 \times 10) = 4.18$. The nominal moment is

$$M_n = A_s f_y \left(d - \frac{a}{2} \right) = 2.37 \times 60,000 (23 - 2.09) = 2,970,000 \text{ in-lb} = 248 \text{ ft-kips}$$

The results of this simple and direct numerical analysis, based on the equivalent rectangular stress distribution, are identical with those previously determined from the general strength analysis described in Section 3.3c.

It is convenient for everyday design to combine Eqs. (3.31) and (3.32) as follows. Noting that $A_s = \rho bd$, Eq. (3.32) can be rewritten as

$$a = \frac{\rho f_y d}{0.85 f'_c} \quad (3.33)$$

This is then substituted into Eq. (3.31) to obtain

$$M_n = \rho f_y b d^2 \left(1 - 0.59 \frac{\rho f_y}{f'_c} \right) \quad (3.34)$$

which is identical to Eq. (3.20b) derived in Section 3.3c. This basic equation can be simplified further as follows:

$$M_n = Rbd^2 \quad (3.35)$$

in which

$$R = \rho f_y \left(1 - 0.59 \frac{\rho f_y}{f'_c} \right) \quad (3.36)$$

The *flexural resistance factor R* depends only on the reinforcement ratio and the strengths of the materials and is easily tabulated. Tables A.5a and A.5b of Appendix A give *R* values for ordinary combinations of steel and concrete and the full practical range of reinforcement ratios.

In accordance with the safety provisions of the ACI Code, the nominal flexural strength M_n is reduced by imposing the strength reduction factor ϕ to obtain the *design strength*

$$\phi M_n = \phi A_s f_y \left(d - \frac{a}{2} \right) \quad (3.37)$$

or, alternatively,

$$\phi M_n = \phi \rho f_y b d^2 \left(1 - 0.59 \frac{\rho f_y}{f'_c} \right) \quad (3.38)$$

or

$$\phi M_n = \phi Rbd^2 \quad (3.39)$$

EXAMPLE 3.4 (continued)

Calculate the design moment capacity ϕM_n for the beam analyzed earlier in Example 3.4.

SOLUTION. Comparing ρ with $\rho_{0.005}$ or c/d , for the beam with the value of c/d , corresponding to $\epsilon_t = 0.005$ demonstrates that $\epsilon_t > 0.005$. Therefore, $\phi = 0.90$ and the design capacity is

$$\phi M_n = 0.9 \times 248 = 223 \text{ ft-kips}$$

e. Minimum Reinforcement Ratio

Another mode of failure may occur in very lightly reinforced beams. If the flexural strength of the cracked section is less than the moment that produced cracking of the previously uncracked section, the beam will fail immediately and without warning of distress upon formation of the first flexural crack. To ensure against this type of

failure, a *lower limit* can be established for the reinforcement ratio by equating the cracking moment, computed from the concrete modulus of rupture (Section 2.9), to the strength of the cracked section.

For a rectangular section having width b , total depth h , and effective depth d (see Fig. 3.2b), the section modulus with respect to the tension fiber is $bd^2/6$. For typical cross sections, it is satisfactory to assume that $h/d = 1.1$ and that the internal lever arm at flexural failure is $0.95d$. If the modulus of rupture is taken as $f_r = 7.5\sqrt{f'_c}$, as usual, then an analysis equating the cracking moment to the flexural strength results in

$$A_{s,\min} = \frac{1.6\sqrt{f'_c}}{f_y} bd \quad (3.40a)$$

This development can be generalized to apply to beams having a T cross section (see Section 3.8 and Fig. 3.16). The corresponding equations depend on the proportions of the cross section and on whether the beam is bent with the flange (slab) in tension or in compression. For T beams of typical proportions that are bent with the flange in compression, analysis will confirm that the minimum steel area should be

$$A_{s,\min} = \frac{2.7\sqrt{f'_c}}{f_y} b_w d \quad (3.40b)$$

where b_w is the width of the web, or stem, projecting below the slab. For T beams that are bent with the flange in tension, from a similar analysis, the minimum steel area is

$$A_{s,\min} = \frac{6.2\sqrt{f'_c}}{f_y} b_w d \quad (3.40c)$$

The ACI Code requirements for minimum steel area are based on the results just discussed, but there are some differences. According to ACI Code 10.5, at any section where tensile reinforcement is required by analysis, with some exceptions as noted below, the area A_s provided must not be less than

$$A_{s,\min} = \frac{3\sqrt{f'_c}}{f_y} b_w d \geq \frac{200b_w d}{f_y} \quad (3.41)$$

This applies to both positive and negative bending sections. The inclusion of the additional limit of $200b_w d/f_y$ is merely for historical reasons; it happens to give the same minimum reinforcement ratio of 0.005 that was imposed in earlier codes for then-common material strengths. Note that in Eq. (3.41) the section width b_w is used; it is understood that for rectangular sections $b_w = b$. Note further that the ACI coefficient of 3 is a conservatively rounded value compared with 2.7 in Eq. (3.40b) for T beams with the flange in compression, and is very conservative when applied to rectangular beam sections, for which a rational analysis gives 1.6 in Eq. (3.40a). This probably reflects the view that the minimum steel for the negative bending sections of a continuous T beam (which are, in effect, rectangular sections, as discussed in Section 3.8c) should be no less than for the positive bending sections, where the moment is generally smaller.

ACI Code 10.5 treats *statically determinate* T beams with the flange in *tension* as a special case, for which the minimum steel area is equal to or greater than the value given by Eq. (3.41) with b_w replaced by either $2b_w$ or the width of the *flange*, whichever is smaller.

Note that ACI Code Eq. (3.41) is conveniently expressed in terms of a *minimum tensile reinforcement ratio* ρ_{\min} by dividing both sides by $b_w d$.

According to ACI Code 10.5, the requirements of Eq. (3.41) need not be imposed if, at every section, the area of tensile reinforcement provided is at least one-third greater than that required by analysis. This provides sufficient reinforcement for large members such as grade beams, where the usual equations would require excessive amounts of steel.

For structural slabs and footings of uniform thickness, the minimum area of tensile reinforcement in the direction of the span is that required for shrinkage and temperature steel (see Section 13.3 and Table 13.2), and the above minimums need not be imposed. The maximum spacing of such steel is the smaller of 3 times the total slab thickness or 18 in.

f. Examples of Rectangular Beam Analysis and Design

Flexural problems can be classified broadly as *analysis problems* or *design problems*. In analysis problems, the section dimensions, reinforcement, and material strengths are known, and the moment capacity is required. In the case of design problems, the required moment capacity is given, as are the material strengths, and it is required to find the section dimensions and reinforcement. Examples 3.5 and 3.6 illustrate analysis and design, respectively.

EXAMPLE 3.5

Flexural strength of a given member. A rectangular beam has width 12 in. and effective depth 17.5 in. It is reinforced with four No. 9 (No. 29) bars in one row. If $f_y = 60,000$ psi and $f'_c = 4000$ psi, what is the nominal flexural strength, and what is the maximum moment that can be utilized in design, according to the ACI Code?

SOLUTION. From Table A.2 of Appendix A, the area of four No. 9 (No. 29) bars is 4.00 in^2 . Assuming that the beam is underreinforced and using Eq. (3.32),

$$a = \frac{4.00 \times 60}{0.85 \times 4 \times 12} = 5.88 \text{ in.}$$

The depth of the neutral axis is $c = a/\beta_1 = 5.88/0.85 = 6.92$, giving

$$\frac{c}{d_t} = \frac{6.92}{17.5} = 0.395$$

which is between 0.429 and 0.375, the values corresponding, respectively, to $\epsilon_t = 0.004$ and $\epsilon_t = 0.005$, as shown in Fig. 3.10. Thus, the beam is, as assumed, underreinforced, and from Eq. (3.31)

$$M_n = 4.00 \times 60 \left(17.5 - \frac{5.88}{2} \right) = 3490 \text{ in-kips}$$

The fact that the beam is unreinforced could also have been established by calculating $\rho = 4.00/(12 \times 17.5) = 0.190$, which just exceeds $\rho_{0.005}$, which is calculated using Eq. (3.30d).

$$\rho_{0.005} = 0.85 \times 0.85 \left(\frac{4}{60} \right) \left(\frac{0.003}{0.003 + 0.005} \right) = 0.0181$$

Because the net tensile strain ϵ_t is between 0.004 and 0.005, ϕ must be calculated: $\epsilon_t = \epsilon_u(d - c)/c = 0.003 \times 17.5 - 6.92/6.92 = 0.00458$. Using linear interpolation from Fig. 3.9, $\phi = 0.87$, and the design strength is taken as

$$\phi M_n = 0.87 \times 3490 = 3040 \text{ in-kips}$$

The ACI Code limits on the reinforcement ratio

$$\rho_{\max} = 0.0206$$

$$\rho_{\min} = \frac{3\sqrt{4000}}{60,000} \geq \frac{200}{60,000} = 0.0033$$

are satisfied for this beam.

EXAMPLE 3.6

Concrete dimensions and steel area to resist a given moment. Find the concrete cross section and the steel area required for a simply supported rectangular beam with a span of 15 ft that is to carry a computed dead load of 1.27 kips/ft and a service live load of 2.15 kips/ft, as shown in Fig. 3.12. Material strengths are $f'_c = 4000$ psi and $f_y = 60,000$ psi.

SOLUTION. Load factors are first applied to the given service loads to obtain the factored load for which the beam is to be designed, and the corresponding moment:

$$w_u = 1.2 \times 1.27 + 1.6 \times 2.15 = 4.96 \text{ kips/ft}$$

$$M_u = \frac{1}{8} \times 4.96 \times 15^2 \times 12 = 1670 \text{ in-kips}$$

The concrete dimensions will depend on the designer's choice of reinforcement ratio. To minimize the concrete section, it is desirable to select the maximum permissible reinforcement ratio. To maintain $\phi = 0.9$, the maximum reinforcement ratio corresponding to a net tensile strain of 0.005 will be selected (see Fig. 3.9). Then, from Eq. (3.30d)

$$\rho_{0.005} = 0.85\beta_1 \frac{f'_c}{f_y} \frac{\epsilon_u}{\epsilon_u + 0.005} = 0.85 \times 0.85 \left(\frac{4}{60} \right) \left(\frac{0.003}{0.003 + 0.005} \right) = 0.0181$$

Using Eq. (3.30c) gives $\rho_{\max} = 0.0206$, but would require a lower strength reduction factor. Setting the required flexural strength equal to the design strength from Eq. (3.38), and substituting the selected values for ρ and material strengths,

$$M_u = \phi M_n$$

$$1670 = 0.90 \times 0.0181 \times 60bd^2 \left(1 - 0.59 \frac{0.0181 \times 60}{4} \right)$$

from which

$$bd^2 = 2040 \text{ in}^3$$

A beam with width $b = 10$ in. and $d = 14.3$ in. will satisfy this requirement. The required steel area is found by applying the chosen reinforcement ratio to the required concrete dimensions:

$$A_s = 0.0181 \times 10 \times 14.3 = 2.59 \text{ in}^2$$

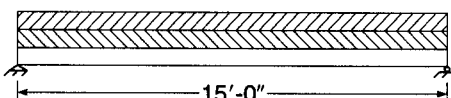
Two No. 10 (No. 32) bars provide 2.54 in², which is very close to the required area.

Assuming 2.5 in. concrete cover from the centroid of the bars, the required total depth is $h = 16.8$ in. In actual practice, however, the concrete dimensions b and h are always rounded up to the nearest inch, and often to the nearest multiple of 2 in. (see Section 3.5). The

FIGURE 3.12

Structural loads for Example 3.6.

Service live load = 2.15 kips/ft
Computed dead load = 1.27 kips/ft
(including beam self-weight)



actual d is then found by subtracting the required concrete cover dimension from h . For the present example, $b = 10$ in. and $h = 18$ in. will be selected, resulting in effective depth $d = 15.5$ in. Improved economy then may be possible, refining the steel area based on the actual, larger, effective depth. One can obtain the revised steel requirement directly by solving Eq. (3.38) for ρ , with $\phi M_n = M_u$. A quicker solution can be obtained by iteration. First a reasonable value of a is assumed, and A_s is found from Eq. (3.37). From Eq. (3.32) a revised estimate of a is obtained, and A_s is revised. This method converges very rapidly. For example, assume $a = 5$ in. Then

$$A_s = \frac{1670}{0.90 \times 60(15.5 - 2.5)} = 2.38 \text{ in}^2$$

Checking the assumed a gives

$$a = \frac{2.38 \times 60}{0.85 \times 4 \times 10} = 4.20 \text{ in.}$$

This is close enough to the assumed value that no further calculation is required. The required steel area of 2.38 in^2 could be provided using three No. 8 (No. 25) bars, but for simplicity of construction, two No. 10 (No. 32) bars will be used as before.

A somewhat larger beam cross section using less steel may be more economical, and will tend to reduce deflections. As an alternative solution, the beam will be redesigned with a lower reinforcement ratio of $\rho = 0.60\rho_{\max} = 0.60 \times 0.0206 = 0.0124$. Setting the required strength equal to the design strength [Eq. (3.38)] as before,

$$1670 = 0.90 \times 0.0124 \times 60bd^2 \left(1 - 0.59 \frac{0.0124 \times 60}{4} \right)$$

and

$$bd^2 = 2800 \text{ in}^3$$

A beam with $b = 10$ in. and $d = 16.7$ in. will meet the requirement, for which

$$A_s = 0.0124 \times 10 \times 16.7 = 2.07 \text{ in}^2$$

Two No. 9 (No. 29) bars are almost sufficient, providing an area of 2.00 in^2 . If the total concrete height is rounded up to 20 in., a 17.5 in. effective depth results, reducing the required steel area to 1.96 in^2 . Two No. 9 (No. 29) bars remain the best choice.

It is apparent that an infinite number of solutions to the stated problem are possible, depending upon the reinforcement ratio selected. That ratio may vary from an upper limit of ρ_{\max} to a lower limit of $3\sqrt{f'_c/f_y} \geq 200/f_y$ for beams, according to the ACI Code. To compare the two solutions (using the theoretical dimensions, unrounded for the comparison, and assuming h is 2.5 in. greater than d in each case), increasing the concrete section area by 14 percent achieves a steel saving of 20 percent. The second solution would certainly be more economical and would be preferred, unless beam dimensions must be minimized for architectural or functional reasons. Economical designs will typically have reinforcement ratios between $0.50\rho_{0.005}$ and $0.75\rho_{0.005}$.

There is a type of problem, occurring frequently, that does not fall strictly into either the analysis or the design category. The concrete dimensions are given and are known to be adequate to carry the required moment, and it is necessary only to find the steel area. Typically, this is the situation at critical design sections of continuous beams, in which the concrete dimensions are often kept constant, although the steel reinforcement varies along the span according to the required flexural resistance. Dimensions b , d , and h are determined at the maximum moment section, usually at one of the supports. At other supports, and at midspan locations, where moments are

usually smaller, the concrete dimensions are known to be adequate and only the tensile steel remains to be found. An identical situation was encountered in the design problem of Example 3.6, in which concrete dimensions were rounded up from the minimum required values, and the required steel area was to be found. In either case, the iterative approach demonstrated in Example 3.6 is convenient.

EXAMPLE 3.7

Determination of steel area. Using the same concrete dimensions as were used for the second solution of Example 3.6 ($b = 10$ in., $d = 17.5$ in., and $h = 20$ in.) and the same material strengths, find the steel area required to resist a moment M_u of 1300 in-kips.

SOLUTION. Assume $a = 4.0$ in. Then

$$A_s = \frac{1300}{0.90 \times 60(17.5 - 2.0)} = 1.55 \text{ in}^2$$

Checking the assumed a gives

$$a = \frac{1.55 \times 60}{0.85 \times 4 \times 10} = 2.74 \text{ in.}$$

Next assume $a = 2.6$ in. and recalculate A_s :

$$A_s = \frac{1300}{0.90 \times 60(17.5 - 1.3)} = 1.49 \text{ in}^2$$

No further iteration is required. Use $A_s = 1.49$ in 2 . Two No. 8 (No. 25) bars, $A_s = 1.58$ in. 2 , will be used. A check of the reinforcement ratio shows $\rho < \rho_{0.005}$ and $\phi = 0.9$.

As seen in Example 3.5, the strength reduction factor becomes a variable at high reinforcement ratios. Example 3.8 demonstrates how the variation in strength reduction factor affects the design process.

EXAMPLE 3.8

Determination of steel area and variable strength reduction factor. Architectural considerations limit the height of a 20 ft long simple span beam to 16 in. and the width to 12 in. The following loads and material properties are given: $w_d = 0.79$ kips/ft, $w_l = 1.65$ kips/ft, $f'_c = 5000$ psi, and $f_y = 60,000$ psi. Determine the reinforcement for the beam.

SOLUTION. Calculating the factored loads gives

$$w_u = 1.2 \times 0.79 + 1.6 \times 1.65 = 3.59 \text{ kips/ft}$$

$$M_u = 3.59 \times \frac{20^2}{8} = 179 \text{ ft-kips} = 2150 \text{ in-kips}$$

Assume $a = 4.0$ in. and $\phi = 0.90$. The structural depth is $(16 - 2.5)$ in. = 13.5 in. Calculating A_s gives

$$A_s = \frac{M_u/\phi}{f_y(d - a/2)} = \frac{2150/0.90}{60(13.5 - 2.0)} = 3.46 \text{ in}^2$$

Try two No. 10 (No. 32) and one No. 9 (No. 29) bar, $A_s = 3.54$ in 2 .

Check $a = 3.54 \times 60/(0.85 \times 5 \times 12) = 4.16$ in. from Eq. (3.32). This is more than assumed; therefore, continue to check the moment capacity.

$$M_n = 3.54 \times 60(13.5 - 4.16/2) = 2426 \text{ in-kips}$$

Using a ϕ of 0.90 gives $\phi M_n = 2183$ in-kips, which is adequate; however, the net tensile strain must be checked to validate the selection of $\phi = 0.9$. In this case $c = a/\beta_1 = 4.16/0.80 = 5.20$ in. The c/d ratio is $0.385 > 0.375$, so $\epsilon_t > 0.005$ is not satisfied. The corresponding net tensile strain is

$$\epsilon_t = 0.003 \frac{13.5 - 5.2}{5.2} = 0.00479$$

A value of $\epsilon_t = 0.00479$ is allowed by the ACI Code, but only if the strength reduction factor is adjusted. A linear interpolation from Fig. 3.9 gives $\phi = 0.88$ and $M_u = \phi M_n = 2140$ in-kips, which is less than the required capacity. Try increasing the reinforcement to three No. 10 (No. 32) bars, $A_s = 3.81$ in². Repeating the calculations,

$$a = \frac{3.81 \times 60}{0.85 \times 5 \times 12} = 4.48 \text{ in.}$$

$$c = \frac{4.48}{0.80} = 5.60 \text{ in.}$$

$$M_n = 3.81 \times 60 \left(13.5 - \frac{4.48}{2} \right) = 2574 \text{ in-kips}$$

$$\epsilon_t = \frac{0.003(13.5 - 5.60)}{5.60} = 0.00423$$

$$\phi = 0.483 + 83.3 \times 0.00423 = 0.835$$

$$M_u = \phi M_n = 0.835 \times 2574 = 2150 \text{ in-kips}$$

which meets the design requirements.

In actuality, the first solution deviates less than 1 percent from the desired value and would likely be acceptable. The remaining portion of the example demonstrates the design implications of requiring a variable strength reduction factor when the net tensile strain falls between 0.005 and 0.004. In this example, the reinforcement increased nearly 8 percent, yet the design moment capacity ϕM_n only increased 0.5 percent due to the decreasing strength reduction factor. For this reason, designs with $\rho < \rho_{0.005}$ are desirable.

In solving these examples, the basic equations have been used to develop familiarity with them. In actual practice, however, design aids such as Table A.4 of Appendix A, giving values of maximum and minimum reinforcement ratios, and Table A.5, providing values of flexural resistance factor R , are more convenient. The example problems will be repeated in Section 3.5 to demonstrate use of these aids.

g. Overreinforced Beams

According to the ACI Code, all beams are to be designed for yielding of the tension steel with ϵ_t not less than 0.004 and thus $\rho \leq \rho_{\max}$. Occasionally, however, such as when analyzing the capacity of existing construction, it may be necessary to calculate the flexural strength of an overreinforced compression-controlled member, for which f_s is less than f_y at flexural failure.

In this case, the steel strain, in Fig. 3.11b, will be less than the yield strain, but can be expressed in terms of the concrete strain ϵ_u and the still-unknown distance c to the neutral axis:

$$\epsilon_s = \epsilon_u \frac{d - c}{c} \quad (3.42)$$

From the equilibrium requirement that $C = T$, one can write

$$0.85\beta_1 f'_c bc = \rho\epsilon_s E_s bd$$

Substituting the steel strain from Eq. (3.42) in the last equation, and defining $k_u = c/d$, one obtains a quadratic equation in k_u as follows:

$$k_u^2 + m\rho k_u - m\rho = 0$$

Here, $\rho = A_s/bd$ as usual, and m is a material parameter given by

$$m = \frac{E_s \epsilon_u}{0.85\beta_1 f'_c} \quad (3.43)$$

Solving the quadratic equation for k_u ,

$$k_u = \sqrt{m\rho + \left(\frac{m\rho}{2}\right)^2} - \frac{m\rho}{2} \quad (3.44)$$

The neutral axis depth for the overreinforced beam can then easily be found from $c = k_u d$, after which the stress-block depth $a = \beta_1 c$. With steel strain ϵ_s then computed from Eq. (3.42), and with $f_s = E_s \epsilon_s$, the nominal flexural strength is

$$M_n = A_s f_s \left(d - \frac{a}{2} \right) \quad (3.45)$$

The strength reduction factor ϕ will equal 0.65 for beams in this range.

3.5 DESIGN AIDS

Basic equations were developed in Section 3.4 for the analysis and design of reinforced concrete beams, and these were used directly in the examples. In practice, the design of beams and other reinforced concrete members is greatly facilitated by the use of aids such as those in Appendix A of this text and in Refs. 3.7 through 3.9. Tables A.1, A.2, A.4 through A.7, and Graph A.1 of Appendix A relate directly to this chapter, and the student can scan this material to become familiar with the coverage. Other aids will be discussed, and their use demonstrated, in later chapters.

Equation (3.39) gives the flexural design strength ϕM_n of an underreinforced rectangular beam with a reinforcement ratio at or below ρ_{max} . The flexural resistance factor R , from Eq. (3.36), is given in Table A.5a for lower reinforcement ratios or Table A.5b for higher reinforcement ratios. Alternatively, R can be obtained from Graph A.1. For *analysis* of the capacity of a section with known concrete dimensions b and d , having known reinforcement ratio ρ , and with known materials strengths, the design strength ϕM_n can be obtained directly by Eq. (3.39).

For *design* purposes, where concrete dimensions and reinforcement are to be found and the factored load moment M_u is to be resisted, there are two possible approaches. One starts with selecting the optimum reinforcement ratio and then calculating concrete dimensions, as follows:

1. Set the required strength M_u equal to the design strength ϕM_n from Eq. (3.39):

$$M_u = \phi Rbd^2$$

2. With the aid of Table A.4, select an appropriate reinforcement ratio between ρ_{\max} and ρ_{\min} . Often a ratio of about $0.60\rho_{\max}$ will be an economical and practical choice. Selection of $\rho \leq \rho_{0.005}$, ($\epsilon_t \geq 0.005$) ensures that ϕ will remain equal to 0.90. For $\rho_{0.005} < \rho < \rho_{\max}$, an iterative solution will be necessary.
3. From Table A.5, for the specified material strengths and selected reinforcement ratio, find the flexural resistance factor R . Then

$$bd^2 = \frac{M_u}{\phi R}$$

4. Choose b and d to meet that requirement. Unless construction depth must be limited or other constraints exist (see Section 12.6), an effective depth about 2 to 3 times the width is often appropriate.
5. Calculate the required steel area

$$A_s = \rho bd$$

Then, referring to Table A.2, choose the size and number of bars, giving preference to the larger bar sizes to minimize placement costs.

6. Refer to Table A.7 to ensure that the selected beam width will provide room for the bars chosen, with adequate concrete cover and spacing. (These points will be discussed further in Section 3.6.)

The alternative approach starts with selecting concrete dimensions (see Section 12.6 for practical guidelines), after which the required reinforcement is found, as follows:

1. Select beam width b and effective depth d . Then calculate the required R :

$$R = \frac{M_u}{\phi bd^2}$$

2. Using Table A.5 for specified material strengths, find the reinforcement ratio $\rho < \rho_{\max}$ that will provide the required value of R and verify the selected value of ϕ .
3. Calculate the required steel area

$$A_s = \rho bd$$

and from Table A.2 select the size and number of bars.

4. Using Table A.7, confirm that the beam width is sufficient to contain the selected reinforcement.

Use of design aids to solve the example problems of Section 3.4 will be illustrated as follows.

EXAMPLE 3.9

Flexural strength of a given member. Find the nominal flexural strength and design strength of the beam in Example 3.5, which has $b = 12$ in. and $d = 17.5$ in. and is reinforced with four No. 9 (No. 29) bars. Make use of the design aids of Appendix A. Material strengths are $f'_c = 4000$ psi and $f_y = 60,000$ psi.

SOLUTION. From Table A.2, four No. 9 (No. 29) bars provide $A_s = 4.00 \text{ in}^2$, and with $b = 12$ in. and $d = 17.5$ in., the reinforcement ratio is $\rho = 4.00/(12 \times 17.5) = 0.0190$. According to Table A.4, this is below $\rho_{\max} = 0.0206$ and above $\rho_{\min} = 0.0033$. Then from Table A.5b, with

$f'_c = 4000$ psi, $f_y = 60,000$ psi, and $\rho = 0.019$, the value $R = 949$ psi is found. The nominal and design strengths are (with $\phi = 0.87$ from Example 3.5), respectively,

$$M_n = Rbd^2 = 949 \times 12 \times \frac{17.5^2}{1000} = 3490 \text{ in-kips}$$

$$\phi M_n = 0.87 \times 3490 = 3040 \text{ in-kips}$$

as before.

EXAMPLE 3.10

Concrete dimensions and steel area to resist a given moment. Find the cross section of concrete and the area of steel required for the beam in Example 3.6, making use of the design aids of Appendix A. $M_u = 1670$ in-kips, $f'_c = 4000$ psi, and $f_y = 60,000$ psi. Use a reinforcement ratio of $0.60\rho_{\max}$.

SOLUTION. From Table A.4, the maximum reinforcement ratio is $\rho_{\max} = 0.0206$. For economy, a value of $\rho = 0.60\rho_{\max} = 0.0124$ will be used. For that value, by interpolation from Table A.5a, the required value of R is 663. Then

$$bd^2 = \frac{M_u}{\phi R} = \frac{1670 \times 1000}{0.90 \times 663} = 2800 \text{ in}^3$$

Concrete dimensions $b = 10$ in. and $d = 16.7$ in. will satisfy this, but the depth will be rounded to 17.5 in. to provide a total beam depth of 20.0 in. It follows that

$$R = \frac{M_u}{\phi bd^2} = \frac{1670 \times 1000}{0.90 \times 10 \times 17.5^2} = 606 \text{ psi}$$

and from Table A.5a, by interpolation, $\rho = 0.0112$. This leads to a steel requirement of $A_s = 0.0112 \times 10 \times 17.5 = 1.96 \text{ in}^2$ as before.

EXAMPLE 3.11

Determination of steel area. Find the steel area required for the beam in Example 3.7, with concrete dimensions $b = 10$ in. and $d = 17.5$ in. known to be adequate to carry the factored load moment of 1300 in-lb. Material strengths are $f'_c = 4000$ psi and $f_y = 60,000$ psi.

SOLUTION. Note that in cases in which the concrete dimensions are known to be adequate and only the reinforcement must be found, the iterative method used earlier is not required. The necessary flexural resistance factor is

$$R = \frac{M_u}{\phi bd^2} = \frac{1300 \times 1000}{0.90 \times 10 \times 17.5^2} = 472 \text{ psi}$$

According to Table A.5a, with the specified material strengths, this corresponds to a reinforcement ratio of $\rho = 0.0085$, giving a steel area of

$$A_s = 0.0085 \times 10 \times 17.5 = 1.49 \text{ in}^2$$

as before. Two No. 8 (No. 25) bars will be used.

The tables and graphs of Appendix A give basic information and are used extensively throughout this text for illustrative purposes. The reader should be aware, however, of the greatly expanded versions of these tables, plus many other useful aids, that are found in Refs. 3.7 through 3.9 and in commercial design software.

3.6 PRACTICAL CONSIDERATIONS IN THE DESIGN OF BEAMS

To focus attention initially on the basic aspects of flexural design, the preceding examples were carried out with only minimum regard for certain practical considerations that always influence the actual design of beams. These relate to optimal concrete proportions for beams, rounding of dimensions, standardization of dimensions, required cover for main and auxiliary reinforcement, and selection of bar combinations. Good judgment on the part of the design engineer is particularly important in translating from theoretical requirements to practical design. Several of the more important aspects are discussed here; much additional guidance is provided by the publications of ACI (Refs. 3.7 and 3.8) and CRSI (Refs. 3.9 to 3.11).

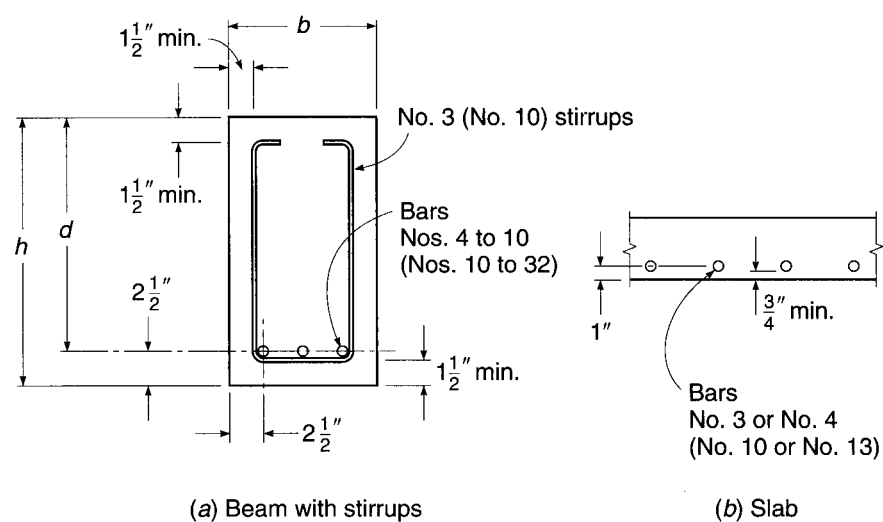
a. Concrete Protection for Reinforcement

To provide the steel with adequate concrete protection against fire and corrosion, the designer must maintain a certain minimum thickness of concrete cover outside of the outermost steel. The thickness required will vary, depending upon the type of member and conditions of exposure. According to ACI Code 7.7, for cast-in-place concrete, concrete protection at surfaces not exposed directly to the ground or weather should be not less than $\frac{3}{4}$ in. for slabs and walls and $1\frac{1}{2}$ in. for beams and columns. If the concrete surface is to be exposed to the weather or in contact with the ground, a protective covering of at least 2 in. is required [$1\frac{1}{2}$ in. for No. 5 (No. 16) and smaller bars], except that if the concrete is cast in direct contact with the ground without the use of forms, a cover of at least 3 in. must be furnished.

In general, the centers of main flexural bars in beams should be placed $2\frac{1}{2}$ to 3 in. from the top or bottom surface of the beam to furnish at least $1\frac{1}{2}$ in. of clear cover for the bars and the stirrups (see Fig. 3.13). In slabs, 1 in. to the center of the bar is ordinarily sufficient to give the required $\frac{3}{4}$ in. cover.

To simplify construction and thereby to reduce costs, the overall concrete dimensions of beams, b and h , are almost always rounded up to the nearest inch, and often to the next multiple of 2 in. As a result, the actual effective depth d , found by subtracting the sum of cover distance, stirrup diameter, and one-half the main

FIGURE 3.13
Requirements for concrete cover in beams and slabs.



reinforcing bar diameter from the total depth h , is seldom an even dimension. For slabs, the total depth is generally rounded up to the nearest $\frac{1}{2}$ in. up to 6 in. in depth, and to the nearest inch above that thickness. The differences between h and d shown in Fig. 3.13 are not exact, but are satisfactory for design purposes for beams with No. 3 (No. 10) stirrups and No. 10 (No. 32) longitudinal bars or smaller, and for slabs using No. 4 (No. 13) or smaller bars. If larger bars are used for the main flexural reinforcement or for the stirrups, as is frequently the case, the corresponding dimensions are easily calculated.

Recognizing the closer tolerances that can be maintained under plant-control conditions, ACI Code 7.7.3 permits some reduction in concrete protection for reinforcement in precast concrete.

b. Concrete Proportions

Reinforced concrete beams may be wide and shallow, or relatively narrow and deep. Consideration of maximum material economy often leads to proportions with effective depth d in the range from about 2 to 3 times the width b (or web width b_w for T beams). However, constraints may dictate other choices, and as will be discussed in Section 12.6, maximum material economy may not translate to maximum structural economy. For example, with one-way concrete joists supported by monolithic beams (see Chapter 18), use of beams and joists with the same total depth will permit use of a single flat-bottom form, resulting in fast, economical construction and permitting level ceilings. The beams will generally be wide and shallow, with heavier reinforcement than otherwise, but the result will be an overall saving in construction cost. In other cases, it may be necessary to limit the total depth of floor or roof construction for architectural or other reasons. An advantage of reinforced concrete is its adaptability to such special needs.

c. Selection of Bars and Bar Spacing

As noted in Section 2.14, common reinforcing bar sizes range from No. 3 to No. 11 (No. 10 to No. 36), the bar number corresponding closely to the number of eighth-inches (millimeters) of bar diameter. The two larger sizes, No. 14 (No. 43) [$1\frac{3}{4}$ in. (43 mm) diameter] and No. 18 (No. 57) [$2\frac{1}{4}$ in. (57 mm) diameter] are used mainly in columns.

It is often desirable to mix bar sizes to meet steel area requirements more closely. In general, mixed bars should be of comparable diameter, for practical as well as theoretical reasons, and generally should be arranged symmetrically about the vertical centerline. Many designers limit the variation in diameter of bars in a single layer to two bar sizes, using, say, No. 10 and No. 8 (No. 32 and No. 25) bars together, but not Nos. 11 and 6 (Nos. 36 and 19). There is some practical advantage to minimizing the number of different bar sizes used for a given structure.

Normally, it is necessary to maintain a certain minimum distance between adjacent bars to ensure proper placement of concrete around them. Air pockets below the steel are to be avoided, and full surface contact between the bars and the concrete is desirable to optimize bond strength. ACI Code 7.6 specifies that the minimum clear distance between adjacent bars not be less than the nominal diameter of the bars, or 1 in. (For columns, these requirements are increased to $1\frac{1}{2}$ bar diameters and $1\frac{1}{2}$ in.) Where beam reinforcement is placed in two or more layers, the clear distance between layers must not be less than 1 in., and the bars in the upper layer should be placed directly above those in the bottom layer.

The maximum number of bars that can be placed in a beam of given width is limited by bar diameter and spacing requirements and is also influenced by stirrup diameter, by concrete cover requirement, and by the maximum size of concrete aggregate specified. Table A.7 of Appendix A gives the maximum number of bars that can be placed in a single layer in beams, assuming $1\frac{1}{2}$ in. concrete cover and the use of No. 4 (No. 13) stirrups. When using the minimum bar spacing in conjunction with a large number of bars in a single plane of reinforcement, the designer should be aware that problems may arise in the placement and consolidation of concrete, especially when multiple layers of bars are used or when the bar spacing is smaller than the size of the vibrator head.

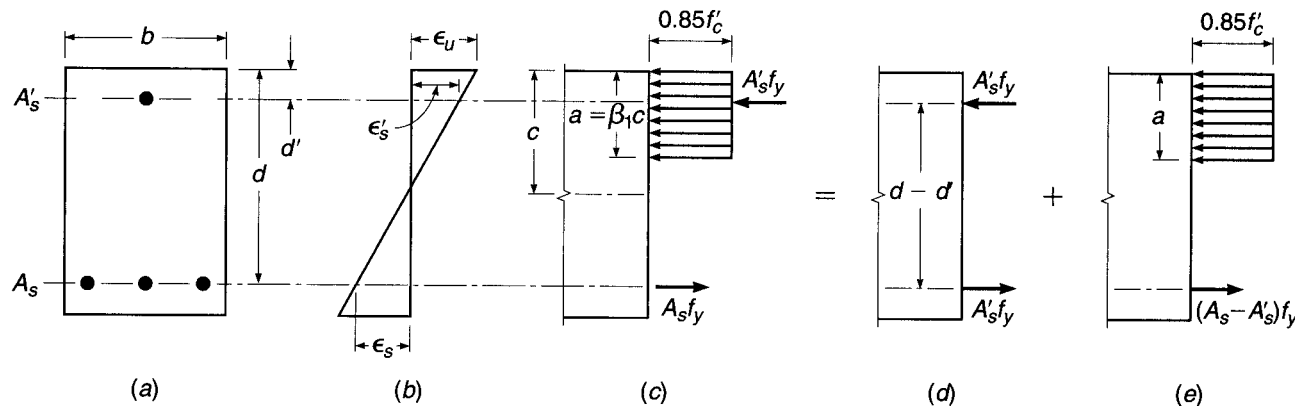
There are also restrictions on the *minimum* number of bars that can be placed in a single layer, based on requirements for the distribution of reinforcement to control the width of flexural cracks (see Section 6.3). Table A.8 gives the minimum number of bars that will satisfy ACI Code requirements, which will be discussed in Chapter 6.

In large girders and columns, it is sometimes advantageous to "bundle" tensile or compressive reinforcement with two, three, or four bars in contact to provide for better deposition of concrete around and between adjacent bundles. These bars may be assumed to act as a unit, with not more than four bars in any bundle, provided that stirrups or ties enclose the bundle. No more than two bars should be bundled in one plane; typical bundle shapes are triangular, square, or L-shaped patterns. Individual bars in a bundle, cut off within the span of flexural members, should terminate at different points. ACI Code 7.6.6 requires at least 40 bar diameters stagger between points of cutoff. Where spacing limitations and minimum concrete cover requirements are based on bar diameter, a unit of bundled bars is treated as a single bar with a diameter that provides the same total area.

ACI Code 7.6.6 states that bars larger than No. 11 (No. 36) shall not be bundled in beams, although the AASHTO Specifications permit bundling of No. 14 and No. 18 (No. 43 and No. 57) bars in highway bridges.

3.7 RECTANGULAR BEAMS WITH TENSION AND COMPRESSION REINFORCEMENT

If a beam cross section is limited because of architectural or other considerations, it may happen that the concrete cannot develop the compression force required to resist the given bending moment. In this case, reinforcement is added in the compression zone, resulting in a *doubly reinforced* beam, i.e., one with compression as well as tension reinforcement (see Fig. 3.14). The use of compression reinforcement has decreased markedly with the use of strength design methods, which account for the full-strength potential of the concrete on the compressive side of the neutral axis. However, there are situations in which compressive reinforcement is used for reasons other than strength. It has been found that the inclusion of some compression steel will reduce the long-term deflections of members (see Section 6.5). In addition, in some cases, bars will be placed in the compression zone for minimum-moment loading (see Section 12.2) or as stirrup support bars continuous throughout the beam span (see Chapter 4). It may be desirable to account for the presence of such reinforcement in flexural design, although in many cases they are neglected in flexural calculations.

**FIGURE 3.14**

Doubly reinforced rectangular beam.

a. Tension and Compression Steel Both at Yield Stress

If, in a doubly reinforced beam, the tensile reinforcement ratio ρ is less than or equal to ρ_b , the strength of the beam may be approximated within acceptable limits by disregarding the compression bars. The strength of such a beam will be controlled by tensile yielding, and the lever arm of the resisting moment will ordinarily be little affected by the presence of the compression bars.

If the tensile reinforcement ratio is larger than ρ_b , a somewhat more elaborate analysis is required. In Fig. 3.14a, a rectangular beam cross section is shown with compression steel A'_s placed a distance d' from the compression face and with tensile steel A_s at effective depth d . It is assumed initially that both A'_s and A_s are stressed to f_y at failure. The total resisting moment can be thought of as the sum of two parts. The first part, M_{n1} , is provided by the couple consisting of the force in the compression steel A'_s and the force in an equal area of tension steel

$$M_{n1} = A'_s f_y (d - d') \quad (3.46a)$$

as shown in Fig. 3.14d. The second part, M_{n2} , is the contribution of the remaining tension steel $A_s - A'_s$ acting with the compression concrete:

$$M_{n2} = (A_s - A'_s) f_y \left(d - \frac{a}{2} \right) \quad (3.46b)$$

as shown in Fig. 3.14e, where the depth of the stress block is

$$a = \frac{(A_s - A'_s) f_y}{0.85 f'_c b} \quad (3.47a)$$

With the definitions $\rho = A_s/bd$ and $\rho' = A'_s/bd$, this can be written

$$a = \frac{(\rho - \rho') f_y d}{0.85 f'_c} \quad (3.47b)$$

The total nominal resisting moment is then

$$M_n = M_{n1} + M_{n2} = A'_s f_y (d - d') + (A_s - A'_s) f_y \left(d - \frac{a}{2} \right) \quad (3.48)$$

In accordance with the safety provisions of the ACI Code, the net tensile strain is checked; and if $\epsilon_t \geq 0.005$, this nominal capacity is reduced by the factor $\phi = 0.90$ to obtain the design strength. For ϵ_t between 0.005 and 0.004, ϕ must be adjusted, as discussed earlier.

It is highly desirable, for reasons given earlier, that failure, should it occur, be precipitated by tensile yielding rather than crushing of the concrete. This can be ensured by setting an *upper limit* on the tensile reinforcement ratio. By setting the tensile steel strain in Fig. 3.14b equal to ϵ_y to establish the location of the neutral axis for the failure condition and then summing horizontal forces shown in Fig. 3.14c (still assuming the compressive steel to be at the yield stress at failure), it is easily shown that the balanced reinforcement ratio $\bar{\rho}_b$ for a doubly reinforced beam is

$$\bar{\rho}_b = \rho_b + \rho' \quad (3.49)$$

where ρ_b is the balanced reinforcement ratio for the corresponding singly reinforced beam and is calculated from Eq. (3.28). The ACI Code limits the net tensile strain, not the reinforcement ratio. To provide the same margin against brittle failure as for singly reinforced beams, the maximum reinforcement ratio should be limited to

$$\bar{\rho}_{\max} = \rho_{\max} + \rho' \quad (3.50a)$$

Because ρ_{\max} establishes the location of the neutral axis, the limitation in Eq. (3.50a) will provide acceptable net tensile strains. A check of ϵ_t is required to determine the strength reduction factor ϕ and to verify net tensile strain requirements are satisfied. Substituting $\rho_{0.005}$ for ρ_{\max} in Eq. (3.50a) will give the maximum reinforcement ratio for $\phi = 0.90$.

$$\bar{\rho}_{0.005} = \rho_{0.005} + \rho' \quad (3.50b)$$

b. Compression Steel below Yield Stress

The preceding equations, through which the fundamental analysis of doubly reinforced beams is developed clearly and concisely, are valid *only* if the compression steel has yielded when the beam reached its nominal capacity. In many cases, such as for wide, shallow beams, beams with more than the usual concrete cover over the compression bars, beams with high yield strength steel, or beams with relatively small amounts of tensile reinforcement, the compression bars will be below the yield stress at failure. It is necessary, therefore, to develop more generally applicable equations to account for the possibility that the compression reinforcement has not yielded when the doubly reinforced beam fails in flexure.

Whether or not the compression steel will have yielded at failure can be determined as follows. Referring to Fig. 3.14b, and taking as the limiting case $\epsilon'_s = \epsilon_y$, one obtains, from geometry,

$$\frac{c}{d'} = \frac{\epsilon_u}{\epsilon_u - \epsilon_y} \quad \text{or} \quad c = \frac{\epsilon_u}{\epsilon_u - \epsilon_y} d'$$

Summing forces in the horizontal direction (Fig. 3.14c) gives the *minimum* tensile reinforcement ratio $\bar{\rho}_{cy}$ that will ensure yielding of the compression steel at failure:

$$\bar{\rho}_{cy} = 0.85\beta_1 \frac{f'_c}{f_y} \frac{d'}{d} \frac{\epsilon_u}{\epsilon_u - \epsilon_y} + \rho' \quad (3.51)$$

If the *tensile reinforcement ratio* is less than this limiting value, the neutral axis is sufficiently high that the compression steel stress at failure is less than the yield stress. In this case, it can easily be shown on the basis of Fig. 3.14b and c that the balanced reinforcement ratio is

$$\bar{\rho}_b = \rho_b + \rho' \frac{f'_s}{f_y} \quad (3.52)$$

where

$$f'_s = E_s \epsilon'_s = E_s \left[\epsilon_u - \frac{d'}{d} (\epsilon_u + \epsilon_y) \right] \leq f_y \quad (3.53a)$$

To determine ρ_{\max} , $\epsilon_t = 0.004$ is substituted for ϵ_y in Eq. (3.53a), giving

$$f'_s = E_s \left[\epsilon_u - \frac{d'}{d} (\epsilon_u + 0.004) \right] \leq f_y \quad (3.53b)$$

Likewise, for $\epsilon_t = 0.005$,

$$f'_s = E_s \left[\epsilon_u - \frac{d'}{d} (\epsilon_u + 0.005) \right] \leq f_y \quad (3.53c)$$

Hence, the maximum reinforcement ratio permitted by the ACI Code is

$$\bar{\rho}_{\max} = \rho_{\max} + \rho' \frac{f'_s}{f_y} \quad (3.54a)$$

and the maximum reinforcement ratio for $\phi = 0.90$ is

$$\bar{\rho}_{0.005} = \rho_{0.005} + \rho' \frac{f'_s}{f_y} \quad (3.54b)$$

where f'_s is given in Eq. (3.53b). A simple comparison shows that Eqs. (3.52), (3.54a), and (3.54b), with f'_s given by Eqs. (3.53a), (3.53b), and (3.53c), respectively, are the generalized forms of Eqs. (3.49), (3.50a), and (3.50b).

It should be emphasized that Eqs. (3.53a), (3.53b), and (3.53c) for compression steel stress apply *only for beams with exact strain values in the extreme tensile steel of ϵ_y , $\epsilon_t = 0.004$, or $\epsilon_t = 0.005$* .

If the tensile reinforcement ratio is less than $\bar{\rho}_b$, as given by Eq. (3.52), and less than $\bar{\rho}_{cy}$, as given by Eq. (3.51), then the tensile steel is at the yield stress at failure but the compression steel is not, and new equations must be developed for compression steel stress and flexural strength. The compression steel stress can be expressed in terms of the still-unknown neutral axis depth as

$$f'_s = \epsilon_u E_s \frac{c - d'}{c} \quad (3.55)$$

Consideration of horizontal force equilibrium (Fig. 3.14c with compression steel stress equal to f'_s) then gives

$$A_s f_y = 0.85 \beta_1 f'_s b c + A'_s \epsilon_u E_s \frac{c - d'}{c} \quad (3.56)$$

This is a quadratic equation in c , the only unknown, and is easily solved for c . The nominal flexural strength is found using the value of f'_s from Eq. (3.55), and $a = \beta_1 c$ in the expression

$$M_n = 0.85 f'_s ab \left(d - \frac{a}{2} \right) + A'_s f'_s (d - d') \quad (3.57)$$

TABLE 3.2
Minimum beam depths for compression reinforcement to yield

f_y , psi	$\epsilon_t = 0.004$		$\epsilon_t = 0.005$	
	Maximum d'/d	Minimum d for $d' = 2.5$ in., in.	Maximum d'/d	Minimum d for $d' = 2.5$ in., in.
40,000	0.23	10.8	0.20	12.3
60,000	0.13	18.8	0.12	21.5
75,000	0.06	42.7	0.05	48.8

This nominal capacity is reduced by the strength reduction factor ϕ to obtain the design strength.

If compression bars are used in a flexural member, precautions must be taken to ensure that these bars will not buckle outward under load, spalling off the outer concrete. ACI Code 7.11.1 imposes the requirement that such bars be anchored in the same way that compression bars in columns are anchored by lateral ties (Section 8.2). Such ties must be used throughout the distance where the compression reinforcement is required.

For the compression steel to yield, the reinforcement ratio must lie below $\bar{\rho}_{\max}$ and above $\bar{\rho}_{cy}$. The ratio between d' and the steel centroidal depth d to allow yielding of the compression reinforcement can be found by equating $\bar{\rho}_{cy}$ to $\bar{\rho}_{\max}$ (or $\bar{\rho}_{0.005}$) and solving for d'/d . Furthermore, if d' is assumed to be 2.5 in., as is often the case, the minimum depth of beam necessary for the compression steel to yield may be found for each grade of steel. The ratios and minimum beam depths are summarized in Table 3.2. Values are included for $\epsilon_t = 0.004$, the minimum tensile yield strain permitted for flexural members, and $\epsilon_t = 0.005$, the net tensile strain needed to ensure that $\phi = 0.90$. For beams with less than the minimum depth, the compression reinforcement cannot yield unless the tensile reinforcement exceeds ρ_{\max} . The compression reinforcement may yield in beams that exceed the minimum depth in Table 3.2, depending on the relative distribution of the tensile and compressive reinforcement.

c. Examples of Analysis and Design of Beams with Tension and Compression Steel

As was the case for beams with only tension reinforcement, doubly reinforced beam problems can be placed in one of two categories: analysis problems or design problems. For *analysis*, in which the concrete dimensions, reinforcement, and material strengths are given, one can find the flexural strength directly from the equations in Section 3.7a or 3.7b. First, it must be confirmed that the tensile reinforcement ratio is less than $\bar{\rho}_b$ given by Eq. (3.52), with compression steel stress from Eq. (3.53a). Once it is established that the tensile steel has yielded, the tensile reinforcement ratio defining compression steel yielding is calculated from Eq. (3.51), and the actual tensile reinforcement ratio is compared. If it is greater than $\bar{\rho}_{cy}$, then $f'_s = f_y$, and M_n is found from Eq. (3.48). If it is less than $\bar{\rho}_{cy}$, then $f'_s < f_y$. In this case, c is calculated by solving Eq. (3.56), f'_s comes from Eq. (3.55), and M_n is found from Eq. (3.57).

For the *design* case, in which the factored load moment M_u to be resisted is known and the section dimensions and reinforcement are to be found, a direct solution is impossible. The steel areas to be provided depend on the steel stresses, which are

not known before the section is proportioned. It can be assumed that the compression steel stress is equal to the yield stress, but this must be confirmed; if it has not yielded, the design must be adjusted. The design procedure can be outlined as follows:

1. Calculate the maximum moment that can be resisted by the underreinforced section with $\rho = \rho_{\max}$, or $\rho_{0.005}$ to ensure that $\phi = 0.90$. The corresponding tensile steel area is $A_s = \rho bd$, and, as usual,

$$M_n = A_s f_y \left(d - \frac{a}{2} \right)$$

with

$$a = \frac{A_s f_y}{0.85 f'_c b}$$

2. Find the excess moment, if any, that must be resisted, and set $M_2 = M_n$, as calculated in step 1.

$$M_1 = \frac{M_u}{\phi} - M_2$$

Now A_s from step 1 is defined as A_{s2} , i.e., that part of the tension steel area in the doubly reinforced beam that works with the compression force in the concrete. In Fig. 3.14e, $A_s - A'_s = A_{s2}$.

3. Tentatively assume that $f'_s = f_y$. Then

$$A'_s = \frac{M_1}{f_y(d - d')}$$

Alternatively, if from Table 3.2 the compression reinforcement is known not to yield, go to step 6.

4. Add an additional amount of tensile steel $A_{s1} = A'_s$. Thus, the total tensile steel area A_s is A_{s2} from step 2 plus A_{s1} .
5. Analyze the doubly reinforced beam to see if $f'_s = f_y$; that is, check the tensile reinforcement ratio against $\bar{\rho}_{cy}$.
6. If $\rho < \bar{\rho}_{cy}$, then the compression steel stress is less than f_y and the compression steel area must be increased to provide the needed force. This can be done as follows. The stress block depth is found from the requirement of horizontal equilibrium (Fig. 3.14e),

$$a = \frac{(A_s - A'_s)f_y}{0.85 f'_c b} \quad \text{or} \quad a = \frac{\left[A_s - A'_s (f'_s/f_y) \right] f_y}{0.85 f'_c b}$$

and the neutral axis depth is $c = a/\beta_1$. From Eq. (3.55),

$$f'_s = \epsilon_u E_s \frac{c - d'}{c}$$

The revised compression steel area, acting at f'_s , must provide the same force as the trial steel area that was assumed to act at f_y . Therefore,

$$A'_{s,\text{revised}} = A'_{s,\text{trial}} \frac{f_y}{f'_s}$$

The tensile steel area need not be revised, because it acts at f_y as assumed.

EXAMPLE 3.12 Flexural strength of a given member. A rectangular beam, shown in Fig. 3.15, has a width of 12 in. and an effective depth to the centroid of the tension reinforcement of 24 in. The tension reinforcement consists of six No. 10 (No. 32) bars in two rows. Compression reinforcement consisting of two No. 8 (No. 25) bars is placed 2.5 in. from the compression face of the beam. If $f_y = 60,000$ psi and $f'_c = 5000$ psi, what is the design moment capacity of the beam?

SOLUTION. The steel areas and ratios are

$$A_s = 7.62 \text{ in}^2 \quad \rho = \frac{7.62}{12 \times 24} = 0.0265$$

$$A'_s = 1.58 \text{ in}^2 \quad \rho' = \frac{1.58}{12 \times 24} = 0.0055$$

Check the beam first as a singly reinforced beam to see if the compression bars can be disregarded,

$$\rho_{\max} = 0.0243 \quad \text{from Table A.4 or Eq. (3.30c)}$$

The actual $\rho = 0.0265$ is larger than ρ_{\max} , so the beam must be analyzed as doubly reinforced. From Eq. (3.51), with $\beta_1 = 0.80$,

$$\bar{\rho}_{cy} = 0.85 \times 0.80 \times \frac{5}{60} \times \frac{2.5}{24} \times \frac{0.003}{0.003 - 0.00207} + 0.0055 = 0.0245$$

The tensile reinforcement ratio is greater than this, so the compression bars will yield when the beam fails. The maximum reinforcement ratio thus can be found from Eq. (3.50),

$$\bar{\rho}_{\max} = 0.0243 + 0.0055 = 0.0298$$

The actual tensile reinforcement ratio is below the maximum value, as required. Then, from Eq. (3.47a),

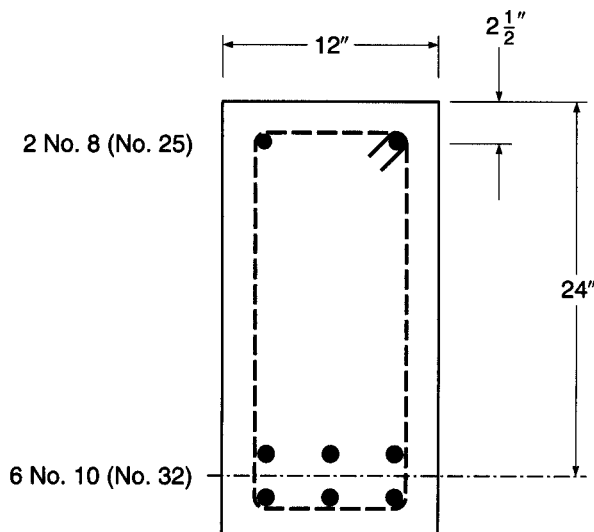
$$a = \frac{(7.62 - 1.58)60}{0.85 \times 5 \times 12} = 7.11 \text{ in.}$$

$$c = a/\beta_1 = \frac{7.11}{0.80} = 8.89 \text{ in.}$$

$$\epsilon_t = 0.003 \left(\frac{24 - 8.89}{8.89} \right) = 0.0051$$

FIGURE 3.15

Doubly reinforced beam of Example 3.12.



and

$$\phi = 0.90$$

and from Eq. (3.48),

$$M_n = 1.58 \times 60(24 - 2.5) + 6.04 \times 60 \left(24 - \frac{7.11}{2} \right) = 9450 \text{ in-kips}$$

The design strength is

$$\phi M_n = 0.90 \times 9450 = 8500 \text{ in-kips}$$

EXAMPLE 3.13

Design of a doubly reinforced beam. A rectangular beam that must carry a service live load of 2.47 kips/ft and a calculated dead load of 1.05 kips/ft on an 18 ft simple span is limited in cross section for architectural reasons to 10 in. width and 20 in. total depth. If $f_y = 60,000$ psi and $f'_c = 4000$ psi, what steel area(s) must be provided?

SOLUTION. The service loads are first increased by load factors to obtain the factored load of $1.2 \times 1.05 + 1.6 \times 2.47 = 5.21$ kips/ft. Then $M_u = 5.21 \times 18^2/8 = 211$ ft-kips = 2530 in-kips. To satisfy spacing and cover requirements (see Section 3.6), assume that the tension steel centroid will be 4 in. above the bottom face of the beam and that compression steel, if required, will be placed 2.5 in. below the beam's top surface. Then $d = 16$ in. and $d' = 2.5$ in.

First, check the capacity of the section if singly reinforced. Table A.4 shows that $\rho_{0.005}$, the maximum value of ρ for $\phi = 0.90$, to be 0.0181. While the maximum reinforcement ratio is slightly higher, Example 3.8 demonstrated there was no economic efficiency of using $\epsilon_t \leq 0.005$. So $A_s = 10 \times 16 \times 0.0181 = 2.90$ in 2 . Then with

$$a = \frac{2.90 \times 60}{0.85 \times 4 \times 10} = 5.12 \text{ in.}$$

$c = a/\beta_1 = 5.12/0.85 = 6.02$ in., and the maximum nominal moment that can be developed is

$$M_n = 2.90 \times 60(16 - 5.12/2) = 2340 \text{ in-kips}$$

Alternatively, using $R = 913$ from Table A.5b, the nominal moment is $M_n = 913 \times 10 \times 16^2/1000 = 2340$ in-kips. Because the corresponding design moment $\phi M_n = 2100$ in-kips is less than the required capacity 2530 in-kips, compression steel is needed as well as additional tension steel.

The remaining moment to be carried by the compression steel couple is

$$M_1 = \frac{2530}{0.90} - 2340 = 470 \text{ in-kips}$$

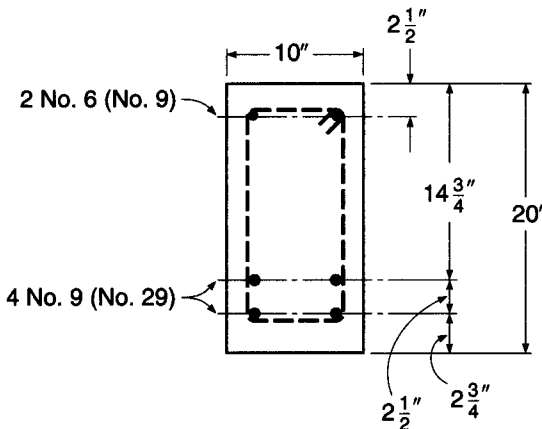
As d is less than the value required to develop the compression reinforcement yield stress (Table 3.2), a reduced stress in the compression reinforcement will be used. Using the strain distribution in Fig. 3.14b, ϵ'_s and f'_c can be computed as

$$\epsilon'_s = 0.003 \frac{6.02 - 2.5}{6.02} = 0.00175 \quad \text{and} \quad f'_s = 0.00175 \times 29,000 = 50.9 \text{ ksi}$$

Try $f'_s = 50$ ksi for the compression reinforcement to obtain the required area of compression steel.

$$A'_s = \frac{470}{50(16 - 2.5)} = 0.70 \text{ in}^2$$

FIGURE 3.16
Doubly reinforced beam of Example 3.13.



The total area of tensile reinforcement at 60 ksi is

$$A_s = 2.90 + 0.70 \left(\frac{50}{60} \right) = 3.48 \text{ in}^2$$

Two No. 6 (No. 19) bars will be used for the compression reinforcement and four No. 9 (No. 29) bars will provide the tensile steel area, as shown in Fig. 3.16. To place the tension bars in a 10 in. beam width, two rows of two bars each are used.

A final check is made to ensure that the selection of reinforcement does not create a lower compressive stress than the assumed 50 ksi.

$$A_s - A'_s \left(\frac{f'_s}{f_y} \right) = 4.0 - 0.88 \left(\frac{50}{60} \right) = 3.27 \text{ in}^2$$

which is greater than 2.90 in² for $\epsilon_t = 0.005$, so $\phi < 0.90$.

$$a = \frac{3.27 \times 60}{0.85 \times 4 \times 10} = 5.77 \text{ in.}$$

$$c = \frac{5.77}{0.85} = 6.79 \text{ in.}$$

$$\epsilon'_s = 0.003 \frac{6.79 - 2.5}{6.79} = 0.0019$$

$$f'_s = 29,000 \times 0.0019 = 55.0 \text{ ksi}$$

which is greater than assumed. Check ϕ , using $d_t = 17.25$ from the strain distribution in Fig. 3.14b, and compute the revised M_u . For simplicity, the area of tensile reinforcement is not modified.

$$\epsilon_t = 0.003 \frac{17.25 - 6.79}{6.79} = 0.0046$$

for which $\phi = 0.87$. Then

$$M_u = 0.87 \left[3.27 \times 60 \left(16.0 - \frac{5.77}{2} \right) + 0.88 \times 55.0 (16 - 2.5) \right] = 2810 \text{ in-kips}$$

This is greater than M_u , so no further refinement is necessary.

d. Tensile Steel below the Yield Stress

All doubly reinforced beams designed according to the ACI Code must be underreinforced, in the sense that the tensile reinforcement ratio is limited to ensure yielding at beam failure. Two cases were considered in Sections 3.7a and 3.7b, respectively: (a) both tension steel and compression steel yield and (b) tension steel yields but compression steel does not. Two other combinations may be encountered in analyzing the capacity of existing beams: (c) tension steel does not yield, but compression steel does, and (d) neither tension steel nor compression steel yields. The last two cases are unusual, and in fact, it would be difficult to place sufficient tension reinforcement to create such conditions, but it is possible. The solution in such cases is obtained as a simple extension of the treatment of Section 3.7b. An equation for horizontal equilibrium is written, in which both tension and compression steel stress are expressed in terms of the unknown neutral axis depth c . The resulting quadratic equation is solved for c , after which steel stresses can be calculated and the nominal flexural strength determined.

3.8 T BEAMS

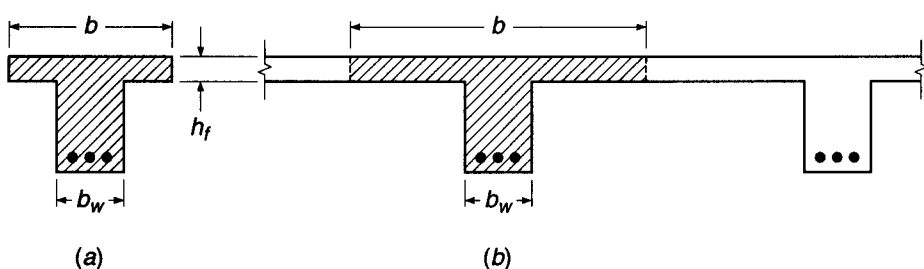
With the exception of precast systems, reinforced concrete floors, roofs, decks, etc., are almost always monolithic. Forms are built for beam soffits and sides and for the underside of slabs, and the entire construction is cast at once, from the bottom of the deepest beam to the top of the slab. Beam stirrups and bent bars extend up into the slab. It is evident, therefore, that a part of the slab will act with the upper part of the beam to resist longitudinal compression. The resulting beam cross section is T-shaped rather than rectangular. The slab forms the beam flange, while the part of the beam projecting below the slab forms what is called the *web* or *stem*. The upper part of such a T-beam is stressed laterally due to slab action in that direction. Although transverse compression at the level of the bottom of the slab may increase the longitudinal compressive strength by as much as 25 percent, transverse tension at the top surface reduces the longitudinal compressive strength (see Section 2.10). Neither effect is usually taken into account in design.

a. Effective Flange Width

The next issue to be resolved is that of the effective width of flange. In Fig. 3.17a, it is evident that if the flange is but little wider than the stem width, the entire flange can be considered effective in resisting compression. For the floor system shown in Fig. 3.17b, however, it may be equally obvious that elements of the flange midway between the beam stems are less highly stressed in longitudinal compression than those elements directly over the stem. This is so because of shearing deformation of the flange, which relieves the more remote elements of some compressive stress.

FIGURE 3.17

Effective flange width of T beams.



Although the actual longitudinal compression varies because of this effect, it is convenient in design to make use of an *effective flange width*, which may be smaller than the actual flange width but is considered to be uniformly stressed at the maximum value. This effective width has been found to depend primarily on the beam span and on the relative thickness of the slab.

The criteria for effective width given in ACI Code 8.12 are as follows:

1. For symmetric T beams, the effective width b shall not exceed one-fourth the span length of the beam. The overhanging slab width on either side of the beam web shall not exceed 8 times the thickness of the slab or go beyond one-half the clear distance to the next beam.
2. For beams having a slab on one side only, the effective overhanging slab width shall not exceed one-twelfth the span length of the beam, 6 times the slab thickness, or one-half the clear distance to the next beam.
3. For isolated beams in which the flange is used only for the purpose of providing additional compressive area, the flange thickness shall not be less than one-half the width of the web, and the total flange width shall not be more than 4 times the web width.

b. Strength Analysis

The neutral axis of a T beam may be either in the flange or in the web, depending upon the proportions of the cross section, the amount of tensile steel, and the strengths of the materials. If the calculated depth to the neutral axis is less than or equal to the flange thickness h_f , the beam can be analyzed as if it were a rectangular beam of width equal to b , the effective flange width. The reason is illustrated in Fig. 3.18a, which shows a T beam with the neutral axis in the flange. The compressive area is indicated by the shaded portion of the figure. If the additional concrete indicated by areas 1 and 2 had been added when the beam was cast, the physical cross section would have been rectangular with a width b . No bending strength would have been added because areas 1 and 2 are entirely in the tension zone, and tension concrete is disregarded in flexural calculations. The original T beam and the rectangular beam are equal in flexural strength, and rectangular beam analysis for flexure applies.

When the neutral axis is in the web, as in Fig. 3.18b, the preceding argument is no longer valid. In this case, methods must be developed to account for the actual T-shaped compressive zone.

In treating T beams, it is convenient to adopt the same equivalent stress distribution that is used for beams of rectangular cross section. The rectangular stress block, having a uniform compressive-stress intensity $0.85f'_c$, was devised originally on the

FIGURE 3.18

Effective cross sections of T beams.

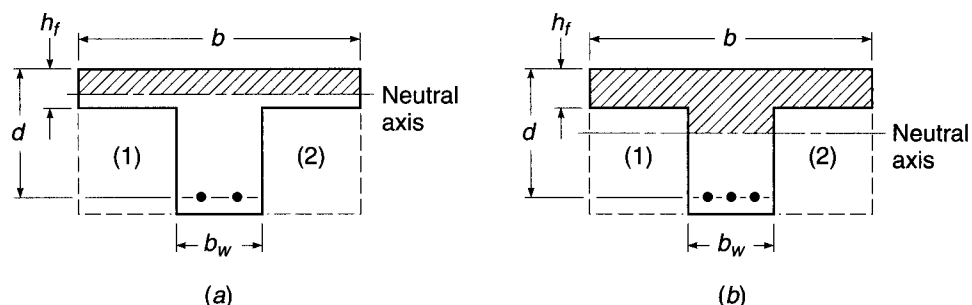
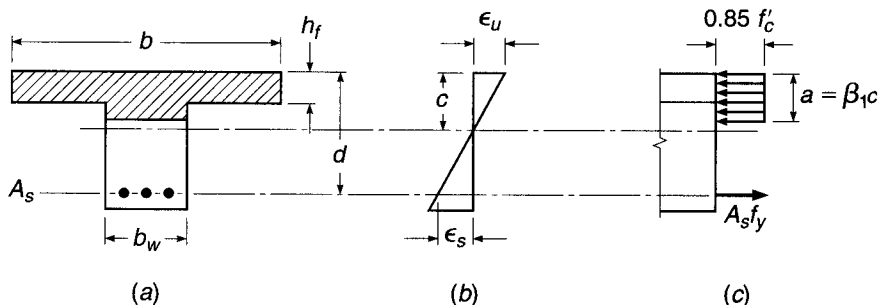


FIGURE 3.19

Strain and equivalent stress distributions for T beams.



basis of tests of rectangular beams (see Section 3.4a), and its suitability for T beams may be questioned. However, extensive calculations based on actual stress-strain curves (reported in Ref. 3.12) indicate that its use for T beams, as well as for beams of circular or triangular cross section, introduces only minor error and is fully justified.

Accordingly, a T beam may be treated as a rectangular beam if the depth of the equivalent stress block is less than or equal to the flange thickness. Figure 3.19 shows a tensile-reinforced T beam with effective flange width b , web width b_w , effective depth to the steel centroid d , and flange thickness h_f . If for trial purposes the stress block is assumed to be completely within the flange,

$$a = \frac{A_s f_y}{0.85 f'_c b} = \frac{\rho f_y d}{0.85 f'_c} \quad (3.58)$$

where $\rho = A_s/bd$. If a is less than or equal to the flange thickness h_f , the member may be treated as a rectangular beam of width b and depth d . If a is greater than h_f , a T beam analysis is required as follows.

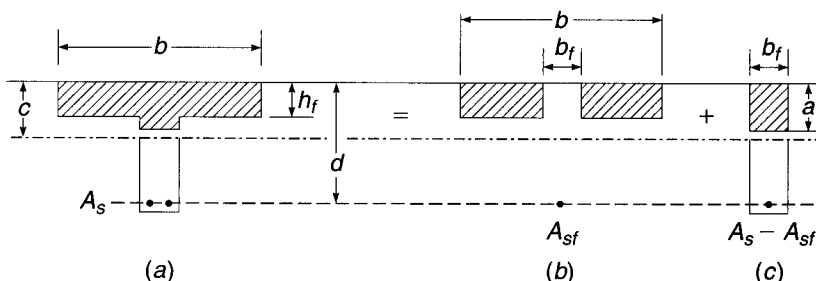
It will be assumed that the strength of the T beam is controlled by yielding of the tensile steel. This will nearly always be the case because of the large compressive concrete area provided by the flange. In addition, an upper limit can be established for the reinforcement ratio to ensure that this is so, as will be shown.

As a computational device, it is convenient to divide the total tensile steel into two parts, as shown in Fig. 3.20. The first part, A_{sf} , represents the steel area that, when stressed to f_y , is required to balance the longitudinal compressive force in the overhanging portions of the flange that are stressed uniformly at $0.85 f'_c$ (Fig. 3.20b). Thus,

$$A_{sf} = \frac{0.85 f'_c (b - b_w) h_f}{f_y} \quad (3.59)$$

FIGURE 3.20

Computational model for design and analysis of T beams.



The force $A_{sf}f_y$ and the equal and opposite force $0.85 f'_c(b - b_w)h_f$ act with a lever arm $d - h_f/2$ to provide the nominal resisting moment

$$M_{n1} = A_{sf}f_y \left(d - \frac{h_f}{2} \right) \quad (3.60)$$

The remaining steel area $A_s - A_{sf}$, at a stress f_y , is balanced by the compression in the rectangular portion of the beam (Fig. 3.20c). The depth of the equivalent rectangular stress block in this zone is found from horizontal equilibrium.

$$a = \frac{(A_s - A_{sf})f_y}{0.85f'_c b_w} \quad (3.61)$$

An additional moment M_{n2} is thus provided by the forces $(A_s - A_{sf})f_y$ and $0.85f'_c ab_w$ acting at the lever arm $d - a/2$.

$$M_{n2} = (A_s - A_{sf})f_y \left(d - \frac{a}{2} \right) \quad (3.62)$$

and the total nominal resisting moment is the sum of the parts:

$$M_n = M_{n1} + M_{n2} = A_{sf}f_y \left(d - \frac{h_f}{2} \right) + (A_s - A_{sf})f_y \left(d - \frac{a}{2} \right) \quad (3.63)$$

This moment is reduced by the strength reduction factor ϕ in accordance with the safety provisions of the ACI Code to obtain the design strength.

As for rectangular beams, the tensile steel should yield prior to sudden crushing of the compression concrete, as assumed in the preceding development. Yielding of the tensile reinforcement and Code compliance are ensured if the net tensile strain is greater than 0.004. From the geometry of the section,

$$\frac{c}{d_t} \leq \frac{\epsilon_u}{\epsilon_u + \epsilon_t} \quad (3.64)$$

Setting $\epsilon_u = 0.003$ and $\epsilon_t = 0.004$ provides a maximum c/d_t ratio of 0.429, as seen in Fig. 3.10. Thus, as long as the depth to the neutral axis is less than $0.429d_t$, the net tensile strain requirements are satisfied, as they are for rectangular beam sections. This will occur if $\rho_w = A_s/b_w d$ is less than

$$\rho_{w,\max} = \rho_{\max} + \rho_f \quad (3.65)$$

where $\rho_f = A_{sf}/b_w d$ and ρ_{\max} is as previously defined for a rectangular cross section [Eq. (3.30c)]. For c/d_t ratios between 0.429 and 0.375, equivalent to ρ_w between the $\rho_{w,\max}$ from Eq. (3.65) and $\rho_{w,0.005}$, calculated by substituting $\rho_{0.005}$ from Eq. (3.30d) for ρ_{\max} in Eq. (3.65), the strength reduction factor ϕ must be adjusted for ϵ_t , as shown in Fig. 3.9. For $\rho_w \leq \rho_{w,0.005}$ or $c/d_t \leq 0.375$, $\phi = 0.90$.

The practical result of applying Eq. (3.65) is that the stress block of T beams will almost always be within the flange, except for unusual geometry or combinations of material strength. Consequently, rectangular beam equations may be applied in most cases.

The ACI Code restriction that the tensile reinforcement ratio for beams not be less than $\rho_{\min} = 3\sqrt{f'_c}/f_y$ and $\geq 200/f_y$ (see Section 3.4d) applies to T beams as well as rectangular beams. For T beams, the ratio ρ should be computed for this purpose based on the web width b_w .

c. Proportions of Cross Section

When designing T beams, in contrast to analyzing the capacity of a given section, normally the slab dimensions and beam spacing will have been established by transverse flexural requirements. Consequently, the only additional section dimensions that must be determined from flexural considerations are the width and depth of the web and the area of the tensile steel.

If the stem dimensions were selected on the basis of concrete stress capacity in compression, they would be very small because of the large compression flange width furnished by the presence of the slab. Such a design would not represent the optimum solution because of the large tensile steel requirement resulting from the small effective depth, because of the excessive web reinforcement that would be required for shear, and because of large deflections associated with such a shallow member. It is better practice to select the proportions of the web (1) so as to keep an arbitrarily low web reinforcement ratio ρ_w or (2) so as to keep web-shear stress at desirably low limits (Chapter 4) or (3) for continuous T beams, on the basis of the flexural requirements at the supports, where the effective cross section is rectangular and of width b_w .

In addition to the main reinforcement calculated according to the preceding requirements, it is necessary to ensure the integrity of the compressive flange of T beams by providing steel in the flange in the direction transverse to the main span. In typical construction, the slab steel serves this purpose. In other cases, additional bars must be added to permit the overhanging flanges to carry, as cantilever beams, the loads directly applied. According to ACI Code 8.12.5, the spacing of such bars must not exceed 5 times the thickness of the flange or in any case exceed 18 in.

d. Examples of Analysis and Design of T Beams

For *analyzing* the capacity of a T beam with known concrete dimensions and tensile steel area, it is reasonable to start with the assumption that the stress block depth a does not exceed the flange thickness h_f . In that case, all ordinary rectangular beam equations (see Section 3.4) apply, with beam width taken equal to the effective width of the flange. If, upon checking that assumption, a proves to exceed h_f , then T beam analysis must be applied. Equations (3.59) through (3.63) can be used, in sequence, to obtain the nominal flexural strength, after which the design strength is easily calculated.

For *design*, the following sequence of calculations may be followed:

1. Establish flange thickness h_f based on flexural requirements of the slab, which normally spans transversely between parallel T beams.
2. Determine the effective flange width b according to ACI limits.
3. Choose web dimensions b_w and d based on either of the following:
 - (a) Negative bending requirements at the supports, if a continuous T beam
 - (b) Shear requirements, setting a reasonable upper limit on the nominal unit shear stress v_u in the beam web (see Chapter 4)
4. With all concrete dimensions thus established, calculate a trial value of A_s , assuming that a does not exceed h_f , with beam width equal to flange width b . Use ordinary rectangular beam design methods.
5. For the trial A_s , check the depth of stress block a to confirm that it does not exceed h_f . If it should exceed that value, revise A_s , using the T beam equations.
6. Check to ensure that $\epsilon_i \geq 0.005$ or $c/d \leq 0.375$ to ensure that $\phi = 0.90$. (This will almost invariably be the case.)
7. Check to ensure that $\rho_w \geq \rho_{w,\min}$.

EXAMPLE 3.14

Moment capacity of a given section. The isolated T beam shown in Fig. 3.21 is composed of a flange 28 in. wide and 6 in. deep cast monolithically with a web of 10 in. width that extends 24 in. below the bottom surface of the flange to produce a beam of 30 in. total depth. Tensile reinforcement consists of six No. 10 (No. 32) bars placed in two horizontal rows separated by 1 in. clear spacing. The centroid of the bar group is 26 in. from the top of the beam. The concrete has a strength of 3000 psi, and the yield strength of the steel is 60,000 psi. What is the design moment capacity of the beam?

SOLUTION. It is easily confirmed that the flange dimensions are satisfactory according to the ACI Code for an isolated beam. The entire flange can be considered effective. For six No. 10 (No. 32) bars, $A_s = 7.62 \text{ in}^2$. First check the location of the neutral axis, on the assumption that rectangular beam equations may be applied. Using Eq. (3.32)

$$a = \frac{7.62 \times 60}{0.85 \times 3 \times 28} = 6.40 \text{ in.}$$

This exceeds the flange thickness, and so a T beam analysis is required. From Eq. (3.59) and Fig. 3.19b,

$$A_{sf} = 0.85 \times \frac{3}{60} (28 - 10) \times 6 = 4.59 \text{ in}^2$$

Then, from Eq. (3.60),

$$M_{n1} = 4.59 \times 60(26 - 3) = 6330 \text{ in-kips}$$

Then, from Fig. 3.19c,

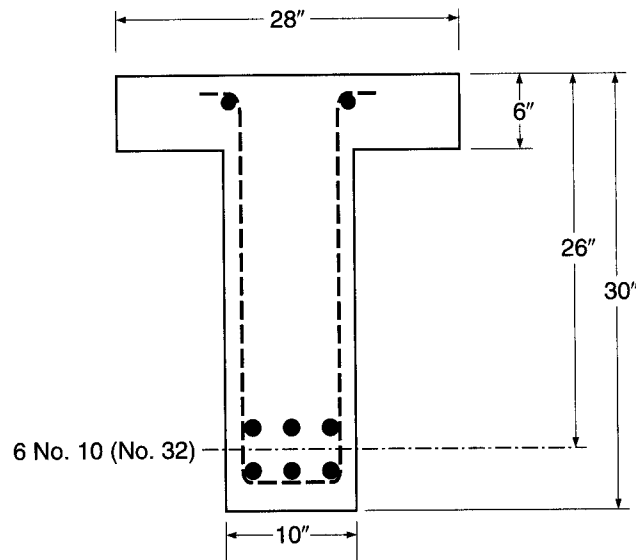
$$A_s - A_{sf} = 7.62 - 4.59 = 3.03 \text{ in}^2$$

and from Eqs. (3.58) and (3.59)

$$a = \frac{3.03 \times 60}{0.85 \times 3 \times 10} = 7.13 \text{ in.}$$

$$M_{n2} = 3.03 \times 60(26 - 3.56) = 4080 \text{ in-kips}$$

FIGURE 3.21
T beam of Example 3.14.



The depth to the neutral axis is $c = a/\beta_1 = 7.13/0.85 = 8.39$ and $d_t = 27.5$ in. to the lowest bar. The c/d_t ratio is $8.39/27.5 = 0.305 < 0.375$, so the $\epsilon_t > 0.005$ requirement is met and $\phi = 0.90$. When the ACI strength reduction factor is incorporated, the design strength is

$$\phi M_n = 0.90(6330 + 4080) = 9370 \text{ in-kips}$$

EXAMPLE 3.15

Determination of steel area for a given moment. A floor system, shown in Fig. 3.22, consists of a 3 in. concrete slab supported by continuous T beams with a 24 ft span, 47 in. on centers. Web dimensions, as determined by negative-moment requirements at the supports, are $b_w = 11$ in. and $d = 20$ in. What tensile steel area is required at midspan to resist a factored moment of 6400 in-kips if $f_y = 60,000$ psi and $f'_c = 3000$ psi?

SOLUTION. First determining the effective flange width,

$$16h_f + b_w = 16 \times 3 + 11 = 59 \text{ in.}$$

$$\frac{\text{Span}}{4} = 24 \times \frac{12}{4} = 72 \text{ in.}$$

Centerline beam spacing = 47 in.

The centerline T beam spacing controls in this case, and $b = 47$ in. The concrete dimensions b_w and d are known to be adequate in this case, since they have been selected for the larger negative support moment applied to the effective rectangular section $b_w d$. The tensile steel at midspan is most conveniently found by trial. Assuming the stress-block depth a is equal to the flange thickness of $h_f = 3$ in., one gets

$$d - \frac{a}{2} = 20 - 1.50 = 18.50 \text{ in.}$$

Trial:

$$A_s = \frac{M_u}{\phi f_y(d - a/2)} = \frac{6400}{0.90 \times 60 \times 18.50} = 6.41 \text{ in}^2$$

Checking the assumed value for a ,

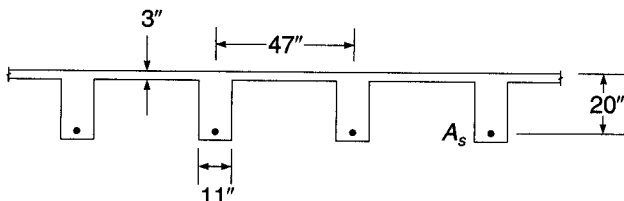
$$a = \frac{A_s f_y}{0.85 f'_c b} = \frac{6.41 \times 60}{0.85 \times 3 \times 47} = 3.21 \text{ in.}$$

Since a is greater than h_f , a T beam design is required and $\phi = 0.90$ is assumed.

$$A_{sf} = \frac{0.85 f'_c (b - b_w) h_f}{f_y} = \frac{0.85 \times 3 \times 36 \times 3}{60} = 4.59 \text{ in}^2$$

FIGURE 3.22

T beam of Example 3.15.



$$\phi M_{n1} = \phi A_{sf} f_y \left(d - \frac{h_f}{2} \right) = 0.90 \times 4.59 \times 60 \times 18.50 = 4590 \text{ in-kips}$$

$$\phi M_{n2} = M_u - \phi M_{n1} = 6400 - 4590 = 1810 \text{ in-kips}$$

Assume $a = 4.00$ in.:

$$A_s - A_{sf} = \frac{\phi M_{n2}}{\phi f_y(d - a/2)} = \frac{1810}{0.90 \times 60 \times (20 - 4.0/2)} = 1.86 \text{ in}^2$$

Check:

$$a = \frac{(A_s - A_{sf})f_y}{0.85f'_c b_w} = \frac{1.86 \times 60}{0.85 \times 3 \times 11} = 3.98 \text{ in.}$$

This is satisfactorily close to the assumed value of 4 in. Then

$$A_s = A_{sf} + A_s - A_{sf} = 4.59 + 1.86 = 6.45 \text{ in}^2$$

Checking to ensure that the net tensile strain of 0.005 is met to allow $\phi = 0.90$,

$$c = \frac{a}{\beta_1} = \frac{3.98}{0.85} = 4.68$$

$$\frac{c}{d_t} = \frac{4.68}{20} = 0.23 < 0.325$$

indicating that the design is satisfactory.

The close agreement should be noted between the approximate tensile steel area of 6.41 in² found by assuming the stress-block depth equal to the flange thickness and the more exact value of 6.45 in² found by T beam analysis. The approximate solution would be satisfactory in most cases.

REFERENCES

- 3.1. H. Rusch, "Researches toward a General Flexural Theory of Structural Concrete," *J. ACI*, vol. 32, no. 1, 1960, pp. 1-28.
- 3.2. L. B. Kriz, "Ultimate Strength Criteria for Reinforced Concrete," *J. Eng. Mech. Div. ASCE*, vol. 85, no. EM3, 1959, pp. 95-110.
- 3.3. L. B. Kriz and S. L. Lee, "Ultimate Strength of Overreinforced Beams," *Proc. ASCE*, vol. 86, no. EM3, 1960, pp. 95-106.
- 3.4. C. S. Whitney, "Design of Reinforced Concrete Members under Flexure or Combined Flexure and Direct Compression," *J. ACI*, vol. 33, Mar-Apr. 1937, pp. 483-498.
- 3.5. A. H. Mattock, L. B. Kriz, and E. Hogenstad, "Rectangular Concrete Stress Distribution in Ultimate Strength Design," *J. ACI*, vol. 32, no. 8, 1961, pp. 875-928.
- 3.6. P. H. Kaar, N. W. Hanson, and H. T. Capell, "Stress-Strain Curves and Stress Block Coefficients for High-Strength Concrete," *Proc. Douglas McHenry Symposium*, ACI Special Publication SP-55, 1978.
- 3.7. *ACI Design Handbook: Beams, One-Way Slabs, Brackets, Footings, Pile Caps, Columns, Two-Way Slabs, and Seismic Design in Accordance with the Strength Design Method of 318-95*, SP-17, American Concrete Institute, Farmington Hills, MI, 1997.
- 3.8. *ACI Detailing Manual*, ACI Special Publication SP-66, American Concrete Institute, Farmington Hills, MI, 2004.
- 3.9. *CRSI Design Handbook*, 9th ed., Concrete Reinforcing Steel Institute, Schaumburg, IL, 2008.
- 3.10. *Economical Concrete Construction*, Engineering Data Report No. 30, Concrete Reinforcing Steel Institute, Schaumburg, IL, 1988.
- 3.11. *Manual of Standard Practice*, 27th ed., Concrete Reinforcing Steel Institute, Schaumburg, IL, 2001.
- 3.12. C. W. Dolan, *Ultimate Capacity of Reinforced Concrete Sections Using a Continuous Stress-Strain Function*, M.S. Thesis, Cornell University, Ithaca, NY, June 1967.

PROBLEMS

- 3.1.** A rectangular beam made using concrete with $f'_c = 6000$ psi and steel with $f_y = 60,000$ psi has a width $b = 20$ in., an effective depth of $d = 17.5$ in., and a total depth of $h = 20$ in. The concrete modulus of rupture $f_r = 530$ psi. The elastic moduli of the concrete and steel are, respectively, $E_c = 4,030,000$ psi and $E_s = 29,000,000$ psi. The tensile steel consists of four No. 11 (No. 36) bars.
- (a) Find the maximum service load moment that can be resisted without stressing the concrete above $0.45f'_c$ or the steel above $0.40f_y$.
 - (b) Determine whether the beam will crack before reaching the service load.
 - (c) Compute the nominal flexural strength of the beam.
 - (d) Compute the ratio of the nominal flexural strength of the beam to the maximum service load moment, and compare your findings to the ACI load factors and strength reduction factor.
- 3.2.** A rectangular, tension-reinforced beam is to be designed for dead load of 500 lb/ft plus self-weight and service live load of 1200 lb/ft, with a 22 ft simple span. Material strengths will be $f_y = 60$ ksi and $f'_c = 3$ ksi for steel and concrete, respectively. The total beam depth must not exceed 16 in. Calculate the required beam width and tensile steel requirement, using a reinforcement ratio of $0.60\rho_{\max}$. Use ACI load factors and strength reduction factors. The effective depth may be assumed to be 2.5 in. less than the total depth.
- 3.3.** A beam with a 20 ft simple span has cross-sectional dimensions $b = 12$ in., $d = 23$ in., and $h = 25$ in. (see Fig. 3.2b for notation). It carries a uniform service load of 2450 lb/ft in addition to its own weight. Material strengths are $f'_c = 4000$ psi and $f_y = 60,000$ psi. Assume a weight of 150 pcf for reinforced concrete.
- (a) Check whether this beam, if reinforced with three No. 9 (No. 29) bars, is adequate to carry this load with a minimum factor of safety against flexural failure of 1.85. If this requirement is not met, select a three-bar reinforcement of diameter or diameters adequate to provide this safety.
 - (b) Determine the maximum stress in the steel and in the concrete under service load, i.e., when the beam carries its own weight and the specified uniform load.
 - (c) Will the beam show hairline cracks on the tension side under service load?
- 3.4.** A rectangular reinforced concrete beam with dimensions $b = 14$ in., $d = 25$ in., and $h = 28$ in. is reinforced with three No. 10 (No. 32) bars. Material strengths are $f_y = 60,000$ psi and $f'_c = 5000$ psi.
- (a) Find the moment that will produce the first cracking at the bottom surface of the beam, basing your calculation on I_g , the moment of inertia of the gross concrete section.
 - (b) Repeat the calculation, using I_{ut} , the moment of inertia of the uncracked transformed section.
 - (c) Determine the maximum moment that can be carried without stressing the concrete beyond $0.45f'_c$ or the steel beyond $0.60f_y$.
 - (d) Find the nominal flexural strength of this beam.
 - (e) Compute the ratio of the flexural strength from part (d) to the service capacity from part (c).
 - (f) Comment on your results, paying particular attention to comparing parts (a) and (b) and comparing the result in part (e) with the load factors in the ACI Code.

- 3.5.** A tensile-reinforced beam has $b = 12$ in. and $d = 20$ in. to the center of the bars, which are placed all in one row. If $f_y = 60,000$ psi and $f'_c = 5000$ psi, find the nominal flexural strength M_n for (a) A_s = two No. 8 (No. 25) bars, (b) A_s = two No. 10 (No. 32) bars, (c) A_s = three No. 10 (No. 32) bars.
- 3.6.** A singly reinforced rectangular beam is to be designed, with effective depth approximately 1.5 times the width, to carry a service live load of 2000 lb/ft in addition to its own weight, on a 24 ft simple span. The ACI Code load factors are to be applied as usual. With $f_y = 60,000$ psi and $f'_c = 4000$ psi, determine the required concrete dimensions b , d , and h , and steel reinforcing bars (a) for $\rho = 0.6\rho_{\max}$ and (b) for $\rho = \rho_{0.005}$. Include a sketch of each cross section drawn to scale. Allow for No. 4 (No. 13) stirrups. Comment on your results.
- 3.7.** A four-span continuous beam of constant rectangular cross section is supported at A , B , C , D , and E . The factored moments resulting from analysis are as follows:

At Supports, ft-kips	At Midspan, ft-kips
$M_a = 138$	$M_{ab} = 158$
$M_b = 220$	$M_{bc} = 138$
$M_c = 200$	$M_{cd} = 138$
$M_d = 220$	$M_{de} = 158$
$M_e = 138$	

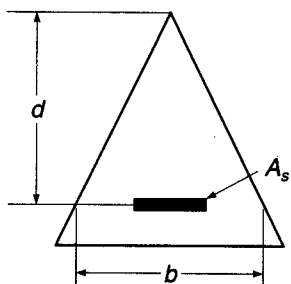
Determine the required final concrete dimensions for this beam, using $d = 1.75b$, and determine the reinforcement requirements at each critical moment section. Your final reinforcement ratio should not exceed $= 0.6\rho_{0.005}$. Use $f_y = 60,000$ psi and $f'_c = 6000$ psi.

- 3.8.** A two-span continuous concrete beam is to be supported by three concrete walls spaced 30 ft on centers. A service live load of 1.5 kips/ft is to be carried in addition to the self-weight of the beam. Use pattern loading; i.e., consider two loading conditions: (1) live load on both spans and (2) live load on a single span. A constant rectangular cross section is to be used with $d = 2b$, but reinforcement is to be varied according to requirements. Find the required concrete dimensions and reinforcement at all critical sections. Allow for No. 3 (No. 10) stirrups. Use a span-to-depth ratio of 15 as the first estimate of the depth. Adjust the depth if the reinforcement ratio is too high. Include sketches, drawn to scale, of the critical cross sections. Use $f_y = 60,000$ psi and $f'_c = 6000$ psi.
- 3.9.** A rectangular concrete beam measures 12 in. wide and has an effective depth of 18 in. Compression steel consisting of two No. 8 (No. 25) bars is located 2.5 in. from the compression face of the beam. If $f'_c = 4000$ psi and $f_y = 60,000$ psi, what is the design moment capacity of the beam, according to the ACI Code, for the following alternative tensile steel areas? (a) A_s = three No. 10 (No. 32) bars in one layer, (b) A_s = four No. 10 (No. 32) bars in two layers, (c) A_s = six No. 9 (No. 29) bars in two layers. (Note: Check for yielding of compression steel in each case.) Plot M_n versus ρ and comment on your findings.
- 3.10.** A rectangular concrete beam of width $b = 24$ in. is limited by architectural considerations to a maximum total depth $h = 16$ in. It must carry a total factored load moment $M_u = 400$ ft-kips. Design the flexural reinforcement for this member, using compression steel if necessary. Allow 3 in. to the center of the bars from the compression or tension face of the beam. Material strengths are $f_y = 60,000$ psi and $f'_c = 4000$ psi. Select reinforcement to provide the

needed areas, and show a sketch of your final design, including provision for No. 4 (No. 13) stirrups.

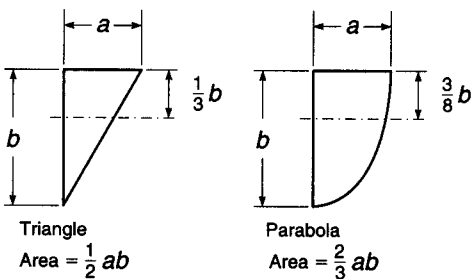
- 3.11.** For the beam with the triangular cross section shown in Fig. P3.11, determine (a) the balanced reinforcement ratio and (b) the maximum reinforcement ratio if $\epsilon_t = 0.005$. The dimensions of the triangle are such that the width of the triangle equals the distance from the apex. Thus, the width at the effective depth b equals the effective depth d . Express the reinforcement ratio ρ in terms of b and d . Draw the strain distribution, and stress distribution, and define your notation.

FIGURE P3.11



- 3.12.** Develop a design table and graph for the moment capacity of rectangular concrete beams based on the use of the flexural resistance factor R . (See Table A.5a and Graph A.1a for examples.) Material strengths are $f_y = 60,000$ psi and $f'_c = 8000$ psi. The table and graph should begin with ρ_{\min} and end at ρ_{\max} . Your work must show how the maximum and minimum values of ρ were computed. You may use Excel or MathCAD to perform your calculations. Your submittal must include a table, a graph, and commentary on how you checked the work.
- 3.13.** A rectangular beam made using concrete with $f'_c = 5000$ psi and steel with $f_y = 60,000$ psi has a width $b = 18$ in., an effective depth $d = 21$ in., and a total depth $h = 24$ in. The beam is reinforced with four No. 9 (No. 29) bars. Compute the nominal moment capacity, assuming (a) an equivalent rectangular stress block, (b) a triangular stress block with a peak value of f'_c , and (c) a parabolic stress block with a peak value of f'_c (see Fig. P3.13). Compare and comment on your results, knowing that the rectangular stress block correlates within 4 percent with test results.

FIGURE P3.13



- 3.14.** A precast T beam is to be used as a bridge over a small roadway. Concrete dimensions are $b = 48$ in., $b_w = 16$ in., $h_f = 5$ in., and $h = 25$ in. The effective depth $d = 20$ in. Concrete and steel strengths are 6000 psi and 60,000 psi,

respectively. Using approximately one-half the maximum tensile reinforcement permitted by the ACI Code (select the actual size of bar and number to be used), determine the design moment capacity of the girder. If the beam is used on a 30 ft simple span, and if in addition to its own weight it must support railings, curbs, and suspended loads totaling 0.475 kip/ft, what uniform service live load limit should be posted?

- 3.15. A rectangular beam with a width of 8 in., an effective depth of 10 in., and a total depth of 12 in. is reinforced with a single fiberglass reinforcing bar that has a cross-sectional area of 0.45 in². The bar has a nominal tensile strength of 140,000 psi, a linear stress-strain curve to failure, and a strain at failure of 1.8 percent. The concrete strength $f'_c = 6000$ psi. Determine the nominal flexural strength of the section.
- 3.16. Compute the maximum and minimum reinforcement ratios for reinforcement with an 80 ksi yield point and $f'_c = 4000$ to 8000 psi in 1000 psi increments, similar to those shown in Table A.4. Using the maximum and minimum reinforcement ratios, develop resistance factors and design graphs similar to Table A.5b and Graph A.1a.

4

Shear and Diagonal Tension in Beams

4.1 INTRODUCTION

Chapter 3 dealt with the flexural behavior and flexural strength of beams. Beams must also have an adequate safety margin against other types of failure, some of which may be more dangerous than flexural failure. This may be so because of greater uncertainty in predicting certain other modes of collapse, or because of the catastrophic nature of some other types of failure, should they occur.

Shear failure of reinforced concrete, more properly called *diagonal tension failure*, is one example. Shear failure is difficult to predict accurately. In spite of many decades of experimental research (Refs. 4.1 to 4.6) and the use of highly sophisticated analytical tools (Refs. 4.7 and 4.8), it is not yet fully understood. Furthermore, if a beam without properly designed shear reinforcement is overloaded to failure, shear collapse is likely to occur suddenly, with no advance warning of distress. This is in strong contrast with the nature of flexural failure. For typically underreinforced beams, flexural failure is initiated by gradual yielding of the tension steel, accompanied by obvious cracking of the concrete and large deflections, giving ample warning and providing the opportunity to take corrective measures. Because of these differences in behavior, reinforced concrete beams are generally provided with special *shear reinforcement* to ensure that flexural failure would occur before shear failure if the member were severely overloaded.

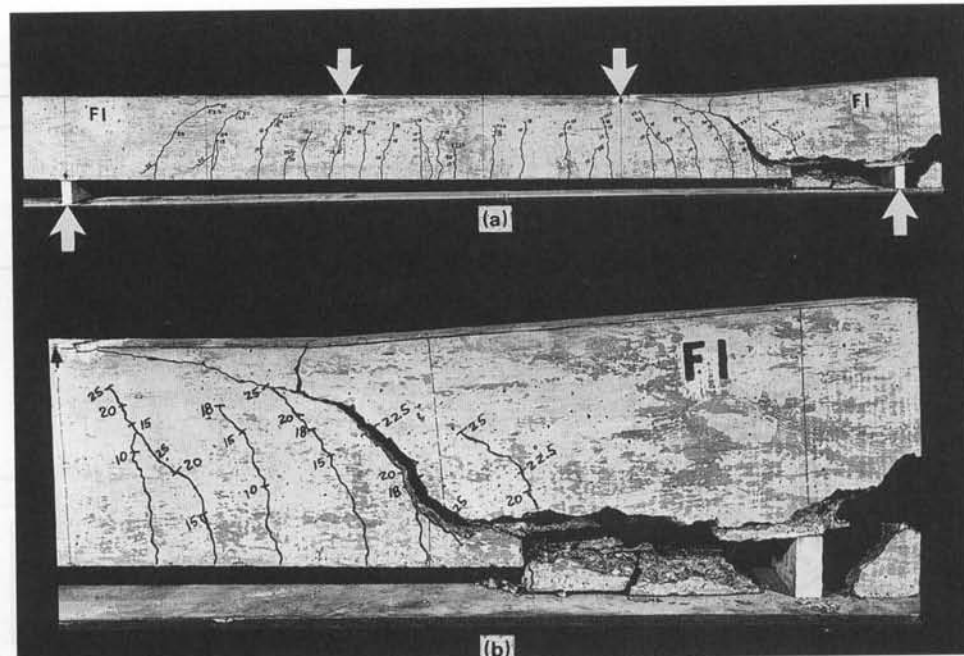
Figure 4.1 shows a shear-critical beam tested under third point loading. With no shear reinforcement provided, the member failed immediately upon formation of the critical crack in the high-shear region near the right support.

It is important to realize that shear analysis and design are not really concerned with shear as such. The shear stresses in most beams are far below the direct shear strength of the concrete. The real concern is with *diagonal tension stress*, resulting from the combination of shear stress and longitudinal flexural stress. Most of this chapter deals with analysis and design for diagonal tension, and it provides background for understanding and using the shear provisions of the 2008 ACI Code. Members without web reinforcement are studied first to establish the location and orientation of cracks and the diagonal cracking load. Methods are then developed for the design of shear reinforcement according to the present ACI Code, both in ordinary beams and in special types of members, such as deep beams.

Over the years, alternative methods of shear design have been proposed, based on variable angle truss models and diagonal compression field theory (Refs. 4.9 and 4.10). These approaches will be reviewed briefly later in this chapter, with one such approach, the modified compression field theory, presented in detail.

FIGURE 4.1

Shear failure of reinforced concrete beam: (a) overall view, (b) detail near right support.



Finally, there are some circumstances in which consideration of direct shear is appropriate. One example is in the design of composite members combining precast beams with a cast-in-place top slab. Horizontal shear stresses on the interface between components are important. The shear-friction theory, useful in this and other cases, will be presented following development of methods for the analysis and design of beams for diagonal tension.

4.2 DIAGONAL TENSION IN HOMOGENEOUS ELASTIC BEAMS

The stresses acting in homogeneous beams were briefly reviewed in Section 3.2. It was pointed out that when the material is elastic (stresses proportional to strains), shear stresses

$$\tau = \frac{VQ}{Ib} \quad (3.4)$$

act at any section in addition to the bending stresses

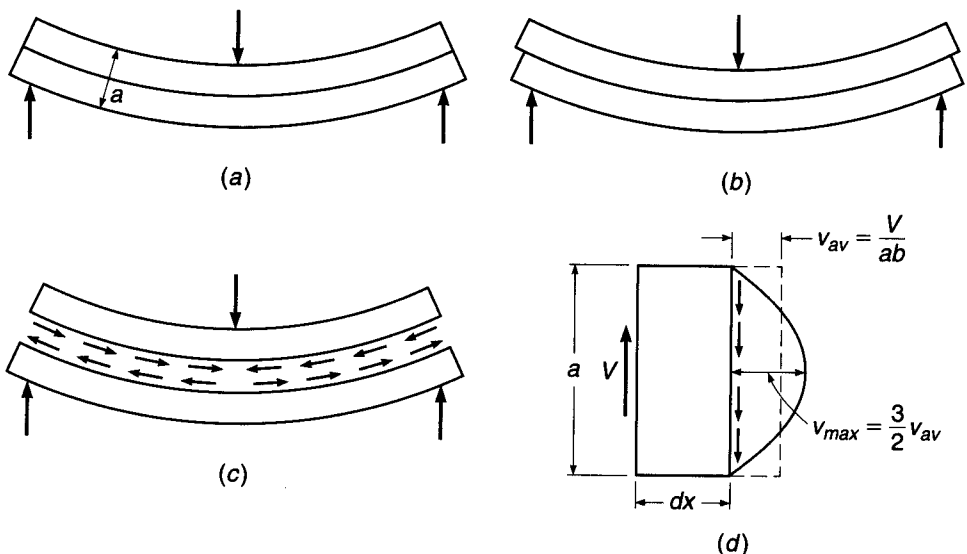
$$f = \frac{My}{I} \quad (3.2)$$

except for those locations at which the shear force V happens to be zero.

The role of shear stresses is easily visualized by the performance under load of the laminated beam of Fig. 4.2; it consists of two rectangular pieces bonded together along the contact surface. If the adhesive is strong enough, the member will deform as one single beam, as shown in Fig. 4.2a. On the other hand, if the adhesive is weak, the two pieces will separate and slide relative to each other, as shown in Fig. 4.2b.

FIGURE 4.2

Shear in homogeneous rectangular beams.



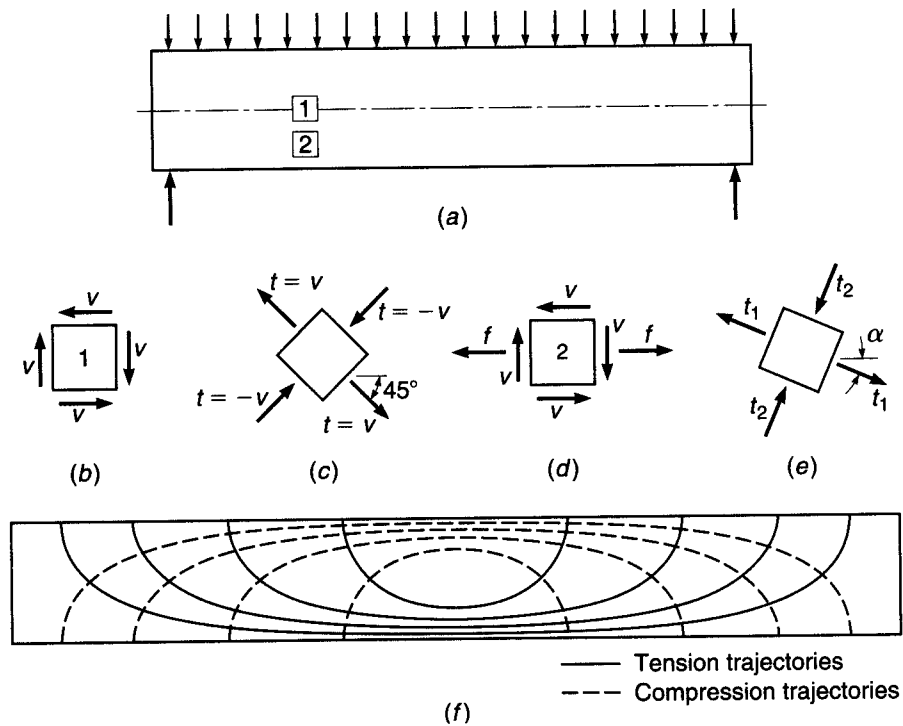
Evidently, then, when the adhesive is effective, there are forces or stresses acting in it that prevent this sliding or shearing. These horizontal shear stresses are shown in Fig. 4.2c as they act, separately, on the top and bottom pieces. The same stresses occur in horizontal planes in single-piece beams; they are different in intensity at different distances from the neutral axis.

Figure 4.2d shows a differential length of a single-piece rectangular beam acted upon by a shear force of magnitude V . Upward translation is prevented; i.e., vertical equilibrium is provided by the vertical shear stresses v . Their average value is equal to the shear force divided by the cross-sectional area $v_{av} = V/ab$, but their intensity varies over the depth of the section. As is easily computed from Eq. (3.4), the shear stress is zero at the outer fibers and has a maximum of $1.5v_{av}$ at the neutral axis, the variation being parabolic as shown. Other values and distributions are found for other shapes of the cross section, the shear stress always being zero at the outer fibers and of maximum value at the neutral axis. If a small square element located at the neutral axis of such a beam is isolated, as shown in Fig. 4.3b, the vertical shear stresses on it, equal and opposite on the two faces for reasons of equilibrium, act as shown. However, if these were the only stresses present, the element would not be in equilibrium; it would spin. Therefore, on the two horizontal faces there exist equilibrating horizontal shear stresses of the same magnitude. That is, at any point within the beam, the horizontal shear stresses of Fig. 4.3b are equal in magnitude to the vertical shear stresses of Fig. 4.2d.

It is proved in any strength-of-materials text that on an element cut at 45° these shear stresses combine in such a manner that their effect is as shown in Fig. 4.3c. That is, the action of the two pairs of shear stresses on the vertical and horizontal faces is the same as that of two pairs of normal stresses, one tensile and one compressive, acting on the 45° faces and of numerical value equal to that of the shear stresses. If an element of the beam is considered that is located neither at the neutral axis nor at the outer edges, its vertical faces are subject not only to the shear stresses but also to the familiar bending stresses whose magnitude is given by Eq. (3.2) (Fig. 4.3d). The six stresses that now act on the element can again be combined into a pair of inclined

FIGURE 4.3

Stress trajectories in homogeneous rectangular beam.



compressive stresses and a pair of inclined tensile stresses that act at right angles to each other. They are known as *principal stresses* (Fig. 4.3e). Their value, as mentioned in Section 3.2, is given by

$$t = \frac{f}{2} \pm \sqrt{\frac{f^2}{4} + v^2} \quad (3.1)$$

and their inclination α by $\tan 2\alpha = 2v/f$.

Since the magnitudes of the shear stresses v and the bending stresses f change both along the beam and vertically with distance from the neutral axis, the inclinations as well as the magnitudes of the resulting principal stresses t also vary from one place to another. Figure 4.3f shows the inclinations of these principal stresses for a rectangular beam uniformly loaded. That is, these stress trajectories are lines which, at any point, are drawn in that direction in which the particular principal stress, tension or compression, acts at that point. It is seen that at the neutral axis the principal stresses in a beam are always inclined at 45° to the axis. In the vicinity of the outer fibers they are horizontal near midspan.

An important point follows from this discussion. Tensile stresses, which are of particular concern in view of the low tensile strength of the concrete, are not confined to the horizontal bending stresses f that are caused by bending alone. Tensile stresses of various inclinations and magnitudes, resulting from shear alone (at the neutral axis) or from the combined action of shear and bending, exist in all parts of a beam and can impair its integrity if not adequately provided for. It is for this reason that the inclined tensile stresses, known as *diagonal tension*, must be carefully considered in reinforced concrete design.

4.3 REINFORCED CONCRETE BEAMS WITHOUT SHEAR REINFORCEMENT

The discussion of shear in a homogeneous elastic beam applies very closely to a plain concrete beam *without* reinforcement. As the load is increased in such a beam, a tension crack will form where the tensile stresses are largest and will immediately cause the beam to fail. Except for beams of very unusual proportions, the largest tensile stresses are those caused at the outer fiber by bending alone, at the section of maximum bending moment. In this case, shear has little, if any, influence on the strength of a beam.

However, when tension reinforcement is provided, the situation is quite different. Even though tension cracks form in the concrete, the required flexural tension strength is furnished by the steel, and much higher loads can be carried. Shear stresses increase proportionally to the loads. In consequence, diagonal tension stresses of significant intensity are created in regions of high shear forces, chiefly close to the supports. The longitudinal tension reinforcement has been so calculated and placed that it is chiefly effective in resisting longitudinal tension near the tension face. It does not reinforce the tensionally weak concrete against the diagonal tension stresses that occur elsewhere, caused by shear alone or by the combined effect of shear and flexure. Eventually, these stresses attain magnitudes sufficient to open additional tension cracks in a direction perpendicular to the local tension stress. These are known as *diagonal cracks*, in distinction to the vertical flexural cracks. The latter occur in regions of large moments, the former in regions in which the shear forces are high. In beams in which no reinforcement is provided to counteract the formation of large diagonal tension cracks, their appearance has far-reaching and detrimental effects. For this reason, methods of predicting the loads at which these cracks will form are desired.

a. Criteria for Formation of Diagonal Cracks

It is seen from Eq. (3.1) that the diagonal tension stresses t represent the combined effect of the shear stresses v and the bending stresses f . These in turn are, respectively, proportional to the shear force V and the bending moment M at the particular location in the beam [Eqs. (3.2) and (3.4)]. Depending on configuration, support conditions, and load distribution, a given location in a beam may have a large moment combined with a small shear force, or the reverse, or large or small values for both shear and moment. Evidently, the relative values of M and V will affect the magnitude as well as the direction of the diagonal tension stresses. Figure 4.4 shows a few typical beams and their moment and shear diagrams and draws attention to locations at which various combinations of high or low V and M occur.

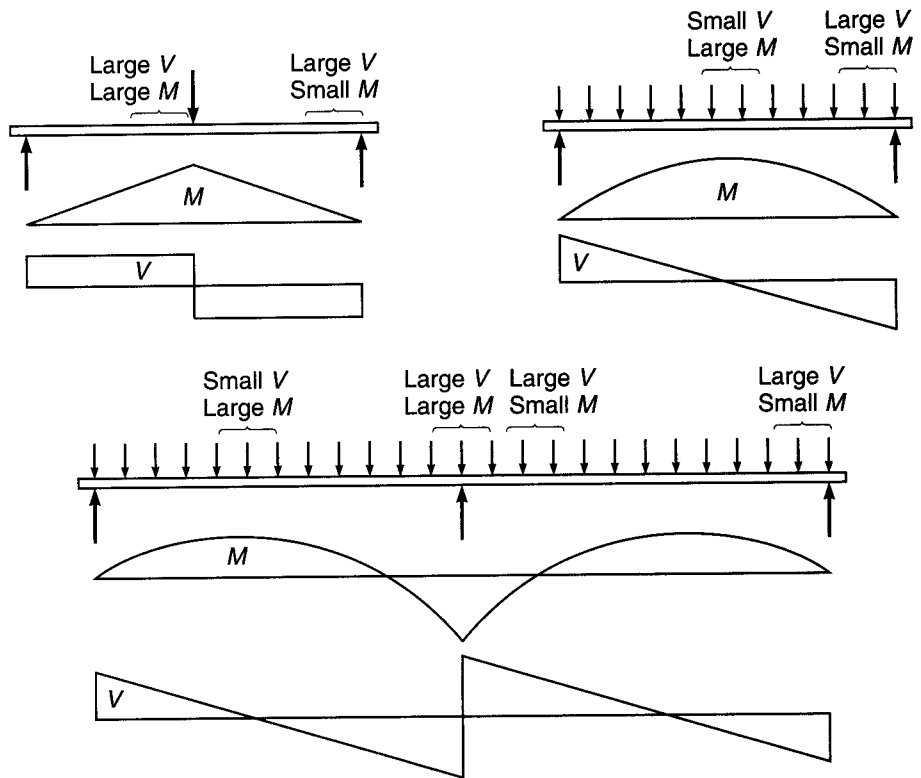
At a location of large shear force V and small bending moment M , there will be little flexural cracking, if any, prior to the development of a diagonal tension crack. Consequently, the average shear stress prior to crack formation is

$$v = \frac{V}{bd} \quad (4.1)$$

The exact distribution of these shear stresses over the depth of the cross section is not known. It cannot be computed from Eq. (3.4) because this equation does not account for the influence of the reinforcement and because concrete is not an elastic homogeneous material. The value computed from Eq. (4.1) must therefore be regarded merely as a measure of the average intensity of shear stresses in the section. The maximum

FIGURE 4.4

Typical locations of critical combinations of shear and moment.



value, which occurs at the neutral axis, will exceed this average by an unknown but moderate amount.

If flexural stresses are negligibly small at the particular location, the diagonal tensile stresses, as in Fig. 4.3b and c, are inclined at about 45° and are numerically equal to the shear stresses, with a maximum at the neutral axis. Consequently, diagonal cracks form mostly at or near the neutral axis and propagate from that location, as shown in Fig. 4.5a. These *web-shear* cracks can be expected to form when the diagonal tension stress in the vicinity of the neutral axis becomes equal to the tensile strength of the concrete. The former, as was indicated, is of the order of, and somewhat larger than, $v = V/bd$; the latter, as discussed in Section 2.9, varies from about $3\sqrt{f'_c}$ to about $5\sqrt{f'_c}$. An evaluation of a very large number of beam tests is in fair agreement with this reasoning (Ref. 4.1). It was found that in regions with large shear and small moment, diagonal tension cracks form at an average or nominal shear stress v_{cr} of about $3.5\sqrt{f'_c}$, that is,

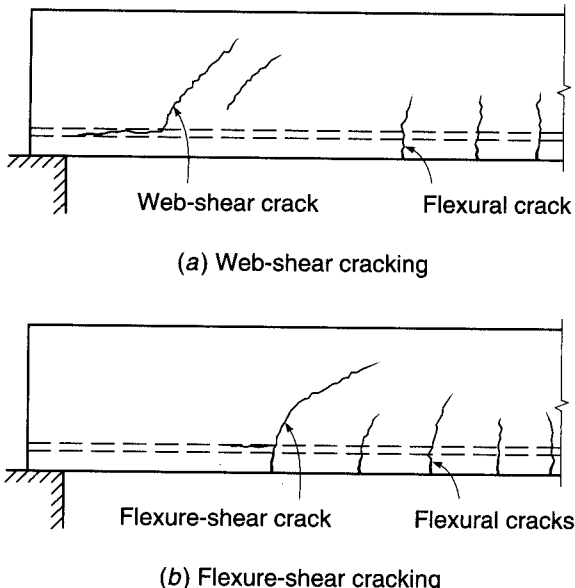
$$v_{cr} = \frac{V_{cr}}{bd} = 3.5\sqrt{f'_c} \quad (4.2a)$$

where V_{cr} is that shear force at which the formation of the crack was observed.[†] Web-shear cracking is relatively rare and occurs chiefly near supports of deep, thin-webbed beams or at inflection points of continuous beams.

[†] Actually, diagonal tension cracks form at places where a compressive stress acts in addition to and perpendicular to the diagonal tension stress, as shown in Fig. 4.3d and e. The crack, therefore, occurs at a location of biaxial stress rather than uniaxial tension. However, the effect of this simultaneous compressive stress on the cracking strength appears to be small, in agreement with the information in Fig. 2.8.

FIGURE 4.5

Diagonal tension cracking in reinforced concrete beams.



The situation is different when both the shear force and the bending moment have large values. At such locations, in a well-proportioned and reinforced beam, flexural tension cracks form first. Their width and length are well controlled and kept small by the presence of longitudinal reinforcement. However, when the diagonal tension stress at the upper end of one or more of these cracks exceeds the tensile strength of the concrete, the crack bends in a diagonal direction and continues to grow in length and width (see Fig. 4.5b). These cracks are known as *flexure-shear* cracks and are more common than web-shear cracks.

It is evident that at the instant at which a diagonal tension crack of this type develops, the average shear stress is larger than that given by Eq. (4.1). This is so because the preexisting tension crack has reduced the area of uncracked concrete that is available to resist shear to a value smaller than that of the uncracked area bd used in Eq. (4.1). The amount of this reduction will vary, depending on the unpredictable length of the preexisting flexural tension crack. Furthermore, the simultaneous bending stress f combines with the shear stress v to increase the diagonal tension stress t further [see Eq. (3.1)]. No way has been found to calculate reliable values of the diagonal tension stress under these conditions, and recourse must be made to test results.

A large number of beam tests have been evaluated for this purpose (Ref. 4.1). They show that in the presence of large moments (for which adequate longitudinal reinforcement has been provided) the nominal shear stress at which diagonal tension cracks form and propagate is, in most cases, conservatively given by

$$v_{cr} = \frac{V_{cr}}{bd} = 1.9\sqrt{f'_c} \quad (4.2b)$$

Comparison with Eq. (4.2a) shows that large bending moments can reduce the shear force at which diagonal cracks form to roughly one-half the value at which they would form if the moment were zero or nearly so. This is in qualitative agreement with the discussion just given.

It is evident, then, that the shear at which diagonal cracks develop depends on the ratio of shear force to bending moment, or, more precisely, on the ratio of shear stress v to bending stress f near the top of the flexural crack. Neither of these can be accurately calculated. It is clear, though, that $v = K_1(V/bd)$, where, by comparison with Eq. (4.1), constant K_1 depends chiefly on the depth of penetration of the flexural crack. On the other hand [see Eq. (3.10)], $f = K_2(V/bd^2)$, where K_2 also depends on crack configuration. Hence, the ratio

$$\frac{v}{f} = \frac{K_1}{K_2} \frac{Vd}{M}$$

must be expected to affect that load at which flexural cracks develop into flexure-shear cracks, the unknown quantity K_1/K_2 to be explored by tests. Equation (4.2a) gives the cracking shear for very large values of Vd/M , and Eq. (4.2b) for very small values. Moderate values of Vd/M result in magnitudes of v_{cr} intermediate between these extremes. Again, from evaluations of large numbers of tests (Ref. 4.1), it has been found that the nominal shear stress at which diagonal flexure-shear cracking develops can be predicted from

$$v_{cr} = \frac{V_{cr}}{bd} = 1.9\sqrt{f'_c} + 2500 \frac{\rho Vd}{M} \leq 3.5\sqrt{f'_c} \quad (4.3a)$$

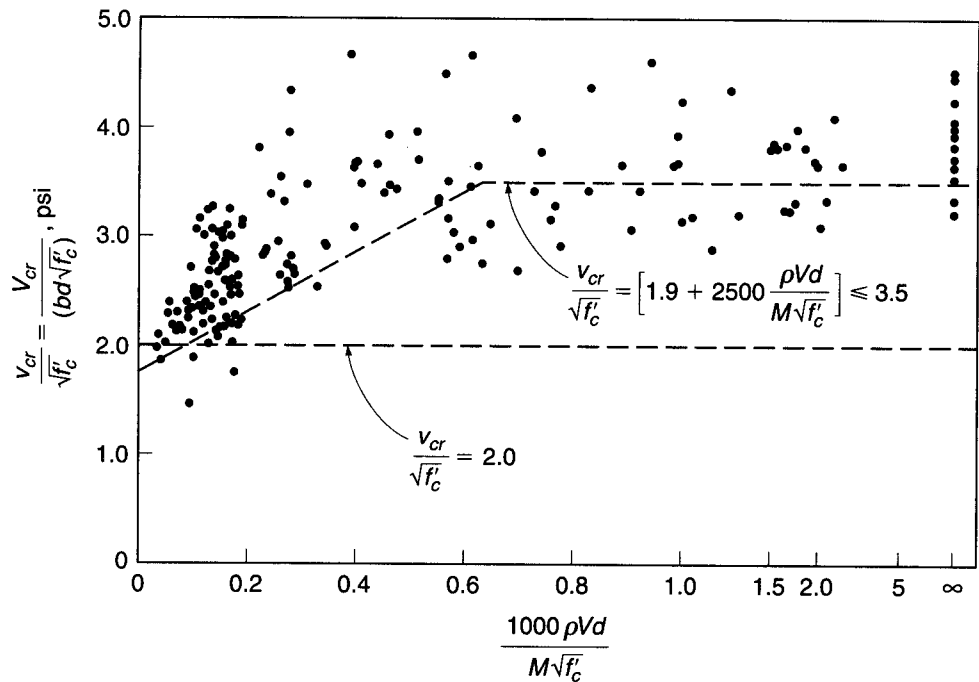
where

$$V_{cr} = v_{cr} bd$$

and $\rho = A_s/bd$, as before, and 2500 is an empirical constant in psi units. A graph of this relation and comparison with test data are given in Fig. 4.6.

FIGURE 4.6

Correlation of Eq. (4.3a) with test results.



Apart from the influence of Vd/M , it is seen from Eq. (4.3a) that increasing amounts of tension reinforcement, i.e., increasing values of the reinforcement ratio ρ , have a beneficial effect in that they increase the shear at which diagonal cracks develop. This is so because larger amounts of longitudinal steel result in smaller and narrower flexural tension cracks prior to the formation of diagonal cracking, leaving a larger area of uncracked concrete available to resist shear. [For more details on the development of Eq. (4.3a), see Ref. 4.1.]

A brief study of Fig. 4.6 will show that although Eq. (4.3a) captures the overall effects of the controlling variables on v_{cr} , the match with actual data is far from perfect. Of particular concern is the tendency of Eq. (4.3a) to overestimate the shear strength of beams with reinforcement ratios $\rho < 1.0$ percent, values that are commonly used in practice. The cracking stress predicted in Eq. (4.3a) becomes progressively less conservative as f'_c increases above 5000 psi and as beam depth d increases above 18 in. On the other hand, Eq. (4.3a) underestimates the effect of Vd/M on v_{cr} and ignores the positive effect of flanges (present on most reinforced concrete beams) on shear strength. The conservatism of Eq. (4.3a) increases as both flange thickness and web width increase (Ref. 4.3), although these factors have less of an effect than f'_c , ρ , or Vd/M on v_{cr} .

Considering the three main variables, an improved match with test results is obtained with the empirical relationship (Ref. 4.11)

$$v_{cr} = \frac{V_{cr}}{bd} = 59 \left(f'_c \rho \frac{Vd}{M} \right)^{1/3} \quad (4.3b)$$

Equation (4.3b) was calibrated based on beams with $d \approx 12$ in. It can be modified to account for the lower average shear cracking stress exhibited by deeper beams with the addition of one term.

$$v_{cr} = \frac{V_{cr}}{bd} = 59 \left(\frac{12}{d} \right)^{1/4} \left(f'_c \rho \frac{Vd}{M} \right)^{1/3} \quad (4.3c)$$

b. Behavior of Diagonally Cracked Beams

In regard to flexural cracks, as distinct from diagonal tension cracks, it was explained in Section 3.3 that cracks on the tension side of a beam are permitted to occur and are in no way detrimental to the strength of the member. One might expect a similar situation in regard to diagonal cracking caused chiefly by shear. The analogy, however, is not that simple. Flexural tension cracks are harmless only because adequate longitudinal reinforcement has been provided to resist the flexural tension stresses that the cracked concrete is no longer able to transmit. In contrast, the beams now being discussed, although furnished with the usual longitudinal reinforcement, are not equipped with any other reinforcement to offset the effects of diagonal cracking. This makes the diagonal cracks much more decisive in subsequent performance and strength of the beam than the flexural cracks.

Two types of behavior have been observed in the many tests on which present knowledge is based:

1. The diagonal crack, once formed, spreads either immediately or at only slightly higher load, traversing the entire beam from the tension reinforcement to the compression face, splitting it in two and failing the beam. This process is sudden and without warning and occurs chiefly in the shallower beams, i.e., beams with

span-depth ratios of about 8 or more. Beams in this range of dimensions are very common. Complete absence of shear reinforcement would make them very vulnerable to accidental large overloads, which would result in catastrophic failures without warning. For this reason it is good practice to provide a minimum amount of shear reinforcement even if calculation does not require it, because such reinforcement restrains growth of diagonal cracks, thereby increasing ductility and providing warning in advance of actual failure. Only in situations where an unusually large safety factor against inclined cracking is provided, i.e., where actual shear stresses are very small compared with v_{cr} , as in some slabs and most footings, is it permissible to omit shear reinforcement.

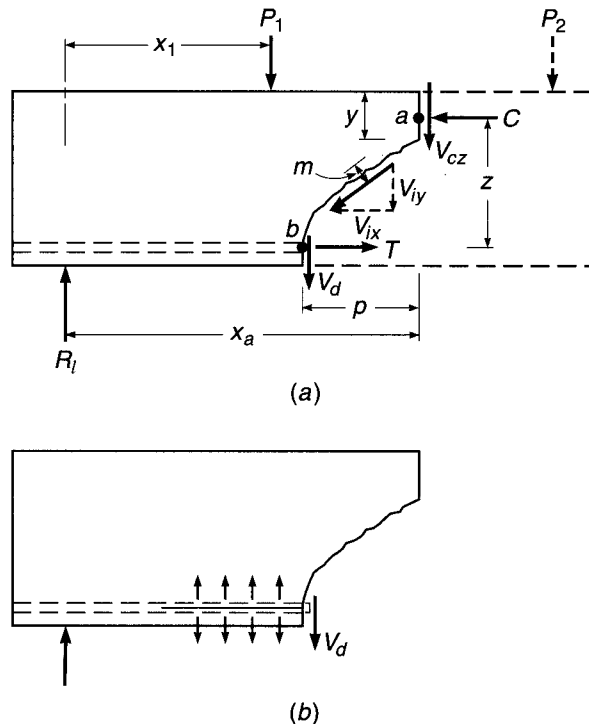
2. Alternatively, the diagonal crack, once formed, spreads toward and partially into the compression zone but stops short of penetrating to the compression face. In this case no sudden collapse occurs, and the failure load may be significantly higher than that at which the diagonal crack first formed. This behavior is chiefly observed in the deeper beams with smaller span-depth ratios and will be analyzed now.

Figure 4.7a shows a portion of a beam, arbitrarily loaded, in which a diagonal tension crack has formed. Consider the part of the beam to the left of the crack, shown in solid lines. There is an external upward shear force $V_{ext} = R_l - P_1$ acting on this portion.

Once a crack is formed, no tension force perpendicular to the crack can be transmitted across it. However, as long as the crack is narrow, it can still transmit forces in its own plane through interlocking of the surface roughnesses. Sizable interlock forces V_i of this kind have in fact been measured, amounting to one-third and more of the total shear force. The components V_{ix} and V_{iy} of V_i are shown in Fig. 4.7a. The other

FIGURE 4.7

Forces at a diagonal crack in a beam without web reinforcement.



internal vertical forces are those in the uncracked portion of the concrete V_{cz} and across the longitudinal steel, acting as a dowel, V_d . Thus, the internal shear force is

$$V_{int} = V_{cz} + V_d + V_{iy}$$

Equilibrium requires that $V_{int} = V_{ext}$ so that the part of the shear resisted by the uncracked concrete is

$$V_{cz} = V_{ext} - V_d - V_{iy} \quad (4.4)$$

In a beam provided with longitudinal reinforcement only, the portion of the shear force resisted by the steel in dowel action is usually quite small. In fact, the reinforcing bars on which the dowel force V_d acts are supported against vertical displacement chiefly by the thin concrete layer below. The bearing pressure caused by V_d creates, in this concrete, vertical tension stresses as shown in Fig. 4.7b. Because of these stresses, diagonal cracks often result in splitting of the concrete along the tension reinforcement, as shown. (See also Fig. 4.1.) This reduces the dowel force V_d and also permits the diagonal crack to widen. This, in turn, reduces the interface force V_i and frequently leads to immediate failure.

Next consider moments about point a at the intersection of V_{cz} and C ; the external moment $M_{ext,a}$ acts at a and happens to be $R_l x_a - P_1(x_a - x_1)$ for the loading shown. The internal moment is

$$M_{int,a} = T_b z + V_d p - V_i m$$

Here p is the horizontal projection of the diagonal crack and m is the moment arm of the force V_i with respect to point a . The designation T_b for T is meant to emphasize that this force in the steel acts at point b rather than vertically below point a . Equilibrium requires that $M_{int,a} = M_{ext,a}$ so that the longitudinal tension in the steel at b is

$$T_b = \frac{M_{ext,a} - V_d p + V_i m}{z} \quad (4.5)$$

Neglecting the forces V_d and V_i , which decrease with increasing crack opening, one has, with very little error,

$$T_b = \frac{M_{ext,a}}{z} \quad (4.6)$$

The formation of the diagonal crack, then, is seen to produce the following redistribution of internal forces and stresses:

1. At the vertical section through point a , the average shear stress before crack formation was V_{ext}/bd . After crack formation, the shear force is resisted by a combination of the dowel shear, the interface shear, and the shear force on the much smaller area by of the remaining uncracked concrete. As tension splitting develops along the longitudinal bars, V_d and V_i decrease; this, in turn, increases the shear force and the resulting shear stress on the remaining uncracked concrete area.
2. The diagonal crack, as described previously, usually rises above the neutral axis and traverses some part of the compression zone before it is arrested by the compression stresses. Consequently, the compression force C also acts on an area by smaller than that on which it acted before the crack was formed. Correspondingly, formation of the crack has increased the compression stresses in the remaining uncracked concrete.
3. Prior to diagonal cracking, the tension force in the steel at point b was caused by, and was proportional to, the bending moment in a vertical section through the

same point b . As a consequence of the diagonal crack, however, Eq. (4.6) shows that the tension in the steel at b is now caused by, and is proportional to, the bending moment at a . Since the moment at a is evidently larger than that at b , formation of the crack has caused a sudden increase in the steel stress at b .

If the two materials are capable of resisting these increased stresses, equilibrium will establish itself after internal redistribution and further load can be applied before failure occurs. Such failure can then develop in various ways. For one, if only enough steel has been provided at b to resist the moment at that section, the increase of the steel force, described in item 3, will cause the steel to yield because of the larger moment at a , thus failing the beam. If the beam is properly designed to prevent this occurrence, it is usually the concrete at the head of the crack that will eventually crush. This concrete is subject simultaneously to large compression and shear stresses, and this biaxial stress combination is conducive to earlier failure than would take place if either of these stresses were acting alone. Finally, if there is splitting along the reinforcement, it will cause the bond between steel and concrete to weaken to such a degree that the reinforcement may pull loose. This either may be the cause of failure of the beam or may occur simultaneously with crushing of the remaining uncracked concrete.

It was noted earlier that relatively deep beams will usually show continued and increasing resistance after formation of a critical diagonal tension crack, but relatively shallow beams will fail almost immediately upon formation of the crack. The amount of reserve strength, if any, was found to be erratic. In fact, in several test series in which two specimens as identical as one can make them were tested, one failed immediately upon formation of a diagonal crack, while the other reached equilibrium under the described redistribution and failed at a higher load.

For this reason, this reserve strength is discounted in modern design procedures. As previously mentioned, most beams are furnished with at least a minimum of web reinforcement. For those flexural members that are not, such as slabs, footings, and others, design is based on that shear force V_{cr} or shear stress v_{cr} , at which formation of inclined cracks must be expected. Thus, Eq. (4.3a), or some equivalent of it, has become the design criterion for such members.

4.4 REINFORCED CONCRETE BEAMS WITH WEB REINFORCEMENT

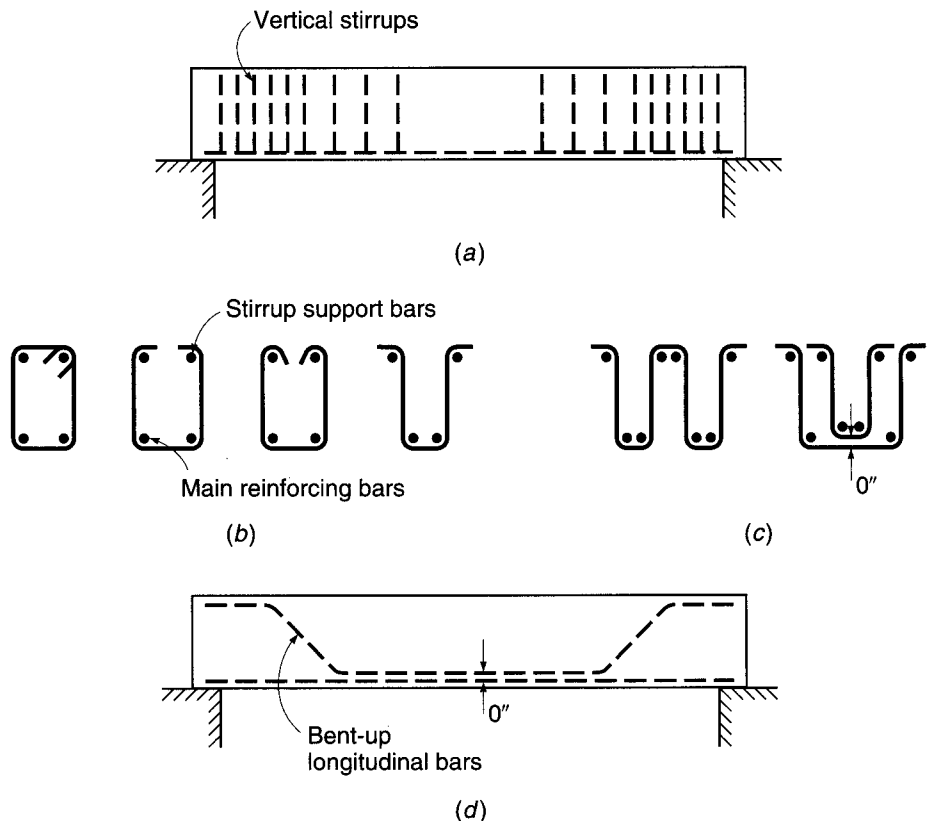
Economy of design demands, in most cases, that a flexural member be capable of developing its full moment capacity rather than having its strength limited by premature shear failure. This is also desirable because structures, if overloaded, should not fail in the sudden and explosive manner characteristic of many shear failures, but should show adequate ductility and warning of impending distress. The latter, as pointed out earlier, is typical of flexural failure caused by yielding of the longitudinal bars, which is preceded by gradual excessively large deflections and noticeable widening of cracks. Therefore, if a fairly large safety margin relative to the available shear strength as given by Eq. (4.3a) or its equivalent does not exist, special shear reinforcement, known as *web reinforcement*, is used to increase this strength.

a. Types of Web Reinforcement

Typically, web reinforcement is provided in the form of vertical *stirrups*, spaced at varying intervals along the axis of the beam depending on requirements, as shown in Fig. 4.8a. Relatively small bars are used, generally Nos. 3 to 5 (Nos. 10 to 16). Simple

FIGURE 4.8

Types of web reinforcement.



U-shaped bars similar to Fig. 4.8b are most common, although multiple-leg stirrups such as shown in Fig. 4.8c are sometimes necessary. Stirrups are formed to fit around the main longitudinal bars at the bottom and hooked or bent around longitudinal bars at the top of the member to improve anchorage and provide support during construction. Detailed requirements for anchorage of stirrups will be discussed in Chapter 5.

Alternatively, shear reinforcement may be provided by bending up a part of the longitudinal steel where it is no longer needed to resist flexural tension, as suggested by Fig. 4.8d. In continuous beams, these bent-up bars may also provide all or part of the necessary reinforcement for negative moments. The requirements for longitudinal flexural reinforcement often conflict with those for diagonal tension, and because the savings in steel resulting from use of the capacity of bent bars as shear resistance is small, most designers prefer to include vertical stirrups to provide for all the shear requirement, counting on the bent part of the longitudinal bars, if bent bars are used, only to increase the overall safety against diagonal tension failure.

Welded wire reinforcement is also used for shear reinforcement, particularly for small, lightly loaded members with thin webs, and for certain types of precast, prestressed beams.

b. Behavior of Web-Reinforced Concrete Beams

Web reinforcement has no noticeable effect prior to the formation of diagonal cracks. In fact, measurements show that the web steel is practically free of stress prior to crack

formation. After diagonal cracks have developed, web reinforcement augments the shear resistance of a beam in four separate ways:

1. Part of the shear force is resisted by the bars that traverse a particular crack. The mechanism of this added resistance is discussed below.
2. The presence of these same bars restricts the growth of diagonal cracks and reduces their penetration into the compression zone. This leaves more uncracked concrete available at the head of the crack for resisting the combined action of shear and compression, already discussed.
3. The stirrups also counteract the widening of the cracks, so that the two crack faces stay in close contact. This makes for a significant and reliable interface force V_i (see Fig. 4.7).
4. As shown in Fig. 4.8, the stirrups are arranged so that they tie the longitudinal reinforcement into the main bulk of the concrete. This provides some measure of restraint against the splitting of concrete along the longitudinal reinforcement, shown in Figs. 4.1 and 4.7b, and increases the share of the shear force resisted by dowel action.

From this it is clear that failure will be imminent when the stirrups start yielding. This not only exhausts their own resistance but also permits a wider crack opening with consequent reduction of the beneficial restraining effects, points 2 to 4, above.

It becomes clear from this description that member behavior, once a crack is formed, is quite complex and dependent in its details on the particulars of crack configuration (length, inclination, and location of the main or critical crack). The latter, in turn, is quite erratic and has so far defied purely analytical prediction. For this reason, the concepts that underlie present design practice are not wholly rational. They are based partly on rational analysis, partly on test evidence, and partly on successful long-time experience with structures in which certain procedures for designing web reinforcement have resulted in satisfactory performance.

BEAMS WITH VERTICAL STIRRUPS. Since web reinforcement is ineffective in the uncracked beam, the magnitude of the shear force or stress that causes cracking to occur is the same as in a beam without web reinforcement and is approximated by Eq. (4.3a). Most frequently, web reinforcement consists of *vertical stirrups*; the forces acting on the portion of such a beam between the crack and the nearby support are shown in Fig. 4.9. They are the same as those of Fig. 4.7, except that each stirrup traversing the crack exerts a force $A_v f_v$ on the given portion of the beam. Here A_v is the cross-sectional area of the stirrup (in the case of the U-shaped stirrup of Fig. 4.8b it is

FIGURE 4.9

Forces at a diagonal crack in a beam with vertical stirrups.

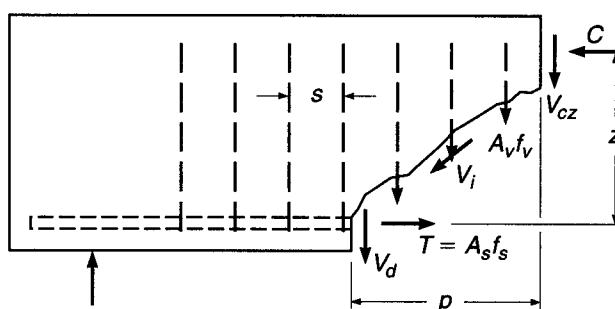
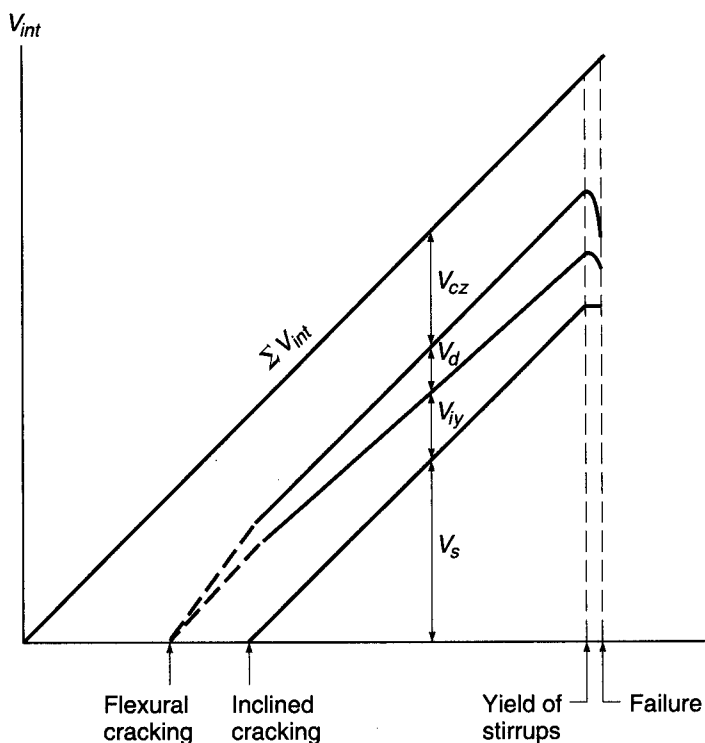


FIGURE 4.10

Redistribution of internal shear forces in a beam with stirrups. (Adapted from Ref. 4.3.)



twice the area of one bar), and f_v is the tensile stress in the stirrup. Equilibrium in the vertical direction requires

$$V_{\text{ext}} = V_{cz} + V_d + V_{iy} + V_s \quad (a)$$

where $V_s = nA_vf_v$ is the vertical force in the stirrups, n being the number of stirrups traversing the crack. If s is the stirrup spacing and p the horizontal projection of the crack, as shown, then $n = p/s$.

The approximate distribution of the four components of the internal shear force with increasing external shear V_{ext} is shown schematically in Fig. 4.10. It is seen that after inclined cracking, the portion of the shear $V_s = nA_vf_v$ carried by the stirrups increases linearly, while the sum of the three other components, $V_{cz} + V_d + V_{iy}$, stays nearly constant. When the stirrups yield, their contribution remains constant at the yield value $V_s = nA_vf_{yt}$, where f_{yt} represents the yield strength of the stirrup (or transverse) reinforcement. However, because of widening of the inclined cracks and longitudinal splitting, V_{iy} and V_d fall off rapidly. This overloads the remaining uncracked concrete and very soon precipitates failure.

While total shear carried by the stirrups at yielding is known, the individual magnitudes of the three other components are not. Limited amounts of test evidence have led to the conservative assumption in present-day methods that just prior to failure of a web-reinforced beam, the sum of these three internal shear components is equal to the cracking shear V_{cr} , as given by Eq. (4.3a). This sum is generally (somewhat loosely) referred to as the *contribution of the concrete* to the total shear resistance and is denoted V_c . Thus $V_c = V_{cr}$ and

$$V_c = V_{cz} + V_d + V_{iy} \quad (b)$$

The number of stirrups n spaced a distance s apart was seen to depend on the length p of the horizontal projection of the diagonal crack. This length is conservatively assumed to be equal to the effective depth of the beam; thus $n = d/s$, implying a crack somewhat flatter than 45° . Then, at failure, when $V_{\text{ext}} = V_n$, Eqs. (a) and (b) yield for the nominal shear strength

$$V_n = V_c + \frac{A_v f_y t}{s} d \quad (4.7a)$$

where V_c is taken equal to the cracking shear V_{cr} given by Eq. (4.3a); that is,

$$V_c = \left(1.9 \sqrt{f'_c} + 2500 \frac{\rho V d}{M} \right) b d \leq 3.5 \sqrt{f'_c} b d \quad (4.3a)$$

Dividing both sides of Eq. (4.7a) by $b d$, the same relation is expressed in terms of the nominal shear stress:

$$\nu_n = \frac{V_n}{b d} = \nu_c + \frac{A_v f_y}{b s} \quad (4.7b)$$

In Ref. 4.1, the results of 166 beam tests are compared with Eq. (4.7b). It is shown that the equation predicts the actual shear strength quite conservatively, the observed strength being on average 45 percent larger than predicted; a very few of the individual test beams developed strength just slightly below that of Eq. (4.7b).

BEAMS WITH INCLINED BARS. The function of *inclined web reinforcement* (Fig. 4.8d) can be discussed in very similar terms. Figure 4.11 again indicates the forces that act on the portion of the beam to one side of the diagonal crack that results in eventual failure. The crack with horizontal projection p and inclined length $i = p/\cos \theta$ is crossed by inclined bars horizontally spaced a distance s apart. The inclination of the bars is α and that of the crack θ , as shown. The distance between bars measured parallel to the direction of the crack is seen from the irregular triangle to be

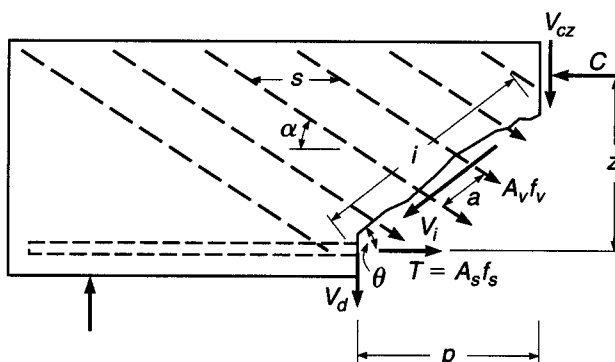
$$a = \frac{s}{\sin \theta (\cot \theta + \cot \alpha)} \quad (a)$$

The number of bars crossing the crack $n = i/a$, after some transformation, is

$$n = \frac{p}{s} (1 + \cot \alpha \tan \theta) \quad (b)$$

FIGURE 4.11

Forces at a diagonal crack in a beam with inclined web reinforcement.



The vertical component of the force in one bar or stirrup is $A_v f_v \sin \alpha$, so that the total vertical component of the forces in all bars that cross the crack is

$$V_s = n A_v f_v \sin \alpha = A_v f_v \frac{P}{s} (\sin \alpha + \cos \alpha \tan \theta) \quad (4.8)$$

As in the case of vertical stirrups, shear failure occurs when the stress in the web reinforcement reaches the yield point. Also, the same assumptions are made as in the case of stirrups, namely, that the horizontal projection of the diagonal crack is equal to the effective depth d , and that $V_{cz} + V_d + V_{iy}$ is equal to V_c . Lastly, the inclination θ of the diagonal crack, which varies somewhat depending on various influences, is generally assumed to be 45° . On this basis, when failure is caused by shear, the nominal strength is

$$V_n = V_c + \frac{A_v f_y t d (\sin \alpha + \cos \alpha)}{s} \quad (4.9)$$

It is seen that Eq. (4.7a), developed for vertical stirrups, is only a special case, for $\alpha = 90^\circ$, of the more general expression (4.9).

Note that Eqs. (4.7) and (4.9) apply only if web reinforcement is so spaced that any conceivable diagonal crack is traversed by at least one stirrup or inclined bar. Otherwise web reinforcement would not contribute to the shear strength of the beam, because diagonal cracks that could form between widely spaced web reinforcement would fail the beam at the load at which it would fail if no web reinforcement were present. This imposes upper limits on the permissible spacing s to ensure that the web reinforcement is actually effective as calculated.

To summarize, at this time the nature and mechanism of diagonal tension failure are clearly understood qualitatively, but some of the quantitative assumptions that have been made in the preceding development cannot be proved by rational analysis. However, the calculated results are in acceptable and generally conservative agreement with a very large body of empirical data, and structures designed on this basis have proved satisfactory. Newer methods, introduced in Section 4.8, provide alternatives that are slowly being incorporated into the ACI Code and the AASHTO Bridge Specifications (Ref. 4.12). Chapter 10 presents a detailed description of one such alternative, the so-called strut-and-tie model, which appears in Appendix A of the 2008 ACI Code.

4.5 ACI CODE PROVISIONS FOR SHEAR DESIGN

According to ACI Code 11.1.1, the design of beams for shear is to be based on the relation

$$V_u \leq \phi V_n \quad (4.10)$$

where V_u is the total shear force applied at a given section of the beam due to factored loads and $V_n = V_c + V_s$ is the nominal shear strength, equal to the sum of the contributions of the concrete and the web steel if present. Thus for vertical stirrups

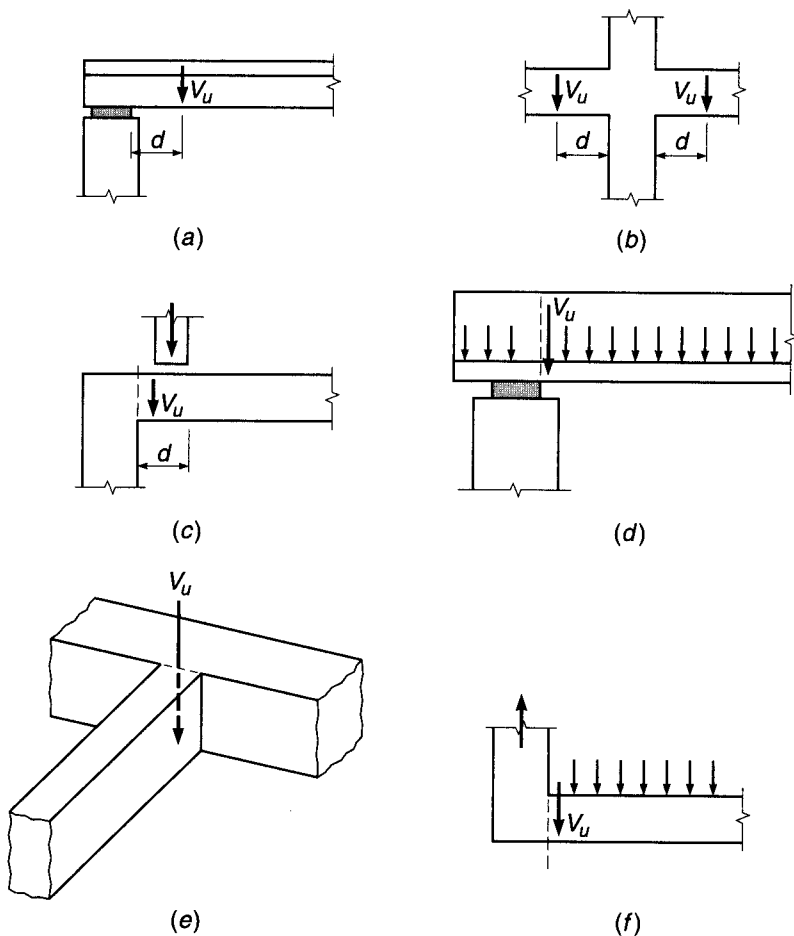
$$V_u \leq \phi V_c + \frac{\phi A_v f_y t d}{s} \quad (4.11a)$$

and for inclined bars

$$V_u \leq \phi V_c + \frac{\phi A_v f_y t d (\sin \alpha + \cos \alpha)}{s} \quad (4.11b)$$

FIGURE 4.12

Location of critical section for shear design: (a) end-supported beam; (b) beam supported by columns; (c) concentrated load within d of the face of the support; (d) member loaded near the bottom; (e) beam supported by girder of similar depth; (f) beam supported by monolithic vertical element.



where all terms are as previously defined. The strength reduction factor ϕ is to be taken equal to 0.75 for shear. The additional conservatism, compared with the value of $\phi = 0.90$ for bending for typical beam designs, reflects both the sudden nature of diagonal tension failure and the large scatter of test results.

For typical support conditions, where the reaction from the support surface or from a monolithic column introduces vertical compression at the end of the beam, sections located less than a distance d from the face of the support may be designed for the same shear V_u as that computed at a distance d , as shown in Fig. 4.12a and b. However, the critical design section should be taken at the face of the support if concentrated loads act within that distance (Fig. 4.12c), if the beam is loaded near its bottom edge (as may occur for an inverted T beam, as shown in Fig. 4.12d), or if the reaction causes vertical tension rather than compression [e.g., if the beam is supported by a girder of similar depth (Fig. 4.12e) or at the end of a monolithic vertical element (Fig. 4.12f)].

a. Shear Strength Provided by the Concrete

The nominal shear strength contribution of the concrete (including the contributions from aggregate interlock, dowel action of the main reinforcing bars, and that of the uncracked concrete) is basically the same as Eq. (4.3a) with slight notational changes.

To permit application of Eq. (4.3a) to T beams having web width b_w , the rectangular beam width b is replaced by b_w with the understanding that for rectangular beams b is used for b_w . For T beams with a tapered web width, such as typical concrete joists, the average web width is used, unless the narrowest part of the web is in compression, in which case b_w is taken as the minimum width. Further, in Eq. (4.3a), the shear V and moment M are designated V_u and M_u to emphasize that they are the values computed at factored loads. Thus, for members subject to shear and flexure, according to ACI Code 11.2.2, the concrete contribution to shear strength is

$$V_c = \left(1.9\lambda\sqrt{f'_c} + 2500 \frac{\rho_w V_u d}{M_u} \right) b_w d \leq 3.5\lambda\sqrt{f'_c} b_w d \quad (4.12a)$$

where ρ_w = longitudinal reinforcement ratio $A_s/b_w d$ or A_s/bd . With the section dimension b_w and d in inches and $V_u d$ and M_u in consistent units, V_c is expressed in pounds. In Eq. (4.12a), the quantity $V_u d/M_u$ is not to be taken greater than 1.0.

The term λ in Eq. (4.12a) is a modification factor reflecting the lower tensile strength of lightweight concrete compared with normalweight concrete of the same compressive strength (see Table 2.2 and Ref. 4.13). Lightweight aggregate concretes having densities from 90 to 120 pcf are used widely, particularly for precast elements. In accordance with ACI Code 8.6.1, $\lambda = 0.85$ for "sand-lightweight" concrete and 0.75 for "all-lightweight" concrete. Linear interpolation between 0.75 and 0.85, based on volumetric fractions, is permitted when a portion of the lightweight fine aggregate is replaced by normalweight fine aggregate. Linear interpolation between 0.85 and 1.0 is also permitted for concretes containing normalweight fine aggregate and a blend of lightweight and normalweight coarse aggregate. If the average split-cylinder strength of lightweight concrete (a good measure of its direct tensile strength) is specified, $\lambda = f_{ct}/(6.7\sqrt{f'_c}) \leq 1.0$. For normalweight concert, $\lambda = 1.0$.

While Eq. (4.12a) is perfectly well suited to computerized design or for research, for manual calculations its use is tedious because ρ_w , V_u , and M_u generally change along the span, requiring that V_c be calculated at frequent intervals. For this reason, an alternative equation for V_c is permitted by ACI Code 11.2.1:

$$V_c = 2\lambda\sqrt{f'_c} b_w d \quad (4.12b)$$

Referring to Fig. 4.6, it is clear that Eq. (4.12b) is very conservative in regions where the shear-moment ratio is high, such as near the ends of simple spans or near the inflection points of continuous spans; however, because of its simplicity, it is often used in practice.

For members with a circular cross section, ACI Code 11.2.3 provides that the area used to calculate V_c in Eqs. (4.12a) and (4.12b) be the product of the diameter and the effective depth. The latter may be taken as 0.8 times the diameter of the member.

The tests on which Eqs. (4.12a) and (4.12b) are based used beams with concrete compressive strength mostly in the range of 3000 to 5000 psi. More recent experimental results (Refs. 4.14 to 4.17) have shown that in beams constructed using high-strength concrete (see Section 2.12) with f'_c above 6000 psi, the concrete contribution to shear strength V_c is less than predicted by those equations. Differences become increasingly significant, the higher the concrete strength. For this reason, ACI Code 11.1.2 places an upper limit of 100 psi on the value of $\sqrt{f'_c}$ to be used in Eqs. (4.12a) and (4.12b), as well as in all other ACI Code shear provisions. However, values of $\sqrt{f'_c}$ greater than 100 psi may be used in computing V_c if a minimum amount of web reinforcement is used (see Section 4.5b).

b. Minimum Web Reinforcement

If V_u , the shear force at factored loads, is no larger than ϕV_c , calculated by Eq. (4.12a) or alternatively by Eq. (4.12b), then theoretically no web reinforcement is required. Even in such a case, however, ACI Code 11.4.6 requires provision of at least a minimum area of web reinforcement equal to

$$A_{v,\min} = 0.75 \sqrt{f'_c} \frac{b_w s}{f_{yt}} \geq 50 \frac{b_w s}{f_{yt}} \quad (4.13)$$

where s = longitudinal spacing of web reinforcement, in.

f_{yt} = yield strength of web steel, psi

$A_{v,\min}$ = total cross-sectional area of web steel within distance s , in²

This provision holds unless V_u is one-half or less of the design shear strength provided by the concrete ϕV_c . Specific exceptions to this requirement for minimum web steel are made for slabs and footings; for concrete joist floor construction; for beams with total depth h not greater than 10 in.; and for beams integral with slabs with h not greater than 24 in. and not greater than the larger of 2.5 times the thickness of the flange and 0.5 times the thickness of the web. These members are excluded because of their capacity to redistribute internal forces before diagonal tension failure, as confirmed by both tests and successful design experience. In addition, beams constructed of steel fiber reinforced, normalweight concrete with f'_c not exceeding 6000 psi, total depth h not greater than 24 in., and V_u not greater than $\phi 2\sqrt{f'_c} b_w d$ are not required to meet the requirements for minimum web reinforcement because beams meeting these requirements have been shown to have shear strength in excess of $3.5\sqrt{f'_c} b_w d$ (Ref. 4.18).†

For high-strength concrete beams, the limitation of 100 psi imposed on the value of $\sqrt{f'_c}$ used in calculating V_c by Eq. (4.12a) or (4.12b) is waived by ACI Code 11.1.2.1 if such beams are designed with minimum web reinforcement equal to the amount required by Eq. (4.13). In this case, the concrete contribution to shear strength may be calculated based on the full concrete compressive strength. Tests described in Refs. 4.14 and 4.17 indicate that for beams with concrete strength above about 6000 psi, the concrete contribution V_c was significantly less than predicted by the ACI Code equations, although the steel contribution V_s was higher. The total nominal shear strength V_n was greater than predicted by ACI Code methods in all cases. The use of minimum web steel for high-strength concrete beams is intended to enhance the post-cracking capacity, thus resulting in safe designs even though the concrete contribution to shear strength is overestimated.‡

EXAMPLE 4.1

Beam without web reinforcement. A rectangular beam is to be designed to carry a shear force V_u of 27 kips. No web reinforcement is to be used, and f'_c is 4000 psi. What is the minimum cross section if controlled by shear?

† To qualify, the fiber-reinforced concrete must conform to requirements in ACI Code 5.6.6.2 that specify a minimum deformed steel fiber content of 100 lb/yd³ and minimum residual flexural strength values when the concrete is tested in accordance with ASTM C1609, "Standard Test Method for Flexural Performance of Fiber-Reinforced Concrete (Using Beam with Third-Point Loading)."

‡ The shortcomings of the ACI Code " $V_c + V_s$ " approach to shear design, particularly the provisions relating to the concrete contribution V_c , have provided motivation for the development of more rational procedures, as will be discussed in Section 4.8.

SOLUTION. If no web reinforcement is to be used, the cross-sectional dimensions must be selected so that the applied shear V_u is no larger than one-half the design shear strength ϕV_c . The calculations will be based on Eq. (4.12b). Thus,

$$V_u = \frac{1}{2} \phi (2\lambda \sqrt{f'_c} b_w d)$$

$$b_w d = \frac{27,000}{0.75 \times 1.0 \sqrt{4000}} = 569 \text{ in}^2$$

A beam with $b_w = 18$ in. and $d = 32$ in. is required. Alternately, if the minimum amount of web reinforcement given by Eq. (4.13) is used, the concrete shear resistance may be taken at its full value ϕV_c , and it is easily confirmed that a beam with $b_w = 12$ in. and $d = 24$ in. will be sufficient.

c. Region in Which Web Reinforcement Is Required

If the required shear strength V_u is greater than the design shear strength ϕV_c provided by the concrete in any portion of a beam, there is a theoretical requirement for web reinforcement. Elsewhere in the span, web steel at least equal to the amount given by Eq. (4.13) must be provided, unless the factored shear force is less than $\frac{1}{2}\phi V_c$.

The portion of any span through which web reinforcement is theoretically necessary can be found from the shear diagram for the span, superimposing a plot of the shear strength of the concrete. Where the shear force V_u exceeds ϕV_c , shear reinforcement must provide for the excess. The additional length through which at least the minimum web steel is needed can be found by superimposing a plot of $\phi V_c/2$.

EXAMPLE 4.2

Limits of web reinforcement. A simply supported rectangular beam 16 in. wide having an effective depth of 22 in. carries a total factored load of 9.4 kips/ft on a 20 ft clear span. It is reinforced with 7.62 in^2 of tensile steel, which continues uninterrupted into the supports. If $f'_c = 4000$ psi, throughout what part of the beam is web reinforcement required?

SOLUTION. The maximum external shear force occurs at the ends of the span, where $V_u = 9.4 \times 20/2 = 94$ kips. At the critical section for shear, a distance d from the support, $V_u = 94 - 9.4 \times 1.83 = 76.8$ kips. The shear force varies linearly to zero at midspan. The variation of V_u is shown in Fig. 4.13a. Adopting Eq. (4.12b) gives

$$V_c = 2\lambda \sqrt{f'_c} b_w d = 2 \times 1.0 \sqrt{4000} \times 16 \times 22 = 44,500 \text{ lb}$$

Hence $\phi V_c = 0.75 \times 44.5 = 33.4$ kips. This value is superimposed on the shear diagram, and, from geometry, the point at which web reinforcement theoretically is no longer required is

$$10 \left(\frac{94.0 - 33.4}{94.0} \right) = 6.45 \text{ ft}$$

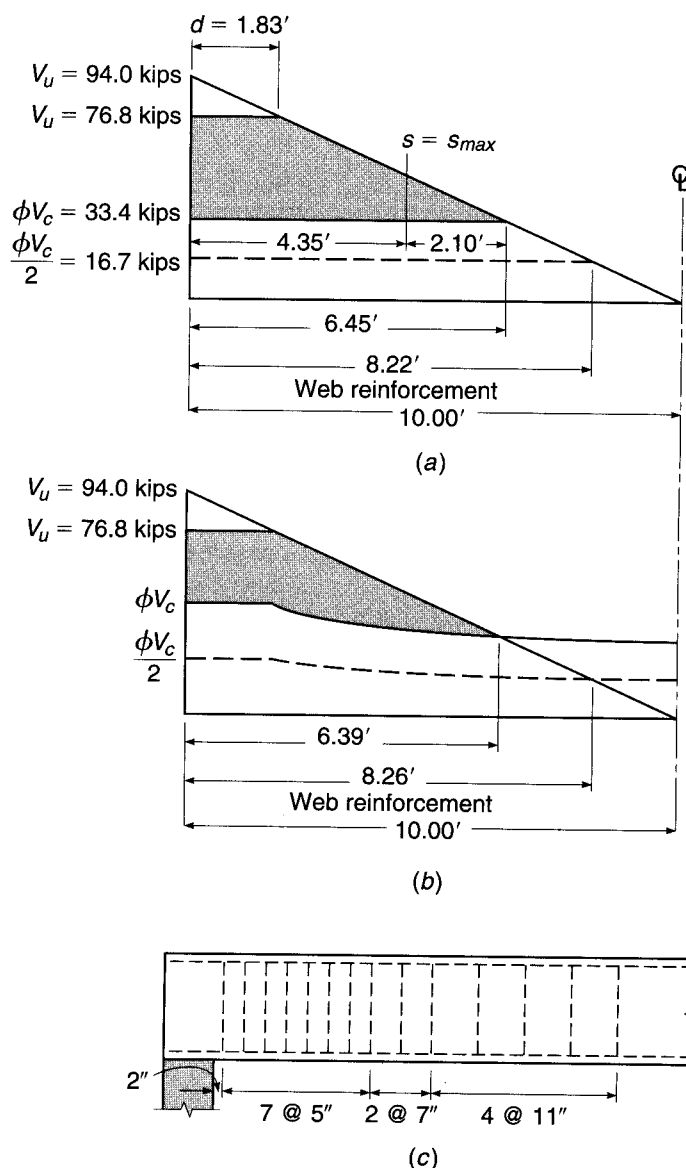
from the support face. However, according to the ACI Code, at least a minimum amount of web reinforcement is required wherever the shear force exceeds $\phi V_c/2$, or 16.7 kips in this case. As seen from Fig. 4.13a, this applies to a distance

$$10 \left(\frac{94.0 - 16.7}{94.0} \right) = 8.22 \text{ ft}$$

from the support face. To summarize, at least the minimum web steel must be provided within a distance of 8.22 ft from the supports, and within 6.45 ft the web steel must provide for the shear force corresponding to the shaded area.

FIGURE 4.13

Shear design example.



If the alternative Eq. (4.12a) is used, the variation along the span of ρ_w , V_u , and M_u must be known so that V_c can be calculated. This is shown in tabular form in Table 4.1.

The factored shear V_u and the design shear capacity ϕV_c are plotted in Fig. 4.13b. From the graph it is found that stirrups are theoretically no longer required 6.39 ft from the support face. However, from the plot of $\phi V_c/2$ it is found that at least the minimum web steel is to be provided within a distance of 8.26 ft.

When Figs. 4.13a and b are compared, it is evident that the length over which web reinforcement is needed is nearly the same for this example whether Eq. (4.12a) or (4.12b) is used. However, the smaller shaded area of Fig. 4.13b indicates that substantially less web-steel area would be needed within that required distance if the more accurate Eq. (4.12a) were adopted.

TABLE 4.1
Shear design example

Distance from Support, ft	M_u , ft-kips	V_u , kips	V_c^a	ϕV_c
0	0	94.0	61.3	46.0
1	89	84.6	61.3	46.0
2	169	75.2	57.8	43.4
3	240	65.8	51.9	38.9
4	301	56.4	48.8	36.6
5	353	47.0	47.0	35.2
6	395	37.6	45.6	34.2
7	428	28.2	44.6	33.5
8	451	18.8	43.8	32.8
9	465	9.4	43.0	32.3
10	470	0	42.3	31.7

$$^a V_c = (1.9\lambda\sqrt{f'_c} + 2500\rho_w V_u d / M_u) b_w d \leq 3.5\lambda\sqrt{f'_c} b_w d \text{ and } V_u d / M_u \leq 1.0$$

d. Design of Web Reinforcement

The design of web reinforcement, under the provisions of the ACI Code, is based on Eq. (4.11a) for vertical stirrups and Eq. (4.11b) for inclined stirrups or bent bars. In design, it is usually convenient to select a trial web-steel area A_v , based on standard stirrup sizes [usually in the range from No. 3 to 5 (No. 10 to 16) for stirrups, and according to the longitudinal bar size for bent-up bars], for which the required spacing s can be found. Equating the design strength ϕV_n to the required strength V_u and transposing Eqs. (4.11a) and (4.11b) accordingly, one finds that the required spacing of web reinforcement is, for vertical stirrups,

$$s = \frac{\phi A_v f_{yt} d}{V_u - \phi V_c} \quad (4.14a)$$

and for bent bars

$$s = \frac{\phi A_v f_{yt} d (\sin \alpha + \cos \alpha)}{V_u - \phi V_c} \quad (4.14b)$$

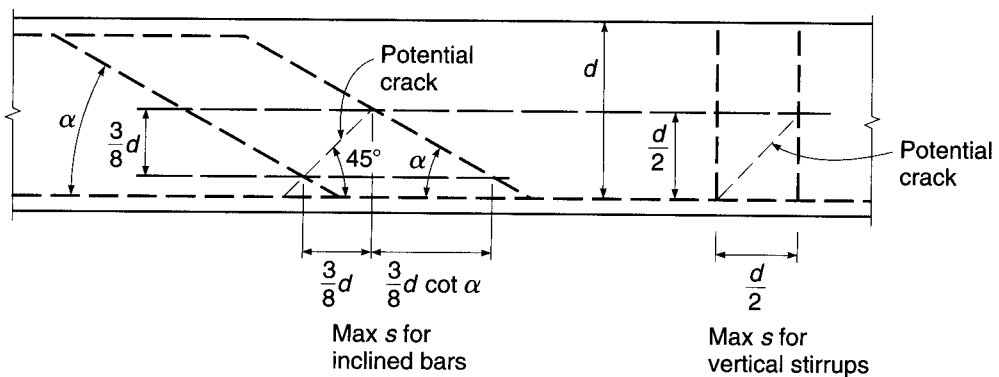
It should be emphasized that when conventional U stirrups such as in Fig. 4.8b are used, the web area A_v provided by each stirrup is *twice* the cross-sectional area of the bar; for stirrups such as those of Fig. 4.8c, A_v is 4 times the area of the bar used. Equation (4.14a) is applicable to members with circular, as well as rectangular, cross sections. For circular members, d is taken as the effective depth, as defined earlier in Section 4.5a, and A_v is taken as 2 times the area of the bar, hoop, or spiral.

While the ACI Code requires only that the inclined part of a bent bar make an angle of at least 30° with the longitudinal part, bars are usually bent at a 45° angle. Only the center three-fourths of the inclined part of any bar is to be considered effective as web reinforcement.

It is undesirable to space vertical stirrups closer than about 4 in.; the size of the stirrups should be chosen to avoid a closer spacing. When vertical stirrups are required over a comparatively short distance, it is good practice to space them uniformly over the entire distance, the spacing being calculated for the point of greatest shear

FIGURE 4.14

Maximum spacing of web reinforcement as governed by diagonal crack interception.



(minimum spacing). If the web reinforcement is required over a long distance, and if the shear varies materially throughout this distance, it is more economical to compute the spacings required at several sections and to place the stirrups accordingly, in groups of varying spacing.

Where web reinforcement is needed, the Code requires it to be spaced so that every 45° line, representing a potential diagonal crack and extending from the middepth $d/2$ of the member to the longitudinal tension bars, is crossed by at least one line of web reinforcement; in addition, the Code specifies a maximum spacing of 24 in. When V_s exceeds $4\sqrt{f'_c} b_w d$, these maximum spacings are halved. These limitations are shown in Fig. 4.14 for both vertical stirrups and inclined bars, for situations in which the excess shear does not exceed the stated limit.

For design purposes, Eq. (4.13) giving the minimum web-steel area A_v is more conveniently inverted to permit calculation of maximum spacing s for the selected A_v . Thus, for the usual case of vertical stirrups, with $V_s \leq 4\sqrt{f'_c} b_w d$, the maximum spacing of stirrups is the smallest of

$$s_{\max} = \frac{A_v f_{yt}}{0.75 \sqrt{f'_c} b_w} \leq \frac{A_v f_{yt}}{50 b_w} \quad (4.15a)$$

$$s_{\max} = \frac{d}{2} \quad (4.15b)$$

$$s_{\max} = 24 \text{ in.} \quad (4.15c)$$

For longitudinal bars bent at 45° , Eq. (4.15b) is replaced by $s_{\max} = 3d/4$, as confirmed by Fig. 4.14.

To avoid excessive crack width in beam webs, the ACI Code limits the yield strength of the reinforcement to $f_{yt} = 60,000$ psi or less for reinforcing bars and 80,000 psi or less for welded wire reinforcement. In no case, according to the ACI Code, is V_s to exceed $8\sqrt{f'_c} b_w d$, regardless of the amount of web steel used.

EXAMPLE 4.3

Design of web reinforcement. Using vertical U stirrups with $f_{yt} = 60,000$ psi, design the web reinforcement for the beam in Example 4.2.

SOLUTION. The solution will be based on the shear diagram in Fig. 4.13a. The stirrups must be designed to resist that part of the shear shown shaded. With No. 3 (No. 10) stirrups used for trial, the three maximum spacing criteria are first applied. For $\phi V_s = V_u - \phi V_c = 43,400$ lb,

which is less than $4\phi\sqrt{f'_c}b_wd = 66,800$ lb, the maximum spacing must exceed neither $d/2 = 11$ in. nor 24 in. Also, from Eq. (4.15a),

$$s_{\max} = \frac{A_v f_{yt}}{0.75\sqrt{f'_c} b_w} = \frac{0.22 \times 60,000}{0.75\sqrt{4000} \times 16} = 17.4 \text{ in.}$$

$$\leq \frac{A_v f_{yt}}{50b_w} = \frac{0.22 \times 60,000}{50 \times 16} = 16.5 \text{ in.}$$

The first criterion controls in this case, and a maximum spacing of 11 in. is imposed. From the support to a distance d from the support, the excess shear $V_u - \phi V_c$ is 43,400 lb. In this region, the required spacing is

$$s = \frac{\phi A_v f_{yt} d}{V_u - \phi V_c} = \frac{0.75 \times 0.22 \times 60,000 \times 22}{43,400} = 5.0 \text{ in.}$$

This is neither so small that placement problems would result nor so large that maximum spacing criteria would control, and the choice of No. 3 (No. 10) stirrups is confirmed. Solving Eq. (4.14a) for the excess shear at which the maximum spacing can be used gives

$$V_u - \phi V_c = \frac{\phi A_v f_{yt} d}{s} = \frac{0.75 \times 0.22 \times 60,000 \times 22}{11} = 19,800 \text{ lb}$$

With reference to Fig. 4.13a, this is attained at a distance x_1 from the point of zero excess shear, where $x_1 = 6.45 \times 19,800/60,600 = 2.10$ ft. This is 4.35 ft from the support face. With this information, a satisfactory spacing pattern can be selected. The first stirrup is usually placed at a distance $s/2$ from the support. The following spacing pattern is satisfactory:

1 space at 2 in. = 2 in.

7 spaces at 5 in. = 35 in.

2 spaces at 7 in. = 14 in.

4 spaces at 11 in. = 44 in.

Total = 95 in. = 7 ft 11 in.

The resulting stirrup pattern is shown in Fig. 4.13c. As an alternative solution, it is possible to plot a curve showing required spacing as a function of distance from the support. Once the required spacing at some reference section, say at the support, is determined,

$$s_0 = \frac{0.75 \times 0.22 \times 60,000 \times 22}{94,000 - 33,400} = 3.59 \text{ in.}$$

it is easy to obtain the required spacings elsewhere. In Eq. (4.14a), only $V_u - \phi V_c$ changes with distance from the support. For uniform load, this quantity is a linear function of distance from the point of zero excess shear, 6.45 ft from the support face. Hence, at 1 ft intervals,

$$s_1 = 3.59 \times 6.45/5.45 = 4.25 \text{ in.}$$

$$s_2 = 3.59 \times 6.45/4.45 = 5.20 \text{ in.}$$

$$s_3 = 3.59 \times 6.45/3.45 = 6.70 \text{ in.}$$

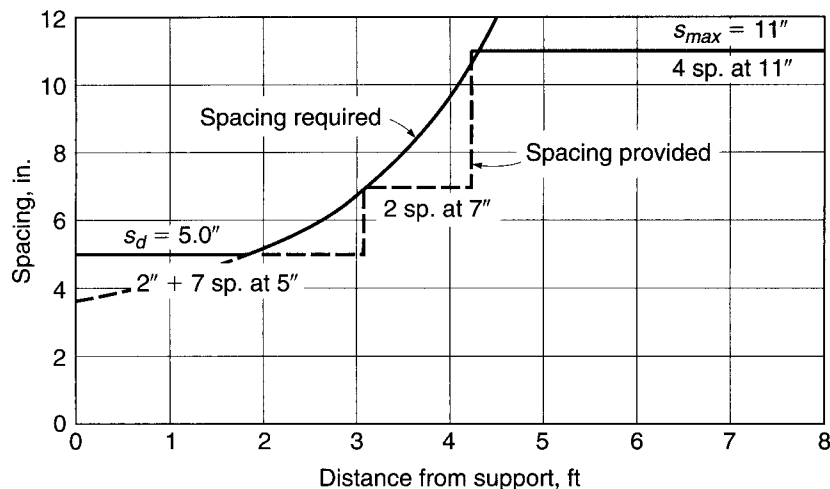
$$s_4 = 3.59 \times 6.45/2.45 = 9.45 \text{ in.}$$

$$s_5 = 3.59 \times 6.45/1.45 = 15.97 \text{ in.}$$

This is plotted in Fig. 4.15 together with the maximum spacing of 11 in., and a practical spacing pattern is selected. The spacing at a distance d from the support face is selected as the minimum

FIGURE 4.15

Required stirrup spacings for Example 4.3.



requirement, in accordance with the ACI Code. The pattern of No. 3 (No. 10) U-shaped stirrups selected (shown on the graph) is identical with the previous solution. In most cases, the experienced designer would find it unnecessary actually to plot the spacing diagram of Fig. 4.15 and would select a spacing pattern directly after calculating the required spacing at intervals along the beam.

If the web steel were to be designed on the basis of the excess-shear diagram in Fig. 4.13b, the second approach illustrated above would necessarily be selected, and spacings would be calculated at intervals along the span. In this particular case, a spacing of 7.07 in. is calculated up to 20 in. from the face of the support. The calculated spacing drops to 6.76 in. at d from the face of the support, and then increases to 11 in., the maximum permissible spacing, 4 ft from the support. The following practical spacing could be used:

$$1 \text{ space at 3 in.} = 3 \text{ in.}$$

$$6 \text{ spaces at 7 in.} = 42 \text{ in.}$$

$$4 \text{ spaces at 11 in.} = 44 \text{ in.}$$

$$\text{Total} = 89 \text{ in.} = 7 \text{ ft 5 in.}$$

Thus, 11 No. 3 (No. 10) stirrups would be used, rather than the 14 previously calculated, in each half of the span.

The number of stirrups just calculated represents the minimum for each of the two expressions for V_c . Although not required by the ACI Code, it is good design practice to continue the stirrups (at maximum spacing) through the middle region of the beam, even though the calculated shear is low. Doing so satisfies the dual purposes of providing continuing support for the top longitudinal reinforcement that is required wherever stirrups are used and providing additional shear capacity in the region to handle load cases not considered in developing the shear diagram. If this were done, the number of stirrups would increase from 14 and 11 to $16\frac{1}{2}$ and $13\frac{1}{2}$ per half-span (i.e., one stirrup at midspan), respectively.

4.6 EFFECT OF AXIAL FORCES

The beams considered in the preceding sections were subjected to shear and flexure only. Reinforced concrete beams may also be subjected to axial forces, acting simultaneously with shear and flexure, due to a variety of causes. These include external

axial loads, longitudinal prestressing, and restraint forces introduced as a result of shrinkage of the concrete or temperature changes. Beams may have their strength in shear significantly modified in the presence of axial tension or compression, as is evident from a review of Sections 4.1 through 4.4.

Prestressed concrete members are treated by somewhat specialized methods, according to present practice, based largely on results of testing prestressed concrete beams. They will be considered separately in Chapter 19, and only nonprestressed reinforced concrete beams will be treated here.

The main effect of axial load is to modify the diagonal cracking load of the member. It was shown in Section 4.3 that diagonal tension cracking will occur when the principal tensile stress in the web of a beam, resulting from combined action of shear and bending, reaches the tensile strength of the concrete. It is clear that the introduction of longitudinal force, which modifies the magnitude and direction of the principal tensile stresses, may significantly alter the diagonal cracking load. Axial compression will increase the cracking load, while axial tension will decrease it.

For members carrying only flexural and shear loading, the shear force at which diagonal cracking occurs V_{cr} is predicted by Eq. (4.3a), based on a combination of theory and experimental evidence. Furthermore, for reasons that were explained in Section 4.4b, in beams with web reinforcement, the contribution of the concrete to shear strength V_c is taken equal to the diagonal cracking load V_{cr} . Thus, according to the ACI Code, the concrete contribution is calculated by Eq. (4.12a) or (4.12b). For members carrying flexural and shear loading plus axial loads, V_c can be calculated by suitable modifications of these equations as follows.

a. Axial Compression

In developing Eq. (4.3a) for V_{cr} , it was pointed out that the diagonal cracking load depends on the ratio of shear stress v to bending stress f at the top of the flexural crack. While these stresses were never actually determined, they were conveniently expressed as

$$v = K_1 \left(\frac{V}{bd} \right) \quad (a)$$

and

$$f = K_2 \left(\frac{M}{bd^2} \right) \quad (b)$$

Equation (a) relates the concrete shear stress at the top of the flexural crack to the average shear stress; Eq. (b) can be used to relate the flexural tension in the concrete at the top of the crack to the tension in the flexural steel, through the modular ratio $n = E_s/E_c$, as follows:

$$f = K_0 \frac{f_s}{n} = K_0 \frac{M}{nA_s jd}$$

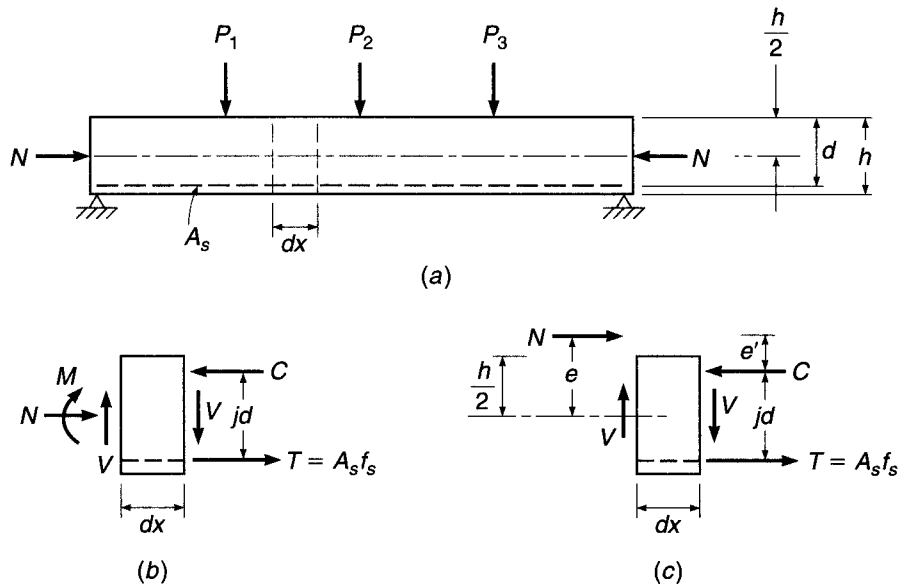
or

$$f = K_0 \frac{M}{n\rho j bd^2} \quad (c)$$

where jd is the internal lever arm between C and T , and K_0 is an unknown constant. Thus, the previous constant K_2 is equal to $K_0/n\rho j$.

FIGURE 4.16

Beams subject to axial compression plus bending and shear loads.



Now consider a beam subject to axial compression N as well as M and V , as shown in Fig. 4.16a. In Fig. 4.16b, the external moment, shear, and thrust acting on the left side of a small element of the beam, having length dx , are equilibrated by the internal stress resultants T , C , and V acting on the right. It is convenient to replace the external loads M and N with the statically equivalent load N acting at eccentricity $e = M/N$ from the middepth, as shown in Fig. 4.16c. The lever arm of the eccentric force N with respect to the compressive resultant C is

$$e' = e + d - \frac{h}{2} - jd \quad (d)$$

The steel stress f_s can now be found taking moments about the point of application of C .

$$f_s = \frac{Ne'}{A_s jd}$$

from which

$$f_s = \frac{M + N(d - h/2 - jd)}{A_s jd}$$

Noting that j is very close to $\frac{7}{8}$ for loads up to that producing diagonal cracking, the term in parentheses in the last equation above can be written as $(d - 4h)/8$. Then with $f = K_0 f_s/n$ as before, the concrete tensile stress at the head of the flexural crack is

$$f = K_0 \frac{M - N(4h - d)/8}{n \rho j b d^2} = K_2 \frac{M - N(4h - d)/8}{b d^2} \quad (e)$$

Comparing Eq. (e) with Eqs. (c) and (b) makes it clear that the previous derivation for flexural tension f holds for the present case including axial loads if a modified moment $M - N(4h - d)/8$ is substituted for M . It follows that Eq. (4.3a) can be used to calculate V_{cr} with the same substitution of modified for actual moment.

The ACI Code provisions are based on this development. The concrete contribution to shear strength V_c is taken equal to V_{cr} and is given by Eq. (4.12a) as before:

$$V_c = \left(1.9\lambda\sqrt{f'_c} + 2500 \frac{\rho_w V_u d}{M_u} \right) b_w d \quad (4.12a)$$

except that the modified moment

$$M_m = M_u - N_u \frac{4h - d}{8} \quad (4.16)$$

is to be substituted for M_u and $V_u d/M_u$ need not be limited to 1.0 as before. The thrust N_u is to be taken positive for compression. For beams with axial compression, the upper limit of $3.5\lambda\sqrt{f'_c} b_w d$ is replaced by

$$V_c = 3.5\lambda\sqrt{f'_c} b_w d \sqrt{1 + \frac{N_u}{500A_g}} \quad (4.17)$$

where A_g is the gross area of the concrete and N_u/A_g is expressed in psi units.

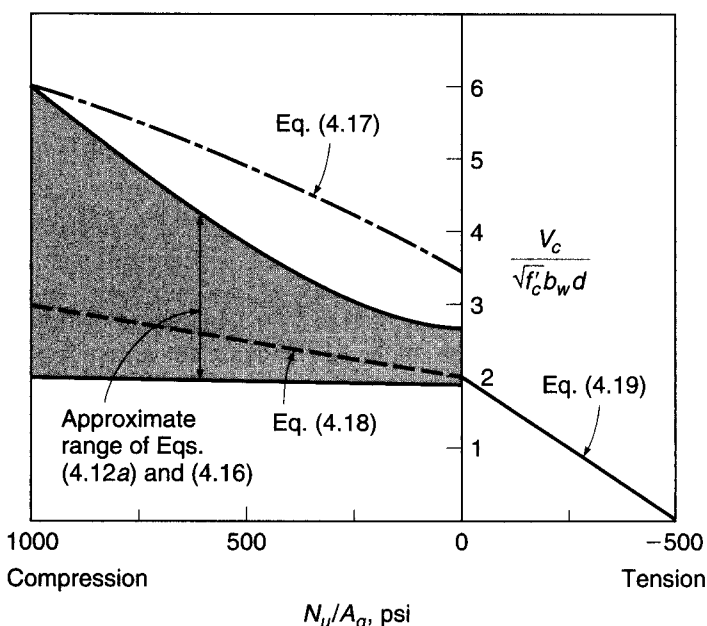
As an alternative to the rather complicated determination of V_c using Eqs. (4.12a), (4.16), and (4.17), ACI Code 11.2.1.2 permits the use of an alternative simplified expression:

$$V_c = 2 \left(1 + \frac{N_u}{2000A_g} \right) \lambda\sqrt{f'_c} b_w d \quad (4.18)$$

Figure 4.17 shows a comparison of V_c calculated by the more complex and simplified expressions for beams with compression load. Equation (4.18) is seen to be generally quite conservative, particularly for higher values of N_u/A_g . However, because of its simplicity, it is widely used in practice.

FIGURE 4.17

Comparison of equations for V_c for members subject to axial loads.



b. Axial Tension

The approach developed above for beams with axial compression does not correlate well with experimental evidence for beams subject to axial tension, and often predicts strengths V_c higher than actually measured. For this reason, the ACI Code provides that, for members carrying significant axial tension as well as bending and shear, the contribution of the concrete be taken as

$$V_c = 2 \left(1 + \frac{N_u}{500A_g} \right) \lambda \sqrt{f'_c} b_w d \quad (4.19)$$

but not less than zero, where N_u is negative for tension. As a simplifying alternative, the Commentary to the Code suggests that, for beams carrying axial tension, V_c be taken equal to zero and the shear reinforcement be required to carry the total shear. The variation of V_c with N_u/A_g for beams with tension is shown in Fig. 4.17 also.

EXAMPLE 4.4

Effect of axial forces on V_c . A beam with dimensions $b = 12$ in., $d = 24$ in., and $h = 27$ in., with $f'_c = 4000$ psi, carries a single concentrated factored load of 100 kips at midspan. Find the maximum shear strength of the concrete V_c at the first critical section for shear at a distance d from the support (a) if no axial forces are present, (b) if axial compression of 60 kips acts, and (c) if axial tension of 60 kips acts. In each case, compute V_c by both the more complex and simplified expressions of the ACI Code. Neglect the self-weight of the beam. At the section considered, tensile reinforcement consists of three No. 10 (No. 32) bars with a total area of 3.81 in^2 .

SOLUTION. At the critical section, $V_u = 50$ kips and $M_u = 50 \times 2 = 100$ ft-kips, while $\rho = 3.81/(12 \times 24) = 0.013$.

(a) If $N_u = 0$, Eq. (4.12a) predicts

$$V_c = \left(1.9 \times 1.0 \sqrt{4000} + 2500 \frac{0.013 \times 50 \times 2}{100} \right) 12 \times \frac{24}{1000} = 44.0 \text{ kips}$$

not to exceed the value of

$$V_c = 3.5 \times 1.0 \sqrt{4000} \times 12 \times \frac{24}{1000} = 63.8 \text{ kips}$$

If the simplified Eq. (4.12b) is used,

$$V_c = 2 \times 1.0 \sqrt{4000} \times 12 \times \frac{24}{1000} = 36.4 \text{ kips}$$

which is about 17 percent below the more exact value of Eq. (4.12a).

(b) With a compression of 60 kips introduced, the modified moment is found from Eq. (4.16) to be

$$M_m = 100 - 60 \frac{4 \times 27 - 24}{8 \times 12} = 47.5 \text{ ft-kips}$$

After introduction of that value into Eq. (4.12a) in place of M_u , the concrete shear strength is

$$V_c = \left(1.9 \times 1.0 \sqrt{4000} + 2500 \frac{0.013 \times 50 \times 2}{47.5} \right) 12 \times \frac{24}{1000} = 54.3 \text{ kips}$$

and, according to Eq. (4.17), should not exceed

$$V_c = 63.8 \sqrt{1 + \frac{60,000}{500 \times 12 \times 27}} = 74.6 \text{ kips}$$

If the simplified Eq. (4.18) is used,

$$V_c = 2 \left(1 + \frac{60,000}{2000 \times 12 \times 27} \right) \times 1.0 \sqrt{4000} \times 12 \times \frac{24}{1000} = 39.8 \text{ kips}$$

Comparing the results of the more exact calculation for (a) and (b), one sees that the introduction of an axial compressive stress of $60,000/(12 \times 27) = 185$ psi increases the concrete shear V_c by about 25 percent.

- (c) With an axial tension of 60 kips acting, the reduced V_c is found from Eq. (4.19) to be

$$V_c = 2 \left(1 - \frac{60,000}{500 \times 12 \times 27} \right) \times 1.0 \sqrt{4000} \times 12 \times \frac{24}{1000} = 22.9 \text{ kips}$$

a reduction of almost 50 percent from the value for $N_u = 0$. The alternative of using Eq. (4.19) for this case, according to the ACI Commentary, would be to set $V_c = 0$.

In all cases above, the strength reduction factor $\phi = 0.75$ would be applied to V_c to obtain the design strength.

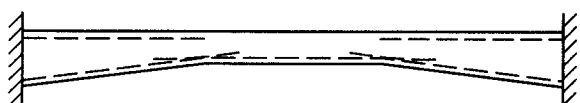
4.7 BEAMS WITH VARYING DEPTH

Reinforced concrete members having varying depth are frequently used in the form of haunched beams for bridges or portal frames, as shown in Fig. 4.18a, as precast roof girders such as shown in Fig. 4.18b, or as cantilever slabs. Generally the depth increases in the direction of increasing moments. For beams with varying depth, the inclination of the internal compressive and tensile stress resultants may significantly affect the shear for which the beam should be designed. In addition, the shear resistance of such members may differ from that of prismatic beams.

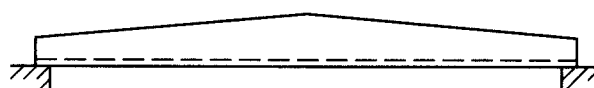
Figure 4.18c shows a cantilever beam, with fixed support at the left end, carrying a single concentrated load P at the right. The depth increases linearly in the direction

FIGURE 4.18

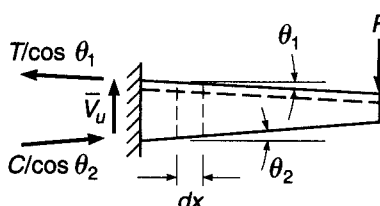
Effect of varying beam depth on shear.



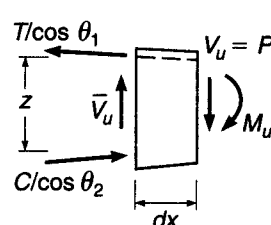
(a)



(b)



(c)



(d)

of increasing moment. In such cases, the internal tension in the steel and the compressive stress resultant in the concrete are inclined, and introduce components transverse to the axis of the member. With reference to Fig. 4.18d, showing a short length dx of the beam, if the slope of the top surface is θ_1 and that of the bottom is θ_2 , the net shear force \bar{V}_u for which the beam should be designed is very nearly equal to

$$\bar{V}_u = V_u - T \tan \theta_1 - C \tan \theta_2$$

where V_u is the external shear force equal to the load P here, and $C = T = M_u/z$. The internal lever arm $z = d - a/2$ as usual. Thus, in a case for which the beam depth increases in the direction of increasing moment, the shear for which the member should be designed is approximately

$$\bar{V}_u = V_u - \frac{M_u}{z} (\tan \theta_1 + \tan \theta_2) \quad (4.20a)$$

For the infrequent case in which the member depth decreases in the direction of increasing moment, it is easily confirmed that the corresponding equation is

$$\bar{V}_u = V_u + \frac{M_u}{z} (\tan \theta_1 + \tan \theta_2) \quad (4.20b)$$

These equations are approximate because the direction of the internal forces is not exactly as assumed; however, the equations may be used without significant error provided the slope angles do not exceed about 30° .

There has been very little research studying the shear strength of beams having varying depth. Tests reported in Ref. 4.19 on simple span beams with haunches at slopes up to about 15° and with depths both increasing and decreasing in the direction of increasing moments indicate no appreciable change in the cracking load V_{cr} compared with that for prismatic members. Furthermore, the strength of the haunched beams, which contained vertical stirrups as web reinforcement, was not significantly decreased or increased, regardless of the direction of decreasing depth. Based on this information, *it appears safe to design beams with varying depth for shear using equations for V_c and V_s developed for prismatic members*, provided the actual depth d at the section under consideration is used in the calculations.

4.8 ALTERNATIVE MODELS FOR SHEAR ANALYSIS AND DESIGN

The ACI Code method of design for shear and diagonal tension in beams, presented in preceding sections of this chapter, is essentially empirical. While generally leading to safe designs, the ACI Code " $V_c + V_s$ " approach lacks a physical model for the behavior of beams subject to shear combined with bending, and its shortcomings are now generally recognized. The "concrete contribution" V_c is generally considered to be some combination of force transfer by dowel action of the main steel, aggregate interlock along a diagonal crack, and shear in the uncracked concrete beyond the end of the crack. The values of each contribution are not identified. A rather vague rationalization is followed in adopting the diagonal cracking load of a member *without* web steel as the concrete contribution to the shear strength of an otherwise identical beam *with* web steel (see Section 4.4). Furthermore, as discussed in Section 4.3, Eqs. (4.3a) and (4.12a), used to predict the diagonal cracking load, overestimate concrete shear strength for beams with low reinforcement ratios ($\rho < 1.0$ percent), overestimate the gain in shear strength

resulting from the use of high-strength concrete (Refs. 4.14 to 4.17), and underestimate the influence of $V_u d/M_u$ (Ref. 4.3). The expressions also ignore the fact that shear strength decreases as member size increases (Refs. 4.20 to 4.21).

Ad hoc procedures are built into the ACI Code to adjust for some of these deficiencies, but it follows that it is necessary to include equations, also empirically developed for the most part, for specific classes of members (e.g., deep beams vs. normal beams, beams with axial loads, prestressed vs. nonprestressed beams, high-strength concrete beams)—with restrictions on the range of applicability of such equations. And it is necessary to incorporate seemingly arbitrary provisions for the maximum nominal shear stress and for the extension of flexural reinforcement past the theoretical point of need. The end result is that the number of ACI Code equations for shear design has grown from 4 prior to 1963 to 38 in 2008.

With this as background, attention has been given to the development of design approaches based on rational behavioral models, generally applicable, rather than on empirical evidence alone (Ref. 4.6).

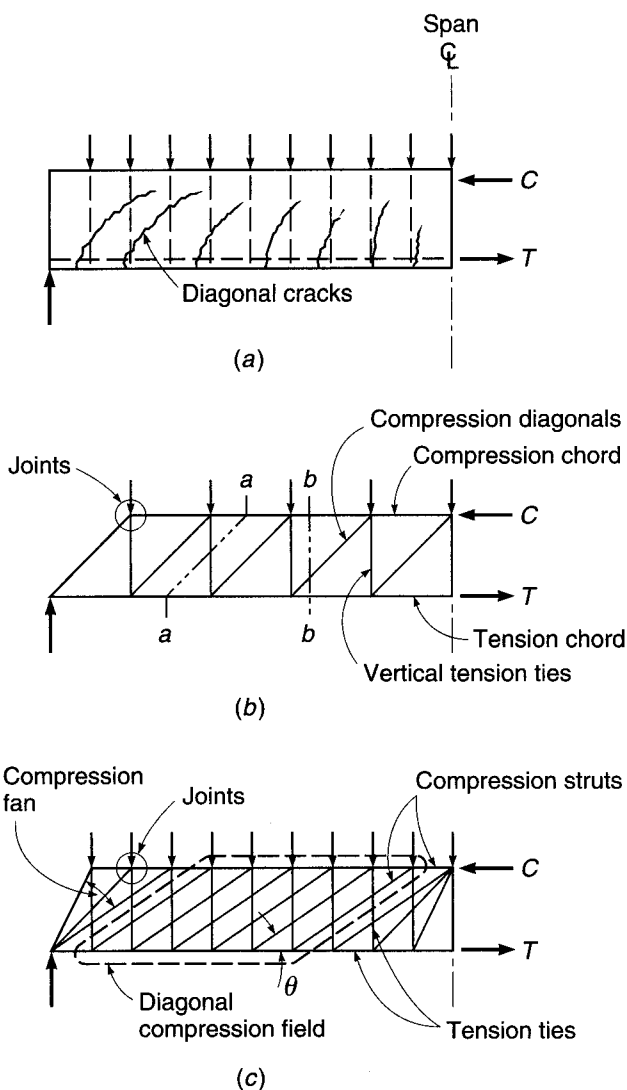
The *truss model* was originally introduced by Ritter (Ref. 4.22) and Morsch (Ref. 4.23) at the turn of the last century. A simplified version has long provided the basis for the ACI Code design of shear steel. The essential features of the truss model are reviewed with reference to Fig. 4.19a, which shows one-half the span of a simply supported, uniformly loaded beam. The combined action of flexure and shear produces the pattern of cracking shown. Reinforcement consists of the main flexural steel near the tension face and vertical stirrups distributed over the span.

The structural action can be represented by the truss of Fig. 4.19b, with the main steel providing the tension chord, the concrete top flange acting as the compression chord, the stirrups providing the vertical tension web members, and the concrete between inclined cracks acting as 45° compression diagonals. The truss is formed by lumping all the stirrups cut by section *a-a* into one vertical member and all the diagonal concrete struts cut by section *b-b* into one compression diagonal. Experience shows that for typical cases, the results of the model described are quite conservative, particularly for beams with small amounts of web reinforcement. As noted above, in the ACI Code the observed excess shear capacity is taken equal to the shear at the commencement of diagonal cracking and is referred to as the *concrete contribution* V_c .

Over the past 25 years, the truss concept has been greatly extended by the work of Schlaich, Marti, Collins, MacGregor, and others (Refs. 4.6, 4.24 to 4.29). It was realized that the angle of inclination of the concrete struts is generally not 45° but may range between about 25° and 65°, depending to a large extent on the arrangement of reinforcement. This led to what has become known as the *variable-angle truss model*, shown in Fig. 4.19c, which illustrates the five basic components of the improved model: (a) struts, or concrete compression members uniaxially loaded; (b) ties, or steel tension members; (c) joints at the intersection of truss members, assumed to be pin-connected; (d) compression fans, which form at “disturbed” regions, such as at the supports or under concentrated loads, transmitting the forces into the beam; and (e) diagonal compression fields, occurring where parallel compression struts transmit force from one stirrup to another. As in the ACI Code development, stirrups are typically assumed to reach yield stress at failure. With the force in all the verticals known and equal to $A_{sv} f_y$, the truss of Fig. 4.19c becomes statically determinate. Direct design equations can be based on the variable-angle truss model for ordinary cases. The model also permits direct numerical solution for the required reinforcement for special cases. The truss model does not include components of the shear failure mechanism such as aggregate interlock and friction, dowel action of the longitudinal steel, and shear carried across uncracked concrete. Furthermore, in the format originally proposed, the truss

FIGURE 4.19

Truss model for beams with web reinforcement:
 (a) uniformly loaded beam;
 (b) simple truss model;
 (c) more realistic model.



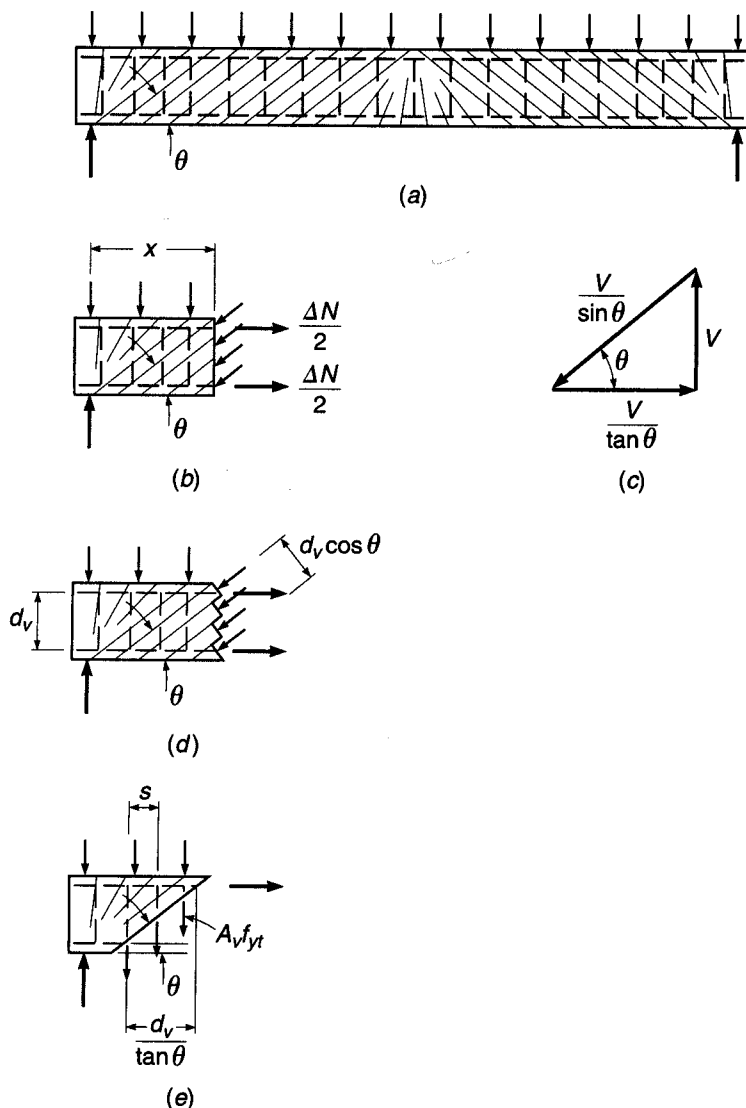
model does not account for compatibility requirements; i.e., it is based on *plasticity theory*. One form of the truss model is incorporated in Appendix A of the ACI Code; strut-and-tie models are discussed in detail in Chapter 10.

a. Compression Field Theory

The Canadian National Standard for reinforced concrete (Ref. 4.30) includes a method of shear design that is essentially the same as the present ACI method but also includes an alternative “general method” based on the variable-angle truss and the *compression field theory* (Refs. 4.27 and 4.31). The latter is incorporated in *AASHTO LRFD Bridge Design Specifications* (Ref. 4.12), where its use is mandatory for shear design. In its complete form, known as the *modified compression field theory*, it accounts for requirements of compatibility as well as equilibrium and incorporates stress-strain characteristics of both materials. Thus, it is capable of predicting not only the failure

FIGURE 4.20

Basis of compression field theory for shear: (a) beam with shear and longitudinal steel; (b) tension in horizontal bars due to shear; (c) diagonal compression on beam web; (d) vertical tension in stirrups; (e) equilibrium diagram of forces due to shear. (Adapted from Ref. 4.27.)



load but also the complete load-deformation response. The most basic elements of the compression field theory, applied to members carrying combined flexure and shear, will be clear from Fig. 4.20. Figure 4.20a shows a simple-span concrete beam, reinforced with longitudinal bars and transverse stirrups, and carrying a uniformly distributed loading along the top face. The light diagonal lines are an idealized representation of potential tensile cracking in the concrete.

Figure 4.20b illustrates that the net shear V at a section a distance x from the support is resisted by the vertical component of the diagonal compression force in the concrete struts. The horizontal component of the compression in the struts must be equilibrated by the total tension force ΔN in the longitudinal steel. Thus, with reference to Fig. 4.20b and c, the magnitude of the longitudinal tension resulting from shear is

$$\Delta N = \frac{V}{\tan \theta} = V \cot \theta \quad (4.21)$$

where θ is the angle of inclination of the diagonal struts. These forces superimpose on the longitudinal forces owing to flexure, not shown in Fig. 4.20b.

The effective depth for shear calculations, according to this method, is taken at the distance between longitudinal force resultants d_v . Thus, from Fig. 4.20d, the diagonal compressive stress in a web having width b_v is

$$f_d = \frac{V}{b_v d_v \sin \theta \cos \theta} \quad (4.22)$$

The tensile force in the vertical stirrups, each having area A_v and assumed to act at the yield stress f_{yt} , can be found from the free body of Fig. 4.20e. With stirrups assumed to be at uniform spacing s ,

$$A_v f_{yt} = \frac{Vs \tan \theta}{d_v} \quad (4.23)$$

Note, with reference to the free-body diagram, that the transverse reinforcement within the length $d_v/\tan \theta$ can be designed to resist the lowest shear that occurs within this length, i.e., the shear at the right end.

In the ACI Code method developed in Section 4.4, it was assumed that the angle θ was 45° . With that assumption, and if d is substituted for d_v , Eq. (4.23) is identical to that used earlier for the design of vertical stirrups. It is generally recognized, however, that the slope angle of the compression struts is not necessarily 45° , and following Refs. 4.12 and 4.30 that angle can range from 20 to 75° , provided the same value of θ is used in satisfying all requirements at a section. It is evident from Eqs. (4.21) and (4.23) that if a lower slope angle is selected, less vertical reinforcement but more horizontal reinforcement will be required. In addition, the compression in the concrete diagonals will be increased. Conversely, if a higher slope angle is used, more vertical steel but less horizontal steel will be needed, and the diagonal thrust will be less. It is generally economical to use a slope angle θ somewhat less than 45° , with the limitation that the concrete diagonal struts not be overstressed in compression.

In addition to providing an improved basis for the design of reinforcement for shear, the variable angle truss model gives important insights into detailing needs. For example, it becomes clear from the above that the increase in longitudinal steel tension resulting from the diagonal compression in the struts requires that flexural steel be extended beyond the point at which it is theoretically not needed for flexure, to account for the increased horizontal tensile force resulting from the thrust in the compression diagonals. This is not recognized explicitly in the ACI Code method for beam design. (However, the ACI Code does contain the arbitrary requirement that the flexural steel be extended a distance d or 12 bar diameters beyond the point indicated by flexural requirements.) Also, it is clear from the basic concept of the truss model that stirrups must be capable of developing their full tensile strength throughout the entire stirrup height. For wide beams, focus on truss action indicates that special attention should be given to lateral distribution of web reinforcement. It is often the practice to use conventional U stirrups for wide beams, with the vertical tension from the stirrups concentrated around the outermost bars. According to the discussion above, diagonal compression struts transmit forces only at the joints. Lack of stirrup joints at the interior of the wide-beam web would force joints to form only at the exterior longitudinal bars, which would concentrate the diagonal compression at the outer faces of the beam and possibly result in premature failure. It is best to form a truss joint at each of the longitudinal bars, and multiple leg stirrups should always be used in wide beams (see Fig. 4.8c).

References 4.12 and 4.30 incorporate a refined version of the approach just described, known as the modified compression field theory (MCFT), in which the cracked concrete is treated as a new material with its own stress-strain characteristics, including the ability to carry tension following crack formation. The compressive strength and the stress-strain curve of the concrete in the diagonal compression struts decrease as the diagonal tensile strain in the concrete increases. Equilibrium, compatibility, and constitutive relationships are formulated in terms of average stresses and average strains. Variability in the angle of inclination of the compression struts and stress-strain softening effects in the response of the concrete are taken into account. Consideration is also given to local stress conditions at crack locations. The method is capable of accurately predicting the response of complex elements such as shear walls, diaphragms, and membrane elements subjected to in-plane shear and axial loads through the full range of loading, from zero load to failure (Refs. 4.28 and 4.29). The version of the method adopted in Ref. 4.12 has been simplified to allow its use for routine design.

b. Design Provisions

The version of the MCFT adopted in the *AASHTO LRFD Bridge Design Specifications* (Ref. 4.12) is, like the shear provisions in the ACI Code, based on nominal shear capacity, with V_n equal to the lesser of

$$V_n = V_c + V_s \quad (4.24)$$

$$V_n = 0.25f'_c b_v d_v \quad (4.25)$$

where b_v = web width (the same as b_w in the ACI Code) and d_v = effective depth in shear, taken as equal to the flexural lever arm (the distance between the centroids of the tensile and compressive forces), but not less than the greater of $0.9d$ or $0.7h$.

The values of V_c and V_s differ from those used by the ACI, with

$$V_c = \beta \sqrt{f'_c} b_v d_v \quad (4.26)$$

and

$$V_s = \frac{A_w f_{yv} d_v (\cot \theta + \cot \alpha) \sin \alpha}{s} \quad (4.27)$$

where A_v , f_{yv} , s , α , and θ are as defined before. β is the *concrete tensile stress factor* and is based on the ability of diagonally cracked concrete to resist tension, which also controls the angle of the diagonal tension crack θ . In Ref. 4.12, the values of β and θ are determined based on the strain in the longitudinal tension reinforcement, which can be approximated by[†]

$$\epsilon_s = \frac{|M_u|/d_v - 0.5N_u + |V_u|}{E_s A_s} \leq 0.006 \quad (4.28)$$

The sign convention for N_u is the same as used in Section 4.6 and the ACI Code: compression is positive and tension is negative (the opposite sign convention is used in Ref. 4.12). M_u should not be taken less than $V_u d_v$; when calculating A_s , the area of bars terminated less than their development length (see Chapter 5) from the section

[†] Equation (4.28) is a simplification of $\epsilon_s = \frac{|M_u|/d_v - 0.5N_u + 0.5|V_u| \cot \theta}{E_s A_s}$, with $0.5|V_u| \cot \theta$ approximated by $|V_u|$. The simplification eliminates the need for an iterative solution between ϵ_s and θ .

under consideration should be reduced in proportion to the decreased development; ϵ_s should be taken as zero if the value calculated in Eq. (4.28) is negative; and ϵ_s should be doubled if N_u is high enough to cause cracking to the flexural compression face of the member. For sections closer than d_v to the face of the support, ϵ_s calculated at d_v from the face of the support may be used to determine β and θ .

For members with at least the minimum shear reinforcement, the concrete tensile stress factor is given by

$$\beta = \frac{4.8}{1 + 750\epsilon_s} \quad (4.29)$$

The angle θ , in degrees, is given by

$$\theta = 29 + 3500\epsilon_s \quad (4.30)$$

As shown in Eq. (4.21), the strength of the *longitudinal* reinforcement must be adequate to carry the additional forces induced by shear. Referring to Fig. 4.21, this leads to

$$A_s f_y \geq T = \frac{|M_u|}{\phi_f} - \frac{0.5N_u}{\phi_c} + \left(\frac{|V_u|}{\phi_v} - 0.5V_s \right) \cot \theta \quad (4.31)$$

where ϕ_f , ϕ_c , and ϕ_v are, respectively, the capacity reduction factors for flexure, axial load (tension or compression), and shear. V_s need not be taken greater than V_u/ϕ . Since the inclination of the compression struts changes, tension in the longitudinal reinforcement does not exceed that required to resist the maximum moment alone.

For members with less than the minimum transverse reinforcement, the angle θ is given by Eq. (4.30), while the value of β becomes a function of ϵ_s and a crack spacing parameter s_{xe} .

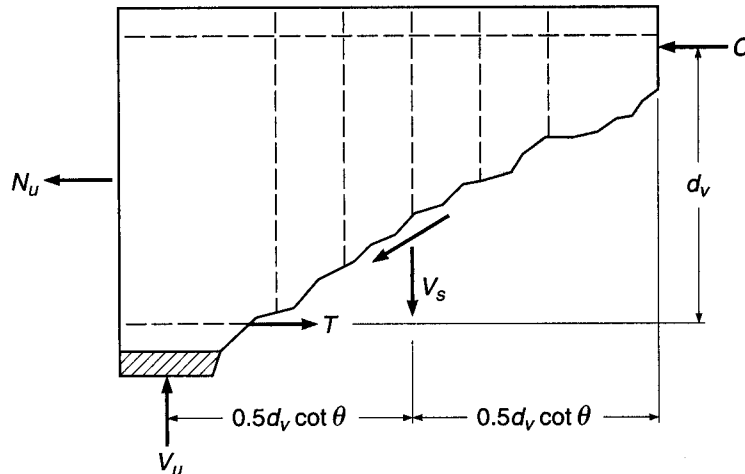
$$\beta = \frac{4.8}{1 + 750\epsilon_s} \quad \frac{51}{39 + s_{xe}} \quad (4.32)$$

The crack spacing parameter is

$$s_{xe} = s_x \frac{1.38}{a_g + 0.63} \quad (4.33)$$

FIGURE 4.21

Equilibrium diagram for calculating tensile force in reinforcement. (Adapted from Ref. 4.12.)



where $12.0 \text{ in.} \leq s_{xe} \leq 80.0 \text{ in.}$, $s_x = \text{lesser of the shear depth } d_v \text{ or the spacing between layers of longitudinal crack control reinforcement, each layer with an area of steel of at least } 0.003b_v s_x$, and $a_g = \text{maximum size of the coarse aggregate}$. Note that $s_{xe} = s_x$ for $\frac{3}{4}\text{-in.}$ coarse aggregate.

Since θ is not, in general, equal to 45° , the critical section might appropriately be taken as $d_v \cot \theta$ from the face of the support if all the load were applied to the upper surface of the member. For simplicity, however, the critical section is taken a distance d_v from the face of the support when the reaction introduces compression into the end region of the member, similar to the loading cases shown in Fig. 4.12a and b. For all other cases, the crucial section is taken at the face of the support, as shown in Fig. 4.12c to f.

AASHTO requires a minimum amount of transverse reinforcement $A_v = \sqrt{f'_c} b_v s / f_{yt}$ (compared to $0.75\sqrt{f'_c} b_w s / f_{yt}$ for ACI), when $V_u > 0.5\phi V_c$, and specifies maximum spacings of transverse reinforcement of $s \leq 0.8d_v \leq 24 \text{ in.}$ when $v_u < 0.125f'_c$ and $s \leq 0.4d_v \leq 12 \text{ in.}$ when $v_u \geq 0.125f'_c$. Because the predictions obtained with the MCFT are generally more accurate than those obtained with the ACI method, AASHTO allows the use of $\phi = 0.90$ for shear, the same as for flexure.

EXAMPLE 4.5

Design by modified compression field approach. Re-solve the problem given in Examples 4.2 and 4.3 based on the MCFT. Use ACI load factors and $\phi = 0.9$ for shear, as used in *AASHTO LRFD Bridge Design Specifications* (Ref. 4.12). Assume an aggregate size a_g of $\frac{3}{4}$ in.

SOLUTION. For simplicity, the effective depth for shear d_v will be set at the minimum allowable value = $0.9d = 0.9 \times 22 = 19.8 \text{ in.}$ Both M_u and V_u are as tabulated previously in Table 4.1.

The critical section for shear is located a distance $d_v = 19.8 \text{ in.} = 1.65 \text{ ft}$ from the support where $V_u = 94 - 9.4 \times 1.65 = 78.5 \text{ kips}$. Calculating $0.125f'_c b_v d_v = 0.125 \times 4000 \times 16 \times 19.8 = 158,400 \text{ lb}$ leads to maximum spacing criteria for No. 3 (No. 10) stirrups equal to the smaller of $0.8d_v = 0.8 \times 19.8 = 15.8 \text{ in.}, 24 \text{ in.}$, or

$$s_{\max} = \frac{A_v f_{yt}}{\sqrt{f'_c} b_v} = \frac{0.22 \times 60,000}{\sqrt{4000} \times 16} = 13.0 \text{ in.}$$

Using Eq. (4.28), the strain in the longitudinal tension steel is approximated as

$$\epsilon_s = \frac{|M_u|/19.8 + |V_u|}{29,000 \times 7.62}$$

with M_u and V_u in in-kips and kips, respectively.

The values of ϵ_s are tabulated along with M_u and V_u in Table 4.2. These values are used to calculate θ using Eq. (4.30) and β using Eqs. (4.29) and (4.32) for sections with and without minimum stirrups, respectively. Where the section meets the minimum stirrup criterion, the values of β are used to calculate the values of V_c , which are then used, along with the values of θ , to calculate V_s and the required stirrup spacing s (see Table 4.2).

For transverse reinforcement less than the minimum, the values of β are based on ϵ_s and s_x . The latter may be taken as the lesser of d_v or the spacing of longitudinal crack control reinforcement. In this case, $d_v = 19.8 \text{ in.}$ controls since crack control reinforcement is not used. The equivalent crack spacing parameter $s_{xe} = s_x$ because $a_g = 0.75 \text{ in.}$ These values of β are used to determine the point where $\phi V_c/2 \geq V_u$, the point at which stirrups may be terminated (Table 4.2). The values of V_u , ϕV_c with at least minimum stirrups, and $\phi V_c/2$ for less than minimum stirrups are plotted in Fig. 4.22a. The following stirrup spacings can be used for this case:

1 space at 6 in. = 6 in.

6 spaces at 13 in. = 78 in.

Total = 84 in. = 7 ft

TABLE 4.2**Modified compression field design example using $\phi = 0.9$ for shear**

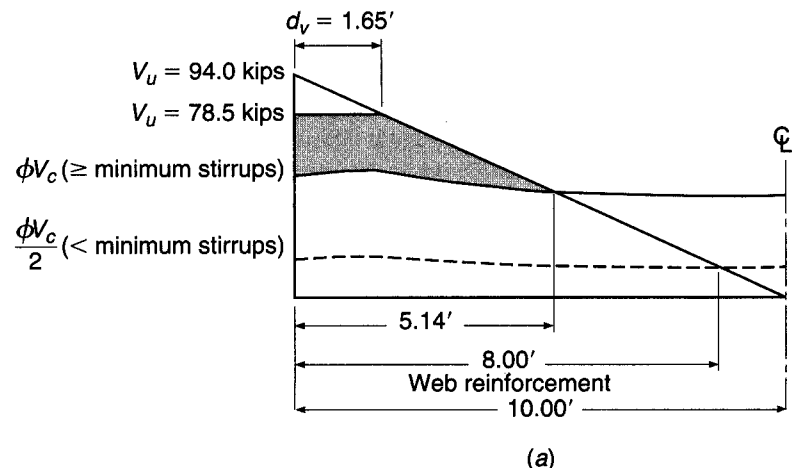
Distance from Support, ft	M_u , ft-kips	V_u , kips	$\epsilon_s \times 1000$	θ	β	ϕV_c for at Least Minimum Stirrups			ϕV_c for Less Than Minimum Stirrups		
						ϕV_c , kips	V_s , kips	s , in.	β	ϕV_c , kips	$\phi V_c/2$, kips
0	0	94.0	0.85	32.0	2.93	52.8	45.7	9.2	2.54	45.8	22.9
1	89	84.6	0.77	31.7	3.05	55.0	32.9	12.9	2.64	47.7	23.8
1.65 [†]	144	78.5	0.75	31.6	3.07	55.4	25.6	16.5	2.66	48.1	24.0
2	169	75.2	0.80	31.8	2.99	54.0	23.6	17.9	2.60	46.8	23.4
3	240	65.8	0.96	32.3	2.80	50.4	17.1	24.2	2.43	43.7	21.9
4	301	56.4	1.08	32.8	2.65	47.8	9.5	42.6	2.30	41.5	20.7
5	353	47.0	1.18	33.1	2.55	45.9	1.2	336	2.21	39.8	19.9
6	395	37.6	1.25	33.4	2.47	44.6	—	—	2.15	38.7	19.4
7	428	28.2	1.30	33.6	2.43	43.8	—	—	2.11	38.0	19.0
8	451	18.8	1.32	33.6	2.41	43.5	—	—	2.09	37.7	18.8
9	465	9.4	1.32	33.6	2.41	43.5	—	—	2.09	37.7	18.9
10	470	0.0	1.29	33.5	2.44	44.0	—	—	2.12	38.2	19.1

[†] d_v from face of support.

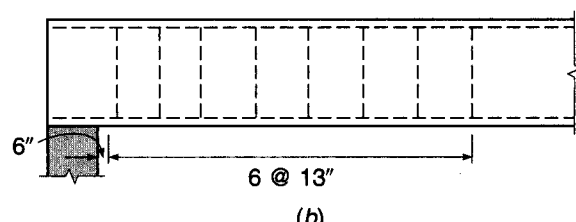
For this example, V_s is selected based on V_u at each point, not the minimum V_u on a crack with angle θ . This simplifies the design procedure and results in a somewhat more conservative design. Even so, only 7 No. 3 (No. 10) stirrups are needed, or 9 stirrups if the stirrups are continued at the maximum spacing through the middle region of the beam. These values compare favorably with the minimum number of stirrups per half-span, 11 and 14, previously

FIGURE 4.22

Modified compression field design for Example 4.5.



(a)



(b)

calculated (Example 4.3) using the two methods required by the ACI Code. The resulting stirrup pattern is shown in Fig. 4.22b.

By way of comparison, had $\phi_{\text{shear}} = 0.75$ been used in this example, the stirrup spacing would have been

$$\begin{aligned} \text{1 space at 5 in.} &= 5 \text{ in.} \\ \text{3 spaces at 10 in.} &= 30 \text{ in.} \\ \text{4 spaces at 13 in.} &= 52 \text{ in.} \\ \text{Total} &= 87 \text{ in.} = 7 \text{ ft 3 in.} \end{aligned}$$

for a total of 8 stirrups.

The MCFT recognizes that shear increases the force in the flexural steel, although, as explained earlier, the maximum tensile force in the steel is not affected. Equation (4.31) should be used to calculate the tensile force T along the span, which will then govern the locations where tensile steel may be terminated. This will be discussed further in Chapter 5.

The MCFT is not included in the 2008 ACI Code. ACI Code 1.4, however, permits the use of “any system of design or construction . . . , the adequacy of which has been shown by successful use or by analysis or test,” if approved by the appropriate building official. The application of the MCFT in Canada and in U.S. bridge practice provides the evidence needed to demonstrate “successful use.”

4.9 SHEAR-FRICTION DESIGN METHOD

Generally, in reinforced concrete design, shear is used merely as a convenient measure of diagonal tension, which is the real concern. In contrast, there are circumstances such that direct shear may cause failure of reinforced concrete members. Such situations occur commonly in precast concrete structures, particularly in the vicinity of connections, as well as in composite construction combining cast-in-place concrete with either precast concrete or structural steel elements. Potential failure planes can be established for such cases along which direct shear stresses are high, and failure to provide adequate reinforcement across such planes may produce disastrous results.

The necessary reinforcement may be determined on the basis of the *shear-friction method* of design (Refs. 4.32 to 4.38). The basic approach is to assume that the concrete may crack in an unfavorable manner, or that slip may occur along a predetermined plane of weakness. Reinforcement must be provided crossing the potential or actual crack or shear plane to prevent direct shear failure.

The shear-friction theory is very simple, and the behavior is easily visualized. Figure 4.23a shows a cracked block of concrete, with the crack crossed by reinforcement. A shear force V_n acts parallel to the crack, and the resulting tendency for the upper block to slip relative to the lower is resisted largely by friction along the concrete interface at the crack. Since the crack surface is naturally rough and irregular, the effective coefficient of friction may be quite high. In addition, the irregular surface will cause the two blocks of concrete to separate slightly, as shown in Fig. 4.23b.

If reinforcement is present normal to the crack, then slippage and subsequent separation of the concrete will stress the steel in tension. Tests have confirmed that well-anchored steel will be stressed to its yield strength when shear failure is obtained (Ref. 4.34). The resulting tensile force sets up an equal and opposite pressure between the concrete faces on either side of the crack. It is clear from the free body of Fig. 4.23c that the maximum value of this interface pressure is $A_{vf}f_y$, where A_{vf} is the total area of steel crossing the crack and f_y is its yield strength.

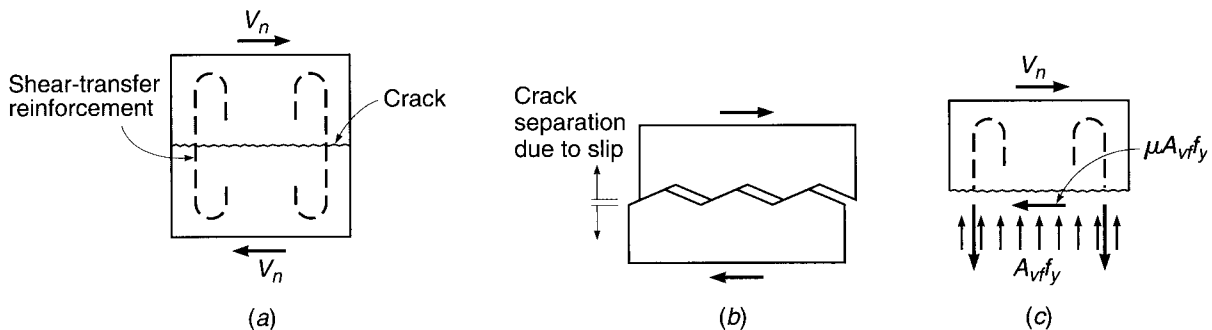


FIGURE 4.23

Basis of shear-friction design method: (a) applied shear; (b) enlarged representation of crack surface; (c) free-body sketch of concrete above crack.

The concrete resistance to sliding may be expressed in terms of the normal force times a coefficient of friction μ . By setting the summation of horizontal forces equal to zero

$$V_n = \mu A_{vf} f_y \quad (4.34)$$

Based on tests, μ may be taken as 1.4 for cracks in monolithic concrete, but V_n should not be assumed to be greater than $0.2f'_c A_c$, $(480 + 0.08f'_c)A_c$, or $1600A_c$ (Refs. 4.32, 4.37, and 4.38).

The relative movement of the concrete on opposite sides of the crack also subjects the individual reinforcing bars to shearing action, and the dowel resistance of the bars to this shearing action contributes to shear resistance. However, it is customary to neglect the dowel effect for simplicity in design and to compensate for this by using an artificially high value of the friction coefficient.

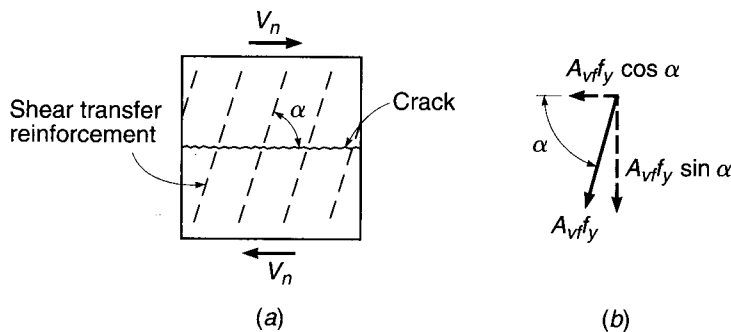
The provisions of ACI Code 11.6 are based on Eq. (4.34). The design strength is equal to ϕV_n , where $\phi = 0.75$ for shear-friction design, and V_n must not exceed the smallest of $0.2f'_c A_c$, $(480 + 0.08f'_c)A_c$, and $1600A_c$ for monolithic or intentionally roughened normalweight concrete or the smaller of $0.2f'_c A_c$ and $800A_c$ lb for other cases. When concretes of different strengths are cast against each other, V_n should be based on the lower value of f'_c . Recommendations for friction factor μ are as follows:

Concrete placed monolithically	1.4 λ
Concrete placed against hardened concrete with surface intentionally roughened	1.0 λ
Concrete placed against hardened concrete not intentionally roughened	0.6 λ
Concrete anchored to as-rolled structural steel by headed studs or reinforcing bars	0.7 λ

where λ is 1.0 for normalweight concrete and 0.75 for both sand-lightweight and all-lightweight concrete. In other cases, λ is determined based on volumetric proportions of lightweight and normalweight aggregates, as described in Section 4.5a and specified in ACI Code 8.6.1, but not greater than 0.85. The yield strength of the reinforcement f_y may not exceed 60,000 psi. Direct tension across the shear plane, if present, must be carried by additional reinforcement, and permanent net compression across the shear plane may be taken as additive to the force in the shear-friction reinforcement $A_{vf} f_y$ when calculating the required A_{vf} .

FIGURE 4.24

Shear-friction reinforcement inclined with respect to crack face.



When shear is transferred between concrete newly placed against hardened concrete, the surface roughness is an important variable; an intentionally roughened surface is defined to have a full amplitude of approximately $\frac{1}{4}$ in. In any case, the old surface must be clean and free of laitance. When shear is to be transferred between as-rolled steel and concrete, the steel must be clean and without paint, according to ACI Code 11.6.

If V_u is the shear force to be resisted at factored loads, then with $V_u = \phi V_n$, the required steel area is found by transposition of Eq. (4.34):

$$A_{vf} = \frac{V_u}{\phi \mu f_y} \quad (4.35)$$

In some cases, the shear-friction reinforcement may not cross the shear plane at 90° as described in the preceding paragraphs. If the shear-friction reinforcement is inclined to the shear plane so that the shear force is applied in the direction to increase tension in the steel, as in Fig. 4.24a, then the component of that tension parallel to the shear plane, shown in Fig. 4.24b, contributes to the resistance to slip. Then the shear strength may be computed from

$$V_n = A_{vf} f_y (\mu \sin \alpha + \cos \alpha) \quad (4.36)$$

in lieu of Eq. (4.34). Here α is the angle between the shear-friction reinforcement and the shear plane. If α is larger than 90° , i.e., if the inclination of the steel is such that the tension in the bars tends to be reduced by the shear force, then the assumption that the steel stress equals f_y is not valid, and a better arrangement of bars should be made.

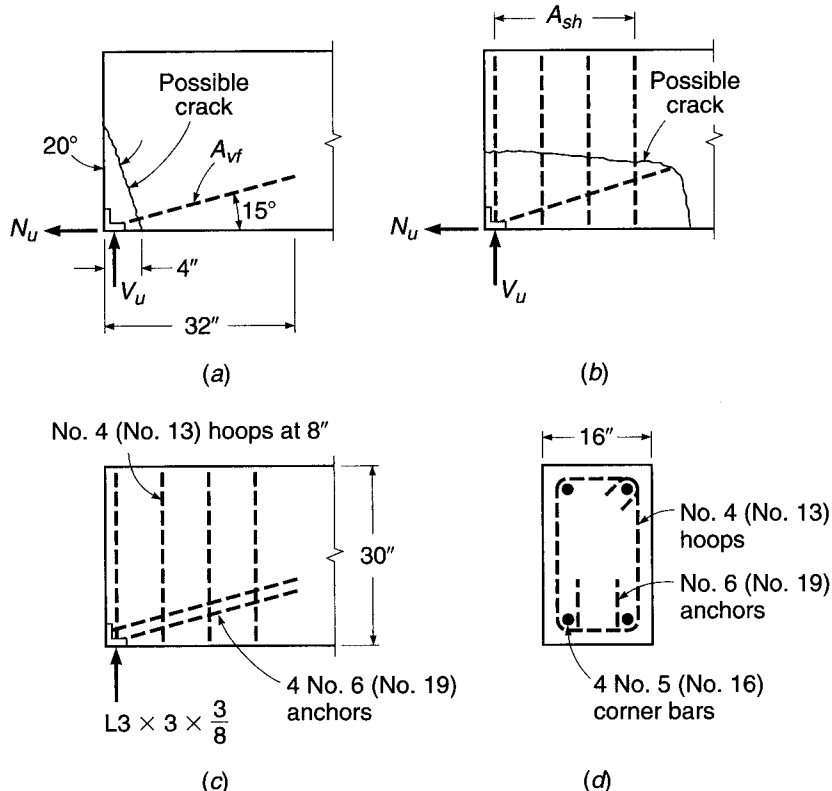
Certain precautions should be observed in applying the shear-friction method of design. Reinforcement, of whatever type, should be well anchored to develop the yield strength of the steel, by the full development length or by hooks or bends, in the case of reinforcing bars, or by proper heads and welding, in the case of studs joining concrete to structural steel. The concrete should be well confined, and the liberal use of hoops has been recommended (Ref. 4.32). Care must be taken to consider all possible failure planes and to provide sufficient well-anchored steel across these planes.

EXAMPLE 4.6

Design of beam bearing detail. A precast beam must be designed to resist a support reaction, at factored loads, of $V_u = 100$ kips applied to a 3×3 steel angle, as shown in Fig. 4.25. In lieu of a calculated value, a horizontal force N_u , owing to restrained volume change, will be assumed to be 20 percent of the vertical reaction, or 20 kips. Determine the required auxiliary reinforcement, using steel of yield strength $f_y = 60,000$ psi. Concrete strength $f'_c = 5000$ psi.

FIGURE 4.25

Design of beam bearing shoe: (a) diagonal crack; (b) horizontal crack; (c) reinforcement; (d) cross section.



SOLUTION. A potential crack will be assumed at 20° , initiating at a point 4 in. from the end of the beam, as shown in Fig. 4.25a. The total required steel A_{vf} is the sum of that required to resist the resultant of V_u and N_u acting parallel to the cracks = $V_u \cos 20^\circ + N_u \sin 20^\circ$. Equation (4.35) is modified accordingly:

$$A_{vf} = \frac{V_u \cos 20^\circ + N_u \sin 20^\circ}{\phi \mu f_y}$$

$$= \frac{100 \times 0.940 + 20 \times 0.340}{0.75 \times 1.4 \times 60} = \frac{101 \text{ kips}}{63 \text{ ksi}}$$

$$= 1.60 \text{ in}^2$$

The net compression normal to the potential crack would be no less than $V_u \sin 20^\circ - N_u \cos 20^\circ = 15.4$ kips. This could be counted upon to reduce the required shear-friction steel, according to the ACI Code, but it will be discounted conservatively here. Four No. 6 (No. 19) bars will be used, providing an area of 1.76 in^2 . They will be welded to the 3×3 angle and will extend into the beam a sufficient distance to develop the yield strength of the bars. According to the ACI Code, the development length for a No. 6 (No. 19) bar is 26 in., 32 in. without the ψ_s factor (see Chapter 5). Considering the uncertainty of the exact crack location, the bars will be extended 32 in. into the beam as shown in Fig. 4.25a. The bars will be placed at an angle of 15° with the bottom face of the member. For the crack oriented at an angle of 20° , as assumed, the area of the crack is

$$A_c = 16 \left(\frac{4}{\sin 20^\circ} \right) = 187 \text{ in}^2$$

Thus, according to the ACI Code, the maximum nominal shear strength of the surface is not to exceed $V_n = 0.2f'_c A_c = 187$ kips, $V_n = (480 + 0.08f'_c)A_c = 165$ kips, or $V_n = 1600A_c = 299$ kips. The maximum design strength to be used is $\phi V_n = 0.75 \times 165 = 124$ kips. As calculated earlier, the applied shear on the interface at factored loads is

$$V_u = 100 \cos 20^\circ + 20 \sin 20^\circ = 101 \text{ kips}$$

and so the design is judged satisfactory to this point.

A second possible crack must be considered, as shown in Fig. 4.25b, resulting from the tendency of the entire anchorage weldment to pull horizontally out of the beam.

The required steel area A_{sh} and the concrete shear stress will be calculated based on the development of the full yield tension in the bars A_{vf} . (Note that the factor ϕ need not be used here because it has already been introduced in computing A_{vf} .)

$$\begin{aligned} A_{sh} &= \frac{A_{vf}f_y \cos 15^\circ}{\mu f_y} \\ &= \frac{1.76 \times 0.966}{1.4} \\ &= 1.21 \text{ in}^2 \end{aligned}$$

Four No. 4 (No. 13) hoops will be used, providing an area of 1.60 in².

The maximum shear force that can be transferred, according to the ACI Code limits, will be based conservatively on a horizontal plane 32 in. long. No strength reduction factor need be included in the calculation of this maximum value because it was already introduced in determining the steel area A_{vf} by which the shear force is applied. Accordingly,

$$V_n \leq (480 + 0.08f'_c) \times 16 \times 32 = 451 \text{ kips}$$

The maximum shear force that could be applied in the given instance is the value used to calculate A_{sh} ,

$$V_u = 1.76 \times 60 \cos 15^\circ = 102 \text{ kips}$$

which is well below the specified maximum.

The first hoop will be placed 2 in. from the end of the member, with the others spaced at 8 in., as shown in Fig. 4.25c. Also shown in Fig. 4.25d are four No. 5 (No. 16) bars that will provide anchorage for the hoop steel.

REFERENCES

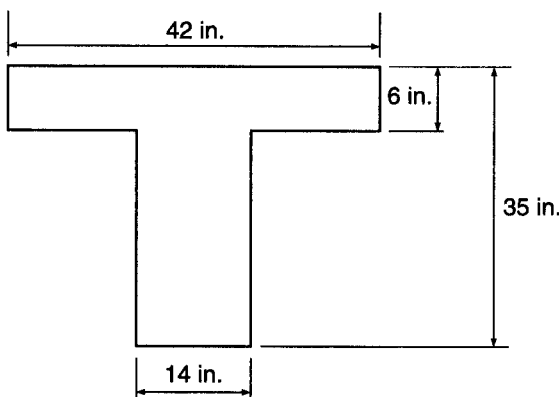
- 4.1. "Shear and Diagonal Tension," pt. 2, ACI-ASCE Committee 326, *J. ACI*, vol. 59, no. 2, 1962, pp. 277–333.
- 4.2. B. Bresler and J. G. MacGregor, "Review of Concrete Beams Failing in Shear," *J. Struct. Div.*, ASCE, vol. 93, no. ST1, 1967, pp. 343–372.
- 4.3. "The Shear Strength of Reinforced Concrete Members," ASCE-ACI Committee 426, *Proc. ASCE*, vol. 99, no. ST6, 1973, pp. 1091–1187 (with extensive bibliography).
- 4.4. "The Shear Strength of Reinforced Concrete Members—Slabs," ASCE-ACI Task Committee 426, *Proc. ASCE*, vol. 100, no. ST8, 1974, pp. 1543–1591.
- 4.5. *Shear in Reinforced Concrete*, vols. 1 and 2, *Special Publication SP-42*, American Concrete Institute, Detroit, 1974.
- 4.6. "Recent Approaches to Shear Design of Structural Concrete," ASCE-ACI Committee 445, *J. Struct. Eng.*, ASCE, vol. 124, no. 12, 1998, pp. 1375–1417.
- 4.7. A. H. Nilson (ed.), *Finite Element Analysis of Reinforced Concrete*, American Society of Civil Engineers, New York, 1982.
- 4.8. J. Isenberg (ed.), *Finite Element Analysis of Reinforced Concrete Structures II*, American Society of Civil Engineers, New York, 1993, pp. 203–232.

- 4.9. M. P. Collins, "Toward a Rational Theory for RC Members in Shear," *J. Struct. Div.*, ASCE, vol. 104, no. ST4, April 1978, pp. 649–666.
- 4.10. T. T. C. Hsu, *Unified Theory of Reinforced Concrete*, CRC Press, Inc., Boca Raton, FL, 1993.
- 4.11. T. C. Zsutty, "Shear Strength Prediction for Separate Categories of Simple Beam Tests," *J. ACI*, vol. 68, no. 2, 1971, pp. 138–143.
- 4.12. *AASHTO LRFD Bridge Design Specifications*, 4th ed., American Association of State Highway and Transportation Officials (AASHTO), Washington, DC, 2007, with interim update 2008.
- 4.13. S. Martinez, A. H. Nilson, and F. O. Slate, "Short-Term Mechanical Properties of High-Strength Lightweight Concrete," *Research Report No. 82-9*, Department of Structural Engineering, Cornell University, August 1982.
- 4.14. A. H. Elzantaty, A. H. Nilson, and F. O. Slate, "Shear Capacity of Reinforced Concrete Beams Using High-Strength Concrete," *J. ACI*, vol. 83, no. 2, 1986, pp. 290–296.
- 4.15. J. J. Roller and H. G. Russell, "Shear Strength of High-Strength Concrete Beams with Web Reinforcement," *ACI Struct. J.*, vol. 87, no. 2, 1990, pp. 191–198.
- 4.16. S. H. Ahmad, A. R. Khaloo, and A. Proveda, "Shear Capacity of Reinforced High-Strength Concrete Beams," *J. ACI*, vol. 83, no. 2, 1986, pp. 297–305.
- 4.17. M. P. Collins and D. Kuchma, "How Safe Are Our Large, Lightly Reinforced Concrete Beams, Slabs, and Footings?" *ACI Struct. J.*, vol. 96, no. 4, 1999, pp. 282–290.
- 4.18. G. J. Parra-Montesinos, "Shear Strength of Beams with Deformed Steel Fibers," *Concr. Int.*, vol. 28, no. 11, 2006, pp. 57–66.
- 4.19. S. Y. Debaiky and E. I. Elmehia, "Behavior and Strength of Reinforced Concrete Haunched Beams in Shear," *J. ACI*, vol. 79, no. 3, 1982, pp. 184–194.
- 4.20. G. N. J. Kani, "How Safe Are Our Large Reinforced Concrete Beams?" *J. ACI*, vol. 64, no. 3, 1967, pp. 128–141.
- 4.21. T. Shioya, M. Iguro, Y. Akiyama, and T. Okada, "Shear Strength of Large Reinforced Concrete Beams, Fracture Mechanics: Application to Concrete," *Special Publication SP-118*, American Concrete Institute, Detroit, 1989, pp. 259–279.
- 4.22. W. Ritter, "Die Bauweise Hennebique" (The Hennebique System), *Schweizerische Bauzeitung*, XXXIII, no. 7, 1899.
- 4.23. E. Morsch, *Der Eisenbetonbau, seine Theorie und Anwendung* (Reinforced Concrete Theory and Application), Verlag Konrad Wittner, Stuttgart, 1912.
- 4.24. J. Schlaich, K. Schafer, and M. Jennewein, "Toward a Consistent Design of Structural Concrete," *J. Prestressed Concr. Inst.*, vol. 32, no. 3, 1987, pp. 74–150.
- 4.25. P. Marti, "Truss Models in Detailing," *Concr. Int.*, vol. 7, no. 12, 1985, pp. 66–73. (See also P. Marti, "Basic Tools of Reinforced Concrete Beam Design," *J. ACI*, vol. 82, no. 1, 1985, pp. 46–56.)
- 4.26. J. G. MacGregor and J. K. Wight, *Reinforced Concrete*, 4th ed., Prentice-Hall, Englewood Cliffs, NJ, 2005.
- 4.27. M. P. Collins and D. Mitchell, *Prestressed Concrete Structures*, Prentice-Hall, Englewood Cliffs, NJ, 1991.
- 4.28. F. J. Vecchio and M. P. Collins, "Modified Compression Field Theory for Reinforced Concrete Elements Subjected to Shear," *J. ACI*, vol. 83, no. 2, 1986, pp. 219–231.
- 4.29. F. J. Vecchio and M. P. Collins, "Predicting the Response of Reinforced Concrete Beams Subjected to Shear Using the Modified Compression Field Theory," *J. ACI*, vol. 85, no. 3, 1988, pp. 258–268.
- 4.30. CSA Committee A23.3, *Design of Concrete Structures*, Canadian Standards Association, Etobicoke, Ontario, 2004.
- 4.31. M. P. Collins, D. Mitchell, P. Adebar, and F. J. Vecchio, "A General Shear Design Method," *ACI Struct. J.*, vol. 93, no. 1, 1996, pp. 36–45.
- 4.32. P. W. Birkeland and H. W. Birkeland, "Connections in Precast Concrete Construction," *J. ACI*, vol. 63, no. 3, 1966, pp. 345–368.
- 4.33. R. F. Mast, "Auxiliary Reinforcement in Precast Concrete Connections," *J. Struct. Div.*, ASCE, vol. 94, no. ST6, June 1968, pp. 1485–1504.
- 4.34. A. H. Mattock and N. M. Hawkins, "Shear Transfer in Reinforced Concrete—Recent Research," *J. Prestressed Concr. Inst.*, vol. 17, no. 2, 1972, pp. 55–75.
- 4.35. A. H. Mattock, "Shear Transfer in Concrete Having Reinforcement at an Angle to the Shear Plane," *Special Publication SP-42*, American Concrete Institute, Detroit, 1974.
- 4.36. *PCI Design Handbook*, 6th ed., Precast Prestressed Concrete Institute, Chicago, 2004.
- 4.37. L. F. Kahn and A. D. Mitchell, "Shear Friction Tests with High-Strength Concrete," *ACI Struct. J.*, vol. 99, no. 1, 2002, pp. 98–103.
- 4.38. A. H. Mattock, "Shear Friction and High-Strength Concrete," *ACI Struct. J.*, vol. 98, no. 1, 2001, pp. 50–59.

PROBLEMS

- 4.1.** A beam is to be designed for loads causing a maximum factored shear of 60.0 kips, using concrete with $f'_c = 5000$ psi. Proceeding on the basis that the concrete dimensions will be determined by diagonal tension, select the appropriate width and effective depth (a) for a beam in which no web reinforcement is to be used, (b) for a beam in which only the minimum web reinforcement is provided, as given by Eq. (4.13), and (c) for a beam in which web reinforcement provides shear strength $V_s = 2V_c$. Follow the ACI Code requirements, and let $d = 2b$ in each case. Calculations may be based on the more approximate value of V_c given by Eq. (4.12b).
- 4.2.** A rectangular beam having $b = 10$ in. and $d = 17.5$ in. spans 15 ft face to face of simple supports. It is reinforced for flexure with three No. 9 (No. 29) bars that continue uninterrupted to the ends of the span. It is to carry service dead load $D = 1.27$ kips/ft (including self-weight) and service live load $L = 3.70$ kips/ft, both uniformly distributed along the span. Design the shear reinforcement, using No. 3 (No. 10) vertical U stirrups. The more approximate Eq. (4.12b) for V_c may be used. Material strengths are $f'_c = 4000$ psi and $f_y = 60,000$ psi.
- 4.3.** Redesign the shear reinforcement for the beam of Problem 4.2, basing V_c on the more accurate Eq. (4.12a). Comment on your results, with respect to design time and probable construction cost difference.
- 4.4.** Design the shear reinforcement, using No. 4 (No. 13) vertical U stirrups for the independent T beam shown in Fig. P4.4. The beam spans 24 ft face to face between simple supports, has an effective depth $d = 31$ in., and is reinforced for flexure with six No. 10 (No. 32) bars in two layers that continue uninterrupted to the ends of the span. It is to carry service dead load $D = 2.67$ kips/ft (including self-weight) and service live load $L = 5.36$ kips/ft, both uniformly distributed along the span. The more approximate Eq. (4.12b) for V_c may be used. Material strengths are $f'_c = 5000$ psi and $f_y = 60,000$ psi.

FIGURE P4.4



- 4.5.** A beam of 11 in. width and effective depth of 16 in. carries a factored uniformly distributed load of 5.3 kips/ft, including its own weight, in addition to a central, concentrated factored load of 12 kips. It spans 18 ft, and restraining end moments at full factored load are 137 ft-kips at each support. It is reinforced with three No. 9 (No. 29) bars for both positive and negative bending. If $f'_c = 4000$ psi, through what part of the beam is web reinforcement theoretically required (a) if Eq. (4.12b) is used and (b) if Eq. (4.12a) is used? Comment.

- 4.6. What effect would an additional clockwise moment of 176 ft-kips at the right support have on the requirement for shear reinforcement determined in part (a) of Problem 4.5?
- 4.7. Design the web reinforcement for the beam of Problem 4.5, with V_c determined by the more approximate ACI equation, using No. 3 (No. 10) vertical stirrups with $f_y = 60,000$ psi.
- 4.8. Design the web reinforcement for the beam of Problem 4.6, with V_c determined by the more approximate ACI equation, using No. 3 (No. 10) vertical stirrups with $f_y = 60,000$ psi.
- 4.9. The beam of Problem 4.2 will be subjected to a factored axial compression load of 88 kips on the 10×20 in. gross cross section, in addition to the loads described earlier. What is the effect on concrete shear strength V_c (a) by the more accurate ACI equation and (b) by the more approximate ACI equation?
- 4.10. The beam of Problem 4.2 will be subjected to a factored axial tension load of 44 kips on the 10×20 in. gross cross section, in addition to the loads described earlier. What is the effect on concrete shear strength V_c (a) by the more accurate ACI equation and (b) by the more conservative ACI approach?
- 4.11. Redesign the shear reinforcement for the beam of Problem 4.2, using the modified compression field theory with (a) $\phi_{\text{shear}} = 0.90$ and (b) $\phi_{\text{shear}} = 0.75$.
- 4.12. Redesign the shear reinforcement for the beam of Problem 4.4, using the modified compression field theory with (a) $\phi_{\text{shear}} = 0.90$ and (b) $\phi_{\text{shear}} = 0.75$.
- 4.13. A precast concrete beam having cross-sectional dimensions $b = 10$ in. and $h = 24$ in. is designed to act in a composite sense with a cast-in-place top slab having depth $h_f = 5$ in. and width 48 in. At factored loads, the maximum compressive stress in the flange at midspan is 2400 psi; at the supports of the 28 ft simple span the flange force must be zero. Vertical U stirrups provided for flexural shear will be extended into the slab and suitably anchored to provide also for transfer of the flange force by shear friction. Find the minimum number of No. 4 (No. 13) stirrups that must be provided, based on shear-friction requirements. Concrete in both precast and cast-in-place parts will have $f'_c = 4000$ psi and $f_y = 60,000$ psi. The top surface of the precast web will be intentionally roughened according to the ACI Code definition.
- 4.14. Redesign the beam-end reinforcement of Example 4.6, given that a roller support will be provided so that $N_u = 0$.

5

Bond, Anchorage, and Development Length

5.1 FUNDAMENTALS OF FLEXURAL BOND

If the reinforced concrete beam of Fig. 5.1a were constructed using plain round reinforcing bars, and, furthermore, if those bars were to be greased or otherwise lubricated before the concrete were cast, the beam would be very little stronger than if it were built of plain concrete, without reinforcement. If a load were applied, as shown in Fig. 5.1b, the bars would tend to maintain their original length as the beam deflected. The bars would slip longitudinally with respect to the adjacent concrete, which would experience tensile strain due to flexure. Proposition 2 of Section 1.8, the assumption that the strain in an embedded reinforcing bar is the same as that in the surrounding concrete, would not be valid. For reinforced concrete to behave as intended, it is essential that *bond forces* be developed on the interface between concrete and steel, such as to prevent significant slip from occurring at that interface.

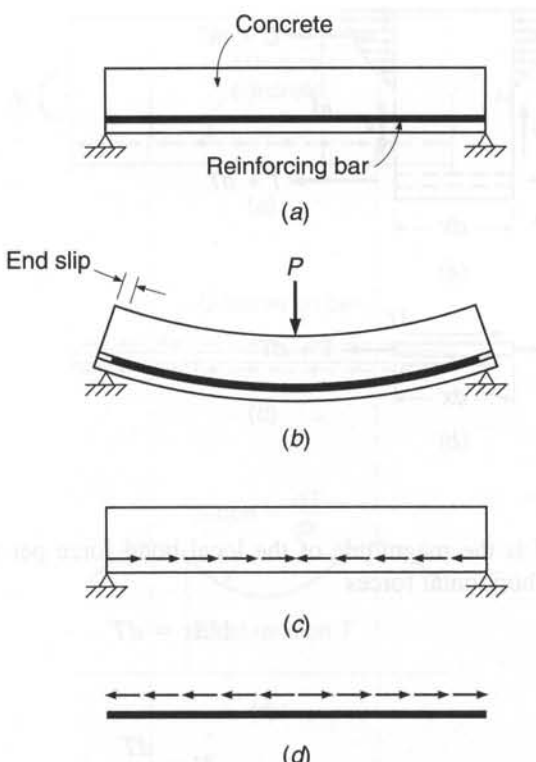
Figure 5.1c shows the bond forces that act on the concrete at the interface as a result of bending, while Fig. 5.1d shows the equal and opposite bond forces acting on the reinforcement. It is through the action of these interface bond forces that the slip indicated in Fig. 5.1b is prevented.

Some years ago, when plain bars without surface deformations were used, initial bond strength was provided only by the relatively weak chemical adhesion and mechanical friction between steel and concrete. Once adhesion and static friction were overcome at larger loads, small amounts of slip led to interlocking of the natural roughness of the bar with the concrete. However, this natural bond strength is so low that in beams reinforced with plain bars, the bond between steel and concrete was frequently broken. Such a beam will collapse as the bar is pulled through the concrete. To prevent this, end anchorage was provided, chiefly in the form of hooks, as in Fig. 5.2. If the anchorage is adequate, such a beam will not collapse, even if the bond is broken over the entire length between anchorages. This is so because the member acts as a tied arch, as shown in Fig. 5.2, with the uncracked concrete shown shaded representing the arch and the anchored bars the tie-rod. In this case, over the length in which the bond is broken, bond forces are zero. This means that over the entire unbonded length the force in the steel is constant and equal to $T = M_{\max}/jd$. As a consequence, the total steel elongation in such beams is larger than in beams in which bond is preserved, resulting in larger deflections and greater crack widths.

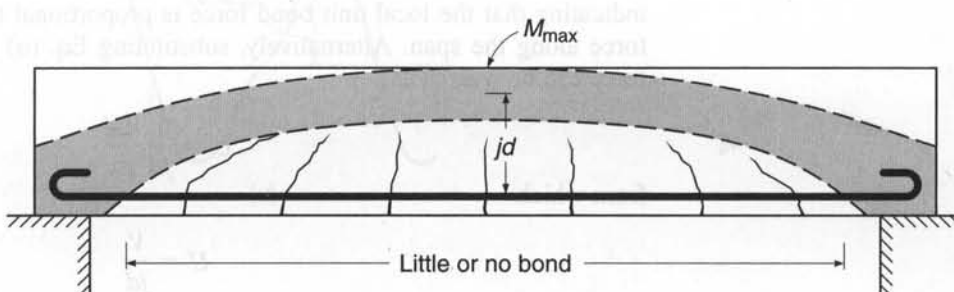
To improve this situation, deformed bars are now universally used in the United States and many other countries (see Section 2.14). With such bars, the shoulders of the projecting deformations bear on the surrounding concrete and result in greatly increased bond strength. It is then possible in most cases to dispense with special anchorage devices such as hooks. In addition, crack widths as well as deflections are reduced.

FIGURE 5.1

Bond forces due to flexure:
 (a) beam before loading;
 (b) unrestrained slip between concrete and steel; (c) bond forces acting on concrete;
 (d) bond forces acting on steel.

**FIGURE 5.2**

Tied-arch action in a beam with little or no bond.



a. Bond Force Based on Simple Cracked Section Analysis

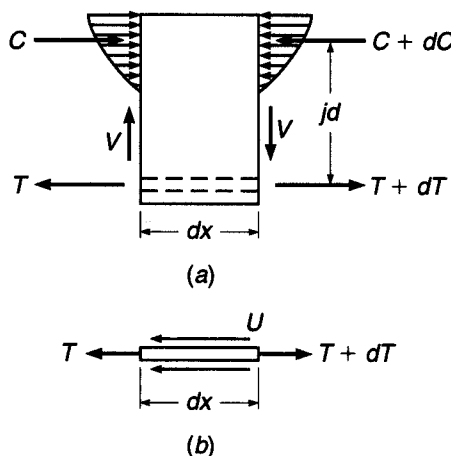
In a short piece of a beam of length dx , such as shown in Fig. 5.3a, the moment at one end will generally differ from that at the other end by a small amount dM . If this piece is isolated, and if one assumes that, after cracking, the concrete does not resist any tension stresses, the internal forces are those shown in Fig. 5.3a. The change in bending moment dM produces a change in the bar force

$$dT = \frac{dM}{jd} \quad (a)$$

where jd is the internal lever arm between tensile and compressive force resultants. Since the bar or bars must be in equilibrium, this change in bar force is resisted at the contact surface between steel and concrete by an equal and opposite force produced by bond, as indicated by Fig. 5.3b.

FIGURE 5.3

Forces acting on elemental length of beam: (a) free-body sketch of reinforced concrete element; (b) free-body sketch of steel element.



If U is the magnitude of the local bond force per unit length of bar, then, by summing horizontal forces

$$U dx = dT \quad (b)$$

Thus

$$U = \frac{dT}{dx} \quad (5.1)$$

indicating that the local unit bond force is proportional to the rate of change of bar force along the span. Alternatively, substituting Eq. (a) in Eq. (5.1), the unit bond force can be written as

$$U = \frac{1}{jd} \frac{dM}{dx} \quad (c)$$

from which

$$U = \frac{V}{jd} \quad (5.2)$$

Equation (5.2) is the “elastic cracked section equation” for flexural bond force, and it indicates that the bond force per unit length is proportional to the shear at a particular section, i.e., to the rate of change of bending moment.

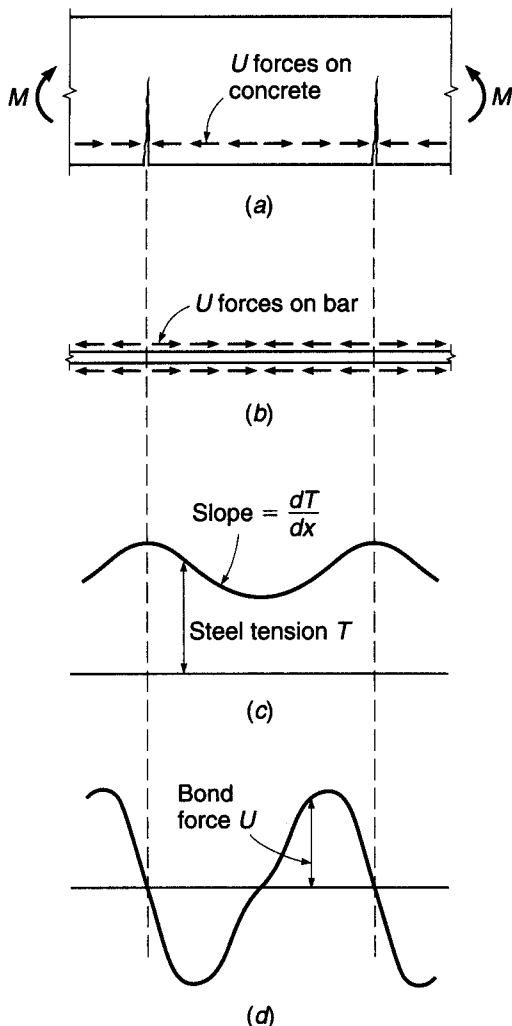
Note that Eq. (5.2) applies to the *tension* bars in a concrete zone that is assumed to be fully cracked, with the concrete resisting no tension. It applies, therefore, to the tensile bars in simple spans, or, in continuous spans, either to the bottom bars in the positive bending region between inflection points or to the top bars in the negative bending region between the inflection points and the supports. It does not apply to compression reinforcement, for which it can be shown that the flexural bond forces are very low.

b. Actual Distribution of Flexural Bond Force

The actual distribution of bond force along deformed reinforcing bars is much more complex than that represented by Eq. (5.2), and Eq. (5.1) provides a better basis for understanding beam behavior. Figure 5.4 shows a beam segment subject to pure

FIGURE 5.4

Variation of steel and bond forces in a reinforced concrete member subject to pure bending: (a) cracked concrete segment; (b) bond forces acting on reinforcing bar; (c) variation of tensile force in steel; (d) variation of bond force along steel.

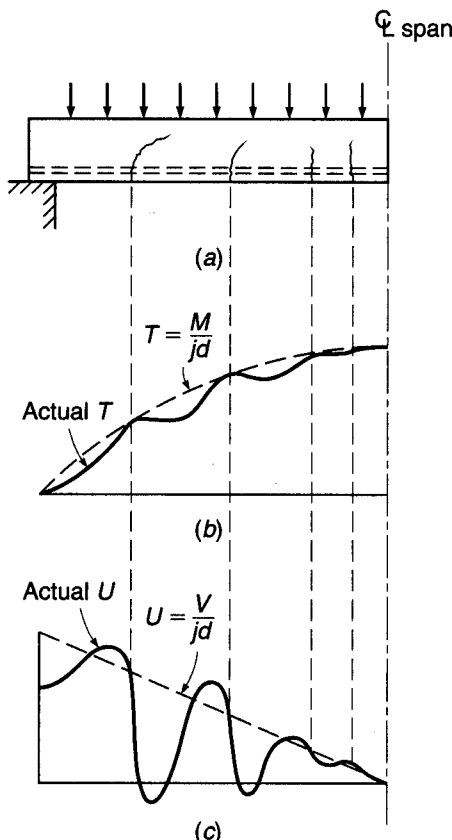


bending. The concrete fails to resist tensile stresses only where the actual crack is located; there the steel tension is maximum and has the value predicted by simple theory: $T = M/jd$. Between cracks, the concrete *does* resist moderate amounts of tension, introduced by bond forces acting along the interface in the direction shown in Fig. 5.4a. This reduces the tensile force in the steel, as illustrated by Fig. 5.4c. From Eq. (5.1), it is clear that U is proportional to the rate of change of bar force, and thus will vary as shown in Fig. 5.4d; unit bond forces are highest where the slope of the steel force curve is greatest and are zero where the slope is zero. Very high local bond forces adjacent to cracks have been measured in tests (Refs. 5.1 and 5.2). They are so high that inevitably some slip occurs between concrete and steel adjacent to each crack.

Beams are seldom subject to pure bending moment; they generally carry transverse loads producing shear and moment that vary along the span. Figure 5.5a shows a beam carrying a distributed load. The cracking indicated is typical. The steel force T predicted by simple cracked section analysis is proportional to the moment diagram and is as shown by the dashed line in Fig. 5.5b. However, the actual value of

FIGURE 5.5

Effect of flexural cracks on bond forces in beam:
 (a) beam with flexural cracks; (b) variation of tensile force T in steel along span; (c) variation of bond force per unit length U along span.



T is less than that predicted by the simple analysis everywhere except at the actual crack locations. The actual variation of T is shown by the solid line of Fig. 5.5b. In Fig. 5.5c, the bond forces predicted by the simplified theory are shown by the dashed line, and the actual variation is shown by the solid line. Note that the value of U is equal to that given by Eq. (5.2) only at those locations where the slope of the steel force diagram equals that of the simple theory. Elsewhere, if the slope is greater than assumed, the local bond force is greater; if the slope is less, local bond force is less. Just to the left of the cracks, for the present example, U is much higher than predicted by Eq. (5.2), and in all probability will result in local bond failure. Just to the right of the cracks, U is much lower than predicted and in fact is generally negative very close to the crack; i.e., the bond forces act in the reverse direction.

It is evident that actual bond forces in beams bear very little relation to those predicted by Eq. (5.2), except in the general sense that they are highest in the regions of high shear.

5.2 BOND STRENGTH AND DEVELOPMENT LENGTH

For reinforcing bars in tension, two types of bond failure have been observed. The first is *direct pullout* of the bar, which occurs when ample confinement is provided by the surrounding concrete. This could be expected when relatively small-diameter bars are used with sufficiently large concrete cover distances and bar spacing. The second type

of failure is *splitting* of the concrete along the bar when cover, confinement, or bar spacing is insufficient to resist the lateral concrete tension resulting from the wedging effect of the bar deformations. Present-day design methods require that both possible failure modes be accounted for.

a. Bond Strength

If the bar is sufficiently confined by a mass of surrounding concrete, then as the tensile force on the bar is increased, adhesive bond and friction are overcome, the concrete eventually crushes locally ahead of the bar deformations, and bar pullout results. The surrounding concrete remains intact, except for the crushing that takes place ahead of the ribs immediately adjacent to the bar interface. For modern deformed bars, adhesion and friction are much less important than the mechanical interlock of the deformations with the surrounding concrete.

Bond failure resulting from splitting of the concrete is more common in beams than direct pullout. Such splitting comes mainly from wedging action when the ribs of the deformed bars bear against the concrete (Refs. 5.3 and 5.4). It may occur either in a vertical plane as in Fig. 5.6a or horizontally in the plane of the bars as in Fig. 5.6b. The horizontal type of splitting of Fig. 5.6b frequently begins at a diagonal crack. In this case, as discussed in connection with Fig. 4.7b and shown in Fig. 4.1, dowel action increases the tendency toward splitting. This indicates that shear and bond failures are often intricately interrelated.

When pullout resistance is overcome or when splitting has spread all the way to the end of an unanchored bar, complete bond failure occurs. Sliding of the steel relative to the concrete leads to immediate collapse of the beam.

If one considers the large local variations of bond force caused by flexural and diagonal cracks (see Figs. 5.4 and 5.5), it becomes clear that local bond failures immediately adjacent to cracks will often occur at loads considerably below the failure load of the beam. These local failures result in small local slips and some widening of cracks and increase of deflections, but will be harmless as long as failure does not propagate all along the bar, with resultant total slip. In fact, as discussed in connection with Fig. 5.2, when end anchorage is reliable, bond can be severed along the entire length of the bar, excluding the anchorages, without endangering the carrying capacity of the beam. End anchorage can be provided by hooks as suggested by Fig. 5.2 or,

FIGURE 5.6

Splitting of concrete along reinforcement.

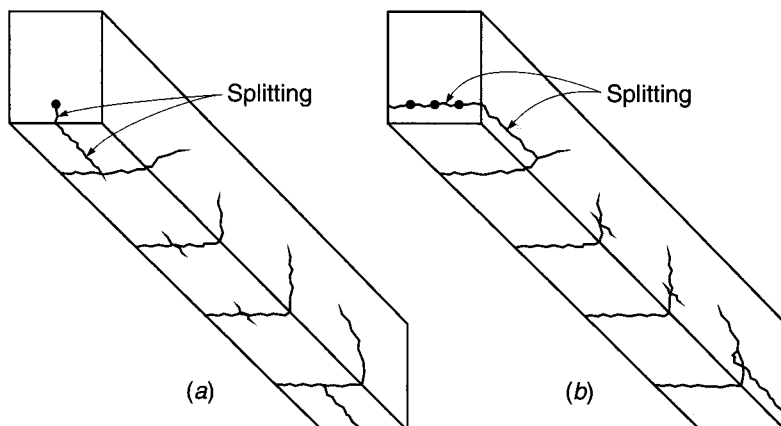
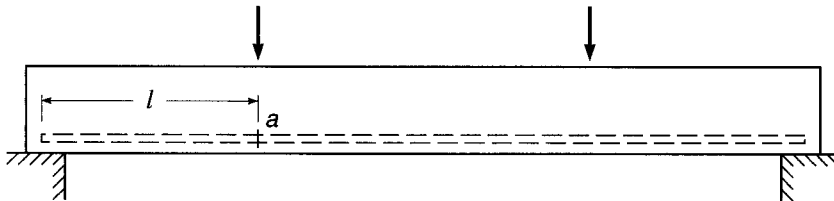


FIGURE 5.7

Development length.



much more commonly, by extending the straight bar a sufficient distance from the point of maximum stress.

Extensive testing (Refs. 5.5 to 5.11), using beam specimens, has established limiting values of bond strength. This testing provides the basis for current design requirements.

b. Development Length

The preceding discussion suggests the concept of *development length* of a reinforcing bar. The development length is defined as that length of embedment necessary to develop the full tensile strength of the bar, controlled by either pullout or splitting. With reference to Fig. 5.7, the moment, and therefore the steel stress, is evidently maximum at point *a* (neglecting the weight of the beam) and zero at the supports. If the bar stress is f_s at *a*, then the total tension force $A_b f_s$ must be transferred from the bar to the concrete in the distance *l* by bond forces. To fully develop the strength of the bar $A_b f_y$, the distance *l* must be at least equal to the development length of the bar, established by tests. In the beam of Fig. 5.7, if the actual length *l* is equal to or greater than the development length l_d , no premature bond failure will occur. That is, the beam will fail in bending or shear rather than by bond failure. This will be so even if in the vicinity of cracks local slip may have occurred over small regions along the beam.

It is seen that the main requirement for safety against bond failure is this: the length of the bar, from any point of given steel stress (f_s or at most f_y) to its nearby free end, must be at least equal to its development length. If this requirement is satisfied, the magnitude of the nominal flexural bond force along the beam, as given by Eq. (5.2), is of only secondary importance, since the integrity of the member is ensured even in the face of possible minor local bond failures. However, if the actual available length is inadequate for full development, special anchorage, such as by hooks, must be provided.

c. Factors Influencing Development Length

Experimental research has identified the factors that influence development length, and analysis of the test data has resulted in the empirical equations used in present design practice. The most basic factors will be clear from review of the preceding paragraphs and include concrete tensile strength, cover distance, spacing of the reinforcing bars, and the presence of transverse steel reinforcement.

Clearly, the *tensile strength* of the concrete is important because the most common type of bond failure in beams is the type of splitting shown in Fig. 5.6. Although tensile strength does not appear explicitly in experimentally derived equations for development length (see Section 5.3), the term $\sqrt{f'_c}$ appears in the denominator of those equations and reflects the influence of concrete tensile strength.

As discussed in Section 2.9, the fracture energy of concrete plays an important role in bond failure because a splitting crack must propagate after it has formed. Since fracture energy is largely independent of compressive strength, bond strength increases more slowly than $\sqrt{f'_c}$, and as data for higher-strength concretes have become available, $f_c'^{1/4}$ has been shown to provide a better representation of the effect of concrete strength on bond than $\sqrt{f'_c}$ (Refs. 5.12 to 5.14). This point is recognized by ACI Committee 408, Bond and Development of Reinforcement (Ref. 5.15), in proposed design expressions based on $f_c'^{1/4}$ and within the ACI Code, which sets an upper limit on the value of $\sqrt{f'_c}$ for use in design.

For lightweight concretes, the tensile strength is usually less than for normal-density concrete having the same compressive strength; accordingly, if lightweight concrete is used, development lengths must be increased. Alternatively, if split-cylinder strength is known or specified for lightweight concrete, it can be incorporated in development length equations as follows. For normal concrete, the split-cylinder tensile strength f_{ct} is generally taken as $f_{ct} = 6.7\sqrt{f'_c}$. If the split-cylinder strength f_{ct} is known for a particular lightweight concrete, then $\sqrt{f'_c}$ in the development length equations can be replaced by $f_{ct}/6.7$.

Cover distance—conventionally measured from the *center* of the bar to the nearest concrete face and measured either in the plane of the bars or perpendicular to that plane—also influences splitting. Clearly, if the vertical or horizontal cover is increased, more concrete is available to resist the tension resulting from the wedging effect of the deformed bars, resistance to splitting is improved, and development length is less.

Similarly, Fig. 5.6b illustrates that if the *bar spacing* is increased (e.g., if only two instead of three bars are used), more concrete per bar will be available to resist horizontal splitting (Ref. 5.16). In beams, bars are typically spaced about one or two bar diameters apart. On the other hand, for slabs, footings, and certain other types of member, bar spacings are typically much greater, and the required development length is reduced.

Transverse reinforcement, such as that provided by stirrups of the types shown in Fig. 4.8, improves the resistance of tensile bars to both vertical or horizontal splitting failure because the tensile force in the transverse steel tends to prevent opening of the actual or potential crack. The effectiveness of such transverse reinforcement depends on its cross-sectional area and spacing along the development length. Its effectiveness does not depend on its yield strength f_{yt} , because transverse reinforcement rarely yields during a bond failure (Refs. 5.12 to 5.15). The yield strength of the transverse steel f_{yt} , however, is presently used in the bond provisions of the ACI Code.

Based on the results of a statistical analysis of test data (Ref. 5.10), with appropriate simplifications, the length l_d needed to develop stress f_s in a reinforcing bar may be expressed as

$$l_d = \left(\frac{3}{40} \frac{f_s}{\sqrt{f'_c} \left[\frac{(c + K_{tr})}{d_b} \right]} \right) d_b \quad (5.3)$$

where d_b = bar diameter

c = smaller of minimum cover or one-half of bar spacing *measured to center of bar*

$K_{tr} = 40A_{tr}/sn$, which represents effect of confining reinforcement

- A_{tr} = area of transverse reinforcement normal to plane of splitting through the bars being developed
 s = spacing of transverse reinforcement
 n = number of bars developed or spliced at same location

Equation (5.3) captures the effects of concrete strength, concrete cover, and transverse reinforcement on l_d and serves as the basis for design in the 2008 ACI Code. For full development of the bar, f_s is set equal to f_y .

In addition to the factors just discussed, other influences have been identified. The vertical location of horizontal bars relative to beam depth has been found to have an effect (Ref. 5.17). If bars are placed in the forms during construction such that a substantial *depth of concrete is placed below those bars*, there is a tendency for excess water, often used in the mix for workability, and for entrapped air to rise to the top of the concrete during consolidation. Air and water tend to accumulate on the underside of the bars. Tests have shown a significant loss in bond strength for bars with more than 12 in. of fresh concrete cast beneath them, and accordingly the development length must be increased. This effect increases as the slump of the concrete increases and is greatest for bars cast near the upper surface of a concrete placement (Ref. 5.18).

Epoxy-coated reinforcing bars are used regularly in projects where the structure may be subjected to corrosive environmental conditions or deicing chemicals, such as for highway bridge decks and parking garages. Studies have shown that bond strength is reduced because the epoxy coating reduces the friction between the concrete and the bar, and the required development length must be increased substantially (Refs. 5.19 to 5.23). Early evidence showed that if cover and bar spacing were large, the effect of the epoxy coating would not be so pronounced, and as a result, a smaller increase was felt justified under these conditions (Ref. 5.20). Although later research (Ref. 5.12) does not support this conclusion, provisions to allow for a smaller increase remain in the ACI Code. Since the bond strength of epoxy-coated bars is already reduced because of lack of adhesion, an upper limit has been established for the product of development length factors accounting for the depth of concrete cast below horizontal bars and epoxy coating.

Not infrequently, tensile reinforcement somewhat in excess of the calculated requirement will be provided, e.g., as a result of upward rounding A_s when bars are selected or when minimum steel requirements govern. Logically, in this case, the required development length may be reduced by the ratio of steel area required to steel area actually provided. The modification for *excess reinforcement* should be applied only where anchorage or development for the full yield strength of the bar is not required.

Finally, based on bars with very short development lengths (most with values of $l_d/d_b < 15$), it was observed that *smaller-diameter bars* required lower development lengths than predicted by Eq. (5.3). As a result, the required development lengths for No. 6 (No. 19) and smaller bars were reduced below the values required by Eq. (5.3).†

Reference 5.15 presents a detailed discussion of the factors that control the bond and development of reinforcing bars in tension. Except as noted, these influences are accounted for in the basic equation for development length in the 2008 ACI Code.

† The use of Eq. (5.3) for low values of l_d/d_b greatly underestimates the actual value of bond strength and makes it appear that a lower value of l_d can be used safely. An evaluation of test results for small bars with more realistic development lengths ($l_d/d_b \geq 16$), however, has shown that the special provision in the ACI Code for smaller bars is not justified (Refs. 5.14, 5.15, and 5.24). Because of the unconservative nature of the small bar provision, ACI Committee 408 (Ref. 5.15) recommends that it not be applied in design.

All modification factors for development length are defined explicitly in the Code, with appropriate restrictions. Details are given next.

5.3 ACI CODE PROVISIONS FOR DEVELOPMENT OF TENSION REINFORCEMENT

The approach to bond strength incorporated in the ACI Code follows from the discussion presented in Section 5.2. The fundamental requirement is that the calculated force in the reinforcement at each section of a reinforced concrete member be developed on each side of that section by adequate embedment length, hooks, mechanical anchorage, or a combination of these, to ensure against pullout. Local high bond forces, such as are known to exist adjacent to cracks in beams, are not considered to be significant. Generally, the force to be developed is calculated based on the yield stress in the reinforcement; i.e., the bar strength is to be fully developed.

In the ACI Code, the required development length for deformed bars in tension is based on Eq. (5.3). A single basic equation is given that includes *all* the influences discussed in Section 5.2 and thus appears highly complex because of its inclusiveness. However, it does permit the designer to see the effects of all the controlling variables and allows more rigorous calculation of the required development length when it is critical. The ACI Code also includes simplified equations that can be used for most cases in ordinary design, provided that some restrictions are accepted on bar spacing, cover values, and minimum transverse reinforcement. These alternative equations can be further simplified for normal-density concrete and uncoated bars.[†]

In the following presentation of development length, the basic ACI equation is given first and its terms are defined and discussed. After this, the alternative equations, also part of the ACI Code, are presented. Note that, in any case, development length l_d must not be less than 12 in.

a. Basic Equation for Development of Tension Bars

According to ACI Code 12.2.3, for deformed bars or deformed wires,

$$l_d = \left(\frac{3}{40} \frac{f_y}{\lambda \sqrt{f'_c}} \frac{\psi_t \psi_e \psi_s}{\left[\frac{(c_b + K_{tr})}{d_b} \right]} \right) d_b \quad (5.4)$$

in which the term $(c + K_{tr})/d_b$ shall not be taken greater than 2.5. In Eq. (5.4), terms are defined and values established as follows.

ψ_t = reinforcement location factor

Horizontal reinforcement so placed that more than 12 in. of fresh concrete is cast in the member below the development length or splice:

1.3

Other situations:

1.0

[†] This two-tier approach to development length corresponds exactly to the ACI Code treatment for V_c , the contribution of concrete in shear calculations. The more detailed calculation by Eq. (4.12a) is useful for computerized design or research but is tedious for manual calculations because of the need to recalculate the governing variables at close intervals along the span. For ordinary design, recognizing that overall economy is but little affected, the simpler but more approximate and more conservative Eq. (4.12b) is used.

ψ_e = coating factor	
Epoxy-coated bars or wires with cover less than $3d_b$ or clear spacing less than $6d_b$:	1.5
All other epoxy-coated bars or wires:	1.2
Uncoated and zinc-coated (galvanized) reinforcement:	1.0
However, the product of $\psi_t \psi_e$ need not be taken greater than 1.7.	
ψ_s = reinforcement size factor	
No. 6 (No. 19) and smaller bars and deformed wires:	0.8 [†]
No. 7 (No. 22) and larger bars:	1.0
λ = lightweight aggregate concrete factor	
When lightweight aggregate concrete is used:	0.75
However, when f_{ct} is specified, $\lambda = f_{ct}/(6.7\sqrt{f'_c}) \leq 1.0$.	
When normalweight concrete is used:	1.0
c = spacing or cover dimension, in.	
Use the smaller of either the distance from the center of the bar to the nearest concrete surface or one-half the center-to-center spacing of the bars being developed.	
K_{tr} = transverse reinforcement index: $40A_{tr}/sn$	
where A_{tr} = total cross-sectional area of all transverse reinforcement that is within the spacing s and that crosses the potential plane of splitting through the reinforcement being developed, in ²	
s = maximum spacing of transverse reinforcement within l_d center to center, in.	
n = number of bars or wires being developed along the plane of splitting	
As a simplification, the designer is permitted to use $K_{tr} = 0$ even if transverse reinforcement is present.	
The limit of 2.5 on $(c + K_{tr})/d_b$ is imposed to avoid pullout failure. With that term taken equal to its limit of 2.5, evaluation of Eq. (5.4) results in $l_d = 0.03d_b f_y/\sqrt{f'_c}$, the experimentally derived limit found in earlier ACI Codes when pullout failure controls. Note that in Eq. (5.4) and in all other ACI Code equations relating to the development length and splices of reinforcement, values of $\sqrt{f'_c}$ are not to be taken greater than 100 psi because of the lack of experimental evidence on bond strengths obtainable with concretes having compressive strength in excess of 10,000 psi at the time that Eqs. (5.3) and (5.4) were formulated. More recent tests with concrete with values of f'_c to 16,000 psi justify this limitation.	

b. Simplified Equations for Development Length

Calculation of required development length (in terms of bar diameter) by Eq. (5.4) requires that the term $(c + K_{tr})/d_b$ be calculated for each particular combination of cover, spacing, and transverse reinforcement. Alternatively, according to the Code, a simplified form of Eq. (5.4) may be used in which $(c + K_{tr})/d_b$ is set equal to 1.5, provided that certain restrictions are placed on cover, spacing, and transverse reinforcement. Two cases of practical importance are:

1. Minimum clear cover of $1.0d_b$, minimum clear spacing of $1.0d_b$, and at least the Code required minimum stirrups or ties (see Section 4.5b) throughout l_d
2. Minimum clear cover of $1.0d_b$ and minimum clear spacing of $2d_b$

[†] ACI Committee 408 recommends a value of 1.0 for all bar sizes based on experimental evidence. The ACI Code value of 0.8, however, will be used in what follows.

TABLE 5.1**Simplified tension development length in bar diameters according to the ACI Code**

	No. 6 (No. 19) and Smaller Bars and Deformed Wires[†]	No. 7 (No. 22) and Larger Bars
Clear spacing of bars being developed or spliced $\geq d_b$, clear cover $\geq d_b$, and stirrups or ties throughout l_d not less than the Code minimum	$l_d = \left(\frac{f_y \psi_t \psi_e}{25\lambda \sqrt{f'_c}} \right) d_b$	$l_d = \left(\frac{f_y \psi_t \psi_e}{20\lambda \sqrt{f'_c}} \right) d_b$
Clear spacing of bars being developed or spliced $\geq 2d_b$, and clear cover $\geq d_b$	Same as above	Same as above
Other cases	$l_d = \left(\frac{3f_y \psi_t \psi_e}{50\lambda \sqrt{f'_c}} \right) d_b$	$l_d = \left(\frac{3f_y \psi_t \psi_e}{40\lambda \sqrt{f'_c}} \right) d_b$

[†] For reasons discussed in Section 5.3a, ACI Committee 408 recommends that l_d for No. 7 (No. 22) and larger bars be used for all bar sizes.

For either of these common cases, it is easily confirmed from Eq. (5.4) that for No. 7 (No. 22) and larger bars

$$l_d = \left(\frac{f_y \psi_t \psi_e}{20\lambda \sqrt{f'_c}} \right) d_b \quad (5.5a)$$

and for No. 6 (No. 19) bars and smaller (with $\gamma = 0.8$)

$$l_d = \left(\frac{f_y \psi_t \psi_e}{25\lambda \sqrt{f'_c}} \right) d_b \quad (5.5b)$$

If these restrictions on spacing are not met, then, provided that Code-imposed minimum spacing requirements are met (see Section 3.6c), the term $(c + K_{tr})/d_b$ will have a value not less than 1.0 (rather than 1.5 as before) whether or not transverse steel is used. The values given by Eqs. (5.5a) and (5.5b) are then multiplied by the factor 1.5/1.0.

Thus if the designer accepts certain restrictions on bar cover, spacing, and transverse reinforcement, simplified calculation of development requirements is possible. The simplified equations are summarized in Table 5.1.

Further simplification is possible for the most common condition of normal-density concrete and uncoated reinforcement. Then λ and ψ_e in Table 5.1 take the value 1.0, and the development lengths, in terms of bar diameters, are simply a function of f_y , f'_c , and the bar location factor ψ_t . Thus development lengths are easily tabulated for the usual combinations of material strengths and bottom or top bars and for the restrictions on bar spacing, cover, and transverse steel defined.[†] Results are given in Table A.10 of Appendix A.

Regardless of whether development length is calculated using the basic Eq. (5.4) or the more approximate Eqs. (5.5a) and (5.5b), development length may be reduced where reinforcement in a flexural member is in excess of that required by analysis,

[†] Note that, for convenient reference, the term top bar is used for any horizontal reinforcing bar placed with more than 12 in. of fresh concrete cast below the development length or splice. This definition may require that bars relatively near the bottom of a deep member be treated as top bars.

except where anchorage or development for f_y is specifically required or the reinforcement is designed for a region of high seismic risk. According to the ACI Code, the reduction is made according to the ratio (A_s required/ A_s provided).

EXAMPLE 5.1

Development length in tension. Figure 5.8 shows a beam-column joint in a continuous building frame. Based on frame analysis, the negative steel required at the end of the beam is 2.90 in^2 ; two No. 11 (No. 36) bars are used, providing $A_s = 3.12 \text{ in}^2$. Beam dimensions are $b = 10 \text{ in.}$, $d = 18 \text{ in.}$, and $h = 21 \text{ in.}$. The design will include No. 3 (No. 10) stirrups spaced four at 3 in., followed by a constant 5 in. spacing in the region of the support, with 1.5 in. clear cover. Normalweight concrete is to be used, with $f'_c = 4000 \text{ psi}$, and reinforcing bars have $f_y = 60,000 \text{ psi}$. Find the minimum distance l_d at which the negative bars can be cut off, based on development of the required steel area at the face of the column, (a) using the simplified equations of Table 5.1, (b) using Table A.10, of Appendix A, and (c) using the basic Eq. (5.4).

SOLUTION. Checking for lateral spacing in the No. 11 (No. 36) bars determines that the clear distance between the bars is $10 - 2(1.50 + 0.38 + 1.41) = 3.42 \text{ in.}$, or 2.43 times the bar diameter d_b . The clear cover of the No. 11 (No. 36) bars to the side face of the beam is $1.50 + 0.38 = 1.88 \text{ in.}$, or 1.33 bar diameters, and that to the top of the beam is $3.00 - 1.41/2 = 2.30 \text{ in.}$, or 1.63 bar diameters. These dimensions meet the restrictions stated in the second row of Table 5.1. Then for top bars, uncoated, and with normal-density concrete, we have the values of $\psi_t = 1.3$, $\psi_e = 1.0$, and $\lambda = 1.0$. From Table 5.1,

$$l_d = \frac{60,000 \times 1.3 \times 1.0}{20 \times 1.0 \sqrt{4000}} \cdot 1.41 = 62 \times 1.41 = 87 \text{ in.}$$

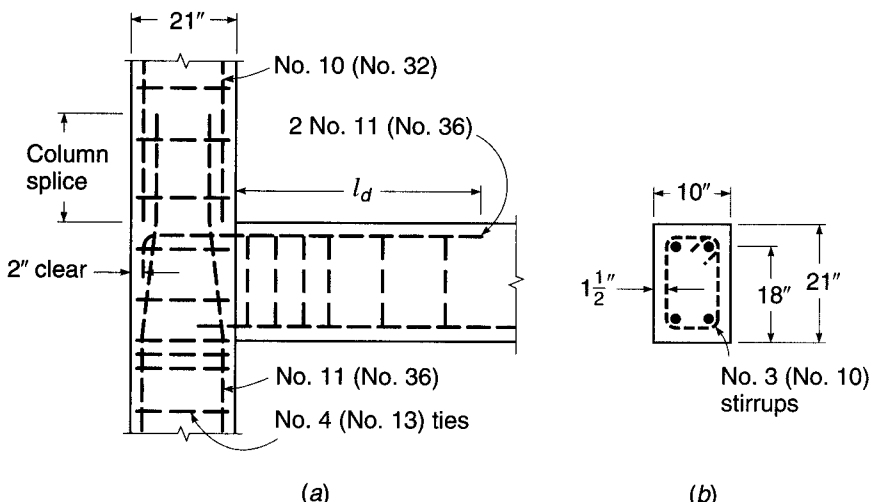
This can be reduced by the ratio of steel required to that provided, so that the final development length is $87 \times 2.90/3.12 = 81 \text{ in.}$

Alternatively, from the lower portion of Table A.10, $l_d/d_b = 62$. The required length to point of cutoff is $62 \times 1.41 \times 2.90/3.12 = 81 \text{ in.}$, as before.

The more accurate Eq. (5.4) will now be used. The center-to-center spacing of the No. 11 (No. 36) bars is $10 - 2(1.50 + 0.38 + 1.41/2) = 4.83$, one-half of which is 2.42 in. The side cover to bar centerline is $1.50 + 0.38 + 1.41/2 = 2.59 \text{ in.}$, and the top cover is 3.00 in. The smallest of these three distances controls, and $c = 2.42 \text{ in.}$ Potential splitting would be in the

FIGURE 5.8

Bar details at beam-column joint for bar development examples.



horizontal plane of the bars, and in calculating A_{tr} , two times the stirrup bar area is used.[†] Based on the No. 3 (No. 10) stirrups at 5 in. spacing:

$$K_{tr} = \frac{40 \times 0.11 \times 2}{5 \times 2} = 0.88 \quad \text{and} \quad \frac{c + K_{tr}}{d_b} = \frac{2.42 + 0.88}{1.41} = 2.34$$

This is less than the limit value of 2.5. Then from Eq. (5.4)

$$l_d = \frac{3 \times 60,000 \times 1.3}{40 \times 1.0 \sqrt{4000 \times 2.34}} 1.41 = 40 \times 1.41 = 55.7 \text{ in.}$$

and the required development length is $55.7 \times 2.90/3.12 = 52$ in. rather than 81 in. as before. Clearly, the use of the more accurate Eq. (5.4) permits a considerable reduction in development length. Even though its use requires much more time and effort, it is justified if the design is to be repeated many times in a structure.

5.4 ANCHORAGE OF TENSION BARS BY HOOKS

a. Standard Dimensions

In the event that the desired tensile stress in a bar cannot be developed by bond alone, it is necessary to provide special anchorage at the ends of the bar, usually by means of a 90° or a 180° hook or a headed bar (the latter is discussed in Section 5.5). The dimensions and bend radii for hooks have been standardized in ACI Code 7.1 as follows (see Fig. 5.9):

1. A 180° bend plus an extension of at least 4 bar diameters, but not less than $2\frac{1}{2}$ in. at the free end of the bar, or
2. A 90° bend plus an extension of at least 12 bar diameters at the free end of the bar, or
3. For stirrup and tie anchorage only:
 - (a) For No. 5 (No. 16) bars and smaller, a 90° bend plus an extension of at least 6 bar diameters at the free end of the bar, or
 - (b) For Nos. 6, 7, and 8 (Nos. 19, 22, and 25) bars, a 90° bend plus an extension of at least 12 bar diameters at the free end of the bar, or
 - (c) For No. 8 (No. 25) bars and smaller, a 135° bend plus an extension of at least 6 bar diameters at the free end of the bar.

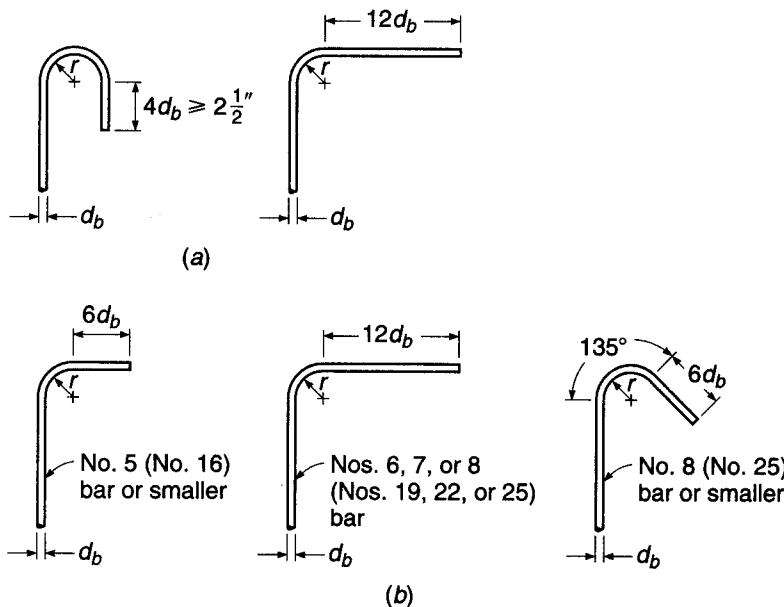
The minimum diameter of bend, measured on the inside of the bar, for standard hooks other than for stirrups or ties in sizes Nos. 3 through 5 (Nos. 10 through 16), should be not less than the values shown in Table 5.2. For stirrup and tie hooks, for bar sizes No. 5 (No. 16) and smaller, the inside diameter of bend should not be less than 4 bar diameters, according to the ACI Code.

When welded wire reinforcement (smooth or deformed wires) is used for stirrups or ties, the inside diameter of bend should not be less than 4 wire diameters for deformed wire larger than D6 and 2 wire diameters for all other wires. Bends with an inside diameter of less than 8 wire diameters should not be less than 4 wire diameters from the nearest welded intersection.

[†] If the top cover had controlled, the potential splitting plane would be vertical and one times the stirrup bar area would be used in calculating A_{tr} .

FIGURE 5.9

Standard bar hooks: (a) main reinforcement; (b) stirrups and ties.

**TABLE 5.2**

Minimum diameters of bend for standard hooks

Bar Size	Minimum Diameter
Nos. 3 through 8 (Nos. 10 through 25)	6 bar diameters
Nos. 9, 10, and 11 (Nos. 29, 32, and 36)	8 bar diameters
Nos. 14 and 18 (Nos. 43 and 57)	10 bar diameters

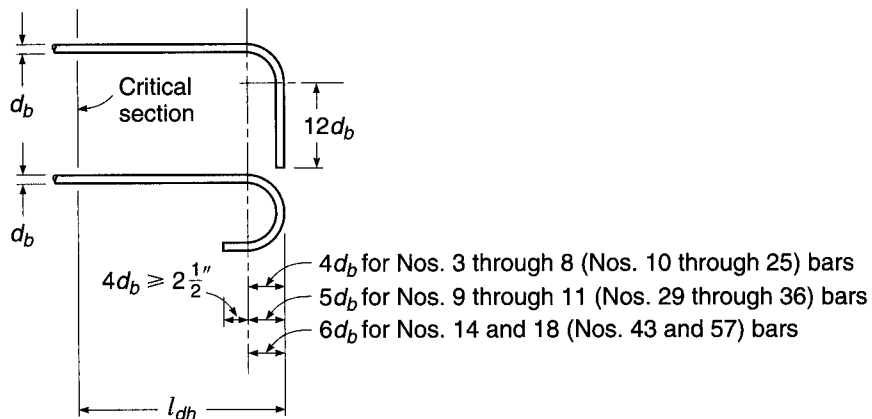
b. Development Length and Modification Factors for Hooked Bars

Hooked bars resist pullout by the combined actions of bond along the straight length of bar leading to the hook and anchorage provided by the hook. Tests indicate that the main cause of failure of hooked bars in tension is splitting of the concrete in the plane of the hook. This splitting is due to the very high stresses in the concrete inside of the hook; these stresses are influenced mainly by the bar diameter d_b for a given tensile force, and the radius of bar bend. Resistance to splitting has been found to depend on the concrete cover for the hooked bar, measured laterally from the edge of the member to the bar perpendicular to the plane of the hook, and measured to the top (or bottom) of the member from the point where the hook starts, parallel to the plane of the hook. If these distances must be small, the strength of the anchorage can be substantially increased by providing confinement steel in the form of closed stirrups or ties.

ACI Code 12.5 provisions for hooked bars in tension are based on research summarized in Refs. 5.8 and 5.9. The Code requirements account for the combined contribution of bond along the straight bar leading to the hook, plus the hooked anchorage. A total development length l_{dh} is defined as shown in Fig. 5.10 and is

FIGURE 5.10

Bar details for development of standard hooks.



measured from the critical section to the farthest point on the bar, parallel to the straight part of the bar. For standard hooks, as shown in Fig. 5.9, the development length is

$$l_{dh} = \left(\frac{0.02 \psi_e f_y}{\lambda \sqrt{f'_c}} \right) d_b \quad (5.6)$$

with $\psi_e = 1.2$ for epoxy-coated reinforcement and $\lambda = 0.75$ for lightweight aggregate concrete. For other cases, ψ_e and λ are taken as 1.0.

The development length l_{dh} should be multiplied by certain applicable modifying factors, summarized in Table 5.3. These factors are combined as appropriate; e.g., if side cover of at least $2\frac{1}{2}$ in. is provided for a 180° hook and if, in addition, ties are provided, the development length is multiplied by the product of 0.7 and 0.8. In any case, the length l_{dh} is not to be less than 8 bar diameters and not less than 6 in.

Transverse confinement steel is essential if the full bar strength must be developed with minimum concrete confinement, such as when hooks may be required at the ends of a simply supported beam or where a beam in a continuous structure frames into an end column and does not extend past the column or when bars must be anchored in a short cantilever, as shown in Fig. 5.11 (Ref. 5.11). According to ACI Code 12.5.4, for bars hooked at the discontinuous ends of members with both side

FIGURE 5.11

Transverse reinforcement requirements at discontinuous ends of members with small cover distances.

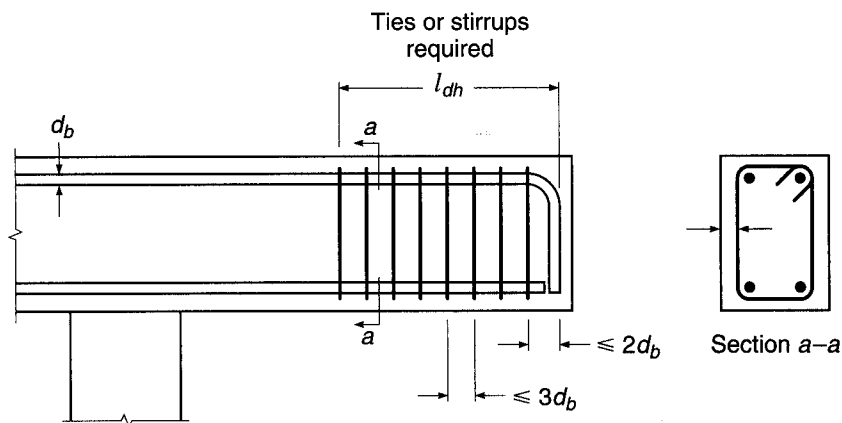


TABLE 5.3
Development lengths for hooked deformed bars in tension

A. Development length l_{dh} for hooked bars	$\left(\frac{0.02\psi_e f_y}{\lambda \sqrt{f'_c}} \right) d_b$
B. Modification factors applied to l_{dh}	
For No. 11 (No. 36) and smaller bar hooks with side cover (normal to plane of hook) not less than $2\frac{1}{2}$ in., and for 90° hooks with cover on bar extension beyond hook not less than 2 in.	0.7
For 90° hooks of No. 11 (No. 36) and smaller bars that are either enclosed within ties or stirrups perpendicular to the bar being developed, spaced not greater than $3d_b$ along the development length l_{dh} of the hook; or enclosed within ties or stirrups parallel to the bar being developed, spaced not greater than $3d_b$ along the length of the tail extension of the hook plus bend	0.8
For 180° hooks of No. 11 (No. 36) and smaller bars that are enclosed within ties or stirrups perpendicular to the bar being developed, spaced not greater than $3d_b$ along the development length l_{dh} of the hook	0.8
Where anchorage or development for f_y is not specifically required, reinforcement in excess of that required by analysis	$\frac{A_s \text{ required}}{A_s \text{ provided}}$
ψ_e :	
For epoxy-coated bars	1.2
For other bars	1.0
λ :	
For lightweight concrete	0.75
For normalweight concrete	1.0

cover and top or bottom cover less than $2\frac{1}{2}$ in., hooks *must* be enclosed with closed stirrups or ties along the full development length, as shown in Fig. 5.11. The spacing of the confinement steel must not exceed 3 times the diameter of the hooked bar d_b , and the first stirrup or tie must enclose the bent portion of the hook within a distance equal to $2d_b$ of the outside of the bend. In such cases, the factor 0.8 of Table 5.3 does not apply.

EXAMPLE 5.2

Development of hooked bars in tension. Referring to the beam-column joint shown in Fig. 5.8, the No. 11 (No. 36) negative bars are to be extended into the column and terminated in a standard 90° hook, keeping 2 in. clear to the outside face of the column. The column width in the direction of beam width is 16 in. Find the minimum length of embedment of the hook past the column face, and specify the hook details.

SOLUTION. The development length for hooked bars, measured from the critical section along the bar to the far side of the vertical hook, is given by Eq. (5.6):

$$l_{dh} = \frac{0.02 \times 1.0 \times 60,000}{1.0 \times \sqrt{4000}} \cdot 1.41 = 27 \text{ in.}$$

In this case, side cover for the No. 11 (No. 36) bars exceeds 2.5 in. and cover beyond the bent bar is adequate, so a modifying factor of 0.7 can be applied. The only other factor applicable is for excess reinforcement, which is 0.93 as for Example 5.1. Accordingly, the minimum development length for the hooked bars is

$$l_{dh} = 27 \times 0.7 \times 0.93 = 18 \text{ in.}$$

With $21 - 2 = 19$ in. available, the required length is contained within the column. The hook will be bent to a minimum diameter of $8 \times 1.41 = 11.28$ in. The bar will continue for 12 bar diameters, or 17 in. past the end of the bend in the vertical direction.

5.5 ANCHORAGE IN TENSION USING HEADED BARS

a. Requirements for Headed Bars

Headed bars provide an alternative to hooks when the desired tensile stress in the bar cannot be developed by bond alone. ACI Code 3.5.9 requires that headed deformed bars conform to ASTM A970 and, in addition, that obstructions or interruptions of the bar deformations not extend more than 2 bar diameters from the bearing face of the head, as shown in Fig. 5.12. While heads come in many configurations and sizes, ACI Code 12.6.1 requires that the bearing area of the head A_{brg} be equal to at least 4 times the area of the bar A_b .

Obstructions, such as shown in Fig. 5.12, are not counted as part of the bearing area according to the Commentary to ACI Code 3.5.9, and thus, the net bearing area of the head may be less than the gross area of the head minus the area of the bar.

b. Development Length and Modification Factors for Headed Bars

Differences between the mode of failure of headed bars loaded in tension and those exhibited by straight bars and hooks, coupled with the fact that only limited test data are available for headed bars, have resulted in the ACI Code adding restrictions to the design criteria for headed bars.

The bond strength of headed bars results from a combination of bond along the length of the bar and bearing at the face of the head. Prior to failure, the bond force along the bar increases and then decreases as slip occurs, while the bearing force on

FIGURE 5.12

Headed deformed reinforcing bar with an obstruction of the deformations that extends less than 2 bar diameters from the bearing face of the head.

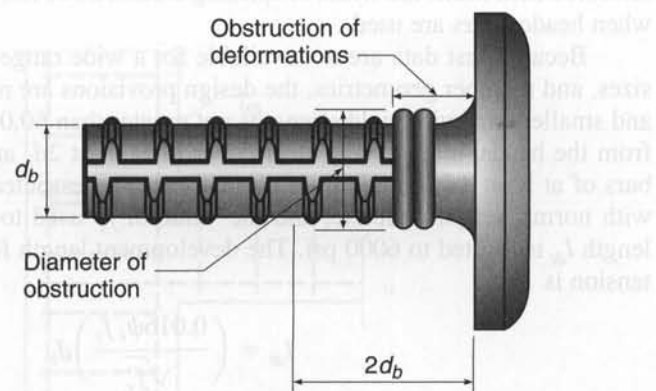


FIGURE 5.13

Headed deformed bars showing conical concrete wedges. (Photograph courtesy of Michael Keith Thompson.)



the head increases. In some cases, the contribution of bond along the length of the bar may become negligible prior to failure. Unlike straight reinforcing bars, which tend to fail in bond due to the formation of splitting cracks between bars or between the bar and the surface of the concrete, and hooks, which tend to fail in bond by cracking in the plane of the hook, headed bars fail in bond due to the formation of a conical wedge, as shown in Fig. 5.13, which causes radial splitting cracks in the concrete. In addition to radial splitting, failure can also occur due to the formation of a flat concrete cone near the surface (shallow pullout), if the development is relatively short, or a breakout cone, if the development length is long, and due to spalling or side-face blowout, if the side cover is low (Refs. 5.25 to 5.28). Transverse confining reinforcement, such as stirrups and ties, which increase the bond strength of both straight and hooked bars, provides little additional capacity to headed bars and is, thus, not considered when calculating the development length of headed bars. Because transverse reinforcement limits the width of splitting cracks, however, its use is still recommended when headed bars are used.

Because test data are not available for a wide range of concrete properties, bar sizes, and member geometries, the design provisions are restricted to No. 11 (No. 36) and smaller bars with yield strengths not greater than 60,000 psi. The bars, as distinct from the heads, must have a clear cover of at least $2d_b$ and a clear spacing between bars of at least $4d_b$. In addition, headed bars are restricted by ACI Code 12.6 to use with normalweight concrete, and the value of f'_c used to calculate the development length l_{dt} is limited to 6000 psi. The development length for headed deformed bars in tension is

$$l_{dt} = \left(\frac{0.016\psi_e f_y}{\sqrt{f'_c}} \right) d_b \quad (5.7)$$

where $\psi_e = 1.2$ for epoxy-coated reinforcement and 1.0 for other cases.

TABLE 5.4
Development lengths for headed deformed bars in tension

A. Development length l_{dt} for headed bars	$\left(\frac{0.016\psi_e f_y}{\sqrt{f'_c}} \right) d_b$
B. Modification factors applied to l_{dt}	
Where anchorage or development for f_y is not specifically required, reinforcement in excess of that required by analysis	$\frac{A_s \text{ required}}{A_s \text{ provided}}$
ψ_e	
For epoxy-coated bars	1.2
For other bars	1.0

Where the reinforcement provided exceeds that required by analysis, except when development of the yield strength f_y is specifically required, the value of l_{dt} in Eq. (5.7) may be multiplied by the factor $(A_s \text{ required})/(A_s \text{ provided})$. Under any circumstances, l_{dt} may not be less than 8 bar diameters or less than 6 in. Calculation of the development length l_{dt} and the applicable modifying factors are summarized in Table 5.4.

The development length l_{dt} should be measured from the bearing face of the head to the critical section, as shown in Fig. 5.14. When headed bars from a flexural member, such as a beam or a slab, terminate in a supporting member, such as the column shown in Fig. 5.15, the commentary to ACI Code 12.6 recommends that the bar be extended "through the joint to the far face of the confined core of the supporting member, allowing for cover and avoidance of interference with column reinforcement," even if the resulting anchorage length is greater than l_{dt} . Doing so helps to adequately anchor

FIGURE 5.14
Development length of headed deformed bars.

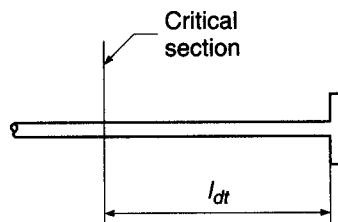
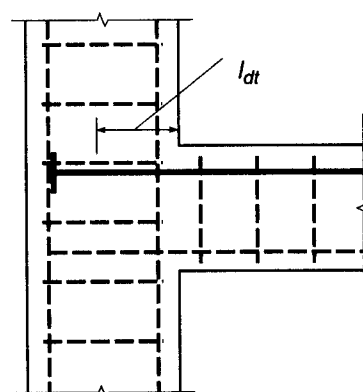


FIGURE 5.15
Headed deformed bar extended to far side of column with anchorage length that exceeds l_{dt} .



the compressive forces that are developed at the face of the head and improves the performance of the beam-column connection.

c. Mechanical Anchorage

In cases where headed bars do not meet the requirements specified in Section 12.6 or in cases where bars are terminated by mechanisms such as welded plates or other manufactured devices, ACI Code 12.6.4 allows such devices to be used to develop the reinforcement if the adequacy of the devices is established by tests. In such cases, the development of the reinforcement may consist of the combined contributions of bond along the length of the bar leading to the critical section, plus that of the mechanical anchorage, much in the way that the total resistance of headed bars is provided.

EXAMPLE 5.3

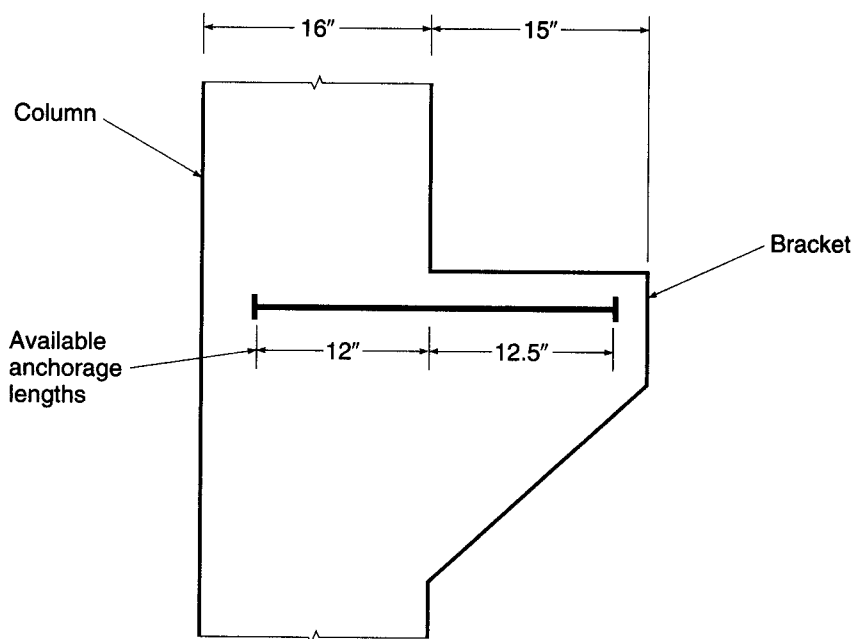
Development of headed deformed bars in tension. Three No. 7 (No. 22) bars serve as top reinforcement for a bracket framing into a 16 × 16 in. column (Fig. 5.16). The bracket projects 15 in. from the column and is the same width as the column. The top cover to the center of the bars is 3 in., and the side cover to the center of the bars is 3.5 in. The bars are spaced laterally at 4.5 in. These dimensions are inadequate for straight development length or for standard hooks. Based on other reinforcement, cover requirements, and head thickness, total development lengths for headed bars of 12 in. in the column and 12.5 in. in the bracket are available. The reinforcing bars have $f_y = 60,000$ psi, and the concrete is normalweight with $f'_c = 5000$ psi. Determine if a bar with heads at both ends can be used in this application.

SOLUTION. The minimum head size is $A_{b,rg} = 4A_b = 2.4 \text{ in}^2$. The smaller available anchorage length in the column governs. Assuming that the bars will be used at the full yield strength, the development length l_{dt} calculated using Eq. (5.7) is

$$l_{dt} = \left(\frac{0.016\psi_e f_y}{\sqrt{f'_c}} \right) d_b = \left(\frac{0.016 \times 1.0 \times 60,000}{\sqrt{5000}} \right) 0.875 = 11.9 \text{ in.}$$

FIGURE 5.16

Column and bracket for headed deformed bar development example.



which must be checked against the minimum values for l_{dt} , which are

$$\begin{aligned} l_{dt} &\geq 8d_b = 7 \text{ in.} \\ l_{dt} &\geq 6 \text{ in.} \end{aligned}$$

Thus, the value of l_{dt} obtained using Eq. (5.7) governs and is less than the available anchorage length. Thus, a bar with heads at both ends can be used, with a distance between heads of 24.5 in., as shown in Fig. 5.16.

5.6 ANCHORAGE REQUIREMENTS FOR WEB REINFORCEMENT

Stirrups should be carried as close as possible to the compression and tension faces of a beam, and special attention must be given to proper anchorage. The truss model (see Section 4.8 and Fig. 4.19) for design of shear reinforcement indicates the development of diagonal compressive struts, the thrust from which is equilibrated, near the top and bottom of the beam, by the tension web members (i.e., the stirrups). Thus, at the factored load, the tensile strength of the stirrups must be developed for almost their full height. Clearly, it is impossible to do this by development length. For this reason, stirrups normally are provided with 90° or 135° hooks at their upper end (see Fig. 5.9b for standard hook details) and at their lower end are bent 90° to pass around the longitudinal reinforcement. In simple spans, or in the positive bending region of continuous spans, where no top bars are required for flexure, stirrup support bars must be used. These are usually about the same diameter as the stirrups themselves, and they not only provide improved anchorage of the hooks but also facilitate fabrication of the reinforcement cage, holding the stirrups in position during placement of the concrete.

ACI Code 12.13 includes special provisions for anchorage of web reinforcement. The ends of single-leg, simple-U, or multiple-U stirrups are to be anchored by one of the following means:

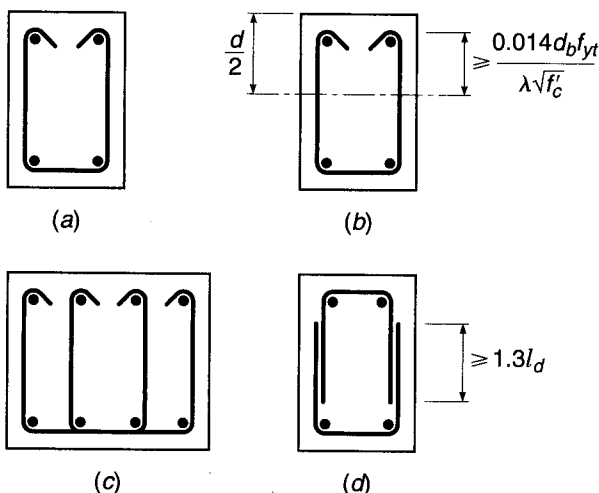
1. For No. 5 (No. 16) bars and smaller, and for Nos. 6, 7, and 8 (Nos. 19, 22, and 25) bars with f_{yt} of 40,000 psi or less, a standard hook around longitudinal reinforcement, as shown in Fig. 5.17a.
2. For Nos. 6, 7, and 8 (Nos. 19, 22, and 25) stirrups with f_{yt} greater than 40,000 psi, a standard hook around a longitudinal bar, plus an embedment between midheight of the member and the outside end of the hook equal to or greater than $0.014d_b f_{yt}/\lambda \sqrt{f_c}$ in., as shown in Fig. 5.17b.

ACI Code 12.13 specifies further that, between anchored ends, each bend in the continuous portion of a simple-U or multiple-U stirrup shall enclose a longitudinal bar, as in Fig. 5.17c. Longitudinal bars bent to act as shear reinforcement, if extended into a region of tension, shall be continuous with longitudinal reinforcement and, if extended into a region of compression, shall be anchored beyond middepth $d/2$ as specified for development length. Pairs of U stirrups or ties so placed as to form a closed unit shall be considered properly spliced when length of laps are $1.3l_d$ as in Fig. 5.17d. In members at least 18 in. deep, such splices are considered adequate if $A_b f_{yt} \leq 9000$ lb and the stirrup legs extend the full depth of the member. As will be discussed in Section 5.11, pairs of U stirrups may not be used in perimeter beams.

Other provisions are contained in the ACI Code relating to the use of welded wire reinforcement, which is sometimes used for web reinforcement in precast and prestressed concrete beams.

FIGURE 5.17

ACI requirements for stirrup anchorage: (a) No. 5 (No. 16) stirrups and smaller, and Nos. 6, 7, and 8 (Nos. 19, 22, and 25) stirrups with yield stress not exceeding 40,000 psi; (b) Nos. 6, 7, and 8 (Nos. 19, 22, and 25) stirrups with yield stress exceeding 40,000 psi; (c) wide beam with multiple-leg U stirrups; (d) pairs of U stirrups forming a closed unit. See Fig. 5.9 for alternative standard hook details.



5.7 WELDED WIRE REINFORCEMENT

Tensile steel consisting of welded wire reinforcement (often referred to as welded wire fabric), with either deformed or smooth wires, is commonly used in one-way and two-way slabs and certain other types of members (see Section 2.15). For *deformed* wire reinforcement, some of the development is assigned to the welded cross wires and some to the embedded length of the deformed wire. According to ACI Code 12.7, the development length of welded deformed wire reinforcement measured from the point of the critical section to the end of the wire is computed as the product of the development length l_d from Table 5.1 or from the more accurate Eq. (5.4) and the appropriate modification factor or factors related to those equations, except that the development length is not to be less than 8 in. For welded deformed wire reinforcement with at least one cross wire within the development length and not less than 2 in. from the point of the critical section, a *deformed wire factor* ψ_w equal to the greater of

$$\frac{f_y - 35,000}{f_y} \quad (5.8a)$$

or

$$\frac{5d_b}{s} \quad (5.8b)$$

is applied, where s is the lateral spacing of the wires being developed; but this factor need not exceed 1.0. When ψ_w from Eq. (5.8a) or (5.8b) is used, the epoxy coating factor ψ_e is taken as 1.0. For welded wire deformed reinforcement with no cross wires within the development length or with a single cross wire less than 2 in. from the point of the critical section, the wire fabric factor is taken to be equal to 1.0 and the development length determined as for the deformed wire.

For welded *plain* wire reinforcement, development is considered to be provided by embedment of two cross wires, with the closer wire not less than 2 in. from the

critical section. However, the development length measured from the critical section to the outermost cross wire is not to be less than

$$l_d = 0.27 \frac{A_b}{s} \frac{f_y}{\lambda \sqrt{f'_c}} \quad (5.9)$$

according to ACI Code 12.8, where A_b is the cross-sectional area of an individual wire to be developed or spliced. The modification factor for excess reinforcement may be applied, but l_d is not to be less than 6 in. for the welded plain wire reinforcement.[†]

5.8 DEVELOPMENT OF BARS IN COMPRESSION

Reinforcement may be required to develop its compressive strength by embedment under various circumstances, e.g., where bars transfer their share of column loads to a supporting footing or where lap splices are made of compression bars in column (see Section 5.13). In the case of bars in compression, a part of the total force is transferred by bond along the embedded length, and a part is transferred by end bearing of the bars on the concrete. Because the surrounding concrete is relatively free of cracks and because of the beneficial effect of end bearing, shorter basic development lengths are permissible for compression bars than for tension bars. If transverse confinement steel is present, such as spiral column reinforcement or special spiral steel around an individual bar, the required development length is further reduced. Hooks and heads such as are shown in Figs. 5.9 and 5.12 are *not* effective in transferring compression from bars to concrete, and, if present for other reasons, should be disregarded in determining required embedment length.

According to ACI Code 12.3, the development length in compression is the greater of

$$l_{dc} = \left(\frac{0.02 f_y}{\lambda \sqrt{f'_c}} \right) d_b \quad (5.10a)$$

and

$$l_{dc} = 0.0003 f_y d_b \quad (5.10b)$$

Modification factors summarized in part *B* of Table 5.5, as applicable, are applied to the development length in compression to obtain the value of development length l_{dc} to be used in design. In no case is l_d to be less than 8 in., according to the ACI Code. Basic and modified compressive development lengths are given in Table A.11 of Appendix A.

5.9 BUNDLED BARS

It was pointed out in Section 3.6c that it is sometimes advantageous to “bundle” tensile reinforcement in large beams, with two, three, or four bars in contact, to provide for improved placement of concrete around and between bundles of bars. Bar bundles are typically triangular or L-shaped for three bars, and square for four. When bars are cut off in a bundled group, the cutoff points must be staggered at least 40 diameters.

[†] The ACI Code offers no explanation as to why $l_{d,min} = 6$ in. for welded plain wire reinforcement, but 8 in. for welded deformed wire reinforcement.

TABLE 5.5
Development lengths for deformed bars in compression

A. Basic development length l_{dc}	$\begin{cases} \geq \left(\frac{0.02 f_y}{\lambda \sqrt{f'_c}} \right) d_b \\ \geq 0.0003 f_y d_b \end{cases}$
B. Modification factors to be applied to l_{dc}	
Reinforcement in excess of that required by analysis	$\frac{A_s \text{ required}}{A_s \text{ provided}}$
Reinforcement enclosed within spiral reinforcement not less than $\frac{1}{4}$ in. diameter and not more than 4 in. pitch or within No. 4 (No. 13) ties spaced at not more than 4 in. on centers	0.75

According to ACI Code 12.4, the development length of individual bars within a bundle, for both tension and compression, is that of the individual bar increased by 20 percent for a three-bar bundle and by 33 percent for a four-bar bundle, to account for the probable deficiency of bond at the inside of the bar group.

For bundled bars, to determine the appropriate spacing and cover values (1) for use in Table 5.1, (2) when calculating the confinement term K_r in Eq. (5.4), or (3) when selecting the epoxy coating factor ψ_e , the unit of bundled bars is treated as a single bar with a diameter derived from the equivalent total area and having a centroid that coincides with that of the bar group.

5.10 BAR CUTOFF AND BEND POINTS IN BEAMS

Chapter 3 dealt with moments, flexural stresses, concrete dimensions, and longitudinal bar areas at the critical moment sections of beams. These critical moment sections are generally at the face of the supports (negative bending) and near the middle of the span (positive bending). Occasionally, haunched members having variable depth or width are used so that the concrete flexural capacity will agree more closely with the variation of bending moment along a span or series of spans. Usually, however, prismatic beams with constant concrete cross-sectional dimensions are used to simplify formwork and thus to reduce cost.

The steel requirement, on the other hand, is easily varied in accordance with requirements for flexure, and it is common practice either to cut off bars where they are no longer needed to resist stress or, sometimes in the case of continuous beams, to bend up the bottom steel (usually at 45°) so that it provides tensile reinforcement at the top of the beam over the supports.

a. Theoretical Points of Cutoff or Bend

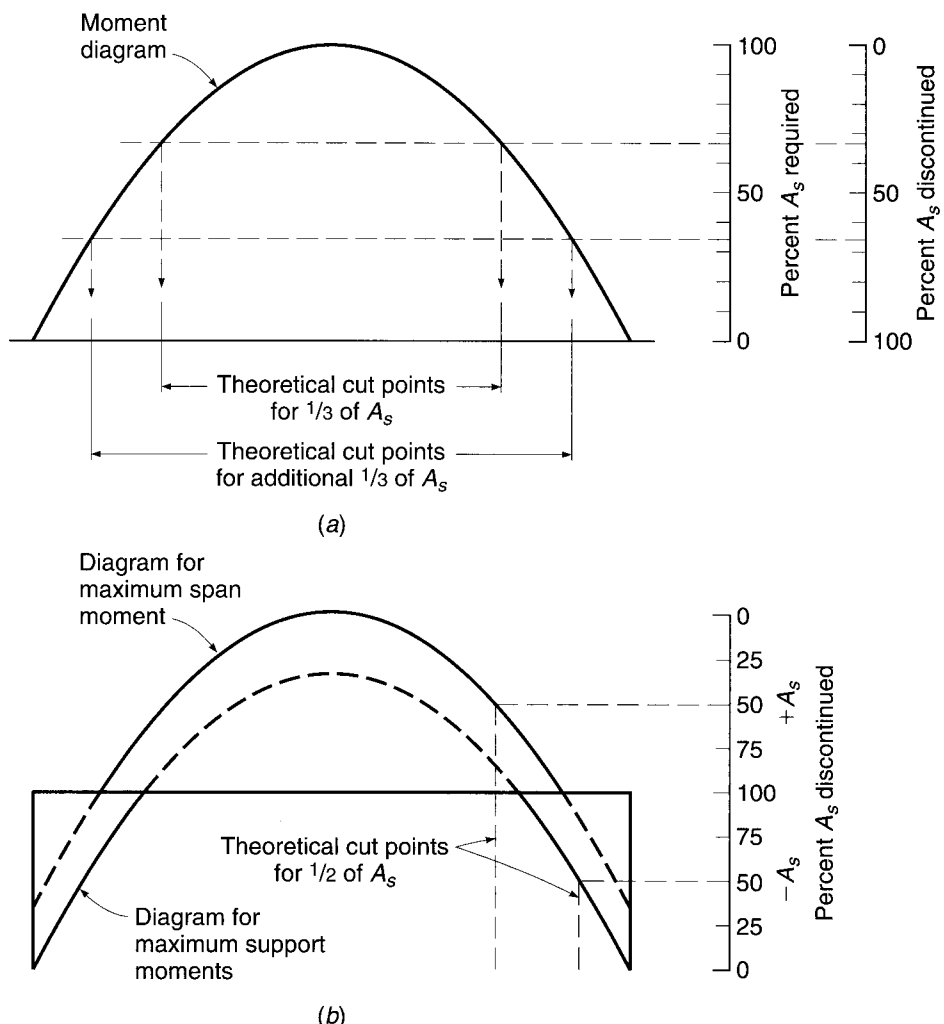
The tensile force to be resisted by the reinforcement at any cross section is

$$T = A_s f_s = \frac{M}{z}$$

where M is the value of bending moment at that section and z is the internal lever arm of the resisting moment. The lever arm z varies only within narrow limits and is never

FIGURE 5.18

Bar cutoff points from moment diagrams.



less than the value at the maximum-moment section. Consequently, the tensile force can be taken with good accuracy directly proportional to the bending moment. Since it is desirable to design so that the steel everywhere in the beam is as nearly fully stressed as possible, it follows that the required steel area is very nearly proportional to the bending moment.

To illustrate, the moment diagram for a uniformly loaded simple-span beam shown in Fig. 5.18a can be used as a steel requirement diagram. At the maximum-moment section, 100 percent of the tensile steel is required (0 percent can be discontinued or bent), while at the supports, 0 percent of the steel is theoretically required (100 percent can be discontinued or bent). The percentage of bars that could be discontinued elsewhere along the span is obtainable directly from the moment diagram, drawn to scale. To facilitate the determination of cutoff or bend points for simple spans, Graph A.2 of Appendix A has been prepared. It represents a half-moment diagram for a uniformly loaded simple span.

To determine cutoff or bend points for continuous beams, the moment diagrams resulting from loading for maximum span moment and maximum support moment are drawn. A moment envelope results that defines the range of values of moment at any

section. Cutoff or bend points can be found from the appropriate moment curve as for simple spans. Figure 5.18b illustrates, for example, a continuous beam with moment envelope resulting from alternate loadings to produce maximum span and maximum support moments. The locations of the points at which 50 percent of the bottom and top steel may theoretically be discontinued are shown.

According to ACI Code 8.3, uniformly loaded, continuous reinforced concrete beams of fairly regular span may be designed using moment coefficients (see Table 12.1). These coefficients, analogous to the numerical constant in the expression $\frac{1}{8}wL^2$ for simple-beam bending moment, give a conservative approximation of span and support moments for continuous beams. When such coefficients are used in design, cutoff and bend points may conveniently be found from Graph A.3 of Appendix A. Moment curves corresponding to the various span and support-moment coefficients are given at the top and bottom of the chart, respectively.

Alternatively, if moments are found by frame analysis rather than from ACI moment coefficients, the location along the span where bending moment reduces to any particular value (e.g., as determined by the bar group after some bars are cut off), or to zero, is easily computed by statics.

b. Practical Considerations and ACI Code Requirements

Actually, in no case should the tensile steel be discontinued exactly at the theoretically described points. As described in Section 4.3 and shown in Fig. 4.7, when diagonal tension cracks form, an internal redistribution of forces occurs in a beam. Prior to cracking, the steel tensile force at any point is proportional to the moment at a vertical section passing through the point. However, after the crack has formed, the tensile force in the steel at the crack is governed by the moment at a section nearer midspan, which may be much larger. Furthermore, the actual moment diagram may differ from that used as a design basis, due to approximation of the real loads, approximations in the analysis, or the superimposed effect of settlement or lateral loads. In recognition of these facts, ACI Code 12.10 requires that every bar be continued at least a distance equal to the effective depth of the beam or 12 bar diameters (whichever is larger) beyond the point at which it is theoretically no longer required to resist stress, except at supports of simple spans and at the free end of cantilevers.

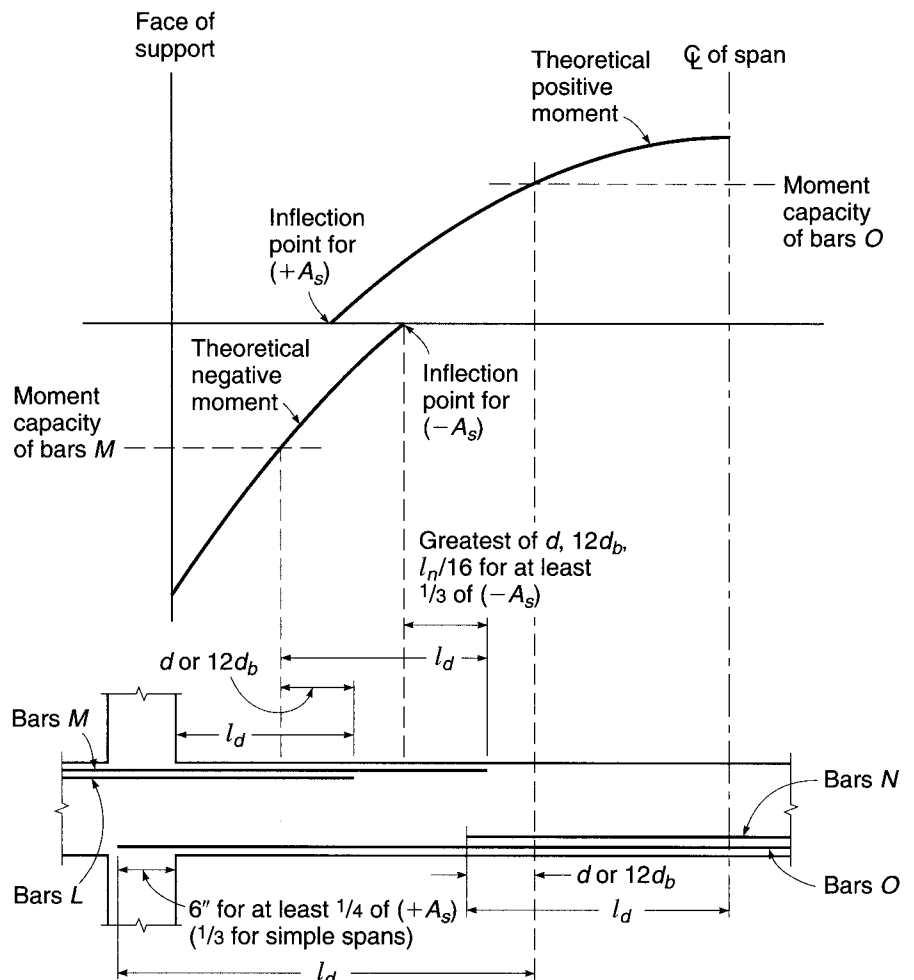
In addition, it is necessary that the calculated stress in the steel at each section be developed by adequate embedded length or end anchorage, or a combination of the two. For the usual case, with no special end anchorage, this means that the full development length l_d must be provided beyond critical sections at which peak stress exists in the bars. These critical sections are located at points of maximum moment and at points where adjacent terminated reinforcement is no longer needed to resist bending.[†]

Further reflecting the possible change in peak stress location, ACI Code 12.11 requires that at least one-third of the positive-moment steel (one-fourth in continuous spans) be continued uninterrupted along the same face of the beam a distance at least 6 in. into the support. When a flexural member is a part of a primary lateral load resisting system, positive-moment reinforcement required to be extended into the support must be anchored to develop the yield strength of the bars at the face of support to account for

[†]The ACI Code is ambiguous as to whether or not the extension length d or $12d_b$ is to be added to the required development length l_d . The Code Commentary presents the view that these requirements need not be superimposed, and Fig. 5.19 has been prepared on that basis. However, the argument just presented regarding possible shifts in moment curves or steel stress distribution curves leads to the conclusion that these requirements should be superimposed. In such cases, each bar should be continued a distance l_d plus the greater of d or $12d_b$ beyond the peak stress location.

FIGURE 5.19

Bar cutoff requirements of the ACI Code.



the possibility of reversal of moment at the supports. According to ACI Code 12.12, at least one-third of the total reinforcement provided for negative moment at the support must be extended beyond the extreme position of the point of inflection a distance not less than one-sixteenth the clear span, or d , or $12d_b$, whichever is greatest.

Requirements for bar cutoff or bend point locations are summarized in Fig. 5.19. If negative bars L are to be cut off, they must extend a full development length l_d beyond the face of the support. In addition, they must extend a distance d or $12d_b$ beyond the theoretical point of cutoff defined by the moment diagram. The remaining negative bars M (at least one-third of the total negative area) must extend at least l_d beyond the theoretical point of cutoff of bars L and in addition must extend d , $12d_b$, or $l_n/16$ (whichever is greatest) past the point of inflection of the negative-moment diagram.

If the positive bars N are to be cut off, they must project l_d past the point of theoretical maximum moment, as well as d or $12d_b$ beyond the cutoff point from the positive-moment diagram. The remaining positive bars O must extend l_d past the theoretical point of cutoff of bars N and must extend at least 6 in. into the face of the support.

When bars are cut off in a tension zone, there is a tendency toward the formation of premature flexural and diagonal tension cracks in the vicinity of the cut end. This may result in a reduction of shear capacity and a loss in overall ductility of the beam.

ACI Code 12.10 requires special precautions, specifying that no flexural bar shall be terminated in a tension zone unless *one* of the following conditions is satisfied:

1. The shear is not over two-thirds of the design strength ϕV_n .
2. Stirrups in excess of those normally required are provided over a distance along each terminated bar from the point of cutoff equal to $\frac{3}{4}d$. These "binder" stirrups shall provide an area $A_v \geq 60b_{w,s}/f_y$. In addition, the stirrup spacing shall not exceed $d/8\beta_b$, where β_b is the ratio of the area of bars cut off to the total area of bars at the section.
3. The continuing bars, if No. 11 (No. 36) or smaller, provide twice the area required for flexure at that point, and the shear does not exceed three-quarters of the design strength ϕV_n .

As an alternative to cutting off the steel, tension bars may be anchored by bending them across the web and making them continuous with the reinforcement on the opposite face. Although this leads to some complication in detailing and placing the steel, thus adding to construction cost, some engineers prefer the arrangement because added insurance is provided against the spread of diagonal tension cracks. In some cases, particularly for relatively deep beams in which a large percentage of the total bottom steel is to be bent, it may be impossible to locate the bend-up point for bottom bars far enough from the support for the same bars to meet the requirements for top steel. The theoretical points of bend should be checked carefully for both bottom and top steel.

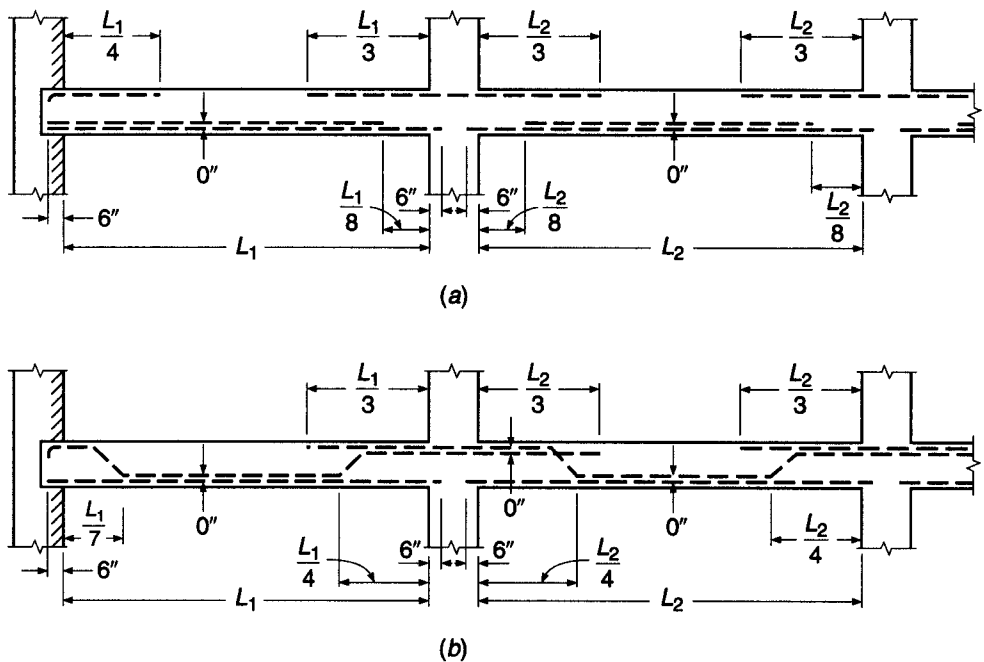
Because the determination of cutoff or bend points may be rather tedious, particularly for frames that have been analyzed by elastic methods rather than by moment coefficients, many designers specify that bars be cut off or bent at more or less arbitrarily defined points that experience has proved to be safe. For nearly equal spans, uniformly loaded, in which not more than about one-half the tensile steel is to be cut off or bent, the locations shown in Fig. 5.20 are satisfactory. Note, in Fig. 5.20, that the beam at the exterior support at the left is shown to be simply supported. If the beam is monolithic with exterior columns or with a concrete wall at that end, details for a typical interior span could be used for the end span as well.

c. Special Requirements near the Point of Zero Moment

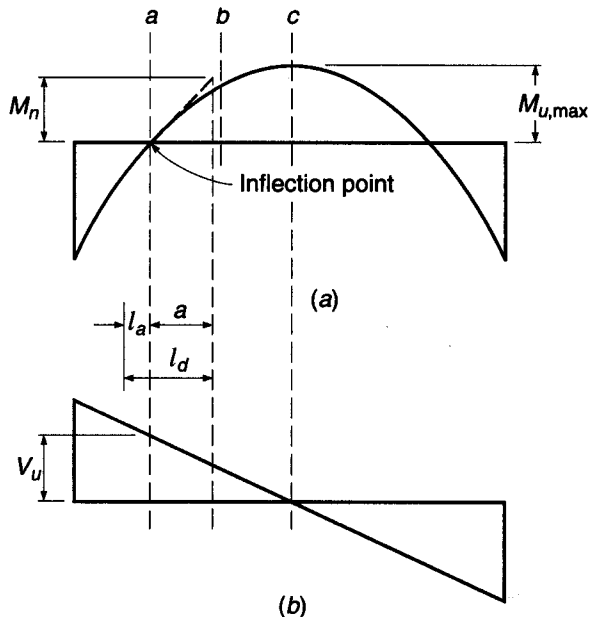
While the basic requirement for flexural tensile reinforcement is that a full development length l_d be provided beyond the point where the bar is assumed fully stressed to f_y , this requirement may *not* be sufficient to ensure safety against bond distress. Figure 5.21 shows the moment and shear diagram representative of a uniformly loaded continuous beam. Positive bars provided to resist the maximum moment at c are required to have a full development length beyond the point c , measured in the direction of decreasing moment. Thus l_d in the limiting case could be exactly equal to the distance from point c to the point of inflection. However, if that requirement were exactly met, then at point b , halfway from c to the point of inflection, those bars would have only one-half their development length remaining, whereas the moment would be three-quarters of that at point c , and three-quarters of the bar force must yet be developed. This situation arises whenever the moments over the development length are greater than those corresponding to a linear reduction to zero. Therefore, the problem is a concern in the positive-moment region of continuous uniformly loaded spans, but not in the negative-moment region.

FIGURE 5.20

Cutoff or bend points for bars in approximately equal spans with uniformly distributed loads.

**FIGURE 5.21**

Development length requirement at point of inflection.



The bond force U per unit length along the tensile reinforcement in a beam is $U = dT/dx$, where dT is the change in bar tension in the length dx . Since $dT = dM/z$, this can be written

$$U = \frac{dM}{z dx} \quad (a)$$

that is, the bond force per unit length of bar, generated by bending, is proportional to the slope of the moment diagram. In reference to Fig. 5.21a, the maximum bond force U in the positive-moment region would therefore be at the point of inflection, and U would gradually diminish along the beam toward point c . Clearly, a conservative approach in evaluating adequacy in bond for those bars that are continued as far as the point of inflection (not necessarily the full A_s provided for M_u at point c) would be to require that the bond resistance, which is assumed to increase linearly along the bar from its end, be governed by the maximum rate of moment increase, i.e., the maximum slope dM/dx of the moment diagram, which for positive bending is seen to occur at the inflection point.

From elementary mechanics, it is known that the slope of the moment diagram at any point is equal to the value of the shear force at that point. Therefore, with reference to Fig. 5.21, the slope of the moment diagram at the point of inflection is V_u . A dashed line may therefore be drawn tangent to the moment curve at the point of inflection having the slope equal to the value of shear force V_u . Then if M_n is the nominal flexural strength provided by those bars that extend to the point of inflection, and if the moment diagram were conservatively assumed to vary linearly along the dashed line tangent to the actual moment curve, from the basic relation that $M_n/a = V_u$, a distance a is established:

$$a = \frac{M_n}{V_u} \quad (b)$$

If the bars in question were fully stressed at a distance a to the right of the point of inflection, and if the moments diminished linearly to the point of inflection, as suggested by the dashed line, then bond failure would not occur if the development length l_d did not exceed the distance a . The actual moments are less than indicated by the dashed line, so the requirement is on the safe side.

If the bars extend past the point of inflection toward the support, as is always required, then the extension can be counted as contributing toward satisfying the requirement for embedded length. Arbitrarily, according to ACI Code 12.11, a length past the point of inflection not greater than the larger of the beam depth d or 12 times the bar diameter d_b may be counted toward satisfying the requirement. Thus, the requirement for tensile bars at the point of inflection is that

$$l_d \leq \frac{M_n}{V_u} + l_a \quad (5.11)$$

where M_n = nominal flexural strength assuming all reinforcement at section to be stressed to f_y

V_u = factored shear force at section

l_a = embedded length of bar past point of zero moment, but not to exceed the greater of d or $12d_b$

A corresponding situation occurs near the supports of simple spans carrying uniform loads, and similar requirements must be imposed. However, because of the beneficial effect of vertical compression in the concrete at the end of a simply supported span, which tends to prevent splitting and bond failure along the bars, the value M_n/V_u may be increased 30 percent for such cases, according to ACI Code 12.11. Thus, at the ends of a simply supported span, the requirement for tension reinforcement is

$$l_d \leq 1.3 \frac{M_n}{V_u} + l_a \quad (5.12)$$

The consequence of these special requirements at the point of zero moment is that, in some cases, smaller bar sizes must be used to obtain smaller l_d , even though requirements for development past the point of maximum stress are met.

It may be evident from review of Sections 5.10b and 5.10c that the determination of cutoff or bend points in flexural members is complicated and can be extremely time-consuming in design. It is important to keep the matter in perspective and to recognize that the overall cost of construction will be increased very little if some bars are slightly longer than absolutely necessary, according to calculation, or as dictated by ACI Code provisions. In addition, simplicity in construction is a desired goal, and can, in itself, produce compensating cost savings. Accordingly, many engineers in practice continue *all* positive reinforcement into the face of the supports the required 6 in. and extend *all* negative reinforcement the required distance past the points of inflection, rather than using staggered cutoff points.

5.11 STRUCTURAL INTEGRITY PROVISIONS

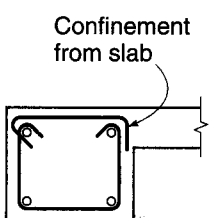
Experience with structures that have been subjected to damage to a major supporting element, such as a column, owing to accident or abnormal loading has indicated that total collapse can be prevented through relatively minor changes in bar detailing. If some reinforcement, properly confined, is carried continuously through a support, then even if that support is damaged or destroyed, catenary action of the beams can prevent total collapse. In general, if beams have bottom and top steel meeting or exceeding the requirements summarized in Sections 5.10b and 5.10c, and if binding steel is provided in the form of properly detailed stirrups, then that catenary action can usually be ensured.

According to ACI Code 7.13.2, beams at the perimeter of the structure (spandrel beams) must have continuous reinforcement passing through the region bounded by the longitudinal reinforcement of the columns consisting of at least one-sixth of the tension reinforcement required for negative moment at the support, but not less than two bars, and at least one-quarter of the tension reinforcement required for positive moment at midspan, but not less than two bars. At noncontinuous supports, the reinforcement must be anchored using a standard hook or a headed deformed bar to develop f_y at the face of the support. The continuous reinforcement must be enclosed by closed stirrups or closed ties perpendicular to the axis of the member, a closed cage of welded wire reinforcement with transverse wires perpendicular to the axis of the member, or spiral reinforcement (see Fig. 1.15). This transverse reinforcement must be anchored by a 135° standard hook (Fig. 5.9b) or a seismic hook (see Section 20.4) around a longitudinal bar, or where the concrete surrounding the anchorage is restrained against spalling by a flange or slab, by either a 90° or 135° standard hook around a longitudinal bar, as shown in Fig. 5.17a and b.

Figure 5.22 shows a two-piece stirrup that meets the requirements of ACI Code 7.13.2. Although the spacing of these stirrups is not specified, the requirements for minimum shear steel given in Section 4.5b provide guidance in regions where shear does not require closer spacing. The stirrups need not be extended through the joints. Overlapping pairs of U stirrups of the type shown in Fig. 5.17d are not permitted in perimeter beams because damage to the side cover concrete may cause both the stirrups and top longitudinal reinforcement to tear out of the concrete, thus preventing the longitudinal reinforcement from acting as a catenary.

FIGURE 5.22

Two-piece stirrup meeting the requirements of ACI Code 7.13.2 for confinement of longitudinal integrity reinforcement in perimeter beams. The 90 degree hook must be placed adjacent to the slab.



The required continuity of longitudinal steel can be provided using top reinforcement spliced at midspan and bottom reinforcement spliced at or near the supports using Class B tension splices, or mechanical or welded splices (see Section 5.13).

In other than perimeter beams, when stirrups of the type shown in Fig. 5.22 are not provided, at least one-quarter of the positive-moment reinforcement required at midspan, but not less than two bars, must pass through the columns' longitudinal reinforcement and must be continuous. The requirements for anchoring this longitudinal reinforcement at noncontinuous supports and for splicing the bars to provide continuity are the same as for perimeter beams.

Note that these provisions require very little additional steel in the structure. At least one-quarter of the bottom bars must be extended 6 in. into the support by other ACI Code provisions; the structural integrity provisions merely require that these bars be made continuous or spliced. Similarly, other ACI Code provisions require that at least one-third of the negative bars be extended a certain minimum distance past the point of inflection; the structural integrity provisions for perimeter beams require only that one-half of those bars be further extended and spliced at midspan.

5.12 INTEGRATED BEAM DESIGN EXAMPLE

In this and in the preceding chapters, the several aspects of the design of reinforced concrete beams have been studied more or less separately: first the flexural design, then design for shear, and finally for bond and anchorage. The following example is presented to show how the various requirements for beams, which are often in some respects conflicting, are satisfied in the overall design of a representative member.

EXAMPLE 5.4

Integrated design of T beam. A floor system consists of single-span T beams 8 ft on centers, supported by 12 in. masonry walls spaced at 25 ft between inside faces. The general arrangement is shown in Fig. 5.23a. A 5 in. monolithic slab carries a uniformly distributed service live load of 165 psf. The T beams, in addition to the slab load and their own weight, must carry two 16,000 lb equipment loads applied over the stem of the T beam 3 ft from the span centerline as shown. A complete design is to be provided for the T beams, using concrete of 4000 psi strength and bars with 60,000 psi yield stress. (Note: Because normalweight concrete is used, $\lambda = 1.0$ and, as such, will be dropped from the calculations for shear and bond.)

SOLUTION. According to the ACI Code, the span length is to be taken as the clear span plus the beam depth, but need not exceed the distance between the centers of supports. The latter

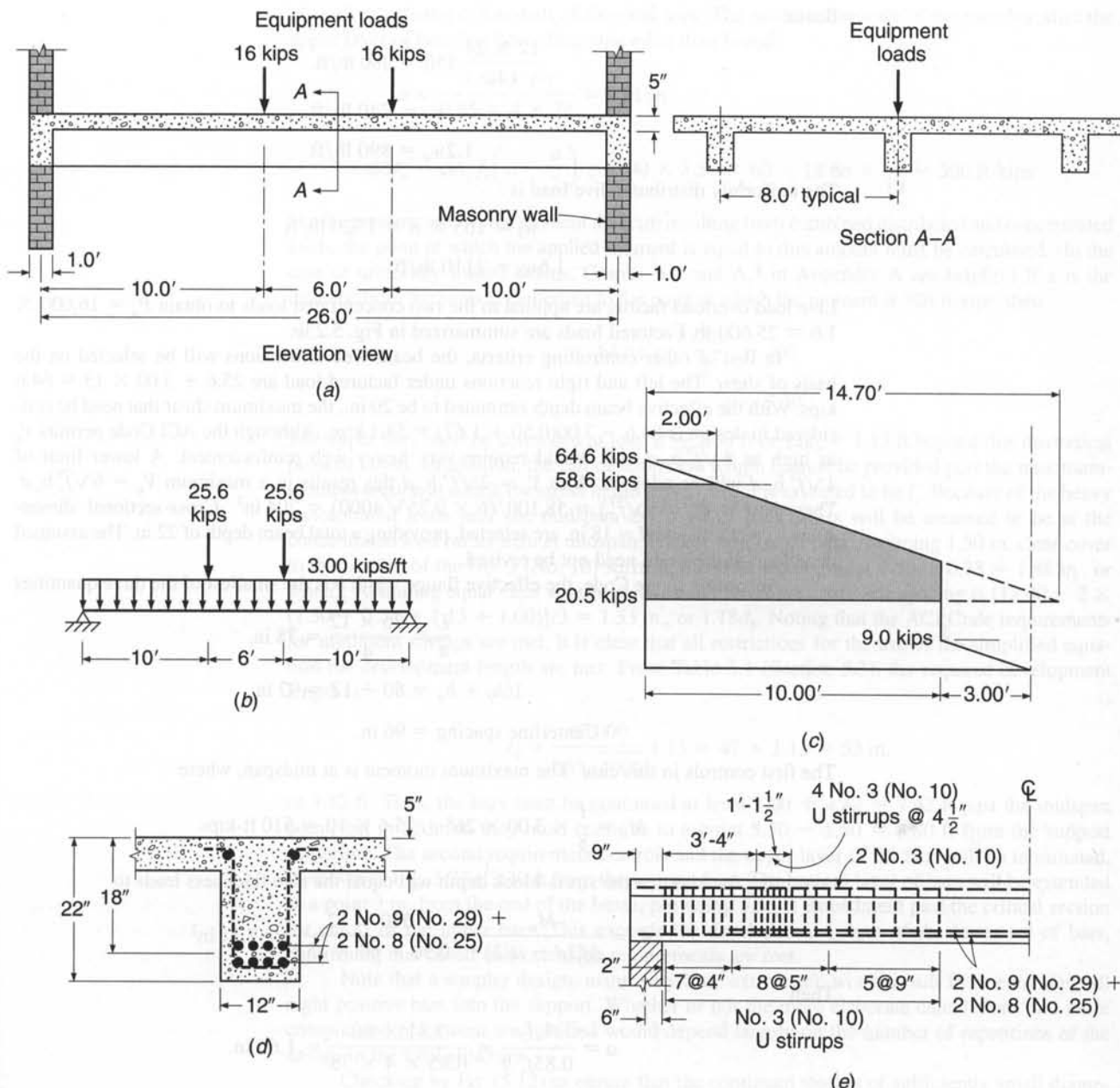


FIGURE 5.23
T beam design for Example 5.4.

provision controls in this case, and the effective span is 26 ft. Estimating the beam web dimensions to be 12 × 24 in., the calculated and factored dead loads are as follows:

Slab:

$$\frac{5}{12} \times 150 \times 7 = 440 \text{ lb/ft}$$

Beam:

$$\frac{12 \times 24}{144} 150 = 300 \text{ lb/ft}$$

$$w_d = 740 \text{ lb/ft}$$

$$1.2w_d = 890 \text{ lb/ft}$$

The uniformly distributed live load is

$$w_l = 165 \times 8 = 1320 \text{ lb/ft}$$

$$1.6w_l = 2110 \text{ lb/ft}$$

Live load overload factors are applied to the two concentrated loads to obtain $P_u = 16,000 \times 1.6 = 25,600 \text{ lb}$. Factored loads are summarized in Fig. 5.23b.

In lieu of other controlling criteria, the beam web dimensions will be selected on the basis of shear. The left and right reactions under factored load are $25.6 + 3.00 \times 13 = 64.6 \text{ kips}$. With the effective beam depth estimated to be 20 in., the maximum shear that need be considered in design is $64.6 - 3.00(0.50 + 1.67) = 58.1 \text{ kips}$. Although the ACI Code permits V_s as high as $8\sqrt{f'_c} b_w d$, this would require very heavy web reinforcement. A lower limit of $4\sqrt{f'_c} b_w d$ will be adopted. With $V_c = 2\sqrt{f'_c} b_w d$ this results in a maximum $V_n = 6\sqrt{f'_c} b_w d$. Then $b_w d = V_u / (6\phi\sqrt{f'_c}) = 58,100 / (6 \times 0.75\sqrt{4000}) = 204 \text{ in}^2$. Cross-sectional dimensions $b_w = 12 \text{ in}$. and $d = 18 \text{ in}$. are selected, providing a total beam depth of 22 in. The assumed dead load of the beam need not be revised.

According to the Code, the effective flange width b is the smallest of the three quantities

$$\frac{L}{4} = \frac{26 \times 12}{4} = 78 \text{ in.}$$

$$16h_f + b_w = 80 + 12 = 92 \text{ in.}$$

$$\text{Centerline spacing} = 96 \text{ in.}$$

The first controls in this case. The maximum moment is at midspan, where

$$M_u = \frac{1}{8} \times 3.00 \times 26^2 + 25.6 \times 10 = 510 \text{ ft-kips}$$

Assuming for trial that the stress-block depth will equal the slab thickness leads to

$$A_s = \frac{M_u}{\phi f_y(d - a/2)} = \frac{510 \times 12}{0.90 \times 60 \times 15.5} = 7.31 \text{ in}^2$$

Then

$$a = \frac{A_s f_y}{0.85 f'_c b} = \frac{7.31 \times 60}{0.85 \times 4 \times 78} = 1.65 \text{ in.}$$

The stress-block depth is seen to be less than the slab depth; rectangular beam equations are valid. An improved determination of A_s is

$$A_s = \frac{510 \times 12}{0.90 \times 60 \times 17.11} = 6.60 \text{ in}^2$$

A check confirms that this is well below the maximum permitted reinforcement ratio. Four No. 9 (No. 29) plus four No. 8 (No. 25) bars will be used, providing a total area of 7.14 in^2 . They will be arranged in two rows, as shown in Fig. 5.23d, with No. 9 (No. 29) bars at the outer end of each row. Beam width b_w is adequate for this bar arrangement.

While the ACI Code permits discontinuation of two-thirds of the longitudinal reinforcement for simple spans, in the present case it is convenient to discontinue only the upper layer

of steel, consisting of one-half of the total area. The moment capacity of the member after the upper layer of bars has been discontinued is then found:

$$a = \frac{3.57 \times 60}{0.85 \times 4 \times 78} = 0.81 \text{ in.}$$

$$\phi M_n = \phi A_s f_y \left(d - \frac{a}{2} \right) = 0.90 \times 3.57 \times 60 \times 18.66 \times \frac{1}{12} = 300 \text{ ft-kips}$$

For the present case, with a moment diagram resulting from combined distributed and concentrated loads, the point at which the applied moment is equal to this amount must be calculated. (In the case of uniformly loaded beams, Graphs A.2 and A.3 in Appendix A are helpful.) If x is the distance from the support centerline to the point at which the moment is 300 ft-kips, then

$$64.6x - \frac{3.00x^2}{2} = 300$$

$$x = 5.30$$

The upper bars must be continued at least $d = 1.50 \text{ ft}$ or $12d_b = 1.13 \text{ ft}$ beyond this theoretical point of cutoff. In addition, the full development length l_d must be provided past the maximum-moment section at which the stress in the bars to be cut is assumed to be f_y . Because of the heavy concentrated loads near the midspan, the point of peak stress will be assumed to be at the concentrated load rather than at midspan. For the four upper bars, assuming 1.50 in. clear cover to the outside of the No. 3 (No. 10) stirrups, the clear side cover is $1.50 + 0.38 = 1.88 \text{ in.}$, or $1.66d_b$. Assuming equal clear spacing between all four bars, that clear spacing is $[12.00 - 2 \times (1.50 + 0.38 + 1.13 + 1.00)]/3 = 1.33 \text{ in.}$, or $1.18d_b$. Noting that the ACI Code requirements for minimum stirrups are met, it is clear that all restrictions for the use of the simplified equation for development length are met. From Table 5.1 (Section 5.3), the required development length is

$$l_d = \frac{60,000}{20\sqrt{4000}} 1.13 = 47 \times 1.13 = 53 \text{ in.}$$

or 4.42 ft. Thus, the bars must be continued at least $3.00 + 4.42 = 7.42 \text{ ft}$ past the midspan point, but in addition they must continue to a point $5.30 - 1.50 = 3.80 \text{ ft}$ from the support centerline. The second requirement controls and the upper layer of the bars will be terminated, as shown in Fig. 5.23e, 3.30 ft from the support face. The bottom layer of bars will be extended to a point 3 in. from the end of the beam, providing 5.55 ft embedment past the critical section for cutoff of the upper bars. This exceeds the development length of the lower set of bars, confirming that cutoff and extension requirements are met.

Note that a simpler design, using very little extra steel, would result from extending all eight positive bars into the support. Whether or not the more elaborate calculations and more complicated placement are justified would depend largely on the number of repetitions of the design in the total structure.

Checking by Eq. (5.12) to ensure that the continued steel is of sufficiently small diameter determines that

$$l_d \leq 1.3 \frac{333 \times 12}{64.6} + 3 = 83 \text{ in.}$$

The actual l_d of 53 in. meets this restriction.

Since the cut bars are located in the tension zone, special binding stirrups will be used to control cracking; these will be selected after the normal shear reinforcement has been determined.

The shear diagram resulting from application of factored loads is shown in Fig. 5.23c. The shear contribution of the concrete is

$$\phi V_c = 0.75 \times 2\sqrt{4000} \times 12 \times 18 = 20,500 \text{ lb}$$

Thus web reinforcement must be provided for that part of the shear diagram shown shaded.

No. 3 (No. 10) stirrups will be selected. The maximum spacings must not exceed $d/2 = 9$ in., 24 in., or $A_v f_y / (0.75 \sqrt{f'_c} b_w) = 0.22 \times 60,000 / (0.75 \sqrt{4000} \times 12) = 23$ in. $\leq A_w f_{yt} / 50 b_w = 0.22 \times 60,000 / 50 \times 12 = 22$ in. The first criterion controls here. For reference, from Eq. (4.14a) the hypothetical stirrup spacing at the support is

$$s_0 = \frac{0.75 \times 0.22 \times 60 \times 18}{64.6 - 20.5} = 4.04 \text{ in.}$$

and at 2 ft intervals along the span,

$$s_2 = 4.68 \text{ in.}$$

$$s_4 = 5.55 \text{ in.}$$

$$s_6 = 6.83 \text{ in.}$$

$$s_8 = 8.87 \text{ in.}$$

$$s_{10} = 12.64 \text{ in.}$$

The spacing need not be closer than that required 2.00 ft from the support centerline. In addition, stirrups are not required past the point of application of concentrated load, since beyond that point the shear is less than one-half of ϕV_c . The final spacing of vertical stirrups selected is

$$1 \text{ space at } 2 \text{ in.} = 2 \text{ in.}$$

$$7 \text{ spaces at } 4 \text{ in.} = 28 \text{ in.}$$

$$8 \text{ spaces at } 5 \text{ in.} = 40 \text{ in.}$$

$$5 \text{ spaces at } 9 \text{ in.} = \underline{45 \text{ in.}}$$

$$\begin{aligned} \text{Total} &= 115 \text{ in.} = 9 \text{ ft } 7 \text{ in. from the face of the} \\ &\quad \text{support (121 in.} = 10 \text{ ft } 1 \text{ in. from} \\ &\quad \text{the support centerline)} \end{aligned}$$

Two No. 3 (No. 10) longitudinal bars will be added to meet anchorage requirements and fix the top of the stirrups.

In addition to the shear reinforcement just specified, it is necessary to provide extra web reinforcement over a distance equal to $\frac{3}{4}d$, or 13.5 in., from the cut ends of the discontinued steel. The spacing of this extra web reinforcement must not exceed $d/8\beta_b = 18/(8 \times \frac{1}{2}) = 4.5$ in. In addition, the area of added steel within the distance s must not be less than $60b_w s / f_{yt} = 60 \times 12 \times 4.5 / 60,000 = 0.054 \text{ in}^2$. For convenience, No. 3 (No. 10) stirrups will be used for this purpose also, providing an area of 0.22 in^2 in the distance s . The placement of the four extra stirrups is shown in Fig. 5.23e.

5.13 BAR SPLICES

In general, reinforcing bars are stocked by suppliers in lengths of 60 ft for bars from No. 5 to No. 18 (No. 16 to No. 57) and in 20 or 40 ft lengths for smaller sizes. For this reason, and because it is often more convenient to work with shorter bar lengths, it is frequently necessary to splice bars in the field. Splices in reinforcement at points of maximum stress should be avoided, and when splices are used, they should be staggered, although neither condition is practical, for example, in compression splices in columns.

Splices for No. 11 (No. 36) bars and smaller are usually made simply by lapping the bars a sufficient distance to transfer stress by bond from one bar to the other. The

lapped bars are usually placed in contact and lightly wired so that they stay in position as the concrete is placed. Alternatively, splicing may be accomplished by welding or by sleeves or mechanical devices. ACI Code 12.14.2 prohibits use of lapped splices for bars larger than No. 11 (No. 36), except that No. 14 and No. 18 (No. 43 and No. 57) bars may be lapped in compression with No. 11 (No. 36) and smaller bars per ACI Code 12.16.2 and 15.8.2.3. For bars that will carry only compression, it is possible to transfer load by end bearing of square cut ends, if the bars are accurately held in position by a sleeve or other device.

Lap splices of bars in bundles are based on the lap splice length required for individual bars within the bundle but must be increased in length by 20 percent for three-bar bundles and by 33 percent for four-bar bundles because of the reduced effective perimeter. Individual bar splices within a bundle should not overlap, and entire bundles must not be lap-spliced.

According to ACI Code 12.14.3, welded splices must develop at least 125 percent of the specified yield strength of the bar. The same requirement applies to full mechanical connections. This ensures that an overloaded spliced bar would fail by ductile yielding in the region away from the splice, rather than at the splice where brittle failure is likely. Mechanical connections of No. 5 (No. 16) and smaller bars not meeting this requirement may be used at points of less than maximum stress, in accordance with ACI Code 12.15.5.

a. Lap Splices in Tension

The required length of lap for tension splices is stated in terms of the development length l_d . In the process of calculating l_d , the usual modification factors are applied except that the reduction factor for excess reinforcement should not be applied because that factor is already accounted for in the splice specification.

Two different classifications of lap splices are established, corresponding to the minimum length of lap required: a Class A splice requires a lap of $1.0l_d$, and a Class B splice requires a lap of $1.3l_d$. In either case, a minimum length of 12 in. applies. For Class B splices, the 12 in. minimum applies to $1.3l_d$, not to the value of l_d used to calculate the lap length. Lap splices, in general, must be Class B splices, according to ACI Code 12.15.2, except that Class A splices are allowed when the area of reinforcement provided is at least twice that required by analysis over the entire length of the splice *and* when one-half or less of the total reinforcement is spliced within the required lap length. The effect of these requirements is to encourage designers to locate splices away from regions of maximum stress, to a location where the actual steel area is at least twice that required by analysis, and to stagger splices.

Spiral reinforcement is spliced with a lap of $48d_b$ for uncoated bars and $72d_b$ for epoxy-coated bars, in accordance with ACI Code 7.10.4.5. The lap for epoxy-coated bars is reduced to $48d_b$ if the bars are anchored with a standard stirrup or tie hook.

b. Compression Splices

Reinforcing bars in compression are spliced mainly in columns, where bars are most often terminated just above each floor or every other floor. This is done partly for construction convenience, to avoid handling and supporting very long column bars, but it is also done to permit column steel area to be reduced in steps, as loads become lighter at higher floors.

Compression bars may be spliced by lapping, by direct end bearing, or by welding or mechanical devices that provide positive connection. The minimum length of lap for compression splices is set according to ACI Code 12.16:

$$\text{For bars with } f_y \leq 60,000 \text{ psi} \quad 0.0005f_y d_b$$

$$\text{For bars with } f_y > 60,000 \text{ psi} \quad (0.0009f_y - 24)d_b$$

but not less than 12 in. For f'_c less than 3000 psi, the required lap is increased by one-third. When bars of different size are lap-spliced in compression, the splice length is to be the larger of the development length of the larger bar and the splice length of the smaller bar. In exception to the usual restriction on lap splices for large-diameter bars, No. 14 and No. 18 bars *may* be lap-spliced to No. 11 and smaller bars.

Direct end bearing of the bars has been found by test and experience to be an effective means for transmitting compression. In such a case, the bars must be held in proper alignment by a suitable device. The bar ends must terminate in flat surfaces within 1.5° of a right angle, and the bars must be fitted within 3° of full bearing after assembly, according to ACI Code 12.16.4. Ties, closed stirrups, or spirals must be used.

c. Column Splices

Lap splices, butt-welded splices, mechanical connections, or end-bearing splices may be used in columns, with certain restrictions. Reinforcing bars in columns may be subjected to compression or tension, or, for different load combinations, both tension and compression. Accordingly, column splices must conform in some cases to the requirements for compression splices only or tension splices only or to requirements for both. ACI Code 12.17 requires that a minimum tension capacity be provided in each face of all columns, even where analysis indicates compression only. Ordinary compressive lap splices provide sufficient tensile resistance, but end-bearing splices may require additional bars for tension, unless the splices are staggered.

For lap splices, where the bar stress due to factored loads is compression, column lap splices must conform to the requirements presented in Section 5.13b for compression splices. Where the stress is tension and does not exceed $0.5f_y$, lap splices must be Class B if more than one-half the bars are spliced at any section, or Class A if one-half or fewer are spliced and alternate lap splices are staggered by l_d . If the stress is tension and exceeds $0.5f_y$, then lap splices must be Class B, according to ACI Code.

If lateral ties are used throughout the splice length having an area of at least $0.0015hs$ in both directions, where s is the spacing of ties and h is the overall thickness of the member, the required splice length may be multiplied by 0.83 but must not be less than 12 in. If spiral reinforcement confines the splice, the length required may be multiplied by 0.75 but again must not be less than 12 in.

End-bearing splices, as described above, may be used for column bars stressed in compression, if the splices are staggered or additional bars are provided at splice locations. The continuing bars in each face must have a tensile strength of not less than $0.25f_y$ times the area of reinforcement in that face.

As mentioned in Section 5.13b, column splices are commonly made just above a floor. However, for frames subjected to lateral loads, a better location is within the center half of the column height, where the moments due to lateral loads are much lower than at floor level. Such placement is mandatory for columns in "special moment frames" designed for seismic loads, as will be discussed in Chapter 20.

EXAMPLE 5.5 **Compression splice of column reinforcement.** In reference to Fig. 5.8, four No. 11 (No. 36) column bars from the floor below are to be lap-spliced with four No. 10 (No. 32) column bars from above, and the splice is to be made just above a construction joint at floor level. The column, measuring 12 in. \times 21 in. in cross section, will be subject to compression only for all load combinations. Transverse reinforcement consists of No. 4 (No. 13) ties at 16 in. spacing. All vertical bars may be assumed to be fully stressed. Calculate the required splice length. Material strengths are $f_y = 60,000$ psi and $f'_c = 4000$ psi.

SOLUTION. The length of the splice must be the larger of the development length of the No. 11 (No. 36) bars and the splice length of the No. 10 (No. 32) bars. For the No. 11 (No. 36) bars, the development length is equal to the larger of the values obtained with Eqs. (5.10a) and (5.10b):

$$l_{dc} = \frac{0.02 \times 60,000}{\sqrt{4000}} 1.41 = 27 \text{ in.}$$

$$l_{dc} = 0.0003 \times 60,000 \times 1.41 = 25 \text{ in.}$$

The first criterion controls. No modification factors apply. For the No. 10 (No. 32) bars, the compression splice length is $0.0005 \times 60,000 \times 1.27 = 38$ in. In the check for use of the modification factor for tied columns, the critical column dimension is 21 in., and the required effective tie area is thus $0.0015 \times 21 \times 16 = 0.50 \text{ in}^2$. The No. 4 (No. 13) ties provide an area of only $0.20 \times 2 = 0.40 \text{ in}^2$, so the reduction factor of 0.83 cannot be applied to the splice length. Thus the compression splice length of 38 in., which exceeds the development length of 27 in. for the No. 11 (No. 36) bars, controls here, and a lap splice of 38 in. is required. Note that if the spacing of the ties at the splice were reduced to 12.8 in. or less (say 12 in.), the required lap would be reduced to $38 \times 0.83 = 32$ in. This would save steel, and, although placement cost would increase slightly, would probably represent the more economical design.

REFERENCES

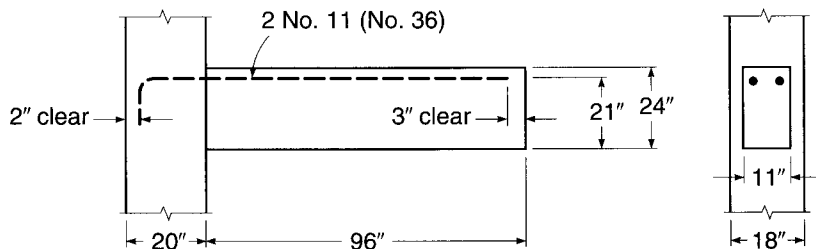
- 5.1. R. M. Mains, "Measurement of the Distribution of Tensile and Bond Stresses along Reinforcing Bars," *J. ACI*, vol. 23, no. 3, 1951, pp. 225–252.
- 5.2. A. H. Nilson, "Internal Measurement of Bond Slip," *J. ACI*, vol. 69, no. 7, 1972, pp. 439–441.
- 5.3. Y. Goto, "Cracks Formed in Concrete around Deformed Tension Bars," *J. ACI*, vol. 68, no. 4, 1971, pp. 244–251.
- 5.4. L. A. Lutz and P. Gergely, "Mechanics of Bond and Slip of Deformed Bars in Concrete," *J. ACI*, vol. 64, no. 11, 1967, pp. 711–721.
- 5.5. P. M. Ferguson and J. N. Thompson, "Development Length of High Strength Reinforcing Bars in Bond," *J. ACI*, vol. 59, no. 7, 1962, pp. 887–922.
- 5.6. R. G. Mathey and D. Watstein, "Investigation of Bond in Beam and Pullout Specimens with High-Strength Reinforcing Bars," *J. ACI*, vol. 32, no. 9, 1961, pp. 1071–1090.
- 5.7. ACI Committee 408, "Bond Stress—The State of the Art," *J. ACI*, vol. 63, no. 11, 1966, pp. 1161–1190.
- 5.8. ACI Committee 408, "Suggested Development, Splice, and Standard Hook Provisions for Deformed Bars in Tension," *Concr. Intl.*, vol. 1, no. 7, 1979, pp. 44–46.
- 5.9. J. O. Jirsa, L. A. Lutz, and P. Gergely, "Rationale for Suggested Development, Splice, and Standard Hook Provisions for Deformed Bars in Tension," *Concr. Intl.*, vol. 1, no. 7, 1979, pp. 47–61.
- 5.10. C. O. Orangun, J. O. Jirsa, and J. E. Breen, "A Reevaluation of the Test Data on Development Length and Splices," *J. ACI*, vol. 74, no. 3, 1977, pp. 114–122.
- 5.11. L. A. Lutz, S. A. Mirza, and N. K. Gosain, "Changes to and Applications of Development and Lap Splice Length Provisions for Bars in Tension," *ACI Struct. J.*, vol. 90, no. 4, 1993, pp. 393–406.
- 5.12. D. Darwin, M. L. Tholen, E. K. Idun, and J. Zuo, "Splice Strength of High Relative Rib Area Reinforcing Bars," *ACI Struct. J.*, vol. 93, no. 1, 1996, pp. 95–107.
- 5.13. D. Darwin, J. Zuo, M. L. Tholen, and E. K. Idun, "Development Length Criteria for Conventional and High Relative Rib Area Reinforcing Bars," *ACI Struct. J.*, vol. 93, no. 3, 1996, pp. 347–359.

- 5.14. J. Zuo and D. Darwin, "Splice Strength of Conventional and High Relative Rib Area Bars in Normal and High Strength Concrete," *ACI Struct. J.*, vol. 97, no. 4, 2000, pp. 630–641.
- 5.15. ACI Committee 408, *Bond and Development of Straight Reinforcement in Tension*, ACI 408R-03, American Concrete Institute, Farmington Hills, MI, 2003.
- 5.16. P. M. Ferguson, "Small Bar Spacing or Cover—A Bond Problem for the Designer," *J. ACI*, vol. 74, no. 9, 1977, pp. 435–439.
- 5.17. P. R. Jeanty, D. Mitchell, and M. S. Mirza, "Investigation of Top Bar Effects in Beams," *ACI Struct. J.*, vol. 85, no. 3, 1988, pp. 251–257.
- 5.18. B. B. Brettmann, D. Darwin, and R. C. Donahey, "Bond of Reinforcement to Superplasticized Concrete," *J. ACI*, vol. 83, no. 1, 1986, pp. 98–107.
- 5.19. R. G. Mathey and J. R. Clifton, "Bond of Coated Reinforcing Bars in Concrete," *J. Struct. Div.*, ASCE, vol. 102, no. ST1, 1976, pp. 215–228.
- 5.20. R. A. Treece and J. O. Jirsa, "Bond Strength of Epoxy-Coated Reinforcing Bars," *ACI Materl. J.*, vol. 86, no. 2, 1989, pp. 167–174.
- 5.21. B. S. Hamad, J. O. Jirsa, and N. I. dePaulo, "Anchorage Strength of Epoxy-Coated Hooked Bars," *ACI Struct. J.*, vol. 90, no. 2, 1993, pp. 210–217.
- 5.22. H. H. Ghaffari, O. C. Choi, D. Darwin, and S. L. McCabe, "Bond of Epoxy-Coated Reinforcement: Cover, Casting Position, Slump, and Consolidation," *ACI Struct. J.*, vol. 91, no. 1, 1994, pp. 59–68.
- 5.23. C. J. Hester, S. Salamizavaregh, D. Darwin, and S. L. McCabe, "Bond of Epoxy-Coated Reinforcement: Splices," *ACI Struct. J.*, vol. 90, no. 1, 1993, pp. 89–102.
- 5.24. D. Darwin and J. Zuo, "Discussion of Proposed Changes to ACI 318 in *ACI 318-02 Discussion and Closure*," *Concr. Intl.*, vol. 24, no. 1, 2002, pp. 91, 93, 97–101.
- 5.25. M. K. Thompson, "The Anchorage Behavior of Headed Reinforcement in CCT Nodes and Lap Splices," Ph.D. Thesis, University of Texas at Austin, 2002.
- 5.26. M. K. Thompson, A. Ledesma, J. O. Jirsa, and J. E. Breen, "Lap Splices Anchored by Headed Bars," *ACI Struct. J.*, vol. 103, no. 2, 2006, pp. 271–279.
- 5.27. M. K. Thompson, J. O. Jirsa, and J. E. Breen, "CCT Nodes Anchored by Headed Bars—Part 2: Capacity of Nodes," *ACI Struct. J.*, vol. 103, no. 1, 2006, pp. 65–73.
- 5.28. M. K. Thompson, M. Ziehl, J. O. Jirsa, and J. E. Breen, "CCT Nodes Anchored by Headed Bars—Part 1: Behavior of Nodes," *ACI Struct. J.*, vol. 103, no. 6, 2006, pp. 808–815.

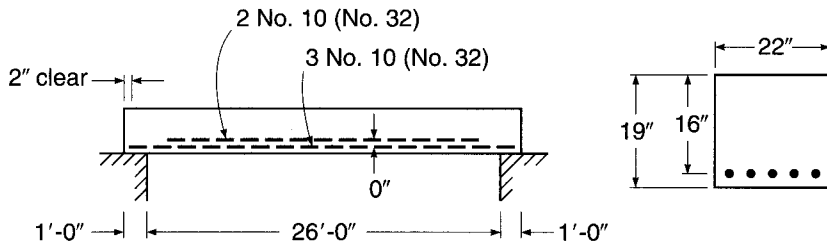
PROBLEMS

- 5.1.** The short beam shown in Fig. P5.1 cantilevers from a supporting column at the left. It must carry a calculated dead load of 2.0 kips/ft including its own weight and a service live load of 2.6 kips/ft. Tensile flexural reinforcement consists of two No. 11 (No. 36) bars at a 21 in. effective depth. Transverse No. 3 (No. 10) U stirrups with 1.5 in. cover are provided at the following spacings from the face of the column: 4 in., 3 at 8 in., 5 at 10.5 in.
- If the flexural and shear steel use $f_y = 60,000$ psi and if the beam uses light-weight concrete having $f'_c = 4000$ psi, check to see if proper development length can be provided for the No. 11 (No. 36) bars. Use the simplified development length equations.
 - Recalculate the required development length for the beam bars using the basic Eq. (5.4). Comment on your results.

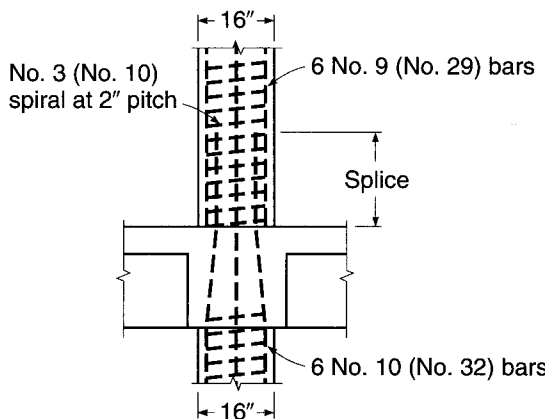
FIGURE P5.1



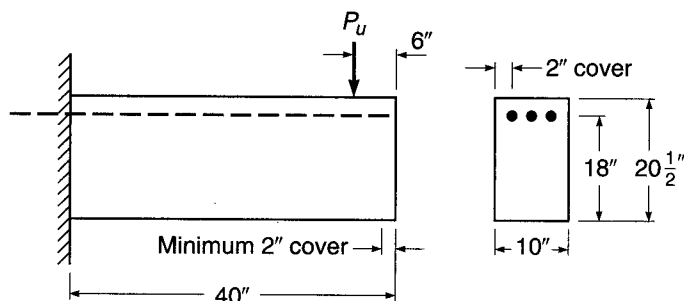
- (c) If the column material strengths are $f_y = 60,000$ psi and $f'_c = 5000$ psi (normalweight concrete), check to see if adequate embedment can be provided within the column for the No. 11 (No. 36) bars. If hooks are required, specify detailed dimensions.
- 5.2.** The beam shown in Fig. P5.2 is simply supported with a clear span of 24.75 ft and is to carry a distributed dead load of 1.05 kips/ft including its own weight and live load of 1.62 kips/ft, unfactored, in service. The reinforcement consists of five No. 10 (No. 32) bars at a 16 in. effective depth, two of which are to be discontinued where no longer needed. Material strengths specified are $f_y = 60,000$ psi and $f'_c = 5000$ psi. No. 3 (No. 10) stirrups are used with a cover of 1.5 in. at spacing less than ACI Code maximum.
- (a) Calculate the point where two bars can be discontinued.
 - (b) Check to be sure that adequate embedded length is provided for continued and discontinued bars.
 - (c) Check special requirements at the support, where $M_u = 0$.
 - (d) If No. 3 (No. 10) bars are used for transverse reinforcement, specify special reinforcing details in the vicinity where the No. 10 (No. 32) bar is cut off.
 - (e) Comment on the practical aspects of the proposed design. Would you recommend cutting off the steel as suggested? Could three bars be discontinued rather than two?

FIGURE P5.2

- 5.3.** Figure P5.3 shows the column reinforcement for a 16 in. diameter concrete column, with $f_y = 75,000$ psi and $f'_c = 8000$ psi. Analysis of the building frame indicates a required $A_s = 7.30 \text{ in}^2$ in the lower column and 5.80 in^2 in the upper column. Spiral reinforcement consists of a $\frac{3}{8}$ in. diameter rod with a 2 in. pitch. Column bars are to be spliced just above the construction joint at the floor level, as shown in the sketch. Calculate the minimum permitted length of splice.

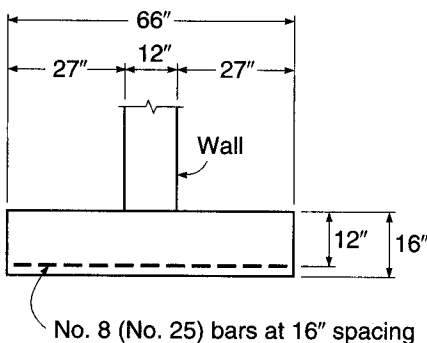
FIGURE P5.3

- 5.4.** The short cantilever shown in Fig. P5.4 carries a heavy concentrated load P_u in. from its outer end. Flexural analysis indicates that three No. 8 (No. 25) bars are required, suitably anchored in the supporting wall and extending to a point no closer than 2 in. from the free end. The bars will be fully stressed to f_y at the fixed support. Investigate the need for hooks and transverse confinement steel at the right end of the member. Material strengths are $f_y = 60,000$ psi and $f'_c = 4000$ psi. If hooks and transverse steel are required, show details in a sketch.

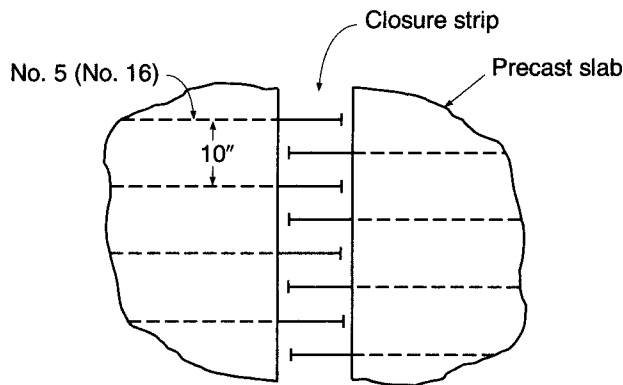
FIGURE P5.4

- 5.5.** A continuous-strip wall footing is shown in cross section in Fig. P5.5. It is proposed that tensile reinforcement be provided using No. 8 (No. 25) bars at 16 in. spacing along the length of the wall, to provide a bar area of $0.59 \text{ in}^2/\text{ft}$. The bars have strength $f_y = 60,000$ psi, and the footing concrete has $f'_c = 4000$ psi. The critical section for bending is assumed to be at the face of the supported wall, and the effective depth to the tensile steel is 12 in. Check to ensure that sufficient development length is available for the No. 8 (No. 25) bars, and if hooks are required, sketch details of the hooks, giving dimensions.

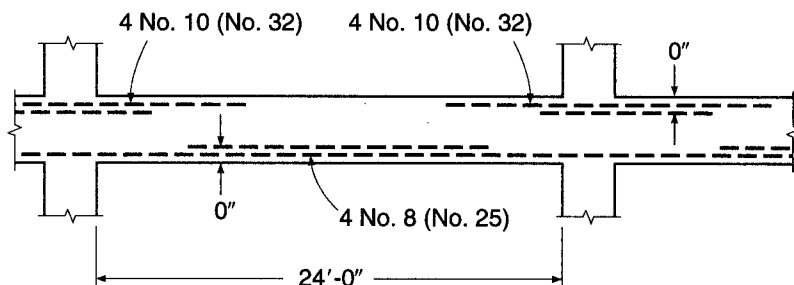
Note: If hooks are required for the No. 8 (No. 25) bars, prepare an alternate design using bars having the same area per foot but of smaller diameter such that hooks could be eliminated; use the largest bar size possible to minimize the cost of steel placement.

FIGURE P5.5

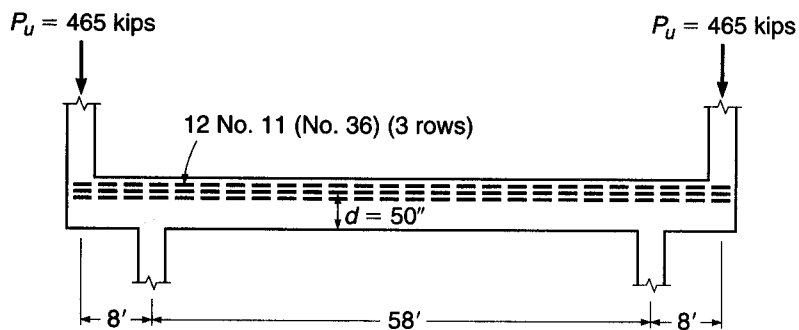
- 5.6.** A closure strip is to be used between two precast slabs (Fig. P5.6). The slabs contain No. 5 (No. 16) bars spaced at 10 in. Determine the minimum width of the closure strip for use with headed bars spliced within the strip. $A_{brg} = 4A_b$. Material strengths are $f_y = 60,000$ psi and $f'_c = 5000$ psi. The maximum size aggregate = $\frac{3}{4}$ in. Assume head thickness = 0.5 in.

FIGURE P5.6

- 5.7.** The continuous beam shown in Fig. P5.7 has been designed to carry a service dead load of 2.25 kips/ft including self-weight and service live load of 3.25 kips/ft. Flexural design has been based on ACI moment coefficients of $\frac{1}{11}$ and $\frac{1}{16}$ at the face of support and midspan, respectively, resulting in a concrete section with $b = 14$ in. and $d = 22$ in. Negative reinforcement at the support face is provided by four No. 10 (No. 32) bars, which will be cut off in pairs where no longer required by the ACI Code. Positive bars consist of four No. 8 (No. 25) bars, which will also be cut off in pairs. Specify the exact point of cutoff for all negative and positive steel. Specify also any supplementary web reinforcement that may be required. Check for satisfaction of ACI Code requirements at the point of inflection, and suggest modifications of reinforcement if appropriate. Material strengths are $f_y = 60,000$ psi and $f'_c = 4000$ psi.

FIGURE P5.7

- 5.8.** Figure P5.8 shows a deep transfer girder that carries two heavy column loads at its outer ends from a high-rise concrete building. Ground-floor columns must be offset 8 ft as shown. The loading produces an essentially constant moment (neglect self-weight of girder) calling for a concrete section with $b = 22$ in. and $b = 50$ in., with main tensile reinforcement at the top of the girder comprised of 12 No. 11 (No. 36) bars in three layers of four bars each. The maximum available bar length is 60 ft, so tensile splices must be provided. Design and detail all splices, following ACI Code provisions. Splices will be

FIGURE P5.8

staggered, with no more than four bars spliced at any section. Also, investigate the need for special anchorage at the outer ends of main reinforcement, and specify details of special anchorage if required. Material strengths are $f_y = 60,000$ psi and $f'_c = 5000$ psi.

6

Serviceability

6.1 INTRODUCTION

Chapters 3, 4, and 5 have dealt mainly with the strength design of reinforced concrete beams. Methods have been developed to ensure that beams will have a proper safety margin against failure in flexure or shear, or due to inadequate bond and anchorage of the reinforcement. The member has been assumed to be at a hypothetical overload state for this purpose.

It is also important that member performance in normal service be satisfactory, when loads are those actually expected to act, i.e., when load factors are 1.0. This is not guaranteed simply by providing adequate strength. Service load deflections under full load may be excessively large, or long-term deflections due to sustained loads may cause damage. Tension cracks in beams may be wide enough to be visually disturbing, and in some cases may reduce the durability of the structure. These and other questions, such as vibration or fatigue, require consideration.

Serviceability studies are carried out based on elastic theory, with stresses in both concrete and steel assumed to be proportional to strain. The concrete on the tension side of the neutral axis may be assumed uncracked, partially cracked, or fully cracked, depending on the loads and material strengths (see Section 3.3).

In early reinforced concrete designs, questions of serviceability were dealt with indirectly, by limiting the stresses in concrete and steel at service loads to the rather conservative values that had resulted in satisfactory performance. In contrast, with current design methods that permit more slender members through more accurate assessment of capacity, and with higher-strength materials further contributing to the trend toward smaller member sizes, such indirect methods no longer work. The current approach is to investigate service load cracking and deflections specifically, after proportioning members based on strength requirements.

In this chapter, methods will be developed to ensure that the cracks associated with flexure of reinforced concrete beams are narrow and well distributed, and that short and long-term deflections at loads up to the full service load are not objectionably large.

6.2 CRACKING IN FLEXURAL MEMBERS

All reinforced concrete beams crack, generally starting at loads well below service level, and possibly even prior to loading due to restrained shrinkage. Flexural cracking due to loads is not only inevitable, but actually necessary for the reinforcement to be used effectively. Prior to the formation of flexural cracks, the steel stress is no more

than n times the stress in the adjacent concrete, where n is the modular ratio E_s/E_c . For materials common in current practice, n is approximately 8. Thus, when the concrete is close to its modulus of rupture of about 500 psi, the steel stress will be only $8 \times 500 = 4000$ psi, far too low to be very effective as reinforcement. At normal service loads, steel stresses 8 or 9 times that value can be expected.

In a well-designed beam, flexural cracks are fine, so-called hairline cracks, almost invisible to the casual observer, and they permit little if any corrosion of the reinforcement. As loads are gradually increased above the cracking load, both the number and the width of cracks increase, and at service load level a maximum width of crack of about 0.016 in. is typical. If loads are further increased, crack widths increase further, although the number of cracks is more or less stable.

Cracking of concrete is a random process, highly variable and influenced by many factors. Because of the complexity of the problem, present methods for predicting crack widths are based primarily on test observations. Most equations that have been developed predict the *probable maximum crack width*, which usually means that about 90 percent of the crack widths in the member are below the calculated value. However, isolated cracks exceeding twice the computed width can sometimes occur (Ref. 6.1).

a. Variables Affecting Width of Cracks

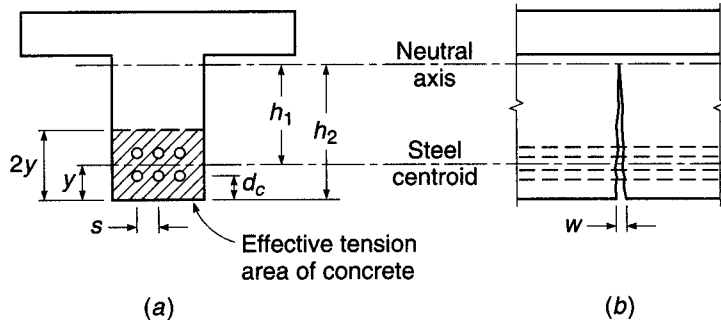
In the discussion of the importance of a good bond between steel and concrete in Section 5.1, it was pointed out that if proper end anchorage is provided, a beam will not fail prematurely, even though the bond is destroyed along the entire span. However, crack widths will be greater than for an otherwise identical beam in which good resistance to slip is provided along the length of the span. In general, beams with smooth round bars will display a relatively small number of rather wide cracks in service, while beams with good slip resistance ensured by proper surface deformations on the bars will show a larger number of very fine, almost invisible cracks. Because of this improvement, reinforcing bars in current practice are always provided with surface deformations, the maximum spacing and minimum height of which are established by ASTM Specifications A615, A706, and A996.

A second variable of importance is the stress in the reinforcement. Studies by Gergely and Lutz and others (Refs. 6.2 to 6.4) have confirmed that crack width is proportional to f_s^n , where f_s is the steel stress and n is an exponent that varies in the range from about 1.0 to 1.4. For steel stresses in the range of practical interest, say from 20 to 36 ksi, n may be taken equal to 1.0. The steel stress is easily computed based on elastic cracked-section analysis (Section 3.3b). Alternatively, f_s may be taken equal to $\frac{2}{3}f_y$ according to ACI Code 10.6.4.

Experiments by Broms (Ref. 6.5) and others have shown that both crack spacing and crack width are related to the concrete cover distance d_c , measured from the center of the bar to the face of the concrete. In general, increasing the cover increases the spacing of cracks and also increases crack width. Furthermore, the distribution of the reinforcement in the tension zone of the beam is important. Generally, to control cracking, it is better to use a larger number of smaller-diameter bars to provide the required A_s than to use the minimum number of larger bars, and the bars should be well distributed over the tensile zone of the concrete. For deep flexural members, this includes additional reinforcement on the sides of the web to prevent excessive surface crack widths above or below the level of the main flexural reinforcement.

FIGURE 6.1

Geometric basis of crack width calculations.



b. Equations for Crack Width

A number of expressions for maximum crack width have been developed based on the statistical analysis of experimental data. Two expressions that have figured prominently in the development of the crack control provisions in the ACI Code are those developed by Gergely and Lutz (Ref. 6.2) and Frosch (Ref. 6.4) for the maximum crack width at the tension face of a beam. They are, respectively,

$$w = 0.076 \beta f_s \sqrt[3]{d_c A} \quad (6.1)$$

and

$$w = 2000 \frac{f_s}{E_s} \beta \sqrt{d_c^2 + \left(\frac{s}{2}\right)^2} \quad (6.2)$$

where w = maximum width of crack, thousandth inches

f_s = steel stress at load for which crack width is to be determined, ksi

E_s = modulus of elasticity of steel, ksi

The geometric parameters are shown in Fig. 6.1 and are as follows:

d_c = thickness of concrete cover measured from tension face to center of bar closest to that face, in.

β = ratio of distances from tension face and from steel centroid to neutral axis, equal to h_2/h_1

A = concrete area surrounding one bar, equal to total effective tension area of concrete surrounding reinforcement and having same centroid, divided by number of bars, in²

s = maximum bar spacing, in.

Equations (6.1) and (6.2), which apply only to beams in which deformed bars are used, include all the factors just named as having an important influence on the width of cracks: steel stress, concrete cover, and the distribution of the reinforcement in the concrete tensile zone. In addition, the factor β is added to account for the increase in crack width with distance from the neutral axis (see Fig. 6.1b).

c. Cyclic and Sustained Load Effects

Both cyclic and sustained loading account for increasing crack width. While there is a large amount of scatter in test data, results of fatigue tests and sustained loading tests indicate that a doubling of crack width can be expected with time (Ref. 6.1). Under

most conditions, the spacing of cracks does not change with time at constant levels of sustained stress or cyclic stress range.

6.3 ACI CODE PROVISIONS FOR CRACK CONTROL

In view of the random nature of cracking and the wide scatter of crack width measurements, even under laboratory conditions, crack width is controlled in the ACI Code by establishing a maximum center-to-center spacing s for the reinforcement closest to the surface of a tension member as a function of the bar stress under service conditions f_s (in psi) and the *clear cover* from the nearest surface in tension to the surface of the flexural tension reinforcement c_c .

$$s = 15 \left(\frac{40,000}{f_s} \right) - 2.5c_c \leq 12 \left(\frac{40,000}{f_s} \right) \quad (6.3)$$

The choice of clear cover c_c , rather than the cover to the center of the bar d_c , was made to simplify design, since this allows s to be independent of bar size. As a consequence, maximum crack widths will be somewhat greater for larger bars than for smaller bars.

As shown in Eq. (6.3), the ACI Code sets an upper limit on s of $12(40,000/f_s)$. The stress f_s is calculated by dividing the service load moment by the product of the area of reinforcement and the internal moment arm, as shown in Eq. (3.8). Alternatively, the ACI Code permits f_s to be taken as two-thirds of the specified yield strength f_y . For members with only a single bar, s is taken as the width of the extreme tension face.

Figure 6.2a compares the values of spacing s obtained using Eqs. (6.1) and (6.2) for a beam containing No. 8 (No. 25) reinforcing bars, for $f_s = 40,000$ psi, $\beta = 1.2$, and a maximum crack width $w = 0.016$ in., to the values calculated using Eq. (6.3). Equations (6.1) and (6.2) give identical spacings for two values of clear cover, but significantly different spacings for other values of c_c . Equation (6.3) provides a practical compromise between the values of s that are calculated using the two experimentally based expressions. The equation is plotted in Fig. 6.2b for $f_s = 26,667$, 40,000, and 50,000 psi, corresponding to $\frac{2}{3}f_y$ for Grade 40, 60, and 75 bars, respectively.

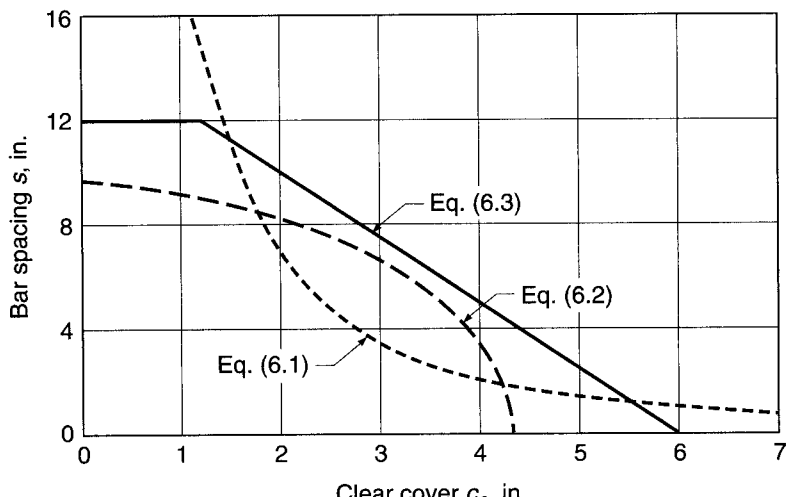
ACI Code 10.6.5 points out that the limitation on s in Eq. (6.3) is not sufficient for structures subject to very aggressive exposure or designed to be watertight. In such cases “special investigations or precautions” are required. These include the use of expressions such as Eqs. (6.1) and (6.2) to determine the probable maximum crack width. Further guidance is given in Ref. 6.1.

When concrete T beam flanges are in tension, as in the negative-moment region of continuous T beams, concentration of the reinforcement over the web may result in excessive crack width in the overhanging slab, even though cracks directly over the web are fine and well distributed. To prevent this, the tensile reinforcement should be distributed over the width of the flange, rather than concentrated. However, because of shear lag, the outer bars in such a distribution would be considerably less highly stressed than those directly over the web, producing an uneconomical design. As a reasonable compromise, ACI Code 10.6.6 requires that the tension reinforcement in such cases be distributed over the effective flange width or a width equal to one-tenth the span, whichever is smaller. If the effective flange width exceeds one-tenth of the span, some longitudinal reinforcement must be provided in the outer portions of the flange. The amount of such additional reinforcement is left to the discretion of the designer; it should at least be the equivalent of temperature reinforcement for the slab (see Section 13.3), and is often taken as twice that amount.

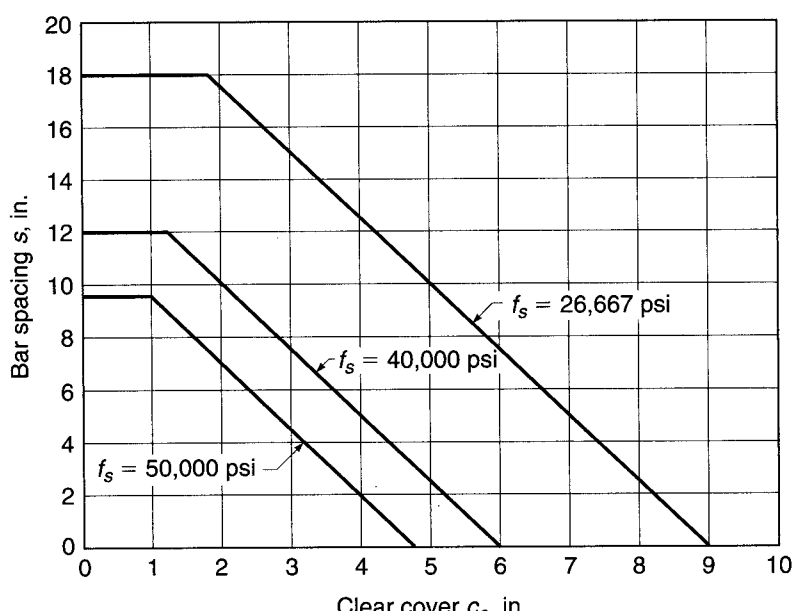
FIGURE 6.2

Maximum bar spacing versus clear cover: (a) Comparison of Eqs. (6.1), (6.2), and (6.3) for $w_c = 0.016$ in., $f_s = 40,000$ psi, $\beta = 1.2$, bar size = No. 8 (No. 25); (b) Eq. (6.3) for $f_s = 26,667$, 40,000, and 50,000 psi, corresponding to $\frac{2}{3}f_y$ for Grades 40, 60, and 75 reinforcement, respectively.

[Part (a) after Ref. 6.6.]



(a)

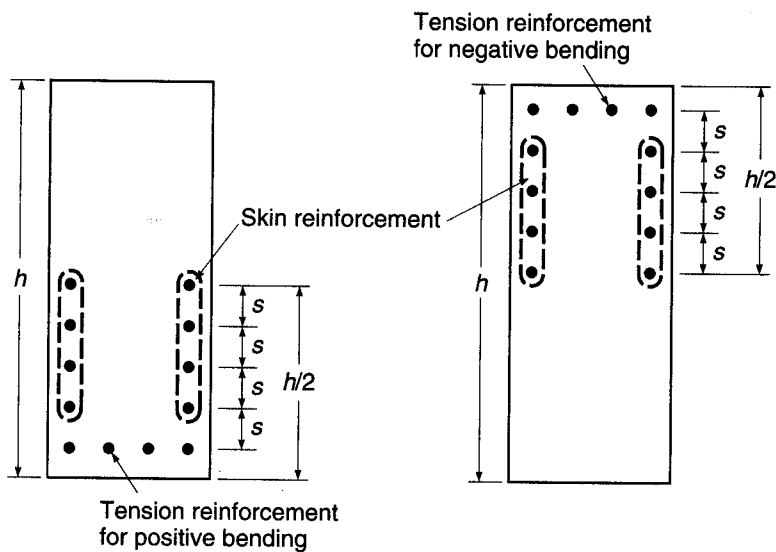


(b)

For beams with relatively deep webs, some reinforcement should be placed near the vertical faces of the web to control the width of cracks in the concrete tension zone above the level of the main reinforcement. Without such steel, crack widths in the web wider than those at the level of the main bars have been observed. According to ACI Code 10.6.7, if the total depth of the beam h exceeds 36 in., longitudinal "skin" reinforcement must be uniformly distributed along both side faces of the member for a distance $h/2$ nearest the flexural tension steel, as shown in Fig. 6.3. The spacing s between longitudinal bars or wires is as specified in Eq. (6.3). The size of the bars or

FIGURE 6.3

Skin reinforcement for flexural members with total depth h greater than 36 in.



wires is not specified, but as indicated in ACI Commentary 10.6.7, No. 3 to No. 5 (No. 10 to No. 16) bars or welded wire reinforcement with a minimum area of 0.1 in² per foot of depth are typically used. The contribution of the skin steel to flexural strength is usually disregarded, although it may be included in the strength calculations if a strain compatibility analysis is used to establish the stress in the skin steel at the flexural failure load.

Figure 6.2b provides a convenient design aid for determining the maximum center-to-center bar spacing as a function of clear cover for the usual case used in design, $f_s = \frac{2}{3}f_y$. From a practical point of view, it is even more helpful to know the minimum number of bars across the width of a beam stem that is needed to satisfy the ACI Code requirements for crack control. That number depends on side cover, as well as clear cover to the tension face, and is dependent on bar size. Table A.8 in Appendix A gives the minimum number of bars across a beam stem for two common cases, 2 in. clear cover on the sides and bottom, which corresponds to using No. 3 or No. 4 (No. 10 or No. 13) stirrups, and 1½ in. clear cover on the sides and bottom, representing beams in which no stirrups are used.

EXAMPLE 6.1

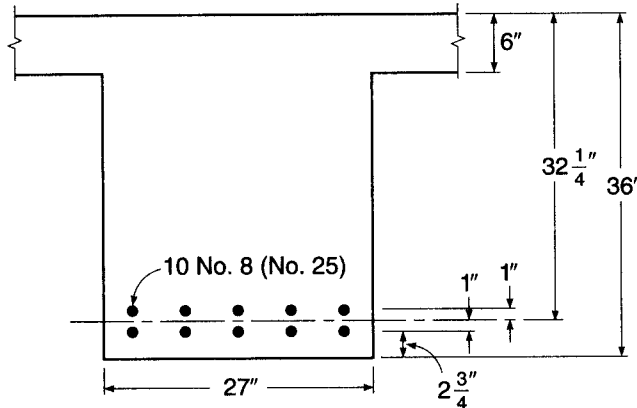
Check crack control criteria. Figure 6.4 shows the main flexural reinforcement at midspan for a T girder in a high-rise building that carries a service load moment of 8630 in-kips. The clear cover on the side and bottom of the beam stem is 2½ in. Determine if the beam meets the crack control criteria in the ACI Code.

SOLUTION. Since the depth of the beam equals but does not exceed 36 in., skin reinforcement is not needed. To check the bar spacing criteria, the steel stress can be estimated closely by taking the internal lever arm equal to the distance $d - h_f/2$:

$$f_s = \frac{M_s}{A_s(d - h_f/2)} = \frac{8630}{7.9 \times 29.25} = 37.3 \text{ ksi}$$

(Alternately, the ACI Code permits using $f_s = \frac{2}{3}f_y$, giving 40.0 ksi.)

FIGURE 6.4
T beam for crack width determination in Example 6.1.



Using f_s in Eq. (6.3) gives

$$s = 15 \left(\frac{40,000}{f_s} \right) - 2.5c_c = 15 \left(\frac{40,000}{37,300} \right) - 2.5 \times 2.25 = 10.5 \text{ in.}$$

By inspection, it is clear that this requirement is satisfied for the beam. If the results had been unfavorable, a redesign using a larger number of smaller-diameter bars would have been indicated.

6.4 CONTROL OF DEFLECTIONS

In addition to limitations on cracking, described in the preceding sections, it is usually necessary to impose certain controls on deflections of beams to ensure serviceability. Excessive deflections can lead to cracking of supported walls and partitions, ill-fitting doors and windows, poor roof drainage, misalignment of sensitive machinery and equipment, or visually offensive sag. It is important, therefore, to maintain control of deflections, in one way or another, so that members designed mainly for strength at prescribed overloads will also perform well in normal service.

There are presently two approaches to deflection control. The first is indirect and consists in setting suitable upper limits on the span-depth ratio. This is simple, and it is satisfactory in many cases where spans, loads and load distributions, and member sizes and proportions fall in the usual ranges. Otherwise, it is essential to calculate deflections and to compare those predicted values with specific limitations that may be imposed by codes or by special requirements.

It will become clear, in the sections that follow, that calculations can, at best, provide a guide to probable actual deflections. This is so because of uncertainties regarding material properties, effects of cracking, and load history for the member under consideration. Extreme precision in the calculations, therefore, is never justified, because highly accurate results are unlikely. However, it is generally sufficient to know, for example, that the deflection under load will be about $\frac{1}{2}$ in. rather than 2 in., while it is relatively unimportant to know whether it will actually be $\frac{5}{8}$ in. rather than $\frac{1}{2}$ in.

The deflections of concern are generally those that occur during the normal service life of the member. In service, a member sustains the full dead load, plus some fraction or all of the specified service live load. Safety provisions of the ACI Code and similar design specifications ensure that, under loads up to the full service load, stresses in both steel and concrete remain within the elastic ranges. Consequently, deflections that occur at once upon application of load, the *immediate deflections*, can be calculated based on the properties of the uncracked elastic member, the cracked elastic member, or some combination of these (see Section 3.3).

It was pointed out in Sections 2.8 and 2.11, however, that in addition to concrete deformations that occur immediately when load is applied, there are other deformations that take place gradually over an extended time. These time-dependent deformations are chiefly due to concrete creep and shrinkage. As a result of these influences, reinforced concrete members continue to deflect with the passage of time. Long-term deflections continue over a period of several years, and may eventually be 2 or more times the initial elastic deflections. Clearly, methods for predicting both instantaneous and time-dependent deflections are essential.

6.5 IMMEDIATE DEFLECTIONS

Elastic deflections can be expressed in the general form

$$\Delta = \frac{f(\text{loads, spans, supports})}{EI}$$

where EI is the flexural rigidity and $f(\text{loads, spans, supports})$ is a function of the particular load, span, and support arrangement. For instance, the deflection of a uniformly loaded simple beam is $5wl^4/384EI$, so that $f = 5wl^4/384$. Similar deflection equations have been tabulated or can easily be computed for many other loadings and span arrangements, simple, fixed, or continuous, and the corresponding f functions can be determined. The particular problem in reinforced concrete structures is therefore the determination of the appropriate flexural rigidity EI for a member consisting of two materials with properties and behavior as widely different as steel and concrete.

If the maximum moment in a flexural member is so small that the tensile stress in the concrete does not exceed the modulus of rupture f_r , no flexural tension cracks will occur. The full, uncracked section is then available for resisting stress and providing rigidity. This stage of loading has been analyzed in Section 3.3a. In agreement with this analysis, the effective moment of inertia for this low range of loads is that of the uncracked transformed section I_{ut} , and E is the modulus of concrete E_c as given by Eq. (2.3). Correspondingly, for this load range,

$$\Delta_{iu} = \frac{f}{E_c I_{ut}} \quad (a)$$

At higher loads, flexural tension cracks are formed. In addition, if shear stresses exceed v_{cr} [see Eq. (4.3)] and web reinforcement is employed to resist them, diagonal cracks can exist at service loads. In the region of flexural cracks, the position of the neutral axis varies: directly at each crack it is located at the level calculated for the cracked transformed section (see Section 3.3b); midway between cracks it dips to a location closer to that calculated for the uncracked transformed section. Correspondingly, flexural-tension cracking causes the effective moment of inertia to be that of the cracked transformed section in the immediate neighborhood of flexural-tension

cracks, and closer to that of the uncracked transformed section midway between cracks, with a gradual transition between these extremes.

The value of the local moment of inertia varies in those portions of the beam in which the bending moment exceeds the cracking moment of the section

$$M_{cr} = \frac{f_r I_{ut}}{y_t} \quad (6.4)$$

where y_t is the distance from the neutral axis to the tension face and f_r is the modulus of rupture. The exact variation of I depends on the shape of the moment diagram and on the crack pattern, and is difficult to determine. This makes an exact deflection calculation impossible.

However, extensively documented studies (Ref. 6.7) have shown that deflections Δ_{ic} occurring in a beam after the maximum moment M_a has reached and exceeded the cracking moment M_{cr} can be calculated by using an effective moment of inertia I_e ; that is,

$$\Delta_{ic} = \frac{f}{E_c I_e} \quad (b)$$

where

$$I_e = \left(\frac{M_{cr}}{M_a} \right)^3 I_{ut} + \left[1 - \left(\frac{M_{cr}}{M_a} \right)^3 \right] I_{cr} \leq I_{ut} \quad (6.5)$$

and I_{cr} is the moment of inertia of the cracked transformed section.

In Fig. 6.5, the effective moment of inertia, given by Eq. (6.5), is plotted as a function of the ratio M_a/M_{cr} (the reciprocal of the moment ratio used in the equation). It is seen that, for values of maximum moment M_a less than the cracking moment M_{cr} , that is, M_a/M_{cr} less than 1.0, $I_e = I_{ut}$. With increasing values of M_a , I_e approaches I_{cr} ; and for values of M_a/M_{cr} of 3 or more, I_e is almost the same as I_{cr} . Typical values of M_a/M_{cr} at full service load range from about 1.5 to 3.

Figure 6.6 shows the growth of deflections with increasing moment for a simple-span beam and illustrates the use of Eq. (6.5). For moments no larger than M_{cr} , deflections are practically proportional to moments, and the deflection at which cracking

FIGURE 6.5
Variation of I_e with moment ratio.

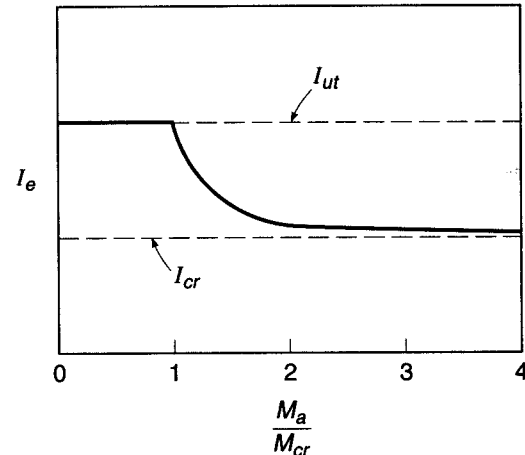
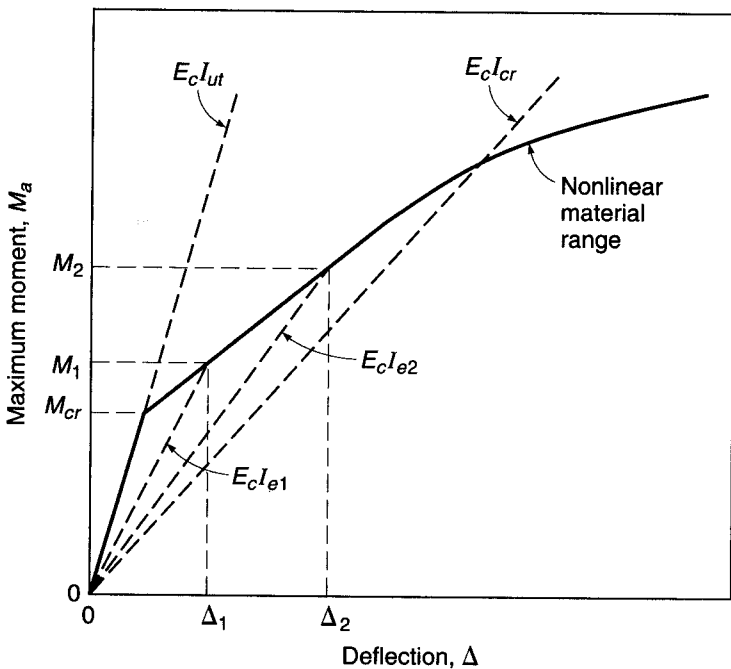


FIGURE 6.6

Deflection of a reinforced concrete beam.



begins is obtained from Eq. (a) with $M = M_{cr}$. At larger moments, the effective moment of inertia I_e becomes progressively smaller, according to Eq. (6.5), and deflections are found by Eq. (b) for the load level of interest. The moment M_2 might correspond to the full service load, for example, while the moment M_1 would represent the dead load moment for a typical case. A moment-deflection curve corresponding to the line $E_c I_{cr}$ represents an upper bound for deflections, consistent with Fig. 6.5, except that at loads somewhat beyond the service load, the nonlinear response of steel or concrete or both causes a further nonlinear increase in deflections.

Note that to calculate the increment of deflection due to live load, causing a moment increase $M_2 - M_1$, a two-step computation is required: the first for deflection Δ_2 due to live and dead load, and the second for deflection Δ_1 due to dead load alone, each with the appropriate value of I_e . Then the deflection increment due to live load is found, equal to $\Delta_2 - \Delta_1$.

Most reinforced concrete spans are continuous, not simply supported. The concepts just introduced for simple spans can be applied, but the moment diagram for a given span will include both negative and positive regions, reflecting the rotational restraint provided at the ends of the spans by continuous frame action. The effective moment of inertia for a continuous span can be found by a simple averaging procedure, according to the ACI Code, that will be described in Section 6.7c.

A fundamental problem for continuous spans is that although the deflections are based on the moment diagram, that moment diagram depends, in turn, on the flexural rigidity EI for each member of the frame. The flexural rigidity depends on the extent of cracking, as has been demonstrated. Cracking, in turn, depends on the moments, which are to be found. The circular nature of the problem is evident.

One could use an iterative procedure, initially basing the frame analysis on uncracked concrete members, determining the moments, calculating effective EI terms for all members, then recalculating moments, adjusting the EI values, etc. The process

could be continued for as many iterations as needed, until changes are not significant. However, such an approach would be expensive and time-consuming, even with computer use.

Usually, a very approximate approach is adopted. Member flexural stiffnesses for the frame analysis are based simply on properties of uncracked rectangular concrete cross sections. This can be defended by noting that the moments in a continuous frame depend only on the *relative* values of EI in its members, not the *absolute* values. Hence, if a consistent assumption, i.e., uncracked section, is used for all members, the results should be valid. Although cracking is certainly more prevalent in beams than in columns, thus reducing the relative EI for the beams, this is compensated to a large extent, in typical cases, by the stiffening effect of the flanges in the positive bending regions of continuous T beam construction. This subject is discussed at greater length in Section 12.5.

6.6 DEFLECTIONS DUE TO LONG-TERM LOADS

Initial deflections are increased significantly if loads are sustained over a long period of time, due to the effects of shrinkage and creep. These two effects are usually combined in deflection calculations. Creep generally dominates, but for some types of members, shrinkage deflections are large and should be considered separately (see Section 6.8).

It was pointed out in Section 2.8 that creep deformations of concrete are directly proportional to the compressive stress up to and beyond the usual service load range. They increase asymptotically with time and, for the same stress, are larger for low-strength than for high-strength concretes. The ratio of additional time-dependent strain to initial elastic strain is given by the creep coefficient C_{cu} (see Table 2.2).

For a reinforced concrete beam, the long-term deformation is much more complicated than for an axially loaded cylinder, because while the concrete creeps under sustained load, the steel does not. The situation in a reinforced concrete beam is illustrated by Fig. 6.7. Under sustained load, the initial strain ϵ_i at the top face of the beam increases, due to creep, by the amount ϵ_t , while the strain ϵ_s in the steel is essentially unchanged. Because the rotation of the strain distribution diagram is therefore about a point at the level of the steel, rather than about the cracked elastic neutral axis, the neutral axis moves down as a result of creep, and

$$\frac{\phi_t}{\phi_i} < \frac{\epsilon_t}{\epsilon_i} \quad (a)$$

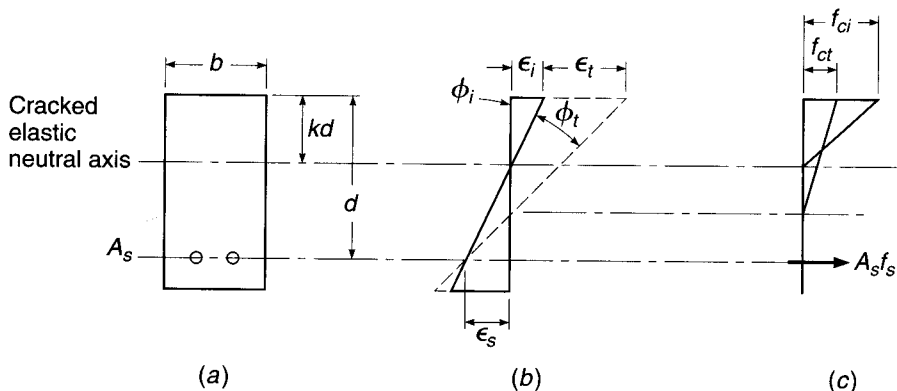
demonstrating that the usual creep coefficients cannot be applied to initial curvatures to obtain creep curvatures (hence deflections).

The situation is further complicated. Due to the lowering of the neutral axis associated with creep (see Fig. 6.7b) and the resulting increase in compression area, the compressive stress required to produce a given resultant C to equilibrate $T = A_s f_s$ is less than before, in contrast to the situation in a creep test of a compressed cylinder, because the beam creep occurs at a gradually diminishing stress. On the other hand, with the new lower neutral axis, the internal lever arm between compressive and tensile resultant forces is less, calling for an increase in both resultants for a constant moment. This, in turn, will require a small increase in stress, and hence strain, in the steel; thus, ϵ_s is not constant as assumed originally.

Because of such complexities, it is necessary in practice to calculate additional, time-dependent deflections of beams due to creep (and shrinkage) using a simplified,

FIGURE 6.7

Effect of concrete creep on curvature: (a) beam cross section; (b) strains; (c) stresses and forces.
(Adapted from Ref. 6.8.)



empirical approach by which the initial elastic deflections are multiplied by a factor λ_Δ to obtain the additional long-time deflections. Values of λ_Δ for use in design are based on long-term deflection data for reinforced concrete beams (Refs. 6.8 to 6.11). Thus

$$\Delta_t = \lambda_\Delta \Delta_i \quad (6.6)$$

where Δ_t is the *additional* long-term deflection due to the combined effect of creep and shrinkage and Δ_i is the initial elastic deflection calculated by the methods described in Section 6.5.

The coefficient λ_Δ depends on the duration of the sustained load. It also depends on whether the beam has only reinforcement A_s on the tension side, or whether additional longitudinal reinforcement A'_s is provided on the compression side. In the latter case, the long-term deflections are much reduced. This is so because when no compression reinforcement is provided, the compression concrete is subject to unrestrained creep and shrinkage. On the other hand, since steel is not subject to creep, if additional bars are located close to the compression face, they will resist and thereby reduce the amount of creep and shrinkage and the corresponding deflection (Ref. 6.11). Compression steel may be included for this reason alone. Specific values of λ_Δ , used to account for the influence of creep and compression reinforcement, will be given in Section 6.7.

If a beam carries a certain sustained load W (e.g., the dead load plus the average traffic load on a bridge) and is subject to a short-term heavy live load P (e.g., the weight of an unusually heavy vehicle), the maximum total deflection under this combined loading is obtained as follows:

1. Calculate the instantaneous deflection Δ_{iw} caused by the sustained load W by methods given in Section 6.5.
2. Calculate the additional long-term deflection caused by W , that is,

$$\Delta_{tw} = \lambda_\Delta \Delta_{iw}$$

3. Then the total deflection caused by the sustained part of the load is

$$\Delta_w = \Delta_{iw} + \Delta_{tw}$$

4. In calculating the additional instantaneous deflection caused by the short-term load P , account must be taken of the fact that the load-deflection relation after cracking is nonlinear, as illustrated by Fig. 6.6. Hence

$$\Delta_{ip} = \Delta_{i(w+p)} - \Delta_{iw}$$

where $\Delta_{i(w+p)}$ is the total instantaneous deflection that would be obtained if W and P were applied simultaneously, calculated by using I_e determined for the moment caused by $W + P$.

5. Then the total deflection under the sustained load plus heavy short-term load is

$$\Delta = \Delta_w + \Delta_{ip}$$

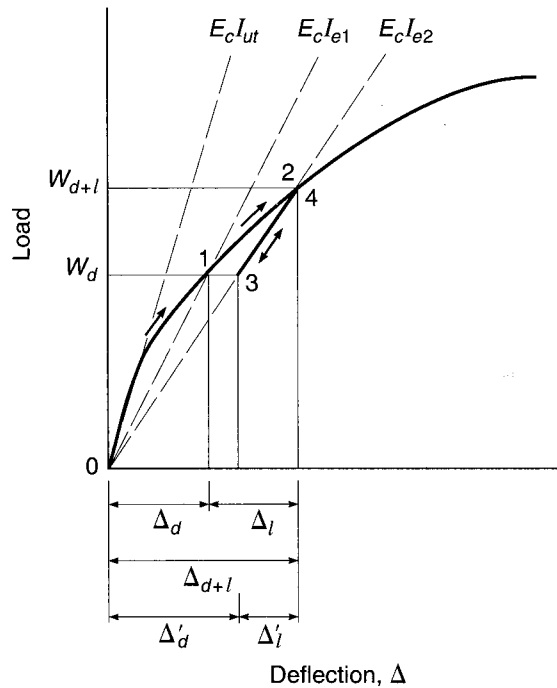
In calculations of deflections, careful attention must be paid to the load history, i.e., the time sequence in which loads are applied, as well as to the magnitude of the loads. The short-term peak load on the bridge girder just described might be applied early in the life of the member, before time-dependent deflections had taken place. Similarly, for buildings, heavy loads such as stacked material are often placed during construction. These temporary loads may be equal to, or even greater than, the design live load. The state of cracking will correspond to the *maximum load* that was carried, and the sustained load deflection, on which the long-term effects are based, would correspond to that cracked condition. I_e for the maximum load reached should be used to recalculate the sustained load deflection before calculating long-term effects.

This will be illustrated referring to Fig. 6.8, showing the load-deflection plot for a building girder that is designed to carry a specified dead and live load. Assume first that the dead and live loads increase monotonically. As the full dead load W_d is applied, the load deflection curve follows the path 0-1, and the dead load deflection Δ_d is found using I_{e1} calculated from Eq. (6.5), with $M_a = M_d$. The time-dependent effect of the dead load would be $\lambda_\Delta \Delta_d$. As live load is then applied, path 1-2 would be followed. Live load deflection Δ_l would be found in two steps, as described in Section 6.5, first finding Δ_{d+l} based on I_{e2} , with M_a in Eq. (6.5) equal to M_{d+l} , and then subtracting dead load deflection Δ_d .

If, on the other hand, short-term construction loads were applied, then removed, the deflection path 1-2-3 would be followed. Then, under dead load only,

FIGURE 6.8

Effect of load history on deflection of a building girder.



the resulting deflection would be Δ'_d . Note that this deflection can be found in one step using W_d , but with I_{e2} corresponding to the maximum load reached. The long-term deflection now would be $\lambda_\Delta \Delta'_d$, significantly *larger* than before. Should the full design *live* load then be applied, the deflection would follow path 3-4, and the live load deflection would be *less* than for the first case. It, too, can be calculated by a simple one-step calculation using W_l alone, in this case, and with moment of inertia equal to I_{e2} .

Clearly, in calculating deflections, the engineer must anticipate, as nearly as possible, both the magnitude and time sequence of the loadings. Although long-term deflections are often calculated assuming monotonic loading, with both immediate and long-term effects of dead load occurring before application of live load, in many cases this is not realistic.

6.7 ACI CODE PROVISIONS FOR CONTROL OF DEFLECTIONS

a. Minimum Depth-Span Ratios

As pointed out in Section 6.4, two approaches to deflection control are in current use, both acceptable under the provisions of the ACI Code, within prescribed limits. The simpler of these is to impose restrictions on the minimum member depth h , relative to the span l , to ensure that the beam will be sufficiently stiff that deflections are unlikely to cause problems in service. Deflections are greatly influenced by support conditions (e.g., a simply supported uniformly loaded beam will deflect 5 times as much as an otherwise identical beam with fixed supports), so minimum depths must vary depending on conditions of restraint at the ends of the spans.

According to ACI Code 9.5.2, the minimum depths of Table 6.1 apply to one-way construction *not* supporting or attached to partitions or other construction likely to be damaged by large deflections, unless computation of deflections indicates a lesser depth can be used without adverse effects. Values given in Table 6.1 are to be used directly for normalweight concrete with $w_c = 145$ pcf and reinforcement with $f_y = 60,000$ psi. For members using lightweight concrete with density in the range from 90 to 115 pcf, the values of Table 6.1 should be multiplied by $1.65 - 0.005w_c \geq 1.09$. For yield strengths other than 60,000 psi, the values should be multiplied by $0.4 + f_y/100,000$.

TABLE 6.1

Minimum thickness of nonprestressed beams or one-way slabs unless deflections are computed

Member	Minimum Thickness h			
	Simply Supported	One End Continuous	Both Ends Continuous	Cantilever
	Members Not Supporting or Attached to Partitions or Other Construction Likely to Be Damaged by Large Deflections			
Solid one-way slabs	$l/20$	$l/24$	$l/28$	$l/10$
Beams or ribbed one-way slabs	$l/16$	$l/18.5$	$l/21$	$l/8$

b. Calculation of Immediate Deflections

When there is need to use member depths shallower than are permitted by Table 6.1, or when members support construction that is likely to be damaged by large deflections, or for prestressed members, deflections must be calculated and compared with limiting values (see Section 6.7e). The calculation of deflections, when required, proceeds along the lines described in Sections 6.5 and 6.6. For design purposes, the moment of the uncracked transformed section I_{ut} can be replaced by that of the gross concrete section I_g , neglecting reinforcement, without serious error. With this simplification, Eqs. (6.4) and (6.5) are replaced by the following:

$$M_{cr} = \frac{f_r I_g}{y_i} \quad (6.7)$$

and

$$I_e = \left(\frac{M_{cr}}{M_a} \right)^3 I_g + \left[1 - \left(\frac{M_{cr}}{M_a} \right)^3 \right] I_{cr} \leq I_g \quad (6.8)$$

The modulus of rupture is to be taken equal to

$$f_r = 7.5\lambda\sqrt{f'_c} \quad (6.9a)$$

As explained in Section 4.5a, in accordance with ACI Code 8.6.1, $\lambda = 1.0$ for normalweight concrete, 0.85 for sand-lightweight concrete, and 0.75 for all-lightweight concrete. If the splitting tensile strength of the concrete f_{ct} is known, $\lambda = f_{ct}/(6.7\sqrt{f'_c}) \leq 1.0$, and Eq. (6.9a) becomes

$$f_r = 7.5 \frac{f_{ct}}{6.7} = 1.12f_{ct} \quad (6.9b)$$

c. Continuous Spans

For continuous spans, ACI Code 9.5.2 calls for a simple average of values obtained from Eq. (6.8) for the critical positive and negative-moment sections, i.e.,

$$I_e = 0.50I_{em} + 0.25(I_{e1} + I_{e2}) \quad (6.10a)$$

where I_{em} is the effective moment of inertia for the midspan section and I_{e1} and I_{e2} are those for the negative-moment sections at the respective beam ends, each calculated from Eq. (6.8) using the applicable value of M_a . It is shown in Ref. 6.12 that a somewhat improved result can be had for continuous prismatic members using a weighted average for beams with both ends continuous of

$$I_e = 0.70I_{em} + 0.15(I_{e1} + I_{e2}) \quad (6.10b)$$

and for beams with one end continuous and the other simply supported of

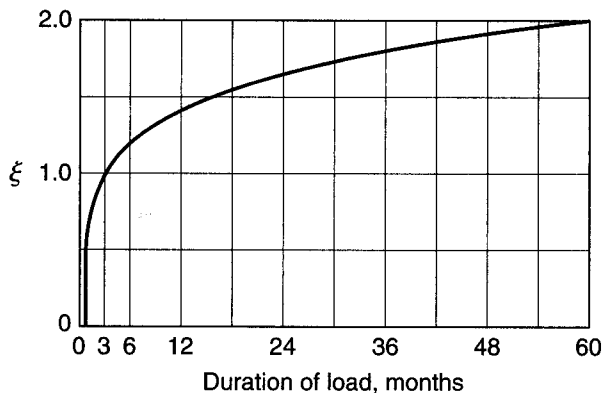
$$I_e = 0.85I_{em} + 0.15I_{e1} \quad (6.10c)$$

where I_{e1} is the effective moment of inertia at the continuous end. The ACI Code, as an option, also permits use of I_e for continuous prismatic beams to be taken equal to the value obtained from Eq. (6.8) at midspan; for cantilevers, I_e calculated at the support section may be used.

After I_e is found, deflections may be computed with due regard for rotations of the tangent to the elastic curve at the supports. In general, in computing the maximum deflection, the loading producing the maximum positive moment may be used, and the

FIGURE 6.9

Time variation of ξ for long-term deflections.



midspan deflection may normally be used as an acceptable approximation of the maximum deflection. Coefficients for deflection calculation such as derived by Branson in Ref. 6.7 are helpful. For members where supports may be considered fully fixed or hinged, handbook equations for deflections may be used.

d. Long-Term Deflection Multipliers

On the basis of empirical studies (Refs. 6.7, 6.9, and 6.11), ACI Code 9.5.2 specifies that *additional* long-term deflections Δ , due to the combined effects of creep and shrinkage be calculated by multiplying the immediate deflection Δ_i by the factor

$$\lambda_{\Delta} = \frac{\xi}{1 + 50\rho'} \quad (6.11)$$

where $\rho' = A'_s/bd$ and ξ is a time-dependent coefficient that varies as shown in Fig. 6.9. In Eq. (6.11), the quantity $1/(1 + 50\rho')$ is a reduction factor that is essentially a section property, reflecting the beneficial effect of compression reinforcement A'_s in reducing long-term deflections, whereas ξ is a material property depending on creep and shrinkage characteristics. For simple and continuous spans, the value of ρ' used in Eq. (6.11) should be that at the midspan section, according to the ACI Code, or that at the support for cantilevers. Equation (6.11) and the values of ξ given by Fig. 6.9 apply to both normalweight and lightweight concrete beams. The additional, time-dependent deflections are thus found using values of λ_{Δ} from Eq. (6.11) in Eq. (6.6).

Values of ξ given in the ACI Code and Commentary are satisfactory for ordinary beams and one-way slabs, but may result in underestimation of time-dependent deflections of two-way slabs, for which Branson has suggested a 5-year value of $\xi = 3.0$ (Ref. 6.7).

Research by Paulson, Nilson, and Hover indicates that Eq. (6.11) does not properly reflect the reduced creep that is characteristic of higher-strength concretes (Ref. 6.13). As indicated in Table 2.2, the creep coefficient for high-strength concrete may be as low as one-half the value for normal concrete. Clearly, the long-term deflection of high-strength concrete beams under sustained load, expressed as a ratio of immediate elastic deflection, correspondingly will be less. This suggests a lower value of the material modifier ξ in Eq. (6.11) and Fig. 6.9. On the other hand, in high-strength concrete beams, the influence of compression

TABLE 6.2
Maximum allowable computed deflections

Type of Member	Deflection to Be Considered	Deflection Limitation
Flat roofs not supporting or attached to nonstructural elements likely to be damaged by large deflections	Immediate deflection due to the live load L	$\frac{l}{180}$
Floors not supporting or attached to nonstructural elements likely to be damaged by large deflections	Immediate deflection due to the live load L	$\frac{l}{360}$
Roof or floor construction supporting or attached to nonstructural elements likely to be damaged by large deflections	That part of the total deflection occurring after attachment of the nonstructural elements (sum of the long-time deflection due to all sustained loads and the immediate deflection due to any additional live load)	$\frac{l}{480}$
Roof or floor construction supporting or attached to nonstructural elements not likely to be damaged by large deflections		$\frac{l}{240}$

steel in reducing creep deflections is less pronounced, requiring an adjustment in the section modifier $1/(1 + 50\rho')$ in that equation.

Based on long-term tests involving six experimental programs, the following modified form of Eq. (6.11) is recommended (Ref. 6.13):

$$\lambda_{\Delta} = \frac{\mu\xi}{1 + 50\mu\rho'} \quad (6.12)$$

in which

$$\begin{aligned} \mu &= 1.4 - f'_c/10,000 \\ 0.4 &\leq \mu \leq 1.0 \end{aligned} \quad (6.13)$$

The proposed equation gives results identical to Eq. (6.11) for concrete strengths of 4000 psi and below, and much improved predictions for concrete strengths between 4000 and 12,000 psi.

e. Permissible Deflections

To ensure satisfactory performance in service, ACI Code 9.5.2 imposes certain limits on deflections calculated according to the procedures just described. These limits are given in Table 6.2. Limits depend on whether or not the member supports or is attached to other nonstructural elements, and whether or not those nonstructural elements are likely to be damaged by large deflections. When long-term deflections are computed, that part of the deflection that occurs before attachment of the nonstructural elements may be deducted; information from Fig. 6.9 is useful for this purpose. The last two limits of Table 6.2 may be exceeded under certain conditions, according to the ACI Code.

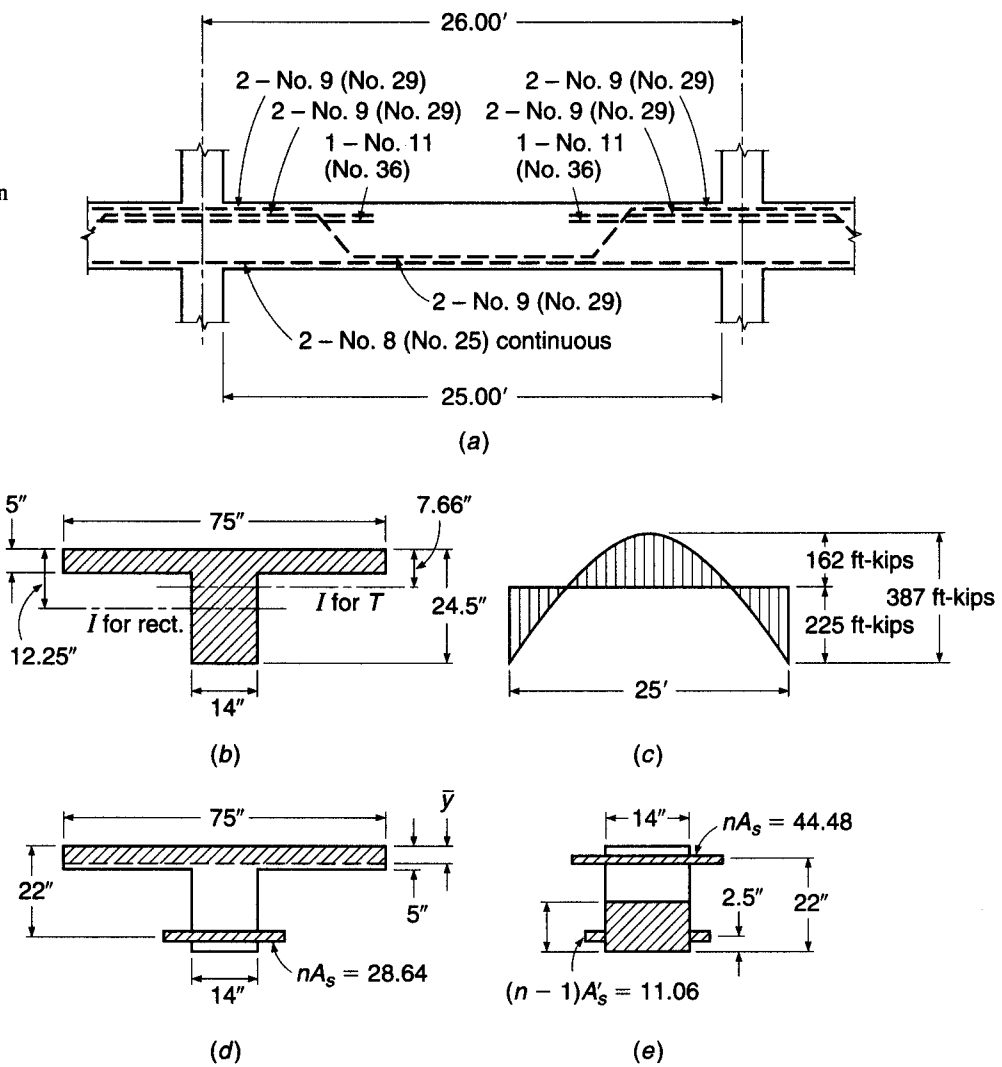
EXAMPLE 6.2

Deflection calculation. The beam shown in Fig. 6.10 is a part of the floor system of an apartment house and is designed to carry calculated dead load w_d of 1.65 kips/ft and a service live load w_l of 3.3 kips/ft. Of the total live load, 20 percent is sustained in nature, while 80 percent will be applied only intermittently over the life of the structure. Under full dead and live load, the moment diagram is as shown in Fig. 6.10c. The beam will support nonstructural partitions that would be damaged if large deflections were to occur. They will be installed shortly after construction shoring is removed and dead loads take effect, but before significant creep occurs. Calculate that part of the total deflection that would adversely affect the partitions, i.e., the sum of long-time deflection due to dead and partial live load plus the immediate deflection due to the nonsustained part of the live load. Material strengths are $f'_c = 4000$ psi and $f_y = 60$ ksi.

SOLUTION. For the specified materials, $E_c = 57,000\sqrt{4000} = 3.60 \times 10^6$ psi, and with $E_s = 29 \times 10^6$ psi, the modular ratio $n = 8$. The modulus of rupture $f_r = 7.5 \times 1.0\sqrt{4000} = 474$ psi. The effective moment of inertia will be calculated for the moment diagram shown in Fig. 6.10c corresponding to the full service load, on the basis that the extent of cracking will be governed by the full service load, even though that load is intermittent. In the positive-moment region, the

FIGURE 6.10

Continuous T beam for deflection calculations in Example 6.2. The uncracked section is shown in (b), the cracked transformed section in the positive moment region is shown in (d), and the cracked transformed section in the negative moment region is shown in (e).



centroidal axis of the uncracked T section of Fig. 6.10b is found by taking moments about the top surface, to be at 7.66 in. depth, and $I_g = 33,160 \text{ in}^4$. By similar means, the centroidal axis of the cracked transformed T section shown in Fig. 6.10d is located 3.73 in. below the top of the slab and $I_{cr} = 10,860 \text{ in}^4$. The cracking moment is then found by means of Eq. (6.7):

$$M_{cr} = 474 \times \frac{33,160}{16.84} \times \frac{1}{12,000} = 78 \text{ ft-kips}$$

With $M_{cr}/M_a = 78/162 = 0.481$, the effective moment of inertia in the positive bending region is found from Eq. (6.8) to be

$$I_e = 0.481^3 \times 33,160 + (1 - 0.481^3) \times 10,860 = 13,340 \text{ in}^4$$

In the negative bending region, the gross moment of inertia will be based on the rectangular section shown in Fig. 6.10b. For this area, the centroid is 12.25 in. from the top surface and $I_g = 17,200 \text{ in}^4$. For the cracked transformed section shown in Fig. 6.10e, the centroidal axis is found, taking moments about the bottom surface, to be 8.65 in. from that level, and $I_{cr} = 11,366 \text{ in}^4$. Then

$$M_{cr} = 474 \times \frac{17,200}{12.25} \times \frac{1}{12,000} = 55.5 \text{ ft-kips}$$

giving $M_{cr}/M_a = 55.5/225 = 0.247$. Thus, for the negative-moment regions,

$$I_e = 0.247^3 \times 17,200 + (1 - 0.247^3) \times 11,366 = 11,450 \text{ in}^4$$

The average value of I_e to be used in calculation of deflection is

$$I_{e,av} = \frac{1}{2}(13,340 + 11,450) = 12,395 \text{ in}^4$$

It is next necessary to find the sustained-load deflection multiplier given by Eq. (6.11) and Fig. 6.9. For the positive bending zone, with no compression reinforcement, $\lambda_{\Delta_{pos}} = 2.00$.

For convenient reference, the deflection of the member under full dead plus live load of 4.95 kips/ft, corresponding to the moment diagram of Fig. 6.10c, will be found. Making use of the moment-area principles,

$$\begin{aligned} \Delta_{d+l} &= \frac{1}{EI} \left[\left(\frac{2}{3} \times 387 \times 12.5 \times \frac{5}{8} \times 12.5 \right) - (225 \times 12.5 \times 6.25) \right] = \frac{7620}{EI} \\ &= \frac{7620 \times 1728}{3600 \times 12,395} = 0.295 \text{ in.} \end{aligned}$$

Using this figure as a basis, the time-dependent portion of dead load deflection (the only part of the total that would affect the partitions) is

$$\Delta_d = 0.295 \times \frac{1.65}{4.95} \times 2.00 = 0.197 \text{ in.}$$

while the sum of the immediate and time-dependent deflection due to the sustained portion of the live load is

$$\Delta_{0.20l} = 0.295 \times \frac{3.3}{4.95} \times 0.20 \times 3.00 = 0.118 \text{ in.}$$

and the instantaneous deflection due to application of the short-term portion of the live load is

$$\Delta_{0.80l} = 0.295 \times \frac{3.3}{4.95} \times 0.80 = 0.157 \text{ in.}$$

Thus the total deflection that would adversely affect the partitions, from the time they are installed until all long-time and subsequent instantaneous deflections have occurred, is

$$\Delta = 0.197 + 0.118 + 0.157 = 0.472 \text{ in.}$$

For comparison, as shown in Table 6.2, the limitation imposed by the ACI Code in such circumstances is $l/480 = 26 \times 12/480 = 0.650$ in., indicating that the stiffness of the proposed member is sufficient.

Note that relatively little error would have been introduced in the above solution if the cracked-section moment of inertia had been used for both positive and negative sections rather than I_e . Significant savings in computational effort would have resulted. If M_{cr}/M_a is less than $\frac{1}{3}$, use of I_{cr} would almost always be acceptable. Note further that computation of the moment of inertia for both uncracked and cracked sections is greatly facilitated by design aids like those included in Ref. 6.14.

6.8 DEFLECTIONS DUE TO SHRINKAGE AND TEMPERATURE CHANGES

Concrete shrinkage will produce compressive stress in the longitudinal reinforcement in beams and slabs and equilibrating tensile stress in the concrete. If, as usual, the reinforcement is not symmetrically placed with respect to the concrete centroid, then shrinkage will produce curvature and corresponding deflection. The deflections will be in the same direction as those produced by the loads, if the reinforcement is mainly on the side of the member subject to flexural tension.

Shrinkage deflection is not usually calculated separately, but is combined with creep deflection, according to ACI Code procedures (see Section 6.7d). However, there are circumstances where a separate and more accurate estimation of shrinkage deflection may be necessary, particularly for thin, lightly loaded slabs. Compression steel, while it has only a small effect in reducing immediate elastic deflections, contributes significantly in reducing deflections due to shrinkage (as well as creep), and is sometimes added for this reason.

Curvatures due to shrinkage of concrete in an unsymmetrically reinforced concrete member can be found by the fictitious tensile force method (Ref. 6.7). Figure 6.11a shows the member cross section, with compression steel area A'_s and tensile steel area A_s , at depths d' and d , respectively, from the top surface. In Fig. 6.11b, the concrete and steel are imagined to be temporarily separated, so that the concrete can assume its free shrinkage strain ϵ_{sh} . Then a fictitious compressive force $T_{sh} = (A_s + A'_s)\epsilon_{sh}E_s$ is applied to the steel, at the centroid of all the bars, a distance e below the concrete centroid, such that the steel shortening will exactly equal the free shrinkage strain of the concrete. The equilibrating tension force T_{sh} is then applied to the recombined section, as in Fig. 6.11c. This produces a moment $T_{sh}e$, and the corresponding shrinkage curvature is

$$\phi_{sh} = \frac{T_{sh}e}{EI}$$

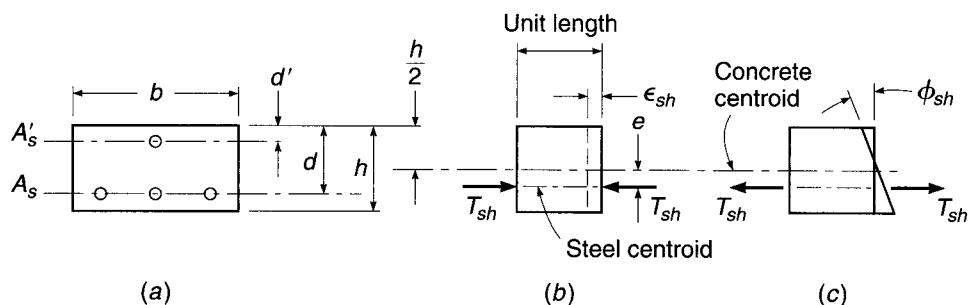
The effects of concrete cracking and creep complicate the analysis, but comparisons with experimental data (Ref. 6.7) indicate that good results can be obtained using e_g and I_g for the uncracked gross concrete section and by using a reduced modulus E_{ct} equal to $\frac{1}{2}E_c$ to account for creep. Thus

$$\phi_{sh} = \frac{2T_{sh}e_g}{E_c I_g} \quad (6.14)$$

where E_c is the usual value of concrete modulus given by Eq. (2.3).

FIGURE 6.11

Shrinkage curvature of a reinforced concrete beam or slab: (a) cross section; (b) free shrinkage strain; (c) shrinkage curvature.



Empirical methods are also used, in place of the fictitious tensile force method, to calculate shrinkage curvatures. These methods are based on the simple but reasonable proposition that the shrinkage curvature is a direct function of the free shrinkage and steel percentage, and an inverse function of the section depth (Ref. 6.7). Branson suggests that for steel percentage $p - p' \leq 3$ percent (where $p = 100A_s/bd$ and $p' = 100A'_s/bd$),

$$\phi_{sh} = 0.7 \frac{\epsilon_{sh}}{h} (p - p')^{1/3} \left(\frac{p - p'}{p} \right)^{1/2} \quad (6.15a)$$

and for $p - p' > 3$ percent,

$$\phi_{sh} = \frac{\epsilon_{sh}}{h} \quad (6.15b)$$

With shrinkage curvature calculated by either method, the corresponding member deflection can be determined by any convenient means such as the moment-area or conjugate-beam method. If steel percentages and eccentricities are constant along the span, the deflection ϵ_{sh} resulting from the shrinkage curvature can be determined from

$$\Delta_{sh} = K_{sh} \phi_{sh} l^2 \quad (6.16)$$

where K_{sh} is a coefficient equal to 0.500 for cantilevers, 0.125 for simple spans, 0.065 for interior spans of continuous beams, and 0.090 for end spans of continuous beams (Ref. 6.7).

EXAMPLE 6.3

Shrinkage deflection. Calculate the midspan deflection of a simply supported beam of 20 ft span due to shrinkage of the concrete for which $\epsilon_{sh} = 780 \times 10^{-6}$. With reference to Fig. 6.11a, $b = 10$ in., $d = 17.5$ in., $h = 20$ in., $A_s = 3.00$ in 2 , and $A'_s = 0$. The elastic moduli are $E_c = 3.6 \times 10^6$ psi and $E_s = 29 \times 10^6$ psi.

SOLUTION. By the fictitious tensile force method,

$$T_{sh} = 3.00 \times 780 \times 10^{-6} \times 29 \times 10^6 = 67,900 \text{ lb}$$

and from Eq. (6.14) with $I_g = 6670$,

$$\phi_{sh} = \frac{2 \times 67,900 \times 7.5}{3.6 \times 10^6 \times 6670} = 42.4 \times 10^{-6}$$

while from Eq. (6.16) with $K_{sh} = 0.125$ for the simple span,

$$\Delta_{sh} = 0.125 \times 42.4 \times 10^{-6} \times 240^2 = 0.305 \text{ in.}$$

Alternatively, by Branson's approximate Eq. (6.15a) with $p = 100 \times 3/175 = 1.7$ percent and $p' = 0$,

$$\phi_{sh} = \frac{0.7 \times 780 \times 10^{-6}}{20} (1.7)^{1/3} = 32.5 \times 10^{-6}$$

compared with 42.4×10^{-6} obtained by the equivalent tensile force method. Considering the uncertainties such as the effects of cracking and creep, the approximate approach can usually be considered satisfactory.

Deflections will be produced as a result of differential temperatures varying from top to bottom of a member also. Such variation will result in a strain variation with member depth that may usually be assumed to be linear. For such cases, the deflection due to differential temperature can be calculated using Eq. (6.16) in which ϕ_{sh} is replaced by $\alpha \Delta T/h$, where the thermal coefficient α for concrete may be taken as 5.5×10^{-6} per °F and ΔT is the temperature differential in degrees Fahrenheit from one side to the other. The presence of the reinforcement has little influence on curvatures and deflections resulting from differential temperatures, because the thermal coefficient for the steel (6.5×10^{-6}) is very close to that for concrete.

6.9 MOMENT VS. CURVATURE FOR REINFORCED CONCRETE SECTIONS

Although it is not needed explicitly in ordinary design and is not a part of ACI Code procedures, the relation between moment applied to a given beam section and the resulting curvature, through the full range of loading to failure, is important in several contexts. It is basic to the study of member ductility, understanding the development of plastic hinges, and accounting for the redistribution of elastic moments that occurs in most reinforced concrete structures before collapse (see Section 12.9).

It will be recalled, with reference to Fig. 6.12, that curvature is defined as the angle change per unit length at any given location along the axis of a member subjected to bending loads:

$$\psi = \frac{1}{r} \quad (6.17)$$

where ψ = unit curvature and r = radius of curvature. With the stress-strain relationships for steel and concrete, represented in idealized form in Fig. 6.13a and b, respectively, and the usual assumptions regarding perfect bond and plane sections, it is possible to calculate the relation between moment and curvature for a typical underreinforced concrete beam section, subject to flexural cracking, as follows.

Figure 6.14a shows the transformed cross section of a rectangular, tensile-reinforced beam in the uncracked elastic stage of loading, with steel represented by the equivalent concrete area nA_s , i.e., with area $(n - 1)A_s$ added outside of the rectangular concrete section.[†] The neutral axis, a distance c_1 below the top surface of the beam, is easily found (see Section 3.3a). In the limiting case, the concrete stress at the tension face is just equal to the modulus of rupture f_r and the strain is $\epsilon_r = f_r/E_c$.

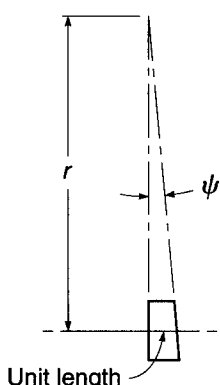


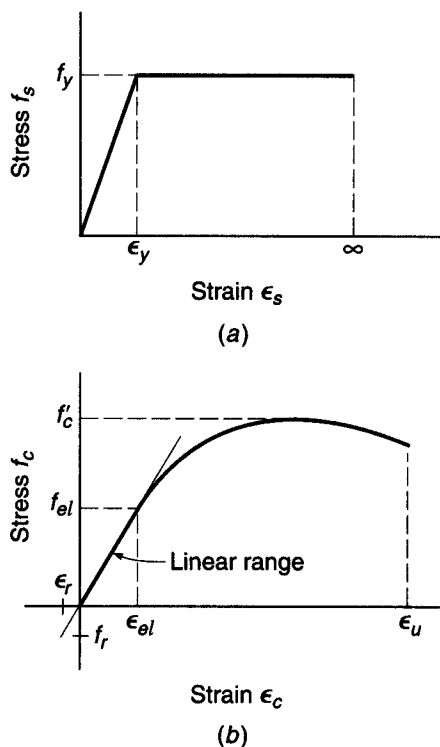
FIGURE 6.12

Unit curvature resulting from bending of beam section.

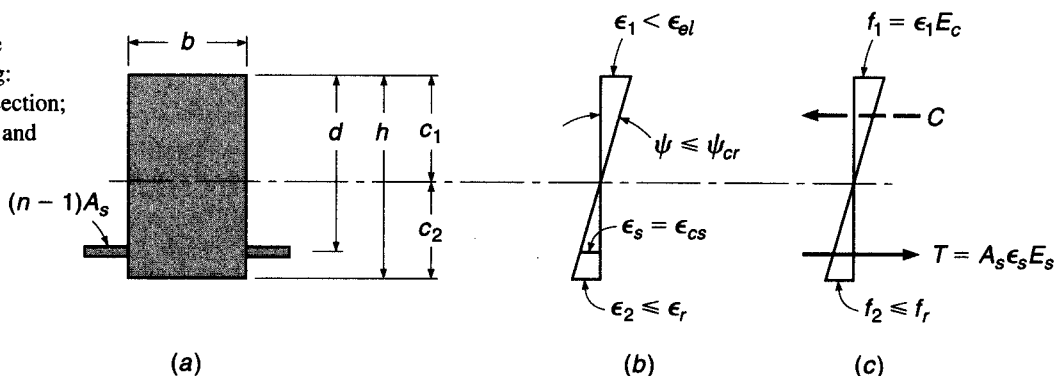
[†] Note that compression reinforcement, or multiple layers of tension reinforcement, can easily be included in the analysis with no essential complication.

FIGURE 6.13

Idealized stress-strain curves:
(a) steel; (b) concrete.

**FIGURE 6.14**

Uncracked beam in the elastic range of loading:
(a) transformed cross section;
(b) strains; (c) stresses and forces.



The steel is well below yield at this stage, which can be confirmed by computing, from the strain diagram, the steel strain $\epsilon_s = \epsilon_{cs}$, where ϵ_{cs} is the concrete strain at the level of the steel. It is easily confirmed, also, that the maximum concrete compressive stress will be well below the proportional limit. The curvature is seen, in Fig. 6.14b, to be

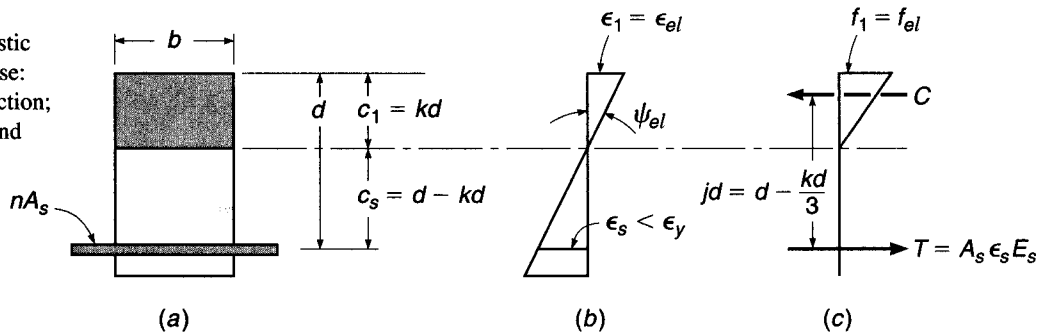
$$\psi_{cr} = \frac{\epsilon_1}{c_1} = \frac{\epsilon_r}{c_2} \quad (6.18)$$

and the corresponding moment is

$$M_{cr} = \frac{f_r I_{ut}}{c_2} \quad (6.19)$$

FIGURE 6.15

Cracked beam in the elastic range of material response:
 (a) transformed cross section;
 (b) strains; (c) stresses and forces.



where I_u is the moment of inertia of the uncracked transformed section. Equations (6.18) and (6.19) provide the information needed to plot point 1 of the moment-curvature graph of Fig. 6.17a.

When tensile cracking occurs at the section, the stiffness is immediately reduced, and curvature increases to point 2 in Fig. 6.17 with no increase in moment. The analysis now is based on the cracked transformed section of Fig. 6.15a, with steel represented by the transformed area nA_s , and tension concrete deleted. The cracked, elastic neutral axis distance $c_1 = kd$ is easily found by the usual methods (see Section 3.3b). In the limiting case, the concrete strain just reaches the proportional limit, as shown in Fig. 6.15b, and typically the steel is still below the yield strain. The curvature is easily computed by

$$\psi_{el} = \frac{\epsilon_1}{c_1} = \frac{\epsilon_{el}}{c_1} \quad (6.20)$$

and the corresponding moment is

$$M_{el} = \frac{1}{2} f_{el} k j b d^2 \quad (6.21)$$

as was derived in Section 3.3b. This provides point 3 in Fig. 6.17. The curvature at point 2 can now be found from the ratio M_{cr}/M_{el} .

Next, the cracked, inelastic stage of loading is shown in Fig. 6.16. Here the concrete is well into the inelastic range, although the steel has not yet yielded. The neutral axis depth c_1 is less than the elastic kd and is changing with increasing load as the shape of the concrete stress distribution changes and the steel stress changes.

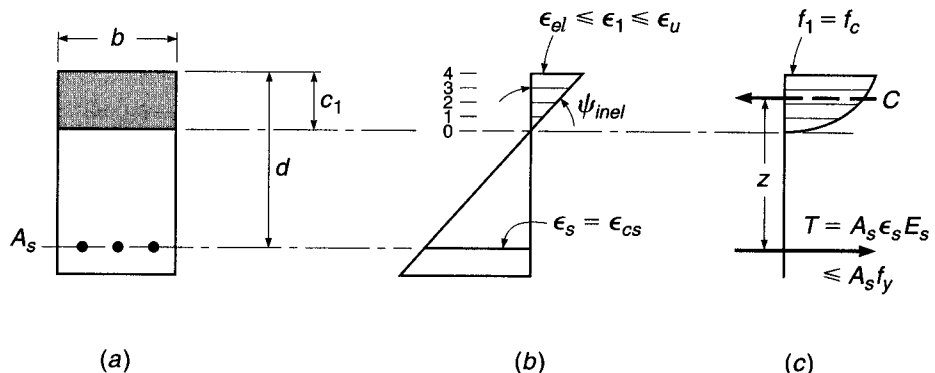
It is now convenient to adopt a numerical representation of the concrete compressive stress distribution, to find both the total concrete compressive force C and the location of its centroid, for any arbitrarily selected value of maximum concrete strain ϵ_1 in this range. The compressive strain diagram is divided into an arbitrary number of steps (e.g., four, in Fig. 6.16b), and the corresponding compressive stresses for each strain are read from the stress-strain curve of Fig. 6.13b. The stepwise representation of the actual continuous stress block is integrated numerically to find C , and its point of application is located, taking moments of the concrete forces about the top of the section. The basic equilibrium requirement $C = T$ then can be used to find the correct location of the neutral axis, for the particular compressive strain selected, following an iterative procedure.

The entire process can be summarized as follows:

1. Select any top face concrete strain ϵ_1 in the inelastic range, i.e., between ϵ_{el} and ϵ_u .
2. Assume the neutral axis depth, a distance c_1 below the top face.
3. From the strain diagram geometry, determine $\epsilon_s = \epsilon_{cs}$.

FIGURE 6.16

Cracked beam with concrete in the inelastic range of loading: (a) cross section; (b) strains; (c) stresses and forces.



4. Compute $f_s = \epsilon_s E_s \leq f_y$ and $T = A_s f_s$.
5. Determine C by integrating numerically under the concrete stress distribution curve.
6. Check to see if $C = T$. If not, the neutral axis must be adjusted upward or downward, for the particular concrete strain that was selected in step 1, until equilibrium is satisfied. This determines the correct value of c_1 .

Curvature can then be found from

$$\psi_{inel} = \frac{\epsilon_1}{c_1} \quad (6.22)$$

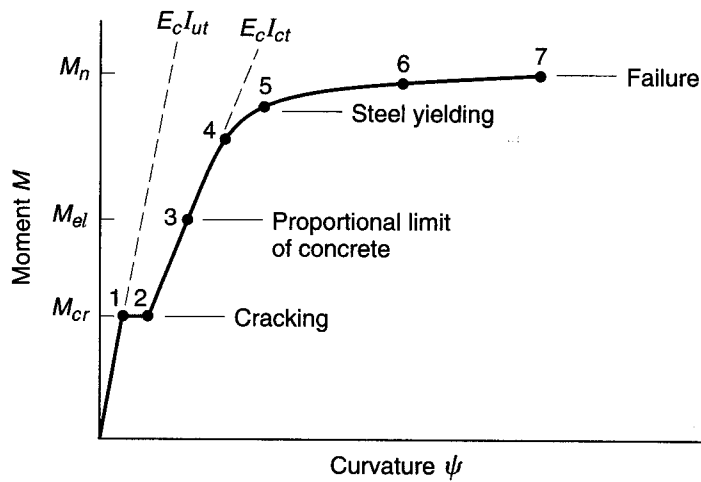
The internal lever arm z from the centroid of the concrete stress distribution to the tensile resultant, Fig. 6.16c, is calculated, after which

$$M_{inel} = Cz = Tz \quad (6.23)$$

The sequence of steps 1 through 6 is then repeated for newly selected values of concrete strain ϵ_1 . The end result will be a series of points, such as 4, 5, 6, and 7 in Fig. 6.17. The limit of the moment-curvature plot is reached when the concrete top face strain equals ϵ_u , corresponding to point 7. The steel would be well past the yield strain at this loading, and at the yield stress.

FIGURE 6.17

Moment-curvature relation for tensile-reinforced beam.



It is important to be aware of the difference between a moment-unit curvature plot, such as Fig. 6.17, and a moment-rotation diagram for the hinging region of a reinforced concrete beam. The hinging region normally includes a number of discrete cracks, but between those cracks, the uncracked concrete reduces the steel strain, leading to what is termed the *tension stiffening* effect. The result is that the total rotation at the hinge is much less than would be calculated by multiplying the curvature per unit length at the cracked section by the observed or assumed length of the hinging region. Furthermore, the sharp increase in unit curvature shown in Fig. 6.17 at cracking would not be seen on the moment-rotation plot, only a small, but progressive, reduction of the slope of the diagram.

REFERENCES

- 6.1. ACI Committee 224, "Control of Cracking in Concrete Structures (ACI 224R-01)," *ACI Manual of Concrete Practice*, Part 1, American Concrete Institute, Farmington Hills, MI, 2008.
- 6.2. P. Gergely and L. A. Lutz, "Maximum Crack Width in Reinforced Concrete Flexural Members," in *Causes, Mechanisms, and Control of Cracking in Concrete*, SP-20, American Concrete Institute, Detroit, MI, 1968, pp. 1-17.
- 6.3. P. H. Kaar and A. H. Mattock, "High-Strength Bars as Concrete Reinforcement—Part 4: Control of Cracking," *Journal*, PCA Research and Development Laboratories, vol. 5, no. 1, 1963, pp. 15-38.
- 6.4. R. J. Frosch, "Another Look at Cracking and Crack Control in Reinforced Concrete," *ACI Struct. J.*, vol. 96, no. 3, 1999, pp. 437-442.
- 6.5. B. B. Broms, "Crack Width and Crack Spacing in Reinforced Concrete Members," *J. ACI*, vol. 62, no. 10, 1965, pp. 1237-1256.
- 6.6. ACI Committee 318, "Discussion of Proposed Revisions to Building Code Requirements for Structural Concrete (ACI 318-95) and Commentary (ACI 318R-95)," *Concr. Int'l.*, vol. 21, no. 5, 1999, pp. 318-1-318-49.
- 6.7. D. E. Branson, *Deformation of Concrete Structures*, McGraw-Hill, New York, 1977.
- 6.8. ACI Committee 435, "Control of Deflection in Concrete Structures (ACI 435R-95)," *ACI Manual of Concrete Practice*, Part 5, American Concrete Institute, Farmington Hills, MI, 2003.
- 6.9. W. W. Yu and G. Winter, "Instantaneous and Long-Time Deflections of Reinforced Concrete Beams under Working Loads," *J. ACI*, vol. 57, no. 1, 1960, pp. 29-50.
- 6.10. ACI Committee 209, "Prediction of Creep, Shrinkage and Temperature Effects in Concrete Structures (ACI 209R-92)," *ACI Manual of Concrete Practice*, Part 1, 2003.
- 6.11. D. E. Branson, "Compression Steel Effect on Long-Time Deflections," *J. ACI*, vol. 68, no. 8, 1971, pp. 555-559.
- 6.12. ACI Committee 435, "Proposed Revisions by Committee 435 to ACI Building Code and Commentary Provisions on Deflections," *J. ACI*, vol. 75, no. 6, June 1978, pp. 229-238.
- 6.13. K. Paulson, A. H. Nilson, and K. C. Hover, "Long-Term Deflection of High-Strength Concrete Beams," *ACI Mater. J.*, vol. 88, no. 2, 1991, pp. 197-206.
- 6.14. *CRSI Handbook*, 10th ed., Concrete Reinforcing Steel Institute, Schaumburg, IL, 2008.

PROBLEMS

- 6.1. A rectangular beam of width $b = 15$ in., effective depth $d = 20.5$ in., and total depth $h = 23$ in. spans 18.5 ft between simple supports. It will carry a computed dead load of 1.08 kips/ft including self-weight, plus a service live load of 2.29 kips/ft. Reinforcement consists of four evenly spaced No. 7 (No. 22) bars in one row. The clear cover on the sides is 2 in. Material strengths are $f_y = 60,000$ psi and $f'_c = 4000$ psi.
 - (a) Compute the stress in the steel at full service load, and using the Gergely-Lutz equation, estimate the maximum crack width.
 - (b) Confirm the suitability of the proposed design based on Eq. (6.3).
- 6.2. To save steel-handling costs, an alternative design is proposed for the beam in Problem 6.1, using two No. 9 (No. 29) Grade 75 bars to provide approximately the same steel strength as the originally proposed four No. 7 (No. 22)

Grade 60 bars. Check to determine if the redesigned beam is satisfactory with respect to cracking according to the ACI Code. What modification could you suggest that would minimize the number of bars to reduce cost, yet satisfy requirements of crack control?

6.3. For the beam in Problem 6.1:

- (a) Calculate the increment of deflection resulting from the first application of the short-term live load.
- (b) Find the creep portion of the sustained load deflection plus the immediate deflection due to live load.
- (c) Compare your results with the limitations imposed by the ACI Code, as summarized in Table 6.2.

Assume that the beam is a part of a floor system and supports cinder block partitions susceptible to cracking if deflections are excessive.

6.4. A beam having $b = 12$ in., $d = 21.5$ in., and $h = 24$ in. is reinforced with three No. 11 (No. 36) bars. Material strengths are $f_y = 60,000$ psi and $f'_c = 4000$ psi.

It is used on a 28 ft simple span to carry a total service load of 2430 lb/ft. For this member, the sustained loads include self-weight of the beam plus additional superimposed dead load of 510 lb/ft, plus 400 lb/ft representing that part of the live load that acts more or less continuously, such as furniture, equipment, and time-average occupancy load. The remaining 1220 lb/ft live load consists of short-duration loads, such as the brief peak load in the corridors of an office building at the end of a workday.

- (a) Find the increment of deflection under sustained loads due to creep.
- (b) Find the additional deflection increment due to the intermittent part of the live load.

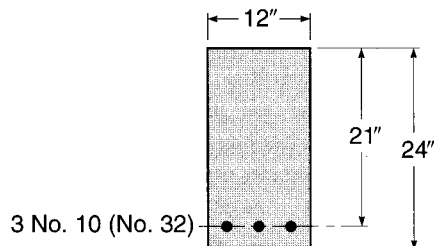
In your calculations, you may assume that the peak load is applied almost immediately after the building is placed in service, then reapplied intermittently. Compare with ACI Code limits from Table 6.2. Assume that, for this long-span floor beam, construction details are provided that will avoid damage to supported elements due to deflections. If ACI Code limitations are not met, what changes would you recommend to improve the design?

6.5. A reinforced concrete beam is continuous over two equal 22 ft spans, simply supported at the two exterior supports, and fully continuous at the interior support. Concrete cross-sectional dimensions are $b = 10$ in., $h = 22$ in., and $d = 19.5$ in. for both positive and negative bending regions. Positive reinforcement in each span consists of two No. 9 (No. 29) bars, and negative reinforcement at the interior support is made up of three No. 10 (No. 32) bars. No compression steel is used. Material strengths are $f_y = 60,000$ psi and $f'_c = 5000$ psi. The beam will carry a service live load, applied early in the life of the member, of 1800 lb/ft distributed uniformly over both spans; 20 percent of this load will be sustained more or less permanently, while the rest is intermittent. The total service dead load is 1000 lb/ft including self-weight.

- (a) Find the immediate deflection when shores are removed and the full dead load is applied.
- (b) Find the long-term deflection under sustained load.
- (c) Find the increment of deflection when the short-term part of the live load is applied.

Compare with ACI Code deflection limits; piping and brittle conduits are carried that would be damaged by large deflections. Note that midspan deflection may be used as a close approximation of maximum deflection.

- 6.6.** Recalculate the deflections of Problem 6.5 based on the assumption that 20 percent of the live load represents the normal service condition of loading and is sustained more or less continuously, while the remaining 80 percent is a short-term peak loading that would probably not be applied until most creep deflections have occurred. Compare with your earlier results.
- 6.7.** The tensile-reinforced rectangular beam shown in Fig. P6.7 is made using steel with $f_y = 60,000$ psi and $E_s = 29,000,000$ psi. A perfectly plastic response after yielding can be assumed. The concrete has a stress-strain curve in compression that may be approximated by the parabola $f_c = f'_c[2\epsilon_c/\epsilon_0 - (\epsilon_c/\epsilon_0)^2]$, where f_c and ϵ_c are the stress and strain in the concrete. The variable ϵ_0 is the strain at the peak stress = 0.002, and $f'_c = 4000$ psi. The ultimate strain in the concrete is 0.003. The concrete responds elastically in tension up to the modulus of rupture $f_r = 475$ psi. Based on this information, plot a curve relating applied moment to unit curvature at a section subjected to flexural cracking. Label points corresponding to first cracking, first yielding of steel, and peak moment.

FIGURE P6.7

7

Analysis and Design for Torsion

7.1 INTRODUCTION

Reinforced concrete members are commonly subjected to bending moments, to transverse shears associated with those bending moments, and, in the case of columns, to axial forces often combined with bending and shear. In addition, torsional forces may act, tending to twist a member about its longitudinal axis. Such torsional forces seldom act alone and are almost always concurrent with bending moment and transverse shear, and sometimes with axial force as well.

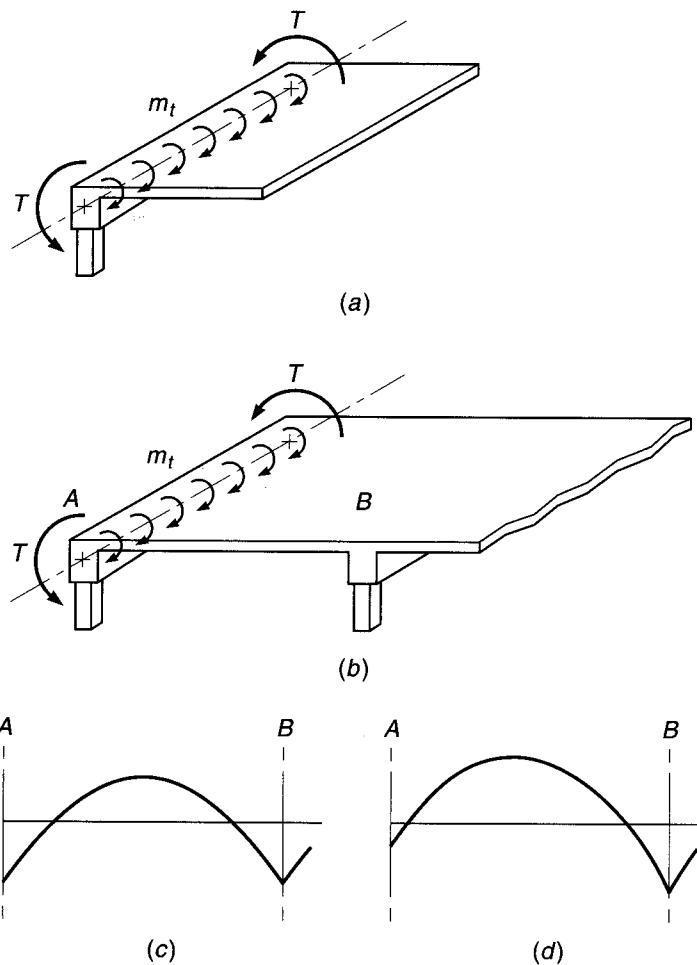
For many years, torsion was regarded as a secondary effect and was not considered explicitly in design, its influence being absorbed in the overall factor of safety of rather conservatively designed structures. Current methods of analysis and design, however, have resulted in less conservatism, leading to somewhat smaller members that, in many cases, must be reinforced to increase torsional strength. In addition, there is increasing use of structural members for which torsion is a central feature of behavior; examples include curved bridge girders, eccentrically loaded box beams, and helical stairway slabs. The design procedures in the ACI Code were first proposed in Switzerland (Refs. 7.1 and 7.2) and are also included in the European and Canadian model codes (Refs. 7.3 and 7.4).

It is useful in considering torsion to distinguish between primary and secondary torsion in reinforced concrete structures. *Primary torsion*, sometimes called *equilibrium torsion* or *statically determinate torsion*, exists when the external load has no alternative load path but must be supported by torsion. For such cases, the torsion required to maintain static equilibrium can be uniquely determined. An example is the cantilevered slab of Fig. 7.1a. Loads applied to the slab surface cause twisting moments m_t to act along the length of the supporting beam. These are equilibrated by the resisting torque T provided at the columns. Without the torsional moments, the structure will collapse.

In contrast to this condition, *secondary torsion*, also called *compatibility torsion* or *statically indeterminate torsion*, arises from the requirements of continuity, i.e., compatibility of deformation between adjacent parts of a structure. For this case, the torsional moments cannot be found based on static equilibrium alone. Disregard of continuity in the design will often lead to extensive cracking, but generally will not cause collapse. An internal readjustment of forces is usually possible and an alternative equilibrium of forces found. An example of secondary torsion is found in the spandrel or edge beam supporting a monolithic concrete slab, shown in Fig. 7.1b. If the spandrel beam is torsionally stiff and suitably reinforced, and if the columns can provide the necessary resisting torque T , then the slab moments will approximate those for a rigid exterior support as shown in Fig. 7.1c. However, if the beam has little torsional stiffness

FIGURE 7.1

Torsional effects in reinforced concrete:
 (a) primary or equilibrium torsion at a cantilevered slab;
 (b) secondary or compatibility torsion at an edge beam; (c) slab moments if edge beam is stiff torsionally; (d) slab moments if edge beam is flexible torsionally.



and inadequate torsional reinforcement, cracking will occur to further reduce its torsional stiffness, and the slab moments will approximate those for a hinged edge, as shown in Fig. 7.1d. If the slab is designed to resist the altered moment diagram, collapse will not occur (see discussion in Section 12.10).

Although current techniques for analysis permit the realistic evaluation of torsional moments for statically indeterminate conditions as well as determinate, designers often neglect secondary torsional effects when torsional stresses are low and alternative equilibrium states are possible. This is permitted according to the ACI Code and many other design specifications. On the other hand, when torsional strength is an essential feature of the design, such as for the bridge shown in Fig. 7.2, special analysis and special torsional reinforcement are required, as described in the remainder of this chapter.

7.2 TORSION IN PLAIN CONCRETE MEMBERS

Figure 7.3 shows a portion of a prismatic member subjected to equal and opposite torques T at the ends. If the material is elastic, St. Venant's torsion theory indicates that

FIGURE 7.2

Curved continuous beam bridge, Las Vegas, Nevada, designed for torsional effects.
(Courtesy of Portland Cement Association.)



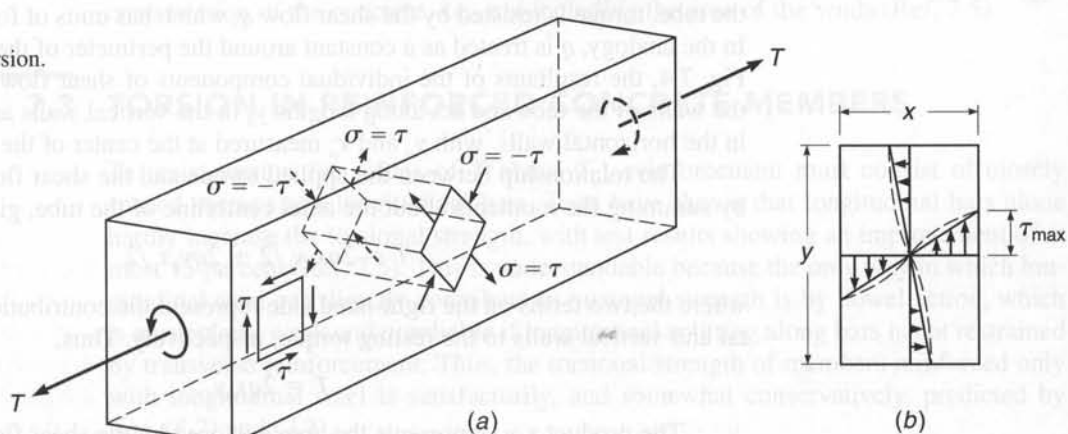
of modulus, which shows that the deflection of a beam occurs to a greater extent than the deflection of a beam with a constant cross section. Thus, the concept will be considered. Consider that a beam is conservatively represented by a beam of constant cross section, which has a deflection of $\delta = \frac{M}{E} = \frac{4V}{G}$.

It is also assumed that the beam is subjected to a uniformly distributed load, which causes the beam to deflect downwards.

Assume that the beam is subjected to a uniformly distributed load, which causes the beam to deflect downwards. The deflection of the beam is given by the shear flow path, which is the geometric center of the beam's cross section. For solid members, the deflection is given by one-fourth of the maximum width-to-depth ratio of 0.5.

FIGURE 7.3

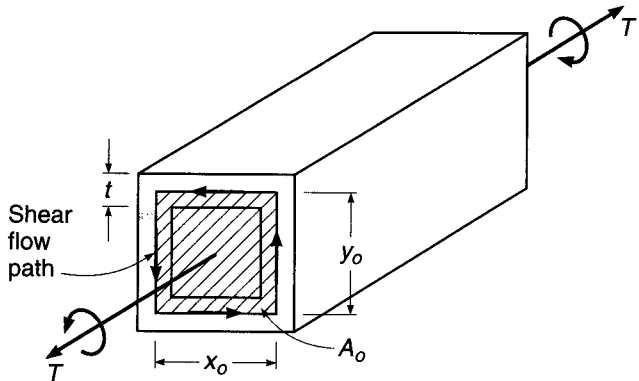
Stresses caused by torsion.



Torsional shear stresses are distributed over the cross section, as shown in Fig. 7.3b. The largest shear stresses occur at the middle of the wide faces. If the material deforms inelastically, as expected for concrete, the stress distribution is closer to that shown by the dashed line.

FIGURE 7.4

Thin-walled tube under torsion.



Shear stresses in pairs act on an element at or near the wide surface, as shown in Fig. 7.3a. As explained in strength of materials texts, this state of stress corresponds to equal tension and compression stresses on the faces of an element at 45° to the direction of shear. These inclined tension stresses are of the same kind as those caused by transverse shear, discussed in Section 4.2. However, in the case of torsion, since the torsional shear stresses are of opposite sign on opposing sides of the member (Fig. 7.3b), the corresponding diagonal tension stresses are at right angles to each other (Fig. 7.3a).

When the diagonal tension stresses exceed the tensile resistance of the concrete, a crack forms at some accidentally weaker location and spreads immediately across the beam. The value of torque corresponding to the formation of this diagonal crack is known as the *cracking torque* T_{cr} .

There are several ways of analyzing members subjected to torsion. The nonlinear stress distribution shown by the dotted lines in Fig. 7.3b lends itself to the use of the *thin-walled tube, space truss analogy*. Using this analogy, the shear stresses are treated as constant over a finite thickness t around the periphery of the member, allowing the beam to be represented by an equivalent tube, as shown in Fig. 7.4. Within the walls of the tube, torque is resisted by the shear flow q , which has units of force per unit length. In the analogy, q is treated as a constant around the perimeter of the tube. As shown in Fig. 7.4, the resultants of the individual components of shear flow are located within the walls of the tube and act along lengths y_o in the vertical walls and along lengths x_o in the horizontal walls, with y_o and x_o measured at the center of the walls.

The relationship between the applied torque and the shear flow can be obtained by summing the moments about the axial centerline of the tube, giving

$$T = 2qx_oy_o/2 + 2qy_ox_o/2 \quad (a)$$

where the two terms on the right-hand side represent the contributions of the horizontal and vertical walls to the resting torque, respectively. Thus,

$$T = 2qx_oy_o \quad (b)$$

The product x_oy_o represents the area enclosed by the shear flow path A_o , giving

$$T = 2qA_o \quad (c)$$

and

$$q = \frac{T}{2A_o} \quad (d)$$

Note that although A_o is an area, it derives from the moment calculation shown in Eq. (a) above. Thus, A_o is applicable for hollow box sections, as well as solid sections, and in such case includes the area of the central void.

For a tube wall thickness t , the unit shear stress acting within the walls of the tube is

$$\tau = \frac{q}{t} = \frac{T}{2A_o t} \quad (7.1)$$

As shown in Fig. 7.3a, the principal tensile stress $\sigma = \tau$. Thus, the concrete will crack only when $\tau = \sigma = f'_t$, the tensile strength of concrete. Considering that concrete is under biaxial tension and compression, f'_t can be conservatively represented by $4\sqrt{f'_c}$ rather than the value typically used for the modulus of rupture of concrete, which is taken as $f_r = 7.5\sqrt{f'_c}$ for normal-density concrete. Substituting $\tau = \tau_{cr} = 4\sqrt{f'_c}$ in Eq. (7.1) and solving for T give the value of the cracking torque:

$$T_{cr} = 4\sqrt{f'_c}(2A_o t) \quad (7.2)$$

Remembering that A_o represents the area enclosed by the shear flow path, A_o must be some fraction of the area enclosed by the outside perimeter of the full concrete cross section A_{cp} . The value of t can, in general, be approximated as a fraction of the ratio A_{cp}/p_{cp} , where p_{cp} is the perimeter of the cross section. For solid members with rectangular cross sections, t is typically one-sixth to one-fourth of the minimum width. Using a value of one-fourth for a member with a width-to-depth ratio of 0.5 yields a value of A_o approximately equal to $\frac{2}{3}A_{cp}$. For the same member, $t = \frac{3}{4}A_{cp}/p_{cp}$. Using these values for A_o and t in Eq. (7.2) gives

$$T_{cr} = 4\sqrt{f'_c} \frac{A_{cp}^2}{p_{cp}} \quad \text{in-lb} \quad (7.3)$$

It has been found that Eq. (7.3) gives a reasonable estimate of the cracking torque of solid reinforced concrete members regardless of the cross-sectional shape. For hollow sections, T_{cr} in Eq. (7.3) should be reduced by the ratio A_g/A_{cp} , where A_g is the gross cross section of the concrete, i.e., not including the area of the voids (Ref. 7.5).

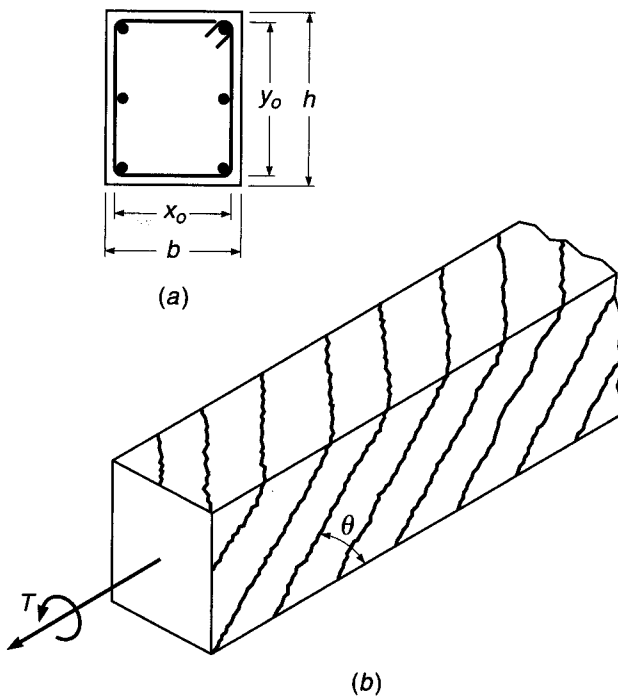
7.3 TORSION IN REINFORCED CONCRETE MEMBERS

To resist torsion for values of T above T_{cr} , reinforcement must consist of closely spaced stirrups and longitudinal bars. Tests have shown that longitudinal bars alone hardly increase the torsional strength, with test results showing an improvement of at most 15 percent (Ref. 7.5). This is understandable because the only way in which longitudinal steel can directly contribute to torsional strength is by dowel action, which is particularly weak and unreliable if longitudinal splitting along bars is not restrained by transverse reinforcement. Thus, the torsional strength of members reinforced only with longitudinal steel is satisfactorily, and somewhat conservatively, predicted by Eqs. (7.2) and (7.3).

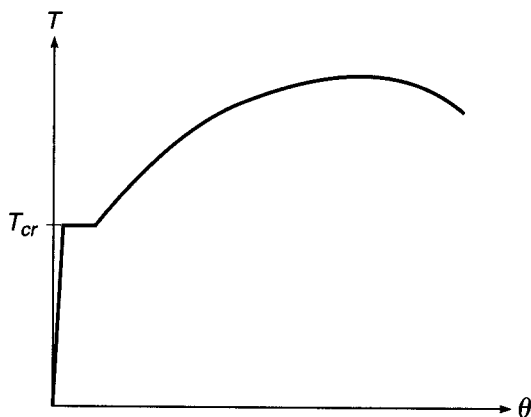
When members are adequately reinforced, as in Fig. 7.5a, the concrete cracks at a torque that is equal to or only somewhat larger than in an unreinforced member, as given by Eq. (7.3). The cracks form a spiral pattern, as shown in Fig. 7.5b. Upon cracking, the torsional resistance of the concrete drops to about one-half of that of the uncracked member, the remainder being now resisted by reinforcement. This redistribution of internal resistance is reflected in the torque-twist curve (Fig. 7.6), which at

FIGURE 7.5

Reinforced concrete beam in torsion: (a) torsional reinforcement; (b) torsional cracks.

**FIGURE 7.6**

Torque-twist curve in reinforced concrete member.



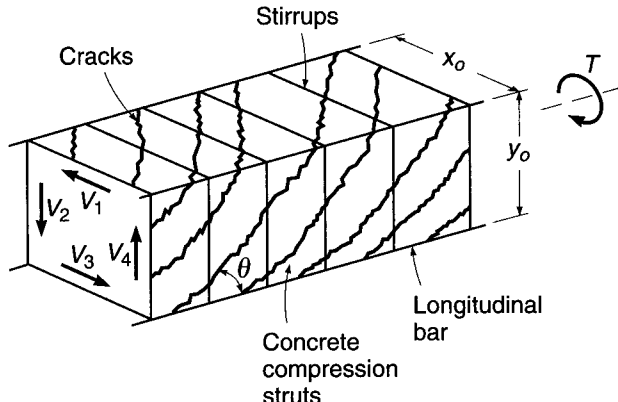
the cracking torque shows continued twist at constant torque until the internal forces have been redistributed from the concrete to the steel. As the section approaches the ultimate load, the concrete outside the reinforcing cage cracks and begins to spall off, contributing progressively less to the torsional capacity of the member.

Tests show that, after cracking, the area enclosed by the shear path is defined by the dimensions x_o and y_o measured to the centerline of the outermost closed transverse reinforcement, rather than to the center of the tube walls as before. These dimensions define the gross area $A_{oh} = x_o y_o$ and the shear perimeter $p_h = 2(x_o + y_o)$ measured at the steel centerline.

Analysis of the torsional resistance of the member is aided by treating the member as a space truss consisting of spiral *concrete diagonals* that are able to take load parallel but not perpendicular to the torsional cracks, transverse *tension tie members*

FIGURE 7.7

Space truss analogy.



that are provided by closed stirrups or ties, and *tension chords* that are provided by longitudinal reinforcement. The hollow-tube, space truss analogy represents a simplification of actual behavior, since, as will be demonstrated, the calculated torsional strength is controlled by the strength of the transverse reinforcement, independent of concrete strength. Such a simplification will be used here because it aids understanding, although it greatly underestimates torsional capacity and does not reflect the higher torsional capacities obtained with higher concrete strengths (Refs. 7.6 and 7.7).

With reference to Fig. 7.7, the torsional resistance provided by a member with a rectangular cross section can be represented as the sum of the contributions of the shears in each of the four walls of the equivalent hollow tube. The contribution of the shear acting in the right-hand vertical wall of the tube to the torsional resistance, for example, is

$$T_4 = \frac{V_4 x_o}{2} \quad (a)$$

Following a procedure similar to that used for analyzing the variable-angle truss shear model discussed in Section 4.8 and shown in Figs. 4.19 and 4.20, the equilibrium of a section of the vertical wall—with one edge parallel to a torsional crack with angle θ —can be evaluated using Fig. 7.8a. Assuming that the stirrups crossing the crack are yielding, the shear in the wall under consideration is

$$V_4 = A_t f_{yt} n \quad (b)$$

where A_t = area of one leg of a closed stirrup

f_{yt} = yield strength of transverse reinforcement

n = number of stirrups intercepted by torsional crack

Since the horizontal projection of the crack is $y_o \cot \theta$ and $n = y_o \cot \theta / s$ where θ is the slope angle of the strut and s is the spacing of the stirrups,

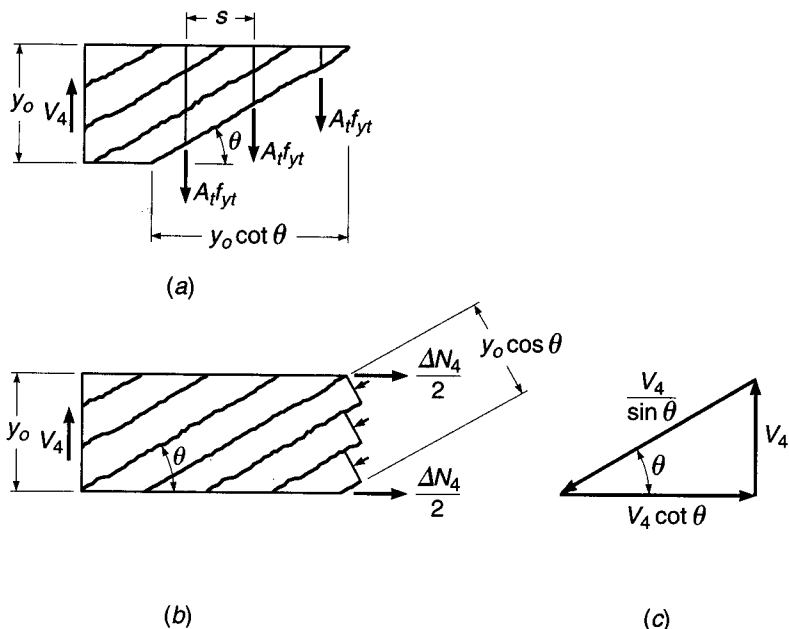
$$V_4 = \frac{A_t f_{yt} y_o}{s} \cot \theta \quad (c)$$

Combining Eqs. (c) and (a) gives

$$T_4 = \frac{A_t f_{yt} y_o x_o}{2s} \cot \theta \quad (d)$$

FIGURE 7.8

Basis for torsional design:
 (a) vertical tension in stirrups; (b) diagonal compression in vertical wall of beam; (c) equilibrium diagram of forces due to shear in vertical wall.



It is easily shown that an identical expression is obtained for each horizontal and vertical wall. Thus, summing over all four sides, the nominal capacity of the section is

$$T_n = \sum_{i=1}^4 T_i = \frac{2A_t f_{yt} y_o x_o}{s} \cot \theta \quad (e)$$

Noting that $y_o x_o = A_{oh}$ and rearranging slightly give

$$T_n = \frac{2A_{oh} A_t f_{yt}}{s} \cot \theta \quad (7.4)$$

The diagonal compression struts that form parallel to the torsional cracks are necessary for the equilibrium of the cross section. As shown in Fig. 7.8b and c, the horizontal component of compression in the struts in the vertical wall must be equilibrated by an axial tensile force ΔN_4 . Based on the assumed uniform distribution of shear flow around the perimeter of the member, the diagonal stresses in the struts must be uniformly distributed, resulting in a line of action of the resultant axial force that coincides with the midheight of the wall. Referring to Fig. 7.8c, the total contribution of the right-hand vertical wall to the change in axial force of the member due to the presence of torsion is

$$\Delta N_4 = V_4 \cot \theta = \frac{A_t f_{yt} y_o}{s} \cot^2 \theta$$

Again, summing over all four sides, the total increase in axial force for the member is

$$\Delta N = \sum_{i=1}^4 \Delta N_i = \frac{A_t f_{yt}}{s} 2(x_o + y_o) \cot^2 \theta \quad (7.5a)$$

$$\Delta N = \frac{A_t f_{yt} p_h}{s} \cot^2 \theta \quad (7.5b)$$

where p_h is the perimeter of the centerline of the closed stirrups.

Longitudinal reinforcement must be provided to carry the added axial force ΔN . If that steel is designed to yield, then

$$A_l f_y = \frac{A_t f_{yt} p_h}{s} \cot^2 \theta \quad (7.6)$$

and

$$A_l = \frac{A_t}{s} p_h \frac{f_{yt}}{f_y} \cot^2 \theta \quad (7.7)$$

where A_l = total area of longitudinal reinforcement to resist torsion, in²
 f_y = yield strength of longitudinal torsional reinforcement, psi

It has been found experimentally that, after cracking, the effective area enclosed by the shear flow path is somewhat less than the value of A_{oh} used in the previous development. It is recommended in Ref. 7.7 that the reduced value be taken as $A_o = 0.85A_{oh}$, where, it will be recalled, A_{oh} is the area enclosed by the centerline of the transverse reinforcement. This recommendation is incorporated in the ACI Code (see Section 7.5) and in a modified form of Eq. (7.4) with A_o substituted for A_{oh} . It has further been found experimentally that the thickness of the equivalent tube at loads near ultimate is closely approximated by $t = A_{oh}/p_h$, where p_h is the perimeter of A_{oh} .

7.4 TORSION PLUS SHEAR

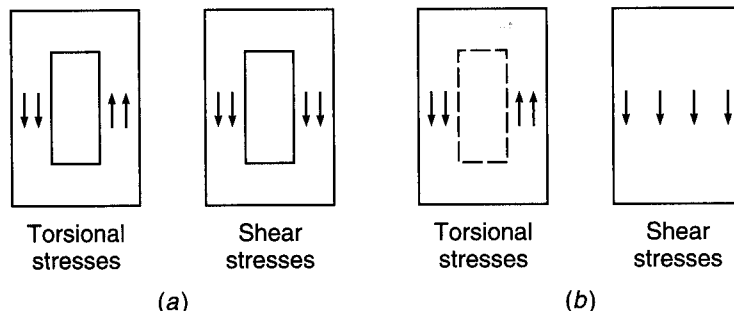
Members are rarely subjected to torsion alone. The prevalent situation is that of a beam subject to the usual flexural moments and shear forces, which, in addition, must resist torsional moments. In an uncracked member, shear forces as well as torque produce shear stresses. In a cracked member, both shear and torsion increase the forces in the diagonal struts (Figs. 4.20d and 7.8b), they increase the width of diagonal cracks, and they increase the forces required in the transverse reinforcement (Figs. 4.20e and 7.8a).

Using the usual representation for reinforced concrete, the nominal shear stress caused by an applied shear force V is $\tau_v = V/b_w d$. The shear stress caused by torsion, given in Eq. (7.1), is $\tau_t = T/(2A_o t)$. As shown in Fig. 7.9a for hollow sections, these stresses are directly additive on one side of the member. Thus, for a cracked concrete cross section with $A_o = 0.85A_{oh}$ and $t = A_{oh}/p_h$, the maximum shear stress can be expressed as

$$\tau = \tau_v + \tau_t = \frac{V}{b_w d} + \frac{T p_h}{1.7 A_{oh}^2} \quad (7.8)$$

FIGURE 7.9

Addition of torsional and shear stresses: (a) hollow section; (b) solid section.
(Adapted from Ref. 7.7.)



For a member with a *solid section*, Fig. 7.9b, τ_t is predominately distributed around the perimeter, as represented by the hollow tube analogy, but the full cross section contributes to carrying τ_v . Comparisons with experimental results show that Eq. (7.8) is somewhat overconservative for solid sections and that a better representation for maximum shear stress is provided by the square root of the sum of the squares of the nominal shear stresses:

$$\tau = \sqrt{\left(\frac{V}{b_w d}\right)^2 + \left(\frac{T p_h}{1.7 A_{oh}^2}\right)^2} \quad (7.9)$$

Equations (7.8) and (7.9) serve as a measure of the shear stresses in the concrete under both service and ultimate loading.

7.5 ACI CODE PROVISIONS FOR TORSION DESIGN

The basic principles upon which ACI Code design provisions are based have been presented in the preceding sections. ACI Code 11.5.3.5 safety provisions require that

$$T_u \leq \phi T_n \quad (7.10)$$

where T_u = required torsional strength at factored loads

T_n = nominal torsional strength of member

The strength reduction factor $\phi = 0.75$ applies for torsion. Strength T_n is based on Eq. (7.4) with A_o substituted for A_{oh} , thus

$$T_n = \frac{2A_o A_i f_y t}{s} \cot \theta \quad (7.11)$$

In accordance with ACI Code 11.5.2, sections located less than a distance d from the face of a support may be designed for the same torsional moment T_u as that computed at a distance d , recognizing the beneficial effects of support compression. However, if a concentrated torque is applied within this distance, the critical section must be taken at the face of the support. These provisions parallel those used in shear design. For beams supporting slabs such as are shown in Fig. 7.1, the torsional loading from the slab may be treated as being uniformly distributed along the beam.

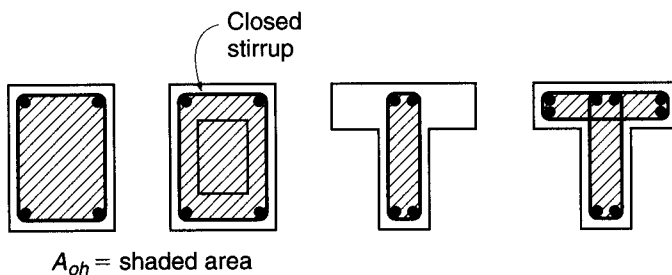
a. T Beams and Box Sections

For T beams, a portion of the overhanging flange contributes to the cracking torsional capacity and, if reinforced with closed stirrups, to the torsional strength. According to ACI Code 11.5.1, the contributing width of the overhanging flange on either side of the web is equal to the smaller of (1) the projection of the beam above or below the slab, whichever is greater, and (2) 4 times the slab thickness. These criteria are the same as those used for two-way slabs with beams, illustrated in Fig. 13.10. As with solid sections, A_{cp} for box sections, with or without flanges, represents the area enclosed by the outside perimeter of the concrete section.

After torsional cracking, the applied torque is resisted by the portion of the section represented by A_{oh} , the area enclosed by the centerline of the outermost closed transverse torsional reinforcement. For rectangular, box, and T sections A_{oh} is illustrated in Fig. 7.10. For sections with flanges, the Code does not require that the section used to establish A_{cp} coincide with that used to establish A_{oh} .

FIGURE 7.10

Definition of A_{oh} . (Adapted from Ref. 7.7.)



b. Minimal Torsion

If the factored torsional moment T_u does not exceed $\phi\lambda\sqrt{f'_c}(A_{cp}^2/p_{cp})$, torsional effects may be neglected, according to ACI Code 11.5.1. This lower limit is 25 percent of the cracking torque, given by Eq. (7.3), reduced by the factor ϕ , as usual, for design purposes. The presence of torsional moment at or below this limit will have a negligible effect on the flexural and shear strength of the member. The value of λ is as specified in ACI Code 8.6.1 and previously described in Section 4.5a, with $\lambda = 0.85, 0.75$, and 1.0 for sand-lightweight, all-lightweight, and normalweight concrete, respectively. Linear interpolation between values is permitted for concretes containing blends of lightweight and normalweight aggregates, and λ may be taken as $f_{ct}/(6.7\sqrt{f'_c})$ if the average split-cylinder strength of lightweight concrete is specified.

For members subjected to an axial load N_u (positive in compression), torsional effects may be neglected when T_u does not exceed $\phi\lambda\sqrt{f'_c}(A_{cp}^2/p_{cp}) \times \sqrt{1 + N_u/(4A_g\lambda\sqrt{f'_c})}$. For hollow sections (with or without axial load), A_{cp} must be replaced by the gross area of the concrete A_g to determine if torsional effects may be neglected. This has the effect of multiplying 25 percent of the cracking torque by the ratio A_g/A_{cp} twice—once to account for the reduction in cracking torque for hollow sections from the value shown in Eq. (7.3) and a second time to account for the transition from the circular interaction of combined shear and torsion stresses in Eq. (7.9) to the linear interaction represented by Eq. (7.8).

c. Equilibrium vs. Compatibility Torsion

A distinction is made in the ACI Code between equilibrium (primary) torsion and compatibility (secondary) torsion. For the first condition, described earlier with reference to Fig. 7.1a, the supporting member *must* be designed to provide the torsional resistance required by static equilibrium. For secondary torsion resulting from compatibility requirements, shown in Fig. 7.1b, it is assumed that cracking will result in a redistribution of internal forces; and according to ACI Code 11.5.2, the maximum torsional moment T_u may be reduced to $4\phi\lambda\sqrt{f'_c}(A_{cp}^2/p_{cp})$ or $4\phi\lambda\sqrt{f'_c}(A_{cp}^2/p_{cp})\sqrt{1 + N_u/(4A_g\lambda\sqrt{f'_c})}$ for members subjected to axial load. In the case of hollow sections, A_{cp} is *not* replaced by A_g . The design moments and shears in the supported member must be adjusted accordingly. The reduced value of T_u permitted by the ACI Code is intended to approximate the torsional cracking strength of the supporting beam, for combined torsional and flexural loading. The large rotations that occur at essentially constant torsional load would result in significant redistribution of internal forces, justifying use of the reduced value for design of the torsional member and the supported elements.

d. Limitations on Shear Stress

Based largely on empirical observations, the width of diagonal cracks caused by combined shear and torsion under *service loads* can be limited by limiting the calculated shear stress under *factored shear and torsion* (Ref. 7.4) so that

$$\nu_{\max} \leq \phi \left(\frac{V_c}{b_w d} + 8\sqrt{f'_c} \right) \quad (7.12)$$

where ν_{\max} in Eq. (7.12) corresponds to the upper limits on shear capacity described in Section 4.5d. Combining Eq. (7.12) with Eq. (7.8) provides limits on the cross-sectional dimensions of *hollow sections*, in accordance with ACI Code 11.5.3.

$$\frac{V_u}{b_w d} + \frac{T_u p_h}{1.7 A_{oh}^2} \leq \phi \left(\frac{V_c}{b_w d} + 8\sqrt{f'_c} \right) \quad (7.13)$$

Likewise, for *solid sections*, combining Eq. (7.12) with Eq. (7.9) gives

$$\sqrt{\left(\frac{V_u}{b_w d} \right)^2 + \left(\frac{T_u p_h}{1.7 A_{oh}^2} \right)^2} \leq \phi \left(\frac{V_c}{b_w d} + 8\sqrt{f'_c} \right) \quad (7.14)$$

Either member dimensions or concrete strength must be increased if the criteria in Eq. (7.13) or (7.14) are not satisfied.

ACI Code 11.5.3 requires that if the wall thickness varies around the perimeter of a hollow section, Eq. (7.13) be evaluated at the location where the left-hand side of the expression is a maximum. If the wall thickness is less than the assumed value of t used in the development of Eq. (7.8) A_{oh}/p_h , the actual value of t must be used in the calculation of torsional shear stress. As a result, the second term on the left-hand side of Eq. (7.13) must be taken as

$$\frac{T_u}{1.7 A_{oh} t}$$

where t is the thickness of the wall of the hollow section at the location where the stresses are being checked.

e. Reinforcement for Torsion

The nominal torsional strength is given by Eq. (7.11).

$$T_n = \frac{2A_o A_t f_{yt}}{s} \cot \theta \quad (7.11)$$

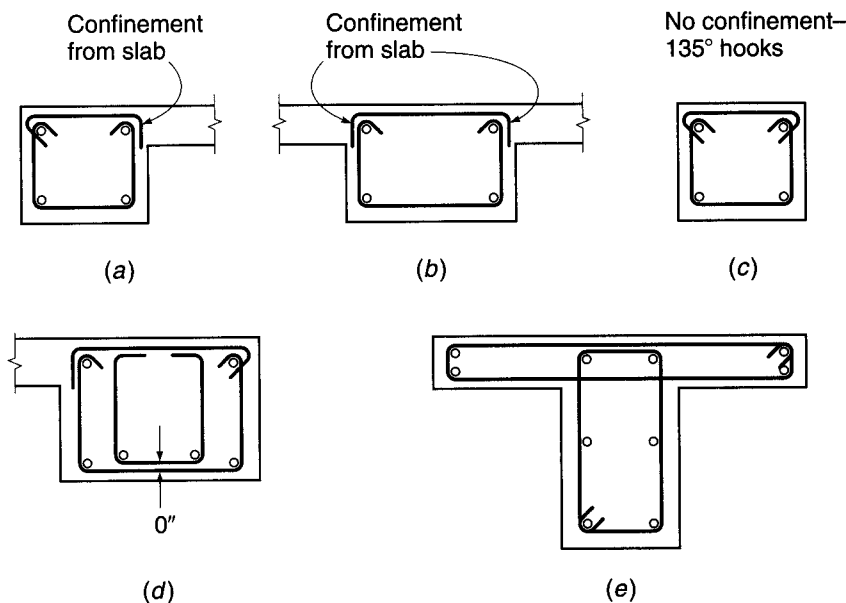
According to ACI Code 11.5.3, the angle θ may assume any value between 30 and 60°, with a value of $\theta = 45^\circ$ suggested. The area enclosed by the shear flow A_o may be determined by analysis using procedures such as suggested in Ref. 7.8, or A_o may be taken as equal to $0.85A_{oh}$. Combining Eq. (7.11) with Eq. (7.10), the required cross-sectional area of one stirrup leg for torsion is

$$A_t = \frac{T_n s}{2\phi A_o f_{yt} \cot \theta} \quad (7.15)$$

The Code limits f_{yt} to a maximum of 60,000 psi for reasons of crack control.

FIGURE 7.11

Stirrup-ties and longitudinal reinforcement for torsion:
 (a) spandrel beam with flanges on one side;
 (b) interior beam; (c) isolated rectangular beam; (d) wide spandrel beam; (e) T beam with torsional reinforcement in flanges.



The reinforcement provided for torsion must be combined with that required for shear. Based on the typical two-leg stirrup, this may be expressed as

$$\frac{A_{v+t}}{s} = \frac{A_v}{s} + 2 \frac{A_t}{s} \quad (7.16)$$

As described in Section 7.3, the transverse stirrups used for torsional reinforcement must be of a closed form to provide the required tensile capacity across the diagonal cracks of all faces of the beam. U-shaped stirrups commonly used for transverse shear reinforcement are not suitable for torsional reinforcement. On the other hand, one-piece closed stirrups make field assembly of beam reinforcement difficult, and for practical reasons torsional stirrups are generally two-piece stirrup-ties, as shown in Fig. 7.11. A U-shaped stirrup is combined with a horizontal top bar, suitably anchored.

Because concrete outside the reinforcing cage tends to spall off when the member is subjected to high torque, transverse torsional reinforcement must be anchored within the concrete core (Ref. 7.9). ACI Code 11.5.4 requires that stirrups or ties used for transverse longitudinal reinforcement be anchored with a 135° standard hook or a seismic hook (described in section 20.4) around a longitudinal bar, unless the concrete surrounding the anchorage is restrained against spalling by a flange or a slab, in which case 90° standard hooks may be used, as shown in Fig. 7.11a, b, and d. Overlapping U-shaped stirrups, such as shown in Fig. 5.12d, may not be used. If flanges are included in the computation of torsional strength for T or L-shaped beams, closed torsional stirrups must be provided in the flanges, as shown in Fig. 7.11e.

The required spacing of closed stirrups, satisfying Eq. (7.16), is selected for the trial design based on standard bar sizes.

To control spiral cracking, the maximum spacing of torsional stirrups should not exceed $p_h/8$ or 12 in., whichever is smaller. In addition, for members requiring both shear and torsion reinforcement, the minimum area of closed stirrups is equal to

$$A_v + 2A_t = 0.75 \sqrt{f'_c} \frac{b_w s}{f_{yt}} \geq 50 \frac{b_w s}{f_{yt}} \quad (7.17)$$

according to ACI Code 11.5.5.

The area of longitudinal bar reinforcement A_t required to resist torsion is given by Eq. (7.7), where θ must have the same value used to calculate A_r . The term A_t/s in Eq. (7.7) should be taken as the value calculated using Eq. (7.15), not modified based on minimum transverse steel requirements. ACI Code 11.5.3 permits the portion of A_t in the flexural compression zone to be reduced by an amount equal to $M_u/(0.9df_y)$, where M_u is the factored moment acting at the section in combination with T_u .

Based on an evaluation of the performance of reinforced concrete beam torsional test specimens, ACI Code 11.5.5 requires that A_t not be less than

$$A_{t,\min} = \frac{5\sqrt{f'_c} A_{cp}}{f_y} - \left(\frac{A_t}{s} \right) p_h \frac{f_{yt}}{f_y} \quad (7.18)$$

where $A_t/s \geq 25b_w/f_{yt}$, with f_{yt} in psi.

The spacing of the longitudinal bars should not exceed 12 in., and they should be distributed around the perimeter of the cross section to control cracking. The bars may not be less than No. 3 (No. 10) in size or have a diameter less than 0.042 times the spacing of the transverse stirrups. At least one longitudinal bar must be placed at each corner of the stirrups. Careful attention must be paid to the anchorage of longitudinal torsional reinforcement so that it is able to develop its yield strength at the face of the supporting columns, where torsional moments are often maximum.

Reinforcement required for torsion may be combined with that required for other forces, provided that the area furnished is the sum of the individually required areas and that the most restrictive requirements of spacing and placement are met. According to ACI Code 11.5.6, torsional reinforcement must be provided at least a distance $b_t + d$ beyond the point theoretically required, where b_t is the width of that part of the cross section containing the closed stirrups resisting torsion. According to the provisions of the ACI Code, the point at which the torsional reinforcement is no longer required is the point at which $T_u < \phi\lambda\sqrt{f'_c}(A_{cp}^2/p_{cp})$, or $T_u < \phi\lambda\sqrt{f'_c}(A_{cp}^2/p_{cp})\sqrt{1 + N_u/(4A_g\lambda\sqrt{f'_c})}$ for members subjected to axial load. The value is 25 percent of the cracking torque, reduced by the factor ϕ , as given in Section 7.5b.

The subject of torsional design of prestressed concrete is not treated here, but as presented in ACI Code 11.5, it differs only in certain details from the above presentation for nonprestressed reinforced concrete beams.

f. Design for Torsion

Designing a reinforced concrete flexural member for torsion involves a series of steps. The following sequence ensures that each is covered:

1. Determine if the factored torque is less than $\phi\lambda\sqrt{f'_c}(A_{cp}^2/p_{cp})$, or $\phi\lambda\sqrt{f'_c}(A_{cp}^2/p_{cp})\sqrt{1 + N_u/(4A_g\lambda\sqrt{f'_c})}$ for members subjected to axial load. If so, torsion may be neglected. If not, proceed with the design. Note that in this step, portions of overhanging flanges, as defined in Section 7.5a, must be included in the calculation of A_{cp} and p_{cp} .
2. If the torsion is compatibility torsion, rather than equilibrium torsion, as described in Sections 7.1 and 7.5c, the maximum factored torque may be reduced to $4\phi\lambda\sqrt{f'_c}(A_{cp}^2/p_{cp})$, or $4\phi\lambda\sqrt{f'_c}(A_{cp}^2/p_{cp})\sqrt{1 + N_u/(4A_g\lambda\sqrt{f'_c})}$ for members subjected to axial load, with the moments and shears in the supported members adjusted accordingly. Equilibrium torsion cannot be adjusted.
3. Check the shear stresses in the section under combined torsion and shear, using the criteria of Section 7.5d.
4. Calculate the required transverse reinforcement for torsion using Eq. (7.15) and shear using Eq. (4.14a). Combine A_t and A_v using Eq. (7.16).

5. Check that the minimum transverse reinforcement requirements are met for both torsion and shear. These include the maximum spacing, as described in Sections 7.5e and 4.5d, and minimum area, as given in Eq. (7.17).
6. Calculate the required longitudinal torsional reinforcement A_t , using the larger of the values given in Eqs. (7.7) and (7.18), and satisfy the spacing and bar size requirements given in Section 7.5e. The portion of A_t in the flexural compression zone may be reduced by $M_u/(0.9df_y)$, providing that Eq. (7.18) and the spacing and bar size requirements are satisfied.
7. Continue torsional reinforcement $b_t + d$ past the point where T_u is less than $\phi\lambda\sqrt{f'_c}(A_{cp}^2/p_{cp})$, or $\phi\lambda\sqrt{f'_c}(A_{cp}^2/p_{cp})\sqrt{1 + N_u/(4A_g\lambda\sqrt{f'_c})}$ for members subjected to axial load.

EXAMPLE 7.1

Design for torsion with shear. The 28 ft span beam shown in Fig. 7.12a and b carries a monolithic slab cantilevering 6 ft past the beam centerline. The resulting L beam supports a live load of 900 lb/ft along the beam centerline plus 50 psf uniformly distributed over the upper slab surface. The effective depth to the flexural steel centroid is 21.5 in., and the distance from the beam surfaces to the centroid of stirrup steel is $1\frac{3}{4}$ in. Material strengths are $f'_c = 5000$ psi and $f_y = 60,000$ psi. Design the torsional and shear reinforcement for the beam.

SOLUTION. Applying ACI load factors gives the slab load as

$$1.2w_d = 1.2 \times 75 \times 5.5 = 495 \text{ lb/ft}$$

$$1.6w_l = 1.6 \times 50 \times 5.5 = \underline{440 \text{ lb/ft}}$$

$$\text{Total} = 935 \text{ lb/ft at } 3.25 \text{ ft eccentricity}$$

while the beam carries directly

$$1.2w_d = 1.2 \times 300 = 360 \text{ lb/ft}$$

$$1.6w_l = 1.6(900 + 50) = \underline{1520 \text{ lb/ft}}$$

$$\text{Total} = 1880 \text{ lb/ft}$$

Thus, the uniformly distributed load on the beam is 2815 lb/ft, acting together with a uniformly distributed torque of $935 \times 3.25 = 3040$ ft-lb/ft. At the face of the column, the design shear force is $V_u = 2.815 \times 28/2 = 39.4$ kips. At the same location, the design torsional moment is $T_u = 3.040 \times 28/2 = 42.6$ ft-kips.

The variation of V_u and T_u with distance from the face of the supporting column is given by Fig. 7.12c and d , respectively. The values of V_u and T_u at the critical design section, a distance d from the column face, are

$$V_u = 39.4 \times \frac{12.21}{14} = 34.4 \text{ kips}$$

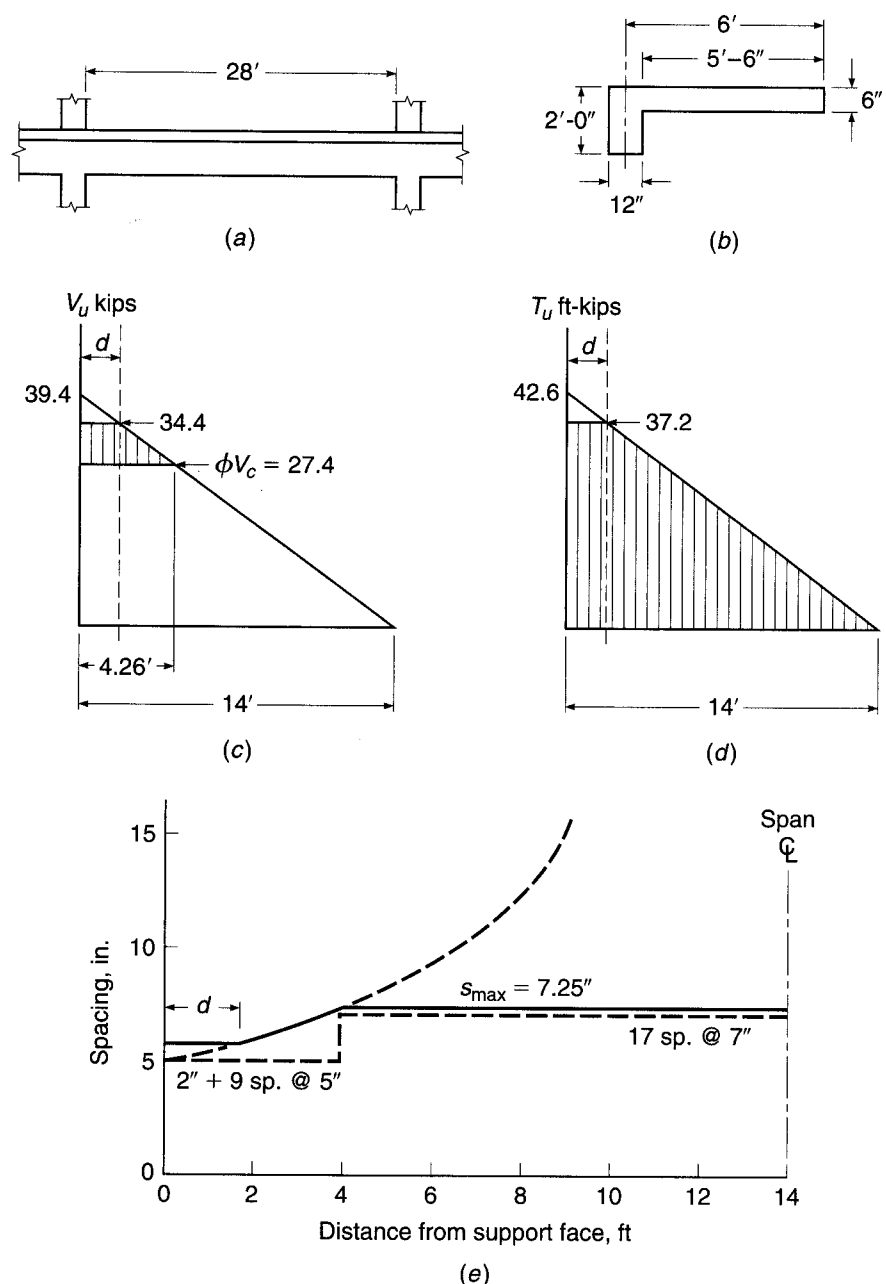
$$T_u = 42.6 \times \frac{12.21}{14} = 37.2 \text{ ft-kips}$$

For the effective beam, $A_{cp} = 12 \times 24 + 6 \times 18 = 396 \text{ in}^2$ and $p_{cp} = 2 \times 24 + 2 \times 30 = 108 \text{ in}$. According to the ACI Code, torsion may be neglected for normalweight concrete ($\lambda = 1.0$) if $T_u \leq 0.75 \times 1.0 \sqrt{5000(396^2/108)/12,000} = 6.4$ ft-kips. Torsion must clearly be considered in the present case. Since the torsional resistance of the beam is required for equilibrium, no reduction in T_u may be made.

Before designing the torsional reinforcement, the section will be checked for adequacy in accordance with Eq. (7.14). Although A_{cp} was calculated considering the flange to check if torsion could be neglected (as required by ACI Code 11.5.1), subsequent calculations for

FIGURE 7.12

Shear and torsion design example.



serviceability and strength will neglect the flange and no torsional reinforcement will be provided in the flange. For reference, $b_w d = 12 \times 21.5 = 258 \text{ in}^2$. With $1\frac{3}{4}$ in. cover to the center of the stirrup bars from all faces, $x_o = 12 - 3.5 = 8.5 \text{ in}$. and $y_o = 24.0 - 3.5 = 20.5 \text{ in}$. Thus, $A_{oh} = 8.5 \times 20.5 = 174 \text{ in}^2$, $A_o = 0.85 \times 174 = 148 \text{ in}^2$, and $p_h = 2(8.5 + 20.5) = 58 \text{ in}$. Using Eq. (7.14),

$$\sqrt{\left(\frac{34.4}{258}\right)^2 + \left(\frac{37.2 \times 12 \times 58}{1.7 \times 174^2}\right)^2} \leq \frac{0.75}{1000} \left(2\sqrt{5000} + 8\sqrt{5000} \right)$$

$$0.520 \text{ ksi} \leq 0.530 \text{ ksi}$$

Therefore, the cross section is of adequate size for the given concrete strength.

The values of A_t and A_v will now be calculated at the column face (for reference only). Using Eq. (7.15) and choosing $\theta = 45^\circ$,

$$\begin{aligned} A_t &= \frac{T_u s}{2\phi A_o f_{yt} \cot \theta} \\ &= \frac{42.6 \times 12s}{2 \times 0.75 \times 148 \times 60 \times 1} = 0.0384s \end{aligned}$$

for one leg of a closed vertical stirrup, or $0.0768s$ for two legs.

The shear capacity of the concrete alone, obtained using Eq. (4.12b), is

$$\begin{aligned} \phi V_c &= 0.75 \times 2\lambda \sqrt{f'_c} b_w d \\ &= \frac{0.75 \times 2 \times 1.0 \sqrt{5000} \times 258}{1000} = 27.4 \text{ kips} \end{aligned}$$

From Eq. (4.14a), the web reinforcement for transverse shear, again computed at the column face, is

$$A_v = \frac{(V_u - \phi V_c)s}{\phi f_{yt} d} = \frac{(39.4 - 27.4)s}{0.75 \times 60 \times 21.5} = 0.0124s$$

to be provided in two vertical legs.

The calculated value of A_t will decrease linearly to zero at the midspan, and the calculated value of A_v will decrease linearly to zero 4.26 ft from the face of the support, the point at which $V_u = \phi V_c$. Thus, the total area to be provided by the two vertical legs is

$$2A_t + A_v = 0.0768s \left(1 - \frac{x}{14}\right) + 0.0124s \left(1 - \frac{x}{4.26}\right)$$

for $0 \leq x \leq 4.26$ ft., where x is the distance from the face of the support, and

$$2A_t + A_v = 0.0768s \left(1 - \frac{x}{14}\right)$$

for $4.26 \leq x \leq 14$ ft.

Number 4 (No. 13) closed stirrups will provide a total area in the two legs of 0.40 in^2 . For $2A_t + A_v = 0.40 \text{ in}^2$, the required spacing at d and at 2 ft intervals along the span can be found using the given relationships between stirrup area and spacing:

$$\begin{aligned} s_d &= 5.39 \text{ in.} \\ s_2 &= 5.52 \text{ in.} \\ s_4 &= 7.19 \text{ in.} \\ s_6 &= 9.11 \text{ in.} \\ s_8 &= 12.2 \text{ in.} \\ s_{10} &= 18.2 \text{ in.} \end{aligned}$$

These values of s are plotted in Fig. 7.12e. ACI provisions for maximum spacing should now be checked. For torsion reinforcement, the maximum spacing is the smaller of

$$\frac{P_h}{8} = \frac{58}{8} = 7.25 \text{ in.}$$

or 12 in., whereas for shear reinforcement, the maximum spacing is $d/2 = 10.75 \text{ in.} \leq 24 \text{ in.}$ The most restrictive provision is the first, and the maximum spacing of 7.25 in. is plotted in Fig. 7.12e. Stirrups between the face of the support and the distance d can be spaced at s_d . The

resulting spacing requirements are shown by the solid line in the figure. These requirements are met in a practical way by No. 4 (No. 13) closed stirrups, the first placed 2 in. from the face of the column, followed by 9 at 5 in. spacing and 17 at 7 in. spacing. According to the ACI Code, stirrups may be discontinued at the point where $V_u < \phi V_c/2$ (4.9 ft from the span centerline) or $b_t + d = 2.8$ ft past the point at which $T_u < \phi \lambda \sqrt{f'_c} (A_{cp}^2/p_{cp})$. The latter point is past the centerline of the member; therefore, minimum stirrups are required throughout the span. The minimum web steel provided, 0.40 in^2 , satisfies the ACI Code minimum $= 0.75 \sqrt{f'_c} b_w s/f_y = 0.75 \sqrt{5000} (12) \times 7/60,000 = 0.074 \text{ in}^2 \geq 50 b_w s/f_y = 50 \times 12 \times 7/60,000 = 0.070 \text{ in}^2$.

The longitudinal steel required for torsion at a distance d from the column face is computed next. At that location

$$\frac{A_t}{s} = 0.0384 \left(1 - \frac{1.79}{14} \right) = 0.0335$$

and from Eq. (7.7)

$$A_t = 0.0335 \times 58 \times \frac{60}{60} \times 1^2 = 1.94 \text{ in}^2$$

with a total not less than given by Eq. (7.18), in which A_t/s is not to be taken less than $25 \times 12/60,000 = 0.005$.

$$A_{t,\min} = \frac{5\sqrt{5000} \times 396}{60 \times 1000} - 0.0335 \times 58 \times \frac{60}{60} = 0.39 \text{ in}^2$$

According to the ACI Code, the spacing must not exceed 12 in., and the bars may not be less than No. 3 (No. 10) in size or have a diameter less than $0.042s = 0.29$ in. Reinforcement will be placed at the top, middepth, and bottom of the member—each level to provide not less than $1.94/3 = 0.65 \text{ in}^2$. Two No. 6 (No. 19) bars will be used at middepth, and reinforcement to be placed for flexure will be increased by 0.65 in^2 at the top and bottom of the member.

Although A_t reduces in direct proportion to A_t/s and, hence, decreases linearly starting at d from the face of the column to the midspan, for simplicity of construction the added bars and the increment in the flexural steel will be maintained throughout the length of the member. Although ACI Code 11.5.3 states that A_t may be decreased in flexural compression zones by an amount equal to $M_u/(0.9df_y)$, that reduction will not be made here. Adequate embedment must be provided past the face of the column to fully develop f_y in the bars at that location.

REFERENCES

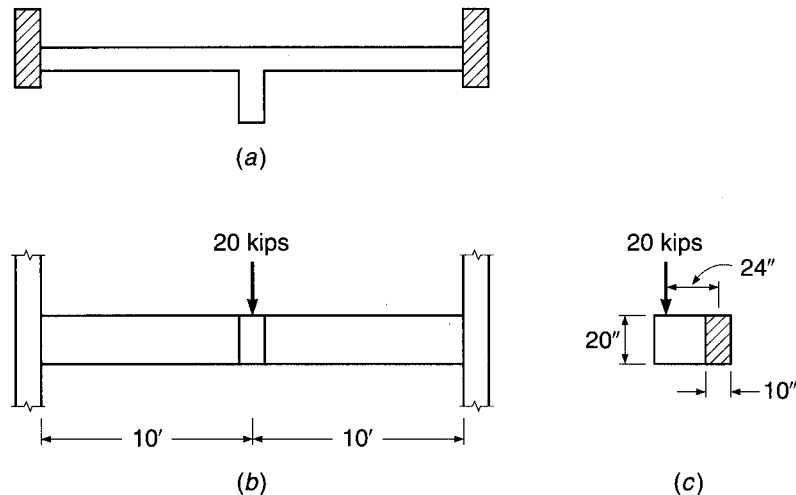
- 7.1. P. Lampert and B. Thurlimann, "Ultimate Strength and Design of Reinforced Concrete Beams in Torsion and Bending," *Int. Assoc. Bridge and Struct. Eng. Publ. 31-I*, Zurich, 1971, pp. 107–131.
- 7.2. B. Thurlimann, "Torsional Strength of Reinforced and Prestressed Beams—CEB Approach," in *Concrete Design: U.S. and European Practices*, SP-59, 1979, American Concrete Institute, Detroit, MI, pp. 117–143.
- 7.3. *CEB-FIP Model Code 1990*, Thomas Telford, London, 1991.
- 7.4. CSA Committee A23.3, *Design of Concrete Structures*, Canadian Standards Association, Etobicoke, Ontario, 2004.
- 7.5. T. T. C. Hsu, "Torsion of Structural Concrete—Behavior of Reinforced Concrete Rectangular Members," in *Torsion of Structural Concrete*, SP-18, 1968, American Concrete Institute, Detroit, MI, pp. 261–306.
- 7.6. A. H. Mattock, Disc. of "Design of Torsion" by J. G. MacGregor and M. G. Ghoneim (Ref 7.7), *ACI Struct. J.*, vol. 93, no. 1, 1996, pp. 142–143.
- 7.7. J. G. MacGregor and M. G. Ghoneim, "Design of Torsion," *ACI Struct. J.*, vol. 92, no. 2, 1995, pp. 218–221.
- 7.8. T. T. C. Hsu, "Shear Flow Zone in Torsion of Reinforced Concrete," *J. Struct. Eng.*, vol. 116, no. 11, 1990, pp. 3206–3226.
- 7.9. D. Mitchell and M. P. Collins, "Detailing for Torsion," *J. ACI*, vol. 73, no. 9, 1976, pp. 506–511.

PROBLEMS

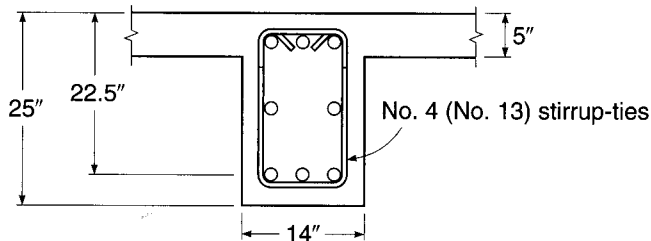
- 7.1.** A beam of rectangular cross section having $b = 22$ in. and $h = 15$ in. is to carry a total factored load of 3500 lb/ft uniformly distributed over its 26 ft span, and in addition the beam will be subjected to a uniformly distributed torsion of 1750 ft-lb/ft at factored loads. Closed stirrup-ties will be used to provide for flexural shear and torsion, placed with the stirrup steel centroid 1.75 in. from each concrete face. The corresponding flexural effective depth will be approximately 12.5 in. Design the transverse reinforcement for this beam and calculate the increment of longitudinal steel area needed to provide for torsion, using $f'_c = 4000$ psi and $f_y = 60,000$ psi.
- 7.2.** Architectural and clearance requirements call for the use of a transfer girder, shown in Fig. P7.2, spanning 20 ft between supporting column faces. The girder must carry from above a concentrated column load of 17.5 kips at midspan, applied with eccentricity 2 ft from the girder centerline. (Load factors are already included, as is an allowance for girder self-weight.) The member is to have dimensions $b = 10$ in., $h = 20$ in., $x_o = 6.5$ in., $y_o = 16.5$ in., and $d = 17$ in. Supporting columns provide full torsional rigidity; flexural rigidity at the ends of the span can be assumed to develop 40 percent of the maximum moment that would be obtained if the girder were simply supported. Design both transverse and longitudinal steel for the beam. Material strengths are $f'_c = 5000$ psi and $f_y = 60,000$ psi.

FIGURE P7.2

Transfer girder: (a) top view; (b) front view; (c) side view.



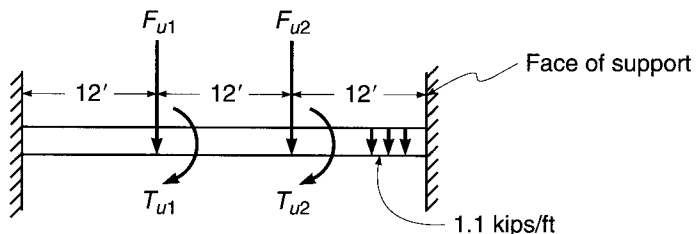
- 7.3.** The beam shown in cross section in Fig. P7.3 is a typical interior member of a continuous building frame, with span 30 ft between support faces. At factored loads, it will carry a uniformly distributed vertical load of 3100 lb/ft, acting simultaneously with a uniformly distributed torsion of 2600 ft-lb/ft. Transverse reinforcement for shear and torsion will consist of No. 4 (No. 13) stirrup-ties, as shown, with 1.5 in. clear to all concrete faces. The effective depth to flexural steel is taken equal to 22.5 in. for both negative and positive bending regions. Design the transverse reinforcement for shear and torsion, and calculate the longitudinal steel to be added to the flexural

FIGURE P7.3

requirements to provide for torsion. Torsional reinforcement will be provided only in the web, not in the flanges. Material strengths are $f'_c = 4000$ psi and $f_y = 60,000$ psi.

- 7.4.** The single-span T beam bridge described in Problem 3.14 is reinforced for flexure with four No. 10 (No. 32) bars in two layers, which continue uninterrupted into the supports, permitting a service live load of 1.50 kips/ft to be carried, in addition to the dead load of 0.93 kip/ft, including self-weight. Assume now that only one-half of that live load acts but that it is applied over only one-half the width of the member, entirely to the right of the section centerline. Design the transverse reinforcement for shear and torsion, and calculate the modified longitudinal steel needed for this eccentric load condition. Torsional reinforcement can be provided in the slab if needed, as well as in the web. Stirrup-ties will be No. 3 or No. 4 (No. 10 or No. 13) bars, with 1.5 in. clear to all concrete faces. Supports provide no restraint against flexural rotations but do provide full restraint against twist. Show a sketch of your final design, detailing all reinforcement. Material strengths are as given for Problem 3.14.
- 7.5.** Design a spandrel (edge) girder for shear and torsion that is loaded with a uniform factored load of 1.1 kips/ft. In addition, beams framing into the girder apply concentrated factored vertical loads F_{u1} and F_{u2} and torsional moments T_{u1} and T_{u2} , as shown in Fig. P7.5. Girder dimensions are $h = 32$ in. and $b_w = 28$ in., and slab thickness (one side of girder only) = 6 in. An analysis of various loading combinations indicates the following results:

Case 1	$F_{u1} = F_{u2} = 80$ kips
	$T_{u1} = T_{u2} = 160$ ft-kips
Case 2	$F_{u1} = 83$ kips; $F_{u2} = 22$ kips
	$T_{u1} = 160$ ft-kips; $T_{u2} = 53$ ft-kips
Case 3	$F_{u1} = 22$ kips; $F_{u2} = 83$ kips
	$T_{u1} = 53$ ft-kips; $T_{u2} = 160$ ft-kips

FIGURE P7.5

To calculate reactions, treat the ends of the girder as fixed. Use $f_y = 60,000$ psi and $f'_c = 4000$ psi. Provide design drawings showing the transverse steel and the longitudinal steel required in addition to the flexural steel.

- 7.6.** A 20-ft long rectangular beam, free-standing except for being fixed at each end against rotation, must carry a midspan live load of 35 kips. The load can be as much as 12 in. off the axis of the beam. Beam dimensions are $b = 12$ in., $d = 20$ in., and $h = 23$ in. Use $f_y = 60,000$ psi and $f'_c = 4000$ psi. Design the shear and torsion reinforcement.

8

Short Columns

8.1 INTRODUCTION: AXIAL COMPRESSION

Columns are defined as members that carry loads chiefly in compression. Usually columns carry bending moments as well, about one or both axes of the cross section, and the bending action may produce tensile forces over a part of the cross section. Even in such cases, columns are generally referred to as compression members, because the compression forces dominate their behavior. In addition to the most common type of compression member, i.e., vertical elements in structures, compression members include arch ribs; rigid frame members inclined or otherwise; compression elements in trusses, shells, or portions thereof that carry axial compression; and other forms. In this chapter the term *column* will be used interchangeably with the term *compression member*, for brevity and in conformity with general usage.

Three types of reinforced concrete compression members are in use:

1. Members reinforced with longitudinal bars and lateral ties.
2. Members reinforced with longitudinal bars and continuous spirals.
3. Composite compression members reinforced longitudinally with structural steel shapes, pipe, or tubing, with or without additional longitudinal bars, and various types of lateral reinforcement.

Types 1 and 2 are by far the most common, and most of the discussion in this chapter will refer to them.

The main reinforcement in columns is longitudinal, parallel to the direction of the load, and consists of bars arranged in a square, rectangular, or circular pattern, as was shown in Fig. 1.15. Figure 8.1 shows an ironworker tightening splices for the main reinforcing steel during construction of the 60-story Bank of America Corporate Center in Charlotte, North Carolina. The ratio of longitudinal steel area A_{st} to gross concrete cross section A_g is in the range from 0.01 to 0.08, according to ACI Code 10.9.1. The lower limit is necessary to ensure resistance to bending moments not accounted for in the analysis and to reduce the effects of creep and shrinkage of the concrete under sustained compression. Ratios higher than 0.08 not only are uneconomical, but also would cause difficulty owing to congestion of the reinforcement, particularly where the steel must be spliced. Most columns are designed with ratios below 0.04. Larger-diameter bars are used to reduce placement costs and to avoid unnecessary congestion. The special large-diameter No. 14 and No. 18 (No. 43 and No. 57) bars are produced mainly for use in columns. According to ACI Code 10.9.2, a minimum of four longitudinal bars is required when the bars are enclosed by spaced rectangular or circular ties, and a minimum of six bars must be used when the longitudinal bars are enclosed by a continuous spiral.

FIGURE 8.1

Reinforcement for primary column of 60-story Bank of America Corporate Center in Charlotte, North Carolina.

(Courtesy of Walter P. Moore and Associates.)

**FIGURE 8.3**

Column sections for square and rectangular columns.

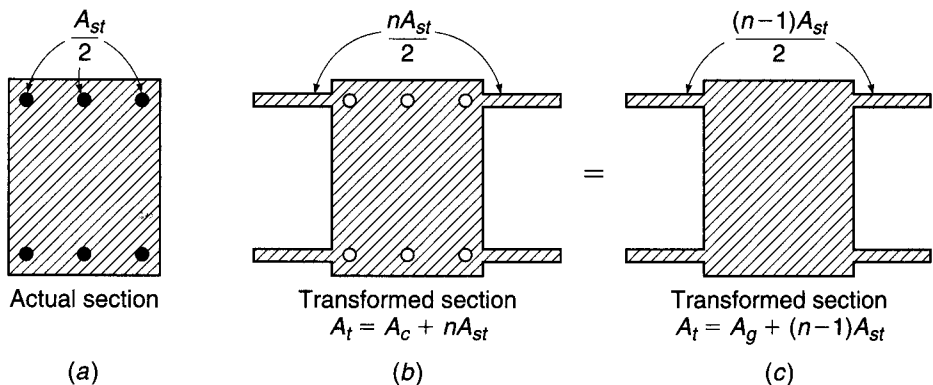
Columns may be divided into two broad categories: *short columns*, for which the strength is governed by the strength of the materials and the geometry of the cross section, and *slender columns*, for which the strength may be significantly reduced by lateral deflections. A number of years ago, an ACI-ASCE survey indicated that 90 percent of columns braced against sidesway and 40 percent of unbraced columns could be designed as short columns. Effective lateral bracing, which prevents relative lateral movement of the two ends of a column, is commonly provided by shear walls, elevator and stairwell shafts, diagonal bracing, or a combination of these. Although slender columns are more common now because of the wider use of high-strength materials and improved methods of dimensioning members, it is still true that most columns in ordinary practice can be considered short columns. Only short columns will be discussed in this chapter; the effects of slenderness in reducing column strength will be covered in Chapter 9.

The behavior of short, axially loaded compression members was discussed in Section 1.9 in introducing the basic aspects of reinforced concrete. It is suggested that the earlier material be reviewed at this point. In Section 1.9, it was demonstrated that, for lower loads at which both materials remain elastic, the steel carries a relatively small portion of the total load. The steel stress f_s is equal to n times the concrete stress:

$$f_s = nf_c \quad (8.1)$$

FIGURE 8.2

Transformed section in axial compression.



where $n = E_s/E_c$ is the modular ratio. In this range the axial load P is given by

$$P = f_c[A_g + (n - 1)A_{st}] \quad (8.2)$$

where A_g is the gross area of the cross section, A_{st} is the total area of the reinforcing steel, and the term in brackets is the area of the transformed section (see Fig. 8.2). Equations (8.2) and (8.1) can be used to find concrete and steel stresses, respectively, for given loads, provided both materials remain elastic. Example 1.1 demonstrated the use of these equations.

In Section 1.9, it was further shown that the nominal strength of an axially loaded column can be found, recognizing the nonlinear response of both materials, by

$$P_n = 0.85f'_cA_c + A_{st}f_y \quad (8.3a)$$

where A_c = net area of concrete, or

$$P_n = 0.85f'_c(A_g - A_{st}) + A_{st}f_y \quad (8.3b)$$

i.e., by summing the strength contributions of the two components of the column. At this stage, the steel carries a significantly larger fraction of the load than was the case at lower total load.

The calculation of the nominal strength of an axially loaded column was demonstrated in Section 1.9.

According to ACI Code 10.3.6, the *design strength* of an axially loaded column is to be found based on Eq. (8.3b) with the introduction of certain strength reduction factors. The ACI factors are lower for columns than for beams, reflecting their greater importance in a structure. A beam failure would normally affect only a local region, whereas a column failure could result in the collapse of the entire structure. In addition, these factors reflect differences in the behavior of tied columns and spirally reinforced columns that will be discussed in Section 8.2. A basic ϕ factor of 0.75 is used for spirally reinforced columns and 0.65 for tied columns, vs. $\phi = 0.90$ for most beams.

A further limitation on column strength is imposed by ACI Code 10.3.6 to allow for accidental eccentricities of loading not considered in the analysis. This is done by imposing an upper limit on the axial load that is less than the calculated design strength. This upper limit is taken as 0.85 times the design strength for spirally

reinforced columns and 0.80 times the calculated strength for tied columns. Thus, according to ACI Code 10.3.6, for spirally reinforced columns

$$\phi P_{n(\max)} = 0.85\phi[0.85f'_c(A_g - A_{st}) + f_y A_{st}] \quad (8.4a)$$

with $\phi = 0.75$. For tied columns

$$\phi P_{n(\max)} = 0.80\phi[0.85f'_c(A_g - A_{st}) + f_y A_{st}] \quad (8.4b)$$

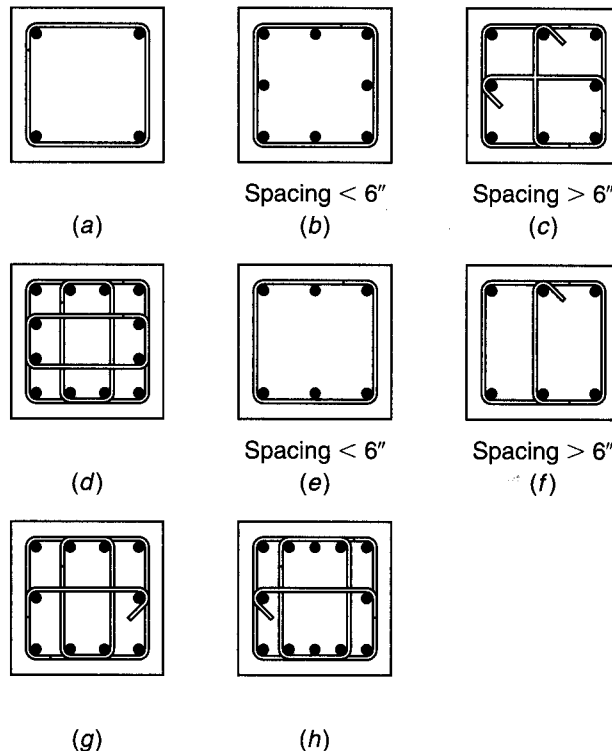
with $\phi = 0.65$.

8.2 LATERAL TIES AND SPIRALS

Figure 1.15 shows cross sections of the simplest types of columns, spirally reinforced or provided with lateral ties. Other cross sections frequently found in buildings and bridges are shown in Fig. 8.3. In general, in members with large axial forces and small moments, longitudinal bars are spaced more or less uniformly around the perimeter (Fig. 8.3a to d). When bending moments are large, much of the longitudinal steel is concentrated at the faces of highest compression or tension, i.e., at maximum distances from the axis of bending (Fig. 8.3e to h). Specific recommended patterns for many combinations and arrangements of bars are found in Refs. 8.1 and 8.2. In heavily loaded columns with large steel percentages, the result of a large number of bars, each of them positioned and held individually by ties, is steel congestion in the forms and

FIGURE 8.3

Tie arrangements for square and rectangular columns.



difficulties in placing the concrete. In such cases, bundled bars are frequently employed. Bundles consist of three or four bars tied in direct contact, wired, or otherwise fastened together. These are usually placed in the corners. Tests have shown that adequately bundled bars act as one unit; i.e., they are detailed as if a bundle constituted a single round bar of area equal to the sum of the bundled bars.

Lateral reinforcement, in the form of individual relatively widely spaced ties or a continuous closely spaced spiral, serves several functions. For one, such reinforcement is needed to hold the longitudinal bars in position in the forms while the concrete is being placed. For this purpose, longitudinal and transverse steel is wired together to form cages, which are then moved into the forms and properly positioned before placing the concrete. For another, transverse reinforcement is needed to prevent the highly stressed, slender longitudinal bars from buckling outward by bursting the thin concrete cover.

Closely spaced spirals serve these two functions. Ties, which can be arranged and spaced in various ways, must be so designed that these two requirements are met. This means that the spacing must be sufficiently small to prevent buckling between ties and that, in any tie plane, a sufficient number of ties must be provided to position and hold all bars. On the other hand, in columns with many longitudinal bars, if the column section is crisscrossed by too many ties, they interfere with the placement of concrete in the forms. To achieve adequate tying yet hold the number of ties to a minimum, ACI Code 7.10.5 gives the following rules for tie arrangement:

All bars of tied columns shall be enclosed by *lateral ties*, at least No. 3 (No. 10) in size for longitudinal bars up to No. 10 (No. 32), and at least No. 4 (No. 13) in size for Nos. 11, 14, and 18 (Nos. 36, 43, and 57) and bundled longitudinal bars. The spacing of the ties shall not exceed 16 diameters of longitudinal bars, 48 diameters of tie bars, nor the least dimension of the column. The ties shall be so arranged that every corner and alternate longitudinal bar shall have lateral support provided by the corner of a tie having an included angle of not more than 135° , and no bar shall be farther than 6 in. clear on either side from such a laterally supported bar. Deformed wire or welded wire fabric of equivalent area may be used instead of ties. Where the bars are located around the periphery of a circle, complete circular ties may be used.

For spirally reinforced columns ACI Code 7.10.4 requirements for lateral reinforcement may be summarized as follows:

Spirals shall consist of a continuous bar or wire not less than $\frac{3}{8}$ in. in diameter, and the clear spacing between turns of the spiral must not exceed 3 in. nor be less than 1 in.

In addition, a minimum ratio of spiral steel is imposed such that the structural performance of the column is significantly improved, with respect to both ultimate load and the type of failure, compared with an otherwise identical tied column.

The structural effect of a spiral is easily visualized by considering as a model a steel drum filled with sand (Fig. 8.4). When a load is placed on the sand, a lateral pressure is exerted by the sand on the drum, which causes hoop tension in the steel wall. The load on the sand can be increased until the hoop tension becomes large enough to burst the drum. The sand pile alone, if not confined in the drum, would have been able to support hardly any load. A cylindrical concrete column, to be sure, does have a definite strength without any lateral confinement. As it is being loaded, it shortens longitudinally and expands laterally, depending on Poisson's ratio. A closely spaced spiral confining the column counteracts the expansion, as

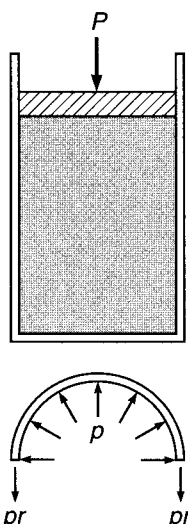


FIGURE 8.4

Model for action of a spiral.

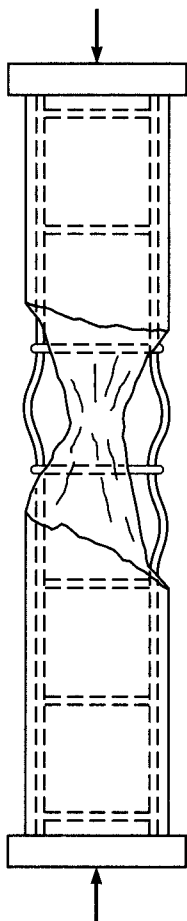


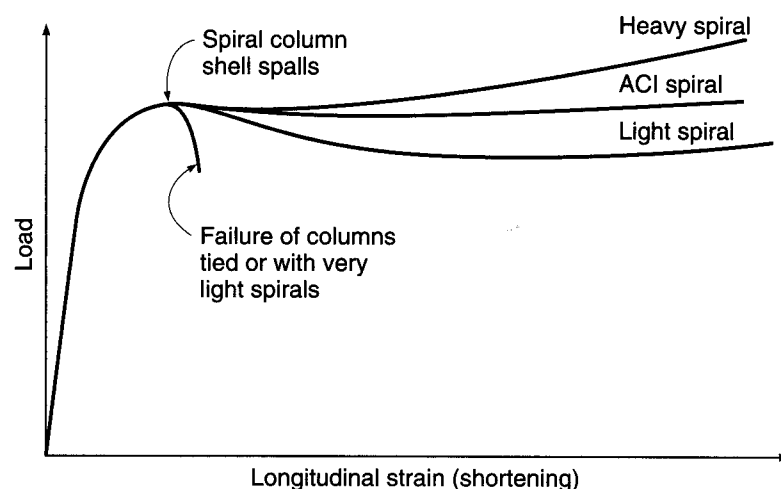
FIGURE 8.5
Failure of a tied column.

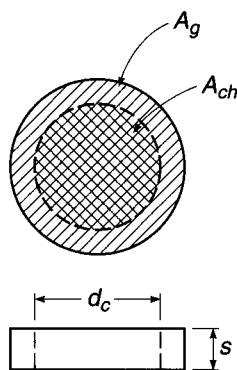
did the steel drum in the model. This causes hoop tension in the spiral, while the carrying capacity of the confined concrete in the core is greatly increased. Failure occurs only when the spiral steel yields, which greatly reduces its confining effect, or when it fractures.

A tied column fails at the load given by Eq. (8.3a or b). At this load the concrete fails by crushing and shearing outward along inclined planes, and the longitudinal steel by buckling outward between ties (Fig. 8.5). In a spirally reinforced column, when the same load is reached, the longitudinal steel and the concrete within the core are prevented from moving outward by the spiral. The concrete in the outer shell, however, not being so confined, does fail; i.e., the outer shell spalls off when the load P_n is reached. It is at this stage that the confining action of the spiral has a significant effect, and if sizable spiral steel is provided, the load that will ultimately fail the column by causing the spiral steel to yield or fracture can be much larger than that at which the shell spalled off. Furthermore, the axial strain limit when the column fails will be much greater than otherwise; the toughness of the column has been much increased.

In contrast to the practice in some foreign countries, it is reasoned in the United States that any excess capacity beyond the spalling load of the shell is wasted because the member, although not actually failed, would no longer be considered serviceable. For this reason, the ACI Code provides a minimum spiral reinforcement of such an amount that its contribution to the carrying capacity is just slightly larger than that of the concrete in the shell. The situation is best understood from Fig. 8.6, which compares the performance of a tied column with that of a spiral column whose spalling load is equal to the ultimate load of the tied column. The failure of the tied column is abrupt and complete. This is true, to almost the same degree, of a spiral column with a spiral so light that its strength contribution is considerably less than the strength lost in the spalled shell. With a heavy spiral the reverse is true, and with considerable prior deformation the spalled column would fail at a higher load. The "ACI spiral," its strength contribution about compensating for that lost in the spalled shell, hardly increases the ultimate load. However, by preventing instantaneous crushing of concrete and buckling of steel, it produces a more gradual and ductile failure, i.e., a tougher column.

FIGURE 8.6
Behavior of spirally reinforced and tied columns.



**FIGURE 8.7**

Confinement of core concrete due to hoop tension.

It has been found experimentally (Refs. 8.3 to 8.5) that the increase in compressive strength of the core concrete in a column provided through the confining effect of spiral steel is closely represented by the equation

$$f_c^* - 0.85f'_c = 4.0f'_2 \quad (a)$$

where f_c^* = compressive strength of spirally confined core concrete

$0.85f'_c$ = compressive strength of concrete if unconfined

f'_2 = lateral confinement stress in core concrete produced by spiral

The confinement stress f'_2 is calculated assuming that the spiral steel reaches its yield stress f_y when the column eventually fails. With reference to Fig. 8.7, a hoop tension analysis of an idealized model of a short segment of column confined by one turn of lateral steel shows that

$$f'_2 = \frac{2A_{sp}f_{yt}}{d_c s} \quad (b)$$

where A_{sp} = cross-sectional area of spiral wire

f_{yt} = yield strength of spiral steel

d_c = outside diameter of spiral

s = spacing or pitch of spiral wire

A *volumetric ratio* is defined as the ratio of the volume of spiral steel to the volume of core concrete:

$$\rho_s = \frac{2\pi d_c A_{sp}}{2} \frac{4}{\pi d_c^2 s}$$

from which

$$A_{sp} = \frac{\rho_s d_c s}{4} \quad (c)$$

Substituting the value of A_{sp} from Eq. (c) into Eq. (b) results in

$$f'_2 = \frac{\rho_s f_{yt}}{2} \quad (d)$$

To find the right amount of spiral steel, one calculates

$$\text{Strength contribution of the shell} = 0.85f'_c(A_g - A_{ch}) \quad (e)$$

where A_g and A_{ch} are, respectively, the gross and core concrete areas. Then substituting the confinement stress from Eq. (d) into Eq. (a) and multiplying by the core concrete area, one finds

$$\text{Strength provided by spiral} = 2\rho_s f_{yt} A_{ch} \quad (f)$$

The basis for the design of the spiral is that the strength gain provided by the spiral should be at least equal to that lost when the shell spalls, so combining Eqs. (e) and (f) yields

$$0.85f'_c(A_g - A_{ch}) = 2\rho_s f_{yt} A_{ch}$$

from which

$$\rho_s = 0.425 \left(\frac{A_g}{A_{ch}} - 1 \right) \frac{f'_c}{f_{yt}} \quad (g)$$

According to the ACI Code, this result is rounded upward slightly, and ACI Code 10.9.3 states that the ratio of spiral reinforcement shall not be less than

$$\rho_s = 0.45 \left(\frac{A_g}{A_{ch}} - 1 \right) \frac{f'_c}{f_{yt}} \quad (8.5)$$

It is further stipulated in the ACI Code that f_{yt} not be taken greater than 100,000 psi and that spiral reinforcement not be spliced if f_{yt} is greater than 60,000 psi.

It follows from this development that two concentrically loaded columns designed in accordance with the ACI Code, one tied and one with spiral but otherwise identical, will fail at about the same load, the former in a sudden and brittle manner, the latter gradually with prior spalling of the shell and with more ductile behavior. This advantage of the spiral column is much less pronounced if the load is applied with significant eccentricity or when bending from other sources is present simultaneously with axial load. For this reason, while the ACI Code permits somewhat larger design loads on spiral than on tied columns when the moments are small or zero ($\phi = 0.75$ for spirally reinforced columns vs. $\phi = 0.65$ for tied), the difference is not large, and it is even further reduced for large eccentricities, for which ϕ approaches 0.90 for both.

The design of spiral reinforcement according to the ACI Code provisions is easily reduced to tabular form, as in Table A.14 of Appendix A.

8.3

COMPRESSION PLUS BENDING OF RECTANGULAR COLUMNS

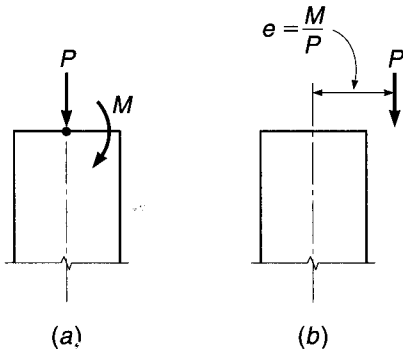
Members that are axially, i.e., concentrically, compressed occur rarely, if ever, in buildings and other structures. Components such as columns and arches chiefly carry loads in compression, but simultaneous bending is almost always present. Bending moments are caused by continuity, i.e., by the fact that building columns are parts of monolithic frames in which the support moments of the girders are partly resisted by the abutting columns, by transverse loads such as wind forces, by loads carried eccentrically on column brackets, or in arches when the arch axis does not coincide with the pressure line. Even when design calculations show a member to be loaded purely axially, inevitable imperfections of construction will introduce eccentricities and consequent bending in the member as built. For this reason members that must be designed for simultaneous compression and bending are very frequent in almost all types of concrete structures.

When a member is subjected to combined axial compression P and moment M , such as in Fig. 8.8a, it is usually convenient to replace the axial load and moment with an equal load P applied at eccentricity $e = M/P$, as in Fig. 8.8b. The two loadings are statically equivalent. All columns may then be classified in terms of the equivalent eccentricity. Those having relatively small e are generally characterized by compression over the entire concrete section, and if overloaded, will fail by crushing of the concrete accompanied by yielding of the steel in compression on the more heavily loaded side. Columns with large eccentricity are subject to tension over at least a part of the section, and if overloaded, may fail due to tensile yielding of the steel on the side farthest from the load.

For columns, load stages below the ultimate are generally not important. Cracking of concrete, even for columns with large eccentricity, is usually not a serious problem, and lateral deflections at service load levels are seldom, if ever, a factor. Design of

FIGURE 8.8

Equivalent eccentricity of column load.



columns is therefore based on the factored load, which must not exceed the design strength, as usual, i.e.,

$$\phi M_n \geq M_u \quad (8.6a)$$

$$\phi P_n \geq P_u \quad (8.6b)$$

8.4 STRAIN COMPATIBILITY ANALYSIS AND INTERACTION DIAGRAMS

Figure 8.9a shows a member loaded parallel to its axis by a compressive force P_n at an eccentricity e measured from the centerline. The distribution of strains at a section $a-a$ along its length, at incipient failure, is shown in Fig. 8.9b. With plane sections assumed to remain plane, concrete strains vary linearly with distance from the neutral axis, which is located a distance c from the more heavily loaded side of the member. With full compatibility of deformations, the steel strains at any location are the same as the strains in the adjacent concrete; thus, if the ultimate concrete strain is ϵ_u , the strain in the bars nearest the load is ϵ'_s , while that in the tension bars at the far side is ϵ_s . Compression steel with area A'_s and tension steel with area A_s are located at distances d' and d , respectively, from the compression face.

The corresponding stresses and forces are shown in Fig. 8.9c. Just as for simple bending, the actual concrete compressive stress distribution is replaced by an equivalent rectangular distribution having depth $a = \beta_1 c$. A large number of tests on columns with a variety of shapes have shown that the strengths computed on this basis are in satisfactory agreement with test results (Ref. 8.6).

Equilibrium between external and internal axial forces shown in Fig. 8.9c requires that

$$P_n = 0.85f'_c ab + A'_s f'_s - A_s f_s \quad (8.7)$$

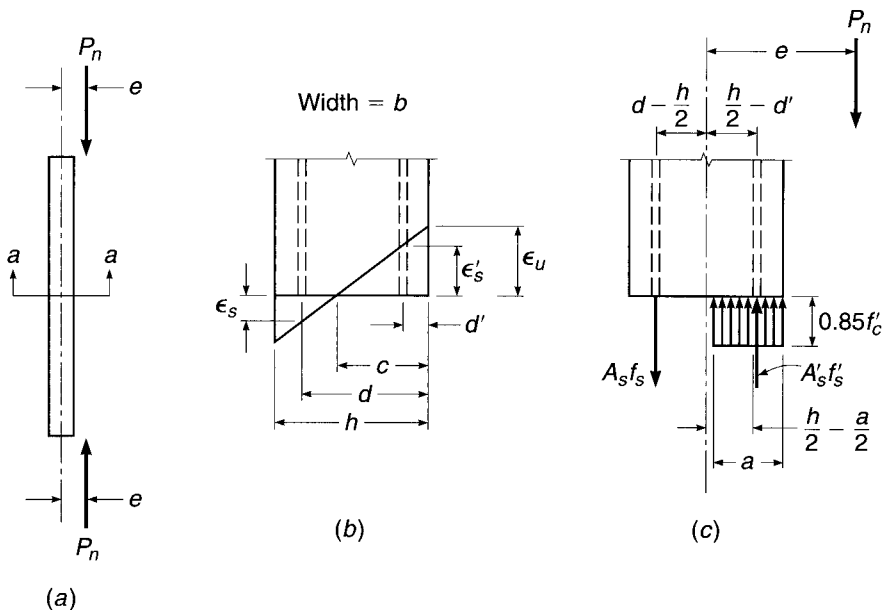
Also, the moment about the centerline of the section of the internal stresses and forces must be equal and opposite to the moment of the external force P_n , so that

$$M_n = P_n e = 0.85f'_c ab \left(\frac{h}{2} - \frac{a}{2} \right) + A'_s f'_s \left(\frac{h}{2} - d' \right) + A_s f_s \left(d - \frac{h}{2} \right) \quad (8.8)$$

These are the two basic equilibrium relations for rectangular eccentrically compressed members.

FIGURE 8.9

Column subject to eccentric compression: (a) loaded column; (b) strain distribution at section $a-a$; (c) stresses and forces at nominal strength.



The fact that the presence of the compression reinforcement A'_s has displaced a corresponding amount of concrete of area A'_s is neglected in writing these equations. If necessary, particularly for large reinforcement ratios, one can account for this very simply. Evidently, in the above equations a nonexistent concrete compression force of amount $A'_s(0.85f'_c)$ has been included as acting in the displaced concrete at the level of the compression steel. This excess force can be removed in both equations by multiplying A'_s by $f'_s - 0.85f'_c$ rather than by f'_s .

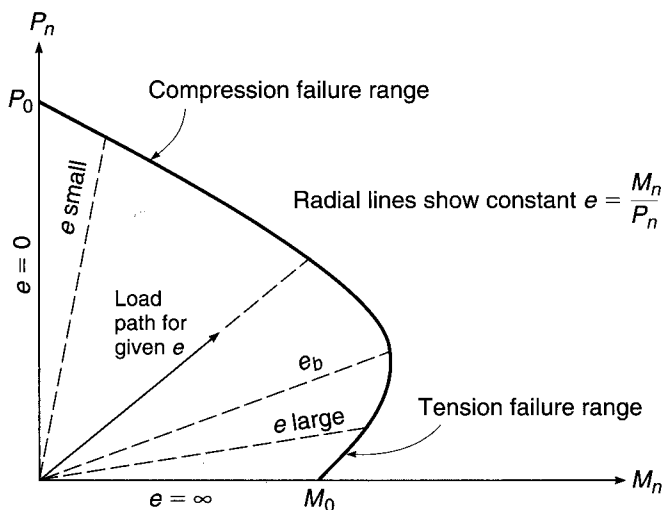
For large eccentricities, failure is initiated by yielding of the tension steel A_s . Hence, for this case, $f_s = f_y$. When the concrete reaches its ultimate strain ϵ_u , the compression steel may or may not have yielded; this must be determined based on compatibility of strains. For small eccentricities the concrete will reach its limit strain ϵ_u before the tension steel starts yielding; in fact, the bars on the side of the column farther from the load may be in compression, not tension. For small eccentricities, too, the analysis must be based on compatibility of strains between the steel and the adjacent concrete.

For a given eccentricity determined from the frame analysis (i.e., $e = M_u/P_u$) it is possible to solve Eqs. (8.7) and (8.8) for the load P_n and moment M_n that would result in failure as follows. In both equations, f'_s , f_s , and a can be expressed in terms of a single unknown c , the distance to the neutral axis. This is easily done based on the geometry of the strain diagram, with ϵ_u taken equal to 0.003 as usual, and using the stress-strain curve of the reinforcement. The result is that the two equations contain only two unknowns, P_n and c , and can be solved for those values simultaneously. However, to do so in practice would be complicated algebraically, particularly because of the need to incorporate the limit f_y on both f'_s and f_s .

A better approach, providing the basis for practical design, is to construct a *strength interaction diagram* defining the failure load and failure moment for a given column for the full range of eccentricities from zero to infinity. For any eccentricity, there is a unique pair of values of P_n and M_n that will produce the state of incipient failure. That pair of values can be plotted as a point on a graph relating P_n and M_n ,

FIGURE 8.10

Interaction diagram for nominal column strength in combined bending and axial load.



such as shown in Fig. 8.10. A series of such calculations, each corresponding to a different eccentricity, will result in a curve having a shape typically as shown in Fig. 8.10. On such a diagram, any radial line represents a particular eccentricity $e = M/P$. For that eccentricity, gradually increasing the load will define a load path as shown, and when that load path reaches the limit curve, failure will result. Note that the vertical axis corresponds to $e = 0$, and P_0 is the capacity of the column if concentrically loaded, as given by Eq. (8.3b). The horizontal axis corresponds to an infinite value of e , i.e., pure bending at moment capacity M_0 . Small eccentricities will produce failure governed by concrete compression, while large eccentricities give a failure triggered by yielding of the tension steel.

For a given column, selected for trial, the interaction diagram is most easily constructed by selecting successive choices of neutral axis distance c , from infinity (axial load with eccentricity 0) to a very small value found by trial to give $P_n = 0$ (pure bending). For each selected value of c , the steel strains and stresses and the concrete force are easily calculated as follows. For the tension steel,

$$\epsilon_s = \epsilon_u \frac{d - c}{c} \quad (8.9)$$

$$f_s = \epsilon_u E_s \frac{d - c}{c} \leq f_y \quad (8.10)$$

while for the compression steel,

$$\epsilon'_s = \epsilon_u \frac{c - d'}{c} \quad (8.11)$$

$$f'_s = \epsilon_u E_s \frac{c - d'}{c} \leq f_y \quad (8.12)$$

The concrete stress block has depth

$$a = \beta_1 c \leq h \quad (8.13)$$

and consequently the concrete compressive resultant is

$$C = 0.85 f'_c ab \quad (8.14)$$

The nominal axial force P_n and nominal moment M_n corresponding to the selected neutral axis location can then be calculated from Eqs. (8.7) and (8.8), respectively, and thus a single point on the strength interaction diagram is established. The calculations are then repeated for successive choices of neutral axis to establish the curve defining the strength limits, such as Fig. 8.10. The calculations, of a repetitive nature, are easily programmed for the computer or performed using a spreadsheet.

8.5 BALANCED FAILURE

As already noted, the interaction curve is divided into a compression failure range and a tension failure range.[†] It is useful to define what is termed a *balanced failure mode* and corresponding eccentricity e_b with the load P_b and moment M_b acting in combination to produce failure, with the concrete reaching its limit strain ϵ_u at precisely the same instant that the tensile steel on the far side of the column reaches yield strain. This point on the interaction diagram is the dividing point between compression failure (small eccentricities) and tension failure (large eccentricities).

The values of P_b and M_b are easily computed with reference to Fig. 8.9. For balanced failure,

$$c = c_b = d \frac{\epsilon_u}{\epsilon_u + \epsilon_y} \quad (8.15)$$

and

$$a = a_b = \beta_1 c_b \quad (8.16)$$

Equations (8.9) through (8.14) are then used to obtain the steel stresses and the compressive resultant, after which P_b and M_b are found from Eqs. (8.7) and (8.8).

Note that, in contrast to beam design, one cannot restrict column designs such that yielding failure rather than crushing failure would always be the result of overloading. The type of failure for a column depends on the value of eccentricity e , which in turn is defined by the load analysis of the building or other structure.

It is important to observe, in Fig. 8.10, that in the region of compression failure the larger the axial load P_n , the smaller the moment M_n that the section is able to sustain before failing. However, in the region of tension failure, the reverse is true; the larger the axial load, the larger the simultaneous moment capacity. This is easily understood. In the compression failure region, failure occurs through overstraining of the concrete. The larger the concrete compressive strain caused by the axial load alone, the smaller the margin of additional strain available for the added compression caused by bending. On the other hand, in the tension failure region, yielding of the steel initiates failure. If the member is loaded in simple bending to the point at which yielding begins in the tension steel, and if an axial compression load is then added, the steel compressive stresses caused by this load will superimpose on the previous tensile stresses. This reduces the total steel stress to a value below its yield strength. Consequently, an additional moment can now be sustained of such magnitude that the combination of the steel stress from the axial load and the increased moment again reaches the yield strength.

[†] The terms *compression failure range* and *tension failure range* are used for the purpose of general description and are distinct from *tension-controlled* and *compression-controlled* failures, as described in Chapter 3 and Section 8.9.

The typical shape of a column interaction diagram shown in Fig. 8.10 has important design implications. In the range of tension failure, a *reduction in axial load* may produce failure for a given moment. In carrying out a frame analysis, the designer must consider all combinations of loading that may occur, including that which would produce minimum axial load paired with a given moment (the specific load combinations are specified in ACI Code 8.10 and described in Section 12.3). Only that amount of compression that is certain to be present should be used in calculating the capacity of a column subject to a given moment.

EXAMPLE 8.1

Column strength interaction diagram. A 12 × 20 in. column is reinforced with four No. 9 (No. 29) bars of area 1.0 in² each, one in each corner as shown in Fig. 8.11a. The concrete cylinder strength is $f'_c = 4000$ psi and the steel yield strength is 60 ksi. Determine (a) the load P_b , moment M_b , and corresponding eccentricity e_b for balanced failure; (b) the load and moment for a representative point in the tension failure region of the interaction curve; (c) the load and moment for a representative point in the compression failure region; (d) the axial load strength for zero eccentricity. Then (e) sketch the strength interaction diagram for this column. Finally, (f) design the transverse reinforcement, based on ACI Code provisions.

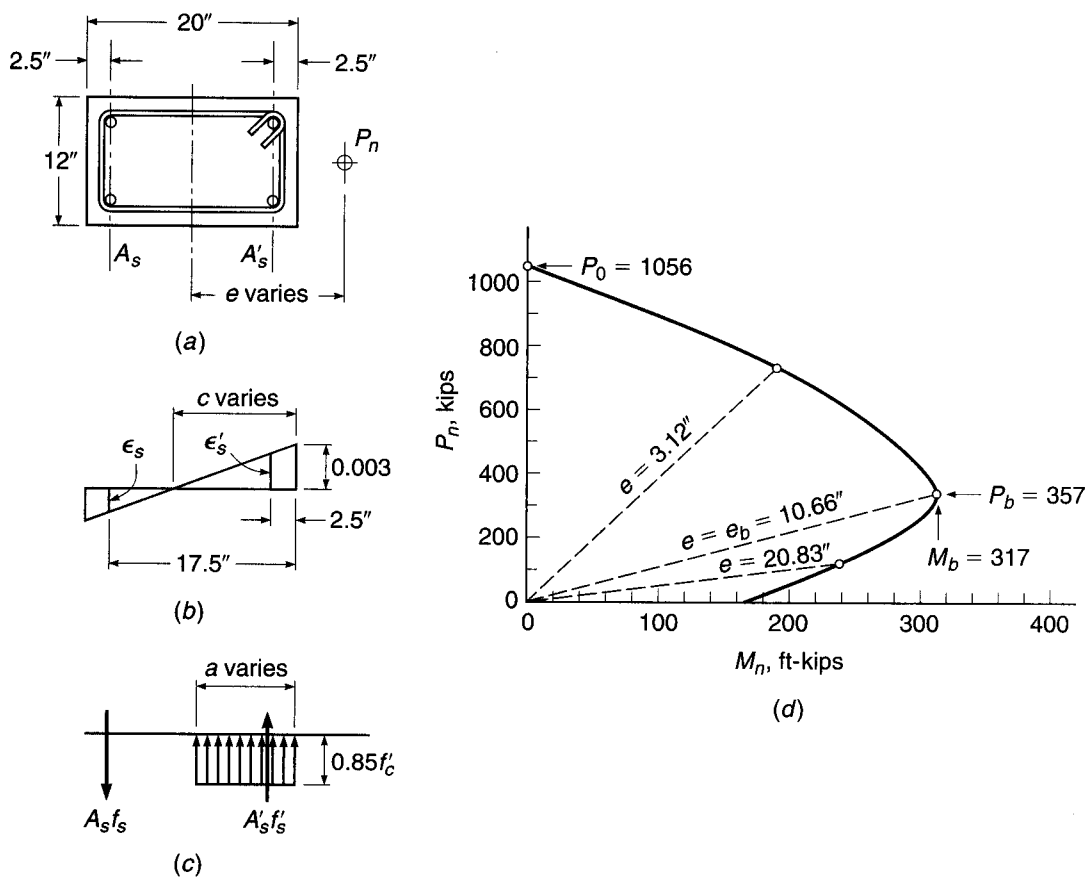


FIGURE 8.11

Column interaction diagram for Example 8.1: (a) cross section; (b) strain distribution; (c) stresses and forces; (d) strength interaction diagram.

SOLUTION.

- (a) The neutral axis for the balanced failure condition is easily found from Eq. (8.15) with $\epsilon_u = 0.003$ and $\epsilon_y = 60/29,000 = 0.0021$

$$c_b = 17.5 \times \frac{0.003}{0.0051} = 10.3 \text{ in.}$$

giving a stress-block depth $a = 0.85 \times 10.3 = 8.76$ in. For the balanced failure condition, by definition, $f_s' = f_y$. The compressive steel stress is found from Eq. (8.12):

$$f_s' = 0.003 \times 29,000 \frac{10.3 - 2.5}{10.3} = 65.9 \text{ ksi} \quad \text{but} \quad \leq 60 \text{ ksi}$$

confirming that the compression steel, too, is at the yield. The concrete compressive resultant is

$$C = 0.85 \times 4 \times 8.76 \times 12 = 357 \text{ kips}$$

The balanced load P_b is then found from Eq. (8.7) to be

$$P_b = 357 + 2.0 \times 60 - 2.0 \times 60 = 357 \text{ kips}$$

and the balanced moment from Eq. (8.8) is

$$\begin{aligned} M_b &= 357(10 - 4.38) + 2.0 \times 60(10 - 2.5) + 2.0 \times 60(17.5 - 10) \\ &= 3806 \text{ in-kips} = 317 \text{ ft-kips} \end{aligned}$$

The corresponding eccentricity of load is $e_b = 10.66$ in.

- (b) Any choice of c smaller than $c_b = 10.3$ in. will give a point in the tension failure region of the interaction curve, with eccentricity larger than e_b . For example, choose $c = 5.0$ in. By definition, $f_s' = f_y$. The compressive steel stress is found to be

$$f_s' = 0.003 \times 29,000 \frac{5.0 - 2.5}{5.0} = 43.5 \text{ ksi}$$

With the stress-block depth $a = 0.85 \times 5.0 = 4.25$, the compressive resultant is $C = 0.85 \times 4 \times 4.25 \times 12 = 173$ kips. Then from Eq. (8.7), the thrust is

$$P_n = 173 + 2.0 \times 43.5 - 2.0 \times 60 = 140 \text{ kips}$$

and the moment capacity from Eq. (8.8) is

$$\begin{aligned} M_n &= 173(10 - 2.12) + 2.0 \times 43.5(10 - 2.5) + 2.0 \times 60(17.5 - 10) \\ &= 2916 \text{ in-kips} = 243 \text{ ft-kips} \end{aligned}$$

giving eccentricity $e = 2916/140 = 20.83$ in., well above the balanced value.

- (c) Now selecting a c value larger than c_b to demonstrate a compression failure point on the interaction curve, choose $c = 18.0$ in., for which $a = 0.85 \times 18.0 = 15.3$ in. The compressive concrete resultant is $C = 0.85 \times 4 \times 15.3 \times 12 = 624$ kips. From Eq. (8.10) the stress in the steel at the left side of the column is

$$f_s = 0.003 \times 29,000 \frac{17.5 - 18.0}{18.0} = -2 \text{ ksi}$$

Note that the negative value of f_s indicates correctly that A_s is in compression if c is greater than d , as in the present case. The compressive steel stress is found from Eq. (8.12) to be

$$f_s' = 0.003 \times 29,000 \frac{18.0 - 2.5}{18.0} = 75 \text{ ksi} \quad \text{but} \quad \leq 60 \text{ ksi}$$

Then the column capacity is

$$P_n = 624 + 2.0 \times 60 + 2.0 \times 2 = 748 \text{ kips}$$

$$\begin{aligned} M_n &= 624(10 - 7.65) + 2.0 \times 60(10 - 2.5) - 2.0 \times 2(17.5 - 10) \\ &= 2336 \text{ in-kips} = 195 \text{ ft-kips} \end{aligned}$$

giving eccentricity $e = 2336/748 = 3.12$ in.

- (d) The axial strength of the column if concentrically loaded corresponds to $c = \infty$ and $e = 0$. For this case,

$$P_n = 0.85 \times 4 \times 12 \times 20 + 4.0 \times 60 = 1056 \text{ kips}$$

Note that, for this as well as the preceding calculations, subtraction of the concrete displaced by the steel has been neglected. For comparison, if the deduction were made in the last calculation,

$$P_n = 0.85 \times 4(12 \times 20 - 4) + (4.0 \times 60) = 1042 \text{ kips}$$

The error in neglecting this deduction is only 1 percent in this case; the difference generally can be neglected, except perhaps for columns with reinforcement ratios close to the maximum of 8 percent. In the case of design aids, however, such as those presented in Refs. 8.2 and 8.7 and discussed in Section 8.10, the deduction is usually included for all reinforcement ratios.

- (e) From the calculations just completed, plus similar repetitive calculations that will not be given here, the strength interaction curve of Fig. 8.11d is constructed. Note the characteristic shape, described earlier, the location of the balanced failure point as well as the "small eccentricity" and "large eccentricity" points just found, and the axial load capacity. In the process of developing a strength interaction curve, it is possible to select the values of steel strain ϵ_s , as done in step a, for use in steps b and c. Selecting ϵ_s uniquely establishes the neutral axis depth c , as shown by Eqs. (8.9) and (8.15), and is useful in determining M_n and P_n for values of steel strain that correspond to changes in the strength reduction factor ϕ , as will be discussed in Section 8.9.
- (f) The design of the column ties will be carried out following the ACI Code restrictions. For the minimum permitted tie diameter of $\frac{3}{8}$ in., used with No. 9 (No. 29) longitudinal bars having a diameter of 1.128 in a column the least dimension of which is 12 in., the tie spacing is not to exceed

$$48 \times \frac{3}{8} = 18 \text{ in.}$$

$$16 \times 1.128 = 18.05 \text{ in.}$$

$$b = 12 \text{ in.}$$

The last restriction controls in this case, and No. 3 (No. 10) ties will be used at 12 in. spacing, detailed as shown in Fig. 8.11a. Note that the permitted spacing as controlled by the first and second criteria, 18 in., must be reduced because of the 12 in. column dimension.

8.6 DISTRIBUTED REINFORCEMENT

When large bending moments are present, it is most economical to concentrate all or most of the steel along the outer faces parallel to the axis of bending. Such arrangements are shown in Fig. 8.3e to h. On the other hand, with small eccentricities so that axial compression is predominant, and when a small cross section is desired, it is often advantageous to place the steel more uniformly around the perimeter, as in Fig. 8.3a to d. In this case, special attention must be paid to the intermediate bars, i.e., those that are not placed along the two faces that are most highly stressed. This is so because when the ultimate load is reached, the stresses in these intermediate bars are usually below the yield point, even though the bars along one or both extreme faces may be yielding. This situation can be analyzed by a simple and obvious extension of the previous analysis based on compatibility of strains. A strength interaction diagram may be constructed just as before. A sequence of

choices of neutral axis location results in a set of paired values of P_n and M_n , each corresponding to a particular eccentricity of load.

EXAMPLE 8.2

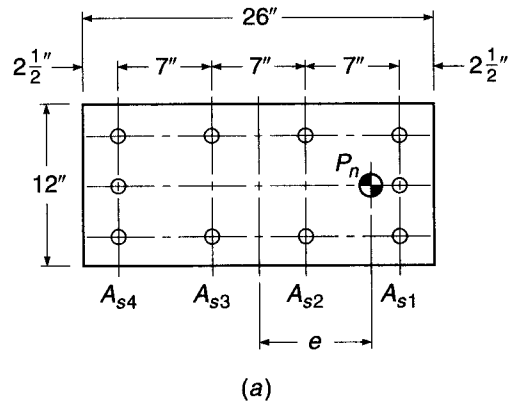
Analysis of eccentrically loaded column with distributed reinforcement. The column in Fig. 8.12a is reinforced with ten No. 11 (No. 36) bars distributed around the perimeter as shown. Load P_n will be applied with eccentricity e about the strong axis. Material strengths are $f'_c = 6000$ psi and $f_y = 75$ ksi. Find the load and moment corresponding to a failure point with neutral axis $c = 18$ in. from the right face.

SOLUTION. When the concrete reaches its limit strain of 0.003, the strain distribution is that shown in Fig. 8.12b, the strains at the locations of the four bar groups are found from similar triangles, after which the stresses are found by multiplying strains by $E_s = 29,000$ ksi applying the limit value f_y :

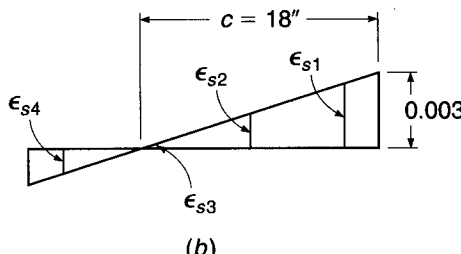
$$\begin{array}{ll} \epsilon_{s1} = 0.00258 & f_{s1} = 75.0 \text{ ksi compression} \\ \epsilon_{s2} = 0.00142 & f_{s2} = 41.2 \text{ ksi compression} \\ \epsilon_{s3} = 0.00025 & f_{s3} = 7.3 \text{ ksi compression} \\ \epsilon_{s4} = 0.00091 & f_{s4} = 26.4 \text{ ksi tension} \end{array}$$

FIGURE 8.12

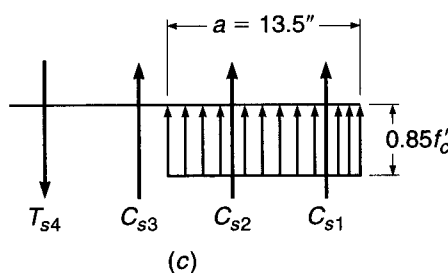
Column in Example 8.2:
(a) cross section; (b) strain distribution; (c) stresses and forces.



(a)



(b)



(c)

For $f'_c = 6000$ psi, $\beta_1 = 0.75$ and the depth of the equivalent rectangular stress block is $a = 0.75 \times 18 = 13.5$ in. The concrete compressive resultant is $C = 0.85 \times 6 \times 13.5 \times 12 = 826$ kips, and the respective steel forces in Fig. 8.12c are

$$C_{s1} = 4.68 \times 75.0 = 351 \text{ kips}$$

$$C_{s2} = 3.12 \times 41.2 = 129 \text{ kips}$$

$$C_{s3} = 3.12 \times 7.3 = 23 \text{ kips}$$

$$T_{s4} = 4.68 \times 26.4 = 124 \text{ kips}$$

The axial load and moment that would produce failure for a neutral axis 18 in. from the right face are found by the obvious extensions of Eqs. (8.7) and (8.8):

$$P_n = 826 + 351 + 129 + 23 - 124 = 1205 \text{ kips}$$

$$\begin{aligned} M_n &= 826(13 - 6.75) + 351(13 - 2.5) + 129(13 - 9.5) - 23(13 - 9.5) \\ &\quad + 124(13 - 2.5) \\ &= 10,520 \text{ in-kips} \\ &= 877 \text{ ft-kips} \end{aligned}$$

The corresponding eccentricity is $e = 10,520/1205 = 8.73$ in. Other points on the interaction diagram can be computed in a similar way.

Two general conclusions can be made from this example:

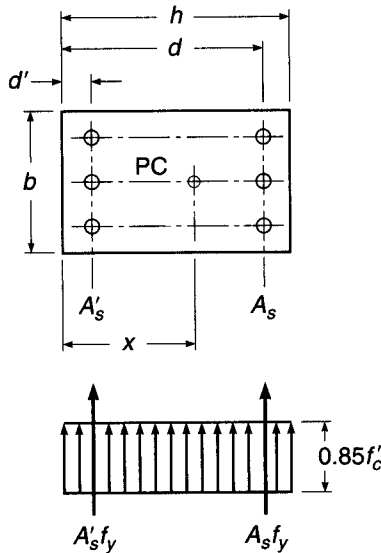
1. Even with the relatively small eccentricity of about one-third of the depth of the section, only the bars of group 1 just barely reached their yield strain, and consequently their yield stress. All other bar groups of the relatively high-strength steel that was used are stressed far below their yield strength, which would also have been true for group 1 for a slightly larger eccentricity. It follows that the use of the more expensive high-strength steel is economical in symmetrically reinforced columns only for very small eccentricities, e.g., in the lower stories of tall buildings.
2. The contribution of the intermediate bars of groups 2 and 3 to both P_n and M_n is quite small because of their low stresses. Again, intermediate bars, except as they are needed to hold ties in place, are economical only for columns with very small eccentricities.

8.7 UNSYMMETRICAL REINFORCEMENT

Most reinforced concrete columns are symmetrically reinforced about the axis of bending. However, for some cases, such as the columns of rigid portal frames in which the moments are uniaxial and the eccentricity is large, it is more economical to use an unsymmetrical pattern of bars, with most of the bars on the tension side such as shown in Fig. 8.13. Such columns can be analyzed by the same strain compatibility approach as described above. However, for an unsymmetrically reinforced column to be loaded concentrically, the load must pass through a point known as the *plastic centroid*. The plastic centroid is defined as the point of application of the resultant force for the column cross section (including concrete and steel forces) if the column is compressed uniformly to the failure strain $\epsilon_u = 0.003$ over its entire cross section. Eccentricity of the applied load must be measured with respect to the plastic centroid, because only then will $e = 0$ correspond to an axial load with no moment. The location of the plastic

FIGURE 8.13

Plastic centroid of an unsymmetrically reinforced column.



centroid for the column of Fig. 8.13 is the resultant of the three internal forces to be accounted for. Its distance from the left face is

$$x = \frac{0.85f'_c b h^2 / 2 + A_s f_y d + A'_s f_y d'}{0.85f'_c b h + A_s f_y + A'_s f_y} \quad (8.17)$$

Clearly, in a symmetrically reinforced cross section, the plastic centroid and the geometric center coincide.

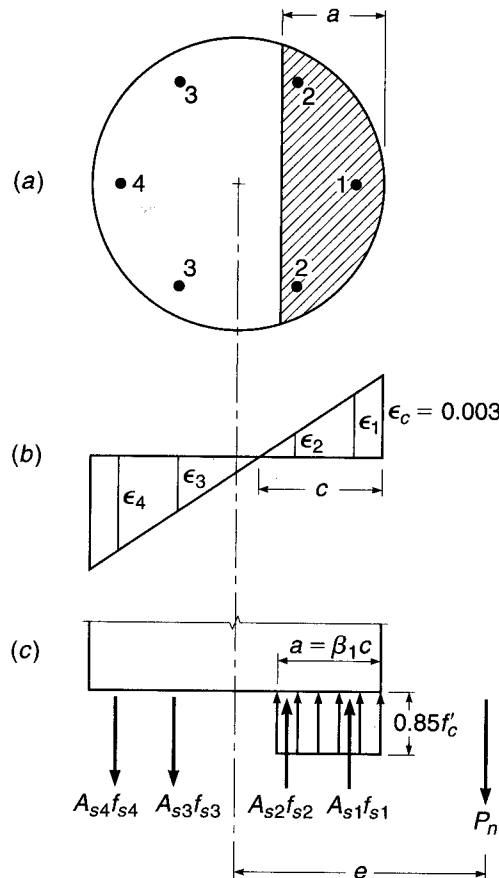
8.8 CIRCULAR COLUMNS

It was mentioned in Section 8.2 that when load eccentricities are small, spirally reinforced columns show greater toughness, i.e., greater ductility, than tied columns, although this difference fades out as the eccentricity is increased. For this reason, as discussed in Section 8.2, the ACI Code provides a more favorable reduction factor $\phi = 0.75$ for spiral columns, compared with $\phi = 0.65$ for tied columns. Also, the maximum stipulated design load for entirely or nearly axially loaded members is larger for spirally reinforced members than for comparable tied members (see Section 8.9). It follows that spirally reinforced columns permit a somewhat more economical utilization of the materials, particularly for small calculated eccentricities. A further advantage lies in the fact that the circular shape is frequently desired by the architect.

Figure 8.14 shows the cross section of a spirally reinforced column. Six or more longitudinal bars of equal size are provided for longitudinal reinforcement, depending on column diameter. The strain distribution at the instant at which the ultimate load is reached is shown in Fig. 8.14b. Bar groups 2 and 3 are seen to be strained to much smaller values than groups 1 and 4. The stresses in the four bar groups are easily found. For any of the bars with strains in excess of yield strain $\epsilon_y = f_y/E_s$, the stress at failure is evidently the yield stress of the bar. For bars with smaller strains, the stress is found from $f_s = \epsilon_s E_s$.

FIGURE 8.14

Circular column with compression plus bending.



One then has the internal forces shown in Fig. 8.14c. They must be in force and moment equilibrium with the nominal strength P_n . Note that the situation is analogous to that discussed in Sections 8.4 to 8.6 for rectangular columns. Calculations can be carried out exactly as in Example 8.1, except that for circular columns the concrete compression zone subject to the equivalent rectangular stress distribution has the shape of a segment of a circle, shown shaded in Fig. 8.14a.

Although the shape of the compression zone and the strain variation in the different groups of bars make longhand calculations awkward, no new principles are involved and computer solutions are easily developed.

Design or analysis of spirally reinforced columns is usually carried out by means of design aids, such as Graphs A.13 to A.16 of Appendix A. Additional tables and graphs are available, e.g., in Ref. 8.7. In developing such design aids, the entire steel area is often assumed to be arranged in a uniform, concentric ring, rather than being concentrated in the actual bar locations; this simplifies calculations without noticeably affecting results if the column contains at least eight longitudinal bars. When fewer bars are used, the interaction curve should be calculated based on the weakest orientation in bending.

Note that to qualify for the more favorable safety provisions for spiral columns, the reinforcement ratio of the spiral must be at least equal to that given by Eq. (8.5) for reasons discussed in Section 8.2.

8.9 ACI CODE PROVISIONS FOR COLUMN DESIGN

For columns, as for all members designed according to the ACI Code, adequate safety margins are established by applying load factors to the service loads and strength reduction factors to the nominal strengths. Thus, for columns, $\phi P_n \geq P_u$ and $\phi M_n \geq M_u$ are the basic safety criteria. For most members subject to axial compression or compression plus flexure (compression-controlled members, as described in Chapter 3), the ACI Code provides basic reduction factors:

$$\phi = 0.65 \text{ for tied columns}$$

$$\phi = 0.75 \text{ for spirally reinforced columns}$$

The spread between these two values reflects the added safety furnished by the greater toughness of spirally reinforced columns.

There are various reasons why the ϕ values for columns are lower than those for flexure or shear (0.90 and 0.75, respectively). One is that the strength of underreinforced flexural members is not much affected by variations in concrete strength, since it depends primarily on the yield strength of the steel, while the strength of axially loaded members depends strongly on the concrete compressive strength. Because the cylinder strength of concrete under site conditions is less closely controlled than the yield strength of mill-produced steel, a larger occasional strength deficiency must be allowed for. This is particularly true for columns, in which concrete, being placed from the top down in a long, narrow form, is more subject to segregation than in horizontally cast beams. Moreover, electrical and other conduits are frequently located in building columns; this reduces their effective cross sections, often to an extent unknown to the designer, even though this is poor practice and restricted by the ACI Code. Finally, the consequences of a column failure, say in a lower story, would be more catastrophic than those of a single beam failure in the same building.

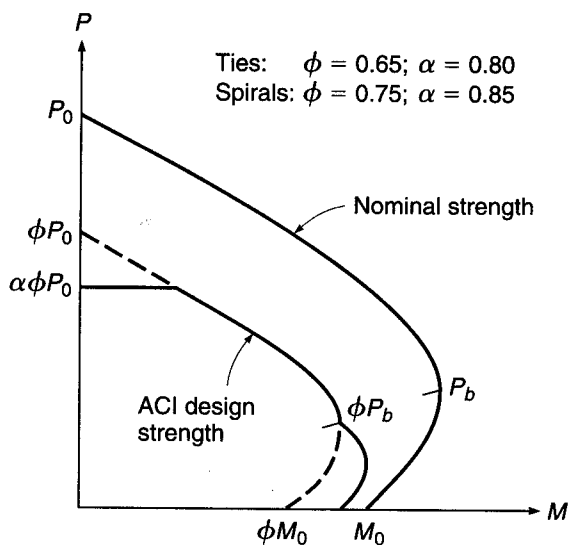
For high eccentricities, as the eccentricity increases from e_b to infinity (pure bending), the ACI Code recognizes that the member behaves progressively more like a flexural member and less like a column. As described in Chapter 3, this is acknowledged in ACI Code 9.3.2 by providing a linear transition in ϕ from values of 0.65 and 0.75 to 0.90 as the net tensile strain in the extreme tensile steel ϵ_t increases from f_y/E_s (which may be taken as 0.002 for Grade 60 reinforcement) to 0.005.

At the other extreme, for columns with very small or zero calculated eccentricities, the ACI Code recognizes that accidental construction misalignments and other unforeseen factors may produce actual eccentricities in excess of these small design values. Also, the concrete strength under high, sustained axial loads may be somewhat smaller than the short-term cylinder strength. Therefore, regardless of the magnitude of the calculated eccentricity, ACI Code 10.3.6 limits the maximum design strength to $0.80\phi P_0$ for tied columns (with $\phi = 0.65$) and to $0.85\phi P_0$ for spirally reinforced columns (with $\phi = 0.75$), where P_0 is the nominal strength of the axially loaded column with zero eccentricity [see Eq. (8.4)].

The effects of the safety provisions of the ACI Code are shown in Fig. 8.15. The solid curve labeled "nominal strength" is the same as Fig. 8.10 and represents the actual carrying capacity, as nearly as can be predicted. The smooth curve shown partially dashed, then solid, then dashed, represents the basic design strength obtained by reducing the nominal strengths P_n and M_n , for each eccentricity, by $\phi = 0.65$ for tied columns and $\phi = 0.75$ for spiral columns. The horizontal cutoff at $\alpha\phi P_0$ represents the maximum design load stipulated in the ACI Code for small eccentricities,

FIGURE 8.15

ACI safety provisions superimposed on column strength interaction diagram.



i.e., large axial loads, as just discussed. At the other end, for large eccentricities, i.e., small axial loads, the ACI Code permits a linear transition of ϕ from 0.65 or 0.75, applicable for $\epsilon_t \leq f_y/E_s$ (or 0.002 for Grade 60 reinforcement) to 0.90 at $\epsilon_t = 0.005$. By definition, $\epsilon_t = f_y/E_s$ at the balanced condition. The effect of the transition in ϕ is shown at the lower right end of the design strength curve.[†]

8.10 DESIGN AIDS

The design of eccentrically loaded columns using the strain compatibility method of analysis described requires that a trial column be selected. The trial column is then investigated to determine if it is adequate to carry any combination of P_u and M_u that may act on it should the structure be overloaded, i.e., to see if P_u and M_u from the analysis of the structure, when plotted on a strength interaction diagram such as Fig. 8.15, fall within the region bounded by the curve labeled "ACI design strength." Furthermore, economical design requires that the controlling combination of P_u and M_u be close to the limit curve. If these conditions are not met, a new column must be selected for trial.

While a simple computer program or spreadsheet can be developed, based on the strain compatibility analysis, to calculate points on the design strength curve, and even to plot the curve, for any trial column, in practice design aids are used such as are available in handbooks and special volumes published by the American Concrete Institute (Ref. 8.7) and the Concrete Reinforcing Steel Institute (Ref. 8.2). They cover the most frequent practical cases, such as symmetrically reinforced rectangular and square columns and circular spirally reinforced columns. There are also a number of commercially available computer programs (e.g., pcaCOLUMN, Portland Cement Association, Skokie, Illinois).

[†] While the general intent of the ACI Code safety provisions relating to eccentric columns is clear and fundamentally sound, the end result is a set of strangely shaped column design curves following no discernible physical law, as is demonstrated in Fig. 8.15. Improved column safety provisions, resulting in a smooth design curve appropriately related to the strength curve, would be simpler to use and more rational as well.

Graphs A.5 through A.16 of Appendix A are representative of column design charts (such as found in Ref. 8.7), in this case for concrete with $f'_c = 4000$ psi and steel with yield strength $f_y = 60$ ksi, for varying cover distances.[†] Reference 8.7 includes charts for a broad range of material strengths. Graphs A.5 through A.8 are drawn for rectangular columns with reinforcement distributed around the column perimeter; Graphs A.9 through A.12 are for rectangular columns with reinforcement along two opposite faces. Circular columns with bars in a circular pattern are shown in Graphs A.13 through A.16.

The graphs are seen to consist of nominal strength interaction curves of the type shown in Fig. 8.15. However, instead of plotting P_n versus M_n , corresponding parameters have been used to make the charts more generally applicable, i.e., load is plotted as $K_n = P_n/(f'_c A_g)$, while moment is expressed as $R_n = P_n e/(f'_c A_g h)$. Families of curves are drawn for various values of $\rho_g = A_{st}/A_g$ between 0.01 and 0.08. The graphs also include radial lines representing different eccentricity ratios e/h , as well as lines representing different ratios of stress f_s/f_y or values of strain $\epsilon_t = 0.002$ and 0.005 in the extreme tension steel.

Charts such as these permit the direct design of eccentrically loaded columns throughout the common range of strength and geometric variables. They may be used in one of two ways as follows. For a given factored load P_u and equivalent eccentricity $e = M_u/P_u$:

1. (a) Select trial cross-sectional dimensions b and h (refer to Fig. 8.9).
 (b) Calculate the ratio γ based on required cover distances to the bar centroids, and select the corresponding column design chart.
 (c) Calculate $K_n = P_u/(\phi f'_c A_g)$ and $R_n = P_u e/(\phi f'_c A_g h)$, where $A_g = bh$.
 (d) From the graph, for the values found in (c), read the required reinforcement ratio ρ_g .
 (e) Calculate the total steel area $A_{st} = \rho_g b h$.
2. (a) Select the reinforcement ratio ρ_g .
 (b) Choose a trial value of h and calculate e/h and γ .
 (c) From the corresponding graph, read $K_n = P_u/(\phi f'_c A_g)$ and calculate the required A_g .
 (d) Calculate $\bar{b} = A_g/h$.
 (e) Revise the trial value of h if necessary to obtain a well-proportioned section.
 (f) Calculate the total steel area $A_{st} = \rho_g b h$.

Use of the column design charts will be illustrated in Examples 8.3 and 8.4.

Other design aids pertaining to ties and spirals, as well as recommendations for standard practice, will be found in Refs. 8.2 and 8.7.

EXAMPLE 8.3

Selection of reinforcement for column of given size. In a three-story structure, an exterior column is to be designed for a service dead load of 222 kips, maximum live load of 297 kips, dead load moment of 136 ft-kips, and live load moment of 194 ft-kips. The minimum live load compatible with the full live load moment is 166 kips, obtained when no live load is placed on the roof but a full live load is placed on the second floor. Architectural considerations require that a rectangular column be used, with dimensions $b = 20$ in. and $h = 25$ in.

[†] Graphs A.5 through A.16 were developed for the specific bar configurations shown on the graphs. The curves exhibit changes in curvature, especially apparent near the balanced load, that result when bars within the cross section yield. The values provided in the graphs, however, are largely insensitive to the exact number of bars in the cross section and may be used for columns with similar bar configurations, but with smaller or larger numbers of bars.

- (a) Find the required column reinforcement for the condition that the full live load acts.
 (b) Check to ensure that the column is adequate for the condition of no live load on the roof. Material strengths are $f'_c = 4000$ psi and $f_y = 60,000$ psi.

SOLUTION.

(a) The column will be designed initially for full load, then checked for adequacy when live load is partially removed. According to the ACI safety provisions, the column must be designed for a factored load $P_u = 1.2 \times 222 + 1.6 \times 297 = 742$ kips and a factored moment $M_u = 1.2 \times 136 + 1.6 \times 194 = 474$ ft-kips. A column 20×25 in. is specified, and reinforcement distributed around the column perimeter will be used. Bar cover is estimated to be 2.5 in. from the column face to the steel centerline for each bar. The column parameters (assuming bending about the strong axis) are

$$K_n = \frac{P_u}{\phi f'_c A_g} = \frac{742}{0.65 \times 4 \times 500} = 0.570$$

$$R_n = \frac{M_u}{\phi f'_c A_g h} = \frac{474 \times 12}{0.65 \times 4 \times 500 \times 25} = 0.175$$

With 2.5 in. cover, the parameter $\gamma = (25 - 5)/25 = 0.80$. For this column geometry and material strengths, Graph A.7 of Appendix A applies. From that figure, with the calculated values of K_n and R_n , $\rho_g = 0.024$. Thus, the required reinforcement is $A_{st} = 0.024 \times 500 = 12.00$ in 2 . Twelve No. 9 (No. 29) bars will be used, one at each corner and two evenly spaced along each face of the column, providing $A_{st} = 12.00$ in 2 .

- (b) With the roof live load absent, the column will carry a factored load $P_u = 1.2 \times 222 + 1.6 \times 166 = 532$ kips and factored moment $M_u = 566$ ft-kips, as before. Thus, the column parameters for this condition are

$$K_n = \frac{P_u}{\phi f'_c A_g} = \frac{532}{0.65 \times 4 \times 500} = 0.409$$

$$R_n = \frac{M_u}{\phi f'_c A_g h} = \frac{474 \times 12}{0.65 \times 4 \times 500 \times 25} = 0.175$$

and $\gamma = 0.80$ as before. From Graph A.7 it is found that a reinforcement ratio of $\rho_g = 0.017$ is sufficient for this condition, less than that required in part (a), so no modification is required.

Selecting No. 3 (No. 10) ties for trial, the maximum tie spacing must not exceed $48 \times 0.375 = 18$ in., $16 \times 1.128 = 18.05$ in., or 20 in. Spacing is controlled by the diameter of the ties, and No. 3 (No. 10) ties will be used at 18 in. spacing, in the pattern shown in Fig. 8.3d.

EXAMPLE 8.4

Selection of column size for a given reinforcement ratio. A column is to be designed to carry a factored load $P_u = 481$ kips and factored moment $M_u = 492$ ft-kips. Material strengths $f_y = 60,000$ psi and $f'_c = 4000$ psi are specified. Cost studies for the particular location indicate that a reinforcement ratio ρ_g of about 0.03 is optimum. Find the required dimensions b and h of the column. Bending will be about the strong axis, and an arrangement of steel with bars concentrated in two layers, adjacent to the outer faces of the column and parallel to the axis of bending, will be used.

SOLUTION. It is convenient to select a trial column dimension h , perpendicular to the axis of bending; a value of $h = 25$ in. will be selected, and assuming a concrete cover of 2.5 in. to the bar centers, the parameter $\gamma = 0.80$. Graph A.11 of Appendix A applies. For the stated loads the eccentricity is $e = 492 \times 12/481 = 12.3$ in., and $e/h = 12.3/25 = 0.49$. From Graph A.11

with $e/h = 0.49$ and $\rho_g = 0.03$, $K_n = P_w/\phi f'_c A_g = 0.51$. For the trial dimension $h = 25$ in., the required column width is

$$b = \frac{P_u}{\phi f'_c K_n h} = \frac{481}{0.65 \times 4 \times 0.51 \times 25} = 14.5 \text{ in.}$$

A column 15×25 in. will be used, for which the required steel area is $A_{st} = 0.03 \times 15 \times 25 = 11.25 \text{ in}^2$. Eight No. 11 (No. 36) bars will be used, providing $A_{st} = 12.48 \text{ in}^2$, arranged in two layers of four bars each, similar to the sketch shown in Graph A.11.

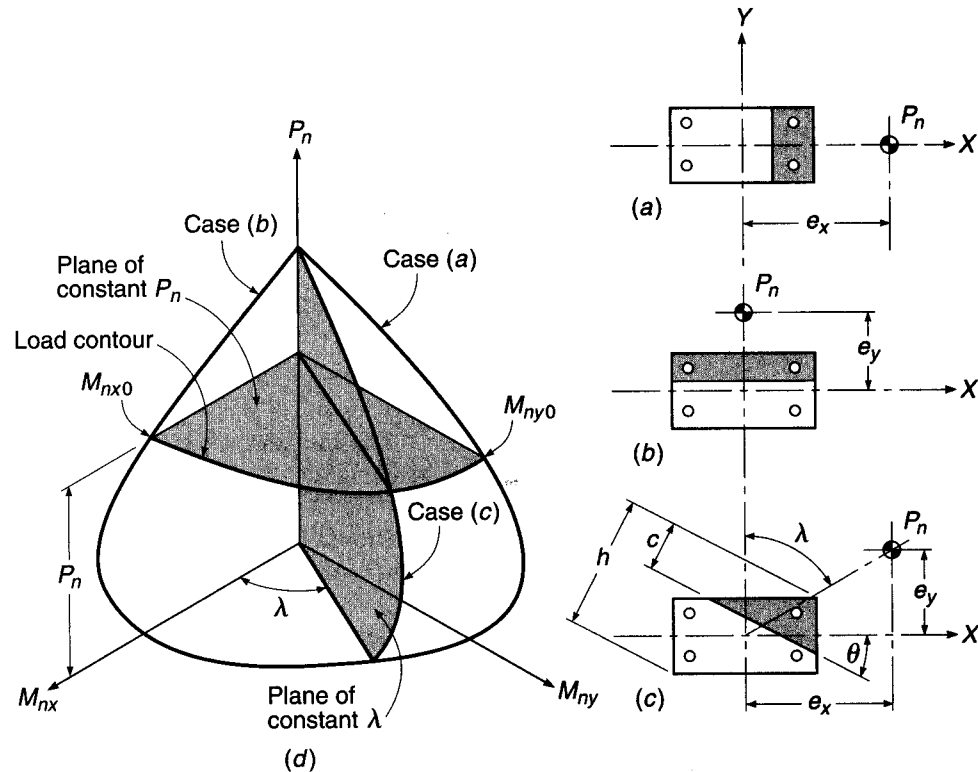
8.11 BIAXIAL BENDING

The methods discussed in the preceding sections permit rectangular or square columns to be designed if bending is present about only one of the principal axes. There are situations, by no means exceptional, in which axial compression is accompanied by simultaneous bending about both principal axes of the section. Such is the case, for instance, in corner columns of buildings where beams and girders frame into the columns in the directions of both walls and transfer their end moments into the columns in two perpendicular planes. Similar loading may occur at interior columns, particularly if the column layout is irregular.

The situation with respect to strength of biaxially loaded columns is shown in Fig. 8.16. Let X and Y denote the directions of the principal axes of the cross section. In Fig. 8.16a, the section is shown subject to bending about the Y axis only, with load

FIGURE 8.16

Interaction diagram for compression plus biaxial bending: (a) uniaxial bending about Y axis; (b) uniaxial bending about X axis; (c) biaxial bending about diagonal axis; (d) interaction surface.



eccentricity e_x measured in the X direction. The corresponding strength interaction curve is shown as case (a) in the three-dimensional sketch in Fig. 8.16d and is drawn in the plane defined by the axes P_n and M_{ny} . Such a curve can be established by the usual methods for uniaxial bending. Similarly, Fig. 8.16b shows bending about the X axis only, with eccentricity e_y measured in the Y direction. The corresponding interaction curve is shown as case (b) in the plane of P_n and M_{nx} in Fig. 8.16d. For case (c), which combines X and Y axis bending, the orientation of the resultant eccentricity is defined by the angle λ :

$$\lambda = \arctan \frac{e_x}{e_y} = \arctan \frac{M_{ny}}{M_{nx}}$$

Bending for this case is about an axis defined by the angle θ with respect to the X axis. The angle λ in Fig. 8.16c establishes a plane in Fig. 8.16d, passing through the vertical P_n axis and making an angle λ with the M_{nx} axis, as shown. In that plane, column strength is defined by the interaction curve labeled case (c). For other values of λ , similar curves are obtained to define a *failure surface* for axial load plus biaxial bending, such as shown in Fig. 8.16d. The surface is exactly analogous to the *interaction curve* for axial load plus uniaxial bending. Any combination of P_u , M_{ux} , and M_{uy} falling inside the surface can be applied safely, but any point falling outside the surface would represent failure. Note that the failure surface can be described either by a set of curves defined by radial planes passing through the P_n axis, such as shown by case (c), or by a set of curves defined by horizontal plane intersections, each for a constant P_n , defining load contours.

Constructing such an interaction surface for a given column would appear to be an obvious extension of uniaxial bending analysis. In Fig. 8.16c, for a selected value of θ , successive choices of neutral axis distance c could be taken. For each, using strain compatibility and stress-strain relations to establish bar forces and the concrete compressive resultant, then using the equilibrium equations to find P_n , M_{nx} , and M_{ny} , one can determine a single point on the interaction surface. Repetitive calculations, easily done by computer, then establish sufficient points to define the surface. The triangular or trapezoidal compression zone, such as shown in Fig. 8.16c, is a complication, and in general the strain in each reinforcing bar will be different, but these features can be incorporated.

The main difficulty, however, is that the neutral axis will not, in general, be perpendicular to the resultant eccentricity, drawn from the column center to the load P_n . For each successive choice of neutral axis, there are unique values of P_n , M_{nx} , and M_{ny} , and only for special cases will the ratio of M_{ny}/M_{nx} be such that the eccentricity is perpendicular to the neutral axis chosen for the calculation. The result is that, for successive choices of c for any given θ , the value of λ in Fig. 8.16c and d will vary. Points on the failure surface established in this way will wander up the failure surface for increasing P_n , not representing a plane intersection, as shown for case (c) in Fig. 8.16d.

In practice, the factored load P_u and the factored moments M_{ux} and M_{uy} to be resisted are known from the frame analysis of the structure. Therefore, the actual value of $\lambda = \arctan(M_{uy}/M_{ux})$ is established, and one needs only the curve of case (c), Fig. 8.16d, to test the adequacy of the trial column. An iterative computer method to establish the interaction line for the particular value of λ that applies will be described in Section 8.14.

Alternatively, simple approximate methods are widely used. These will be described in Sections 8.12 and 8.13.

8.12 LOAD CONTOUR METHOD

The load contour method is based on representing the failure surface of Fig. 8.16d by a family of curves corresponding to constant values of P_n (Ref. 8.8). The general form of these curves can be approximated by a nondimensional interaction equation

$$\left(\frac{M_{nx}}{M_{nx0}} \right)^{\alpha_1} + \left(\frac{M_{ny}}{M_{ny0}} \right)^{\alpha_2} = 1.0 \quad (8.18)$$

where

$$M_{nx} = P_n e_y$$

$$M_{nx0} = M_{nx} \quad \text{when } M_{ny} = 0$$

$$M_{ny} = P_n e_x$$

$$M_{ny0} = M_{ny} \quad \text{when } M_{nx} = 0$$

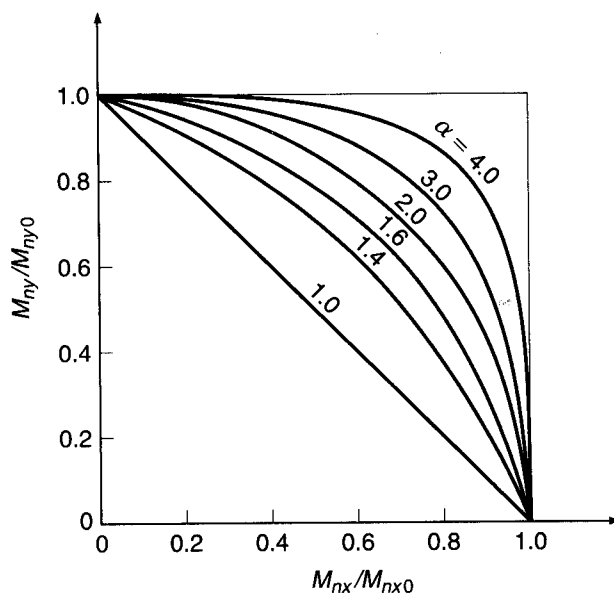
and α_1 and α_2 are exponents depending on column dimensions, amount and distribution of steel reinforcement, stress-strain characteristics of steel and concrete, amount of concrete cover, and size of lateral ties or spiral. When $\alpha_1 = \alpha_2 = \alpha$, the shapes of such interaction contours are as shown in Fig. 8.17 for specific α values.

Calculations reported by Bresler in Ref. 8.9 indicate that α falls in the range from 1.15 to 1.55 for square and rectangular columns. Values near the lower end of that range are the more conservative. Methods and design aids permitting a more defined estimation of α are found in Ref. 8.7.

In practice, the values of P_u , M_{ux} , and M_{uy} are known from the analysis of the structure. For a trial column section, the values of M_{nx0} and M_{ny0} corresponding to the load P_u/ϕ can easily be found by the usual methods for uniaxial bending. Then replacing M_{nx} with M_{ux}/ϕ and M_{ny} with M_{uy}/ϕ and using $\alpha_1 = \alpha_2 = \alpha$ in Eq. (8.18), or alternatively by plotting $(M_{nx}/\phi)/M_{nx0}$ and $(M_{ny}/\phi)/M_{ny0}$ in Fig. 8.17, it can be confirmed that a

FIGURE 8.17

Interaction contours at constant P_n for varying α .
(Adapted from Ref. 8.8.)



particular combination of factored moments falls within the load contour (safe design) or outside the contour (failure), and the design modified if necessary.

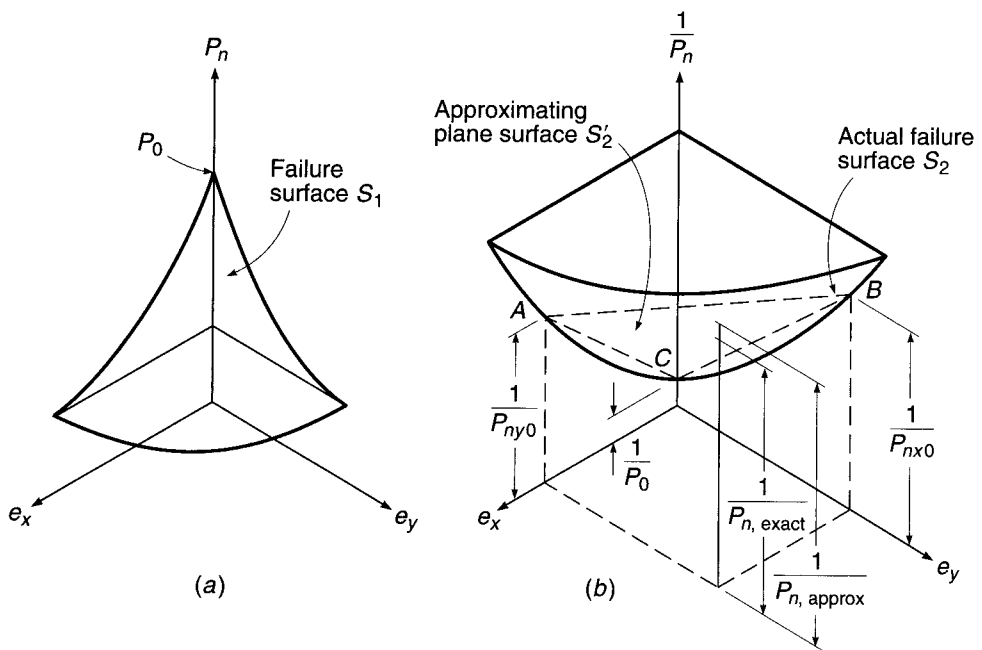
An approximate approach to the load contour method, in which the curved load contour is represented by a bilinear approximation, will be found in Ref. 8.10. It leads to a method of *trial design* in which the biaxial bending moments are represented by an equivalent uniaxial bending moment. Design charts based on this approximate approach will be found in the *ACI Design Handbook* (Ref. 8.7). Trial designs arrived at in this way should be checked for adequacy by the load contour method, described above, or by the method of reciprocal loads that follows.

8.13 RECIPROCAL LOAD METHOD

A simple, approximate design method developed by Bresler (Ref. 8.9) has been satisfactorily verified by comparison with results of extensive tests and accurate calculations (Ref. 8.11). It is noted that the column interaction surface in Fig. 8.16d can, alternatively, be plotted as a function of the axial load P_n and eccentricities $e_x = M_{ny}/P_n$ and $e_y = M_{nx}/P_n$, as is shown in Fig. 8.18a. The surface S_1 of Fig. 8.18a can be transformed into an equivalent failure surface S_2 , as shown in Fig. 8.18b, where e_x and e_y are plotted against $1/P_n$ rather than P_n . Thus, $e_x = e_y = 0$ corresponds to the inverse of the capacity of the column if it were concentrically loaded P_0 , and this is plotted as point C. For $e_y = 0$ and any given value of e_x , there is a load P_{ny0} (corresponding to moment M_{ny0}) that would result in failure. The reciprocal of this load is plotted as point A. Similarly, for $e_x = 0$ and any given value of e_y , there is a certain load P_{nx0} (corresponding to moment M_{nx0}) that would cause failure, the reciprocal of which is point B. The values of P_{nx0} and P_{ny0} are easily established, for known eccentricities of loading applied to a given column, using the methods already established for uniaxial bending, or using design charts for uniaxial bending.

FIGURE 8.18

Interaction surfaces for the reciprocal load method.



An oblique plane S'_2 is defined by the three points: A , B , and C . This plane is used as an approximation of the actual failure surface S_2 . Note that, for any point on the surface S_2 (i.e., for any given combination of e_x and e_y), there is a corresponding plane S'_2 . Thus, the approximation of the true failure surface S_2 involves an infinite number of planes S'_2 determined by particular pairs of values of e_x and e_y , i.e., by particular points A , B , and C .

The vertical ordinate $1/P_{n,\text{exact}}$ to the true failure surface will always be conservatively estimated by the distance $1/P_{n,\text{approx}}$ to the oblique plane ABC (extended), because of the concave upward eggshell shape of the true failure surface. In other words, $1/P_{n,\text{approx}}$ is always greater than $1/P_{n,\text{exact}}$, which means that $P_{n,\text{approx}}$ is always less than $P_{n,\text{exact}}$.

Bresler's reciprocal load equation derives from the geometry of the approximating plane. It can be shown that

$$\frac{1}{P_n} = \frac{1}{P_{nx0}} + \frac{1}{P_{ny0}} - \frac{1}{P_0} \quad (8.19)$$

where P_n = approximate value of nominal load in biaxial bending with eccentricities e_x and e_y

P_{ny0} = nominal load when only eccentricity e_x is present ($e_y = 0$)

P_{nx0} = nominal load when only eccentricity e_y is present ($e_x = 0$)

P_0 = nominal load for concentrically loaded column

Equation (8.19) has been found to be acceptably accurate for design purposes provided $P_n \geq 0.10P_0$. It is not reliable where biaxial bending is prevalent and accompanied by an axial force smaller than $P_0/10$. In the case of such strongly prevalent bending, failure is initiated by yielding of the steel in tension, and the situation corresponds to the lowest tenth of the interaction diagram of Fig. 8.16d. In this range, it is conservative and accurate enough to neglect the axial force entirely and to calculate the section for biaxial bending only.

Over most of the range for which the Bresler method is applicable, above $0.10P_0$, ϕ is constant, although for very small eccentricities the ACI Code imposes an upper limit on the maximum design strength that has the effect of flattening the upper part of the column strength interaction curve (see Section 8.9 and Graphs A.5 through A.16 of Appendix A). When using the Bresler method for biaxial bending, it is necessary to use the uniaxial strength curve *without* the horizontal cutoff (as shown by the lighter lines in the graphs of Appendix A) in obtaining values for use in Eq. (8.19). The value of ϕP_n obtained in this way should then be subject to the restriction, as for uniaxial bending, that it must not exceed $0.80\phi P_0$ for tied columns and $0.85\phi P_0$ for spirally reinforced columns.

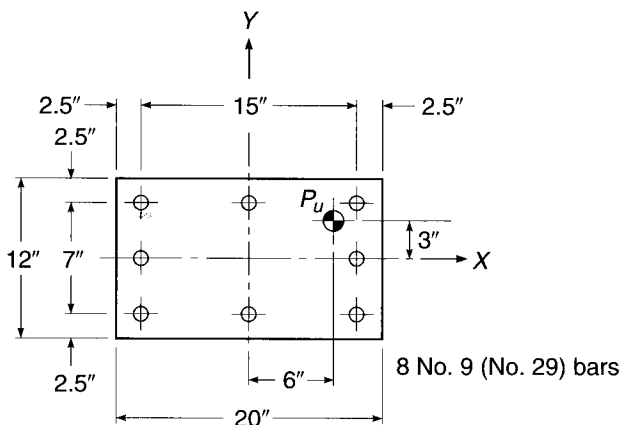
In a typical design situation, given the size and reinforcement of the trial column and the load eccentricities e_y and e_x , one finds by computation or from design charts the nominal loads P_{nx0} and P_{ny0} for uniaxial bending around the X and Y axes, respectively, and the nominal load P_0 for concentric loading. Then $1/P_n$ is computed from Eq. (8.19), and from that P_n is calculated. The design requirement is that the factored load P_u not exceed ϕP_n , as modified by the horizontal cutoff mentioned above, if applicable.

EXAMPLE 8.5

Design of column for biaxial bending. The 12×20 in. column shown in Fig. 8.19 is reinforced with eight No. 9 (No. 29) bars arranged around the column perimeter, providing an area $A_{st} = 8.00 \text{ in}^2$. A factored load P_u of 255 kips is to be applied with eccentricities $e_y = 3$ in. and

FIGURE 8.19

Column cross section for Example 8.5.



$e_x = 6$ in., as shown. Material strengths are $f'_c = 4$ ksi and $f_y = 60$ ksi. Check the adequacy of the trial design (a) using the reciprocal load method and (b) using the load contour method.

SOLUTION.

- (a) By the reciprocal load method, first considering bending about the Y axis, $\gamma = 15/20 = 0.75$, and $e/h = 6/20 = 0.30$. With the reinforcement ratio of $A_{st}/bh = 8.00/240 = 0.033$, using the average of Graphs A.6 ($\gamma = 0.70$) and A.7 ($\gamma = 0.80$),

$$\frac{P_{ny0}}{f'_c A_g} \text{ (avg)} = \frac{0.62 + 0.66}{2} = 0.64 \quad P_{ny0} = 0.64 \times 4 \times 240 = 614 \text{ kips}$$

$$\frac{P_0}{f'_c A_g} = 1.31 \quad P_0 = 1.31 \times 4 \times 240 = 1258 \text{ kips}$$

Then for bending about the X axis, $\gamma = \frac{7}{12} = 0.58$ (say 0.60), and $e/h = \frac{3}{12} = 0.25$. Graph A.5 of Appendix A gives

$$\frac{P_{nx0}}{f'_c A_g} = 0.65 \quad P_{nx0} = 0.65 \times 4 \times 240 = 624 \text{ kips}$$

$$\frac{P_0}{f'_c A_g} = 1.31 \quad P_0 = 1.31 \times 4 \times 240 = 1258 \text{ kips}$$

Substituting these values in Eq. (8.19) results in

$$\frac{1}{P_n} = \frac{1}{624} + \frac{1}{614} - \frac{1}{1258} = 0.00244$$

from which $P_n = 410$ kips. Thus, according to the Bresler method, the design load of $P_u = 0.65 \times 410 = 267$ kips can be applied safely.

- (b) By the load contour method, for Y axis bending with $P_u/(\phi f'_c A_g) = 255/(0.65 \times 4 \times 240) = 0.41$. The average from Graphs A.6 and A.7 of Appendix A is

$$\frac{M_{ny0}}{f'_c A_g h} \text{ (avg)} = \frac{0.212 + 0.235}{2} = 0.224$$

Hence, $M_{ny0} = 0.224 \times 4 \times 240 \times 20 = 4300$ in-kips. Then for X axis bending, with $P_u/(\phi f'_c A_g) = 0.41$, as before, from Graph A.5,

$$\frac{M_{nx0}}{f'_c A_g h} = 0.186$$

So $M_{nx0} = 0.186 \times 4 \times 240 \times 12 = 2140$ in-kips. The factored load moments about the Y and X axes, respectively, are

$$M_{uy} = 255 \times 6 = 1530 \text{ in-kips}$$

$$M_{ux} = 255 \times 3 = 765 \text{ in-kips}$$

Adequacy of the trial design will now be checked using Eq. (8.18) with an exponent α conservatively taken equal to 1.15. Then with $M_{nx} = M_{ux}/\phi$ and $M_{ny} = M_{uy}/\phi$, that equation indicates

$$\left(\frac{765/0.65}{2140} \right)^{1.15} + \left(\frac{1530/0.65}{4300} \right)^{1.15} = 0.502 + 0.500 = 1.002$$

This is close enough to 1.0 that the design would be considered safe by the load contour method also.

In actual practice, the values of α used in Eq. (8.18) should be checked, for the specific column, because predictions of that equation are quite sensitive to changes in α . In Ref. 8.10, it is shown that $\alpha = \log 0.5/\log \beta$, where values of β can be tabulated for specific column geometries, material strengths, and load ranges (see Ref. 8.7). For the present example, it can be confirmed from Ref. 8.7 that $\beta = 0.56$ and hence $\alpha = 1.19$, approximately as chosen.

One observes that, in Example 8.5a, an eccentricity in the Y direction equal to 50 percent of that in the X direction causes a reduction in nominal capacity of 33 percent, i.e., from 614 to 410 kips. For cases in which the ratio of eccentricities is smaller, there is some justification for the frequent practice in framed structures of neglecting the bending moments in the direction of the smaller eccentricity. *In general, biaxial bending should be taken into account when the estimated eccentricity ratio approaches or exceeds 0.2.*

8.14 COMPUTER ANALYSIS FOR BIAXIAL BENDING OF COLUMNS

Although the load contour method and the reciprocal load method are widely used in practice, each has serious shortcomings. With the load contour method, selection of the appropriate value of the exponent α is made difficult by a number of factors relating to column shape and bar distribution. For many cases, the usual assumption that $\alpha_1 = \alpha_2$ is a poor approximation. Design aids are available, but they introduce further approximations, e.g., the use of a bilinear representation of the load contour. The reciprocal load method is very simple to use, but the representation of the curved failure surface by an approximating plane is not reliable in the range of large eccentricities, where failure is initiated by steel yielding.

With the general availability and wide use of computers, it is better to use simpler methods to obtain faster, and more exact, solutions to the biaxial column problem. Such a method is that developed by Ehsani (Ref. 8.12). A column strength interaction curve is established for a trial column, exactly analogous to the curve for axial load plus uniaxial bending, as described in Sections 8.3 to 8.7. However, the curve is generated for the particular value of the eccentricity angle that applies, as determined by the ratio of M_{uy}/M_{ux} from the structural frame analysis [see case (c) of Fig. 8.16d]. This is done by taking successive choices of neutral axis distance, measured in this case along one face of the column from the most heavily compressed corner, from

very small (large eccentricity) to very large (small eccentricity), then calculating the axial force P_n and moments M_{nx} and M_{ny} . For each neutral axis distance, iteration is performed with successive values of the orientation angle θ , Fig. 8.16c, until $\lambda = \arctan(M_{ny}/M_{nx})$ is in agreement with the value of $\lambda = \arctan(M_{uy}/M_{ux})$ from the structural frame analysis. Thus, one point on curve (c) of Fig. 8.16d is established. The sequence of calculations is repeated: another choice of neutral axis distance is made, a value of θ is selected, the axial force and moments are calculated, λ is found, and the value of θ is iterated until λ is correct. Thus, the next point is established, and so on, until the complete strength interaction curve for that particular value of λ is complete. ACI Code safety provisions may then be imposed in the usual way, and the adequacy of the proposed design tested, for the known load and moments, against the design strength curve for the trial column.

The method is obviously impractical for manual calculation, but the iterative steps are easily and quickly performed by computer, which can also provide a graphical presentation of results. Full details will be found in Ref. 8.12.

A number of computer programs for biaxial bending are available commercially, such as pcaCOLUMN (Portland Cement Association, Skokie, Illinois).

8.15 BAR SPLICING IN COLUMNS

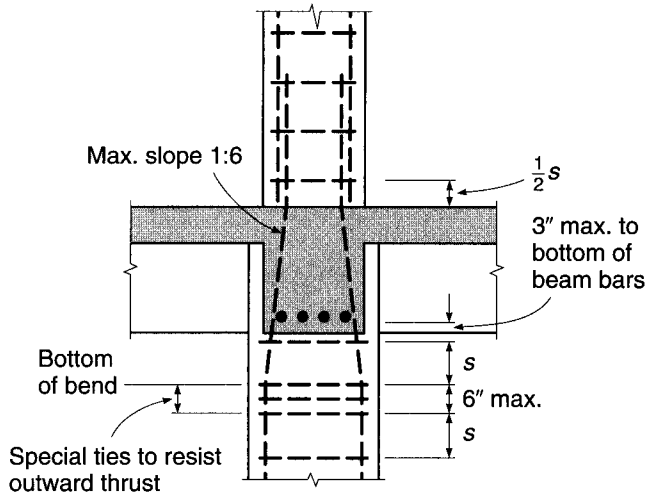
The main vertical reinforcement in columns is usually spliced just above each floor, or sometimes at alternate floors. This permits the column steel area to be reduced progressively at the higher levels in a building, where loads are smaller, and in addition avoids handling and supporting very long column bars. Column steel may be spliced by lapping, by butt welding, by various types of mechanical connections, or by direct end bearing, using special devices to ensure proper alignment of bars.

Special attention must be given to the problem of bar congestion at splices. Lapping the bars, for example, effectively doubles the steel area in the column cross section at the level of the splice and can result in problems placing concrete and meeting the ACI Code requirement for minimum lateral spacing of bars ($1.5d_b$ or 1.5 in.). To avoid difficulty, column steel percentages are often limited in practice to not more than about 4 percent, or the bars are extended two stories and staggered splices are used.

The most common method of splicing column steel is the simple lapped bar splice, with the bars in contact throughout the lapped length. It is standard practice to offset the lower bars, as shown in Fig. 8.20, to permit the proper positioning of the upper bars. To prevent outward buckling of the bars at the bottom bend point of such an offset, with spalling of the concrete cover, it is necessary to provide special lateral reinforcement in the form of extra ties. According to ACI Code 7.8.1, the slope of the inclined part of an offset bar must not exceed 1 in 6, and lateral steel must be provided to resist $1\frac{1}{2}$ times the horizontal component of the computed force in the inclined part of the offset bar. This special reinforcement must be placed not more than 6 in. from the point of bend, as shown in Fig. 8.20. Elsewhere in the column, above and below the floor, the usual spacing requirements described in Section 8.2 apply, except that ties must be located not more than one-half the normal spacing s above the floor. Where beams frame from four directions into a joint, as shown in Fig. 8.20, ties may be terminated not more than 3 in. below the lowest reinforcement in the shallowest of such beams, according to ACI Code 7.10.5. If beams are not present on four sides, such as for exterior columns, ties must be placed vertically at the usual spacing through the depth of the joint to a level not more than one-half the usual spacing s below the lowest reinforcement in the slab.

FIGURE 8.20

Splice details at typical interior column.



Analogous requirements are found in ACI Code 7.10.4 and are illustrated in Ref. 8.1 for spirally reinforced columns.

As discussed in Section 5.11, in frames subjected to lateral loading, a viable alternative to splicing bars just above the floor is to splice them in the center half of the column height, where the moment due to lateral loading is much lower than at floor level. Splicing near midheight is mandatory in “special moment frames” designed for seismic loading (Chapter 20). The use of midheight splices removes the requirement for the special ties shown in Fig. 8.20 because bent bars are not used.

Column splices are mainly compression splices, although load combinations producing moderate to large eccentricity require that splices transmit tension as well. ACI Code 12.17 permits splicing by lapping, butt welding, mechanical connectors, or end bearing. As discussed in Section 5.13, the length of compression lap splices may be reduced in cases where ties or spiral reinforcement throughout the lap length meets specific requirements. If the column bars are in tension, Class A tension lap splices are permitted if the tensile stress does not exceed $0.5f_y$ and less than one-half of the bars are spliced at any section. Class B tension splices are required if the tensile stresses are higher than $0.5f_y$ under factored loads or where more than one-half of the reinforcement is spliced at one location. When end bearing splices are used, they must be staggered or additional reinforcement must be added so that the continuing bars on each column face possess a tensile strength not less than $0.25f_y$ times the area of the vertical reinforcement on that face.

Full requirements for both compression and tension lap splices are discussed in Section 5.13, and the design of a compression splice in a typical column is illustrated in Example 5.5.

8.16 TRANSMISSION OF COLUMN LOADS THROUGH FLOOR SYSTEMS

Quite often, the specified compressive strength of the concrete in columns will exceed that of the floor system. This is especially true for the lower stories in high-rise buildings, where high-strength concrete is used to minimize the cross-sectional area of the

columns and thus maximize the usable floor space. High-strength concrete, however, is not needed for the beams and slabs that make up the floor system.

Floor systems and columns must be cast in separate placements. This not only is good construction practice to allow the concrete in the columns to settle prior to placement of the floor system, but also is required by ACI Code 6.4.6 to prevent cracking at the interface between the floor and the column that would occur if the floor and supporting members were cast at the same time. This standard practice, however, opens the possibility for placement of lower-strength concrete within the portion of a floor system that directly supports the columns above, which would, in turn, significantly reduce their capacity. The high lateral confinement provided by the floor system to the concrete in the vicinity of the column does have a mitigating effect because it places that region in triaxial compression and thus increases its usable compressive strength, as explained in Section 2.10.

To address the effects on performance of using concretes with significantly different compressive strengths in the columns and floor system, ACI Code 10.12 specifies that if f'_c of the column exceeds 1.4 times that of the floor system, one of three requirements must be met:

1. At the time of concrete placement in the floor system, concrete with the strength specified for the column must be placed in the floor at the column location. The concrete must extend 2 ft into the surrounding slab from the face of the column and be well integrated with the floor concrete.
2. The strength of the column through the floor system must be based on the lower compressive strength of the floor concrete. Additional reinforcement may be required.
3. For columns that are laterally supported on four sides by beams of approximately the same depth or by slabs, the strength of the column may be based on a compressive strength equal to 75 percent of the column concrete strength plus 35 percent of the floor concrete strength. The ratio of the column concrete strength to the slab concrete strength may not be taken greater than 2.5 for use in design.

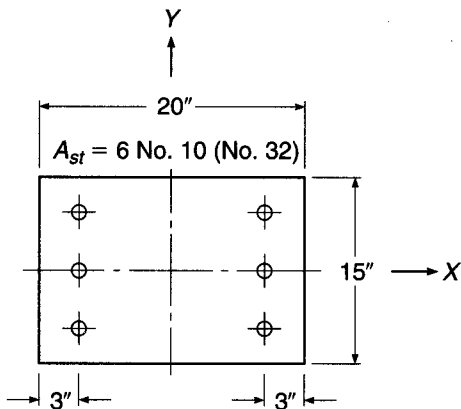
REFERENCES

- 8.1. *ACI Detailing Manual*, SP-66, American Concrete Institute, Farmington Hills, MI, 2004.
- 8.2. *CRSI Design Handbook*, 10th ed., Concrete Reinforcing Steel Institute, Schaumburg, IL, 2008.
- 8.3. F. E. Richart, A. Brandtzaeg, and R. L. Brown, "A Study of the Failure of Concrete under Combined Compressive Stresses," *Univ. Ill. Eng. Exp. Stn. Bull.* 185, 1928.
- 8.4. F. E. Richart, A. Brandtzaeg, and R. L. Brown, "The Failure of Plain and Spirally Reinforced Concrete in Compression," *Univ. Ill. Eng. Exp. Stn. Bull.* 190, 1929.
- 8.5. S. Martinez, A. H. Nilson, and F. O. Slate, "Spirally Reinforced High Strength Concrete Columns," *J. ACI*, vol. 81, no. 5, 1984, pp. 431–442.
- 8.6. A. H. Mattock, L. B. Kriz, and E. Hognestad, "Rectangular Concrete Stress Distribution in Ultimate Strength Design," *J. ACI*, vol. 32, no. 8, 1961, pp. 875–928.
- 8.7. *ACI Design Handbook*, SP-17, American Concrete Institute, Farmington Hills, MI, 1997.
- 8.8. F. N. Pannell, "Failure Surfaces for Members in Compression and Biaxial Bending," *J. ACI*, vol. 60, no. 1, 1963, pp. 129–140.
- 8.9. B. Bresler, "Design Criteria for Reinforced Columns under Axial Load and Biaxial Bending," *J. ACI*, vol. 32, no. 5, 1960, pp. 481–490.
- 8.10. A. L. Parme, J. M. Nieves, and A. Gouwens, "Capacity of Reinforced Concrete Rectangular Members Subject to Biaxial Bending," *J. ACI*, vol. 63, no. 9, 1966, pp. 911–923.
- 8.11. L. N. Ramamurthy, "Investigation of the Ultimate Strength of Square and Rectangular Columns under Biaxially Eccentric Loads," in *Symp. Reinforced Concrete Columns*, SP-13, American Concrete Institute, Detroit, MI, 1966, pp. 263–298.
- 8.12. M. R. Ehsani, "CAD for Columns," *Concr. Int'l.*, vol. 8, no. 9, 1986, pp. 43–47.

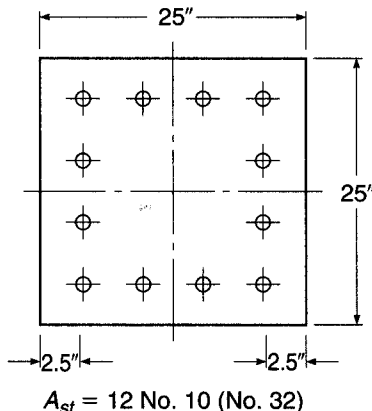
PROBLEMS

- 8.1.** A 16 in. square column is reinforced with four No. 14 (No. 43) bars, one in each corner, with cover distances 3 in. to the steel center in each direction. Material strengths are $f'_c = 5000$ psi and $f_y = 60,000$ psi. Construct the interaction diagram relating axial strength P_n and flexural strength M_n . Bending will be about an axis parallel to one face. Calculate the coordinates for P_o , P_b , and at least three other representative points on the curve.
- 8.2.** Starting with the column in Problem 8.1, perform enough additional calculations to determine the effects of increasing f'_c from 5000 to 8000 psi on column capacity at both high and low axial loads. Assuming that a compressive strength of 8000 psi is appropriate for the lower stories of a high-rise structure, would you recommend using concrete with $f'_c = 8000$ psi for the columns supporting all stories within the building? Use your analysis to support your answer.
- 8.3.** Plot the design strength curve relating ϕP_n and ϕM_n for the column of Problem 8.1. Design and detail the tie steel required by the ACI Code. Is the column a good choice to resist a load $P_u = 540$ kips applied with an eccentricity $e = 4.44$ in.?
- 8.4.** The short column shown in Fig. P8.4 will be subjected to an eccentric load causing uniaxial bending about the Y axis. Material strengths are $f_y = 60$ ksi and $f'_c = 4$ ksi.
- Construct the nominal strength interaction curve for this column, calculating no fewer than five points, including those corresponding to pure bending, pure axial thrust, and balanced failure.
 - Compare the calculated values with those obtained using Graph A.10 in Appendix A.
 - Show on the same drawing the design strength curve obtained through introduction of the ACI ϕ factors.
 - Design the lateral reinforcement for the column, giving key dimensions for ties.

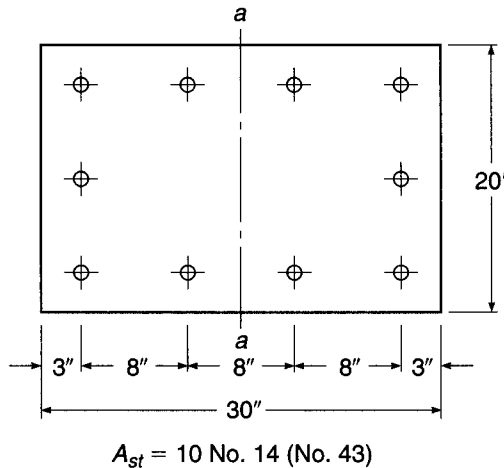
FIGURE P8.4



- 8.5.** The column shown in Fig. P8.5 is subjected to axial load and bending moment, causing bending about an axis parallel to that of the rows of bars. What moment M_n would cause the column to fail if the axial load P_n applied simultaneously was 1250 kips? Material strengths are $f'_c = 4000$ psi and $f_y = 60$ ksi.

FIGURE P8.5

- 8.6. What is the strength M_n of the column of Problem 8.5 if it was loaded in pure bending (axial force = 0) about one principal axis?
- 8.7. Construct the interaction diagram relating P_n to M_n for the building column shown in Fig. P8.7. Bending will be about the axis $a-a$. Calculate specific coordinates for concentric loading ($e = 0$), for P_b , and at least three other points, well chosen, on the curve. Material strengths are $f'_c = 8000$ psi and $f_y = 60,000$ psi.

FIGURE P8.7

- 8.8. A short rectangular reinforced concrete column shown in Fig. P8.8 is to be a part of a long-span rigid frame and will be subjected to high bending moments combined with relatively low axial loads, causing bending about the strong axis. Because of the high eccentricity, steel is placed unsymmetrically as shown, with three No. 14 (No. 43) bars near the tension face and two No. 11 (No. 36) bars near the compression face. Material strengths are $f'_c = 6$ ksi and $f_y = 75$ ksi. Construct the complete strength interaction diagram, plotting P_n vs. M_n , relating eccentricities to the plastic centroid of the column (not the geometric center).

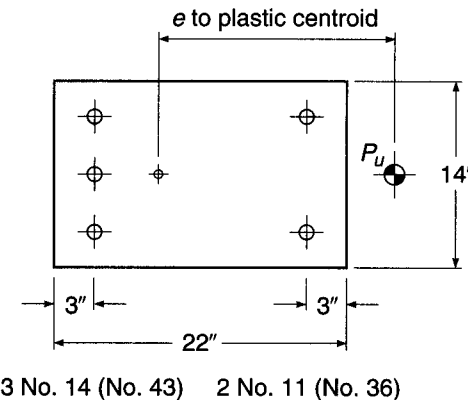


FIGURE P8.8

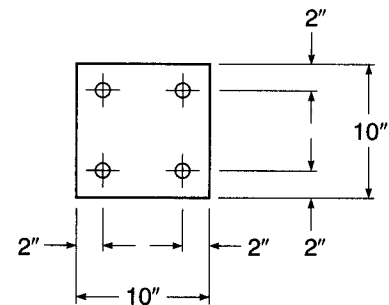


FIGURE P8.9

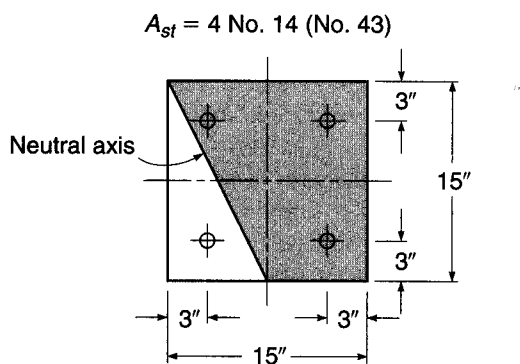
- 8.9.** The square column shown in Fig. P8.9 must be designed for a factored axial load of 130 kips. Material strengths are $f'_c = 4000$ psi and $f_y = 60,000$ psi.

- Select the longitudinal and transverse reinforcement for an eccentricity $e_y = 2.7$ in.
- Select the longitudinal and transverse reinforcement for the same axial load with $e_x = e_y = 2.7$ in.
- Construct the strength interaction diagram and design strength curves for the column designed in part (b), given that the column will be subjected to biaxial bending with equal eccentricities about both principal axes.

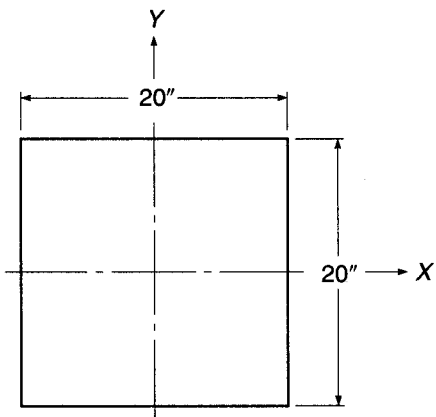
- 8.10.** The square column shown in Fig. P8.10 is a corner column subject to axial load and biaxial bending. Material strengths are $f_y = 60,000$ psi and $f'_c = 4000$ psi.

- Find the unique combination of P_n , M_{nx} , and M_{ny} that will produce incipient failure with the neutral axis located as in the figure. The compressive zone is shown shaded. Note that the actual neutral axis is shown, not the equivalent rectangular stress block limit; however, the rectangular stress block may be used as the basis of calculations.
- Find the angle between the neutral axis and the eccentricity axis, the latter defined as the line from the column center to the point of load.

FIGURE P8.10



- 8.11.** For the axial load P_n found in Problem 8.10, and for the same column, with the same eccentricity ratio e_y/e_x , find the values of M_{nx} and M_{ny} that would produce incipient failure, using the load contour method. Compare with the results of Problem 8.10. Take $\alpha = 1.30$, and use the graphs in Appendix A, as appropriate.
- 8.12.** For the eccentricities e_x and e_y found in Problem 8.10, find the value of axial load P_n that would produce incipient failure, using the reciprocal load (Bresler) method. Use the graphs in Appendix A, as appropriate. Compare with the results of Problems 8.10 and 8.11.
- 8.13.** A 20 in. square lower-story interior building column must be designed for maximum and minimum factored axial loads P_u of 880 and 551 kips, respectively. For both values of P_u , the column will be subjected to simultaneous factored bending moments M_u of 295 and 24 ft-kips about the Y and X axes, respectively (Fig. P8.13). Material strengths are $f_y = 60,000$ psi and $f'_c = 4000$ psi. Using equal reinforcement on all sides, design the longitudinal and transverse reinforcement for this column.

FIGURE P8.13

- 8.14.** A 16 in. square lower-story corner column in the building described in Problem 8.13 will be subjected to maximum and minimum factored axial loads P_u of 209 and 130 kips, respectively. For both values of P_u , the columns must be designed for simultaneous factored bending moments M_u of 110 and 104 ft-kips about the Y and X axes, respectively. Using equal reinforcement on all sides, design the longitudinal and transverse reinforcement for this column.

9

Slender Columns

9.1 INTRODUCTION

The material presented in Chapter 8 pertained to concentrically or eccentrically loaded *short columns*, for which the strength is governed entirely by the strength of the materials and the geometry of the cross section. Most columns in present-day practice fall in that category. However, with the increasing use of high-strength materials and improved methods of dimensioning members, it is now possible, for a given value of axial load, with or without simultaneous bending, to design a much smaller cross section than in the past. This clearly makes for more slender members. It is because of this, together with the use of more innovative structural concepts, that rational and reliable design procedures for slender columns have become increasingly important.

A column is said to be *slender* if its cross-sectional dimensions are small compared with its length. The degree of slenderness is generally expressed in terms of the slenderness ratio l/r , where l is the unsupported length of the member and r is the radius of gyration of its cross section, equal to $\sqrt{I/A}$. For square or circular members, the value of r is the same about either axis; for other shapes r is smallest about the minor principal axis, and it is generally this value that must be used in determining the slenderness ratio of a freestanding column.

It has long been known that a member of great slenderness will collapse under a smaller compression load than a stocky member with the same cross-sectional dimensions. When a stocky member, say with $l/r = 10$ (e.g., a square column of length equal to about 3 times its cross-sectional dimension h), is loaded in axial compression, it will fail at the load given by Eq. (8.3), because at that load both concrete and steel are stressed to their maximum carrying capacity and give way, respectively, by crushing and by yielding. If a member with the same cross section has a slenderness ratio $l/r = 100$ (e.g., a square column hinged at both ends and of length equal to about 30 times its section dimension), it may fail under an axial load equal to one-half or less of that given by Eq. (8.3). In this case, collapse is caused by buckling, i.e., by sudden lateral displacement of the member between its ends, with consequent overstressing of steel and concrete by the bending stresses that are superimposed on the axial compressive stresses.

Most columns in practice are subjected to bending moments as well as axial loads, as was made clear in Chapter 8. These moments produce lateral deflection of a member between its ends and may also result in relative lateral displacement of joints. Associated with these lateral displacements are *secondary moments* that add to the primary moments and that may become very large for slender columns, leading to failure. A practical definition of a slender column is one for which there

is a significant reduction in axial load capacity because of these secondary moments. In the development of ACI Code column provisions, for example, any reduction greater than about 5 percent is considered significant, requiring consideration of slenderness effects.

The ACI Code and Commentary contain detailed provisions governing the design of slender columns. ACI Code 10.10.5, 10.10.6, and 10.10.7 present approximate methods for accounting for slenderness through the use of *moment magnification factors*. The provisions are quite similar to those used for many years for steel columns designed under the American Institute of Steel Construction (AISC) Specification. Alternatively, in ACI Code 10.10.3 and 10.10.4, a more fundamental approach is endorsed, in which the effect of lateral displacements is accounted for directly in the frame analysis. The latter approach, known as *second-order analysis*, is often incorporated as a feature in commercially available structural analysis software.

As noted, most columns in practice continue to be short columns. Simple expressions are included in the ACI Code to determine whether slenderness effects must be considered. These will be presented in Section 9.4 following the development of background information in Sections 9.2 and 9.3 relating to column buckling and slenderness effects.

9.2 CONCENTRICALLY LOADED COLUMNS

The basic information on the behavior of straight, concentrically loaded slender columns was developed by Euler more than 200 years ago. In generalized form, it states that such a member will fail by buckling at the critical load

$$P_c = \frac{\pi^2 E I}{(kl)^2} \quad (9.1)$$

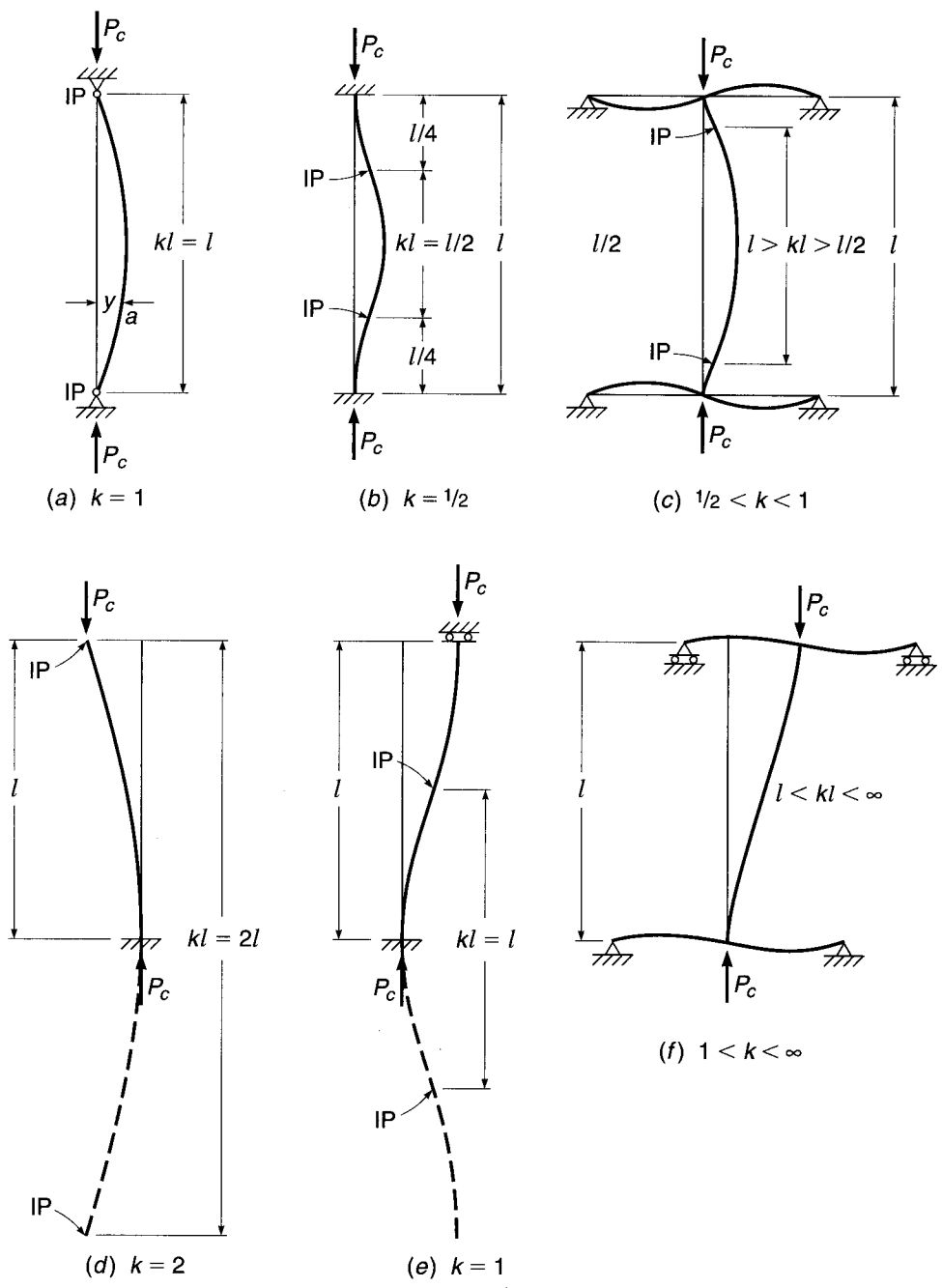
It is seen that the buckling load decreases rapidly with increasing *slenderness ratio* kl/r (Ref. 9.1).

For the simplest case of a column hinged at both ends and made of elastic material, E , simply becomes Young's modulus and kl is equal to the actual length l of the column. At the load given by Eq. (9.1), the originally straight member buckles into a half sine wave, as shown in Fig. 9.1a. In this bent configuration, bending moments P_y act at any section such as a ; y is the deflection at that section. These deflections continue to increase until the bending stress caused by the increasing moment, together with the original compression stress, overstresses and fails the member.

If the stress-strain curve of a short piece of the given member has the shape shown in Fig. 9.2a, as it would be for reinforced concrete columns, E_t is equal to Young's modulus, provided that the buckling stress P_c/A is below the proportional limit f_p . If the strain is larger than f_p , buckling occurs in the inelastic range. In this case, in Eq. (9.1), E_t is the tangent modulus, i.e., the slope of the tangent to the stress-strain curve. As the stress increases, E_t decreases. A plot of the buckling load vs. the slenderness ratio, the so-called column curve, therefore has the shape given in Fig. 9.2b, which shows the reduction in buckling strength with increasing slenderness. For very stocky columns, the value of the buckling load, calculated from Eq. (9.1), exceeds the direct crushing strength of the stocky column P_n , given by Eq. (8.3). This is also shown in Fig. 9.2b. Correspondingly, there is a limiting slenderness ratio $(kl/r)_{lim}$. For values smaller than this, failure occurs by simple crushing, regardless of

FIGURE 9.1

Buckling and effective length of axially loaded columns.

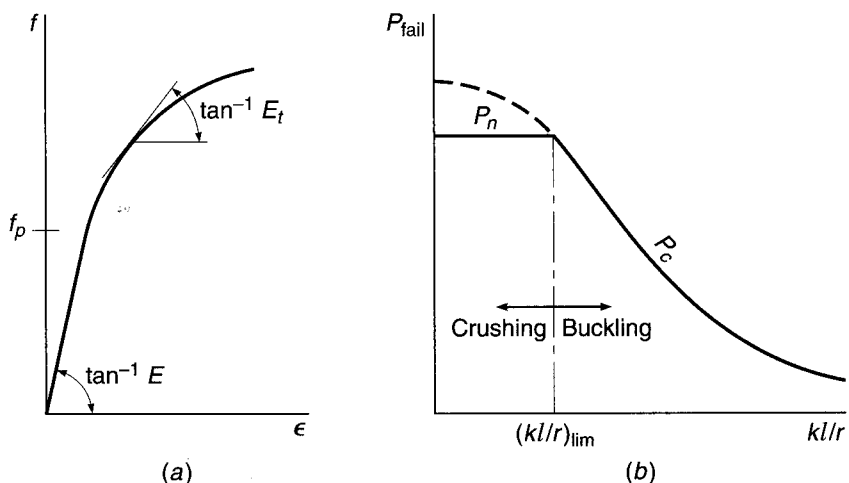


kl/r ; for values larger than $(kl/r)_{\text{lim}}$, failure occurs by buckling, the buckling load or stress decreasing for greater slenderness.

If a member is fixed against rotation at both ends, it buckles in the shape of Fig. 9.1b, with inflection points (IPs) as shown. The portion between the inflection points is in precisely the same situation as the hinge-ended column of Fig. 9.1a, and thus, the *effective length* kl of the fixed-fixed column, i.e., the distance between inflection points, is seen to be $kl = l/2$. Equation (9.1) shows that an elastic column fixed at both ends will carry 4 times as much load as when hinged.

FIGURE 9.2

Effect of slenderness on strength of axially loaded columns.



Columns in real structures are rarely either hinged or fixed but have ends partially restrained against rotation by abutting members. This is shown schematically in Fig. 9.1c, from which it is seen that for such members the effective length kl , i.e., the distance between inflection points, has a value between l and $l/2$. The precise value depends on the degree of end restraint, i.e., on the ratio of the stiffness EI/l of the column to the sum of stiffnesses EI/l of the restraining members at both ends.

In the columns of Fig. 9.1a to c, it was assumed that one end was prevented from moving laterally relative to the other end, by horizontal bracing or otherwise. In this case, it is seen that the effective length kl is always smaller than (or at most it is equal to) the real length l .

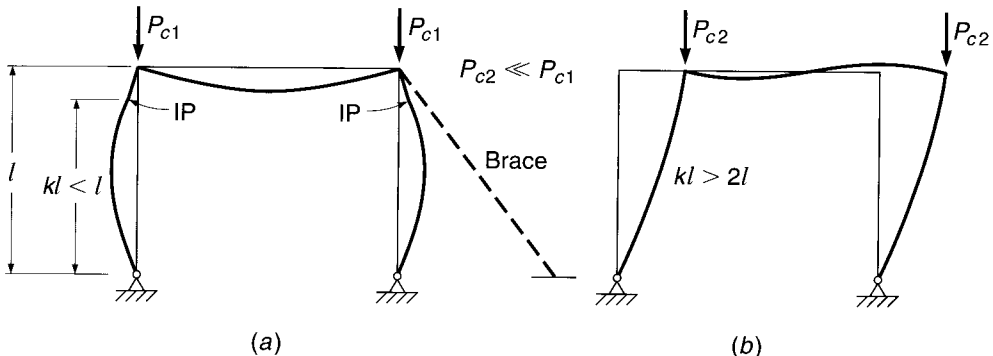
If a column is fixed at one end and entirely free at the other (cantilever column or flagpole), it buckles as shown in Fig. 9.1d. That is, the upper end moves laterally with respect to the lower, a kind of deformation known as *sidesway*. It buckles into a quarter of a sine wave and is therefore analogous to the upper half of the hinged column in Fig. 9.1a. The inflection points, one at the end of the actual column and the other at the imaginary extension of the sine wave, are a distance $2l$ apart, so that the effective length is $kl = 2l$.

If the column is rotationally fixed at both ends but one end can move laterally with respect to the other, it buckles as shown in Fig. 9.1e, with an effective length $kl = l$. If one compares this column, fixed at both ends but free to sidesway, with a fixed-fixed column that is braced against sidesway (Fig. 9.1b), one sees that the effective length of the former is twice that of the latter. By Eq. (9.1), this means that the buckling strength of an elastic fixed-fixed column that is free to sidesway is only one-quarter that of the same column when braced against sidesway. This is an illustration of the general fact that *compression members free to buckle in a sidesway mode are always considerably weaker than when braced against sidesway*.

Again, the ends of columns in actual structures are rarely hinged, fixed, or entirely free but are usually restrained by abutting members. If sidesway is not prevented, buckling occurs as shown in Fig. 9.1f, and the effective length, as before, depends on the degree of restraint. If the cross beams are very rigid compared with the column, the case of Fig. 9.1e is approached and kl is only slightly larger than l . On the other hand, if the restraining members are extremely flexible, a hinged condition is approached at both ends. Evidently, a column hinged at both ends and free to sidesway is unstable. It will simply topple, being unable to carry any load whatever.

FIGURE 9.3

Rigid-frame buckling:
(a) laterally braced;
(b) unbraced.



In reinforced concrete structures, one is rarely concerned with single members but rather with rigid frames of various configurations. The manner in which the relationships just described affect the buckling behavior of frames is illustrated by the simple portal frame shown in Fig. 9.3, with loads applied concentrically to the columns. If sidesway is prevented, as indicated schematically by the brace in Fig. 9.3a, the buckling configuration will be as shown. The buckled shape of the column corresponds to that in Fig. 9.1c, except that the lower end is hinged. It is seen that the effective length kl is smaller than l . On the other hand, if no sidesway bracing is provided to an otherwise identical frame, buckling occurs as shown in Fig. 9.3b. The column is in a situation similar to that shown in Fig. 9.1d, upside down, except that the upper end is not fixed but only partially restrained by the girder. It is seen that the effective length kl exceeds $2l$ by an amount depending on the degree of restraint. The buckling strength depends on kl/r in the manner shown in Fig. 9.2b. As a consequence, even though they are dimensionally identical, the unbraced frame will buckle at a radically smaller load than the braced frame.

In summary, the following can be noted:

1. The strength of concentrically loaded columns decreases with increasing slenderness ratio kl/r .
2. In columns that are *braced against sidesway* or that are parts of frames braced against sidesway, the effective length kl , i.e., the distance between inflection points, falls between $l/2$ and l , depending on the degree of end restraint.
3. The effective lengths of columns that are *not braced against sidesway* or that are parts of frames not so braced are always larger than l , the more so the smaller the end restraint. In consequence, the buckling load of a frame not braced against sidesway is always substantially smaller than that of the same frame when braced.

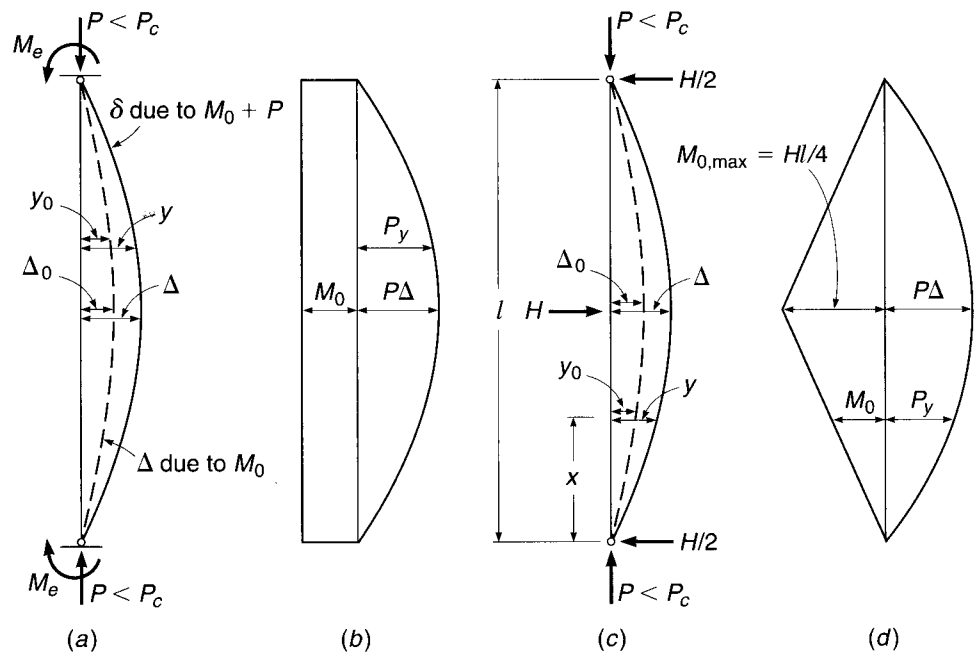
9.3 COMPRESSION PLUS BENDING

Most reinforced concrete compression members are also subject to simultaneous flexure, caused by transverse loads or by end moments owing to continuity. The behavior of members subject to such combined loading also depends greatly on their slenderness.

Figure 9.4a shows such a member, axially loaded by P and bent by equal end moments M_e . If no axial load were present, the moment M_0 in the member would be constant throughout and equal to the end moments M_e . This is shown in Fig. 9.4b. In this situation, i.e., in simple bending without axial compression, the member deflects as shown by the dashed curve of Fig. 9.4a, where y_0 represents the deflection at any

FIGURE 9.4

Moments in slender members with compression plus bending, bent in single curvature.



point caused by bending only. When P is applied, the moment at any point increases by an amount equal to P times its lever arm. The increased moments cause additional deflections, so that the deflection curve under the simultaneous action of P and M_0 is the solid curve of Fig. 9.4a. At any point, then, the total moment is now

$$M = M_0 + Py \quad (9.2)$$

i.e., the total moment consists of the moment M_0 that acts in the presence of P and the additional moment caused by P , equal to P times the deflection. This is one illustration of the so-called $P\Delta$ effect.

A similar situation is shown in Fig. 9.4c, where bending is caused by the transverse load H . When P is absent, the moment at any point x is $M_0 = Hx/2$, with a maximum value at midspan equal to $Hi/4$. The corresponding M_0 diagram is shown in Fig. 9.4d. When P is applied, additional moments Py are caused again, distributed as shown, and the total moment at any point in the member consists of the same two parts as in Eq. (9.2).

The deflections y of elastic columns of the type shown in Fig. 9.4 can be calculated from the deflections y_0 , that is, from the deflections of the corresponding beam without axial load, using the following expression (see, for example, Ref. 9.1).

$$y = y_0 \frac{1}{1 - P/P_c} \quad (9.3)$$

If Δ is the deflection at the point of maximum moment M_{\max} , as shown in Fig. 9.4, M_{\max} can be calculated using Eqs. (9.2) and (9.3).

$$M_{\max} = M_0 + P\Delta = M_0 + P\Delta_0 \frac{1}{1 - P/P_c} \quad (9.4)$$

It can be shown (Ref. 9.2) that Eq. (9.4) can be written

$$M_{\max} = M_0 \frac{1 + \psi P/P_c}{1 - P/P_c} \quad (9.5)$$

where ψ is a coefficient that depends on the type of loading and varies between about ± 0.20 for most practical cases. Because P/P_c is always significantly smaller than 1, the second term in the numerator of Eq. (9.5) is small enough to be neglected. Doing so, one obtains the simplified design equation

$$M_{\max} = M_0 \frac{1}{1 - P/P_c} \quad (9.6)$$

where $1/(1 - P/P_c)$ is known as the *moment magnification factor*, which reflects the amount by which the moment M_0 is magnified by the presence of a simultaneous axial force P .

Since P_c decreases with increasing slenderness ratio, it is seen from Eq. (9.6) that the moment M in the member increases with the slenderness ratio kl/r . The situation is shown schematically in Fig. 9.5. It indicates that, for a given transverse loading (i.e., a given value of M_0), an axial force P causes a larger additional moment in a slender member than in a stocky member.

In the two members in Fig. 9.4, the largest moment caused by P , namely $P\Delta$, adds directly to the maximum value of M_0 ; for example,

$$M_0 = \frac{Hl}{4}$$

in Fig. 9.4d. As P increases, the maximum moment at midspan increases at a rate faster than that of P in the manner given by Eqs. (9.2) and (9.6) and shown in Fig. 9.6. The member will fail when the simultaneous values of P and M become equal to P_n and M_n , the nominal strength of the cross section at the location of maximum moment.

This direct addition of the maximum moment caused by P to the maximum moment caused by the transverse load, clearly the most unfavorable situation, does not result for all types of deformations. For instance, the member in Fig. 9.7a, with equal and opposite end moments, has the M_0 diagram shown in Fig. 9.7b. The deflections caused by M_0 alone are again magnified when an axial load P is applied.

FIGURE 9.5
Effect of slenderness on column moments.

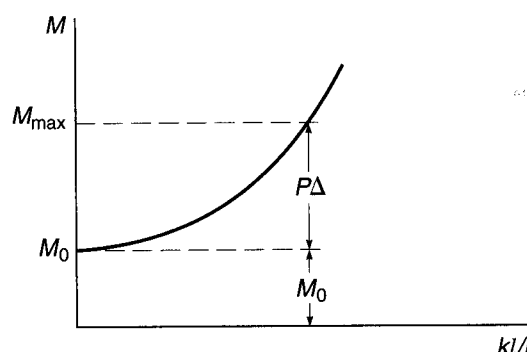
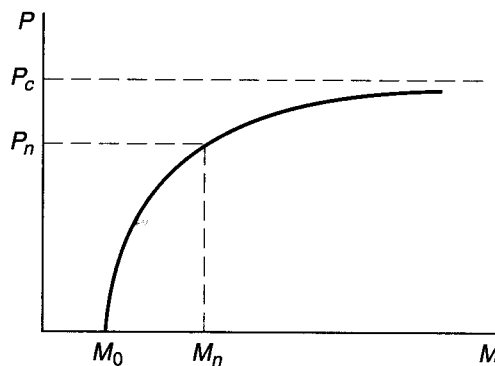


FIGURE 9.6

Effect of axial load on column moments.



In this case, these deflections under simultaneous bending and compression can be approximated by (Ref. 9.1)

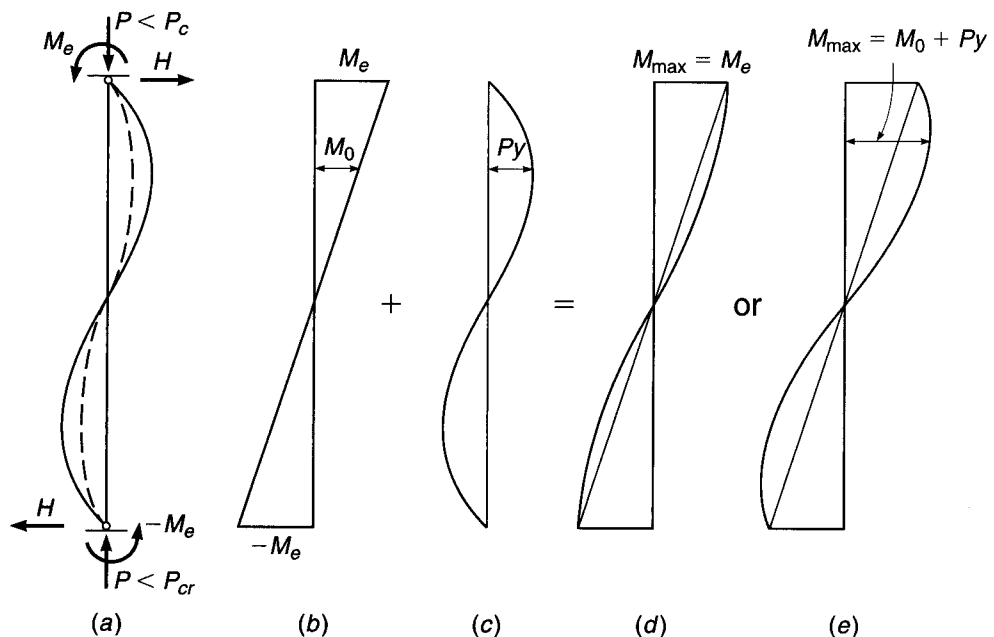
$$y = y_0 \frac{1}{1 - P/4P_c} \quad (9.7)$$

By comparison with Eq. (9.3) it is seen that the deflection magnification here is much smaller.

The additional moments Py caused by the axial load are distributed as shown in Fig. 9.7c. Although the M_0 moments are largest at the ends, the Py moments are seen to be largest at some distance from the ends. Depending on their relative magnitudes, the total moments $M = M_0 + Py$ are distributed as shown in either Fig. 9.7d or e. In the former case, the maximum moment continues to act at the end and to be equal to M_e ; the presence of the axial force, then, does not result in any increase in the maximum moment. Alternatively, in the case of Fig. 9.7e, the maximum moment is

FIGURE 9.7

Moments in slender members with compression plus bending, bent in double curvature.



located at some distance from the end; at that location M_0 is significantly smaller than its maximum value M_e , and for this reason the added moment P_y increases the maximum moment to a value only moderately greater than M_e .

Comparing Figs. 9.4 and 9.7, one can generalize as follows. The moment M_0 will be magnified most strongly when the location where M_0 is largest coincides with that where the deflection y_0 is largest. This occurs in members bent into single curvature by symmetrical loads or equal end moments. If the two end moments of Fig. 9.4a are unequal but of the same sign, i.e., producing single curvature, M_0 will still be strongly magnified, though not quite so much as for equal end moments. On the other hand, as evident from Fig. 9.7, there will be little or possibly no magnification if the end moments are of opposite sign and produce an inflection point along the member.

It can be shown (Ref. 9.2) that the way in which moment magnification depends on the relative magnitude of the two end moments (as in Figs. 9.4a and 9.7a) can be expressed by a modification of Eq. (9.6):

$$M_{\max} = M_0 \frac{C_m}{1 - P/P_c} \quad (9.8)$$

where

$$C_m = 0.6 + 0.4 \frac{M_1}{M_2} \geq 0.4 \quad (9.9)$$

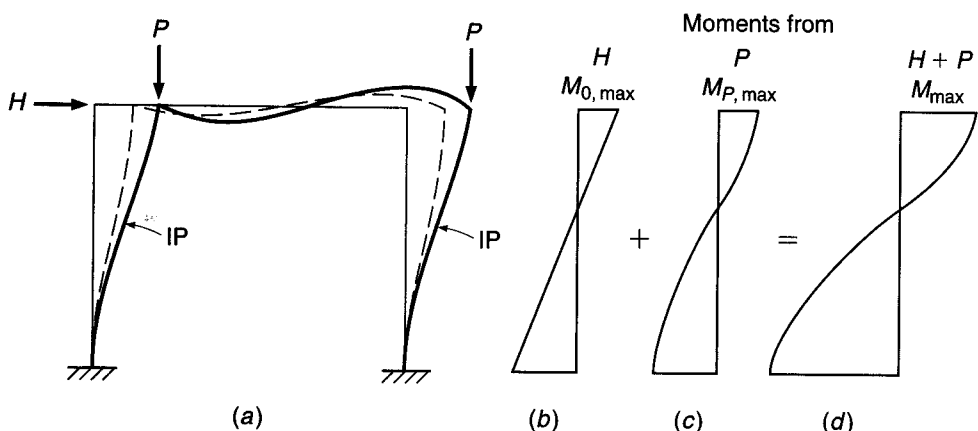
Here M_1 is the numerically smaller and M_2 the numerically larger of the two end moments; hence, by definition, $M_0 = M_2$. The fraction M_1/M_2 is defined as positive if the end moments produce single curvature and negative if they produce double curvature. It is seen that when $M_1 = M_2$, as in Fig. 9.4a, $C_m = 1$, so that Eq. (9.8) becomes Eq. (9.6), as it should. Note that Eq. (9.9) applies only to members braced against sidesway. As will become apparent from the discussion that follows, for members not braced against sidesway, maximum moment magnification usually occurs, that is, $C_m = 1$.

Members that are braced against sidesway include columns that are parts of structures in which sidesway is prevented in one of various ways: by walls sufficiently strong and rigid in their own planes to effectively prevent horizontal displacement; by special bracing in vertical planes; in buildings by designing the utility core to resist horizontal loads and furnish bracing to the frames; or by bracing the frame against some other essentially immovable support.

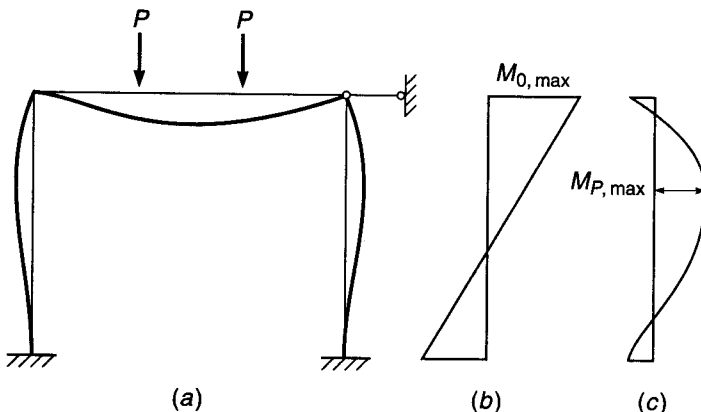
If no such bracing is provided, *sidesway can occur only for the entire frame simultaneously*, not for individual columns in the frame. If this is the case, the combined effect of bending and axial load is somewhat different from that in braced columns. As an illustration, consider the simple portal frame of Fig. 9.8a subject to a horizontal load H , such as a wind load, and compression forces P , such as from gravity loads. The moments M_0 caused by H alone, in the absence of P , are shown in Fig. 9.8b; the corresponding deformation of the frame is given in dashed curves. When P is added, horizontal moments are caused that result in the magnified deformations shown in solid curves and in the moment diagram of Fig. 9.8d. It is seen that the maximum values of M_0 , both positive and negative, and the maximum values of the additional moments M_P of the same sign occur at the same locations, namely, at the ends of the columns. They are therefore fully additive, leading to a large moment magnification. In contrast, if the frame in Fig. 9.8 is laterally braced and vertically loaded, Fig. 9.9 shows that the maximum values of the two different moments occur in different locations; the moment magnification, if any, is therefore much smaller, as correctly expressed by C_m .

FIGURE 9.8

Fixed portal frame, laterally unbraced.

**FIGURE 9.9**

Fixed portal frame, laterally braced.



The moments that cause a frame to sidesway need not be caused by horizontal loads as in Fig. 9.8. Asymmetries, of either frame configuration or vertical loading or both, also result in sidesway displacements. In this case, the presence of axial column loads again results in the increased deflection and moment magnification.

In summary, it can be stated as follows:

1. In flexural members, the presence of axial compression causes additional deflections and additional moments P_y . Other things being equal, the additional moments increase with increasing slenderness ratio kl/r .
2. In members braced against sidesway and bent in single curvature, the maxima of both types of moments, M_0 and P_y , occur at the same or at nearby locations and are fully additive; this leads to large moment magnifications. If the M_0 moments result in double curvature (i.e., in the occurrence of an inflection point), the opposite is true and less or no moment magnification occurs.
3. In members in frames not braced against sidesway, the maximum moments of both kinds, M_0 and P_y , almost always occur at the same locations, the ends of the columns; they are fully additive, regardless of the presence or absence of an inflection point. Here, too, other things being equal, the additional deflections and the corresponding moments increase with increasing kl/r .

This discussion is a simplified presentation of a fairly complex subject. The provisions of the ACI Code regarding slender columns are based on the behavior and

the corresponding equations that have just been presented. They take account, in an approximate manner, of the additional complexities that arise from the fact that concrete is not an elastic material, that tension cracking changes the moment of inertia of a member, and that under sustained load, creep increases the short-term deflections and, thereby, the moments caused by these deflections.

9.4 ACI CRITERIA FOR SLENDERNESS EFFECTS IN COLUMNS

The procedure of designing slender columns is inevitably lengthy, particularly because it involves a trial-and-error process. At the same time, studies have shown that most columns in existing buildings are sufficiently stocky that slenderness effects reduce their capacity only a few percent. As stated in Chapter 8, an ACI-ASCE survey indicated that 90 percent of columns braced against sway, and 40 percent of unbraced columns, could be designed as short columns; i.e., they could develop essentially the full cross-sectional strength with little or no reduction from slenderness (Ref. 9.3). Furthermore, lateral bracing is usually provided by shear walls, elevator shafts, stairwells, or other elements for which resistance to lateral deflection is much greater than for the columns of the building frame. It can be concluded that in most cases in reinforced concrete buildings, slenderness effects may be neglected.

To permit the designer to dispense with the complicated analysis required for slender column design for these ordinary cases, ACI Code 10.10.1 provides limits below which the effects of slenderness are insignificant and may be neglected. These limits are adjusted to result in a maximum unaccounted reduction in column capacity of no more than 5 percent. Separate limits are applied to braced and unbraced structures, alternately described in the ACI Code as *nonsway* and *sway* frames, respectively. For the purpose of determining if slenderness effects may be neglected, ACI Code 10.10.1 permits compression members to be considered as braced against sidesway if the total stiffness of the bracing elements resisting lateral movement of a story is at least 12 times the stiffness of all columns in that story. The Code provisions are as follows:

1. For compression members braced against sidesway (i.e., in nonsway structures), the effects of slenderness may be neglected when $kl_u/r \leq 34 - 12M_1/M_2$, where $34 - 12M_1/M_2$ is not taken greater than 40.
2. For compression members not braced against sidesway (i.e., in sway structures), the effects of slenderness may be neglected when kl_u/r is less than 22.

In these provisions, k is the effective length factor (see Section 9.2); l_u is the unsupported length, taken as the clear distance between floor slabs, beams, or other members providing lateral support; M_1 is the smaller factored end moment on the compression member, positive if the member is bent in single curvature and negative if bent in double curvature; and M_2 is the larger factored end moment on the compression member, always positive.

The radius of gyration r for rectangular columns may be taken as $0.30h$, where h is the overall cross-sectional dimension in the direction in which stability is being considered. For circular members, it may be taken as 0.25 times the diameter. For other shapes, r may be computed for the gross concrete section.

The effective length factor k may be conservatively taken as 1.0 for compression members that are braced against sidesway if a more accurate value is not determined by analysis. By necessity, k must be determined by analysis for compression members that are not braced against sidesway. The ACI criteria for determining k for both braced and unbraced columns are discussed in Section 9.6.

If slenderness effects must be considered, ACI Code 10.10.2 requires that the design of columns, beams restraining those columns, and other supporting members in the structure be based on a second-order analysis. The analysis may be nonlinear (ACI Code 10.10.3) or linear (ACI Code 10.10.4), or may be in accordance with the ACI moment magnifier procedure (ACI Code 10.10.5). To limit the potential for excessive moment magnification, the total moment including second-order effects in compression members may not exceed 1.4 times the moment due to first-order effects. In addition, second-order effects must be considered along the length of a member to cover cases in which the maximum moment may occur away from the ends. If a second-order analysis program is used, checking along the length of a member will require subdividing the member when it is modeled. In lieu of doing so, the ACI moment magnification method may be used. ACI Code 10.10.2 requires that the dimensions of all members used in the analysis be within 10 percent of the final dimensions. If not, the structure must be reanalyzed.

Nonlinear and linear second-order analyses, which are covered in ACI Code 10.10.3 and 10.10.4, are discussed in Section 10.8. The ACI moment magnification method of second-order analysis is discussed next.

9.5 ACI CRITERIA FOR NONSWAY VS. SWAY STRUCTURES

The discussion of Section 9.3 clearly shows important differences in the behavior of slender columns in nonsway (braced) structures and corresponding columns in sway (unbraced) structures. ACI Code provisions and Commentary guidelines for the approximate design of slender columns reflect this, and there are separate provisions in each relating to the important parameters in nonsway vs. sway structures, including moment magnification factors and effective length factors.

In practice, a structure is seldom either completely braced or completely unbraced. It is necessary, therefore, to determine in advance if bracing provided by shear walls, elevator and utility shafts, stairwells, or other elements is adequate to restrain the structure against significant sway effects. Both the ACI Code and Commentary provide guidance.

As suggested in ACI Commentary 10.10.5, a compression member can be assumed braced if it is located in a story in which the bracing elements (shear walls, etc.) have a stiffness substantial enough to limit lateral deflection to the extent that the column strength is not substantially affected. Such a determination can often be made by inspection. If not, ACI Code 10.10.5 provides two alternate criteria for determining if columns and stories are treated as nonsway or sway.

To be considered as a nonsway or braced column, the first criterion requires that the increase in column end moment due to second-order effects not exceed 5 percent of the first-order end moments. The designer is free to select the method for such a determination.

As an alternative, the Code allows a story to be considered nonsway when the *stability index*

$$Q = \frac{\sum P_u \Delta_o}{V_{us} l_c} \quad (9.10)$$

for a story is not greater than 0.05, where $\sum P_u$ and V_{us} are the total factored vertical load and story shear, respectively, for the story; Δ_o is the first-order relative deflection between the top and the bottom of the story due to V_{us} ; and l_c is the length of the compressive member measured center to center of the joints in the frame. ACI

Commentary 10.10.5 provides the guidance that $\sum P_u$ should be based on the lateral loading that maximizes the value of $\sum P_u$; the case of $V_{us} = 0$ is not included. In most cases, this calculation involves the combinations of load factors in Table 1.2 for wind, earthquake, or soil pressure (e.g., $1.2D + 1.6W + 1.0L + 0.5L_r$).

As shown in Refs. 9.3 and 9.4, for Q not greater than 0.6, the stability index closely approximates the ratio P/P_c used in the calculation of the moment magnification factor, so that $1/(1 - P/P_c)$ can be replaced by $1/(1 - Q)$. Thus, for $Q = 0.05$, $M_{max} \approx 1.05M_0$.[†]

The section properties of the frame members used to calculate Q need to account for the effects of axial loads, cracked regions along the length of the member, and the duration of the loads. ACI Code 10.10.4 provides useful guidance that is appropriate for first-order as well as second-order analysis. According to ACI Code 10.10.4, section properties may be represented using the modulus of elasticity E_c given in Eq. (2.3) and the following section properties:

Moments of inertia

Beams	$0.35I_g$
Columns	$0.70I_g$
Walls—uncracked	$0.70I_g$
—cracked	$0.35I_g$
Flat plates and flat slabs	$0.25I_g$

Area	$1.0A_g$
------	----------

where I_g and A_g are based on the gross concrete cross section, neglecting reinforcement. As discussed in Section 12.5, I_g for T beams can be closely approximated as 2 times I_g for the web. The reduced values of I given above take into account the effect of nonlinear material behavior on the effective stiffness of the members. Reference 9.3 shows that these values for moments of inertia underestimate the true moments of inertia and conservatively overestimate second-order effects by 20 to 25 percent for reinforced concrete frames.

Based on work described in Refs. 9.5 and 9.6, ACI Code 10.10.4 indicates that the moments of inertia I of compression members and flexural members may also be computed using alternative expressions. For compression members,

$$I = \left(0.80 + 25 \frac{A_{st}}{A_g} \right) \left(1 - \frac{M_u}{P_u h} - 0.5 \frac{P_u}{P_o} \right) I_g \leq 0.875 I_g \quad (9.11)$$

where P_u and M_u are based on the load combination under consideration, or the combination of P_u and M_u resulting in the smallest value of I . The value of I calculated using Eq. (9.11) need not be taken less than $0.35I_g$.

For flexural members,

$$I = (0.10 + 25 \rho) \left(1.2 - 0.2 \frac{b_w}{d} \right) I_g \leq 0.5 I_g \quad (9.12)$$

The value of I calculated using Eq. (9.12) need not be taken less than $0.25I_g$. For continuous flexural members, I may be taken as the average value of I calculated at

[†]The near equivalence of Q to P/P_{cr} for reinforced concrete columns can be demonstrated using a single-sway column with ends fixed against rotation, as shown in Fig. 9.1e. For this column, $Q = P_u \Delta_o / V_{us} l_c$. Since $V_{us}/\Delta_o =$ the lateral stiffness of the column = $12EI/l_c^3$, the stability index can be expressed as $Q = P_u / (12EI/l_c^2)$. For an unsupported length of the column (the length used to calculate P_u) $l_u = 0.9l_c$ and $P = P_u$, $Q = P_u / (9.72EI/l_u^2)$ compared to $P/P_c = P_u / (\pi^2 EI/l_u^2) = P_u / (9.87EI/l_u^2)$.

critical positive and negative moment locations along the length of the beam. The Code requires that the member dimensions and reinforcement ratios used in Eqs. (9.11) and (9.12) be within 10 percent of the final values.

To account for the effects of creep on Δ_o in Eq. (9.10) when sustained lateral loads act, the moments of inertia for compression members must be divided by $1 + \beta_{ds}$, where β_{ds} is the ratio of the maximum factored sustained shear within a story to the maximum factored shear in that story associated with the same load combination, but not greater than 1.0.

9.6 ACI MOMENT MAGNIFIER METHOD FOR NONSWAY FRAMES

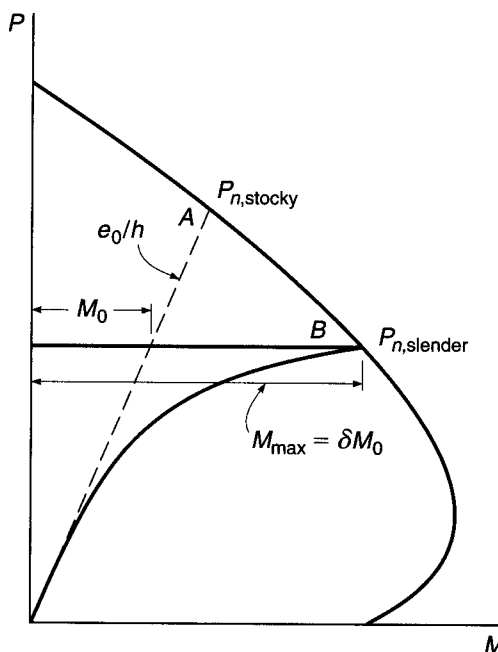
A slender reinforced concrete column reaches the limit of its strength when the combination of P and M at the most highly stressed section causes that section to fail. In general, P is essentially constant along the length of the member. This means that the column approaches failure when, at the most highly stressed section, the axial force P combines with a moment $M = M_{\max}$, as given by Eq. (9.8), so that this combination becomes equal to P_n and M_n , which will cause the section to fail. This is easily visualized by means of Fig. 9.10.

For a column of given cross section, Fig. 9.10 presents a typical interaction diagram. For simplicity, suppose that the column is bent in single curvature with equal eccentricities at both ends. For this eccentricity, the strength of the cross section is given by point A on the interaction curve. If the column is stocky enough for the moment magnification to be negligibly small, then $P_{n,stocky}$ at point A represents the member strength of the column under the simultaneous moment $M_{n,stocky} = e_0 P_{n,stocky}$.

On the other hand, if the same column is sufficiently slender, significant moment magnification will occur with increasing P . Then the moment at the most highly stressed section is M_{\max} , as given by Eq. (9.8), with $C_m = 1$ because of equal end eccentricities. The solid curve in Fig. 9.10 shows the nonlinear increase of M_{\max} as

FIGURE 9.10

Effect of slenderness on carrying capacity.



P increases. The point where this curve intersects the interaction curve, i.e., point B , defines the member strength $P_{n,\text{slender}}$ of the slender column, combined with the simultaneously applied end moments $M_0 = e_0 P_{n,\text{slender}}$. If end moments are unequal, the factor C_m will be less than 1, as discussed in Section 9.3.

For slender column design, the axial load and end moments in a column are first determined using conventional frame analysis (see Chapter 12), typically using the section properties given in Section 9.5. The member is then designed for that axial load and a simultaneous magnified column moment.

For a nonsway frame, the ACI Code equation for magnified moment, acting with the factored axial load P_{ns} is written as

$$M_c = \delta_{ns} M_2 \quad (9.13)$$

where the moment magnification factor is

$$\delta_{ns} = \frac{C_m}{1 - P_u/0.75P_c} \geq 1 \quad (9.14)$$

In Eqs. (9.13) and (9.14), the subscript ns denotes a nonsway frame. The 0.75 term in Eq. (9.14) is a *stiffness reduction factor*, designed to provide a conservative estimate of P_c . The critical load P_c , in accordance with Eq. (9.1), is given as

$$P_c = \frac{\pi^2 EI}{(kl_u)^2} \quad (9.15)$$

where l_u is defined as the unsupported length of the compression member. The value of k in Eq. (9.15) should be set equal to 1.0, unless calculated using the values of E_c and I given in Section 9.5 and procedures described later in this section.

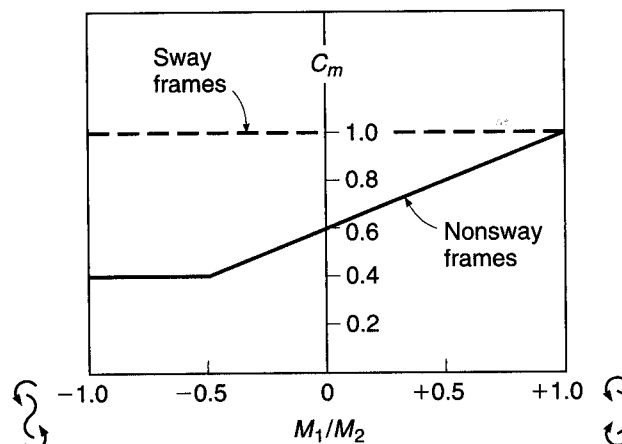
In Eq. (9.14), the value of C_m is as previously given in Eq. (9.9):

$$C_m = 0.6 + 0.4 \frac{M_1}{M_2} \geq 0.4 \quad (9.9)$$

for members braced against sidesway and without transverse loads between supports. Here M_2 is the larger of the two end moments, and M_1/M_2 is positive when the end moments produce single curvature and negative when they produce double curvature. The variation of C_m with M_1/M_2 is shown in Fig. 9.11. In Eq. (9.14), when the calculated value of δ_{ns} is smaller than 1, it indicates that the larger of the two end moments, M_2 , is the largest moment in the column, a situation depicted in Fig. 9.7d.

FIGURE 9.11

Values of C_m for slender columns in sway and nonsway frames.



In this way, the ACI Code provides for the capacity-reducing effects of slenderness in nonsway frames by means of the moment magnification factor δ_{ns} . However, it is well known that for columns with no or very small applied moments, i.e., axially or nearly axially loaded columns, increasing slenderness also reduces the column strength. For this situation, ACI Code 10.10.6.5 provides that the factored moment M_2 in Eq. (9.13) not be taken less than

$$M_{2,\min} = P_u(0.6 + 0.03h) \quad (9.16)$$

about each axis separately, where 0.6 and h are in inches. For members in which $M_{2,\min}$ exceeds M_2 , the value of C_m in Eq. (9.9) is taken equal to 1.0 or is based on the ratio of the computed end moments M_1 and M_2 .

The value of EI used in Eq. (9.15) to calculate P_c for an individual member must be both accurate and reasonably conservative to account for the greater variability inherent in the properties of individual columns, as compared to the properties of the reinforced concrete frame, as a whole. The values of EI provided in Section 9.5 are adequate for general frame analysis but not for establishing P_c for individual columns.

In homogeneous elastic members, such as steel columns, EI is easily obtained from Young's modulus and the usual moment of inertia. Reinforced concrete columns, however, are nonhomogeneous, since they consist of both steel and concrete. Whereas steel is substantially elastic, concrete is not and is, in addition, subject to creep and to cracking if tension occurs on the convex side of the column. All these factors affect the effective value of EI for a reinforced concrete member. It is possible by computer methods to calculate fairly realistic effective section properties, taking account of these factors. Even these calculations are no more accurate than the assumptions on which they are based. On the basis of elaborate studies, both analytical and experimental (Ref. 9.7), the ACI Code requires that EI be determined by either

$$EI = \frac{0.2E_c I_g + E_s I_{se}}{1 + \beta_{dns}} \quad (9.17)$$

or by the simpler expression

$$EI = \frac{0.4E_c I_g}{1 + \beta_{dns}} \quad (9.18)$$

where E_c = modulus of elasticity of concrete, psi

I_g = moment of inertia of gross section of column, in⁴

E_s = modulus of elasticity of steel = 29,000,000 psi

I_{se} = moment of inertia of reinforcement about centroidal axis of member cross section, in⁴

β_{dns} = ratio of maximum factored axial sustained load to maximum factored axial load associated with same load combination, but not greater than 1.0 (this definition differs from that used in Section 9.5 to calculate Δ_o)

The factor β_{dns} accounts approximately for the effects of creep. That is, the larger the sustained loads, the larger are the creep deformations and corresponding curvatures. Consequently, the larger the sustained loads relative to the temporary loads, the smaller the effective rigidity, as correctly reflected in Eqs. (9.17) and (9.18). Because, of the two materials, only concrete is subject to creep, and reinforcing

steel as ordinarily used is not, the argument can be made that the creep parameter $1 + \beta_{dns}$ should be applied only to the term $0.2E_c J_s$ in Eq. (9.17). However, as explained in ACI Commentary 10.10.6.2, the creep parameter is applied to both terms because of the potential for premature yielding of steel in columns under sustained loading.

Both Eqs. (9.17) and (9.18) are conservative lower limits for large numbers of actual members (Ref. 9.3). The simpler but more conservative Eq. (9.18) is not unreasonable for lightly reinforced members, but it greatly underestimates the effect of reinforcement for more heavily reinforced members, i.e., for the range of higher ρ values. Equation (9.17) is more reliable for the entire range of ρ and definitely preferable for medium and high ρ values (Ref. 9.8).

An accurate determination of the effective length factor k is essential in connection with Eqs. (9.13) and (9.15). In Section 9.2, it was shown that, for frames braced against sidesway (nonsway frames), k varies from $\frac{1}{2}$ to 1, whereas for laterally unbraced frames (sway frames), it varies from 1 to ∞ , depending on the degree of rotational restraint at both ends. This was illustrated in Fig. 9.1. For frames, it is seen that this degree of rotational restraint depends on whether the stiffnesses of the beams framing into the column at top and bottom are large or small compared with the stiffness of the column itself. An approximate but generally satisfactory way of determining k is by means of *alignment charts* based on isolating the given column plus all members framing into it at top and bottom, as shown in Fig. 9.12. The *degree of end restraint* at each end is $\psi = \sum(EI/l_c \text{ of columns}) / \sum(EI/l \text{ of floor members})$. Only floor members that are in a plane at either end of the column are to be included. The value of k can be read directly from the chart of Fig. 9.13, as illustrated by the dashed lines.[†]

It is seen that k must be known before a column in a frame can be dimensioned. Yet k depends on the stiffness EI/l of the members to be dimensioned, as well as on that of the abutting members. Thus, the dimensioning process necessarily involves iteration; i.e., one assumes member sizes, calculates member stiffnesses and corresponding k values, and then calculates the critical buckling load and more accurate member sizes on the basis of these k values until assumed and final member sizes coincide or are satisfactorily close. The stiffness EI/l should be calculated based on the values of E_c and I given in Section 9.5, and the span lengths of the members l_c and l should be measured center to center of the joints.

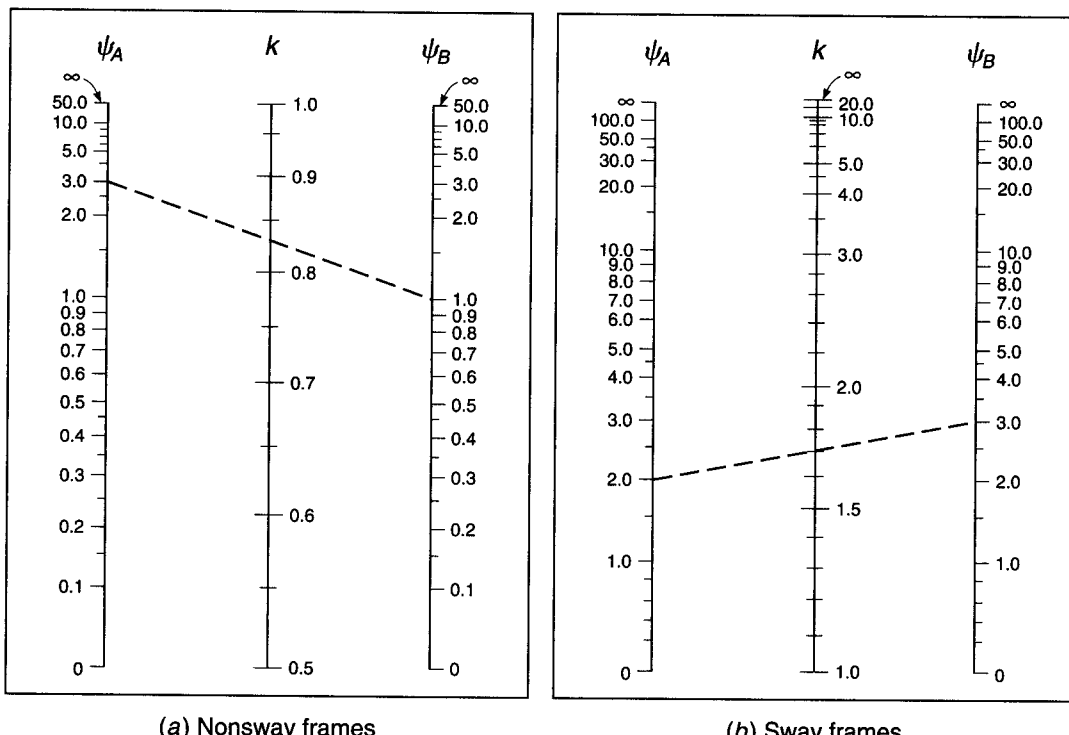
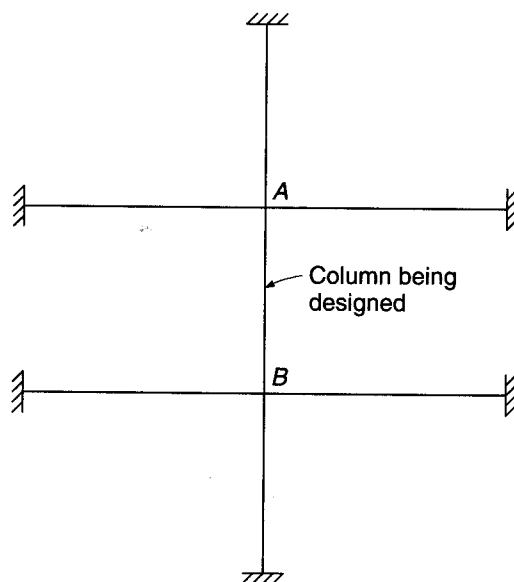
An outline of the separate steps in the analysis/design procedure for nonsway stories or frames follows along these lines:

1. Select a trial column section to carry the factored axial load P_u and moment $M_u = M_2$ from the elastic first-order frame analysis, assuming short column behavior and following the procedures of Chapter 8.
2. Determine if the frame should be considered as nonsway or sway, using the criteria of Section 9.5.
3. Find the unsupported length l_u .
4. For the trial column, check for consideration of slenderness effects, using the criteria of Section 9.4 with $k = 1.0$.
5. If slenderness is tentatively found to be important, refine the calculation of k based on the alignment chart in Fig. 9.13a, with member stiffnesses EI/l (Section 9.5).

[†] Equations for the determination of effective length factors k , more convenient than charts for developing computer solutions, are presented in Refs. 9.9 through 9.12. The expressions in Ref. 9.12 are the most accurate.

FIGURE 9.12

Section of rigid frame including column to be designed.



(a) Nonsway frames

(b) Sway frames

FIGURE 9.13

Alignment charts for effective length factors k .

and rotational restraint factors ψ based on trial member sizes. Recheck against the slenderness criteria.

6. If moments from the frame analysis are small, check to determine if the minimum moment from Eq. (9.16) controls.

7. Calculate the equivalent uniform moment factor C_m from Eq. (9.9).
8. Calculate β_{dns} , EI from Eq. (9.17) or (9.18), and P_c from Eq. (9.15) for the trial column.
9. Calculate the moment magnification factor δ_{ns} from Eq. (9.14) and magnified moment M_c from Eq. (9.13).
10. Check the adequacy of the column to resist axial load and magnified moment, using the column design charts of Appendix A in the usual way. Revise the column section and reinforcement if necessary.
11. If column dimensions are altered, repeat the calculations for k , ψ , and P_c based on the new cross section. Determine the revised moment magnification factor and check the adequacy of the new design.

EXAMPLE 9.1

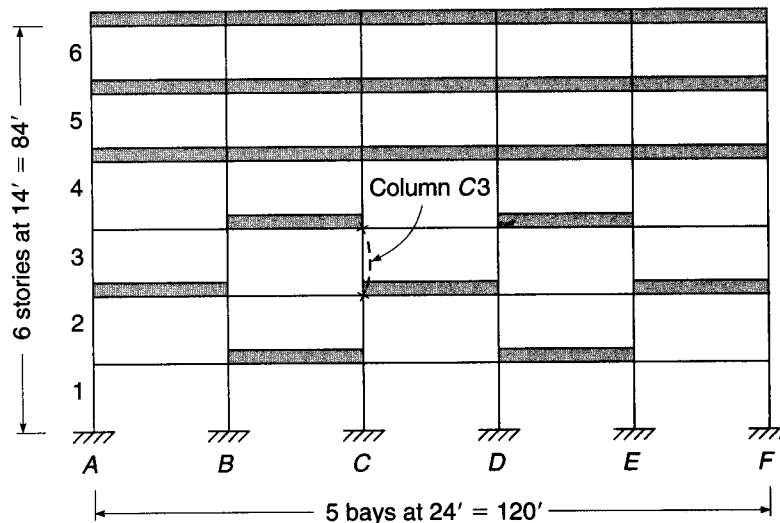
Design of a slender column in a nonsway frame. Figure 9.14 shows an elevation view of a multistory concrete frame building, with 48 in. wide \times 12 in. deep beams on all column lines, carrying two-way slab floors and roof. The clear height of the columns is 13 ft. Interior columns are tentatively dimensioned at 18 \times 18 in., and exterior columns at 16 \times 16 in. The frame is effectively braced against sway by stair and elevator shafts having concrete walls that are monolithic with the floors, located in the building corners (not shown in the figure). The structure will be subjected to vertical dead and live loads. Trial calculations by first-order analysis indicate that the pattern of live loading shown in Fig. 9.14, with full load distribution on roof and upper floors and a checkerboard pattern adjacent to column C3, produces maximum moments with single curvature in that column, at nearly maximum axial load. Dead loads act on all spans. Service load values of dead and live load axial force and moments for the typical interior column C3 are as follows:

Dead load	Live load
$P = 230$ kips	$P = 173$ kips
$M_2 = 2$ ft-kips	$M_2 = 108$ ft-kips
$M_1 = -2$ ft-kips	$M_1 = 100$ ft-kips

The column is subjected to double curvature under dead load alone and single curvature under live load.

FIGURE 9.14

Concrete building frame for Example 9.1.



Design column C3, using the ACI moment magnifier method. Use $f'_c = 4000$ psi and $f_y = 60,000$ psi.

SOLUTION. The column will first be designed as a short column, assuming no slenderness effect. With the application of the usual load factors,

$$P_u = 1.2 \times 230 + 1.6 \times 173 = 553 \text{ kips}$$

$$M_u = 1.2 \times 2 + 1.6 \times 108 = 175 \text{ ft-kips}$$

For an 18×18 in. column, with the 1.5 in. clear to the outside steel, No. 3 (No. 10) stirrups, and (assumed) No. 10 (No. 32) longitudinal steel:

$$\gamma = (18.00 - 2 \times 1.50 - 2 \times 0.38 - 1.27)/18 = 0.72$$

Graph A.6 for $\gamma = 0.70$, with bars arranged around the column perimeter, will be used. Then

$$\frac{P_u}{\phi f'_c A_g} = \frac{553}{0.65 \times 4 \times 324} = 0.656$$

$$\frac{M_u}{\phi f'_c A_g h} = \frac{175 \times 12}{0.65 \times 4 \times 324 \times 18} = 0.138$$

and from the graph $\rho_g = 0.02$. This is low enough that an increase in steel area could be made, if necessary, to allow for slenderness, and the 18×18 in. concrete dimensions will be retained.

For an initial check on slenderness, an effective length factor $k = 1.0$ will be used. Then

$$\frac{kl_u}{r} = \frac{1.0 \times 13 \times 12}{0.3 \times 18} = 28.9$$

For a braced frame, the upper limit for short column behavior is

$$34 - 12 \frac{M_1}{M_2} = 34 - 12 \frac{1.2 \times (-2) + 1.6 \times 100}{1.2 \times 2 + 1.6 \times 108} = 23.2$$

The calculated value of 28.9 exceeds this, so slenderness must be considered in the design. A more refined calculation of the effective length factor k is thus called for.

Because E_c is the same for column and beams, it will be canceled in the stiffness calculations. For this step, the column moment of inertia will be taken as $0.7I_g = 0.7 \times 18 \times 18^3/12 = 6124$ in 4 , giving $I/l_c = 6124/(14 \times 12) = 36.5$ in 3 . For the beams, the moment of inertia will be taken as $0.35I_g$, where I_g is taken as 2 times the gross moment of inertia of the web. Thus, $0.35I_g = 0.35 \times 2 \times 48 \times 12^3/12 = 4838$ in 4 , and $I/l = 4838/(24 \times 12) = 16.8$ in 3 . Rotational restraint factors at the top and bottom of column C3 are the same and are

$$\psi_a = \psi_b = \frac{36.5 + 36.5}{16.8 + 16.8} = 2.17$$

From Fig. 9.13a for the braced frame, the value of k is 0.87, rather than 1.0 as used previously. Consequently,

$$\frac{kl_u}{r} = \frac{0.87 \times 13 \times 12}{0.3 \times 18} = 25.1$$

This is still above the limit value of 23.3, confirming that slenderness must be considered.

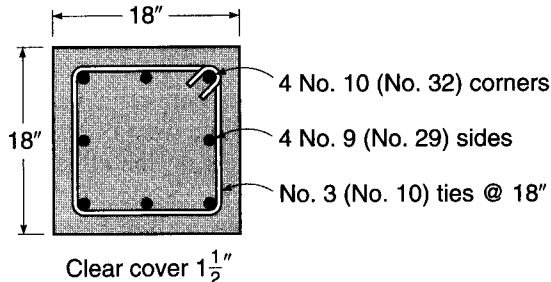
A check will now be made of minimum moment. According to Eq. (9.16), $M_{2,\min} = 553 \times (0.6 + 0.03 \times 18)/12 = 53$ ft-kips. It is seen that this does not control.

The coefficient C_m can now be found from Eq. (9.9) with $M_1 = 1.2 \times (-2) + 1.6 \times 100 = 158$ ft-kips and $M_2 = 1.2 \times 2 + 1.6 \times 108 = 175$ ft-kips:

$$C_m = 0.6 + 0.4 \frac{158}{175} = 0.96$$

FIGURE 9.15

Cross section of column C3,
Example 9.1.



Next the factor β_{dns} will be found based on the ratio of the maximum factored sustained axial load (the factored dead load in this case) to the maximum factored axial load:

$$\beta_{dns} = \frac{1.2 \times 230}{1.2 \times 230 + 1.6 \times 173} = 0.50$$

For a relatively low reinforcement ratio, one estimated to be in the range of 0.02 to 0.03, the more approximate Eq. (9.18) for EI will be used, and

$$EI = \frac{0.4 \times 3.60 \times 10^6 \times 18 \times 18^3/12}{1 + 0.50} = 8.40 \times 10^9 \text{ in}^2\text{-lb}$$

The critical buckling load is found from Eq. (9.15) to be

$$P_c = \frac{\pi^2 EI}{(kl_u)^2} = \frac{\pi^2 \times 8.40 \times 10^9}{(0.87 \times 13 \times 12)^2} = 4.50 \times 10^6 \text{ lb}$$

The moment magnification factor can now be found from Eq. (9.14).

$$\delta_{ns} = \frac{C_m}{1 - P_u/0.75P_c} = \frac{0.96}{1 - 553/(0.75 \times 4500)} = 1.15$$

Thus, the required axial strength of the column is $P_u = 553$ kips (as before), while the magnified design moment is $M_c = \delta_{ns}M_2 = 1.15 \times 175 = 201$ ft-kips. As described in Section 9.5, ACI Code 10.10.2 limits the magnified moment to 1.4 times the moment due to first-order effects. This limitation is clearly satisfied. With reference again to the column design chart A.6 with

$$\frac{P_u}{\phi f'_c A_g} = \frac{553}{0.65 \times 4 \times 324} = 0.656$$

$$\frac{M_u}{\phi f'_c A_g h} = \frac{201 \times 12}{0.65 \times 4 \times 324 \times 18} = 0.159$$

it is seen that the required reinforcement ratio is increased from 0.020 to 0.026 because of slenderness. The steel area now required is

$$A_{st} = 0.026 \times 324 = 8.42 \text{ in}^2$$

which can be provided using four No. 10 (No. 32) and four No. 9 (No. 29) bars ($A_{st} = 9.08 \text{ in}^2$), arranged as shown in Fig. 9.15. No. 3 (No. 10) ties will be used at a spacing not to exceed the least dimension of the column (18 in.), 48 tie diameters (18 in.), or 16 bar diameters (18 in.). Single ties at 18 in. spacing, as shown in the figure, will meet requirements of the ACI Code.

Further refinements in the design could, of course, be made by recalculating the critical buckling load using Eq. (9.17). This extra step is not justified here because the column slenderness is barely above the upper limit for short column behavior and the moment magnification is not great.

9.7 ACI MOMENT MAGNIFIER METHOD FOR SWAY FRAMES

The important differences in behavior between columns braced against sidesway and columns for which sidesway is possible were discussed in Sections 9.2 and 9.3. The critical load for a column P_c depends on the effective length kl_u , and although the effective length factor k falls between 0.5 and 1.0 for braced columns, it is between 1.0 and ∞ for columns that are unbraced (see Figs. 9.1 and 9.13). Consequently, an unbraced column will buckle at a much smaller load than will a braced column that is otherwise identical.

Columns subject to sidesway do not normally stand alone but are part of a structural system including floors and roof. A floor or roof is normally very stiff in its own plane. Consequently, all columns at a given story level in a structure are subject to essentially identical sway displacements; i.e., sidesway of a particular story can occur only by simultaneous lateral motion of all columns of that story. Clearly, all columns at a given level must be considered together in evaluating slenderness effects relating to sidesway.

On the other hand, it is also possible for a single column in a sway frame to buckle individually under gravity loads, the ends of the column being held against relative lateral movement by other, stiffer columns at the same floor level. This possibility, resulting in magnification of nonsway moments due to gravity loads, must also be considered in the analysis and design of slender columns in unbraced frames.

The ACI moment magnifier approach can still be used for frames subject to sidesway, but it is necessary, according to ACI Code 10.10.7, to separate the loads acting on a structure into two categories: loads that result in no appreciable sidesway and loads that result in appreciable sidesway. Clearly two separate frame analyses are required, one for loads of each type. In general, gravity loads acting on reasonably symmetrical frames produce little sway, and the effects of gravity load may therefore be placed in the first category. This is confirmed by tests and analyses in Ref. 9.13 that show that the sway magnification of gravity moments by the sway multiplier is unwarranted.

The maximum magnified moments caused by sway loading occur at the ends of the column, but those due to gravity loads may occur somewhere in the midheight of the column, the exact location of the latter varying depending on the end moments. Because magnified gravity moments and magnified sway moments do not occur at the same location, the argument can be made that, in most cases, no magnification should be applied to the nonsway moments when sway moments are considered; that is, it is unlikely that the actual maximum moment will exceed the sum of the nonmagnified gravity moment and the magnified sway moment. Consequently, for cases involving sidesway, Eq. (9.13) is replaced by

$$M_1 = M_{1ns} + \delta_s M_{1s} \quad (9.19)$$

$$M_2 = M_{2ns} + \delta_s M_{2s} \quad (9.20)$$

where M_1 = smaller factored end moment on compression member

M_2 = larger factored end moment on compression member

M_{1ns} = factored end moment on compression member at end at which M_1 acts, due to loads that cause no appreciable sidesway, calculated using a first-order elastic frame analysis

M_{2ns} = factored end moment on compression member at end at which M_2 acts, due to loads that cause no appreciable sidesway, calculated using a first-order elastic frame analysis

M_{1s} = factored end moment on compression member at end at which M_1 acts, due to loads that cause appreciable sidesway, calculated using a first-order elastic frame analysis

M_{2s} = factored end moment on compression member at end at which M_2 acts, due to loads that cause appreciable sidesway, calculated using a first-order elastic frame analysis

δ_s = moment magnification factor for frames not braced against sidesway, to reflect lateral drift resulting from lateral (and sometimes gravity) loads

ACI Code 10.10.7 provides two alternate methods for calculating the moment magnification factor for frames not braced against sidesway δ_s .

With the first alternative, the moment magnification factor is calculated as

$$\delta_s = \frac{1}{1 - Q} \geq 1 \quad (9.21)$$

where Q is the stability index calculated using Eq. (9.10). The ACI Code limits application of Eq. (9.21) to values of $\delta_s = 1/(1 - Q) \leq 1.5$. An elastic second-order analysis, as described in ACI Code 10.10.4, or the second alternative described in ACI Code 10.10.7 must be used for higher values of δ_s .

For the second alternative, the moment magnification factor is calculated as

$$\delta_s = \frac{1}{1 - \sum P_u / 0.75 \sum P_c} \geq 1 \quad (9.22)$$

in which $\sum P_u$ is the total axial load on all columns and $\sum P_c$ is the total critical buckling load for all columns in the story under consideration. As with Eq. (9.14), the 0.75 factor in Eq. (9.22) is a stiffness reduction factor to provide a conservative estimate of the critical buckling loads P_c . The individual values of P_c are calculated using Eq. (9.15) with effective length factors k for unbraced frames (Fig. 9.13b) and values of EI from Eq. (9.17) or (9.18).

When calculating δ_s , the factor β_{ds} is defined differently than β_{dns} is for non-sway frames. As described earlier, in Section 9.5, β_{ds} is the ratio of the maximum factored sustained shear within a story to the maximum factored shear in that story. Thus, for most applications, $\beta_{ds} = 0$ for the purpose of calculating δ_s . In unusual situations, $\beta_{ds} \neq 0$ will occur, such as a building located on a sloping site that is subjected to soil pressure on a single side (Refs. 9.14 and 9.15).

The sequence of design steps for slender columns in sway frames is similar to that outlined in Section 9.6 for nonsway frames, except for the requirement that loads be separated into gravity loads, which are assumed to produce no sway, and horizontal loads producing sway. Separate frame analyses are required, and different equivalent length factors k and creep coefficients β_{dns} and β_{ds} must be applied. Note that according to ACI Code 9.2 (see also Table 1.2 of Chapter 1), if wind effects W are included in the design, four possible factored load combinations are to be applied:

$$U = 1.2D + 1.6L$$

$$U = 1.2D + 1.6(L_r \text{ or } S \text{ or } R) + 0.8W$$

$$U = 1.2D + 1.6W + 1.0L + 0.5(L_r \text{ or } S \text{ or } R)$$

$$U = 0.9D + 1.6W$$

Similar provisions are included for cases where earthquake loads are to be considered. This represents a significant complication in the sway frame analysis; however, the

factored loads can be separated into gravity effects and sway effects, as required, and a separate analysis can be performed for each.

It is important to realize that, for sway frames, *the beams must be designed for the total magnified end moments of the compression members at the joint*. Even though the columns may be very rigid, if plastic hinges were to form in the restraining beams adjacent to the joints, the effective column length would be greatly increased and the critical column load much reduced.

The choice of which of the methods to use for calculating δ_s depends upon the desired level of accuracy and the available analytical tools.

Second-order analysis (discussed in greater detail in Section 9.8) provides the most accurate estimate of the magnified sway moments but requires more sophisticated techniques. The extra effort required for second-order analysis, however, usually produces a superior design. The first alternative, Eq. (9.21), will in most cases be the easiest to apply, since matrix analysis is used for virtually all frames to determine member forces under gravity and lateral loading. Such an analysis automatically generates the value of Δ_o , the first-order relative deflection within a story, allowing Q to be calculated for each story within a structure. The second alternative, Eq. (9.22), is retained with minor modifications from previous versions of the ACI Code. As will be demonstrated in the following example, calculations using Eq. (9.22) are more tedious than those needed for Eq. (9.21) but do not require knowledge of Δ_o . Application of Eq. (9.21) is limited by the Code to values of $\delta_s \leq 1.5$. For $\delta_s > 1.5$, application of Eq. (9.22) is mandatory if a second-order analysis is not used.

EXAMPLE 9.2

Design of a slender column in a sway frame. Consider now that the concrete building frame of Example 9.1 acts as a *sway frame*, without the stairwells or elevator shafts described earlier. An initial evaluation is carried out using the member dimensions and reinforcement given in Example 9.1. The reinforcement for the interior 18×18 in. columns, shown in Fig. 9.15, consists of four No. 10 (No. 32) bars at the corners and four No. 9 (No. 29) bars at the center of each side. Reinforcement for the exterior 16×16 in. columns consists of eight No. 8 (No. 25) bars distributed in a manner similar to that shown for the longitudinal reinforcement in Fig. 9.15. The building will be subjected to gravity dead and live loads and horizontal wind loads. Elastic first-order analysis of the frame at service loads (all load factors = 1.0) using the values of E and I defined in Section 9.5 gives the following results at the third story:

	Cols. A3 and F3	Cols. B3 and E3	Cols. C3 and D3
P_{dead}	115 kips	230 kips	230 kips
P_{live}	90 kips	173 kips	173 kips
P_{wind}	± 30 kips	± 18 kips	± 6 kips
V_{wind}	5.5 kips	11 kips	11 kips
$M_{2,\text{dead}}$			2 ft-kips
$M_{2,\text{live}}$			108 ft-kips
$M_{2,\text{wind}}$			± 79 ft-kips
$M_{1,\text{dead}}$			-2 ft-kips
$M_{1,\text{live}}$			100 ft-kips
$M_{1,\text{wind}}$			± 70 ft-kips

To simplify the analysis in this example, roof loads will not be considered. The relative lateral deflection for the third story under total wind shear $V_{\text{wind}} = 55$ kips is 0.76 in.

Column C3 is to be designed for the critical loading condition, using $f'_c = 4000$ psi and $f_y = 60,000$ psi as before.

SOLUTION. The column size and reinforcement must satisfy requirements for each of the four load conditions noted above.

Initially, a check is made to see if a sway frame analysis is required. The factored shear $V_{us} = 1.6 \times V_{wind} = 1.6 \times 55 = 88$ kips. The corresponding deflection $\Delta_o = 1.6 \times 0.76 = 1.22$ in. The total factored axial force on the story is obtained using the load table.

$$\text{Columns } A3 \text{ and } F3: \quad P_u = 1.2 \times 115 + 1.0 \times 90 = 228 \text{ kips}$$

$$\text{Columns } B3, C3, D3, \text{ and } E3: \quad P_u = 1.2 \times 230 + 1.0 \times 173 = 449 \text{ kips}$$

Note that in this case the values of P_{wind} in the columns are not considered since they cancel out for the floor as a whole, i.e., $\sum P_{wind} = 0$. Thus, $\sum P_u = 2 \times 228 + 4 \times 449 = 2252$ kips, and the stability index is

$$Q = \frac{\sum P_u \Delta_o}{V_{us} l_c} = \frac{2252 \times 1.22}{88 \times 14 \times 12} = 0.19$$

Since $Q > 0.05$, sway frame analysis is required for this story.

(a) Gravity loads only. All columns in sway frames must first be considered as braced columns under gravity loads acting alone, i.e., for $U = 1.2D + 1.6L$. This check has already been made for column *C3* in Example 9.1.

(b) Gravity plus wind loads. Three additional load combinations must be considered when wind effects are included: $U = 1.2D + 1.6(L_r \text{ or } S \text{ or } R) + 0.8W$, $U = 1.2D + 1.6W + 1.0L + 0.5(L_r \text{ or } S \text{ or } R)$, and $U = 0.9D + 1.6W$. By inspection, the second combination will control for this case, and the others will not be considered further. From Example 9.1, $\psi_a = \psi_b = 2.17$. With reference to the alignment chart in Fig. 9.13b, the effective length factor for an unbraced frame $k = 1.64$ and

$$\frac{kl_u}{r} = \frac{1.64 \times 13 \times 12}{0.3 \times 18} = 47.4$$

This is much above the limit value of 22 for short column behavior in an unbraced frame. (This should be no surprise since $kl_u/r = 25.1$ for column *C3* in the braced condition.) For sway frame analysis, the loads must be separated into gravity loads and sway loads, and the appropriate magnification factor must be computed and applied to the sway moments. The factored end moments resulting from the nonsway loads on column *C3* are

$$M_{1ns} = 1.2 \times (-2) + 1.0 \times 100 = 98 \text{ ft-kips}$$

$$M_{2ns} = 1.2 \times 2 + 1.0 \times 108 = 110 \text{ ft-kips}$$

The sway effects will amplify the moments:

$$M_{1s} = 1.6(-70) = -112 \text{ ft-kips}$$

$$M_{2s} = 1.6 \times 79 = 126 \text{ ft-kips}$$

For the purposes of comparison, the magnified sway moments will be calculated based on both Q [Eq. (9.21)] and $\sum P_u / \sum P_c$ [Eq. (9.22)].

Using Eq. (9.21),

$$\delta_s = \frac{1}{1 - Q} = \frac{1}{1 - 0.19} = 1.23$$

giving

$$\delta_s M_{1s} = 1.23 \times (-112) = -138 \text{ ft-kips}$$

$$\delta_s M_{2s} = 1.23 \times 126 = 155 \text{ ft-kips}$$

To use Eq. (9.22), the critical loads must be calculated for each of the columns as follows. For columns *A3* and *F3*,

$$\begin{aligned} \text{Columns: } I &= 0.7I_g = 0.7 \times 16 \times 16^3 / 12 = 3823 \text{ in}^4 \\ &\text{and } I/l_c = 3823 / (14 \times 12) = 22.8 \text{ in}^3 \end{aligned}$$

$$\text{Beams: } I = 4838 \text{ in}^4 \quad \text{and} \quad I/l_c = 16.8 \text{ in}^3$$

Rotational restraint factors for this case, with two columns and one beam framing into the joint, are

$$\psi_a = \psi_b = \frac{22.8 + 22.8}{16.8} = 2.71$$

which, with reference to the alignment chart for unbraced frames, gives $k = 1.77$. For wind load, $\beta_{ds} = 0$. Since reinforcement has been initially selected for one column, EI will be calculated using Eq. (9.17).

$$\begin{aligned} EI &= 0.2E_c I_g + E_s I_{se} = 0.2 \times 3.6 \times 10^6 \times 16 \times 16^3/12 + 29 \times 10^6 \times 6 \times 0.79 \times 6.6^2 \\ &= 9.92 \times 10^9 \text{ in}^2\text{-lb} \end{aligned}$$

Then the critical load is

$$P_c = \frac{\pi^2 \times 9.92 \times 10^9}{(1.77 \times 13 \times 12)^2} = 1.51 \times 10^6 \text{ lb}$$

For columns *B3*, *C3*, *D3*, and *E3*, from earlier calculations for column *C3*, $k = 1.64$ for the sway loading case. For these columns,

$$\begin{aligned} EI &= 0.2 \times 3.6 \times 10^6 \times 18 \times 18^3/12 + 29 \times 10^6 (4 \times 1.27 \times 6.4^2 + 2 \times 1.0 \times 6.5^2) \\ &= 14.8 \times 10^9 \text{ in}^2\text{-lb} \\ P_c &= \frac{\pi^2 \times 14.8 \times 10^9}{(1.64 \times 13 \times 12)^2} = 2.62 \times 10^6 \text{ lb} \end{aligned}$$

Thus, for all the columns at this level of the structure,

$$\Sigma P_c = 2 \times 1510 + 4 \times 2620 = 13,500 \text{ kips}$$

The sway moment magnification factor is

$$\delta_s = \frac{1}{1 - \Sigma P_u / 0.75 \Sigma P_c} = \frac{1}{1 - 2252 / (0.75 \times 13,500)} = 1.29$$

and the magnified sway moments for the top and bottom of column *C3* are

$$\begin{aligned} \delta_s M_{1s} &= 1.29 \times (-112) = -144 \text{ ft-kips} \\ \delta_s M_{2s} &= 1.29 \times 126 = 163 \text{ ft-kips} \end{aligned}$$

The values of $\delta_s M_s$ are higher based on $\Sigma P_u / \Sigma P_c$ than they are based on Q (163 ft-kips vs. 155 ft-kips for $\delta_s M_{2s}$), emphasizing the conservative nature of the moment magnifier approach based on Eq. (9.22). The design will proceed using the less conservative value of $\delta_s M_s$.

The total magnified moments are

$$M_1 = 98 - 138 = -40 \text{ ft-kips}$$

$$M_2 = 110 + 155 = 265 \text{ ft-kips}$$

The values do not exceed the upper limit of 1.4 times the moments due to first-order effects and will now be combined with factored axial load $P_u = 459$ kips (now including $1.6P_{wind}$). In reference to Graph A.6 with column parameters

$$\frac{P_u}{\phi f'_c A_g} = \frac{459}{0.65 \times 4 \times 324} = 0.545$$

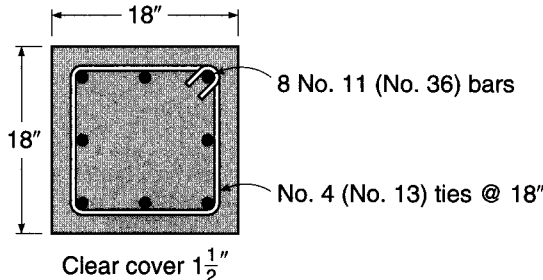
$$\frac{M_u}{\phi f'_c A_g h} = \frac{265 \times 12}{0.65 \times 4 \times 324 \times 18} = 0.211$$

it is seen that $\rho_g = 0.038$. This is considerably higher than the value of 0.026 required for column *C3* in a braced frame. The required steel area of

$$A_{st} = 0.038 \times 324 = 12.31 \text{ in}^2$$

FIGURE 9.16

Cross section of column C3,
Example 9.2.



will be provided using eight No. 11 (No. 36) bars, arranged as shown in Fig. 9.16. Spacing of No. 4 (No. 13) ties must not exceed the least dimension of the column, 48 tie diameters, or 16 main bar diameters. The first criterion controls, and No. 4 (No. 13) ties at 18 in. spacing will be used in the pattern shown in Fig. 9.16.

9.8 SECOND-ORDER ANALYSIS FOR SLENDERNESS EFFECTS

It may be evident from the preceding examples that although the ACI moment magnifier method works well enough for nonsway frames, its application to sway frames is complicated, with many opportunities for error, especially when Eq. (9.22) is used to calculate δ_s .

With the universal availability of computers in design offices, and because of the complexity of the moment magnifier method, it is advantageous to apply rational second-order frame analysis, or $P-\Delta$ analysis, in which the effects of lateral deflection on moments, axial forces, and, in turn, lateral deflections are computed directly. The resulting moments and deflections include the effects of slenderness, and so the problem is strictly nonlinear, whether the model used for the analysis is nonlinear (ACI Code 10.10.3) or elastic (ACI Code 10.10.4).

Nonlinear second-order analysis in accordance with ACI Code 10.10.3 must account for the effects of material nonlinearity, member curvature and lateral drift, load duration, shrinkage and creep, and the interaction between the frame and the supporting foundation. ACI Code 10.10.3 requires that the second-order analysis procedure be one that provides a strength prediction that is in “substantial agreement” with test results for reinforced concrete columns in statically indeterminate frames. ACI Commentary 10.10.3 suggests that a prediction within 15 percent of the test results is satisfactory. It also suggests that a stiffness reduction factor ϕ_K of 0.80 be used to account for variations in actual member properties and for consistency with elastic second-order analysis under ACI Code 10.10.4.

Elastic second-order analysis in accordance with ACI Code 10.10.4 must consider the effects of axial loads, cracked regions within the members, and load duration, and although elastic models are simpler to implement than nonlinear models, as pointed out in Ref. 9.16, the key requirement for EI values for second-order frame analysis, whether elastic or nonlinear, is that they be representative of member stiffness just prior to failure. The values of E and I in Section 9.5, which are taken from ACI Code 10.10.4, meet that requirement and include a stiffness reduction factor of 0.875 (Ref. 9.16). The value of the stiffness reduction factor and the moments of inertia in Section 9.5 are higher than the factor 0.75 in Eqs. (9.14) and (9.21) and the effective values of I in

Eqs. (9.17) and (9.18), respectively, because of the inherently lower variability in the total stiffness of a frame compared to that of an individual member.

As pointed out in Section 9.5, the member dimensions used in any second-order analysis must be within 10 percent of the final dimensions. Otherwise, the frame must be reanalyzed.

A rational second-order analysis gives a better approximation of actual moments and forces than the moment magnifier method. Differences are particularly significant for irregular frames, for frames subject to significant sway forces, and for lightly braced frames. There may be important economies in the resulting design.

Practical methods for performing a full second-order analysis are described in the literature (Refs. 9.3, 9.17, 9.18, 9.19, and 9.20 to name a few), and general-purpose programs that perform a full nonlinear analysis including sway effects are commercially available. Linear first-order analysis programs are also available, but must include an iterative approach to produce acceptable results. This iterative approach can be summarized as follows.

Figure 9.17a shows a simple frame subject to lateral loads H and vertical loads P . The lateral deflection Δ is calculated by ordinary first-order analysis. As the frame is displaced laterally, the column end moments must equilibrate the lateral loads and a moment equal to $(\Sigma P)\Delta$:

$$\Sigma(M_{\text{top}} + M_{\text{bot}}) = Hl_c + \Sigma P \Delta \quad (9.23)$$

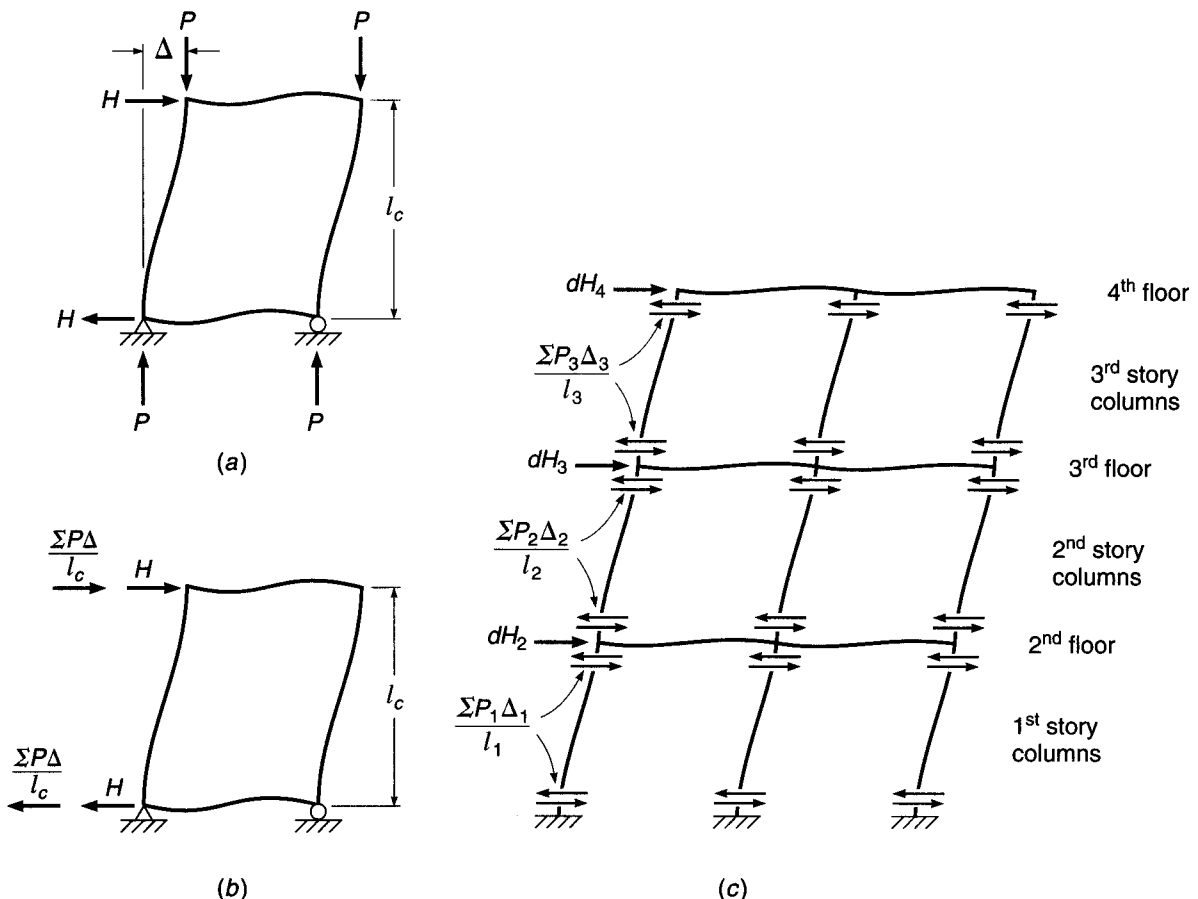
where Δ is the lateral deflection of the top of the frame with respect to the bottom, and ΣP is the sum of the vertical forces acting. The moment $\Sigma P \Delta$ in a given story can be represented by equivalent shear forces $(\Sigma P)\Delta/l_c$, where l_c is the story height, as shown in Fig. 9.17b. These shears give an overturning moment equal to that of the loads P acting at a displacement Δ .

Figure 9.17c shows the story shears acting in a three-story frame. The algebraic sum of the story shears from the columns above and below a given floor corresponds in effect to a sway force dH acting on that floor. For example, at the second floor the sway force is

$$dH_2 = \frac{\Sigma P_1 \Delta_1}{l_1} - \frac{\Sigma P_2 \Delta_2}{l_2} \quad (9.24)$$

The sway forces must be added to the applied lateral force H at any story level, and the structure is then reanalyzed, giving new deflections and increased moments. If the lateral deflections increase significantly (say more than 5 percent), new dH sway forces are computed, and the structure is reanalyzed for the sum of the applied lateral forces and the new sway forces. Iteration is continued until changes are insignificant. Generally one or two cycles of iteration are adequate for structures of reasonable lateral stiffness (Ref. 9.3).

It is noted in Ref. 9.17 that a correction must be made in the analysis to account for the differences in shape between the $P\Delta$ moment diagram that has the same shape as the deflected column, and the moment diagram associated with the $P\Delta/l$ forces, which is linear between the joints at the column ends. The area of the actual $P\Delta$ moment diagram is larger than the linear equivalent representation, and consequently lateral deflections will be larger. The difference will vary depending on the relative stiffnesses of the column and the beams framing into the joints. In Ref. 9.17, it is suggested that the increased deflection can be accounted for by taking the sway forces dH as 15 percent greater than the calculated value for each iteration. Iteration and the

**FIGURE 9.17**

Basis for iterative P - Δ analysis: (a) vertical and lateral loads on rectangular frame; (b) real lateral forces H and fictitious sway forces dH ; (c) three-story frame subject to sway forces. (Adapted from Ref. 9.17.)

15 percent increase in deflection are not required if the program performs a full non-linear geometric analysis, since the $P\Delta$ moments are calculated in full.

The accuracy of the results of a P - Δ analysis will be strongly influenced by the values of member stiffness used, by foundation rotations, if any, and by the effects of concrete creep. In connection with creep effects, lateral loads causing significant sway are usually wind or earthquake loads of short duration, so creep effects are minimal. In general, the use of sway frames to resist *sustained* lateral loads, e.g., from earth or liquid pressures, is not recommended, and it would be preferable to include shear walls or other elements to resist these loads.

REFERENCES

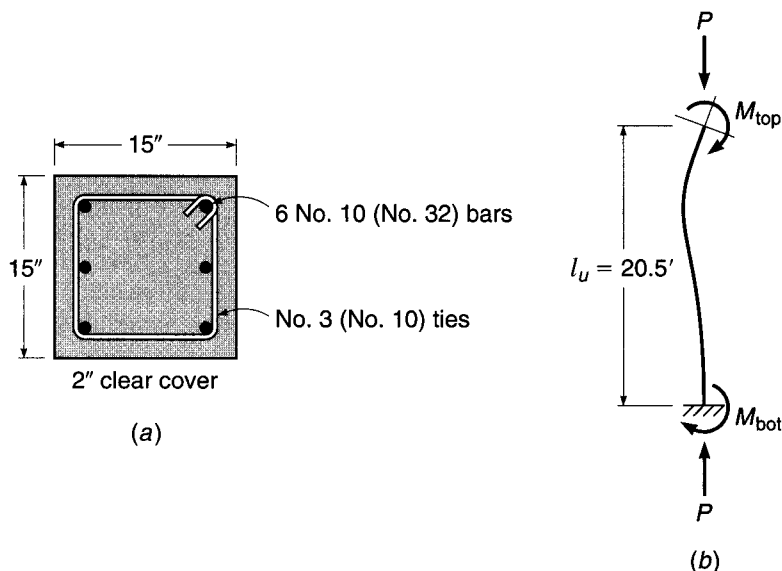
- 9.1. S. P. Timoshenko and J. M. Gere, *Theory of Elastic Stability*, 3d ed., McGraw-Hill, New York, 1969.
- 9.2. T. V. Galambos (ed.), *Guide to Stability Design Criteria for Metal Structures*, 5th ed., John Wiley & Sons, New York, 1998.
- 9.3. J. G. MacGregor and S. E. Hage, "Stability Analysis and Design of Concrete Frames," *J. Struct. Div., ASCE*, vol. 103, no. ST10, 1977, pp. 1953–1977.
- 9.4. S.-M. A. Lai and J. G. MacGregor, "Geometric Nonlinearities in Unbraced Multistory Frames," *J. Struct. Eng., ASCE*, vol. 109, no. 11, 1983, pp. 2528–2545.

- 9.5. M. Khuntia and S. K. Ghosh, "Flexural Stiffness of Reinforced Concrete Columns and Beams: Analytical Approach," *ACI Struct. J.*, vol. 101, no. 3, 2004, pp. 351–363.
- 9.6. M. Khuntia and S. K. Ghosh, "Flexural Stiffness of Reinforced Concrete Columns and Beams: Experimental Verification," *ACI Struct. J.*, vol. 101, no. 3, 2004, pp. 364–374.
- 9.7. J. G. MacGregor, J. E. Breen, and E. O. Pfrang, "Design of Slender Concrete Columns," *J. ACI*, vol. 67, no. 1, 1970, pp. 6–28.
- 9.8. J. G. MacGregor, V. H. Oelhafen, and S. E. Hage, "A Reexamination of the EI Value for Slender Columns," *Reinforced Concrete Columns*, American Concrete Institute, Detroit, MI, 1975, pp. 1–40.
- 9.9. *Code of Practice for the Structural Use of Concrete*, Part 1, "Design Materials and Workmanship," (CP110: Part 1, 1972), British Standards Institution, London, 1972.
- 9.10. W. B. Cranston, "Analysis and Design of Reinforced Concrete Columns," *Research Report No. 20*, Paper 41.020, Cement and Concrete Association, London, 1972.
- 9.11. R. W. Furlong, "Column Slenderness and Charts for Design," *J. ACI*, vol. 68, no. 1, 1971, pp. 9–18.
- 9.12. M. Valley and P. Dumonteil, Disc. of "K-Factor Equation to Alignment Charts for Column Design," by L. Duan, W.-S. King, and W.-F. Chen, *ACI Struct. J.*, vol. 91, no. 2, Mar.-Apr. 1994, pp. 229–230.
- 9.13. J. S. Ford, D. C. Chang, and J. E. Breen, "Design Indications from Tests of Unbraced Multipanel Concrete Frames," *Concr. Intl.*, vol. 3, no. 3, 1981, pp. 37–47.
- 9.14. *Building Code Requirements for Structural Concrete*, ACI 318-02, American Concrete Institute, Farmington Hills, MI, 2002.
- 9.15. *Commentary on Building Code Requirements for Structural Concrete*, ACI 318R-02, American Concrete Institute, Farmington Hills, MI, 2002 (published as part of Ref. 9.14).
- 9.16. J. G. MacGregor, "Design of Slender Concrete Columns—Revisited," *ACI Struct. J.*, vol. 90, no. 3, 1993, pp. 302–309.
- 9.17. J. G. MacGregor, *Reinforced Concrete*, 3d ed., Prentice-Hall, Upper Saddle River, NJ, 1997.
- 9.18. B. R. Wood, D. Beaulieu, and P. F. Adams, "Column Design by P -Delta Model," *Proc. ASCE*, vol. 102, no. ST2, 1976, pp. 487–500.
- 9.19. B. R. Wood, D. Beaulieu, and P. F. Adams, "Further Aspects of Design by P -Delta Model," *J. Struct. Div.*, ASCE, vol. 102, no. ST3, 1976, pp. 487–500.
- 9.20. R. W. Furlong, "Rational Analysis of Multistory Concrete Structures," *Concr. Intl.*, vol. 3, no. 6, 1981, pp. 29–35.

PROBLEMS

- 9.1.** The 15×15 in. column shown in Fig. P9.1 must extend from footing level to the second floor of a braced frame structure with an unsupported length of 20.5 ft. Exterior exposure requires 2 in. clear cover for the outermost steel. Analysis indicates the critical loading corresponds with the following service loads:

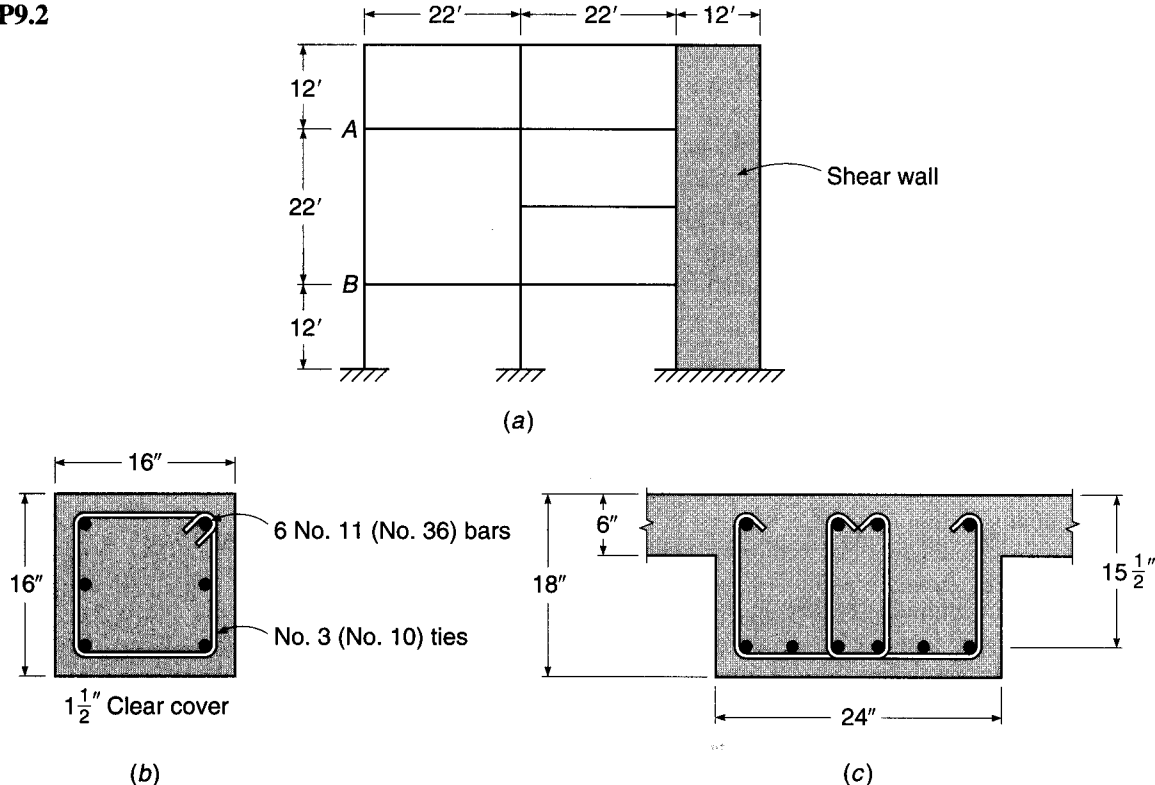
FIGURE P9.1



(a) from dead loads, $P = 170$ kips, $M_{\text{top}} = 29$ ft-kips, $M_{\text{bot}} = 14.5$ ft-kips; (b) from live loads, $P = 100$ kips, $M_{\text{top}} = 50$ ft-kips, $M_{\text{bot}} = 25$ ft-kips, with the column bent in double curvature as shown. The effective length factor k determined using Fig. 9.13a is 0.90. Material strengths are $f'_c = 4000$ psi and $f_y = 60,000$ psi. Using the ACI moment magnifier method, determine whether the column is adequate to resist these loads.

9.2. The structure shown in Fig. P9.2a requires tall slender columns at the left side. It is fully braced by shear walls on the right. All columns are 16×16 in., as shown in Fig. P9.2b, and all beams are 24×18 in. with 6 in. monolithic floor slab, as in Fig. P9.2c. Trial calculations call for column reinforcement as shown. Alternate load analysis indicates the critical condition with column AB bent in single curvature, and service loads and moments as follows: from dead loads, $P = 139$ kips, $M_{\text{top}} = 61$ ft-kips, $M_{\text{bot}} = 41$ ft-kips; from live load, $P = 93$ kips, $M_{\text{top}} = 41$ ft-kips, $M_{\text{bot}} = 27$ ft-kips. Material strengths are $f'_c = 4000$ psi and $f_y = 60,000$ psi. Is the proposed column, reinforced as shown, satisfactory for this load condition? Use Eq. (9.18) to calculate EI for the column.

FIGURE P9.2



- 9.3.** Refine the calculations of Problem 9.2, using Eq. (9.17) to calculate EI for the column. The reinforcement will be as given in Problem 9.2. Comment on your results.
- 9.4.** An interior column in a braced frame has an unsupported length of 20 ft and carries the following service load forces and moments: (a) from dead loads, $P = 180$ kips, $M_{\text{top}} = 28$ ft-kips, $M_{\text{bot}} = -28$ ft-kips; (b) from live loads,

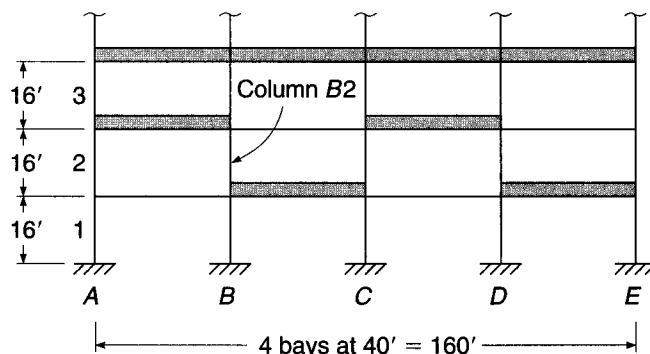
$P = 220$ kips, $M_{\text{top}} = 112$ ft-kips, $M_{\text{bot}} = 112$ ft-kips, with the signs of the moments representing double curvature under dead load and single curvature under live load. Rotational restraint factors at the top and bottom may be taken equal to 1.0. Design a square tied column to resist these loads, with a reinforcement ratio of about 0.02. Use $f'_c = 4000$ psi and $f_y = 60,000$ psi.

- 9.5. The first three floors of a multistory building are shown in Fig. P9.5. The lateral load-resisting frame consists of 20 × 20 in. exterior columns, 24 × 24 in. interior columns, and 36 in. wide × 24 in. deep girders. The center-to-center column height is 16 ft. For the second-story columns, the service gravity dead and live loads and the horizontal wind loads based on an elastic first-order analysis of the frame are:

	Cols. A2 and E2	Cols. B2 and D2	Col. C2
P_{dead}	348 kips	757 kips	688 kips
P_{live}	137 kips	307 kips	295 kips
P_{wind}	±19 kips	±9 kips	0 kips
V_{wind}	6.5 kips	13.5 kips	13.5 kips
$M_{2,\text{dead}}$		31 ft-kips	
$M_{2,\text{live}}$		161 ft-kips	
$M_{2,\text{wind}}$		105 ft-kips	
$M_{1,\text{dead}}$		−34 ft-kips	
$M_{1,\text{live}}$		108 ft-kips	
$M_{1,\text{wind}}$		−98 ft-kips	

A matrix analysis for the total unfactored wind shear of 53.5 kips, using values of E and I specified in Section 9.5, indicates that the relative lateral deflection of the second story is 0.24 in. Design columns B2 and D2 using Eq. (9.21) to calculate δ_s . Material strengths are $f'_c = 4000$ psi and $f_y = 60,000$ psi.

FIGURE P9.5



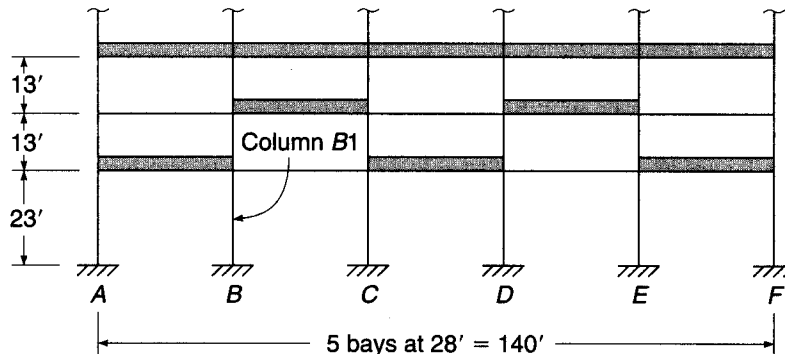
- 9.6. Repeat Problem 9.5, using Eq. (9.22) to calculate δ_s . Comment on your results.
 9.7. Redesign column C3 from Example 9.2 for a story height of 16 ft, a column unsupported length of 15 ft, and a relative lateral displacement of the third story of 1.10 in. Loads and other dimensions remain unchanged.
 9.8. The first four floors of a multistory building are shown in Fig. P9.8. The lateral load-resisting frame consists of 22 × 22 in. exterior columns, 26 × 26 in. interior columns, and 33 in. wide × 18 in. deep girders. The foundation is at ground level, supported on drilled piers, and may be considered as fully fixed

against rotation. The first-story columns have a clear height to the girder soffit of 21 ft 6 in., giving a floor-to-floor height of 23 ft. The upper floors have a center-to-center spacing of 13 ft. For the first-story columns, the service gravity dead and live loads plus the horizontal and vertical wind loads based on an elastic first-order analysis of the frame are:

	<i>Cols. A1 and F1</i>	<i>Cols. B1 and E1</i>	<i>Cols. C1 and D1</i>
P_{dead}	495 kips	1090 kips	989 kips
P_{live}	99 kips	206 kips	188 kips
P_{wind}	± 32 kips	± 19 kips	± 6 kips
V_{wind}	11 kips	22 kips	22 kips
$M_{2,\text{dead}}$		4 ft-kips	
$M_{2,\text{live}}$		70 ft-kips	
$M_{2,\text{wind}}$		240 ft-kips	
$M_{1,\text{dead}}$		-2 ft-kips	
$M_{1,\text{live}}$		-35 ft-kips	
$M_{1,\text{wind}}$		-240 ft-kips	

A matrix analysis for the total unfactored wind shear of 110 kips, using values of E and I specified in Section 9.5, indicates that the relative lateral deflection of the second story is 0.40 in. Design columns *B1* and *E1*, using Eq. (9.21) to calculate δ_s . Material strengths are $f'_c = 4000$ psi and $f_y = 60,000$ psi.

FIGURE P9.8



- 9.9.** Repeat Problem 9.8, using Eq. (9.22) to calculate δ_s . Comment on your results.

10

Strut-and-Tie Models

10.1 INTRODUCTION

Reinforced concrete beam theory is based on equilibrium, compatibility, and the constitutive behavior of the materials, steel and concrete. Of particular importance is the assumption that strain varies linearly through the depth of a member and that, as a result, plane sections remain plane. This assumption is validated by St. Venant's principle, which stipulates that strains induced by discontinuities in load or in member cross section vary in an approximately linear fashion at distances greater than or equal to the greatest cross-sectional dimension h from the point of load application. St. Venant's principle underlies the development of beam theory as presented in Chapters 1 and 3.

St. Venant's principle, however, does not apply at points closer than the distance h to discontinuities in applied load or geometry. This leads to the identification of *discontinuity regions* within reinforced concrete members near concentrated loads, openings, or changes in cross section. Because of their geometry, the full volume of deep beams and column brackets qualify as discontinuity regions. Thus, reinforced concrete structures may be divided into regions where beam theory is valid, often referred to as *B-regions*, and regions where discontinuities affect member behavior, known as *D-regions*. A number of D-regions are illustrated in Fig. 10.1.

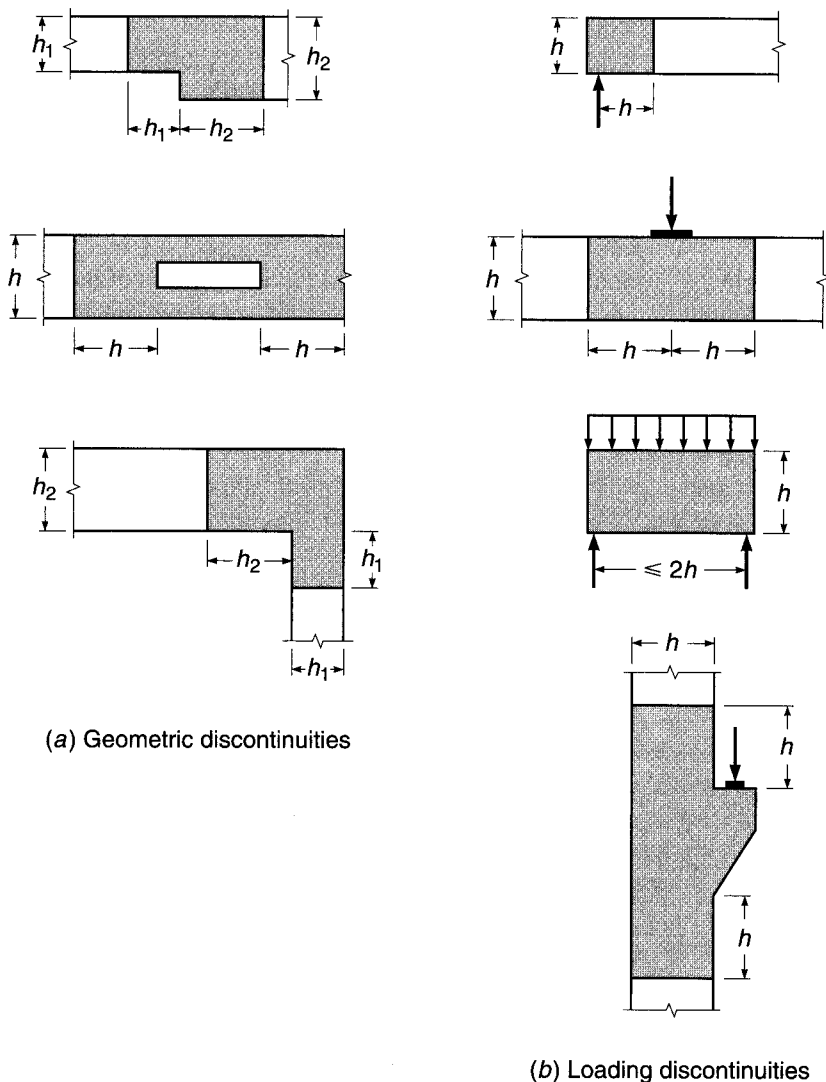
At low stresses, when the concrete is elastic and uncracked, the stresses within D-regions may be computed using finite element analysis or elasticity theory. When concrete cracks, the strain field is disrupted, causing a redistribution of the internal forces. Once this happens, it is possible to represent the internal forces within discontinuity regions using a statically determinate truss, referred to as a *strut-and-tie model*. This allows a complex design problem to be greatly simplified, producing a safe solution that satisfies statics. As shown in Fig. 10.2, strut-and-tie models consist of concrete compression *struts*, steel tension *ties*, and joints that are referred to as *nodal zones* (for consistency of presentation, struts are represented by dashed lines and ties are represented by solid lines).

10.2 DEVELOPMENT OF STRUT-AND-TIE MODELS

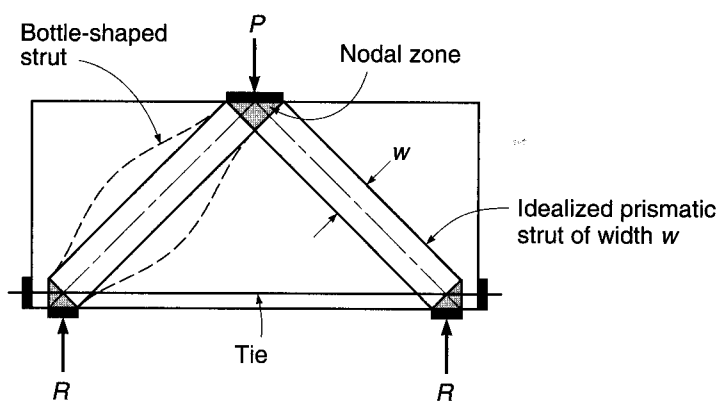
Strut-and-tie models evolved in the early 1980s in Europe (Refs. 10.1 to 10.4). Their use is permitted by ACI Code 8.3.4 and defined in Appendix A of the Code (Ref. 10.5). As defined, strut-and-tie models divide members into D-regions and B-regions. A D-region is that portion of a member that is within a distance equal to the member

FIGURE 10.1

Geometric and load discontinuities for D-regions.

**FIGURE 10.2**

Strut-and-tie model.



height h^{\dagger} from a force or geometric discontinuity, as shown in Fig. 10.1. B-regions are, in general, any portions of a member outside of D-regions. The assumption is that within B-regions strain varies linearly through the member cross section and plane sections remain plane.

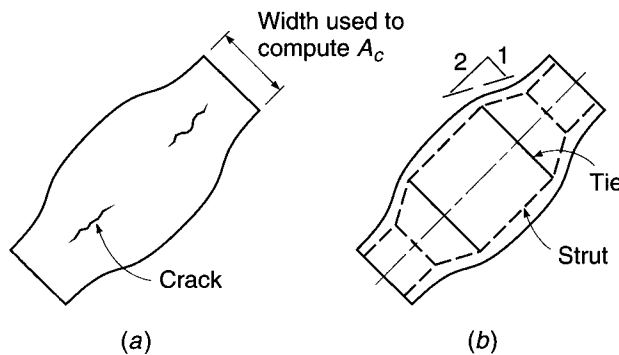
Strut-and-tie models are applied within D-regions. Models consist of struts and ties connected at nodal zones that are capable of transferring loads to the supports or adjacent B-regions. The cross-sectional dimensions of the struts and ties are designated as thickness and width. Thickness b is perpendicular to the plane of the truss model, and width w is measured in the plane of the model, as shown in Fig. 10.2.

a. Struts

A strut is an internal compression member. It may consist of a single element, parallel elements, or a fan-shaped compression field. Along its length, a strut may be rectangular or *bottle-shaped*, in which case the compression field spreads laterally between nodal zones, as shown in Fig. 10.3. For design purposes, a strut is typically idealized as a prismatic member between two nodes. While not preferred, a strut can also be idealized as a uniformly tapered compression member if the design criteria require different widths at the two ends of the strut. The dimensions of the cross section of the strut are established by the contact area between the strut and the nodal zone. Bottle-shaped struts are wider at the center than at the ends and form when the surrounding concrete permits the compression field to spread laterally. As the compression zone spreads along the length of bottle-shaped struts, tensile stresses perpendicular to the axis of the strut may result in longitudinal cracking. For simplicity in design, bottle-shaped struts are idealized as having linearly tapered ends and uniform center sections. The linear taper is taken at a slope of 1:2 to the axis of the compression force, as shown in Fig. 10.3b. The capacity of a strut is a function of the effective concrete compressive strength, which is affected by lateral stresses within the struts. Because of longitudinal splitting, bottle-shaped struts are weaker than rectangular struts, even though they possess a larger cross section at midlength. Transverse reinforcement is designed to control longitudinal splitting and proportioned using a strut-and-tie model that forms within the strut element, as shown in Fig. 10.3b.

FIGURE 10.3

Bottle-shaped strut.



[†] The ACI Code defines a D-region based on the member height h or effective depth d . No guidance is provided when to use h or d . The member height h is used in this text because it is conservative, always defining a larger D-region than that defined by the effective depth d .

b. Ties

A tie is a tension member within a strut-and-tie model. Ties consist of reinforcement (prestressed or nonprestressed) plus a portion of the concrete that is concentric with and surrounds the axis of the tie. The surrounding concrete defines the tie area and the region available to anchor the tie. For design purposes, it is assumed that the concrete within the tie does not carry any tensile force. Even though the tensile capacity of the concrete is not used in design, it assists in reducing tie deformation at service load.

c. Nodal Zones

Nodes are points within strut-and-tie models where the axes of struts, ties, and concentrated loads intersect. A nodal zone is the volume of concrete around a node where force transfer occurs. A nodal zone may be treated as a single region or may be subdivided into two smaller zones to equilibrate forces. For example, the nodal zone shown in Fig. 10.4a is subdivided, as shown in Fig. 10.4b, where two reactions R_1 and R_2 equilibrate the vertical components of strut forces C_1 and C_2 .

For equilibrium, at least three forces must act on a node. Nodes are classified by the sign of these forces (Fig. 10.5). Thus, a *C-C-C* node resists three compressive forces, and a *C-C-T* node resists two compressive forces and one tensile force. Both tensile and compressive forces place nodes in compression because tensile forces are treated as if they pass through the node and apply a compressive force on the far side, or anchorage face. Thus, within the plane of a strut-and-tie model truss, nodal zones

FIGURE 10.4

Subdivision of nodal zones.

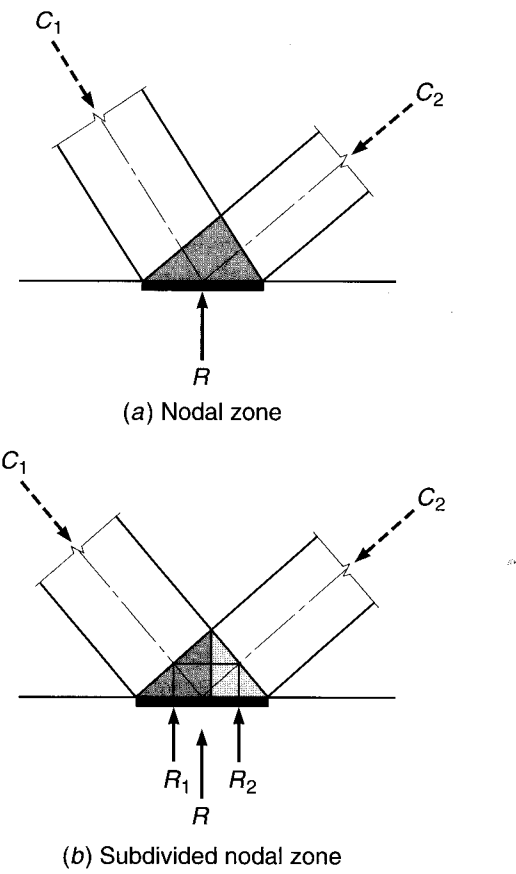
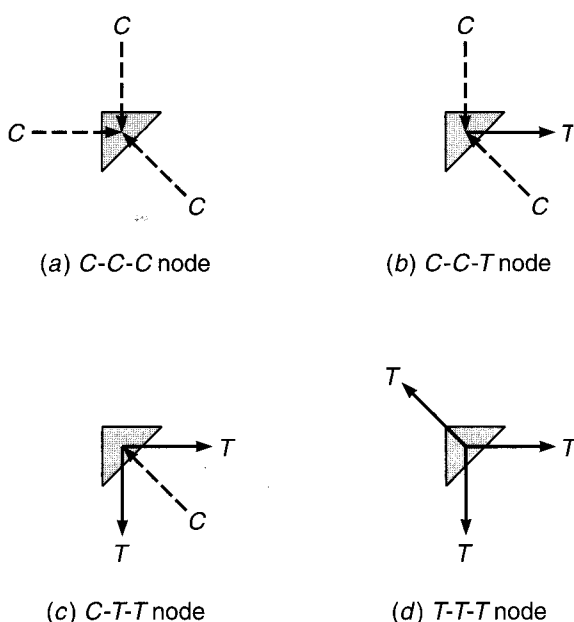


FIGURE 10.5

Classification of nodes.



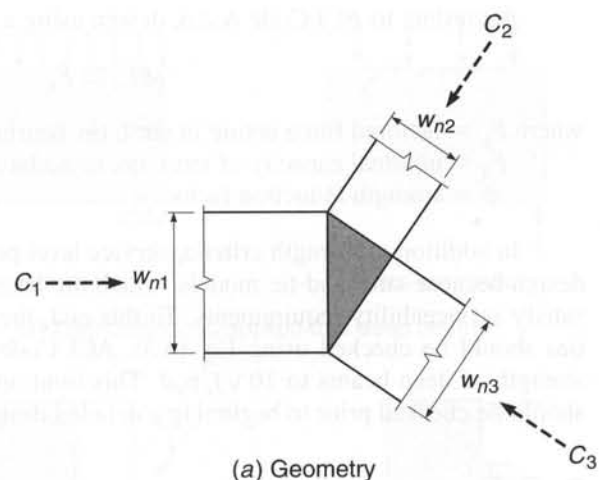
are considered to be in compression, as shown in Fig. 10.6a. If the nodal zone dimensions w_{n1} , w_{n2} , and w_{n3} are proportional to the applied compressive forces, the state of stress becomes one of *hydrostatic* compression. The dimension of one side of a nodal zone is often determined based on the contact area of the load, e.g., by a bearing plate, column base, or beam support. If a hydrostatic state of stress is desired, the dimensions of the remaining sides are selected to maintain a constant level of stress p within the node. By selecting nodal zone dimensions that are proportional to the applied loads, the stresses on the faces of the nodal zone are equal.[†] If, instead, the dimensions are determined based on preselected strut dimensions, e.g., minimum width, the state of stress will no longer be hydrostatic. The decision to use a hydrostatic or a nonhydrostatic state of stress is made by the designer, with the former being more typical because the latter results in a more complex design.

The length of a hydrostatic zone is often not adequate to allow for anchorage of tie reinforcement. For this reason, an *extended nodal zone*, defined by the intersection of the nodal zone and the associated strut (shown in light shading in Fig. 10.6b and c), is used. An extended nodal zone may be regarded as that portion of the overlap region between struts and ties that is not already counted as part of a primary node. It increases the length within which the tensile force from the tie can be transferred to the concrete and, thus, defines the available anchorage length for ties. Ties may be developed outside of the nodal and extended nodal zones if needed, as shown to the left of the node in Fig. 10.6c.

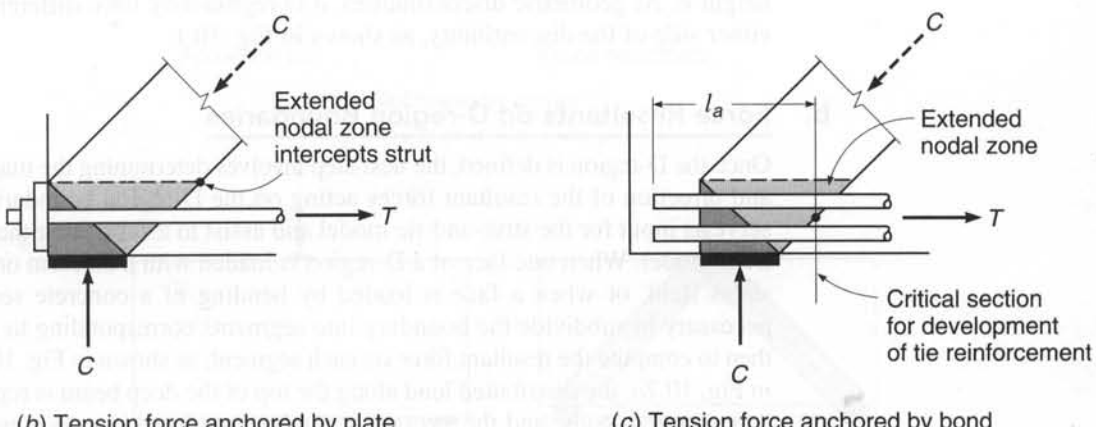
10.3 STRUT-AND-TIE DESIGN METHODOLOGY

Strut-and-tie models are used in several ways during the design process. At the *conceptual* design level, sketching a strut-and-tie model provides insight into structural behavior and detailing requirements. Examples of conceptual design can be seen in the

[†] The state of stress within a nodal zone is not truly hydrostatic since out-of-plane stresses are not considered.



(a) Geometry



(b) Tension force anchored by plate

(c) Tension force anchored by bond

FIGURE 10.6

Nodal zones and extended nodal zones.

development of connection details in Chapter 11. Strut-and-tie models may be used to validate design details, such as for special reinforcement configurations. Finally, strut-and-tie models may form the basis for detailed design of a member.

Application of a detailed strut-and-tie model involves completion of the following steps.

- Define and isolate the D-regions.
- Compute the force resultants on each D-region boundary.
- Select a truss model to transfer the forces across a D-region.
- Select dimensions for strut-and-tie nodal zones.
- Verify the capacity of the node and the strut, the latter both at midlength and at the nodal interface.
- Design the ties and the tie anchorage.
- Prepare design details and check minimum reinforcement requirements.

As will be described shortly, the design process requires interaction between these steps.

According to ACI Code A.2.6, design using a strut-and-tie model requires that

$$\phi F_n \geq F_u \quad (10.1)$$

where F_u = factored force acting in strut, tie, bearing area, or nodal zone

F_n = nominal capacity of strut, tie, or nodal zone

ϕ = strength reduction factor

In addition to strength criteria, service level performance must be considered in design because strut-and-tie models, which are based on strength, do not necessarily satisfy serviceability requirements. To this end, the spacing of reinforcement within ties should be checked using Eq. (6.3). ACI Code 11.7.3 limits the nominal shear strength of deep beams to $10\sqrt{f'_c}b_{w,d}$. This limit applies to strut-and-tie models and should be checked prior to beginning a detailed design, as described in Section 10.4d.

a. D-region

A D-region extends on both sides of a discontinuity by a distance equal to the member height h . At geometric discontinuities, a D-region may have different dimensions on either side of the discontinuity, as shown in Fig. 10.1.

b. Force Resultants on D-region Boundaries

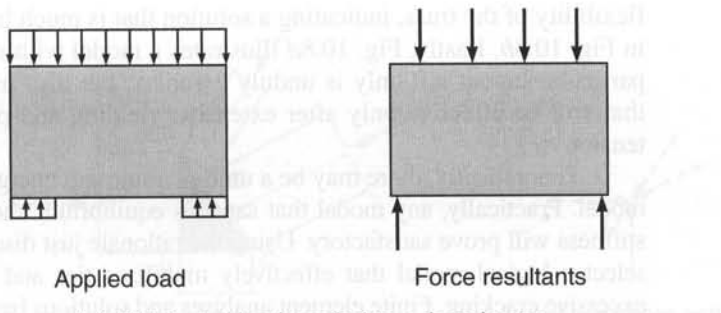
Once the D-region is defined, the next step involves determining the magnitude, location, and direction of the resultant forces acting on the D-region boundaries. These forces serve as input for the strut-and-tie model and assist in establishing the geometry of the truss model. When one face of a D-region is loaded with a uniform or linearly varying stress field, or when a face is loaded by bending of a concrete section, it may be necessary to subdivide the boundary into segments corresponding to struts or ties and then to compute the resultant force on each segment, as shown in Fig. 10.7. For example, in Fig. 10.7a, the distributed load along the top of the deep beam is represented by four concentrated loads, and the stresses at the beam-column interface are represented by concentrated reactions. In Fig. 10.7b, the moments at the faces of the beam-column joint are represented by couples consisting of tensile and compressive forces acting at the interfaces between the members and the joint.

c. The Truss Model

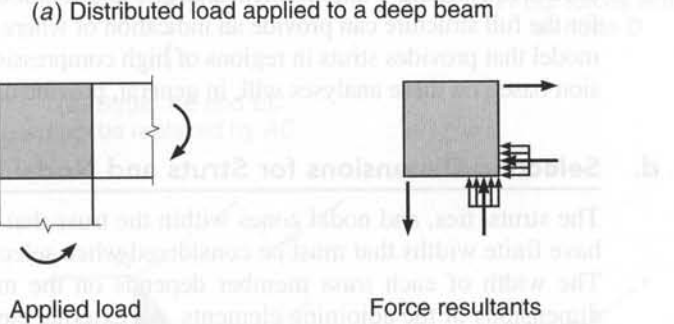
The truss representing the strut-and-tie model must fit within the envelope defined by the D-region. The selection of struts and ties is made at the discretion of the designer, and, therefore, multiple solutions are possible. The axes of the truss members are chosen to coincide with the centroids of the tension and compression fields, and the geometry so established is used to compute the forces in the members. The layout of a truss model is constrained by the geometric requirement that struts must intersect only at nodal zones. Ties may cross struts. An effective model will represent a minimum energy distribution through the D-region (Refs. 10.1 and 10.4); i.e., within the model, forces should follow the stiffest load path. Because struts are typically much stiffer than ties, a model with a minimum number of tension ties is generally preferred. Alternative truss models for a deep beam are compared in Fig. 10.8. Figure 10.8a shows a deep beam subjected to a concentrated load at midspan. Figure 10.8b shows the preferred strut-and-tie model for this beam and loading condition. In this case, struts carry the load directly to nodal regions at the supports, which are, in turn, connected by

FIGURE 10.7

Resolution of forces in a deep beam's D-region.



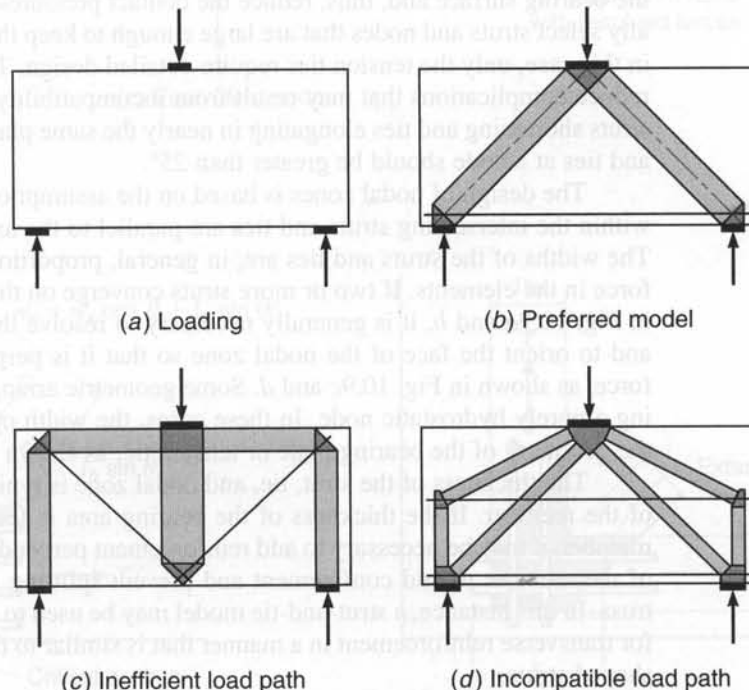
(a) Distributed load applied to a deep beam



(b) Moment resisting corner

FIGURE 10.8

Alternatives for a deep beam truss model.



(a) Loading

(b) Preferred model

(c) Inefficient load path

(d) Incompatible load path

a single tension tie. The model in Fig. 10.8c shows an ineffective load path, with a single strut carrying the load to a node at the bottom of the beam that is supported by two diagonal tension ties, which are, in turn, supported by vertical struts over the supports. In this instance, the number of transfer points and tension ties is greater, as is the

flexibility of the truss, indicating a solution that is much less effective than that shown in Fig. 10.8b. Lastly, Fig. 10.8d illustrates a model with multiple struts and ties. This particular layout not only is unduly complex, but also includes an upper tension tie that will be effective only after extensive yielding and possible failure of the lower tension tie.

Theoretically, there may be a unique minimum energy solution for a strut-and-tie model. Practically, any model that satisfies equilibrium and pays attention to structural stiffness will prove satisfactory. Using the rationale just discussed allows the designer to select a logical model that effectively mobilizes ties and minimizes the potential for excessive cracking. Finite element analyses and solutions based on the theory of elasticity for the full structure can provide an indication of where maximum stresses occur. A truss model that provides struts in regions of high compression and ties in regions of high tension based on these analyses will, in general, provide an efficient load path.

d. Selecting Dimensions for Struts and Nodal Zones

The struts, ties, and nodal zones within the truss that represents a strut-and-tie model have finite widths that must be considered when selecting the dimensions of the truss. The width of each truss member depends on the magnitude of the forces and the dimensions of the adjoining elements. An external element, such as a bearing plate or column, can serve to define a nodal zone. If the bearing area is too small, a high hydrostatic pressure results, and the corresponding width of the node or struts will not be sufficient to carry the applied load. The solution in this case is to increase the size of the bearing surface and, thus, reduce the contact pressures. Some designers intentionally select struts and nodes that are large enough to keep the compressive stresses low; in this case, only the tension ties require detailed design. To minimize cracking and to reduce complications that may result from incompatibility in the deformations due to struts shortening and ties elongating in nearly the same plane, the angle between struts and ties at a node should be greater than 25°.

The design of nodal zones is based on the assumption that the principal stresses within the intersecting struts and ties are parallel to the axes of these truss members. The widths of the struts and ties are, in general, proportional to the magnitude of the force in the elements. If two or more struts converge on the same face, such as shown in Fig. 10.9a and b, it is generally necessary to resolve the forces into a single force and to orient the face of the nodal zone so that it is perpendicular to the combined force, as shown in Fig. 10.9c and d. Some geometric arrangements preclude establishing a purely hydrostatic node. In these cases, the width of the strut is determined by the geometry of the bearing plate or tension tie, as shown in Fig. 10.10a.

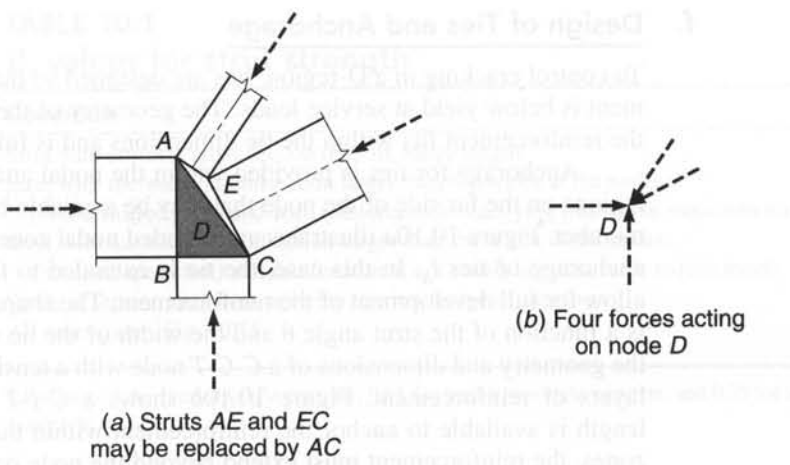
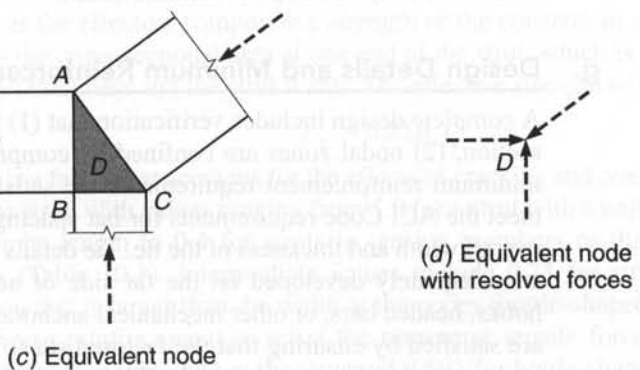
The thickness of the strut, tie, and nodal zone is typically equal to the thickness of the member. If the thickness of the bearing area is less than the thickness of the member, it may be necessary to add reinforcement perpendicular to the principal plane of the member to add confinement and prevent splitting parallel to the plane of the truss. In this instance, a strut-and-tie model may be used to determine the requirements for transverse reinforcement in a manner that is similar to that used to reinforce bottle-shaped struts.

e. Capacity of Struts

Strut capacity is based on both the strength of the strut itself and the strength of the nodal zone. If a strut does not have sufficient capacity, the design must be revised by providing compression reinforcement or by increasing the size of the nodal zone. This may, in turn, affect the size of the bearing plate or column.

FIGURE 10.9

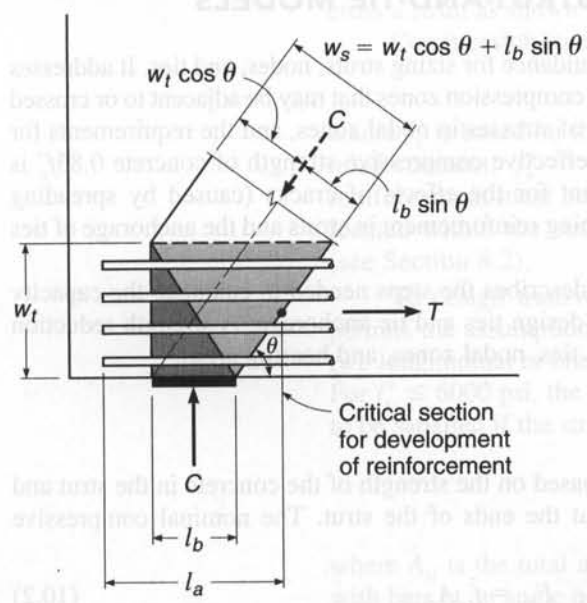
Resolution of forces in nodal zones.

(a) Struts AE and EC
may be replaced by AC(b) Four forces acting
on node D

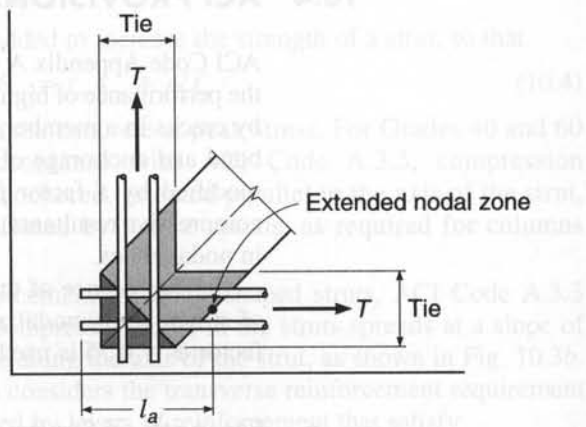
(c) Equivalent node

(d) Equivalent node
with resolved forces**FIGURE 10.10**

Extended nodal zone definition.



(a) C-C-T node with eccentric strut



(b) C-T-T node

f. Design of Ties and Anchorage

To control cracking in a D-region, ties are designed so that the stress in the reinforcement is below yield at service loads. The geometry of the tie must be selected so that the reinforcement fits within the tie dimensions and is fully anchored.

Anchorage for ties is provided within the nodal and extended nodal zones plus regions on the far side of the node that may be available based on the geometry of the member. Figure 10.10a illustrates an extended nodal zone and the length available for anchorage of ties l_a . In this case, the tie is extended to the left of the nodal zone to allow for full development of the reinforcement. The shape of the extended nodal zone is a function of the strut angle θ and the width of the tie w_t . Figure 10.10a illustrates the geometry and dimensions of a C-C-T node with a tension tie that contains multiple layers of reinforcement. Figure 10.10b shows a C-T-T nodal zone. If insufficient length is available to anchor the reinforcement within the nodal and extended nodal zones, the reinforcement must extend beyond the node or a hook or headed bar must be used to fully develop the reinforcement.

g. Design Details and Minimum Reinforcement Requirements

A complete design includes verification that (1) tie reinforcement can be placed in the section, (2) nodal zones are confined by compressive forces or tension ties, and (3) minimum reinforcement requirements are satisfied. Reinforcement within ties must meet the ACI Code requirements for bar spacing (see Section 3.6c) and fit within the overall width and thickness of the tie. Tie details should be reviewed to ensure that ties are adequately developed on the far side of nodes by tension development length, hooks, headed bars, or other mechanical anchorage. Shear reinforcement requirements are satisfied by ensuring that the factored shear is less than the ACI Code maximum, as described in Chapter 4, longitudinal cracking of bottle-shaped struts is controlled, or the minimum reinforcement requirements described in Section 10.4d are met.

10.4 ACI PROVISIONS FOR STRUT-AND-TIE MODELS

ACI Code Appendix A provides guidance for sizing struts, nodes, and ties. It addresses the performance of highly stressed compression zones that may be adjacent to or crossed by cracks in a member, the effect of stresses in nodal zones, and the requirements for bond and anchorage of ties. The effective compressive strength of concrete $0.85f'_c$ is modified by a factor β to account for the effects of cracks (caused by spreading compressive resultants) and confining reinforcement in struts and the anchorage of ties in nodal zones.

The balance of this section describes the steps needed to calculate the capacity of struts, verify nodal zones, and design ties and tie anchorage. A strength reduction factor $\phi = 0.75$ is used for struts, ties, nodal zones, and bearing areas.

a. Strength of Struts

The strength of a strut is limited based on the strength of the concrete in the strut and the strength of the nodal zones at the ends of the strut. The nominal compressive strength of a strut F_{ns} is given as

$$F_{ns} = f_{ce} A_{cs} \quad (10.2)$$

TABLE 10.1
 β_s values for strut strength

Condition	β_s
Strut with uniform cross section over its entire length	1.0
Strut with the width at midsection larger than the width at the nodes (bottle-shaped strut) and with reinforcement satisfying transverse requirements	0.75
Strut with the width at midsection larger than the width at the nodes (bottle-shaped strut) and reinforcement not satisfying transverse requirements	$0.60\lambda^{\dagger}$
Struts in tension members or in the tension flange of members	0.40
All other cases, Fig. 10.11	0.60λ

[†] λ equals 1.0 for normalweight concrete, 0.85 for sand-lightweight concrete, and 0.75 for all-lightweight concrete.

where f_{ce} is the effective compressive strength of the concrete in a strut or nodal zone and A_{cs} is the cross-sectional area at one end of the strut, which is equal to the product of the strut thickness and the strut width. The effective strength of concrete in a strut is

$$f_{ce} = 0.85\beta_s f'_c \quad (10.3)$$

where β_s is a factor that accounts for the effects of cracking and confining reinforcement within the strut, with values ranging from 1.0 for a strut with a uniform cross-sectional area over its length to 0.4 for struts in tension members or the tension flanges of members (Table 10.1). Intermediate values include 0.75 for struts with a width at midsection that is larger than the width at the nodes (bottle-shaped struts) and crossed by transverse reinforcement to resist the transverse tensile force resulting from the compressive force spreading in the strut and 0.60λ for bottle-shaped struts without the required transverse reinforcement, where λ is the correction factor related to the unit weight of concrete: 1.0 for normalweight concrete, 0.85 for sand-lightweight concrete, and 0.75 for all-lightweight concrete. $\beta_s = 0.60\lambda$ for all other cases, as when parallel diagonal cracks divide the web struts or when diagonal cracks are likely to turn and cross a strut, as shown in Fig. 10.11.

Compression steel may be added to increase the strength of a strut, so that

$$F_{ns} = f_{ce}A_{cs} + A'_s f'_s \quad (10.4)$$

where f'_s is based on the strain in the concrete at peak stress. For Grades 40 and 60 reinforcement, $f'_s = f_y$. In accordance with ACI Code A.3.5, compression reinforcement must be properly anchored, oriented parallel to the axis of the strut, located within the strut, and enclosed by ties or spirals, as required for columns (see Section 8.2).

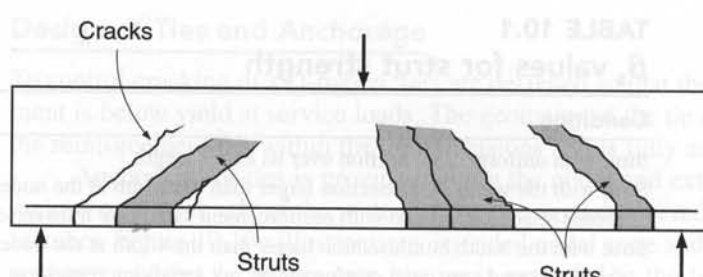
To design transverse reinforcement for bottle-shaped struts, ACI Code A.3.3 permits the assumption that the compressive force in the struts spreads at a slope of two longitudinal to one transverse along the axis of the strut, as shown in Fig. 10.3b. For $f'_c \leq 6000$ psi, the ACI Code considers the transverse reinforcement requirement to be satisfied if the strut is crossed by layers of reinforcement that satisfy

$$\sum \frac{A_{si}}{b_s s_i} \sin \alpha_i \geq 0.003 \quad (10.5)$$

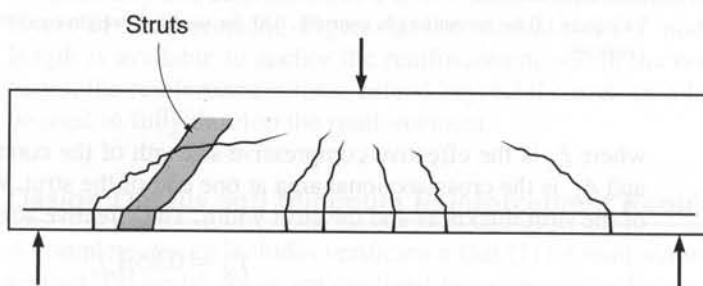
where A_{si} is the total area of reinforcement at spacing s_i in a layer of reinforcement with bars at an angle α_i to the axis of the strut and b_s is the thickness of the strut. The

FIGURE 10.11

Beam cracking conditions for $\beta_s = 0.6\lambda$.



(a) Struts in beam with inclined cracks parallel to strut



(b) Struts crossed by skew cracks

reinforcement may be perpendicular to the strut axis or may be placed in an orthogonal grid pattern. The subscript i denotes the layer of reinforcement. The values s_i and α_i are shown in Fig. 10.12. The minimum reinforcement requirements described for deep beams in Section 10.4d provide additional guidance for selection of reinforcement to satisfy Eq. (10.5).

The ACI Code provides no clear guidance to indicate when a strut should be considered as rectangular or bottle-shaped. Some researchers suggest that horizontal

FIGURE 10.12
Details of reinforcement crossing a strut.

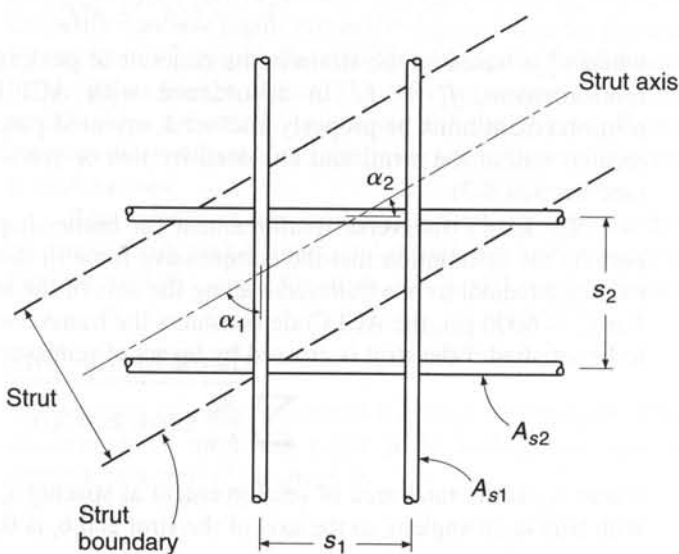


TABLE 10.2
 β_n values for node strength

Nodal Zone Condition	Classification	β_n
Bounded by struts or bearing area	C-C-C	1.0
Anchoring one tie	C-C-T	0.80
Anchoring two or more ties	C-T-T or T-T-T	0.60

struts be represented as rectangular and inclined struts represented as bottle-shaped (Ref. 10.6). Others simply assume a bottle-shaped strut will develop and use the lower values of β_s for design (Ref. 10.7). Examples in this text use rectangular horizontal struts and bottle-shaped inclined struts.

b. Strength of Nodal Zones

The nominal compressive strength of a nodal zone is

$$F_{nn} = f_{ce} A_{nz} \quad (10.6)$$

where f_{ce} is the effective strength of the concrete in the nodal zone and A_{nz} is (1) the area of the face of the nodal zone taken perpendicular to the line of action of the force from the strut or tie or (2) the area of a section through the nodal zone taken perpendicular to the line of action of the resultant force on the section. The latter condition occurs when multiple struts intersect a node, as shown in Fig. 10.9.

The effective concrete strength in a nodal zone is

$$f_{ce} = 0.85 \beta_n f'_c \quad (10.7)$$

where f'_c is the compressive strength of the concrete in the nodal zone and β_n is a factor that reflects the degree of disruption in nodal zones due to the incompatibility of tensile strains in ties with compressive strains in struts. $\beta_n = 1.0$ for C-C-C nodes, 0.80 for C-C-T nodes, and 0.60 for C-T-T or T-T-T nodes. Values of β_n are summarized in Table 10.2. ACI Code A.5.2 permits the strength of a node to be increased above the value given in Eq. (10.7) if the node contains confining reinforcement and the effect of that reinforcement is demonstrated by tests and analysis.

Unless compression reinforcement is used in the struts, the lower value of f_{ce} from Eqs. (10.3) and (10.7) governs and should be used to design both the node and the adjoining struts.

c. Strength of Ties

The nominal strength of ties F_{nt} is the sum of the strengths of the reinforcing steel and prestressing steel within the tie.

$$F_{nt} = A_{ts} f_y + A_{tp} (f_{pe} + \Delta f_p) \quad (10.8)$$

where A_{ts} = area of reinforcing steel

f_y = yield strength of reinforcing steel

A_{tp} = area of prestressing steel, if any

f_{pe} = effective stress in prestressing steel

Δf_p = increase in prestressing steel stress due to factored load

The sum $f_{pe} + \Delta f_p$ must be less than or equal to the yield stress of the prestressing reinforcement f_{py} , and A_{tp} is zero for nonprestressed members. The value of Δf_p may be found by analysis; or, in lieu of formal analysis, ACI Code A.4.1 allows a value 60,000 psi to be used for bonded tendons and 10,000 psi to be used for unbonded tendons.

The effective width of a tie w_t depends on the distribution of the tie reinforcement. If the reinforcement in a tie is placed in a single layer, the effective width of a tie may be taken as the diameter of the largest bars in the tie plus twice the cover to the surface of the bars. Alternatively, the width of a tie may be taken as the width of the anchor plates. The practical upper limit for tie width $w_{t,max}$ is equal to the width corresponding to the width of a hydrostatic nodal zone, given as

$$w_{t,max} = \frac{F_{nt}}{b_s f_{ce}} \quad (10.9)$$

where f_{ce} is the effective nodal zone compressive stress given in Eq. (10.7) and b_s is the thickness of the strut.

Ties must be anchored before they leave the extended nodal zone at a point defined by the centroid of the bars in the tie and the extension of the outlines of either the strut or the bearing area, as shown in Fig. 10.10. If the combined lengths of the nodal zone and extended nodal zone are inadequate to provide for development of the reinforcement, additional anchorage may be obtained by extending the reinforcement beyond the nodal zone, using 90° hooks, or by using a mechanical anchor. If the tie is anchored with a 90° hook, the hooks should be confined by reinforcement extending into the beam from supporting members to avoid splitting of the concrete within the anchorage region.

d. ACI Shear Requirements for Deep Beams

Beams with clear spans less than or equal to 4 times the total member depth or with concentrated loads placed within twice the member depth of a support are classified as deep beams, according to ACI Code 11.7.[†] Examples of deep beams are shown in Fig. 10.13. ACI Code 11.7.2 allows such members to be designed either by using a nonlinear analysis or by applying the strut-and-tie method of ACI Code Appendix A. While solutions based on nonlinear strain distributions are available (Ref. 10.8), the strut-and-tie approach allows a rational design solution.

ACI Code 11.7.3 specifies that the nominal shear in a deep beam may not exceed $10\sqrt{f'_c b_w d}$, where b_w is the width of the web and d is the effective depth. ACI Code 11.7.4 and 11.7.5 provide minimum steel requirements for horizontal and vertical reinforcement within a deep beam. The minimum reinforcement perpendicular to a span is

$$A_v \geq 0.0025 b_w s \quad (10.10)$$

where s is the spacing of the reinforcement. The minimum reinforcement parallel to a span is

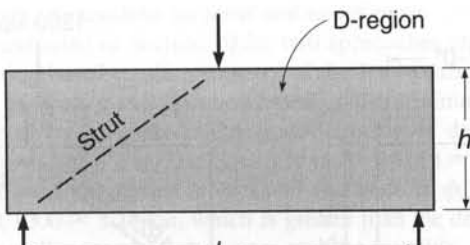
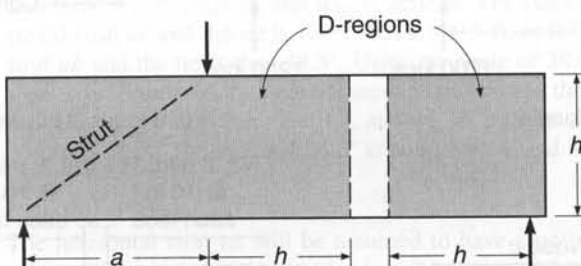
$$A_{vh} \geq 0.0015 b_w s_2 \quad (10.11)$$

where s_2 is the spacing of the reinforcement perpendicular to the longitudinal reinforcement. Spacings s and s_2 may not exceed $d/5$ or 12 in. ACI Code 11.7.6 allows Eq. (10.5) to be used in lieu of Eqs. (10.10) and (10.11). For strut-and-tie models, b_w equals the thickness of the element b .

[†] The ACI Code does not specify the magnitude of the concentrated load at a beam end needed to invoke the deep beam provisions of Section 11.7. A level of professional judgment is required if a low-magnitude concentrated load is placed at the end of a beam. Deep beam design may not be required in this situation.

FIGURE 10.13

Deep beam D-regions.

(a) Deep beam with $L \leq 4h$ (b) Deep beam with $a \leq 2h$

10.5 APPLICATIONS

While there are a number of possible applications for a strut-and-tie model, ACI Code 11.7 and 11.8 specifically allow deep beam and column bracket design to be completed with this method. The following examples examine the details of deep beams and dapped beam end design by the strut-and-tie method. Additional examples of strut-and-tie modeling may be found in Chapter 11 and in Refs. 10.9 through 10.12.

a. Deep Beams

Deep beams represent one of the principal applications of strut-and-tie models, since the alternative under ACI Code 11.7 is a nonlinear analysis. Two examples of deep beam design are presented next, one that includes the application of concentrated loads at the upper surface of a transfer girder and a second that addresses design for distributed as well as concentrated loads.

EXAMPLE 10.1

Deep beam. A transfer girder is to carry two 24 in. square columns, each with factored loads of 1200 kips located at the third points of its 36 ft span, as shown in Fig. 10.14a. The beam has a thickness of 2 ft and a total height of 12 ft. Design the beam for the given loads, ignoring the self-weight, using $f'_c = 5000$ psi and $f_y = 60,000$ psi.

SOLUTION. The span-to-depth ratio for the beam is 3, thereby qualifying it as a deep beam. A strut-and-tie solution will be used.

Definition of D-region

All of the supports and loads are within h of each other or the supports, so the entire structure may be characterized as a D-region. The thickness of the struts and ties is equal to the thickness

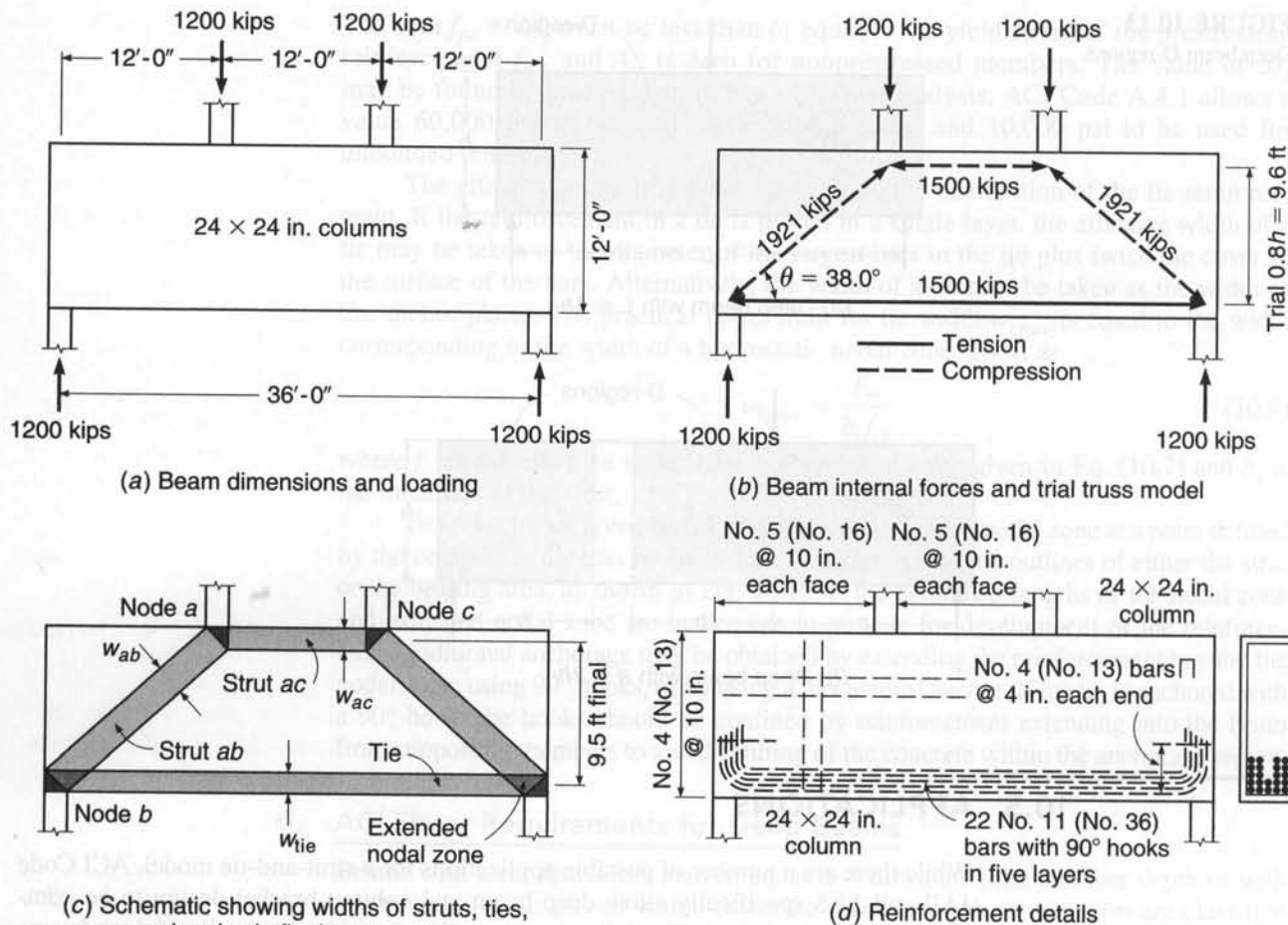


FIGURE 10.14

Deep beam design for Example 10.1.

of the beam $b = 24$ in. Assuming an effective depth $d = 0.9h = 0.9 \times 12 = 10.8$ ft in the middle third of the beam, the maximum design shear capacity of the beam is $\phi V_u = \phi 10\sqrt{f'_c}b_w d = 0.75 \times 10\sqrt{5000} \times 24 \times 10.8 \times 12/1000 = 1650$ kips. This is greater than $V_u = 1200$ kips. Thus, the design may continue.

Force resultants on D-region boundaries

The 1200 kip column loads on the upper face of the beam are equilibrated by 1200 kip reactions at the supports, as shown in Fig. 10.14b. Based on an assumed center-to-center distance between the horizontal strut and the tie of $0.8h$, the trial diagonal struts form at an angle $\theta = 38.66^\circ$ and carry a load of 1921 kips. A horizontal 1500 kip compression strut runs between the two column loads, and a 1500 kip tension tie runs between the bottom nodes.

The truss model

Based on the beam geometry and loading, a single truss is sufficient to carry the column loads, as shown in Fig. 10.14c. The truss has a trapezoidal shape. This is an acceptable solution since the nodes are not true pins and instability within the plane of the truss is not a concern in a strut-and-tie model. The truss geometry is established by the assumed intersection of the struts and ties and used to determine θ .

Selecting dimensions for strut and nodal zones

As mentioned in Section 10.2c, two approaches are used to select strut and nodal zone sizes: selection based on the geometry of the load-bearing transfer elements to maintain a constant level of stress p and selection based on the minimum strut width w . For this example, the first approach will be used. The nodal stress p is determined by the average stress under the columns. Thus, $p = 1200 \text{ kips}/(24 \text{ in.} \times 24 \text{ in.}) = 2.08 \text{ ksi}$. Because this is a C-C-C node, β_n is 1.0, and the design strength of the node is $\phi f_{ce} = \phi 0.85\beta_n f'_c = 0.75 \times 0.85 \times 1.0 \times 5000/1000 = 3.19 \text{ ksi}$, which is greater than the demand from the column. This result implies that smaller truss member sizes may be possible, a point that is discussed at the end of this example. The width of strut ac , found using p , is

$$w_{ac} = F_{ac}/(b_s \times p) = 1500/(24 \times 2.08) = 30.0 \text{ in.}$$

Similarly, $w_{ab} = 38.5 \text{ in.}$ and $w_{tie} = 30.0 \text{ in.}$ The center-to-center distance between the horizontal strut ac and the tie is $12 - 30/12 = 9.5 \text{ ft}$, or $0.79h$. The angle θ between the diagonal strut ab and the tie is thus 38.3° . Using an angle of 38.0° gives a revised force in strut ab of 1949 kips. Similarly, the revised force in strut ac and the tie is 1536 kips, while the widths are revised to $w_{ab} = 39.0 \text{ in.}$, and w_{ac} and $w_{tie} = 30.7 \text{ in.}$ (*Note:* After iteration, the actual angle becomes 38.2° . The value of 38.0° is conservative and is, thus, retained.)

Capacity of struts

The horizontal strut ac will be assumed to have a uniform cross section, while the diagonal struts will be considered as bottle-shaped because of the greater width available. Strut capacity is given in Eqs. (10.2) and (10.3), which, when combined, give $\phi F_{ns} = \phi 0.85\beta_s f'_c w_i b_s$, where w_i is the width of the strut and β_s is 1.0 for a rectangular strut. For strut ac ,

$$\phi F_{ns} = 0.75 \times 0.85 \times 1.0 \times 5000 \times 30.7 \times 24/1000 = 2349 \text{ kips} > 1536 \text{ kips}$$

Therefore, strut ac is adequate. Similarly, for strut ab ,

$$\phi F_{ns} = 0.75 \times 0.85 \times 0.75 \times 5000 \times 39.0 \times 24/1000 = 2238 \text{ kips} > 1949 \text{ kips}$$

From Eqs. (10.6) and (10.7), the capacity of the nodal zone is $\phi F_{nn} = \phi 0.85\beta_n f'_c w_i b_s$. At a , a C-C-C node, $\beta_n = 1.0$, and at b , a C-C-T node, $\beta_n = 0.80$. Thus, the capacity of strut ab is established at node b with $\beta_n = 0.80$ and

$$\phi F_{nn} = 0.75 \times 0.85 \times 0.80 \times 5000 \times 39.0 \times 24/1000 = 2387 \text{ kips} \geq 1949 \text{ kips}$$

Similarly, the nodal end capacity of strut ac is 2349 kips with $\beta_n = 1.0$. The capacity at the end of the struts and at the nodes exceeds the factored loads, and thus, the struts are adequate.

Design ties and anchorage

The tie design consists of three steps: selection of the area of steel, design of the anchorage, and validation that the tie fits within the available tie width. The steel area is computed as $A_{ts} = F_{tu}/\phi f_y = 1536/(0.75 \times 60) = 34.1 \text{ in}^2$. This is satisfied by using 22 No. 11 (No. 36) bars, having a total area of $A_{ts} = 34.3 \text{ in}^2$. Placing the bars in two layers of five bars and three layers of four bars, while allowing for 2.5 in. clear cover to the bottom of the beam and $4\frac{1}{2}$ in. clear spacing between layers, results in a total tie width of $5 \times 1.41 + 4 \times 4.5 + 2 \times 2.5 = 30.0 \text{ in.}$, matching the tie dimension.

The anchorage length l_d for No. 11 (No. 36) bars (from Table A.10 in Appendix A) is $42d_b = 59.2 \text{ in.}$ The length of the nodal zone and extended nodal zone is $24 + 0.5 \times 30.7 \cot 38.0^\circ = 43.6 \text{ in.}$, which is less than l_d . The beam geometry does not allow the tie reinforcement to extend linearly beyond the node; therefore, 90° hooks or mechanical anchors are required on the No. 11 (No. 36) bars. Placement details are covered in the next section. Allowing 1.5 in. cover on the sides, No. 5 (No. 16) transverse and horizontal reinforcement, and $2d_b$ spacing between No. 11 (No. 36) bars, five No. 11 (No. 36) bars require a total thickness of $b_{reqd} = 2 \times 1.5 + 4 \times 0.625 + 4 \text{ spaces} @ 2 \times 1.41 + 5 \text{ bars} \times 1.41 = 23.8 \text{ in.}$, which fits within the 24 in. beam thickness.

Design details and minimum reinforcement requirements

ACI Code 11.8.6 requires that shear reinforcement in deep beams satisfy (1) both Eqs. (10.10) and (10.11) or (2) Eq. (10.5). Using Eq. (10.10), the minimum required vertical steel is $A_v \geq 0.0025b_{ws} = 0.0025 \times 24 \times 12 = 0.72 \text{ in}^2/\text{ft}$. This is satisfied by No. 5 (No. 16) bars at 10 in. placed on each face, giving a total area of reinforcement equal to $0.74 \text{ in}^2/\text{ft}$. Similarly, using Eq. (10.11), the horizontal reinforcement is $A_{vh} \geq 0.0015b_{ws}^2 = 0.0015 \times 24 \times 12 = 0.43 \text{ in}^2/\text{ft}$, which is satisfied using No. 4 (No. 13) bars at 10 in. placed on each face, giving $0.48 \text{ in}^2/\text{ft}$.

Equation (10.5) produces similar steel requirements. Using the reinforcement selected using Eqs. (10.10) and (10.11), two No. 5 (No. 16) bars ($\gamma = 38.0^\circ$) give $A_v = 0.62 \text{ in}^2$ and two No. 4 (No. 13) bars ($\alpha = 52.0^\circ$) give $A_{vh} = 0.40 \text{ in}^2$. Equation (10.5) becomes

$$\sum \frac{A_{si}}{b_s s_i} \sin \alpha_i = \frac{0.62 \sin 52.0^\circ + 0.40 \sin 38.0^\circ}{24 \times 10} = 0.00306 > 0.003 \text{ req'd.}$$

This ensures that sufficient reinforcement is present to control longitudinal splitting in the bottle-shaped struts as well as to satisfy minimum reinforcement requirements.

The large number of No. 11 (No. 36) bars will require either the use of mechanical anchorage or staggering the location of the hooks. Heads require less space than hooks and would be preferable for concrete placement, but because they require a clear spacing of $4d_b$ (see Section 5.5), headed bars will not work in this case. Figure 10.14d shows staggered hooks for the final design. In addition, horizontal U-shaped No. 4 (No. 13) bars are placed at 4 in. ($3d_b = 3 \times 1.41 \text{ in.} = 4.23 \text{ in.}$) across the end of the beam to confine the No. 11 (No. 36) hooks. The final beam details are given in Fig. 10.14d.

Because the ACI Code does not require that hydrostatic pressure be maintained within the nodes, alternate solutions are possible. For example, a bottle-shaped strut ($\beta_s = 0.75$) can carry a maximum stress that is higher than p . Using the design compressive strength ϕf_{ce} , the width of the strut can be reduced to

$$w_{ab} = F_{ab}/(b_s \times \phi 0.85 \beta_s f'_c) = 1991/(24 \times 0.75 \times 0.85 \times 0.70 \times 5000/1000) = 31.6 \text{ in.}$$

compared with the width of 38.5 in. used in this example. Using this reduction would lead to smaller nodes, but also increased complexity in nodal geometry. Such complexity, however, may be warranted if it is necessary to fit a truss into a more confined area.

EXAMPLE 10.2

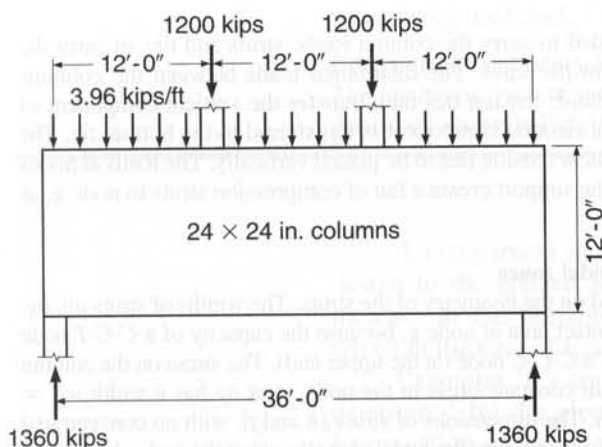
Deep beam with distributed loads. In addition to the concentrated loads, the transfer girder from Example 10.1 carries a distributed factored load of 3.96 kips/ft applied along its top edge, as shown in Fig. 10.15a. Design for the given loads, plus the self-weight, using $f'_c = 5000 \text{ psi}$ and $f_y = 60,000 \text{ psi}$.

SOLUTION. The factored self-weight of the beam is $1.2(12 \text{ ft} \times 2 \text{ ft} \times 0.15 \text{ kips/ft}^3) = 4.32 \text{ kips/ft}$. Thus, the total factored distributed load is $4.32 + 3.96 = 8.28 \text{ kips/ft}$, resulting in a total factored load of $8.28 \text{ kips/ft} \times 37.7 \text{ ft} = 312 \text{ kips}$, approximately 13 percent of the column loads. The solution follows Example 10.1 and accounts for the distributed loads. For this example, the self-weight of the beam is combined with the superimposed dead load. A more conservative solution could place the self-weight at the bottom of the beam and correspondingly increase the vertical tension tie requirements to transfer the load to the top flange. The top placement is used in this case because the self-weight is a small percentage of the total load and the concentrated forces are moved slightly toward the center of the beam for a conservative placement.

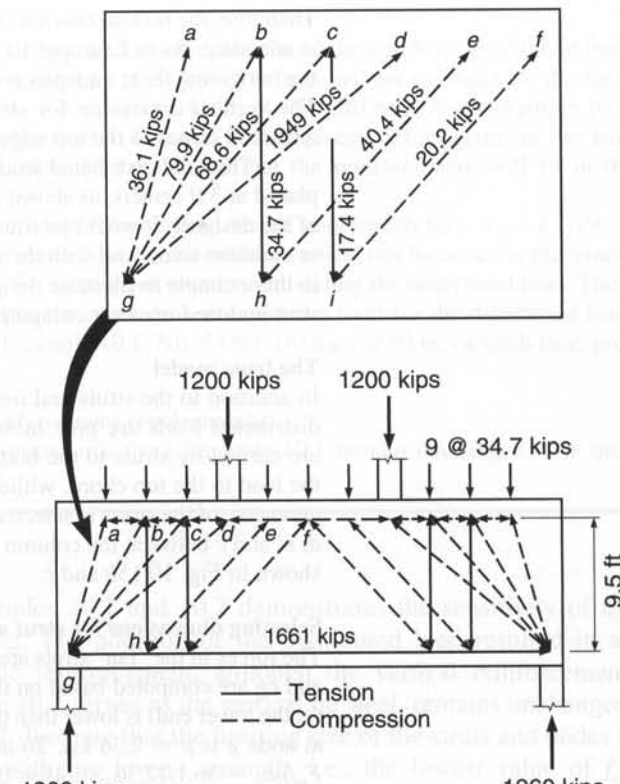
Definition of D-region

The entire beam is a D-region, as shown in Fig. 10.15a. The maximum factored shear in the beam is $V_u = 1200 + 312/2 = 1360 \text{ kips} < \phi 10\sqrt{f'_c} b_w d = 1650 \text{ kips}$, the maximum design shear using $d = 10.8 \text{ ft}$. Thus, the design can continue.

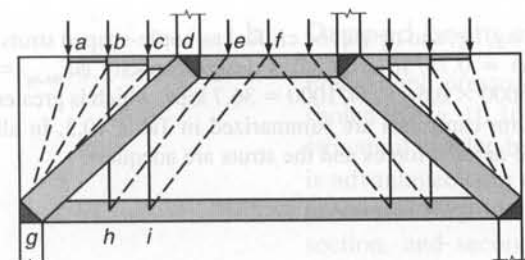
in Fig. 10.15(a) of a 24-in. deep beam having a 12'-0" width. The beam has two 24 × 24-in. columns at the top and two 24-in. square columns at the bottom. The beam is subjected to a total horizontal load of 2400 kips, which is distributed uniformly over the width of the beam. The beam is supported by two 24 × 24-in. columns at the top and two 24-in. square columns at the bottom. The beam is subjected to a total horizontal load of 2400 kips, which is distributed uniformly over the width of the beam.



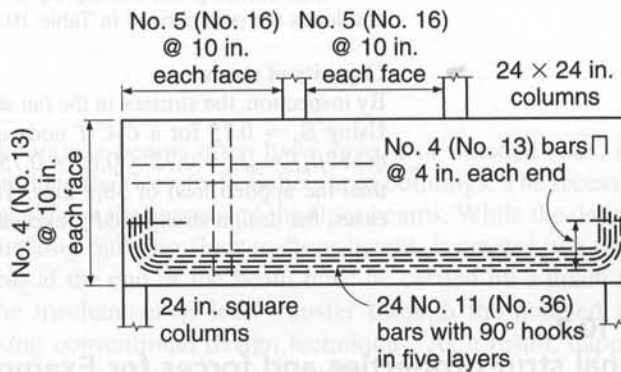
(a) Beam dimensions and loading



(b) Beam internal forces and truss model



(c) Struts, ties, and nodes



(d) Reinforcement details

FIGURE 10.15

Deep beam with distributed loads for Example 10.2.

Force resultants on D-region boundaries

The 1200 kip column loads are the same as in Example 10.1; however, the lower column reactions are equal to 1360 kips. Maintaining the same lower column size gives a stress at the beam-column interface of $p = 1360/(24 \times 24) = 2.36$ ksi.

The stress on the column node cannot exceed the effective concrete strength. For a C-C-T node,

$$p \leq \phi f_{ce} = \phi 0.85 \beta_n f'_c = 0.75 \times 0.85 \times 0.80 \times 5000/1000 = 2.55 \text{ ksi}$$

Therefore, the bottom column of 24×24 in., giving $p = 1360/(24 \times 24) = 2.36$ ksi < 2.55 ksi, is adequate. As in Example 10.1, the center-to-center distance between the horizontal strut and the horizontal tie at midspan is taken as 9.5 ft to compute the slope of the strut dg as $\theta = 38.0^\circ$. The vertical dimension for struts ag , bg , and cg is assumed to be 10.5 ft because they are anchored closer to the top edge of the beam.

The total distributed load of 312 kips is represented by nine 34.7 kip concentrated loads placed at 3 ft centers, as shown in Fig. 10.15b. Distributed loads can be grouped at the discretion of the designer. It would be equally satisfactory to group them into 12 loads, placed one per foot, or combine some load with the column loads. The loads are not combined with the column loads in this example to illustrate design for distributed loads. Using the geometric layout of the loads, strut-and-tie forces are computed and summarized in Fig. 10.15b and Table 10.3.

The truss model

In addition to the struts and ties needed to carry the column loads, struts and ties to carry the distributed loads are now included in the truss. The distributed loads between the columns are carried by struts to the bottom chord; tension ties then transfer the vertical component of the load to the top chord, while the horizontal component is transferred to the bottom tie. The geometry of the struts is selected to allow tension ties to be placed vertically. The loads at nodes a , b , and c between the column and the support create a fan of compression struts to node g , as shown in Fig. 10.15b and c.

Selecting dimensions for strut and nodal zones

The forces in the “fan” struts are based on the geometry of the struts. The widths of struts ag , bg , and cg are computed based on the contact area at node g , because the capacity of a $C-C-T$ node (at the lower end) is lower than that of a $C-C-C$ node (at the upper end). The stress on the column at node g is $p = 2.36$ ksi. To maintain constant stress in the node, strut ag has a width $w_{ag} = F_u/pb_s = 36.1/(2.36 \times 24) = 0.64$ in. The dimensions of struts eh and fi , with no concentrated loads acting directly on either end, are governed by the nodal capacity, since the nodes h and i are $C-T-T$ nodes, with $\beta_n = 0.60$ (Table 10.2). For example, for strut eh , $p = \phi f_{ce} = 0.75 \times 0.85 \times 0.60 \times 5000/1000 = 1.91$ ksi and width $w_{eh} = F_u/pb_s = 47.8/(1.91 \times 24) = 1.04$ in. In this case, the design capacity will exactly equal the factored load. The remaining strut widths, geometries, and loads are summarized in Table 10.3.

Capacity of struts

By inspection, the stresses in the fan struts ag , bg , and cg will be critical as bottle-shaped struts. Using $\beta_n = 0.75$ for a $C-C-T$ node and $\phi = 0.75$, strut ag has a design capacity $\phi F_{ns,ag} = \phi 0.85\beta_s f'_c w_{ab} b_s = 0.75 \times 0.85 \times 0.75 \times 5000 \times 0.64 \times 24/1000 = 36.7$ kips, which is greater than the applied load of 36.1 kips. The strut capacities are summarized in Table 10.3. In all cases, the design strength ϕF_{ns} exceeds the applied forces and the struts are adequate.

TABLE 10.3

Diagonal strut properties and forces for Example 10.2

Design ties and anchorage

Tie design is similar to that in Example 10.1, except that the additional horizontal thrust from the distributed loads increases the force to 1680 kips. The required area of steel for the tie is $A_{ts} = F_{uu}/\phi f_y = 1680/(0.75 \times 60) = 37.3 \text{ in}^2$ or 24 No. 11 (No. 36) bars. As in Example 10.1, 90° hooks will be required to anchor the tie. The steel will be placed in four layers of five bars and one layer of four bars. Example 10.1 validated that the reinforcement will fit in the available space.

The vertical tie bh carries 34.7 kips. The required area of steel for this tie is $A_{ts} = F_{uu}/\phi f_y = 34.7/(0.75 \times 60) = 0.77 \text{ in}^2$. Distributed steel is selected for vertical ties because the placement of the struts was arbitrary due to the assumptions made in modeling the distributed load. Thus, the 0.77 in² is distributed over 3 ft, the center-to-center spacing used for the distributed load. The minimum reinforcement in Example 10.1, No. 5 (No. 16) bars at 10 in. on each face, provides the required steel.

Design details and minimum reinforcement requirements

The minimum reinforcement requirements from Example 10.1 remain unchanged. The final details are shown in Fig. 10.15d.

A comparison of Examples 10.1 and 10.2 demonstrates the sensitivity of the design to the applied loading. The addition of the distributed load resulted in an increase in the horizontal tie reinforcement, although the vertical reinforcement, which in the case of Example 10.2 serves as the vertical tie steel, remains unchanged.

Examples 10.1 and 10.2 illustrate that the limiting size of the struts and nodes is determined by the element with the lowest strength, i.e., the lowest value of f_{ce} . Examination of the β_s and β_n values in Tables 10.3 and 10.4 shows the variation in strength. Recognizing that using the lowest value of β (and f_{ce}) will establish the minimum usable strut and node dimensions allows the designer to minimize the number of iterations needed to construct the truss model.

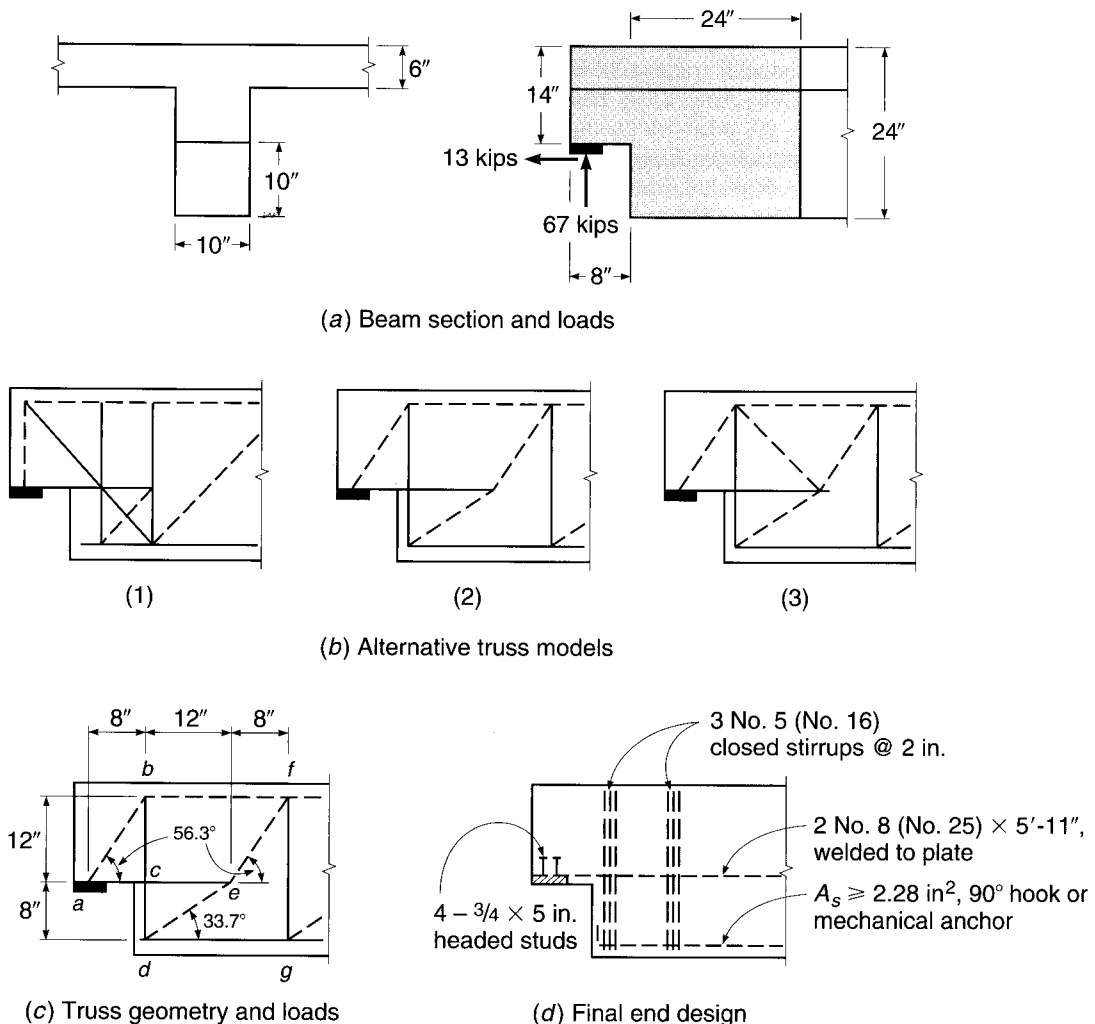
b. Dapped beam ends

Precast and prestressed concrete beams often have *dapped* or notched ends, such as shown in Fig. 10.16, to reduce the floor-to-floor height of buildings. The recess allows structural overlap between the main beams and the floor beams. While the dapped end is advantageous in controlling building floor-to-floor height, it creates two structural problems. First, the shear at the end of the beam must be carried by a much smaller section, and second, the mechanism of load transfer through the notched zone is difficult to represent using conventional design techniques. As a result, dapped-end beams lend themselves to strut-and-tie design methods.

EXAMPLE 10.3

Design of a dapped beam end. A 24 in. deep precast concrete T beam has a 10 in. thick web that carries factored end reactions of 67 kips in the vertical direction and 13 kips in the horizontal direction, as shown in Fig. 10.16a. The beam end is notched 10 in. vertically and 8 in. along the beam axis. The load is transferred to the support through a 4 × 10 in. bearing plate. Design the end reinforcement, using $f'_c = 5000 \text{ psi}$ and $f_y = 60,000 \text{ psi}$.

SOLUTION. The combination of the concentrated load and the geometric discontinuity suggest the use of a strut-and-tie solution.

**FIGURE 10.16**

Dapped beam end design for Example 10.3.

Definition of D-region

The D-region for this beam is approximately one structural depth in from the end of the notch. The bearing plate will have longitudinal reinforcement welded to it to allow for load transfer. Therefore, the effective depth at the notch is taken as 13.0 in. The maximum allowable shear capacity is $V_u = \phi V_n = \phi 10\sqrt{f'_c} b_w d = 0.75 \times 10\sqrt{5000} \times 10 \times 13.0/1000 = 68.9$ kips. This exceeds the 67 kip applied load, so the section is adequate to proceed with the design.

Force resultants on D-region boundaries and the truss model

Three possible truss layouts are considered, as shown in Fig. 10.16b. Option 1 includes a vertical strut and a diagonal tension tie to the lower chord of the beam. The presence of several tension ties in this model suggests that this is not a minimum energy solution. Option 2 includes a diagonal compressive strut and a vertical hanger to transfer the load to the bottom chord of the beam. The compression strut below the dapped end transfers the tensile reaction to the main longitudinal steel. Option 3 includes an internal triangular truss to balance the reaction within the interior of the beam. Balancing nodal forces at an indeterminate interior four-member joint

TABLE 10.4**Strut and tie properties and forces for Example 10.3**

Member				Force, kips	Capacity, kips	A_s Required, in ²	A_s Provided, in ²	Reinforcement
Type	Member	β_s	β_n	w_i , in.				
Strut	<i>ab</i>	0.75	0.8	80.5	4.79	114.6		
	<i>bf</i>	1.0	0.8	44.7	2.66	67.8		
	<i>de</i>	0.75	0.8	120.8	7.19	171.9		
	<i>ef</i>	0.75	0.8	80.5	4.79	114.6		
Tie	<i>ae</i>			57.7	3.43	1.28	1.58	2 No. 8 (No. 25)
	<i>bd</i> [†]			67.0	3.99	1.49	1.86	3 No. 5 (No. 16)
	<i>dg</i> [‡]			100.5	5.98	2.28	2.37	3 No. 8 (No. 25)
	<i>fg</i> [†]			67.0	3.99	1.49	1.86	3 No. 5 (No. 16)

[†] For ties *bd* and *fg*, use three No. 5 (No. 16) stirrups with two legs each, $A_s = 3$ stirrups \times 2 legs \times 0.31 in² = 1.86 in².

[‡] Tie *dg* is an extension of the main longitudinal reinforcement and must have an area ≥ 2.28 in² and a 90° hook or mechanical anchor at node *d*. If the main reinforcement is insufficient, auxiliary reinforcement may be added.

poses difficulties in joint detailing, but may be desirable if concentrated loads are applied to the top flange. Option 2 is selected as the design choice based on its simplicity and limited number of tension ties. The dimensions of the truss are shown in Fig. 10.16c, and the truss forces are summarized in Table 10.4.

Selecting dimensions for strut and nodal zones

The nodal zone stress is established at the bearing plate. The stress is $p = V_u/A_b = 67/(4 \times 10) = 1.68$ ksi. The calculations for strut *ab* follow, and the remaining strut-and-tie widths and capacities are given in Table 10.4. $F_{u,ab} = V_u/\sin \theta = 67/\sin 56.3^\circ = 80.5$ kips. The strut width is $w_{ab} = F_{u,ab}/(p \times 10) = 4.79$ in.

Capacity of struts

The strut design capacity is based on the strength of a bottle-shaped strut ($\beta_s = 0.75$). For strut *ab*, $\phi F_{ns,ab} = \phi 0.85 \beta_s f'_c w_{ab} b_s = 0.75 \times 0.85 \times 0.75 \times 5.0 \times 4.79 \times 10 = 114.5$ kips. This exceeds the applied load of 80.5 kips, so the strut is adequate. The remaining strut design capacities are summarized in Table 10.4. All exceed the applied forces, as would be expected with the low nodal stress used in this design.

Design ties and anchorage

For tie *bd*, $A_{ts} = F_{u,bd}/\phi f_y = 67/(0.75 \times 60) = 1.49$ in². Three No. 5 (No. 16) stirrups provide 1.86 in² of steel. The maximum width for tie *bd* is $w_{bd} = F_{u,bd}/pb = 67.0/(1.68 \times 10) = 3.99$ in. Three No. 5 (No. 16) stirrups may be placed within a total width of 2.7 in. and, thus, fit within the maximum tie width for *bd*. Tie *ae* carries both the horizontal component of strut *ab* and the 13 kip horizontal reaction. Therefore, $F_{u,ae} = 67 \times 8/12 + 13.0 = 57.7$ kips, requiring an area of steel equal to 1.28 in², which is provided by two No. 8 (No. 25) bars. The anchorage length of the ties exceeds the available nodal dimensions. Therefore, tie *ae* is welded to the plate at node *a* and has a full development length to the right of node *f*. Ties *bd* and *fg* are detailed as closed stirrups. The area of steel and the selected bar sizes for the ties are tabulated in Table 10.4. Stirrups for tie *bd* are grouped together and should be added to any normal shear reinforcement from the B-region of the beam.

Design details and minimum reinforcement requirements

Strut *ab* transfers a horizontal thrust to node *a*. Welding the reinforcement for tie *ae* to the plate anchors the tie, but it is not sufficient to ensure that the horizontal component of the strut force is transferred to the tie. Two solutions are possible. First, the plate at node *a* may be replaced with a steel angle. A 3.5 in. tall leg is needed to confine the nodal zone width. Second, a more common practice in the precast industry, headed studs are welded to the plate

and the connection is designed by the shear-friction principles described in Section 4.9. Headed studs have a yield stress of 50,000 psi and a coefficient of friction μ between concrete and steel of 0.7. Thus, the area of studs required to resist the horizontal components of strut *ab* is $A_{vf} = V_{uf}/\phi f_y \mu = 67(8/12)/(0.75 \times 50 \times 0.7) = 1.70 \text{ in}^2$. Four $\frac{3}{4}$ in. diameter \times 5 in. long headed studs will be used to provide 1.76 in^2 . The 5 in. length places the head of the stud outside of the nodal zone width.

Tie *dg* is an extension of the main longitudinal reinforcement. An area of Grade 60 steel $\geq 2.28 \text{ in}^2$ is needed to provide the force in the tie, which should also be checked against the reinforcement requirements for moment in the B-region. A 90° hook or mechanical anchor is required at node *d* to provide full development of the force in tie *dg*. If the beam is prestressed, the prestressing steel and the accompanying compression in the concrete provide an equivalent anchorage.

Minimum reinforcement in the dapped end is $A_{v,\min} = 0.0025 b_w s = 0.0025 \times 10 \times 12 = 0.30 \text{ in}^2/\text{ft}$. This is satisfied by No. 4 (No. 13) bars at 12 in. Since the steel in tie *bd* exceeds this, no further reinforcement is needed. The final connection is detailed in Fig. 10.16d.

The examples in this section illustrate both the methodology of strut-and-tie design and the importance of understanding the detailing requirements needed to transfer forces at nodes. Failure to appreciate the need to provide anchorage for the tie in Example 10.1 or to supply thrust resistance for the struts in Example 10.3 can lead to failure. In the examples, the contact area was used to establish the hydrostatic nodal pressure. As discussed, an equally acceptable solution would have been to select the maximum stress for one of the struts. The remaining strut and tie widths would then be adjusted accordingly.

REFERENCES

- 10.1. J. Schlaich, K. Schäfer, and M. Jennewein, "Toward a Consistent Design of Structural Concrete," *J. PCI*, vol. 32, no. 3, May-June 1987, pp. 74–150.
- 10.2. P. Marti, "Truss Models in Detailing," *Concr. Int'l.*, vol. 7, no. 12, 1985, pp. 66–73.
- 10.3. P. Marti, "Basic Tools for Reinforced Concrete Design," *J. ACI*, vol. 82, no. 1, 1985, pp. 46–56.
- 10.4. J. Schlaich and K. Schäfer, "Design and Detailing of Structural Concrete Using Strut-and-Tie Models," *Struct. Eng.*, vol. 69, no. 6, March 1991, 13 pp.
- 10.5. *Building Code Requirements for Structural Concrete and Commentary*, Appendix A, ACI 318-08, American Concrete Institute, Farmington Hills, MI, 2008.
- 10.6. C. M. Uribe and S. Alcocer, "Example 1a: Deep Beam Design in Accordance with ACI 318-2002," *Examples for the Design of Structural Concrete with Strut-and-Tie Models*, ACI SP 208, Karl-Heinz Reineck (ed.), American Concrete Institute, Farmington Hills, MI, 2002, pp. 65–80.
- 10.7. L. C. Nowak and H. Sprenger, "Example 5: Deep Beam with Opening," *Examples for the Design of Structural Concrete with Strut-and-Tie Models*, ACI SP 208, Karl-Heinz Reineck (ed.), American Concrete Institute, Farmington Hills, MI, 2002, pp. 129–144.
- 10.8. L. Chow, H. Conway, and G. Winter, "Stresses in Deep Beams," *Trans. ASCE*, vol. 118, 1953, p. 686.
- 10.9. *Examples for the Design of Structural Concrete with Strut-and-Tie Models*, ACI SP 208, Karl-Heinz Reineck (ed.), American Concrete Institute, Farmington Hills, MI, 2002.
- 10.10. J. MacGregor, *Reinforced Concrete, Mechanics and Design*, 3rd ed., Prentice-Hall, Upper Saddle River, NJ, 1997.
- 10.11. J. K. Wight and G. J. Parra-Montesinos, "Strut-and-Tie Model for Deep Beam Design," *Concr. Int'l.*, vol. 25, no. 5, 2003, pp. 63–70.
- 10.12. G. J. Klein, "Curved-Bar Nodes," *Concr. Int'l.*, vol. 30, no. 9, 2008, pp. 43–47.

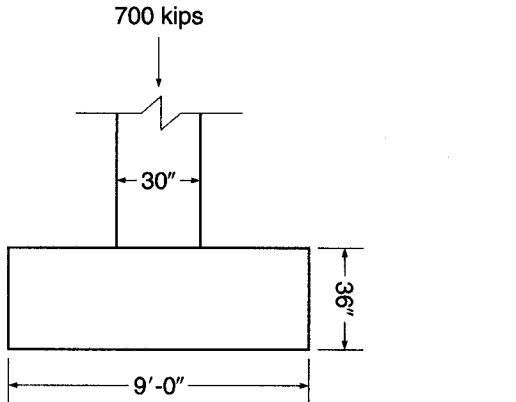
PROBLEMS

- 10.1.** A deep beam with the dimensions and material properties given in Example 10.1 carries a single 24×24 in. column with a factored load of 1600 kips located 12 ft from the left end. Design the beam using a strut-and-tie solution that

includes the self-weight of the beam. In your solution, include (a) a sketch of the load path and truss layout, (b) the sizes and geometry of the struts, ties, and nodal zones, and (c) a complete sketch of the final design.

- 10.2. Redesign the column bracket shown in Example 11.5 using the strut-and-tie method. Your strut-and-tie model may be based on Fig. 11.23. Material properties remain the same as in Example 11.5.
- 10.3. A 36 in. deep single T beam with a dapped end has a web thickness of 6 in. The factored end reactions are 82 kips in the vertical direction and 18 kips in the horizontal direction. The horizontal force places the beam in tension. The beam end is notched 12 in. high by 10 in. along the beam axis. Design the end connection using a bearing plate that is 3 in. wide with a thickness equal to that of the web. Adjust the bearing plate size if necessary. Specified material strengths are $f'_c = 6000$ psi and $f_y = 60,000$ psi.
- 10.4. A transfer girder has an overall depth of 11 ft and spans 22 ft between column supports. In addition to its own weight, it will pick up a uniformly distributed factored load of 3.8 kips/ft from the floor above and will carry a 14 × 14 in. column delivering a concentrated factored load of 1000 kips from floors above at midspan. The girder width must be equal to or less than 16 in. Design the beam for the given loads. Find the girder width and the area and geometry of tie steel, and specify the placement details. Material strengths are $f'_c = 5000$ psi and $f_y = 60,000$ psi.
- 10.5. A column transfers a factored load of 700 kips to the 9-ft square spread footing shown in Fig. P10.5, resulting in a factored uniform soil pressure of 8640 psf. Design the footing reinforcement using strut-and-tie methods. Material strengths are $f'_c = 4000$ psi and $f_y = 60,000$ psi. Because footings typically contain no shear reinforcement, your design should be based on unreinforced bottle-shaped struts.

FIGURE P10.5



- 10.6. Redesign the footing in Problem 10.5 using traditional flexure and shear methods, as described in Chapter 16. Compare your solution to the solution for Problem 10.5, and comment on your results.

11

Design of Reinforcement at Joints

11.1 INTRODUCTION

Most reinforced concrete failures occur not because of any inadequacies in analysis of the structure or in design of the members but because of inadequate attention to the detailing of reinforcement. Most often, the problem is at the connections of main structural elements (Ref. 11.1).

There is an increasing tendency in modern structural practice for the engineer to rely upon a detailer, employed by the reinforcing bar fabricator, to provide the joint design. Certainly, in many cases, standard details such as those found in the ACI Detailing Manual (Ref. 11.2) can be followed, but only the design engineer, with the complete results of analysis of the structure at hand, can make this judgment. In many other cases, special requirements for force transfer require that joint details be fully specified on the engineering drawings, including bend configurations and cutoff points for main bars and provision of supplementary reinforcement.

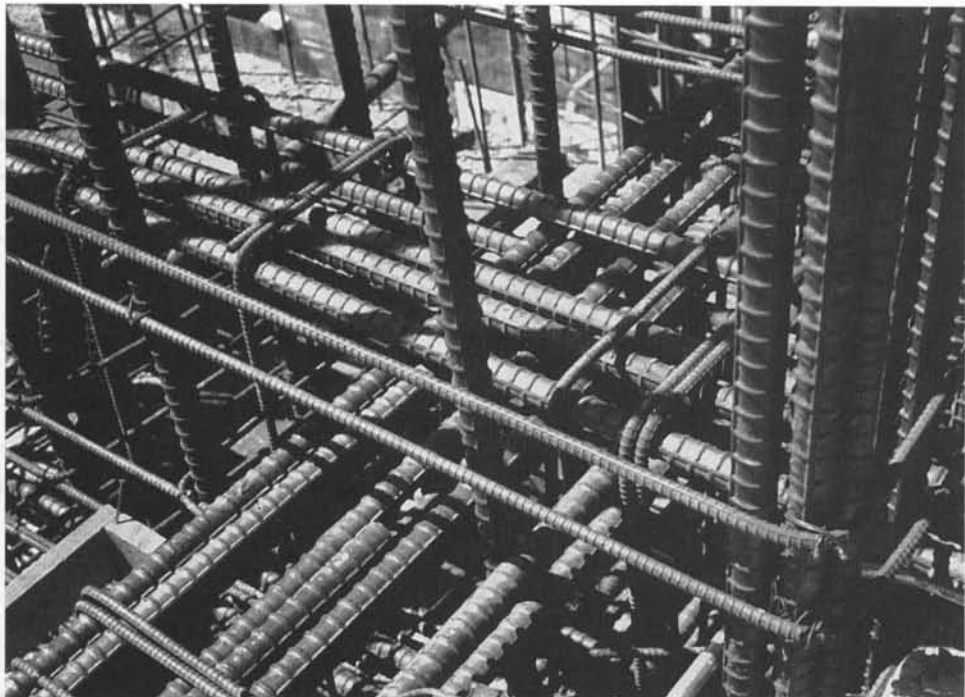
The basic requirement at joints is that all of the forces existing at the ends of the members must be transmitted through the joint to the supporting members. Complex stress states exist at the junction of beams and columns, for example, that must be recognized in designing the reinforcement. Sharp discontinuities occur in the direction of internal forces, and it is essential to place reinforcing bars, properly anchored, to resist the resulting tension. Some frequently used connection details, when tested, have been found to provide as little as 30 percent of the strength required (Refs. 11.1 and 11.3).

Over the years, important research has been directed toward establishing an improved basis for joint design (Refs. 11.4 and 11.5). Full-scale tests of beam-column joints have led to improved design methods such as those described in *Recommendations for Design of Beam-Column Joints in Monolithic Reinforced Concrete Structures*, reported by ACI-ASCE Committee 352 (Ref. 11.6). Although they are not a part of the ACI Code, such recommendations provide a basis for the safe design of beam-column joints both for ordinary construction and for buildings subject to seismic forces. Other tests have given valuable insight into the behavior of beam-girder joints, wall junctions, and other joint configurations, thus providing a sound basis for design.

The practicality of the joint design should not be overlooked. Beam reinforcement entering a beam-column joint must clear the vertical column bars, and timely consideration of this fact in selecting member widths and bar size and spacing can avoid costly delays in the field. Similarly, beam steel and girder steel, intersecting at right angles at a typical beam-girder-column joint, cannot be in the same horizontal plane as they enter the joint. Figure 11.1 illustrates the congestion of reinforcing bars at such an intersection. Concrete placement in such a region is difficult at best, but is assisted with the use of plasticizer admixtures.

FIGURE 11.1

Steel congestion at beam-girder-column joint.



Most of this chapter treats the design of joint regions for typical continuous-frame monolithic structures that are designed according to the strength requirements of the ACI Code for gravity loads or normal wind loads. Joints connecting members that must sustain strength under reversals of deformation into the inelastic range, as in earthquakes, represent a separate category and are covered in Chapter 20. Brackets and corbels, although they are most often a part of precast buildings rather than monolithic construction, have features in common with monolithic joints, and these will be covered here.

11.2 BEAM-COLUMN JOINTS

A *beam-column joint* is defined as the portion of a column within the depth of the beams that frame into it. Formerly, the design of monolithic joints was limited to providing adequate anchorage for the reinforcement. However, the increasing use of high-strength concrete, resulting in smaller member cross sections, and the use of larger-diameter and higher-strength reinforcing bars now require that greater attention be given to joint design and detailing. Although very little guidance is provided by the ACI Code, the ACI-ASCE Committee 352 report *Recommendations for Design of Beam-Column Joints in Monolithic Reinforced Concrete Structures* (Ref. 11.6) provides a basis for the design of joints in both ordinary structures and structures required to resist heavy cyclic loading into the inelastic range.

a. Classification of Joints

Reference 11.6 classifies structural joints into two categories. A *Type 1* joint connects members in an ordinary structure designed on the basis of strength, according to the

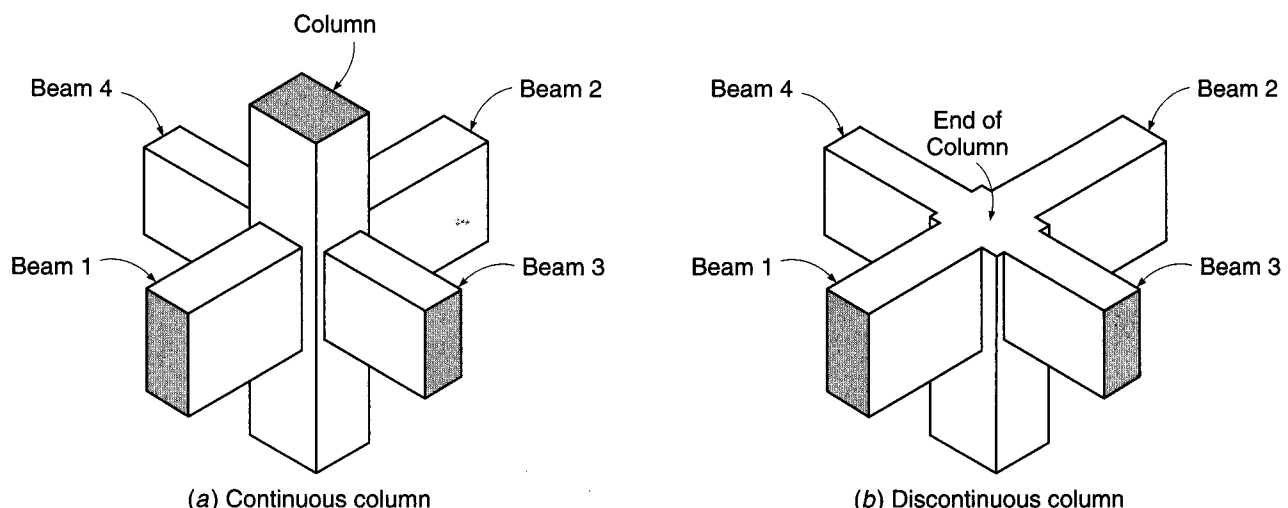


FIGURE 11.2

Typical monolithic interior beam-column joint.

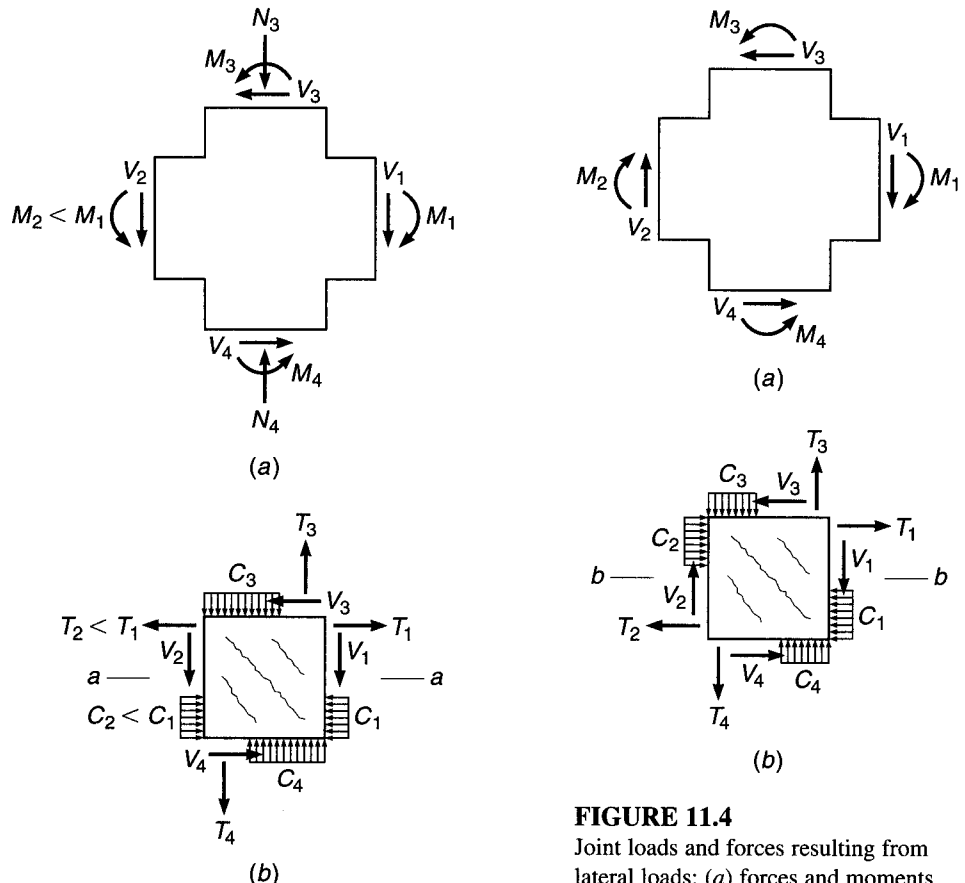
main body of the ACI Code, to resist gravity and normal wind load. A *Type 2* joint connects members designed to have sustained strength under deformation reversals into the inelastic range, such as members in a structure designed for earthquake motions, very high winds, or blast effects. Only Type 1 joints will be considered in this chapter.

Figure 11.2a shows typical *interior joints* in a monolithic reinforced concrete frame, with beams 1 and 2 framing into opposite faces of the column and beams 3 and 4 framing into the column faces in the perpendicular direction. An *exterior joint* would include beams 1, 2, and 3, or in some cases only beams 1 and 2. A *corner joint* would include only beams 1 and 3, or occasionally only a single beam 1. A joint may have beams framing into it from two perpendicular directions as shown, but for purposes of analysis and design each direction can be considered separately. Joint confinement is further affected if the column is discontinuous, as illustrated in Fig. 11.2b.

b. Joint Loads and Resulting Forces

The joint region must be designed to resist forces that the beams and column transfer to the joint, including axial loads, bending, torsion, and shear. Figure 11.3a shows joint loads acting on the free body of a typical joint of a frame subject to gravity loads, with moments M_1 and M_2 acting on opposite faces, in the opposing sense. In general, these moments will be unequal, with their difference equilibrated by the sum of the column moments M_3 and M_4 . Figure 11.3b shows the resulting forces to be transmitted through the joint. Similarly, Fig. 11.4a shows the loads on a joint in a structure subjected to sidesway loading. The corresponding joint forces are shown in Fig. 11.4b. Only for very heavy lateral loading, such as from seismic forces, would the moments acting on opposite faces of the joint act in the same sense, as shown here, producing very high horizontal shears within the joint.

According to the recommendations by Committee 352, the forces to be considered in designing joint regions are not those determined from the conventional frame analysis; rather, they are calculated based on the *nominal strengths of the members*.

**FIGURE 11.3**

Joint loads and forces resulting from gravity loads: (a) forces and moments on the free body of a joint region; (b) resulting internal forces.

FIGURE 11.4

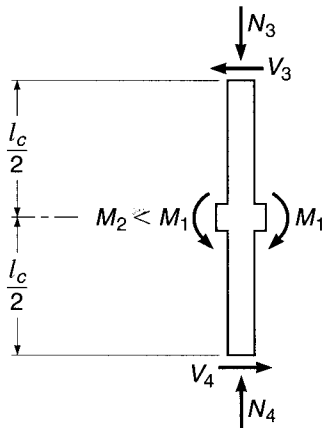
Joint loads and forces resulting from lateral loads: (a) forces and moments on the free body of a joint; (b) resulting internal forces.

Where a typical underreinforced beam meets the column face, the tension force from the negative moment reinforcement at the top of the beam is to be taken as $T = A_{sv}f_y$, and the compression force at the face is from equilibrium $C = T$, not the nominal compressive capacity of the concrete. The design moment applied at the joint face is that corresponding to these maximum forces, $M_u = M_n = A_{sv}f_y(d - a/2)$, rather than that from the overall analysis of the frame. Note that the inclusion of the usual strength reduction factor ϕ would be unconservative in the present case because it would reduce the forces for which the joint is to be designed; it is therefore not included in this calculation.

With the moment applied to each joint face found in this way, the corresponding column forces for joint design are those forces required to keep the connection in equilibrium. To illustrate, the column shears V_3 and V_4 of Figs. 11.3a and 11.4a are calculated based on the free body of the column between inflection points, as shown in Fig. 11.5. The inflection points generally can be assumed at column midheight, as shown.

FIGURE 11.5

Free-body diagram of an interior column and joint region.



c. Shear Strength of a Joint

A joint subject to the forces shown in Fig. 11.3b or 11.4b will develop a pattern of diagonal cracking owing to the diagonal tensile stresses that result from the normal forces and shears, as indicated by those figures. The approach used by Committee 352 is to limit the shear force on a horizontal plane through the joint to a value established by tests. The design basis is

$$V_u \leq \phi V_n \quad (11.1)$$

where V_u is the applied shear force, V_n is the nominal shear strength of the joint, and ϕ is taken equal to 0.75.

The shear force V_u is to be calculated on a horizontal plane at midheight of the joint, such as plane *a-a* of Fig. 11.3b or plane *b-b* of Fig. 11.4b, by summing horizontal forces acting on the joint above that plane. For example, in Fig. 11.3b the joint shear on plane *a-a* is

$$V_u = T_1 - T_2 - V_3$$

and in Fig. 11.4b, the joint shear on plane *b-b* is

$$\begin{aligned} V_u &= T_1 + C_2 - V_3 \\ &= T_1 + T_2 - V_3 \end{aligned}$$

The nominal shear strength V_n is given by the equation

$$V_n = \gamma \sqrt{f'_c} b h_c \quad (11.2)$$

where b is the effective joint width in inches, h_c is the thickness in inches of the column in the direction of the load being considered, and $\sqrt{f'_c}$ is expressed in psi units. According to Committee 352, Eq. (11.2) is conservative for concretes with strengths up to 15,000 psi. As discussed in Chapter 20, ACI Code 21.7 follows similar procedures for the design of joints in moment resistant frames, the only difference being that lower values for the coefficient γ are recommended.

The coefficient γ in Eq. (11.2) depends on the confinement of the joint provided by the beams framing into it and whether the column is continuous or terminates at the level under consideration, as shown in Table 11.1.

TABLE 11.1
Values of γ for beam-to-column connections

Joint	Continuous Columns		Discontinuous Columns	
	Gravity Frames (Type 1)	Moment Resisting Frames (Type 2)	Gravity Frames (Type 1)	Moment Resisting Frames (Type 2)
Interior	24	20	20	15
Exterior	20	15	15	12
Column	15	12	12	8

The definitions of interior, exterior, and corner joints were discussed in Section 11.2a. However, there are restrictions to be applied for purposes of determining γ as follows:

1. An *interior joint* has beams framing into all four sides of the joint. However, to be classified as an interior joint, the beams should cover at least $\frac{3}{4}$ the width of the column, and the total depth of the shallowest beam should not be less than $\frac{3}{4}$ the total depth of the deepest beam. Interior joints that do not satisfy this requirement should be classified as *exterior joints*.
2. An *exterior joint* has at least two beams framing into opposite sides of the joint. However, to be classified as an exterior joint, the widths of the beams on the two opposite faces of the joint should cover at least $\frac{3}{4}$ the width of the column, and the depths of these two beams should be not less than $\frac{3}{4}$ the total depth of the deepest beam framing into the joint. Joints that do not satisfy this requirement should be classified as *corner joints*.

For joints with beams framing in from two perpendicular directions, as for a typical interior joint, the horizontal shear should be checked independently in each direction. Although such a joint is designed to resist shear in two directions, only one classification is made for the joint in this case (i.e., only one value of γ is selected based on the joint classification, and that value is used to compute V_n when checking the design shear capacity in each direction).

According to Committee 352 recommendations, the effective joint width b_j to be used in Eq. (11.2) depends on the transverse width of the beams that frame into the column as well as the transverse width of the column. With regard to the beam width b_b , if there is a single beam framing into the column in the load direction, then b_b is the width of that beam. If there are two beams in the direction of shear, one framing into each column face, then b_b is the average of the two beam widths. In reference to Fig. 11.6a, when the beam width is less than the column width, the effective joint width is equal to the smaller of the average of the beam width and column width,

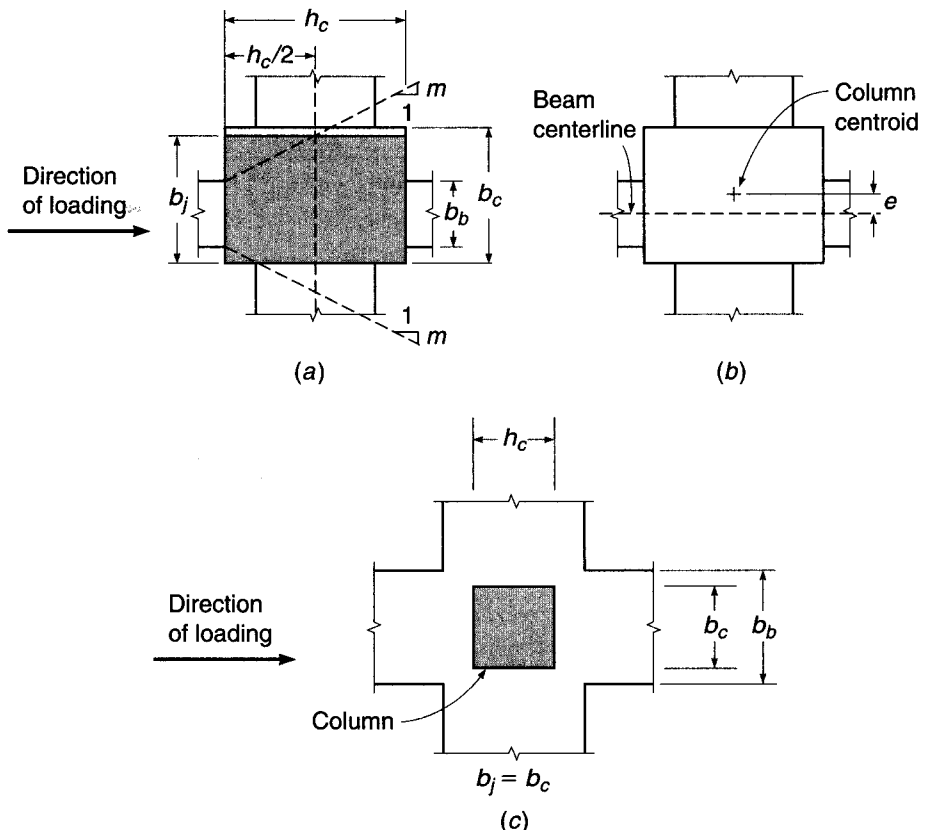
$$b_j = \frac{b_b + b_c}{2} \quad (11.3)$$

and

$$b_j = b_b + \sum \frac{mh_c}{2} \quad (11.4)$$

FIGURE 11.6

Determination of effective joint width b_j : (a) beams narrower than column; (b) eccentricity between beam centerline and column centroid; (c) beam wider than column. (Parts a and b adapted from Ref. 11.6.)



where m is a slope that depends on the eccentricity e of the beam centerline with respect to the column centroid (Fig. 11.6b). If e is greater than $b_c/8$, $m = 0.3$; otherwise, $m = 0.5$. As shown in Fig. 11.6a, the slope m defines a width at the centroid of the column. According to Committee 352, $mh_c/2$ should not be taken as greater than the extension of the column edge beyond the edge of the beam.

If the beam width b_b exceeds the column width b_c , the effective joint width b_j is equal to the column width b_c , as shown in Fig. 11.6c.

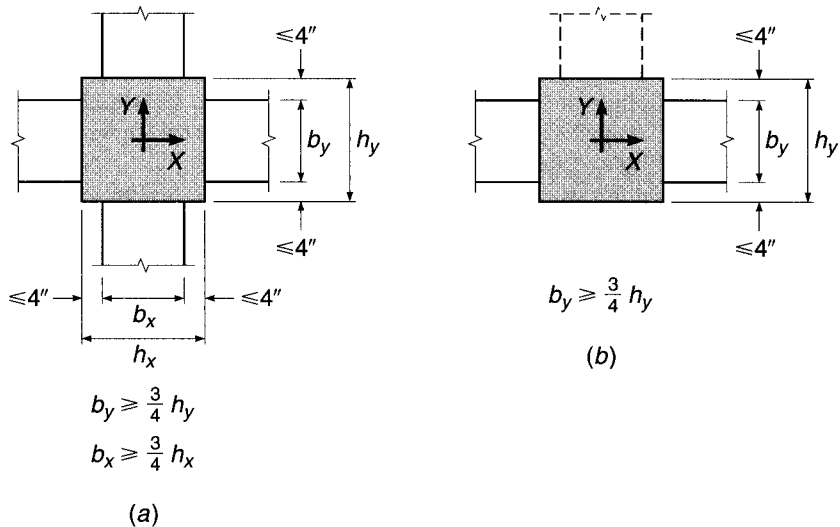
d. Confinement and Transverse Joint Reinforcement

The successful performance of a beam-column joint depends strongly on the lateral confinement of the joint. Confinement has two benefits: (1) the core concrete is strengthened and its strain capacity improved, and (2) the vertical column bars are prevented from buckling outward. Confinement can be provided either by the beams that frame into the joint or by special column ties provided within the joint region.

Confinement by beams is illustrated in Fig. 11.7. According to Committee 352 recommendations, if beams frame into four sides of the joint, as in Fig. 11.7a, adequate confinement is provided if each beam width is at least $\frac{3}{4}$ the width of the intersected column face and if no more than 4 in. of column face is exposed on either side of the beam. Where beams frame into only two sides of the joint, as in Fig. 11.7b, adequate confinement can be assumed *in the direction of the beams* if the beam widths are at least $\frac{3}{4}$ the column width and no more than 4 in. of concrete is exposed on either side

FIGURE 11.7

Confinement of joint concrete by beams: (a) confinement in X and Y directions; (b) confinement in X direction only.



of the beams. In the other direction, transverse reinforcement must be provided for confinement. The presence of a third beam, but not a fourth, in the perpendicular direction does not modify the requirement for transverse reinforcement.

If adequate confinement is not provided by beams according to these criteria, then transverse reinforcement must be provided. If confinement steel is needed, it must meet all the usual requirements for column ties (see Section 8.2). In addition, there must be at least two layers of ties between the top and bottom flexural steel in the beams at the joint, and the vertical center-to-center spacing of these ties must not exceed 12 in. If the beam-column joint is part of the primary system for resisting nonseismic lateral loads, this maximum spacing is reduced to 6 in. For joints that are not confined by beams on four sides, ACI Code 11.10 requires that the ties satisfy Eq. (4.13).

e. Anchorage and Development of Beam Reinforcement

For interior joints, normally the flexural reinforcement in a beam entering one face of the joint is continued through the joint to become the flexural steel for the beam entering the opposite face. Therefore, for loadings associated with Type 1 joints, pullout is unlikely, and no special recommendations are made. However, for exterior or corner joints, where one or more of the beams do not continue beyond the joint, a problem of bar anchorage exists. The critical section for development of the yield strength of the beam steel is at the face of the column. Column dimensions seldom permit development of the steel entering the joint by straight embedment alone, and hooks are usually needed for the negative beam reinforcement. Headed bars or ninety degree hooks are used, with the hook extending toward and beyond the middepth of the joint. If the bottom bars entering the joint need to develop their strength $A_s f_y$ at the face of the joint, as they do if the beam is a part of a primary lateral load-resisting system, they should also be anchored with 90° hooks, in this case turned upward to extend toward the middepth of the joint, or headed bars. Requirements for development of hooked bars given in Chapter 5 are applicable in both cases, including modification factors for concrete cover and for enclosure with ties or stirrups.

EXAMPLE 11.1 Design of exterior Type 1 joint. The exterior joint shown in Fig. 11.8 is a part of a continuous, monolithic, reinforced concrete frame designed to resist gravity loads only. Member section dimensions $b \times h$ and reinforcements are as shown. The frame story height is 12 ft. Material strengths are $f'_c = 4000$ psi and $f_y = 60,000$ psi. Design the joint, following the recommendations of the Committee 352 report.

SOLUTION. First the joint geometry must be carefully laid out, to be sure that beam bars and column bars do not interfere with one another and that placement and vibration of the concrete are practical. In this case, bar layout is simplified by making the column 4 in. wider than the beams. Column steel is placed with the usual 1.5 in. of concrete outside of the No. 4 (No. 13) ties. Beam top and bottom bars are placed just inside the outer column bars. The slight offset of the center top beam bars to avoid the center column bars is of no concern. Top bars of the spandrel beams are placed just under the top normal beam bars, except for the outer spandrel bar, which is above the hook shown in Fig. 11.8b. Bottom bars enter the joint at different levels without interference.

No anchorage problems exist for the spandrel beam top reinforcement, which is continuous through the joint. However, the normal beam top steel must be provided with hooks to develop its yield strength at the face of the column. Referring to Table 5.3, the basic development length for No. 10 (No. 32) hooked bars is

$$l_{dh} = \left(\frac{0.02\psi_e f_y}{\lambda \sqrt{f'_c}} \right) d_b = \left(\frac{0.02 \times 1 \times 60,000}{1 \times \sqrt{4000}} \right) 1.27 = 24.1 \text{ in.}$$

FIGURE 11.8

Exterior beam-column joint for Example 11.1: (a) plan view; (b) cross section through spandrel beam; (c) cross section through normal beam. Note that beam stirrups and column ties outside of the joint are not shown.

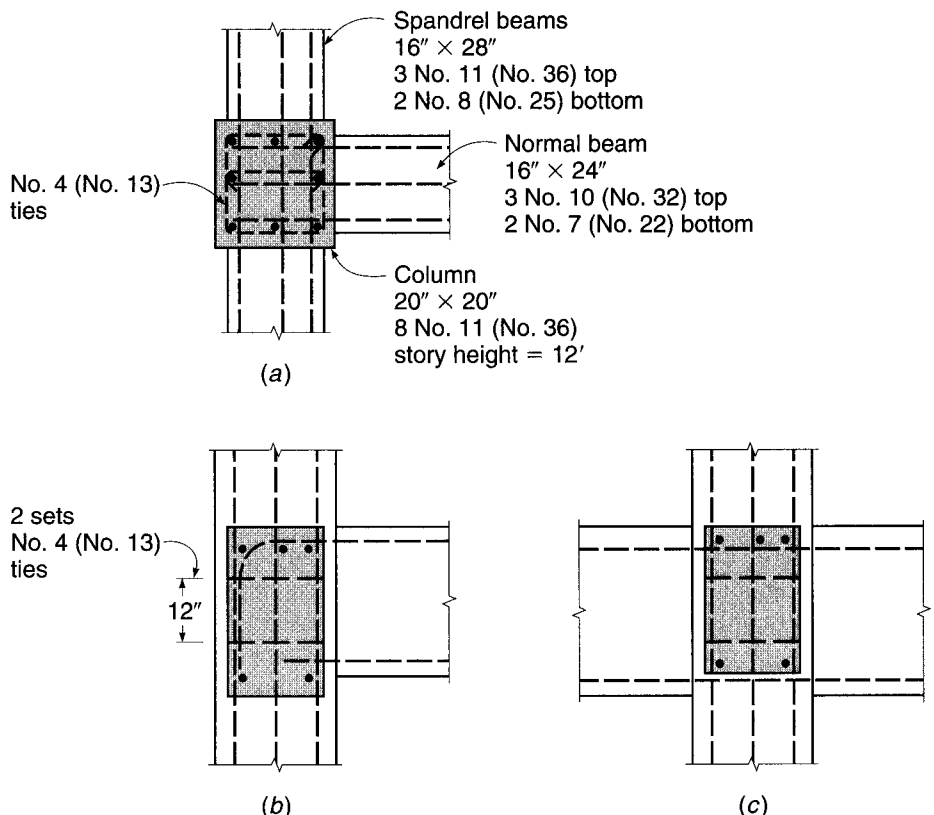
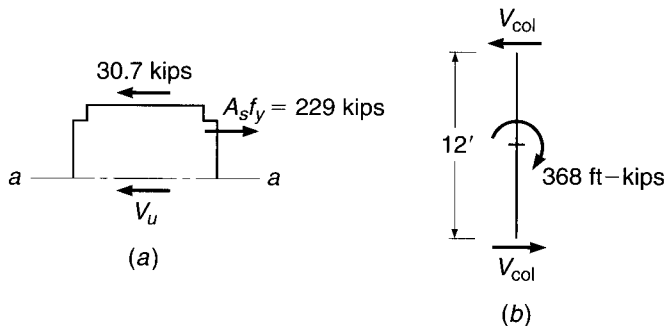


FIGURE 11.9

Basis of column shear for Example 11.1: (a) horizontal forces on joint free-body sketch; (b) free-body sketch of column between inflection points.



Being inside the column bars, the beam top bars have side cover of $1.5 + 0.5 + 1.4 = 3.4$ in. This exceeds 2.5 in., so a modification factor of 0.7 is applicable, and the required hook development length is

$$l_{dh} = 24.1 \times 0.7 = 16.9 \text{ in.}$$

If the hooked bars are carried down just inside the column ties, the actual embedded length is $20.0 - 1.5 - 0.5 = 18.0$ in., exceeding 16.9 in., so development is ensured. None of the beams are a part of the primary, lateral load-resisting system of the frame, so the bottom bars simply can be carried 6 in. into the face of the joint and stopped.

Next the shear strength of the joint must be checked. In the direction of the spandrel beams, moments applied to the joint will be about the same and acting in the opposite sense, so very little joint shear is expected in that direction. However, the normal beam will subject the joint to horizontal shears. In reference to Fig. 11.9a, which shows a free-body sketch of the top half of the joint, the maximum force from the beam top steel is

$$A_s f_y = 3.81 \times 60 = 229 \text{ kips}$$

The joint moment is calculated based on this tensile force. The normal beam effective depth is $d = 24.0 - 1.5 - 0.5 - 1.27/2 = 21.4$ in. and with stress block depth $a = A_s f_y / 0.85 f'_c b_w = 229 / (0.85 \times 4 \times 16) = 4.21$ in., the design moment is

$$M_u = M_n = A_s f_y \left(d - \frac{a}{2} \right) = \frac{229}{12} \left(21.4 - \frac{4.21}{2} \right) = 368 \text{ ft-kips}$$

Column shears corresponding to this joint moment are found based on the free body of the column between assumed midheight inflection points, as shown in Fig. 11.9b: $V_{col} = 368/12 = 30.7$ kips. Then summing horizontal forces on the joint above the middepth plane $a-a$, the joint shear in the direction of the normal beam is

$$V_u = 229 - 30.7 = 198 \text{ kips}$$

For purposes of calculating the joint shear strength, the joint can be classified as exterior, because the 16 in. width of the spandrel beams exceeds $\frac{3}{4}$ the column width of 15 in., and the spandrels are the deepest beams framing into the joint. Thus, $\gamma = 20$. The effective joint width is the smaller of

$$b_j = \frac{b_b + b_c}{2} = \frac{16 + 20}{2} = 18 \text{ in.}$$

and

$$b_j = b_b + \sum \frac{mh_c}{2} = 16 + 2 \left(\frac{0.5 \times 20}{2} \right) = 26 \text{ in.}$$

In the latter case, limiting $mh_c/2$ to be no greater than the extension of the column edge beyond the edge of the beam results in $b_j = b_c = 20$ in.

Using $b_j = 18$ in., the nominal and design shear strengths of the joint are, respectively,

$$V_n = \gamma \sqrt{f'_c} b_j h = 20 \sqrt{4000} \times 18 \times \frac{20}{1000} = 455 \text{ kips}$$

$$\phi V_n = 0.75 \times 455 = 341 \text{ kips}$$

The applied shear $V_u = 198$ kips does not exceed the design strength, so shear is satisfactory.

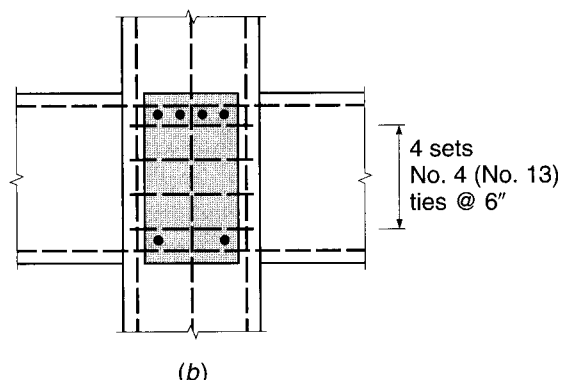
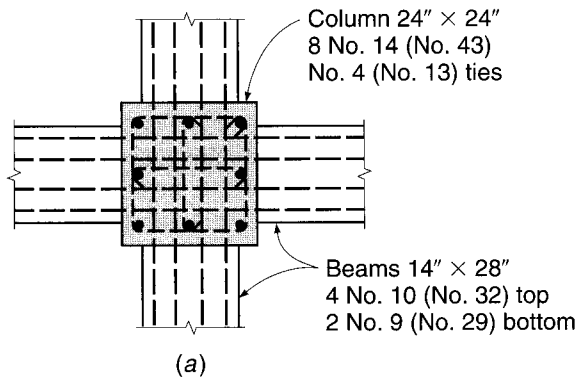
Confinement is provided in the direction of the spandrel beams by the beams themselves because the spandrel width of 16 in. exceeds $\frac{3}{4}$ the column width and no more than 4 in. of column face is exposed on either side. However, in the direction of the normal beam, confinement must be provided by column ties within the joint. Two sets of No. 4 (No. 13) ties will be provided, as shown in Fig. 11.8a and b. The clear distance between column bars is 5.89 in. here, less than 6 in., so strictly speaking the single-leg crosstie is not required. However, it will improve the joint confinement, guard against outward buckling of the central No. 11 (No. 36) column bar, and add little to the cost of construction, so crossties will be specified, as shown in Fig. 11.8a. The ties satisfy Eq. (4.13) several times over. Note that a 90° hook at one end, rather than the 135° bend shown, will meet ACI Code tie anchorage requirements and facilitate steel fabrication as well.

EXAMPLE 11.2

Design of interior Type 1 joint. Figure 11.10 shows a proposed interior joint of a reinforced concrete building, with beam and column dimensions and reinforcement as indicated. The building frame is to carry gravity loads and normal wind loads. Design and detail the joint reinforcement.

FIGURE 11.10

Interior beam-column joint for Example 11.2: (a) plan view; (b) section through beam.



SOLUTION. Because the joint is to be a part of the primary, lateral load-resisting system, beam bottom bars as well as top bars are carried straight through the joint for anchorage. In such cases, it is usually convenient to lap splice the bottom steel near the point of inflection of the beams.

In Fig. 11.10a and b, top and bottom beam bars entering the joint in one direction must pass, respectively, under and over the corresponding bars in the perpendicular direction. It will be assumed that this has been recognized by adjusting the effective depths in designing the beams. Because the column is 10 in. wider than the beams, the outer beam bars can be passed inside the corner column bars without interference. Four bars are used for the beam top steel in order to avoid interference with the center column bar.

Even the combination of normal wind loading with gravity loads should not produce large unbalanced moment on opposite faces of this interior column, and it can be safely assumed that joint shear will not be critical. However, confinement of the joint region by the beams is considered inadequate because (1) the beam width of 14 in. is less than $\frac{3}{4}$ the column width of 24 in. and (2) the exposed column face outside the beam is $(24 - 14)/2 = 5$ in., which exceeds the 4 in. limit. Consequently, transverse column ties must be added within the joint for confinement. For the 24 in. square column, the spacing between the vertical bars exceeds 6 in., so it is necessary, according to the ACI Code, to provide ties to support the intermediate bars as well as the corner bars. Three ties are used per set, as shown in Fig. 11.10a. Since the joint is a part of the lateral load-resisting system, the maximum vertical spacing of these tie sets is 6 in. Four sets within the joint, as indicated in Fig. 11.10b, are adequate to satisfy this requirement.

f. Wide-Beam Joints

In multistory buildings, to reduce the construction depth of each floor and to reduce the overall building height, wide shallow beams are sometimes used. Joint design in cases where the beams are wider than the column introduces some important concepts not addressed in the Committee 352 report. It is important to equilibrate all of the forces applied to the joint. The tension from the top bars in the usual case, with beam width no greater than the column, will be equilibrated by the horizontal component of a diagonal compression strut within the joint. The diagonal compression at the ends of the strut, in turn, is equilibrated by the beam compression and the thrust from the column. (See Section 11.3 for a more complete description of the strut-and-tie model.) If the outer bars of the normal beam pass *outside* of the column, as they often do in wide-beam designs, the diagonal strut will also be outside of the column, with no equilibrating vertical compression at its upper and lower ends. The outer parts of the beam would tend to shear off, resulting in premature failure. The problem is of special concern for Type 2 connections.

To minimize the problem, Committee 352 suggests that satisfactory performance of Type 2 connections with wide beams will result if, to provide satisfactory bond, the reinforcement passing outside the joint core is selected so that the ratio of the column depth h_c to the bar diameter d_b is greater than or equal to 24 and that at least one-third of the steel passes through or is anchored in the column between the vertical bars. In the event that these restrictions cannot be met, two possibilities exist to improve performance. The first solution requires that all of the beam top steel be placed within the width of the column, and preferably inside the outer column bars. If the normal beam bars are carried outside the joint, the second solution is to provide vertical stirrups through the joint region to carry the vertical component of thrust from the compression strut. In addition, Type 2 exterior beams must be designed for equilibrium torsion per ACI Code 11.5, which may require additional transverse reinforcement.

In extreme but not unusual cases, very wide beams are used, several times wider than the column, with beam depth only about 2 times the slab depth. In such cases, a safe basis for joint design is to treat the wide beam as a slab and follow the recommendations for slab-column connections contained in Chapter 13.

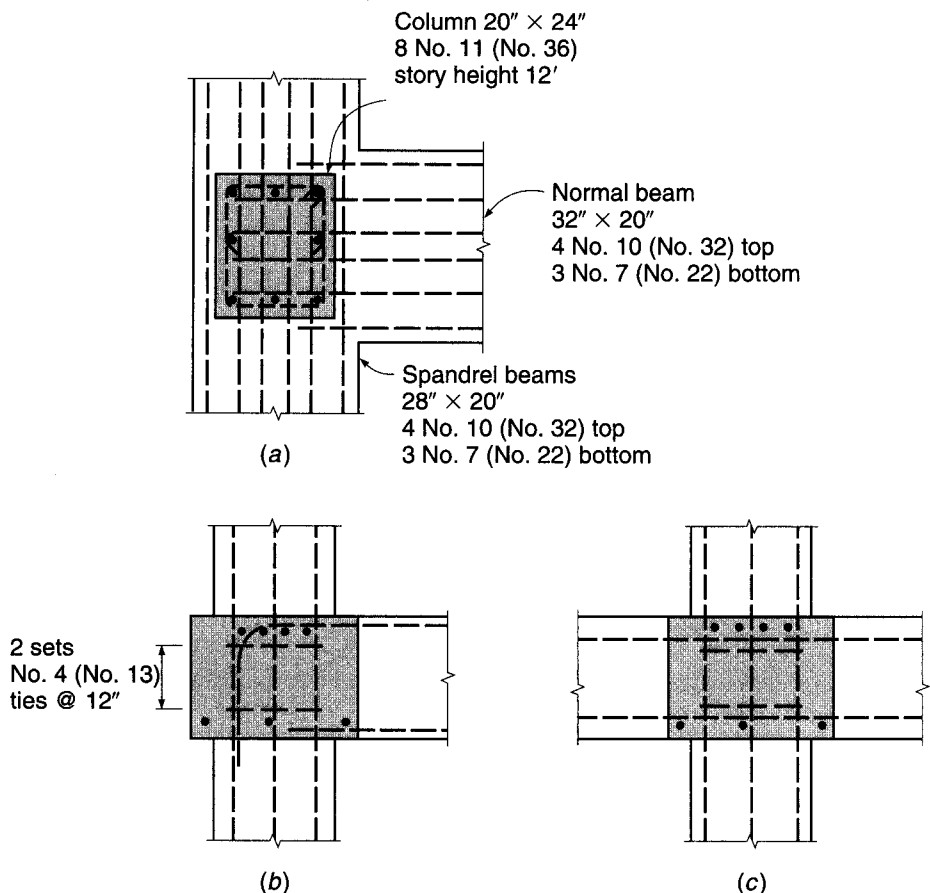
EXAMPLE 11.3

Design of exterior Type 1 joint with wide beams. Figure 11.11 shows a typical exterior joint in the floor of a wide-beam structure, designed to resist gravity loads. Here the beams in each direction are 8 in. wider than the corresponding column dimension. Check the proposed joint geometry and shear strength, and design the transverse joint reinforcement. Material strengths are $f'_c = 4000$ psi and $f_y = 60,000$ psi. Story height is 12 ft.

SOLUTION. For the present case, all normal beam top steel is passed inside the core of the joint, terminating in 90° hooks at the outside of the column. Top steel in the spandrel beams is continuous through the joint but is also carried inside the joint core. Bottom beam bars, in each case, can be spread across the width of the beam, and they are carried only 6 in. into the joint for the normal beam because the joint is not a part of the primary, lateral load-resisting system. The bottom spandrel beam bars are continued to provide structural integrity (ACI Code 7.13). Beam stirrups outside of the joint, not shown in Fig. 11.11, would be carried outside of the outer bottom bars and bent up. They would require small-diameter horizontal bars inside the hooks for proper anchorage at the upper ends of their vertical legs.

FIGURE 11.11

Exterior beam-column joint for Example 11.3: (a) plan view; (b) section through spandrel beam; (c) section through normal beam.



Checking the required development length of the No. 10 (No. 32) top bars of the normal beam gives

$$l_{dh} = \left(\frac{0.02\psi_e f_y}{\lambda \sqrt{f'_c}} \right) d_b = \left(\frac{0.02 \times 1 \times 60,000}{1 \times \sqrt{4000}} \right) 1.27 = 24.1 \text{ in.}$$

With lateral cover well in excess of 2.5 in., a modification factor of 0.7 is applicable, and the necessary hook development length is

$$l_{dh} = 24.1 \times 0.7 = 16.9 \text{ in.}$$

If the hooks are carried down in the plane of the outer column bars, the available embedment is $20.0 - 1.5 - 0.5 = 18.0$ in., exceeding the minimum required embedment.

Moments from the spandrels on either side of the joint will be about equal, so no joint shear problem exists in that direction. In the direction of the normal beam, shear must be checked. The tensile force applied by the top bars is $A_s f_y = 5.08 \times 60 = 305$ kips. The depth of the beam compressive stress block is $a = A_s f_y / 0.85 f'_c b_w = 305 / (0.85 \times 4 \times 32) = 2.80$ in., and the corresponding moment is

$$M_u = M_n = A_s f_y \left(d - \frac{a}{2} \right) = \frac{305}{12} \left(17.6 - \frac{2.80}{2} \right) = 412 \text{ ft-kips}$$

Column shears are based on a free body corresponding to that of Fig. 11.9b, and are equal to $V_{col} = 412/12 = 34.3$ kips. Thus, the joint shear at middepth is $V_u = 305 - 34.3 = 270$ kips.

The spandrel beams provide full-width joint confinement in their direction, and the joint can be classed as exterior, so $\gamma = 20$. In the perpendicular direction, when the beam width exceeds the column width, the joint width b_j is to be taken equal to the column width (24 in. in the present case). The nominal and design shear strengths are, respectively,

$$V_n = \gamma \sqrt{f'_c} b_j h = 20 \sqrt{4000} \times 24 \times 20/1000 = 607 \text{ kips}$$

$$\phi V_n = 0.75 \times 607 = 455 \text{ kips}$$

Because the design strength is well above the applied shear of 270 kips, the shear requirement is met.

Transverse confinement steel must be provided in the direction of the normal beam, between the top and bottom bars of the normal beam, with spacing not to exceed 12 in. Two sets of No. 4 (No. 13) column ties will be used, as shown in Fig. 11.11. In addition to the hoop around the outside bars, a single-leg crosstie is required for the middle column bars because the clear distance between column bars exceeds 6 in. The ties satisfy Eq. (4.13).

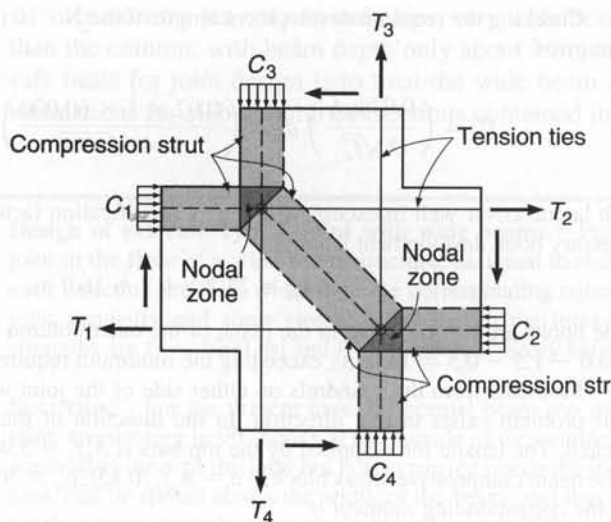
11.3 STRUT-AND-TIE MODEL FOR JOINT BEHAVIOR

Although the Committee 352 report (Ref. 11.6) is an important contribution to the safe design of joints of certain standard configurations, the recommendations are based mainly on test results. Consequently, they must be restricted to joints whose geometry closely matches that of the tested joints. This leads to many seemingly arbitrary geometric limitations, and little guidance is provided for the design of joints that may not meet these limitations. An illustration of this is the wide-beam joint discussed in Section 11.2f.

Good physical models are available for many aspects of reinforced concrete behavior—for example, for predicting the flexural strength of a beam or the strength of an eccentrically loaded column—but no clear physical model is evident in the

FIGURE 11.12

Strut-and-tie model for behavior of a beam-column joint.



Committee 352 recommendations for the behavior of a joint. For this reason, among others, increasing attention is being given to the strut-and-tie models, described in Chapter 10, as a basis for the design of D-regions in joints.

The essential features of a strut-and-tie model of joint behavior may be understood with reference to Fig. 11.12, which shows a joint of a frame subject to lateral loading, with clockwise moments from the beams equilibrated by counterclockwise moments from the columns. The line of action of the horizontal forces C_1 and T_2 intersects that of the vertical forces C_3 and T_4 at a *nodal zone*, where the resultant force is equilibrated by a diagonal *compression strut* within the joint. At the lower end of the strut, the diagonal compression equilibrates the resultant of the horizontal forces T_1 and C_2 and the vertical forces T_3 and C_4 . The tension bars must be well anchored by extension into and through the joint, or in the case of discontinuous bars (such as the top beam steel in an exterior joint) by hooks. The concrete within the nodal zone is subjected to a biaxial or, in many cases, a triaxial state of stress.

With this simple model, the flow of forces in a joint is easily visualized, satisfaction of the requirements of equilibrium is confirmed, and the need for proper anchorage of bars is emphasized. In a complete strut-and-tie model analysis, through proper attention to deformations within the joint, serviceability is ensured through control of cracking.

According to the strut-and-tie model, the main function of the column ties required within the joint region by conventional design procedures, in addition to preventing outward buckling of the vertical column bars, is to confine the concrete in the compression strut, thereby improving both its strength and ductility, and to control the cracking that may occur owing to diagonal tension perpendicular to the axis of the compression strut. The main load is carried by the uniaxially loaded struts and ties.

The strut-and-tie model not only provides valuable insights into the behavior of ordinary beam-column joints but also represents an important tool for the design of joints that fall outside of the limited range of those considered in Ref. 11.6. In the sections of this chapter that follow, a number of types of joints will be considered that occur commonly in reinforced concrete structures, for which the strut-and-tie models provide essential aid in developing proper bar details.

11.4 BEAM-TO-GIRDER JOINTS

Commonly in concrete construction, secondary floor beams are supported by primary girders, as shown in Fig. 11.13a and b. It is often assumed that the reaction from the floor beam is more or less uniformly distributed through the depth of the interface between beam and girder. This incorrect assumption is perhaps encouraged by the ACI Code “ $V_c + V_s$ ” approach to shear design, which makes use of a nominal average shear stress in the concrete, $v_c = V_c/b_w d$, suggesting a uniform distribution of shear stress through the beam web.

The actual behavior of a diagonally cracked beam, as indicated by tests, is quite different, and the flow of forces can be represented in somewhat simplified form by the truss model of the beam shown in Fig. 11.13c (Ref. 11.7). The main reaction is delivered from beam to girder by a diagonal compression strut mn , which applies its thrust near the bottom of the carrying girder. Failure to provide for this thrust may result in splitting off the concrete at the bottom of the girder followed by collapse of the beam. A graphic example of lack of support for diagonal compression at the junction of a beam and its supporting girder is shown in Fig. 11.14.

Proper detailing of steel in the region of such a joint requires the use of well-anchored “hanger” stirrups in the girder, as shown in Fig. 11.13a and b, to provide for the downward thrust of the compression strut at the end of the beam (Refs. 11.8 and 11.9). These stirrups serve as tension ties to transmit the reaction of the beam to the compression zone of the girder, where it can be equilibrated by diagonal compression struts in the girder. The hanger stirrups, which are required *in addition* to the normal girder stirrups required for shear, can be designed based on equilibrating part or all of the reaction from the beam, with the hanger stirrups assumed to be stressed to their yield stress f_y at the factored load stage.

FIGURE 11.13

Main girder supporting secondary beam: (a) cross section through girder showing hanger stirrups; (b) cross section through beam; (c) truss model showing transfer of beam load to girder at load near ultimate; (d) truss model showing transfer of load into the girder.

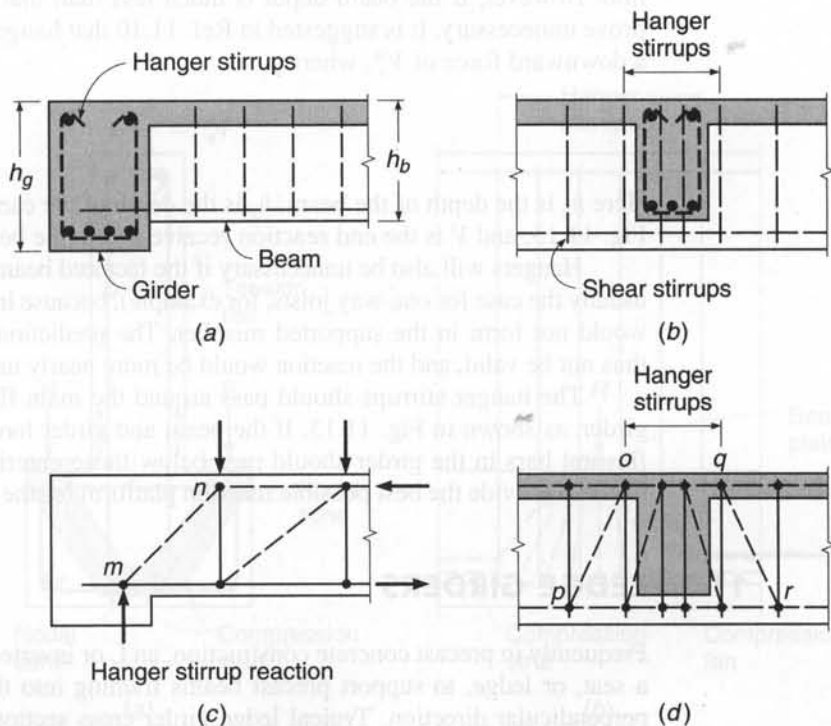
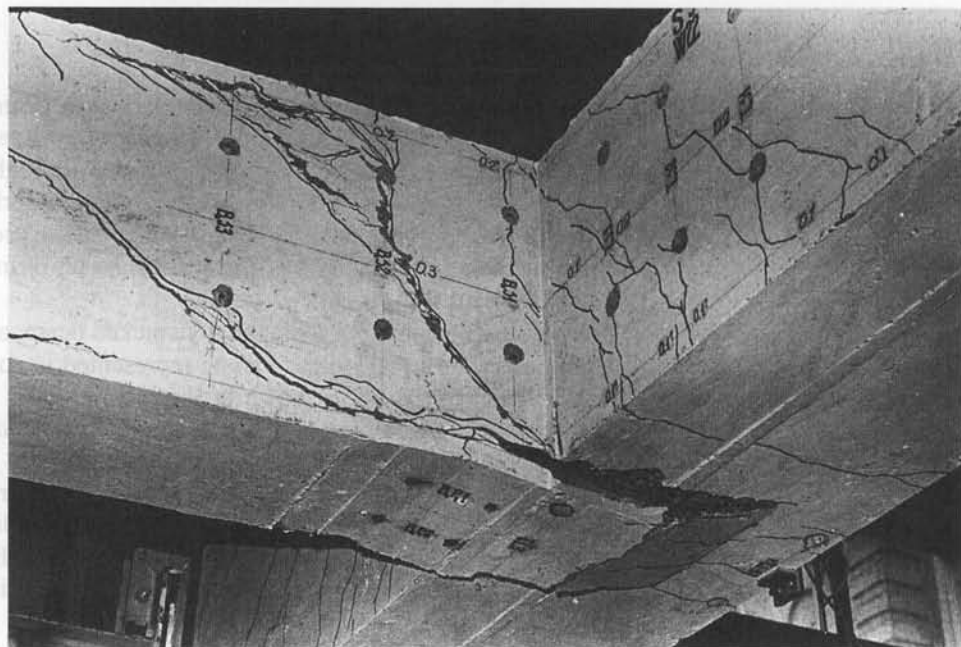


FIGURE 11.14

Failure due to lack of support for diagonal compression in beam-girder joint. (*Courtesy of M. P. Collins, University of Toronto.*)



The strut-and-tie model allows visualization of the transfer of the beam load along the girder as seen in Fig. 11.13d. The compression struts *op* and *qr* complete the shear transfer into the girder. The orientation of these compression struts depends on the location of the beam relative to the girder end.

If the beam and girder are the same depth, the hangers should take the full reaction. However, if the beam depth is much less than that of the girder, hangers may prove unnecessary. It is suggested in Ref. 11.10 that hanger stirrups be placed to resist a downward force of V_s^* , where

$$V_s^* = \frac{h_b}{h_g} V \quad (11.5)$$

Here h_b is the depth of the beam, h_g is the depth of the carrying girder, as indicated by Fig. 11.13, and V is the end reaction received from the beam.

Hangers will also be unnecessary if the factored beam shear is less than ϕV_c (as is usually the case for one-way joists, for example), because in such a case diagonal cracks would not form in the supported member. The predictions of the truss model would thus not be valid, and the reaction would be more nearly uniform through the depth.

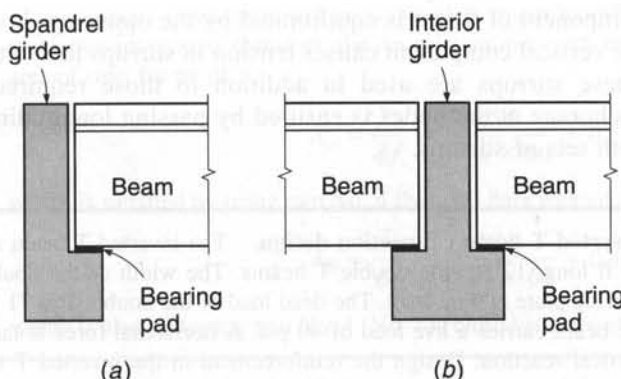
The hanger stirrups should pass around the main flexural reinforcement of the girder, as shown in Fig. 11.13. If the beam and girder have the same depth, the main flexural bars in the girder should pass below those entering the connection from the beam to provide the best possible reaction platform for the diagonal compression strut.

11.5 LEDGE GIRDERS

Frequently in precast concrete construction, an L or inverted T girder is used to provide a seat, or ledge, to support precast beams framing into the carrying girder from the perpendicular direction. Typical ledge girder cross sections are shown in Fig. 11.15.

FIGURE 11.15

Ledge girders carrying precast T beams: (a) L girder providing exterior support for T beam; (b) inverted T girder carrying two T beam reactions.



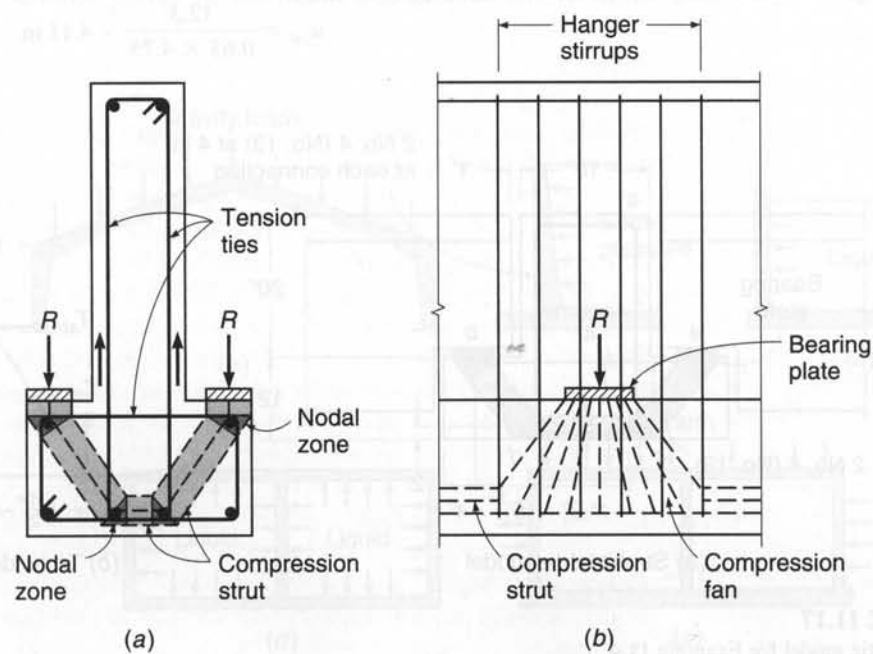
The end reaction of the beams introduces a heavy concentrated load near the bottom of such girders, requiring special reinforcement in the projecting ledge and in the girder web.

The design of such reinforcement is facilitated through use of a strut-and-tie model, as illustrated in Fig. 11.16. The downward reaction of the supported beam creates a compression fan in the ledge that distributes the reaction along a length greater than that of the bearing plate, as shown in Fig. 11.16b. The horizontal components of the fan are equilibrated by a compression strut along the lower flange of the girder.

In the cross section view of Fig. 11.16a, the downward thrust under the bearing plate is equilibrated by a diagonal compression strut, with the outward thrust at the top of the strut causing tension in the upper horizontal leg of closed hoop stirrups in the lower part of the girder. In many cases, a short structural steel angle is used just under the bearing plate, and the main tie at the top of the ledge is welded to the angle to ensure positive anchorage. At the bottom of the diagonal strut, the horizontal

FIGURE 11.16

Strut-and-tie model for behavior of inverted T ledge girder: (a) girder cross section; (b) side elevation.



component of thrust is equilibrated by the opposing thrust from the other side, and the vertical component causes tension in stirrups that extend to the top of the girder. These stirrups are used in addition to those required for girder shear. Proper anchorage at the nodes is ensured by passing longitudinal bars inside the bends of both sets of stirrups.

EXAMPLE 11.4

Inverted T beam connection design. The inverted T beam shown in Fig. 11.17a supports 40 ft long, 12 ft wide double T beams. The width of the double T stem is 4.75 in. and the bearing plate is 6 in. long. The dead load of the double T is 71 psf, including self-weight, and the beam carries a live load of 40 psf. A horizontal force is taken equal to 20 percent of the vertical reaction. Design the reinforcement in the inverted T at the double T bearing point. Material properties are $f'_c = 6000$ psi and $f_y = 60,000$ psi.

SOLUTION. The factored loads on the beam stem for a 6-ft tributary width are

$$q_u = 1.2 \times 71 + 1.6 \times 40 = 149 \text{ psf}$$

$$R_u = 0.149 \text{ psf} \times 6 \text{ ft} \times 40 \text{ ft}/2 = 17.9 \text{ kips}$$

and

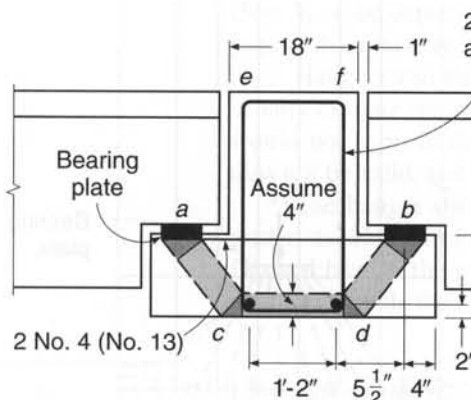
$$T_u = 0.2 \times 17.9 = 3.6 \text{ kips}$$

The bearing area under the double T leg is 6 in. by 4.75 in. = 28.5 in², giving a nodal bearing stress of

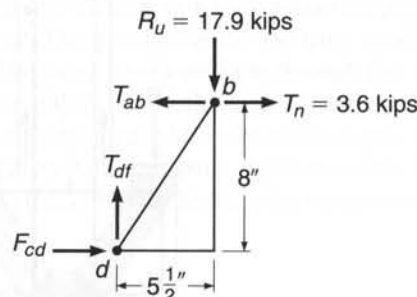
$$f_n = \frac{17.9}{28.5} = 0.63 \text{ ksi}$$

which is well below the nominal capacity of the nodes and bottle-shaped or rectangular struts. The low stress is used to demonstrate an alternative solution methodology. By using the low stress, the node and strut capacities are adequate by inspection; however, the size of strut *cd* must be confirmed. Solving for the geometry and forces in Fig. 11.17b, $T_{ab} = 15.9$ kips, $T_{df} = 17.9$ kips, and strut *cd* carries $F_{cd} = 12.3$ kips. The thickness of the strut is assumed as 4.75 in., the same as the bearing plate. Therefore, the width of strut *cd* is

$$w_{cd} = \frac{12.3}{0.63 \times 4.75} = 4.11 \text{ in.}$$



(a) Strut-and-tie model



(b) Truss detail

FIGURE 11.17

Strut-and-tie model for Example 11.4.

This is slightly more than the 4 in. assumed. A minor modification to the bearing stress would make this acceptable; therefore, the design continues with the selected geometry. The required area of steel for tie *ab* is

$$A_{ts} = \frac{T_{ab}}{\phi f_y} = \frac{15.9}{0.75 \times 60} = 0.35 \text{ in}^2$$

which is satisfied by using two No. 4 (No. 13) bars welded to each bearing plate. For tie *df*,

$$A_{ts} = \frac{T_{df}}{\phi f_y} = \frac{17.9}{0.75 \times 60} = 0.40 \text{ in}^2$$

which is also met using two No. 4 (No. 13) closed stirrups at 4 in. on center at each load point.

11.6 CORNERS AND T JOINTS

In many common types of reinforced concrete structures, moments and other forces must be transmitted around corners. Some examples, shown in Fig. 11.18, include gable frames, retaining walls, liquid storage tanks, and large box culverts. Reinforcement detailing at the corners is rarely obvious. A comprehensive experimental study of such joints by Nilsson and Losberg (Ref. 11.3) showed that many commonly used joint details will transmit only a small fraction of their assumed strength. Ideally, the joint should resist a moment at least as large as the calculated failure moment of the members framing into it (i.e., the *joint efficiency* should be at least 100 percent). Tests have shown that, for common reinforcing details, joint efficiency may be as low as 30 percent.

Corner joints may be subjected to opening moments, causing flexural tension on the inside of the joint, or closing moments, causing tension on the outside. Generally, the first case is the more difficult to detail properly.

Consider, for example, a corner joint subjected to opening moments, such as an exterior corner of the liquid storage tank shown in the plan view in Fig. 11.18d.

FIGURE 11.18

Structures with corners subject to opening or closing moments: (a) gable frame; (b) earth-retaining wall; (c) liquid storage tank; (d) plan view of multicell liquid storage tank; (e) large box culvert.

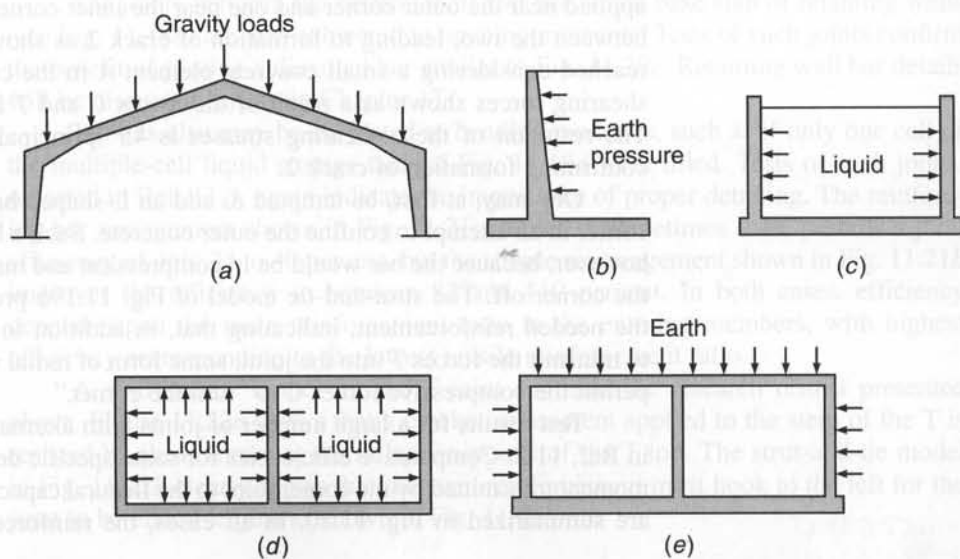
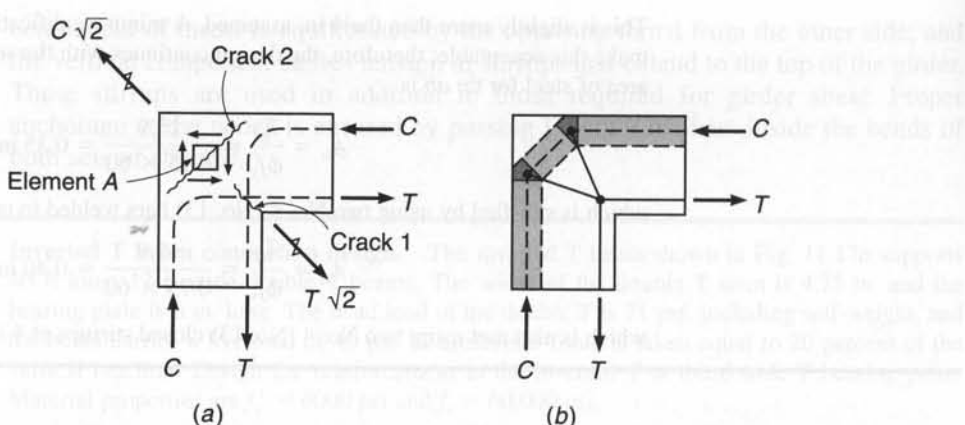


FIGURE 11.19

Corner joint subject to opening moments:
(a) cracking in an improperly designed joint; (b) strut-and-tie model of joint behavior.

**FIGURE 11.20**

Efficiencies of corner joints subject to opening moments for various reinforcing details: (a) 32 percent; (b) 68 percent; (c) 77 percent; (d) 87 percent; (e) 115 percent. (After Ref. 11.3.)

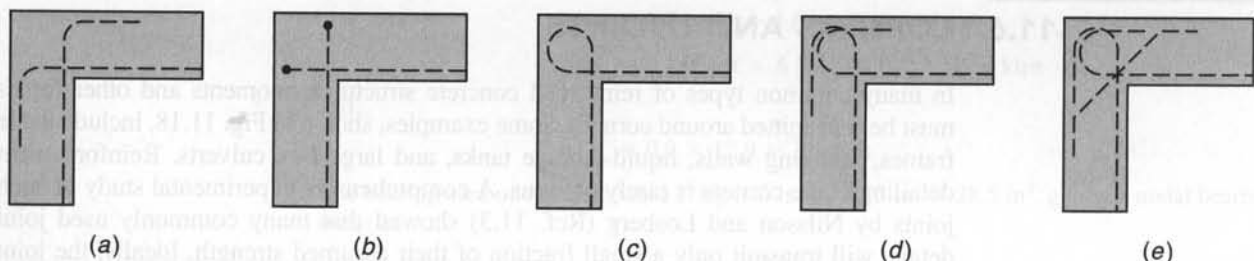


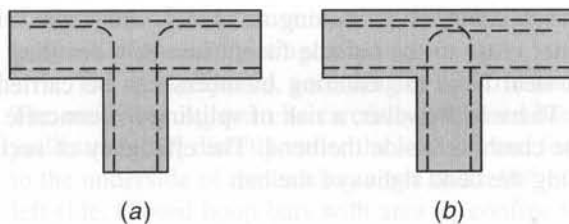
Figure 11.19a shows the system of forces acting on such a corner. The reinforcing bar pattern shown is *not* recommended. Formation of crack 1, radiating inward from the corner, is perhaps obvious. Crack 2, which may lead to splitting off the outside corner, may not be so obvious. However, the resultant of the two compressive forces C , having a magnitude $C\sqrt{2}$, is equilibrated by the resultant tension $T\sqrt{2}$. These two forces, one applied near the outer corner and one near the inner corner, require high tensile stress between the two, leading to formation of crack 2 as shown. The same conclusion is reached considering a small concrete element A in the corner. It is subjected to the shearing forces shown as a result of the forces C and T from the entering members. The resultant of these shearing stresses is 45° principal tension across the corner, confirming formation of crack 2.

One may, at first, be tempted to add an L-shaped bar around the outside of the corner in an attempt to confine the outer concrete. Such a bar would serve no purpose, however, because the bar would be in compression and may actually assist in pushing the corner off. The strut-and-tie model of Fig. 11.19b provides valuable insight into the needed reinforcement, indicating that, in addition to well-anchored tensile bars to transmit the forces T into the joint, some form of radial reinforcement is required to permit the compressive forces C to "turn the corner."

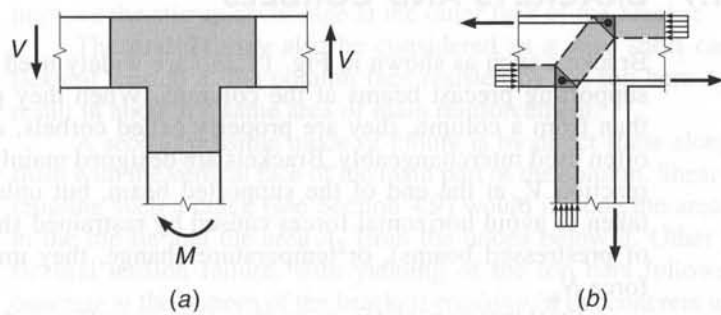
Test results for a large number of joints with alternative bar details are reported in Ref. 11.3. Comparative efficiencies for some specific details, relating the maximum moment transmitted by the corner joint to the flexural capacity of the entering members, are summarized in Fig. 11.20. In all cases, the reinforcement ratio of the entering

FIGURE 11.21

Comparative efficiencies of T joints subject to bending moment: (a) 24 to 40 percent depending on reinforcement ratio; (b) 82 to 110 percent depending on reinforcement ratio. (After Ref. 11.3.)

**FIGURE 11.22**

T joint behavior subjected to moment: (a) bending moment and resulting shear forces; (b) strut-and-tie model.



members is 0.75 percent. Figure 11.20a is a simple detail, probably often used, but it provides joint efficiency of only 32 percent. The details in Fig. 11.20b, reinforced with bent bars in the form of hairpins with the plane of the hooks parallel to the inside face of the joint, provide efficiency of 68 percent. In Fig. 11.20c, the main reinforcement is simply looped and continued out the other leg of the joint, resulting in an efficiency of 77 percent. The somewhat similar detail shown in Fig. 11.20d, in which the bars entering the joint are terminated with separate loops, gives an efficiency of 87 percent. The best performance results from the detail shown in Fig. 11.20e—the same as in Fig. 11.20d except for the addition of a diagonal bar. This improves joint efficiency to 115 percent, so that the joint is actually stronger than the design strength of the members framing into it. It was determined experimentally that the area of the diagonal bar should be about one-half that of the main reinforcement.

The joints between the vertical wall and horizontal base slab of retaining walls (see Fig. 11.18b) are also subjected to opening moments. Tests of such joints confirm the benefit of placing a diagonal bar similar to Fig. 11.20e. Retaining wall bar details will be discussed further in Chapter 17.

T joints also may be subjected to bending moments, such as if only one cell of the multiple-cell liquid storage tank of Fig. 11.18d were filled. Tests of such joints, reported in Ref. 11.3, again indicate the importance of proper detailing. The reinforcing bar arrangement shown in Fig. 11.21a, which is sometimes seen, permits a joint efficiency of only 24 to 40 percent, but the simple rearrangement shown in Fig. 11.21b improves the efficiency to between 82 and 110 percent. In both cases, efficiency depends upon the main reinforcement ratio in the entering members, with highest efficiency corresponding to the lowest tensile reinforcement ratio.

A strut-and-tie model for the T joint confirms the research results presented above. Figure 11.22a shows that a clockwise moment applied to the stem of the T is resisted by shear forces at the inflection points of the T-top. The strut-and-tie model in Fig. 11.22b clearly shows that the stem reinforcement must hook to the left for the joint to be effective, just as shown in Fig. 11.21b.

FIGURE 11.19

Corner joint subject to opening moments
(a) cracking near unsupported
designed joint; (b) joint with
no cracks at lower bending

Joints subjected to closing moments, with main reinforcement passing around the corner close to the outside face, cause few detailing problems because the main tension steel from the entering members can be carried around the outside of the corner. There is, however, a risk of splitting the concrete in the plane of the bend, or concrete crushing inside the bend. The efficiency of such joints can be improved by increasing the bend radius of the bar.

11.7 BRACKETS AND CORBELS

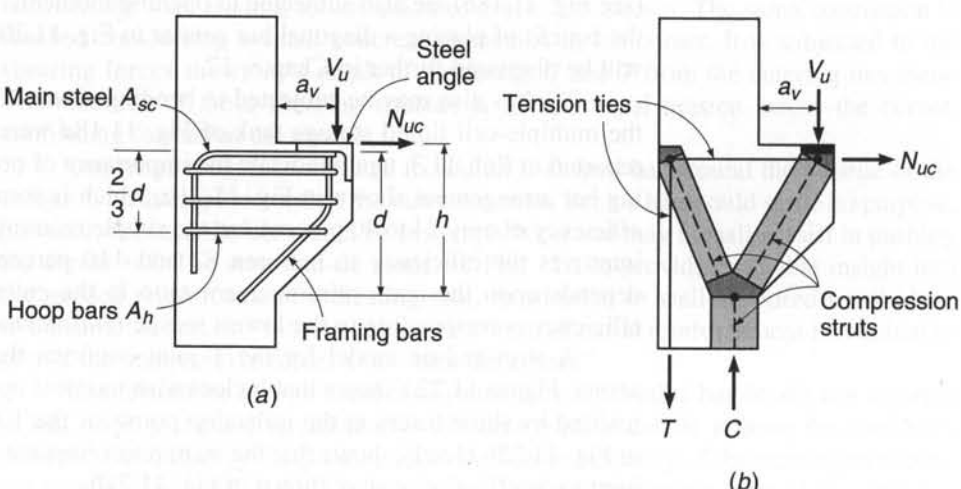
Brackets such as shown in Fig. 11.23a are widely used in precast construction for supporting precast beams at the columns. When they project from a wall, rather than from a column, they are properly called corbels, although the two terms are often used interchangeably. Brackets are designed mainly to provide for the vertical reaction V_u at the end of the supported beam, but unless special precautions are taken to avoid horizontal forces caused by restrained shrinkage, creep (in the case of prestressed beams), or temperature change, they must also resist a horizontal force N_{uc} .

Steel bearing plates or angles are generally used on the top surface of the brackets, as shown, to provide a uniform contact surface and to distribute the reaction. A corresponding steel bearing plate or angle is usually provided at the lower corner of the supported member. If the two plates are welded together, horizontal forces clearly must be allowed for in the design. Even with Teflon or elastomeric bearing pads, frictional forces will develop due to volumetric change.

The structural performance of a bracket can be visualized easily by means of the strut-and-tie model shown in Fig. 11.23b. The downward thrust of the load V_u is equilibrated by the vertical component of the reaction from the diagonal compression strut that carries the load down into the column. The outward thrust at the top of the strut is balanced by the tension in the horizontal tie bars across the top of the bracket; these also take the tension, if any, imparted by the horizontal force N_{uc} . At the left end of the horizontal tie, the tension is equilibrated by the horizontal component of thrust from the second compression strut shown. The vertical

FIGURE 11.23

Typical reinforced concrete bracket: (a) loads and reinforcement; (b) strut-and-tie model for internal forces.



component of this thrust requires the tensile force shown acting downward at the left side of the supporting column.

The steel required, according to the strut-and-tie model, is shown in Fig. 11.23a. The main bars A_{sc} must be carefully anchored because they need to develop their full yield strength f_y directly under the load V_u , and for this reason they are usually welded to the underside of the bearing angle and a 90° hook is provided for anchorage at the left side. Closed hoop bars with area A_h confine the concrete in the two compression struts and resist a tendency for splitting in a direction parallel to the thrust. The framing bars shown are usually of about the same diameter as the stirrups and serve mainly to improve the stirrup anchorage at the outer face of the bracket.

The bracket may also be considered as a very short cantilevered beam, with flexural tension at the column face resisted by the top bars A_{sc} . Either concept will result in about the same area of main reinforcement.

A second possible mode of failure is by direct shear along a plane more or less flush with the vertical face of the main part of the column. Shear-friction reinforcement crossing such a crack (see Section 4.9) would include the area A_{sc} previously placed in the top tie and the area A_h from the hoops below it. Other failure modes include flexural tension failure, with yielding of the top bars followed by crushing of the concrete at the bottom of the bracket; crushing of the concrete under the bearing angle (particularly if end rotation of the supported beam causes the force V_u to be applied too close to the outer corner of the bracket); and direct tension failure, if the horizontal force N_{uc} is larger than anticipated.

The provisions of ACI Code 11.8 for the design of brackets and corbels have been developed mainly based on tests (Refs. 11.9, 11.11, and 11.12) and relate to the flexural model of bracket behavior. They apply to brackets and corbels with a shear span ratio a_v/d of 1.0 or less (see Fig. 11.23a). Brackets and corbels with a_v/d less than 2 may be designed using strut-and-tie models, as described in Chapter 10. The distance d is measured at the column face, and the depth at the outside edge of the bearing area must not be less than $0.5d$. The usual design basis is employed, i.e., $M_u \leq \phi M_n$ and $V_u \leq \phi V_n$, and for brackets and corbels (for which shear dominates the design), ϕ is to be taken equal to 0.75 for all strength calculations, including flexure and direct tension as well as shear.

The section at the face of the supporting column must simultaneously resist the shear V_u , the moment $M_u = V_u a_v + N_{uc}(h - d)$, and the horizontal tension N_{uc} . Unless special precautions are taken, a horizontal tension not less than 20 percent of the vertical reaction must be assumed to act. This tensile force is to be regarded as live load, and a load factor of 1.6 should be applied.

An amount of steel A_f to resist the moment M_u can be found by the usual methods for flexural design. Thus,

$$A_f = \frac{M_u}{\phi f_y(d - a/2)} \quad (11.6)$$

where $a = A_f f_y / 0.85 f_c' b$. An additional area of steel A_n must be provided to resist the tensile component of force:

$$A_n = \frac{N_{uc}}{\phi f_y} \quad (11.7)$$

The total area required for flexure and direct tension at the top of the bracket is thus

$$A_{sc} \geq A_f + A_n \quad (11.8)$$

Design for shear is based on the shear-friction method of Section 4.9, and the total shear-friction reinforcement A_{vf} is found by

$$A_{vf} = \frac{V_u}{\phi \mu f_y} \quad (11.9)$$

where the friction factor μ for monolithic construction is 1.4λ , where $\lambda = 1.0$ for normalweight concrete and 0.75 for both sand-lightweight and all-lightweight concrete, in accordance with ACI Code 11.6. The value of $V_n = V_u/\phi$ must not exceed the smallest of $0.2f'_c b_w d$, $(480 + 0.08f'_c)b_w d$, and $1600b_w d$ at the support face for normalweight concrete or the smaller of $(0.2 - 0.07a_v/d)f'_c b_w d$ and $(800 - 280a_v/d)b_w d$ for lightweight concrete. Then, according to ACI Code 11.8, the total area required for *shear plus direct tension* at the top of the bracket is

$$A_{sc} \geq \frac{2}{3} A_{vf} + A_n \quad (11.10)$$

with the remaining part of A_{vf} placed in form of closed hoops having area A_h in the lower part of the bracket, as shown in Fig. 11.23a.

Thus, the total steel area A_{sc} required at the top of the bracket is equal to the larger of the values given by Eq. (11.8) or (11.10). An additional restriction, that A_{sc} not be less than $0.04(f'_c/f_y)bd$, is intended to avoid the possibility of sudden failure upon formation of a flexural tensile crack at the top of the bracket.

According to the ACI Code, closed hoop stirrups having area A_h (see Fig. 11.23a) not less than $0.5(A_{sc} - A_n)$ must be provided and be uniformly distributed within two-thirds of the effective depth adjacent to and parallel to A_{sc} . This requirement is more clearly stated as follows:

$$A_h \geq 0.5A_f \quad \text{and} \quad \geq \frac{1}{3} A_{vf} \quad (11.11)$$

EXAMPLE 11.5

Design of column bracket. A column bracket having the general features shown in Fig. 11.24 is to be designed to carry the end reaction from a long-span precast girder. Vertical reactions from service dead and live loads are 25 and 51 kips, respectively, applied at $a_v = 5.5$ in. from the column face. A steel bearing plate will be provided for the girder, which will rest directly on a $5 \times 3 \times \frac{3}{8}$ in. steel angle anchored at the outer corner of the bracket. Bracket reinforcement will include main steel A_{sc} welded to the underside of the steel angle, closed hoop stirrups having total area A_h distributed appropriately through the bracket depth, and framing bars in a vertical plane near the outer face. Select appropriate concrete dimensions, and design and detail all reinforcement. Material strengths are $f'_c = 5000$ psi and $f_y = 60,000$ psi.

SOLUTION. The vertical factored load to be carried is

$$V_u = 1.2 \times 25 + 1.6 \times 51 = 112 \text{ kips}$$

In the absence of a roller or low-friction support pad, a horizontal tensile force of

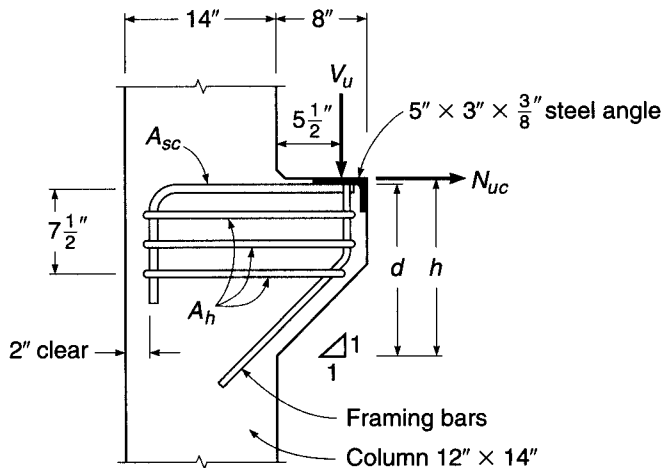
$$N_{uc} = 0.20 \times 112 = 22.4 \text{ kips}$$

will be included. According to the shear friction provisions of the ACI Code, the nominal shear strength V_n must not exceed $0.2f'_c bd$, $(480 + 0.08f'_c)bd$, or $1600bd$. With $f'_c = 5000$ psi, the second limit controls. Then, with $V_u = \phi V_n$ and with the column width $b = 12$ in.,

$$112 = 0.75 \times 0.880 \times 12d$$

FIGURE 11.24

Column bracket design example.



from which $d = 14.14$ in. Estimating 1 in. from the center of the main steel to the top surface of the bracket, a total depth $h = 16$ in. will be selected, with d approximately equal to 15 in., the exact value depending on the bar diameter chosen for A_{sc} . If a 45° slope is used, as indicated in Fig. 11.24, the bracket depth at the outside of the bearing area will be 8 in. This is not less than $0.5d = 7.5$ in., as required. For the bracket geometry selected, $a_v/d = 5.5/15 = 0.36$. This does not exceed the 1.0 limit imposed by the ACI Code.

The total shear friction steel is found from Eq. (11.9):

$$A_{vf} = \frac{V_u}{\phi \mu f_y} = \frac{112}{0.75 \times 1.4 \times 60} = 1.78 \text{ in}^2$$

The bending moment to be resisted is

$$\begin{aligned} M_u &= V_u a_v + N_{uc}(h - d) \\ &= 112 \times 5.5 + 22.4 \times 1 = 638 \text{ kips} \end{aligned}$$

The depth of the flexural compression stress block will be estimated to be 2 in., so, from Eq. (11.6),

$$A_f = \frac{M_u}{\phi f_y(d - a/2)} = \frac{638}{0.75 \times 60(15 - 2.0/2)} = 1.01 \text{ in}^2$$

Checking the stress block depth gives

$$a = \frac{A_f f_y}{0.85 f'_c b} = \frac{1.01 \times 60}{0.85 \times 5 \times 12} = 1.12 \text{ in.}$$

so the revised steel area is

$$A_f = \frac{638}{0.75 \times 60(15 - 1.12/2)} = 0.98 \text{ in}^2$$

The tensile force of 22.4 kips requires an additional steel area, from Eq. (11.7), of

$$A_n = \frac{N_{uc}}{\phi f_y} = \frac{22.4}{0.75 \times 60} = 0.50 \text{ in}^2$$

Thus, from Eqs. (11.8) and (11.10), respectively, the total steel area at the top of the bracket must not be less than

$$A_{sc} \geq A_f + A_n = 0.98 + 0.50 = 1.48 \text{ in}^2$$

or less than

$$A_{sc} \geq \frac{2}{3} A_{vf} + A_n = \frac{2}{3} \times 1.78 + 0.50 = 1.69 \text{ in}^2$$

The second requirement controls here. The minimum steel requirement of

$$A_{sc,min} = 0.04 \frac{f'_c}{f_y} bd = 0.04 \times \frac{5}{60} \times 12 \times 16 = 0.64 \text{ in}^2$$

is seen not to control. A total of three No. 7 (No. 22) bars, providing $A_{sc} = 1.80 \text{ in}^2$, will be used.

Closed hoop steel having a total area A_h not less than $0.5(A_{sc} - A_n)$ must be provided. Thus,

$$A_h \geq 0.5A_f = 0.5 \times 0.92 = 0.46 \text{ in}^2$$

and

$$A_h \geq 0.5 \times \frac{2}{3} A_{vf} = \frac{1}{3} \times 1.78 = 0.60 \text{ in}^2$$

The second requirement controls. Three No. 3 (No. 10) closed hoops will be provided, giving total area $A_h = 0.66 \text{ in}^2$. These must be placed within $\frac{2}{3}$ of the effective depth of the main steel. A spacing of 2.5 in. will be satisfactory, as indicated in Fig. 11.24. A pair of No. 3 (No. 10) framing bars will be added at the inside corner of the hoops to improve anchorage, as shown.

Anchorage of the No. 7 (No. 22) bars will be provided at the right end by welding to the underside of the steel angle and at the left end by a standard 90° bend (see Fig. 5.10). The basic development length for hooked bars (Table 5.3) is

$$l_{dh} = \left(\frac{0.02\psi_e f_y}{\lambda \sqrt{f'_c}} \right) d_b = \left(\frac{0.02 \times 1 \times 60,000}{1 \times \sqrt{5000}} \right) 0.875 = 14.8 \text{ in.}$$

Two modification factors apply here. The first is 0.7, provided at least 2 in. cover is maintained at the end of the hook, and the second is (required A_s)/(provided A_s) = $1.69/1.80 = 0.94$. Thus, the required development length past the face of the column is

$$l_{dh} = 14.8 \times 0.7 \times 0.94 = 9.74 \text{ in.}$$

This requirement is easily met. The hook extension will be $12d_b = 12 \times 0.875 = 10.5 \text{ in.}$ For the hoop bars, a standard 1'35° hook, as shown in Fig. 5.9b, will be used.

REFERENCES

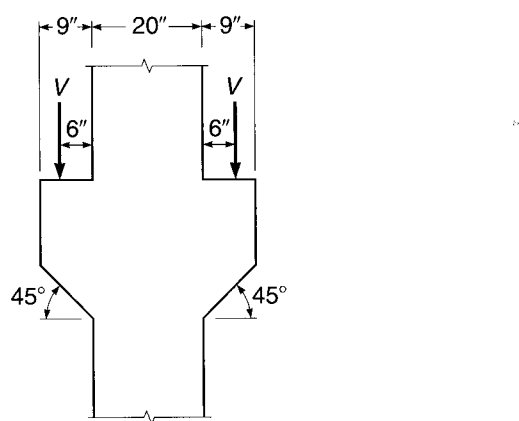
- 11.1. "Reinforced Concrete Design Includes Approval of Details," CRSI Engineering Practice Committee, *Concr. Int.*, vol. 10, no. 1, 1988, pp. 21–22.
- 11.2. *ACI Detailing Manual*, ACI Special Publication SP66, American Concrete Institute, Farmington Hills, MI, 2004.
- 11.3. I. H. E. Nilsson and A. Losberg, "Reinforced Concrete Corners and Joints Subjected to Bending Moment," *J. Struct. Div.*, ASCE, vol. 102, no. ST6, 1976, pp. 1229–1254.
- 11.4. D. F. Meinheit and J. O. Jirsa, "Shear Strength of Reinforced Concrete Beam-Column Connections," *J. Struct. Div.*, ASCE, vol. 107, no. ST11, 1981, pp. 2227–2244.
- 11.5. J. G. L. Marques and J. O. Jirsa, "A Study of Hooked Bar Anchorages in Beam-Column Joints," *J. ACI*, vol. 72, no. 5, 1975, pp. 198–209.
- 11.6. ACI-ASCE Committee 352, Recommendations for Design of Beam-Column Joints in Monolithic Reinforced Concrete Structures (ACI 352R-02), American Concrete Institute, Farmington Hills, MI, 2002.
- 11.7. N. S. Anderson and J. A. Ramirez, "Detailing of Stirrup Reinforcement," *ACI Struct. J.*, vol. 86, no. 5, 1989, pp. 507–515.
- 11.8. R. Park and T. Pauley, *Reinforced Concrete Structures*, John Wiley, New York, 1975.

- 11.9. L. B. Kriz and C. H. Raths, "Connections in Precast Concrete Structures—Strength of Corbels," *J. Prestressed Concr. Inst.*, vol. 10, no. 1, 1965, pp. 16–47.
- 11.10. A. H. Mattock and J. F. Shen, "Joints Between Reinforced Concrete Members of Similar Depth," *ACI Struct. J.*, vol. 89, no. 3, 1992, pp. 290–295.
- 11.11. A. H. Mattock, K. C. Chen, and K. Soongswang, "The Behavior of Reinforced Concrete Corbels," *J. Prestressed Concr. Inst.*, vol. 21, no. 2, 1976, pp. 52–77.
- 11.12. A. H. Mattock, "Design Proposals for Reinforced Concrete Corbels," *J. Prestressed Concr. Inst.*, vol. 21, no. 3, 1976, pp. 18–24.

PROBLEMS

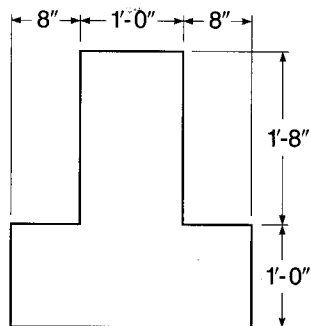
- 11.1.** An interior Type 1 joint, which is to be considered a part of the primary lateral load-resisting system, is to be designed. The 16 in. square column, with main steel consisting of four No. 11 (No. 36) bars, is intersected by two 12 × 18 in. beams in the X direction, reinforced with three No. 10 (No. 32) top bars and three No. 8 (No. 25) bottom bars. In the Y direction, there are two 12 × 22 in. girders, reinforced with three No. 11 (No. 36) top bars and three No. 9 (No. 29) bottom bars. Concrete cover is 2.5 in. to the center of the bars, except for the top steel in the girders, which is carried just under the top steel of the beams. Design and detail the joint, using $f'_c = 4000$ psi and $f_y = 60,000$ psi. Specify placement of all bars and cutoff points.
- 11.2.** A typical exterior joint of the building of Problem 11.1 is identical to the interior joint except that the 12 × 18 in. beam occurs on one side of the column only; the girders frame into two opposite faces, as before. All reinforcement is the same as for the joint of Problem 11.1. Design and detail the joint, specifying bar placement, cutoff points, and details such as bar hook dimensions.
- 11.3.** The precast columns of a proposed parking garage will incorporate symmetrical brackets to carry the end reactions of short girders that, in turn, carry long-span precast, prestressed double T floor units. The girder reactions will be applied 6 in. from the column face, as shown in Fig. P11.3, and a total width of bracket of 9 in. must be provided for proper bearing. Column width in the perpendicular direction is 20 in. Service load reactions applied at the top face of the brackets are 45 kips dead load and 36 kips live load. Select all unspecified concrete dimensions and design and detail the reinforcement. A corner angle is suggested at the outer top edge of the bracket. Column material strengths are $f'_c = 6000$ psi and $f_y = 60,000$ psi.

FIGURE P11.3



- 11.4.** The stem of a 60 ft long, 8 ft wide simply supported single T beam rests on the ledge of the inverted T beam shown in Fig. P11.4. The T beam has a bearing area 6 in. thick and 4 in. parallel to the axis of the T. The applied service load is 85 psf dead load, including self-weight, and 50 psf live load. Design the connection detail under the stem using $f'_c = 5000$ psi and $f_y = 60,000$ psi.

FIGURE P11.4



12

Analysis of Indeterminate Beams and Frames

12.1 CONTINUITY

The individual members that compose a steel or timber structure are fabricated or cut separately and joined together by rivets, bolts, welds, or nails. Unless the joints are specially designed for rigidity, they are too flexible to transfer moments of significant magnitude from one member to another. In contrast, in reinforced concrete structures, as much of the concrete as is practical is placed in one single operation. Reinforcing steel is not terminated at the ends of a member but is extended through the joints into adjacent members. At construction joints, special care is taken to bond the new concrete to the old by carefully cleaning the latter, by extending the reinforcement through the joint, and by other means. As a result, reinforced concrete structures usually represent monolithic, or continuous, units. A load applied at one location causes deformation and stress at all other locations. Even in precast concrete construction, which resembles steel construction in that individual members are brought to the job site and joined in the field, connections are often designed to provide for the transfer of moment as well as shear and axial load, producing at least partial continuity.

The effect of continuity is most simply illustrated by a continuous beam, such as shown in Fig. 12.1a. With simple spans, such as provided in many types of steel construction, only the loaded member *CD* would deform, and all other members of the structure would remain straight. But with continuity from one member to the next through the support regions, as in a reinforced concrete structure, the distortion caused by a load on one single span is seen to spread to all other spans, although the magnitude of deformation decreases with increasing distance from the loaded member. All members of the six-span structure are subject to curvature, and thus also to bending moment, as a result of loading span *CD*.

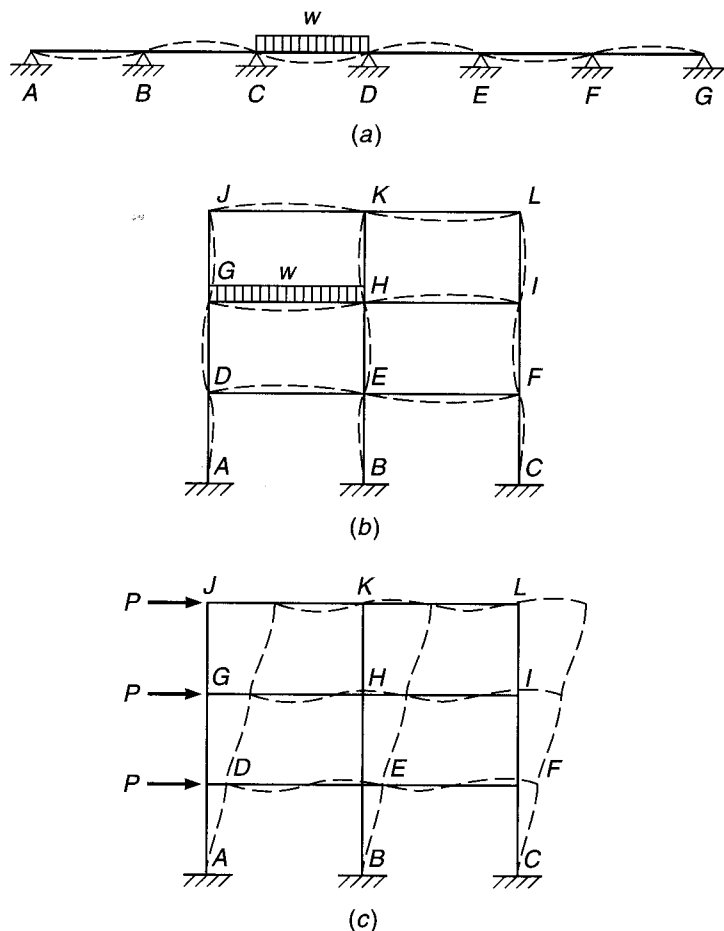
Similarly, for the rigid-jointed frame of Fig. 12.1b, the distortion caused by a load on the single member *GH* spreads to all beams and all columns, although, as before, the effect decreases with increasing distance from the load. All members are subject to bending moment, even though they may carry no transverse load.

If horizontal forces, such as forces caused by wind or seismic action, act on a frame, it deforms as illustrated by Fig. 12.1c. Here, too, all members of the frame distort, even though the forces act only on the left side; the amount of distortion is seen to be the same for all corresponding members, regardless of their distance from the points of loading, in contrast to the case of vertical loading. A member such as *EH*, even without a directly applied transverse load, will experience deformations and associated bending moment.

In *statically determinate structures*, such as simple-span beams, the deflected shape and the moments and shears depend only on the type and magnitude of the loads

FIGURE 12.1

Deflected shape of continuous beams and frames.



and the dimensions of the member. In contrast, inspection of the *statically indeterminate structures* in Fig. 12.1 shows that the deflection curve of any member depends not only on the loads but also on the joint rotations, whose magnitudes in turn depend on the distortion of adjacent, rigidly connected members. For a rigid joint such as joint H in the frame shown in Fig. 12.1b or c, all the rotations at the near ends of all members framing into that joint must be the same. For a correct design of continuous beams and frames, it is evidently necessary to determine moments, shears, and thrusts considering the effect of continuity at the joints.

The determination of these internal forces in continuously reinforced concrete structures is usually based on *elastic analysis* of the structure at factored loads with methods that will be described in Sections 12.2 through 12.5. Such analysis requires knowledge of the cross-sectional dimensions of the members. Member dimensions are initially estimated during preliminary design, which is described in Section 12.6 along with guidelines for establishing member proportions. For checking the results of more exact analysis, the approximate methods of Section 12.7 are useful. For many structures, a full elastic analysis is not justified, and the ACI coefficient method of analysis described in Section 12.8 provides an adequate basis for design moments and shears.

Before failure, reinforced concrete sections are usually capable of considerable inelastic rotation at nearly constant moment, as was described in Section 6.9. This

permits a *redistribution of elastic moments* and provides the basis for *plastic analysis* of beams, frames, and slabs. Plastic analysis will be developed in Section 12.9 for beams and frames and in Chapters 14 and 15 for slabs.

12.2 LOADING

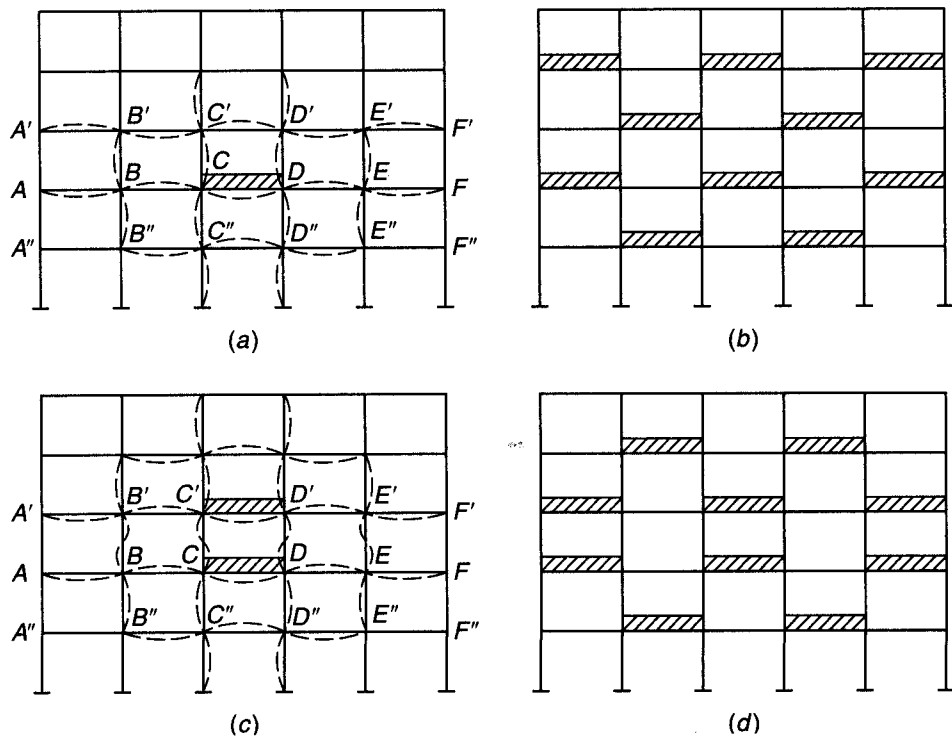
The individual members of a structural frame must be designed for the worst combination of loads that can reasonably be expected to occur during its useful life. Internal moments, shears, and thrusts are brought about by the combined effect of dead and live loads, plus other loads, such as wind and earthquake, as discussed in Section 1.7. While dead loads are constant, live loads such as floor loads from human occupancy can be placed in various ways, some of which will result in larger effects than others. In addition, the various combinations of factored loads specified in Table 1.2 must be used to determine the load cases that govern member design. The subject of load placement will be addressed first.

a. Placement of Loads

In Fig. 12.2a only span CD is loaded by live load. The distortions of the various frame members are seen to be largest in, and immediately adjacent to, the loaded span and to decrease rapidly with increasing distance from the load. Since bending moments are proportional to curvatures, the moments in more remote members are correspondingly smaller than those in, or close to, the loaded span. However, the loading shown in Fig. 12.2a does not produce the maximum possible positive moment in CD . In fact,

FIGURE 12.2

Alternate live loadings for maximum effects.



if additional live load were placed on span *AB*, this span would bend down, *BC* would bend up, and *CD* itself would bend down in the same manner, although to a lesser degree, as it is bent by its own load. Hence, the positive moment in *CD* is increased if *AB* and, by the same reasoning, *EF* are loaded simultaneously. By expanding the same reasoning to the other members of the frame, one can easily see that the checkerboard pattern of live load shown in Fig. 12.2*b* produces the largest possible positive moments, not only in *CD*, but in all loaded spans. Hence, two such checkerboard patterns are required to obtain the maximum positive moments in all spans.

In addition to maximum span moments, it is often necessary to investigate minimum span moments. Dead load, acting as it does on all spans, usually produces only positive span moments. However, live load, placed as in Fig. 12.2*a*, and even more so in Fig. 12.2*b*, is seen to bend the unloaded spans upward, i.e., to produce negative moments in the span. If these negative live load moments are larger than the generally positive dead load moments, a given girder, depending on load position, may be subject at one time to positive span moments and at another to negative span moments. It must be designed to withstand both types of moments; i.e., it must be furnished with tensile steel at both top and bottom. Thus, the loading of Fig. 12.2*b*, in addition to giving maximum span moments in the loaded spans, gives minimum span moments in the unloaded spans.

Maximum negative moments at the supports of the girders are obtained, on the other hand, if loads are placed on the two spans adjacent to the particular support and in a corresponding pattern on the more remote girders. A separate loading scheme of this type is then required for each support for which maximum negative moments are to be computed.

In each column, the largest moments occur at the top or bottom. While the loading shown in Fig. 12.2*c* results in large moments at the ends of columns *CC'* and *DD'*, the reader can easily be convinced that these moments are further augmented if additional loads are placed as shown in Fig. 12.2*d*.

It is seen from this brief discussion that to calculate the maximum possible moments at all critical points of a frame, live load must be placed in a great variety of different schemes. In most practical cases, however, consideration of the relative magnitude of effects will permit limitation of analysis to a small number of significant cases.

b. Load Combinations

The ACI Code requires that structures be designed for a number of load combinations, as discussed in Section 1.7. Thus, for example, factored load combinations might include (1) dead plus live load; (2) dead plus fluid plus temperature plus live plus soil plus snow load; (3) three possible combinations that include dead, live, and wind load; and (4) two combinations that include dead load, live load, and earthquake load, with some of the combinations including snow, rain, soil, and roof live load. While each of the combinations may be considered as an individual loading condition, experience has shown that the most efficient technique involves separate analyses for each of the basic loads without load factors, that is, a full analysis for unfactored dead load only, separate analyses for the various live load distributions described in Section 12.2*a*, and separate analyses for each of the other loads (wind, snow, etc.). Once the separate analyses are completed, it is a simple matter to combine the results using the appropriate load factor for each type of load. This procedure is most advantageous because, for example, live load may require a load factor of 1.6 for one combination, a value of 1.0 for another, and a value of 0.5 for yet another. Once the forces have been calculated

for each combination, the combination of loads that governs for each member can usually be identified by inspection.

12.3 SIMPLIFICATIONS IN FRAME ANALYSIS

Considering the complexity of many practical building frames and the need to account for the possibility of alternative loadings, there is evidently a need to simplify. This can be done by means of certain approximations that allow the determination of moments with reasonable accuracy while substantially reducing the amount of computation.

Numerous trial computations have shown that, for building frames with a reasonably regular outline, not involving unusual asymmetry of loading or shape, the influence of sidesway caused by vertical loads can be neglected. In that case, moments due to vertical loads are determined with sufficient accuracy by dividing the entire frame into simpler subframes. Each of these consists of one continuous beam, plus the top and bottom columns framing into that particular beam. Placing the live loads on the beam in the most unfavorable manner permits sufficiently accurate determination of all beam moments, as well as the moments at the top ends of the bottom columns and the bottom ends of the top columns. For this partial structure, the far ends of the columns are considered fixed, except for such first-floor or basement columns where soil and foundation conditions dictate the assumption of hinged ends. Such an approach is explicitly permitted by ACI Code 8.11, which specifies the following for floor and roof members:

1. The live load may be considered to be applied only to the floor or roof under consideration, and the far ends of columns built integrally with the structure may be considered fixed.
2. The arrangement of live load may be limited to combinations of (a) factored dead load on all spans with full factored live load on two adjacent spans, and (b) factored dead load on all spans with full factored live load on alternate spans.

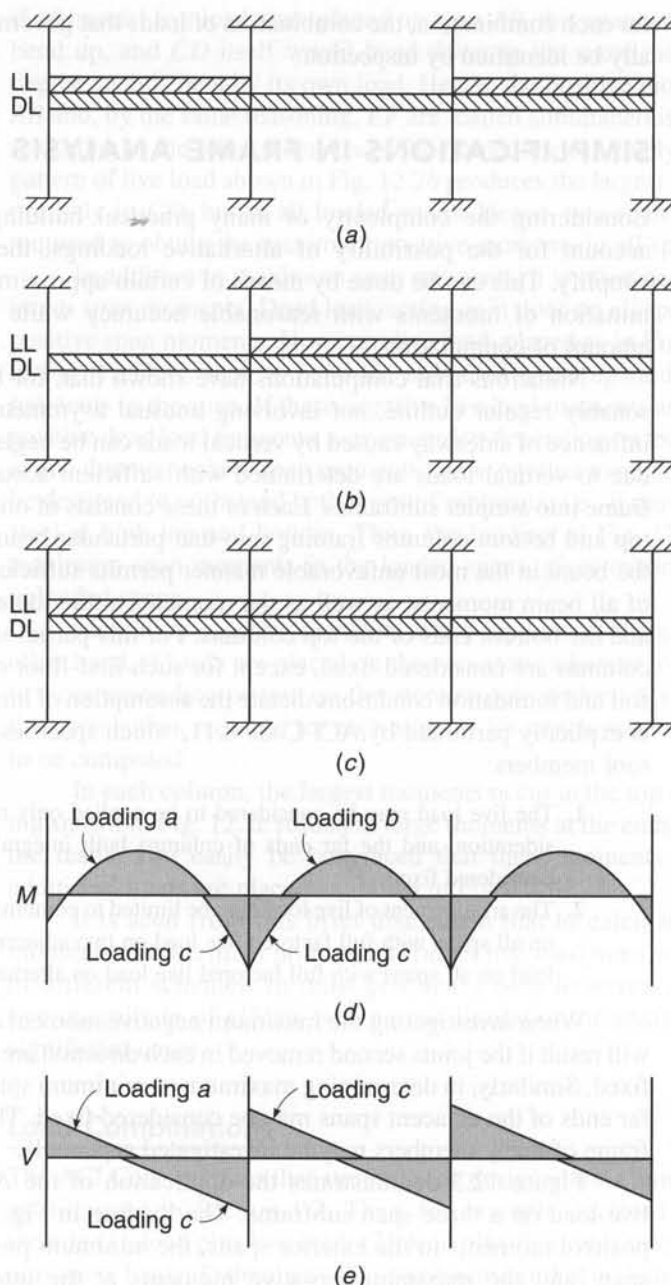
When investigating the maximum negative moment at any joint, negligible error will result if the joints second removed in each direction are considered to be completely fixed. Similarly, in determining maximum or minimum span moments, the joints at the far ends of the adjacent spans may be considered fixed. Thus, individual portions of a frame of many members may be investigated separately.

Figure 12.3 demonstrates the application of the ACI Code requirements for live load on a three-span subframe. The loading in Fig. 12.3a results in maximum positive moments in the exterior spans, the minimum positive moment in the center span, and the maximum negative moments at the interior faces of the exterior columns. The loading shown in Fig. 12.3b results in the maximum positive moment in the center span and minimum positive moments in the exterior spans. The loading in Fig. 12.3c results in maximum negative moment at both faces of the interior columns. Since the structure is symmetrical, values of moment and shear obtained for the loading shown in Fig. 12.3c apply to the right side of the structure as well as the left. Due to the simplicity of this structure, joints away from the spans of interest are not treated as fixed.

Moments and shears used for design are determined by combining the moment and shear diagrams for the individual load cases to obtain the maximum values along each span length. The resulting envelope moment and shear diagrams are shown in Fig. 12.3d and e, respectively. The moment and shear envelopes (note the range of

FIGURE 12.3

Subframe loading as required by ACI Code 8.9: Loading for (a) maximum positive moments in the exterior spans, the minimum positive moment in the center span, and the maximum negative moments at the interior faces of the exterior columns; (b) maximum positive moment in the center span and minimum positive moments in the exterior spans; and (c) maximum negative moment at both faces of the interior columns; (d) envelope moment diagram; (e) envelope shear diagram. (DL and LL represent factored dead and live loads, respectively.)



positions for points of inflection and points of zero shear) are used not only to design the critical sections but to determine cutoff points for flexural reinforcement and requirements for shear reinforcement.

In regard to columns, ACI Code 8.10 indicates

1. Columns shall be designed to resist the axial forces from factored loads on all floors or roof and the maximum moment from factored loads on a single adjacent span of the floor or roof under consideration. The loading condition giving the maximum ratio of moment to axial load shall also be considered.

2. In frames or continuous construction, consideration shall be given to the effect of unbalanced floor or roof loads on both exterior and interior columns and of eccentric loading due to other causes.
3. In computing moments in columns due to gravity loading, the far ends of columns built integrally with the structure may be considered fixed.
4. The resistance to moments at any floor or roof level shall be provided by distributing the moment between columns immediately above and below the given floor in proportion to the relative column stiffness and conditions of restraint.

Although it is not addressed in the ACI Code, axial loads on columns are usually determined based on the column tributary areas, which are defined based on the midspan of flexural members framing into each column. The axial load from the tributary area is used in design, with the exception of first interior columns, which are typically designed for an extra 10 percent axial load to account for the higher shear expected in the flexural members framing into the exterior face of first interior columns. The use of this procedure to determine axial loads due to gravity is conservative (note that the total vertical load exceeds the factored loads on the structure) and is adequately close to the values that would be obtained from a more detailed frame analysis.

12.4 METHODS FOR ELASTIC ANALYSIS

Many methods have been developed over the years for the elastic analysis of continuous beams and frames. The so-called classical methods (Ref. 12.1), such as application of the theorem of three moments, the method of least work (Castiglano's second theorem), and the general method of consistent deformation, will prove useful only in the analysis of continuous beams having few spans or of very simple frames, and are, in fact, rarely used. For the cases generally encountered in practice, such methods prove exceedingly tedious, and alternative approaches are preferred.

For many years moment distribution (Ref. 12.1) provided the basic analytical tool for the analysis of indeterminate concrete beams and frames, originally with the aid of the slide rule and later with handheld programmable calculators. For relatively small problems, moment distribution may still provide the most rapid results, and it is often used in current practice, for example, in the Equivalent Frame Method of design for slabs described in Section 13.9. However, with the widespread availability of computers, manual methods have been replaced largely by matrix analysis, which provides rapid solutions with a high degree of accuracy (Refs. 12.2 and 12.3).

Approximate methods of analysis, based either on careful sketches of the shape of the deformed structure under load or on moment coefficients, still provide a means for rapid estimation of internal forces and moments (Ref. 12.4). Such estimates are useful in preliminary design and in checking more exact solutions for gross errors that might result from input errors. In structures of minor importance, approximations may even provide the basis for final design.

In view of the number of excellent texts now available that treat methods of analysis (Refs. 12.1 to 12.4 to name just a few), the present discussion will be confined to an evaluation of the usefulness of several of the more important of these, with particular reference to the analysis of reinforced concrete structures. Certain idealizations and approximations that facilitate the solution in practical cases will be described in more detail.

a. Moment Distribution

In 1932, Hardy Cross developed the method of moment distribution to solve problems in frame analysis that involve many unknown joint displacements and rotations. For the next three decades, moment distribution provided the standard means in engineering offices for the analysis of indeterminate frames. Even now, it serves as the basic analytical tool if computer facilities are not available.

In the moment distribution method (Ref. 12.1), the fixed-end moments for each member are modified in a series of cycles, each converging on the precise final result, to account for rotation and translation of the joints. The resulting series can be terminated whenever one reaches the degree of accuracy required. After member end moments are obtained, all member stress resultants can be obtained from the laws of statics.

It has been found by comparative analyses that, except in unusual cases, building-frame moments found by modifying fixed-end moments by only two cycles of moment distribution will be sufficiently accurate for design purposes (Ref. 12.5).

b. Matrix Analysis

Use of matrix theory makes it possible to reduce the detailed numerical operations required in the analysis of an indeterminate structure to systematic processes of matrix manipulation that can be performed automatically and rapidly by computer. Such methods permit the rapid solution of problems involving large numbers of unknowns. As a consequence, less reliance is placed on special techniques limited to certain types of problems, and powerful methods of general applicability have emerged, such as the direct stiffness method (Refs. 12.2 and 12.3). By such means, an "exact" determination of internal forces throughout an entire building frame can be obtained quickly and at small expense. Three-dimensional frame analysis is possible where required. A large number of alternative loadings can be considered, including dynamic loads.

Some engineering firms prefer to write and maintain their own programs for structural analysis particularly suited to their needs. However, most make use of readily available programs that can be used for a broad range of problems. Input—including loads, material properties, structural geometry, and member dimensions—is provided by the user, often in an interactive mode. Output includes joint displacements and rotations, plus moment, shear, and thrust at critical sections throughout the structure. Most of these programs perform analysis of two- or three-dimensional framed structures subject to static or dynamic loads, shear walls, and other elements in a small fraction of the time formerly required, providing results to a high degree of accuracy.

12.5 IDEALIZATION OF THE STRUCTURE

It is seldom possible for the engineer to analyze an actual complex redundant structure. Almost without exception, certain idealizations must be made in devising an analytical model, so that the analysis will be practically possible. Thus, three-dimensional members are represented by straight lines, generally coincident with the actual centroidal axis. Supports are idealized as rollers, hinges, or rigid joints. Loads actually distributed over a finite area are assumed to be point loads. In three-dimensional framed structures, analysis is often limited to plane frames, each of which is assumed to act independently.

In the idealization of reinforced concrete frames, certain questions require special comment. The most important of these pertain to effective span lengths, effective moments of inertia, and conditions of support.

a. Effective Span Length

In elastic frame analysis, a structure is usually represented by a simple line diagram, based dimensionally on the centerline distances between columns and between floor beams. Actually, the depths of beams and the widths of columns (in the plane of the frame) amount to sizable fractions of the respective lengths of these members; their clear lengths are therefore considerably smaller than their centerline distances between joints.

It is evident that the usual assumption in frame analysis that the members are prismatic, with constant moment of inertia between centerlines, is not strictly correct. A beam intersecting a column may be prismatic up to the column face, but from that point to the column centerline it has a greatly increased depth, with a moment of inertia that could be considered infinite compared with that of the remainder of the span. A similar variation in width and moment of inertia is obtained for the columns. Thus, to be strictly correct, the actual variation in member depth should be considered in the analysis. Qualitatively, this would increase beam support moments somewhat and decrease span moments. In addition, it is apparent that the critical section for design for negative bending would be at the face of the support, and not at the centerline, since for all practical purposes an unlimited effective depth is obtained in the beam across the width of the support.

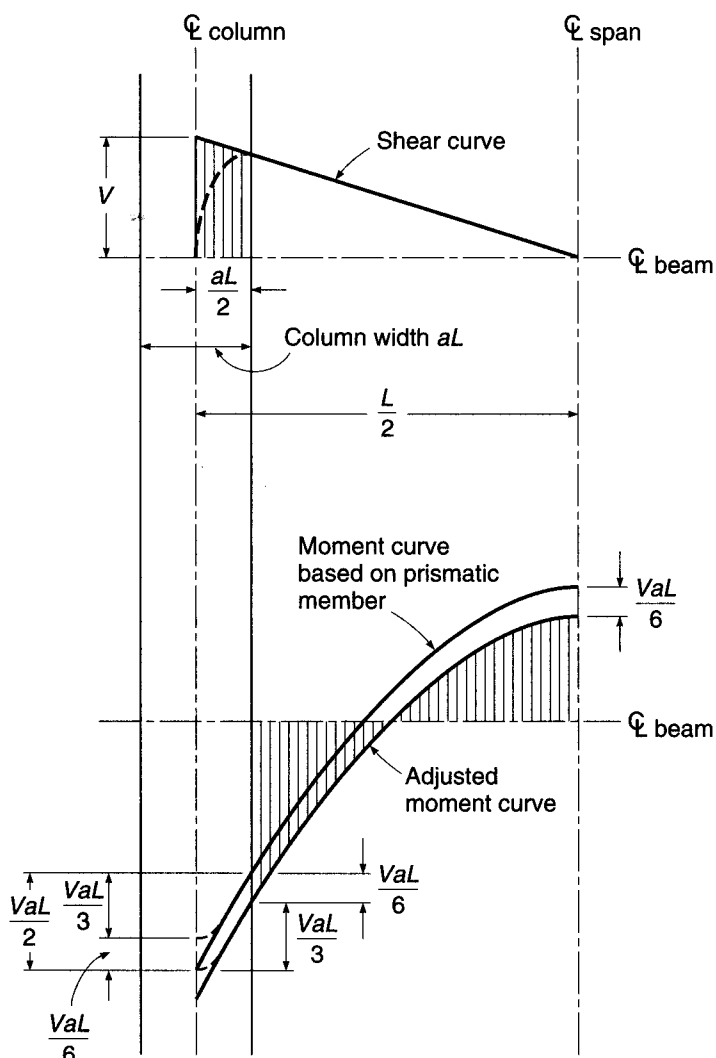
It will be observed that, in the case of the columns, the moment gradient is not very steep, so that the difference between centerline moment and the moment at the top or bottom face of the beam is small and in most cases can be disregarded. However, the slope of the moment diagram for the beam is usually quite steep in the region of the support, and there will be a substantial difference between the support centerline moment and face moment. If the former were used in proportioning the member, an unnecessarily large section would result. It is desirable, then, to reduce support moments found by elastic analysis to account for the finite width of the supports.

In Fig. 12.4, the change in moment between the support centerline and the support face will be equal to the area under the shear diagram between those two points. For knife edge supports, this shear area is seen to be very nearly equal to $VaL/2$. Actually, however, the reaction is distributed in some unknown way across the width of the support. This will have the effect of modifying the shear diagram as shown by the dashed line; it has been proposed that the reduced area be taken as equal to $VaL/3$. The fact that the reaction is distributed will modify the moment diagram as well as the shear diagram, causing a slight rounding of the negative moment peak, as shown in the figure, and the reduction of $VaL/3$ is properly applied to the moment diagram after the peak has been rounded. This will give nearly the same face moment as would be obtained by deducting the amount $VaL/2$ from the peak moment.

Another effect is present, however: the modification of the moment diagram due to the increased moment of inertia of the beam at the column. This effect is similar to that of a haunch, and it will mean slightly increased negative moment and slightly decreased positive moment. For ordinary values of the ratio a , this shift in the moment curve will be on the order of $VaL/6$. Thus, it is convenient simply to deduct the amount $VaL/3$ from the unrounded peak moment obtained from elastic analysis. This allows for (1) the actual rounding of the shear diagram and the negative moment peak due to

FIGURE 12.4

Reduction of negative and positive moments in a frame.



the distributed reaction and (2) the downward shift of the moment curve due to the haunch effect at the supports. The consistent reduction in positive moment of $VaL/6$ is illustrated in Fig. 12.4.

With this said, there are two other approaches that are often used by structural designers. The first is to analyze the structure based on the simple line diagram and to reduce the moment from the column centerline to the face of the support by $VaL/2$ without adjusting for the higher effective stiffness within the thickness width of the column. The moment diagram, although somewhat less realistic than represented by the lower curve in Fig. 12.4, still satisfies statics and requires less flexural reinforcement at the face of the support. As a consequence, there is less congestion in the beam-column joint, a location where it is often difficult to place concrete because of the high quantity of reinforcing steel from the flexural members framing into the column (usually from two different directions) and from the column itself. The somewhat higher percentage of reinforcement required at midspan usually causes little difficulty in concrete placement. The second approach involves representing the portion of the “beam” within the

width of the column as a rigid link that connects the column centerline with the clear span of the flexural member. The portion of the column within the depth of the beam can also be represented using a rigid link. Such a model will produce moment diagrams similar to the lower curve in Fig. 12.4, without additional analysis. The second approach is both realistic and easy to implement in matrix analysis programs.

It should be noted that there are certain conditions of support for which no reduction in negative moment is justified. For example, when a continuous beam is carried by a girder of approximately the same depth, the negative moment in the beam at the centerline of the girder should be used to design the negative reinforcing steel.

b. **Moments of Inertia**

Selection of reasonable values for moments of inertia of beams and columns for use in the frame analysis is far from a simple matter. The design of beams and columns is based on cracked section theory, i.e., on the supposition that tension concrete is ineffective. It might seem, therefore, that moments of inertia to be used should be determined in the same manner, i.e., based on the cracked transformed section, in this way accounting for the effects of cracking and presence of reinforcement. Things are not this simple, unfortunately.

Consider first the influence of cracking. For typical members, the moment of inertia of a cracked beam section is about one-half that of the uncracked gross concrete section. However, the extent of cracking depends on the magnitude of the moments relative to the cracking moment. In beams, no flexural cracks would be found near the inflection points. Columns, typically, are mostly uncracked, except for those having relatively large eccentricity of loading. A fundamental question, too, is the load level to consider for the analysis. Elements that are subject to cracking will have more extensive cracks near ultimate load than at service load. Compression members will be unaffected in this respect. Thus, the relative stiffness depends on load level.

A further complication results from the fact that the effective cross section of beams varies along a span. In the positive bending region, a beam usually has a T section. For typical T beams, with flange width about 4 to 6 times web width and flange thickness from 0.2 to 0.4 times the total depth, the gross moment of inertia will be about 2 times that of the rectangular web with width b_w and depth h . However, in the negative bending region near the supports, the bottom of the section is in compression. The T flange is cracked, and the effective cross section is therefore rectangular.

The amount and arrangement of reinforcement are also influential. In beams, if bottom bars are continued through the supports, as is often done, this steel acts as compression reinforcement and stiffens the section. In columns, reinforcement ratios are generally much higher than in beams, adding to the stiffness.

Given these complications, it is clear that some simplifications are necessary. It is helpful to note that, in most cases, it is only the *ratio* of member stiffnesses that influences the final result, not the absolute value of the stiffnesses. The stiffness ratios may be but little affected by different assumptions in computing moment of inertia if there is consistency for all members.

In practice, it is generally sufficiently accurate to base stiffness calculations for frame analysis on the gross concrete cross section of the columns. In continuous T beams, cracking will reduce the moment of inertia to about one-half that of the uncracked section. Thus, the effect of the flanges and the effect of cracking may nearly cancel in the positive bending region. In the negative moment regions there are no flanges; however, if bottom bars continue through the supports to serve as compression

steel, the added stiffness tends to compensate for lack of compression flange. Thus, for beams, generally a constant moment of inertia can be used, based on the rectangular cross-sectional area $b_w h$.

ACI Code 8.7.1 states that *any* set of reasonable assumptions may be used for computing relative stiffnesses, provided that the assumptions adopted are consistent throughout the analysis. ACI Commentary 8.7.1 notes that *relative* values of stiffness are important and that two common assumptions are to use gross EI values for all members or to use one-half of the gross EI of the beam stem for beams and the gross EI for the columns. Additional guidance is given in ACI Code 10.10.4, which specifies the section properties to be used for frames subject to sidesway. Thirty-five percent of the gross moment of inertia is used for beams and 70 percent for columns. This differs from the guidance provided in ACI Commentary 8.7.1 but, except for a factor of 0.70, matches the guidance provided in the earlier discussion.

c. Conditions of Support

For purposes of analysis, many structures can be divided into a number of two-dimensional frames. Even for such cases, however, there are situations in which it is impossible to predict with accuracy what the conditions of restraint might be at the ends of a span; yet moments are frequently affected to a considerable degree by the choice made. In many other cases, it is necessary to recognize that structures may be three-dimensional. The rotational restraint at a joint may be influenced or even governed by the characteristics of members framing into that joint at right angles. Adjacent members or frames parallel to the one under primary consideration may likewise influence its performance.

If floor beams are cast monolithically with reinforced concrete walls (frequently the case when first-floor beams are carried on foundation walls), the moment of inertia of the wall about an axis parallel to its face may be so large that the beam end could be considered completely fixed for all practical purposes. If the wall is relatively thin or the beam particularly massive, the moment of inertia of each should be calculated, that of the wall being equal to $bt^3/12$, where t is the wall thickness and b the wall width tributary to one beam.

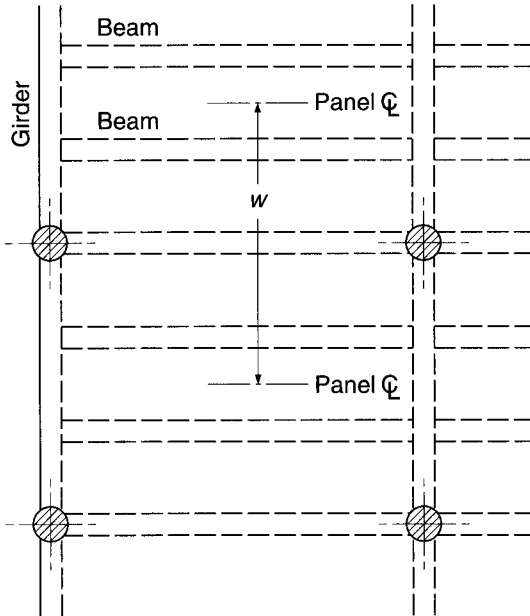
If the outer ends of concrete beams rest on masonry walls, as is sometimes the case, an assumption of zero rotational restraint (i.e., hinged support) is probably closest to the actual case.

For columns supported on relatively small footings, which in turn rest on compressible soil, a hinged end is generally assumed, since such soils offer but little resistance to rotation of the footing. If, on the other hand, the footings rest on solid rock, or if a cluster of piles is used with their upper portion encased by a concrete cap, the effect is to provide almost complete fixity for the supported column, and this should be assumed in the analysis. Columns supported by a continuous foundation mat should likewise be assumed fixed at their lower ends.

If members framing into a joint in a direction perpendicular to the plane of the frame under analysis have sufficient torsional stiffness, and if their far ends are fixed or nearly so, their effect on joint rigidity should be included in the computations. The torsional stiffness of a member of length L is given by the expression GJ/L , where G is the shear modulus of elasticity of concrete (approximately to $E_c/2.2$) and J is the torsional stiffness factor of the member. For beams with rectangular cross sections or with sections made up of rectangular elements, J can be taken equal to $\Sigma(hb^3/3 - b^4/5)$, in which h and b are the cross-sectional dimensions of each rectangular element, b being the lesser dimension in each case. In moment

FIGURE 12.5

Slab, beam, and girder floor system.



distribution, when the effect of torsional rigidity is included, it is important that the absolute flexural stiffness $4EI/L$ be used rather than relative I/L values.

A common situation in beam-and-girder floors and concrete joist floors is illustrated in Fig. 12.5. The sketch shows a beam-and-girder floor system in which longitudinal beams are placed at the third points of each bay, supported by transverse girders, in addition to the longitudinal beams supported directly by the columns. If the transverse girders are quite stiff, it is apparent that the flexural stiffness of all beams in the width w should be balanced against the stiffness of one set of columns in the longitudinal bent. If, on the other hand, the girders have little torsional stiffness, there would be ample justification for making two separate longitudinal analyses, one for the beams supported directly by the columns, in which the rotational resistance of the columns would be considered, and a second for the beams framing into the girders, in which case hinged supports would be assumed. In most cases, it would be sufficiently accurate to consider the girders stiff torsionally and to add directly the stiffness of all beams tributary to a single column. This has the added advantage that all longitudinal beams will have the same cross-sectional dimensions and the same reinforcing steel, which will greatly facilitate construction. Plastic redistribution of loads upon overloading would generally ensure nearly equal restraint moments on all beams before collapse as assumed in design. Torsional moments should not be neglected in designing the girders.

12.6 PRELIMINARY DESIGN AND GUIDELINES FOR PROPORTIONING MEMBERS

In making an elastic analysis of a structural framework, it is necessary to know at the outset the cross-sectional dimensions of the members, so that moments of inertia and stiffnesses can be calculated. Yet the determination of these same cross-sectional dimensions is the precise purpose of the elastic analysis. In terms of load, the dead load

on a structure is often dominated by the weight of the slab. Obviously, a preliminary estimate of member sizes must be one of the first steps in the analysis. Subsequently, with the results of the analysis at hand, members are proportioned, and the resulting dimensions compared with those previously assumed. If necessary, the assumed section properties are modified, and the analysis is repeated. Since the procedure may become quite laborious, it is obviously advantageous to make the best possible original estimate of member sizes, in the hope of avoiding repetition of the analysis.

In this connection, it is worth repeating that in the ordinary frame analysis, one is concerned with relative stiffnesses only, not the absolute stiffnesses. If, in the original estimate of member sizes, the stiffnesses of all beams and columns are overestimated or underestimated by about the same amount, correction of these estimated sizes after the first analysis will have little or no effect. Consequently, no revision of the analysis would be required. If, on the other hand, a nonuniform error in estimation is made, and relative stiffnesses differ from assumed values by more than about 30 percent, a new analysis should be made.

The experienced designer can estimate member sizes with surprising accuracy. Those with little or no experience must rely on trial calculations or arbitrary rules, modified to suit particular situations. In building frames, the depth of one-way slabs (discussed at greater length in Chapter 13) is often controlled by either deflection requirements or the negative moments at the faces of the supporting beams. Minimum depth criteria are reflected in Table 13.1, and negative moments at the face of the support can be estimated using coefficients described in Section 12.8. A practical minimum thickness of 4 in. is often used, except for joist construction meeting the requirements of ACI Code 8.13 (see Section 18.2d).

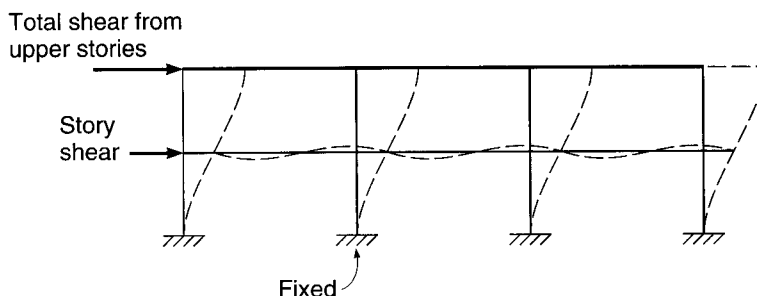
Beam sizes are usually governed by the negative moments and the shears at the supports, where their effective section is rectangular. Moments can be approximated by the fixed-end moments for the particular span, or by using the ACI moment coefficients (see Section 12.8). In most cases, shears will not differ greatly from simple beam shears. Alternatively, many designers prefer to estimate the depth of beams at about $\frac{3}{4}$ in. per foot of span, with the width equal to about one-half the depth.

For most construction, wide, relatively shallow beams and girders are preferred to obtain minimum floor depths, and using the same depth for all flexural members allows the use of simple, low-cost forming systems. Such designs can significantly reduce forming costs, while incurring only small additional costs for concrete and reinforcing steel. It is often wise to check the reinforcement ratio ρ based on the assumed moments to help maintain overall economy. A value of $\rho \approx 0.012$ in preliminary design will give $\rho \approx 0.01$ in a final design, if a more exact analysis is used. Obviously, member dimensions are subject to modification, depending on the type and magnitude of the loads, methods of design, and material strength.

Column sizes are governed primarily by axial loads, which can be estimated quickly, although the presence of moments in the columns is cause for some increase of the area as determined by axial loads. For interior columns, in which unbalanced moments will not be large, a 10 percent increase may be sufficient, while for exterior columns, particularly for upper stories, an increase of 50 percent in area may be appropriate. In deciding on these estimated increases, the following factors should be considered. Moments are larger in exterior than in interior columns, since in the latter dead load moments from adjacent spans will largely balance, in contrast to the case in exterior columns. In addition, the influence of moments, compared with that of axial loads, is larger in upper-floor than in lower-floor columns, because the moments are usually of about the same magnitude, while the axial loads are larger in the latter than in the former.

FIGURE 12.6

Subframe for estimating moments in lower-story columns of lateral load-resisting frames.



For minimum forming costs, it is highly desirable to use the same column dimensions throughout the height of a building. This can be accomplished by using higher-strength concrete on the lower stories (for high-rise buildings, this should be the highest-strength concrete available) and reducing concrete strength in upper stories, as appropriate. For columns in *laterally braced frames*, the preliminary design of the lower-story columns may be based on zero eccentricity using $0.80\phi P_o = P_u$. A total reinforcement ratio $\rho_g \approx 0.02$ should be used for the column with the highest axial load. With a value of $\rho_g \approx 0.01$ for the column with the lowest axial load on higher stories, the column size is maintained, reducing f'_c when ρ_g drops below 1 percent. Although ACI Code 10.9.1 limits ρ_g to a range of 1 to 8 percent, the effective minimum value of ρ_g is 0.005 based on ACI Code 10.8.4, which allows the minimum reinforcement to be calculated based on a reduced effective area A_g not less than one-half the total area (this provision cannot be used in regions of high seismic risk). For columns in lateral load-resisting frames, a subframe may be used to estimate the factored bending moments due to lateral load on the lower-story columns. The subframe illustrated in Fig. 12.6 consists of the lower two stories in the structure, with the appropriate level of fixity at the base. The upper flexural members in the subframe are treated as rigid. Factored lateral loads are applied to the structure. The subframe can be analyzed using matrix analysis or the portal frame method described in Section 12.7. Judicious consideration of factors such as those just discussed, along with simple models, as appropriate, will enable a designer to produce a reasonably accurate preliminary design, which in most cases will permit a satisfactory analysis to be made on the first trial.

12.7 APPROXIMATE ANALYSIS

In spite of the development of refined methods for the analysis of beams and frames, increasing attention is being paid to various approximate methods of analysis (Ref. 12.4). There are several reasons for this. Prior to performing a complete analysis of an indeterminate structure, it is necessary to estimate the proportions of its members to determine their relative stiffness, upon which the analysis depends. These dimensions can be obtained on the basis of approximate analysis. Also, even with the availability of computers, most engineers find it desirable to make a rough check of results, using approximate means, to detect gross errors. Further, for structures of minor importance, it is often satisfactory to design on the basis of results obtained by rough calculation. For these reasons, many engineers at some stage in the design process estimate the values of moments, shears, and thrusts at critical locations, using approximate sketches of the structure deflected by its loads.

Provided that points of inflection (locations in members at which the bending moment is zero and there is a reversal of curvature of the elastic curve) can be located accurately, the stress resultants for a framed structure can usually be found on the basis of static equilibrium alone. Each portion of the structure must be in equilibrium under the application of its external loads and the internal stress resultants.

For the fixed-end beam in Fig. 12.7a, for example, the points of inflection under uniformly distributed load are known to be located $0.211l$ from the ends of the span. Since the moment at these points is zero, imaginary hinges can be placed there without modifying the member behavior. The individual segments between hinges can be analyzed by statics, as shown in Fig. 12.7b. Starting with the center segment, shears equal to $0.289wl$ must act at the hinges. These, together with the transverse load, produce a midspan moment of $0.0417wl^2$. Proceeding next to the outer segments, a downward load is applied at the hinge representing the shear from the center segment. This, together with the applied load, produces support moments of $0.0833wl^2$. Note that, for this example, since the correct position of the inflection points was known at the start,

FIGURE 12.7

Analysis of fixed-end beam by locating inflection points.

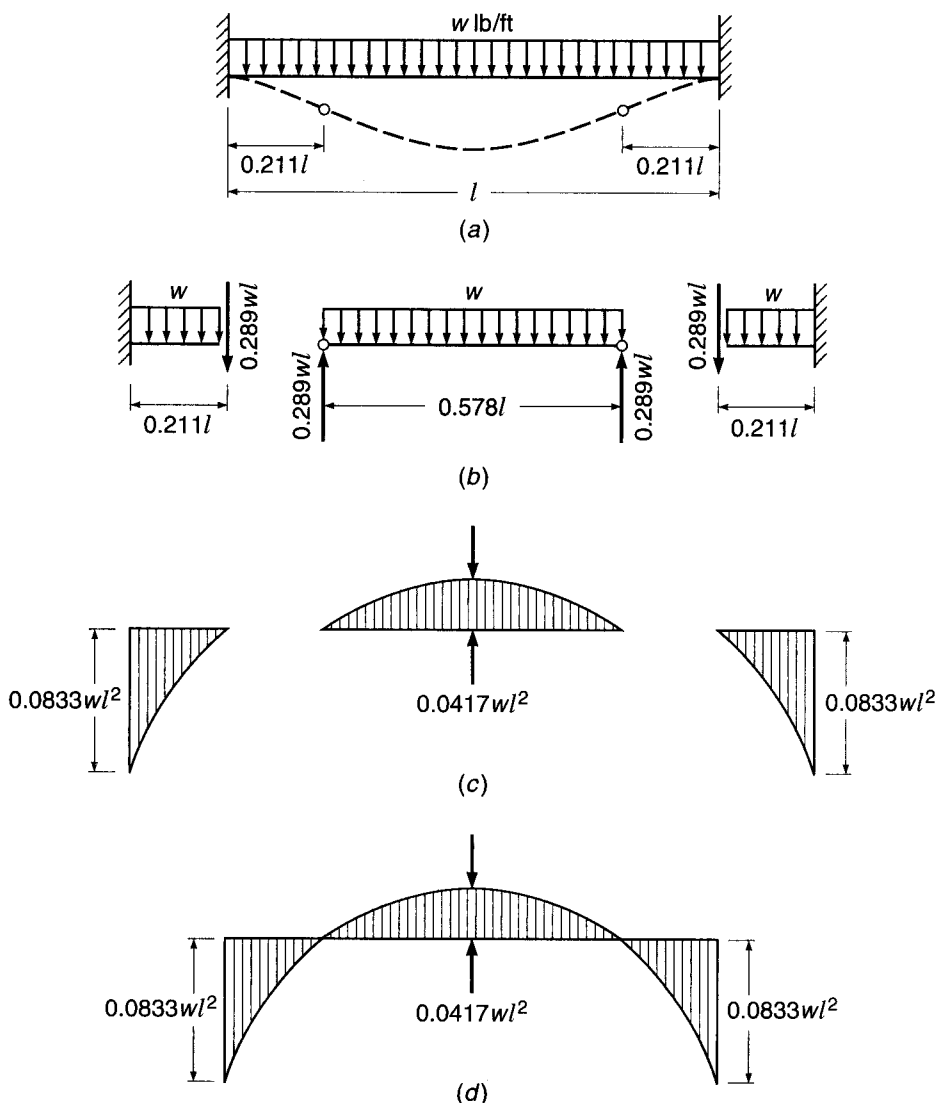
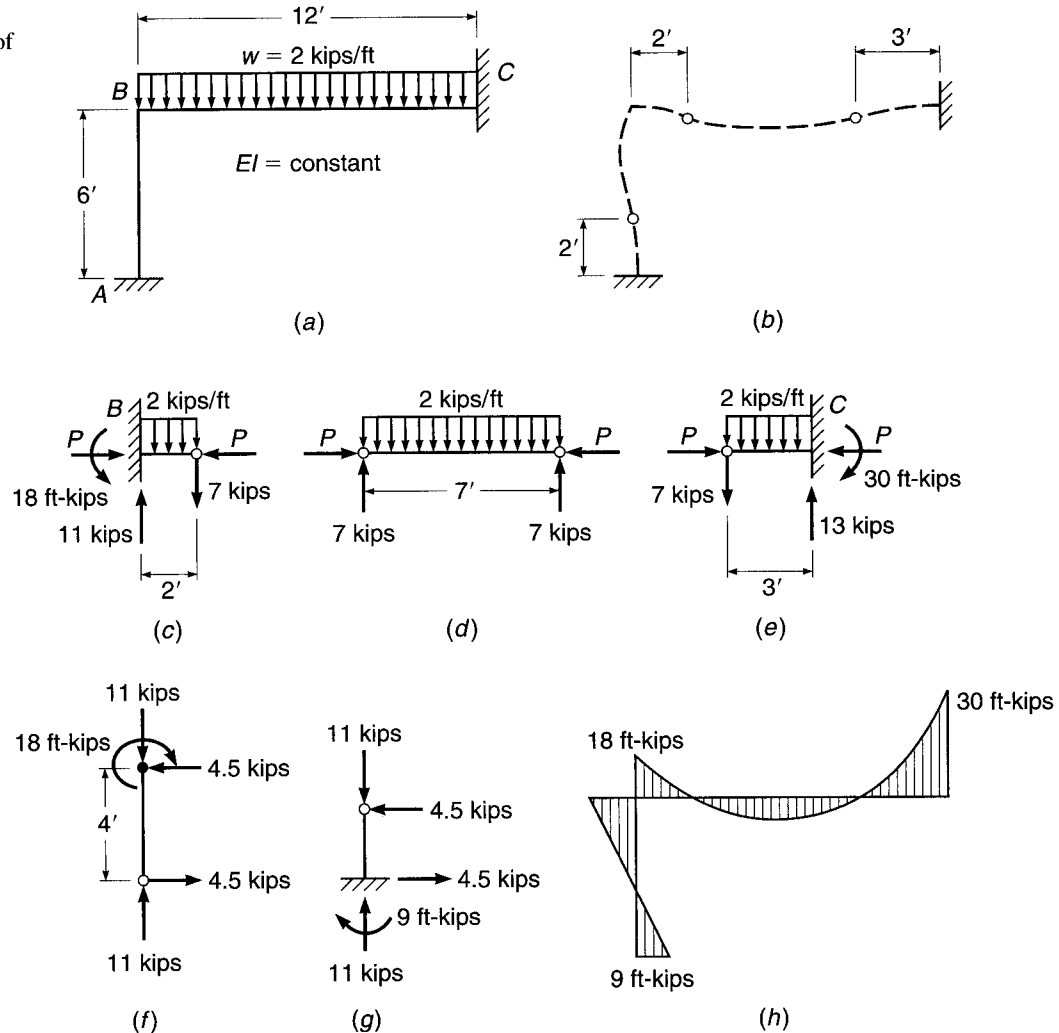


FIGURE 12.8

Approximate analysis of rigid frame.



the resulting moment diagram of Fig. 12.7c agrees exactly with the true moment diagram for a fixed-end beam shown in Fig. 12.7d. In more practical cases, inflection points must be estimated, and the results obtained will only approximate the true values.

The use of approximate analysis in determining stress resultants in frames is illustrated by Fig. 12.8. Figure 12.8a shows the geometry and loading of a two-member rigid frame. In Fig. 12.8b an exaggerated sketch of the probable deflected shape is given, together with the estimated location of points of inflection. On this basis, the central portion of the girder is analyzed by statics, as shown in Fig. 12.8d, to obtain girder shears at the inflection points of 7 kips, acting with an axial load P (still not determined). Similarly, the requirements of statics applied to the outer segments of the girder in Fig. 12.8c and e give vertical shears of 11 and 13 kips at B and C, respectively, and end moments of 18 and 30 ft-kips at the same locations. Proceeding then to the upper segment of the column, shown in Fig. 12.8f, with known axial load of 11 kips and top moment of 18 ft-kips acting, a horizontal shear of 4.5 kips at the inflection point is required for equilibrium. Finally, static analysis of the lower part of the column indicates a requirement of 9 ft-kips moment at A, as shown in Fig. 12.8g. The value of P equal to 4.5 kips is obtained by summing horizontal forces at joint B.

The moment diagram resulting from approximate analysis is shown in Fig. 12.8*h*. For comparison, an exact analysis of the frame indicates member end moments of 8 ft-kips at *A*, 16 ft-kips at *B*, and 28 ft-kips at *C*. The results of the approximate analysis would be satisfactory for design in many cases; if a more exact analysis is to be made, a valuable check is available on the magnitude of results.

A specialization of the approximate method described, known as the *portal method*, is commonly used to estimate the effects of sidesway due to lateral forces acting on multistory building frames. For such frames, it is usual to assume that horizontal loads are applied at the joints only. If this is true, moments in all members vary linearly and, except in hinged members, have opposite signs close to the midpoint of each member.

For a simple rectangular portal frame having three members, the shear forces are the same in both legs and are each equal to one-half the external horizontal load. If one of the legs is more rigid than the other, it will require a larger horizontal force to displace it horizontally the same amount as the more flexible leg. Consequently, the portion of the total shear resisted by the stiffer column is larger than that of the more flexible column.

In multistory building frames, moments and forces in the girders and columns of each individual story are distributed in substantially the same manner as just discussed for single-story frames. The portal method of computing approximate moments, shears, and axial forces from horizontal loads is, therefore, based on the following three simple propositions:

1. The total horizontal shear in all columns of a given story is equal and opposite to the sum of all horizontal loads acting above that story.
2. The horizontal shear is the same in both exterior columns; the horizontal shear in each interior column is twice that in an exterior column.
3. The inflection points of all members, columns and girders, are located midway between joints.

Although the last of these propositions is commonly applied to all columns, including those of the bottom floor, the authors prefer to deal with the latter separately, depending on conditions of foundation. If the actual conditions are such as practically to prevent rotation (foundation on rock, massive pile foundations, etc.), the inflection points of the bottom columns are above midpoint and may be assumed to be at a distance $2h/3$ from the bottom. If little resistance is offered to rotation, e.g., for relatively small footings on compressible soil, the inflection point is located closer to the bottom and may be assumed to be at a distance $h/3$ from the bottom, or even lower. (With ideal hinges, the inflection point is at the hinge, i.e., at the very bottom.) Since shears and corresponding moments are largest in the bottom story, a judicious evaluation of foundation conditions as they affect the location of inflection points is of considerable importance.

The first of the three cited propositions follows from the requirement that horizontal forces be in equilibrium at any level. The second takes account of the fact that in building frames interior columns are generally more rigid than exterior ones because (1) the larger axial loads require a larger cross section and (2) exterior columns are restrained from joint rotation only by one abutting girder, while interior columns are so restrained by two such members. The third proposition is very nearly true because, except for the top and bottom columns and, to a minor degree, for the exterior girders, each member in a building frame is restrained about equally at both ends. For this reason, members deflect under horizontal loads in an antisymmetrical manner, with the inflection point at midlength.

The actual computations in this method are extremely simple. Once column shears are determined from propositions 1 and 2 and inflection points located from proposition 3, all moments, shears, and forces are simply computed by statics. The process is illustrated in Fig. 12.9a.

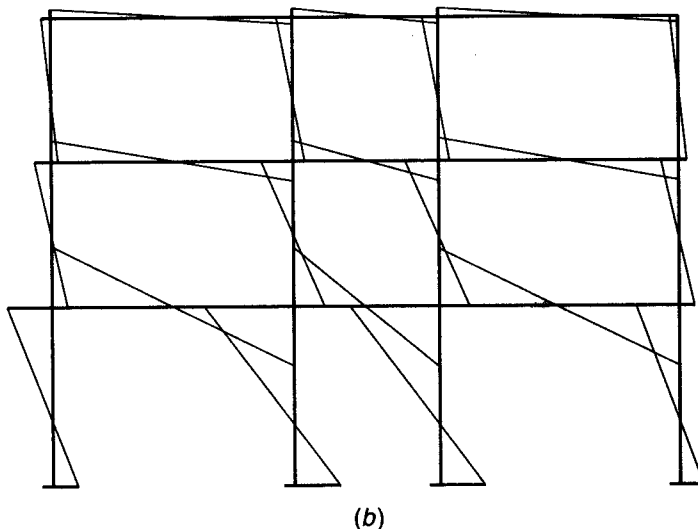
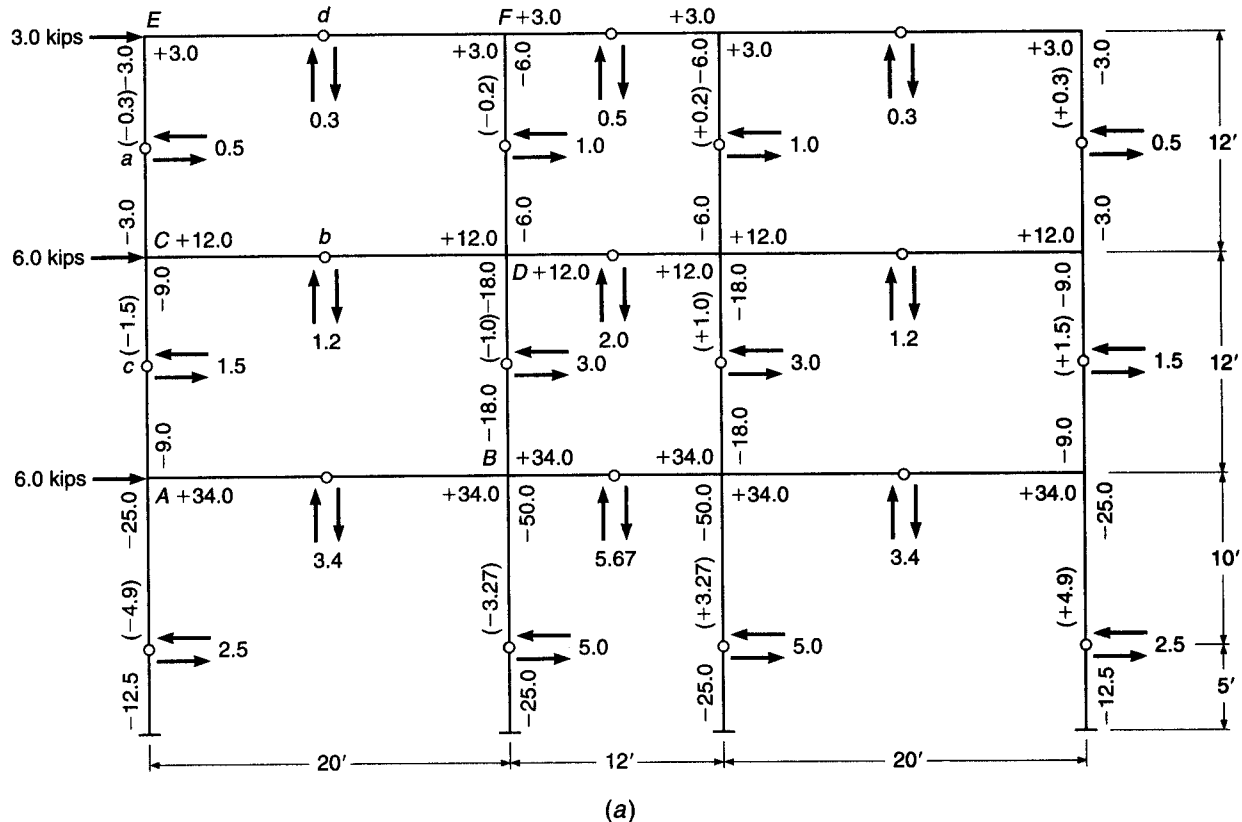


FIGURE 12.9

Portal method for determining moments from wind load in a building frame: (a) moments, shears, and thrusts; (b) variations of moments.

Consider joints *C* and *D*. The total shear in the second story is $3 + 6 = 9$ kips. According to proposition 2, the shear in each exterior column is $9/6 = 1.5$ kips, and in each interior column $2 \times 1.5 = 3.0$ kips. The shears in the other floors, obtained in the same manner, act at the hinges as shown. Consider the equilibrium of the rigid structure between hinges *a*, *b*, and *c*; the column moments, 3.0 and 9.0 ft-kips, respectively, are obtained directly by multiplying the shears by their lever arms, 6 ft. The girder moment at *C*, to produce equilibrium, is equal and opposite to the sum of the column moments. The shear in the girder is obtained by recognizing that its moment (i.e., shear times one-half the girder span) must be equal to the girder moment at *C*. Hence, this shear is $12.0/10 = 1.2$ kips. The moment at end *D* is equal to that at *C*, since the inflection point is at midspan. At *D*, column moments are computed in the same manner from the known column shears and lever arms. The sum of the two girder moments, to produce equilibrium, must be equal and opposite to the sum of the two column moments, from which the girder moment to the right of *C* is $18.0 + 6.0 - 12.0 = 12.0$ ft-kips. Axial forces in the columns also follow from statics. Thus, for the rigid body *aEd*, a vertical shear of 0.3 kip is seen to act upward at *d*. To equilibrate it, a tensile force of -0.3 kip is required in the column *CE*. In the rigid body *abc*, an upward shear of 1.2 kips at *b* is added to the previous upward tension of 0.3 kip at *a*. To equilibrate these two forces, a tension force of -1.5 kips is required in column *AC*. If the equilibrium of all other partial structures between hinges is considered in a similar manner, all moments, forces, and shears are rapidly determined.

In the present case, relatively flexible foundations were assumed, and the location of the lowermost inflection points was estimated to be at $h/3$ from the bottom. The general character of the resulting moment distribution is shown in Fig. 12.9b.

12.8 ACI MOMENT COEFFICIENTS

ACI Code 8.3 includes expressions that may be used for the approximate calculation of maximum moments and shears in continuous beams and one-way slabs. The expressions for moment take the form of a coefficient multiplied by $w_u l_n^2$, where w_u is the total factored load per unit length on the span and l_n is the clear span from face to face of supports for positive moment, or the average of the two adjacent clear spans for negative moment. Shear is taken equal to a coefficient multiplied by $w_u l_n/2$. The coefficients, found in ACI Code 8.3.3, are shown in Table 12.1 and summarized in Fig. 12.10.

The ACI moment coefficients were derived by elastic analysis, considering alternative placement of live load to yield maximum negative or positive moments at the critical sections, as was described in Section 12.2. They are applicable within the following limitations:

1. There are two or more spans.
2. Spans are approximately equal, with the longer of two adjacent spans not greater than the shorter by more than 20 percent.
3. Loads are uniformly distributed.
4. The unfactored live load does not exceed 3 times the unfactored dead load.
5. Members are prismatic.

As discussed in Section 12.3 for more general loading conditions, the alternative loading patterns considered in applying the Code moment coefficients result in an envelope of maximum moments, as illustrated in Fig. 12.11 for one span of a continuous

TABLE 12.1
Moment and shear values using ACI coefficients[†]

Positive moment	
End spans	
If discontinuous end is unrestrained	$\frac{1}{11} w_u l_n^2$
If discontinuous end is integral with the support	$\frac{1}{14} w_u l_n^2$
Interior spans	$\frac{1}{16} w_u l_n^2$
Negative moment at exterior face of first interior support	
Two spans	$\frac{1}{9} w_u l_n^2$
More than two spans	$\frac{1}{10} w_u l_n^2$
Negative moment at other faces of interior supports	$\frac{1}{11} w_u l_n^2$
Negative moment at face of all supports for (1) slabs with spans not exceeding 10 ft and (2) beams and girders where ratio of sum of column stiffness to beam stiffness exceeds 8 at each end of the span	$\frac{1}{12} w_u l_n^2$
Negative moment at interior faces of exterior supports for members built integrally with their supports	
Where the support is a spandrel beam or girder	$\frac{1}{24} w_u l_n^2$
Where the support is a column	$\frac{1}{16} w_u l_n^2$
Shear in end members at first interior support	$1.15 \frac{w_u l_n}{2}$
Shear at all other supports	$\frac{w_u l_n}{2}$

[†] w_u = total factored load per unit length of beam or per unit area of slab.

l_n = clear span for positive moment and shear and the average of the two adjacent clear spans for negative moment.

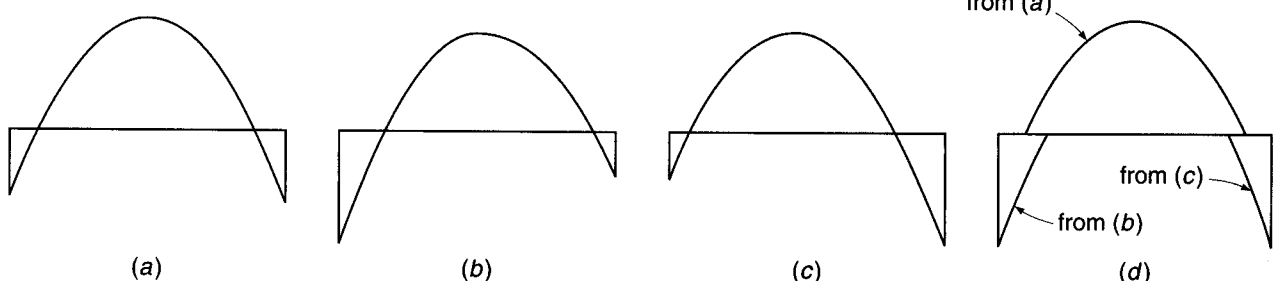
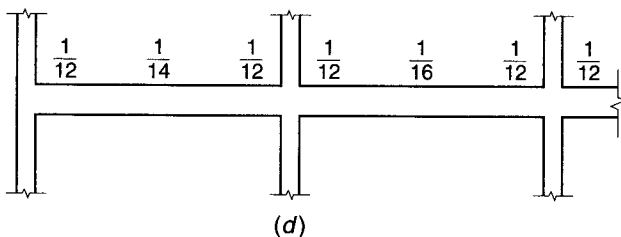
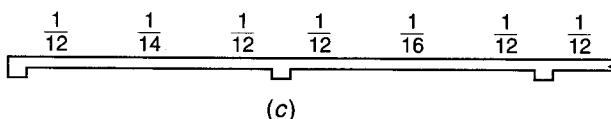
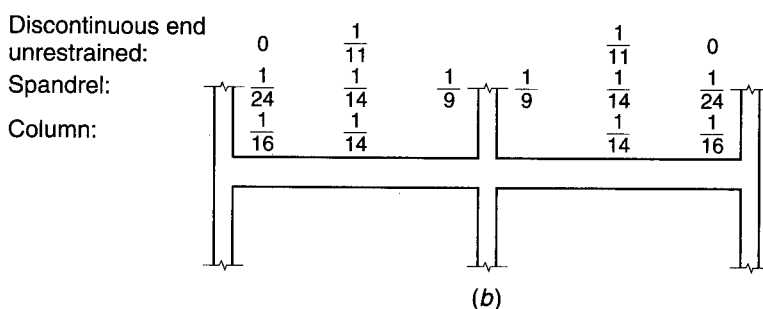
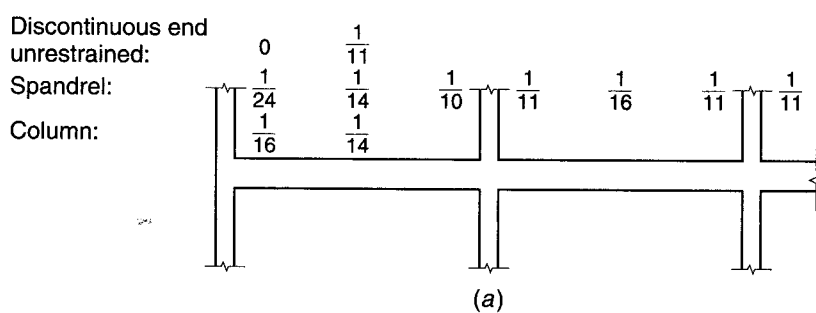
frame. For maximum positive moment, that span would carry dead and live loads, while adjacent spans would carry dead load only, producing the diagram of Fig. 12.11a. For maximum negative moment at the left support, dead and live loads would be placed on the given span and that to the left, while the adjacent span on the right would carry only dead load, with the result shown in Fig. 12.11b. Figure 12.11c shows the corresponding results for maximum moment at the right support.

The composite moment diagram formed from the controlling portions of those just developed (Fig. 12.11d) provides the basis for design of the span. As observed in Section 12.3, there are a range of positions for the points of inflection resulting from alternate loadings. The extreme locations, required to determine bar cutoff points, can be found with the aid of Graph A.3 of Appendix A. In the region of the inflection point, it is evident from Fig. 12.11d that there may be a reversal of moments for alternative load patterns. However, within the stated limits for use of the coefficients, there should be no reversal of moments at the critical design sections near midspan or at the support faces.

Comparison of the moments found using the ACI coefficients with those calculated by more exact analysis will usually indicate that the coefficient moments are quite conservative. Actual elastic moments may be considerably smaller. Consequently, in many reinforced concrete structures, significant economy can be achieved by making a more precise analysis. This is mandatory for beams and slabs with spans differing by more than 20 percent, sustaining loads that are not uniformly distributed, or carrying live loads greater than 3 times the dead load.

FIGURE 12.10

Summary of ACI moment coefficients: (a) beams with more than two spans; (b) beams with two spans only; (c) slabs with spans not exceeding 10 ft; (d) beams in which the sum of column stiffnesses exceeds 8 times the sum of beam stiffnesses at each end of the span.

**FIGURE 12.11**

Maximum moment diagrams and moment envelope for a continuous beam: (a) maximum positive moment; (b) maximum negative moment at left end; (c) maximum negative moment at right end; (d) composite moment envelope.

Because the load patterns in a continuous frame that produce critical moments in the columns are different from those for maximum negative moments in the beams, column moments must be found separately. According to ACI Code 8.10, columns must be designed to resist the axial load from factored dead and live loads on all floors above and on the roof plus the maximum moment from factored loads on a single adjacent span of the floor or roof under consideration. In addition, because of the characteristic shape of the column strength interaction diagram (see Chapter 8), it is necessary to consider the case that gives the maximum ratio of moment to axial load. In multistory structures, this results from a checkerboard loading pattern (see Fig. 12.2d), which gives maximum column moments but at a less-than-maximum axial force. As a simplification, in computing moments resulting from gravity loads, the far ends of the columns may be considered fixed. The moment found at a column-beam joint for a given loading is to be assigned to the column above and the column below in proportion to the relative column stiffness and conditions of restraint.

The shears at the ends of the spans in a continuous frame are modified from the value of $w_u l_n / 2$ for a simply supported beam because of the usually unbalanced end moments. For interior spans, within the limits of the ACI coefficient method, this effect will seldom exceed about 8 percent, and it may be neglected, as suggested in Table 12.1. However, for end spans, at the face of the first interior support, the additional shear is significant, and a 15 percent increase above the simple beam shear is indicated in Table 12.1. The corresponding reduction in shear at the face of the exterior support is conservatively neglected.

12.9 LIMIT ANALYSIS

a. Introduction

Most reinforced concrete structures are designed for moments, shears, and axial forces found by elastic theory with methods such as those described in Sections 12.1 through 12.8. On the other hand, the actual proportioning of members is done by strength methods, with the recognition that inelastic section and member response would result upon overloading. Factored loads are used in the elastic analysis to find moments in a continuous beam, for example, after which the critical beam sections are designed with the knowledge that the steel would be well into the yield range and the concrete stress distribution very nonlinear before final collapse. Clearly this is an inconsistent approach to the total analysis-design process, although it can be shown to be both safe and conservative. A beam or frame so analyzed and designed will not fail at a load lower than the value calculated in this way.[†]

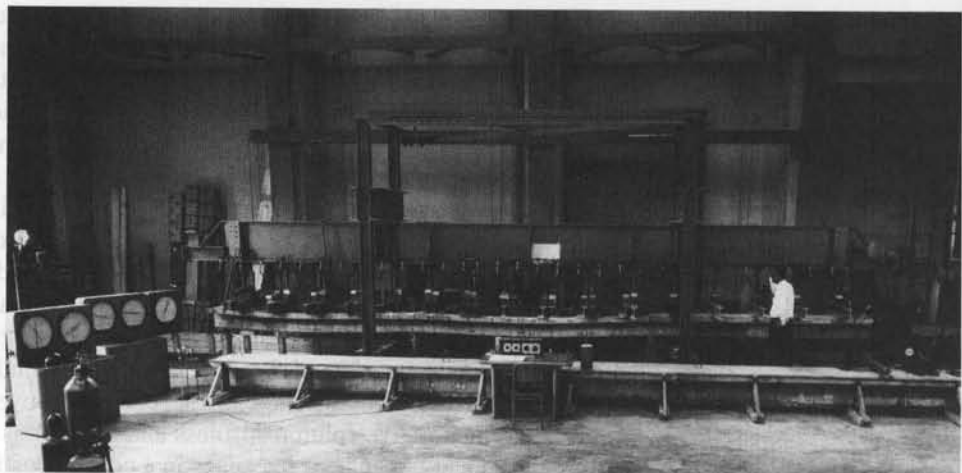
On the other hand, it is known that a continuous beam or frame normally will not fail when the nominal moment capacity of just one critical section is reached. A *plastic hinge* will form at that section, permitting large rotation to occur at essentially constant resisting moment and thus transferring load to other locations along the span where the limiting resistance has not yet been reached. Normally in a continuous beam or frame, excess capacity will exist at those other locations because they would have been reinforced for moments resulting from different load distributions selected to produce maximum moments at those other locations.

As loading is further increased, additional plastic hinges may form at other locations along the span and eventually result in collapse of the structure, but only

[†] See the discussion of upper and lower bound theorems of the theory of plasticity, Section 14.2, for an elaboration on this point.

FIGURE 12.12

Three-span continuous beam after the formation of plastic hinges at the interior supports.



after a significant *redistribution of moments* has occurred. The ratio of negative to positive moments found from elastic analysis is no longer correct, for example, and the true ratio after redistribution depends upon the flexural strengths actually provided at the hinging sections.

Recognition of redistribution of moments can be important because it permits a more realistic appraisal of the actual load-carrying capacity of a structure, thus leading to improved economy. In addition, it permits the designer to modify, within limits, the moment diagrams for which members are to be designed. Certain sections can be deliberately underreinforced if moment resistance at adjacent critical sections is increased correspondingly. Adjustment of design moments in this way enables the designer to reduce the congestion of reinforcement that often occurs in high-moment areas, such as at the beam-column joints.

The formation of plastic hinges is well established by tests such as that pictured in Fig. 12.12. The three-span continuous beam illustrates the inelastic response typical of heavily overloaded members. It was reinforced in such a way that plastic hinges would form at the interior support sections before the limit capacity of sections elsewhere was reached. The beam continued to carry increasing load well beyond the load that produced first yielding at the supports. The extreme deflections and sharp changes in slope of the member axis that are seen here were obtained only slightly before final collapse.

The *inconsistency* of the present approach to the total analysis-design process, the possibility of using the *reserve strength* of concrete structures resulting from moment redistribution, and the opportunity to *reduce steel congestion* in critical regions have motivated considerable interest in limit analysis for reinforced concrete based on the concepts just described. For beams and frames, ACI Code 8.4 permits limited redistribution of moments, depending upon the strain in the tensile steel ϵ_t . For slabs, which generally use very low reinforcement ratios and consequently have great ductility, plastic design methods are especially suitable.

b. Plastic Hinges and Collapse Mechanisms

If a short segment of a reinforced concrete beam is subjected to a bending moment, curvature of the beam axis will result, and there will be a corresponding rotation of one face of the segment with respect to the other. It is convenient to express this in

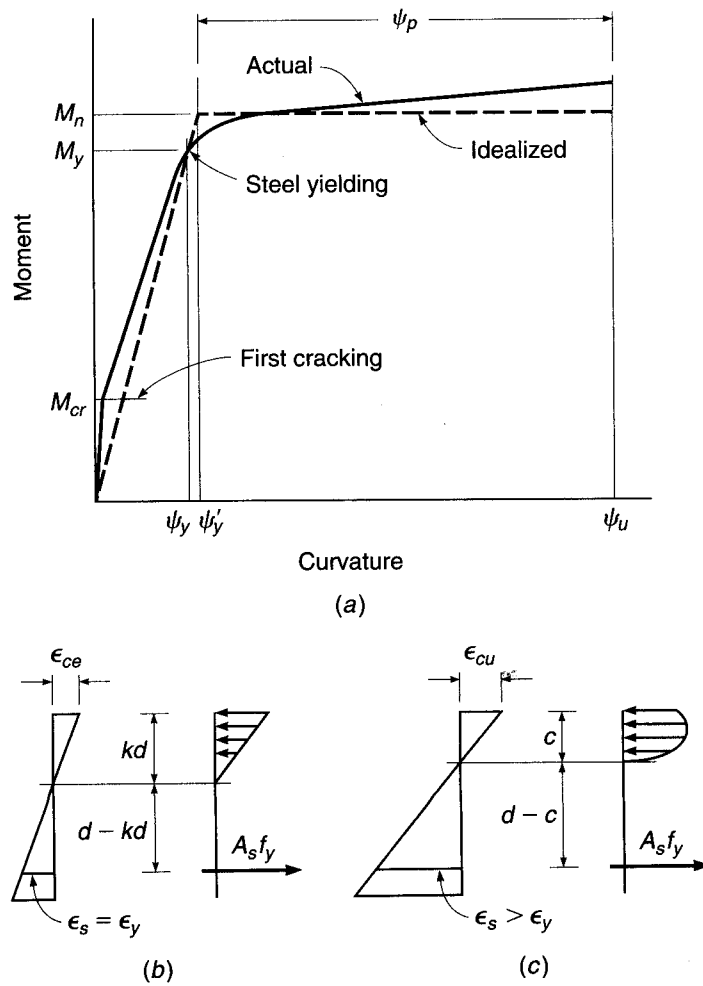
terms of an angular change per unit length of the member. The relation between moment and angle change per unit length of beam, or curvature, at a reinforced concrete beam section subject to tensile cracking was developed in Section 6.9. Methods were presented there by which the theoretical moment-curvature graph might be drawn for a given beam cross section, as in Fig. 6.17.

The actual moment-curvature relationship measured in beam tests differs somewhat from that shown in Fig. 6.17, mainly because, from tests, curvatures are calculated from average strains measured over a finite gage length, usually about equal to the effective depth of the beam. In particular, the sharp increase in curvature upon concrete cracking shown in Fig. 6.17 is not often seen because the crack occurs at only one discrete location along the gage length. Elsewhere, the uncracked concrete shares in resisting flexural tension, resulting in what is known as *tension stiffening*. This tends to reduce curvature. Furthermore, the exact shape of the moment-curvature relation depends strongly upon the reinforcement ratio as well as upon the exact stress-strain curves for the concrete and steel.

Figure 12.13 shows a somewhat simplified moment-curvature diagram for an actual concrete beam section having a tensile reinforcement ratio equal to about one-half the balanced value. The diagram is linear up to the cracking moment M_{cr} , after which a nearly straight line of somewhat flatter slope is obtained. At the moment

FIGURE 12.13

Plastic hinge characteristics in a reinforced concrete member: (a) typical moment-curvature diagram; (b) strains and stresses at start of yielding; (c) strains and stresses at incipient failure.



that initiates yielding M_y , the curvature starts to increase disproportionately. Further increase in applied moment causes extensive inelastic rotation until, eventually, the compressive strain limit of the concrete is reached at the ultimate rotation ψ_u . The maximum moment is often somewhat above the calculated flexural strength M_n , due largely to strain hardening of the reinforcement.

The effect of inelastic concrete response prior to steel yielding is small for typically underreinforced sections, as is indicated in Fig. 6.17, and the yield moment can be calculated based on the elastic concrete stress distribution shown in Fig. 12.13b:

$$M_y = A_s f_y \left(d - \frac{kd}{3} \right) \quad (12.1)$$

where kd is the distance from the compression face to the cracked elastic neutral axis (see Section 3.3b). The nominal moment capacity M_n , based on Fig. 12.13c, is calculated by the usual expression

$$M_n = A_s f_y \left(d - \frac{a}{2} \right) = A_s f_y \left(d - \frac{\beta_1 c}{2} \right) \quad (12.2)$$

For purposes of limit analysis, the $M-\psi$ curve is usually idealized, as shown by the dashed line in Fig. 12.13a. The slope of the elastic portion of the curve is obtained with satisfactory accuracy using the moment of inertia of the cracked transformed section. After the nominal moment M_n is reached, continued plastic rotation is assumed to occur with no change in applied moment. The elastic curve of the beam will show an abrupt change in slope at such a section. The beam behaves as if there were a hinge at that point. However, the hinge will not be "friction-free," but will have a constant resistance to rotation.

If such a plastic hinge forms in a determinate structure, as shown in Fig. 12.14, uncontrolled deflection takes place, and the structure will collapse. The resulting system is referred to as a *mechanism*, an analogy to linkage systems in mechanics. Generalizing, one can say that a statically determinate system requires the formation of only one plastic hinge to become a mechanism.

This is not so for indeterminate structures. In this case, stability may be maintained even though hinges have formed at several cross sections. The formation of such hinges in indeterminate structures permits a redistribution of moments within the beam or frame. It will be assumed for simplicity that the indeterminate beam of Fig. 12.15a is symmetrically reinforced, so that the negative bending capacity is the same as the positive. Let the load P be increased gradually until the elastic moment at the fixed support, $\frac{3}{16}PL$, is just equal to the plastic moment capacity of the section M_n . This load is

$$P = P_{el} = \frac{16}{3} \frac{M_n}{L} = 5.33 \frac{M_n}{L} \quad (a)$$

FIGURE 12.14

Statically indeterminate member after the formation of plastic hinge.

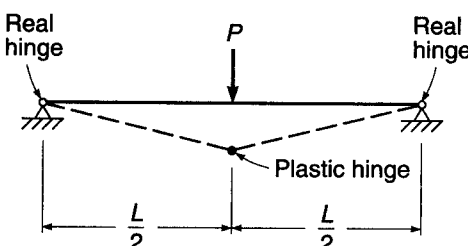
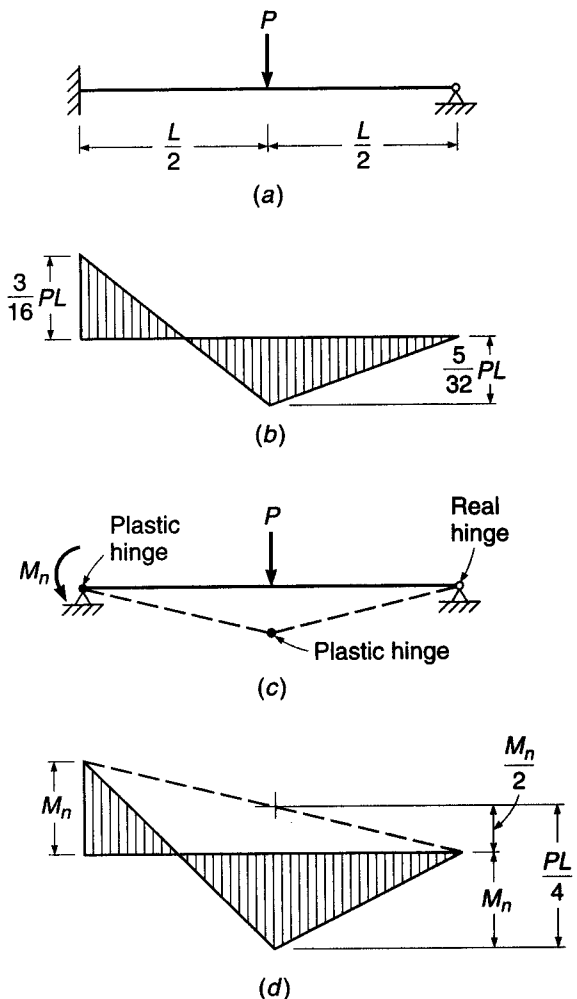


FIGURE 12.15

Indeterminate beam with plastic hinges at support and midspan.



At this load, the positive moment under the load is $\frac{5}{32}PL$, as shown in Fig. 12.15b. The beam still responds elastically everywhere but at the left support. At that point the actual fixed support can be replaced for purposes of analysis with a plastic hinge offering a known resisting moment M_n . Because a redundant reaction has been replaced by a known moment, the beam is now determinate.

The load can be increased further until the moment under the load also becomes equal to M_n , at which load the second hinge forms. The structure is converted into a mechanism, as shown in Fig. 12.15c, and collapse occurs. The moment diagram at collapse load is shown in Fig. 12.15d.

The magnitude of load causing collapse is easily calculated from the geometry of Fig. 12.15d:

$$M_n + \frac{M_n}{2} = \frac{PL}{4}$$

from which

$$P = P_n = \frac{6M_n}{L} \quad (b)$$

By comparison of Eqs. (b) and (a), it is evident that an increase in P of 12.5 percent is possible, beyond the load that caused the formation of the first plastic hinge, before the beam will actually collapse. Due to the formation of plastic hinges, a redistribution of moments has occurred such that, at failure, the ratio between the positive moment and negative moment is equal to that assumed in reinforcing the structure.

c. Rotation Requirement

It may be evident that there is a direct relation between the amount of redistribution desired and the amount of inelastic rotation at the critical sections of a beam required to produce the desired redistribution. In general, the greater the modification of the elastic moment ratio, the greater the required rotation capacity to accomplish that change. To illustrate, if the beam of Fig. 12.15a had been reinforced according to the elastic moment diagram of Fig. 12.15b, no inelastic-rotation capacity at all would be required. The beam would, at least in theory, yield simultaneously at the left support and at midspan. On the other hand, if the reinforcement at the left support had been deliberately reduced (and the midspan reinforcement correspondingly increased), inelastic rotation at the support would be required before the strength at midspan could be realized.

The amount of rotation required at plastic hinges for any assumed moment diagram can be found by considering the requirements of compatibility. The member must be bent, under the combined effects of elastic moment and plastic hinges, so that the correct boundary conditions are satisfied at the supports. Usually, zero support deflection is to be maintained. Moment-area and conjugate-beam principles are useful in quantitative determination of rotation requirements (Ref. 12.6). In deflection calculations, it is convenient to assume that plastic hinging occurs at a point, rather than being distributed over a finite *hinging length*, as is actually the case. Consequently, in loading the conjugate beam with unit rotations, plastic hinges are represented as concentrated loads.

Calculation of rotation requirements will be illustrated by the two-span continuous beam shown in Fig. 12.16a. The elastic moment diagram resulting from a single concentrated load is shown in Fig. 12.16b. The moment at support B is $0.096Pl$, while that under the load is $0.182Pl$. If the deflection of the beam at support C were calculated using the unit rotations equal to M/EI , based on this elastic moment diagram, a zero result would be obtained.

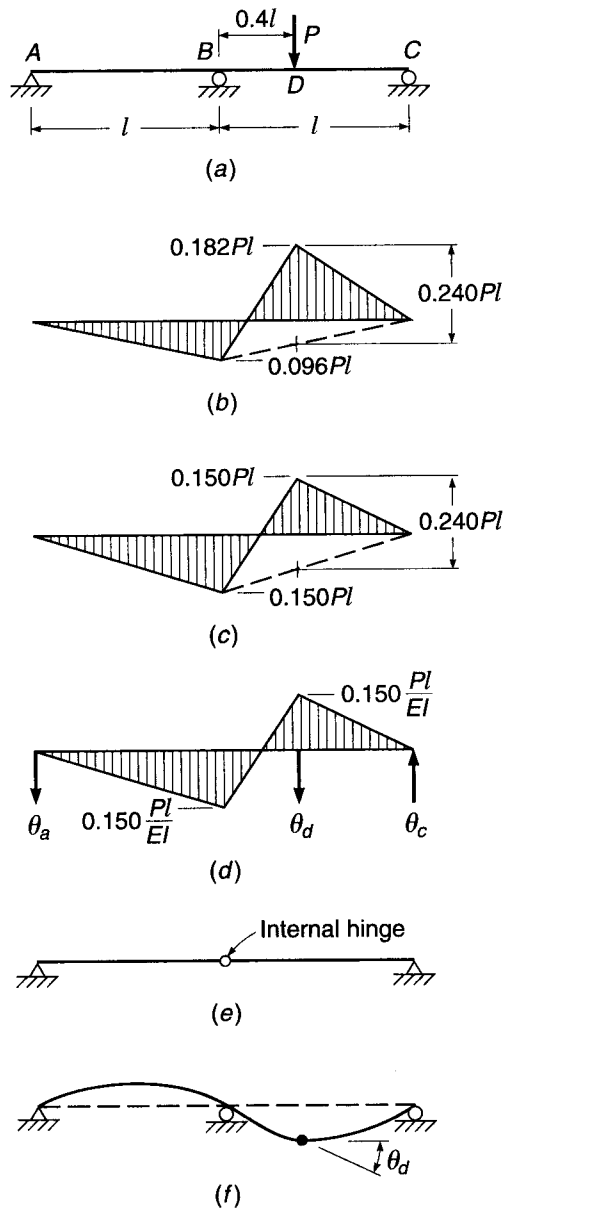
Figure 12.16c shows an alternative, statically admissible moment diagram that was obtained by arbitrarily increasing the support moment from $0.096Pl$ to $0.150Pl$. If the beam deflection at C were calculated using this moment diagram as a basis, a nonzero value would be obtained. This indicates the necessity for inelastic rotation at one or more points to maintain geometric compatibility at the right support.

If the beam were reinforced according to Fig. 12.16c, increasing loads would produce the first plastic hinge at D , where the beam has been deliberately made understrength. Continued loading would eventually result in formation of the second plastic hinge at B , creating a mechanism and leading to collapse of the structure.

Limit analysis requires calculation of rotation at all plastic hinges up to, but not including, the last hinge that triggers actual collapse. Figure 12.16d shows the M/EI load to be imposed on the conjugate beam of Fig. 12.16e. Also shown is the concentrated angle change θ_d , which is to be evaluated. Starting with the left span,

FIGURE 12.16

Moment redistribution in a two-span beam: (a) loaded beam; (b) elastic moments; (c) modified moments; (d) M/EI loads; (e) conjugate beam; (f) deflection curve.



taking moments of the M/EI loads about the internal hinge of the conjugate beam at B , one obtains the left reaction of the conjugate beam (equal to the slope of the real beam):

$$\theta_a = 0.025 \frac{Pl^2}{EI}$$

With that reaction known, moments are taken about the support C of the conjugate beam and set equal to zero to obtain

$$\theta_d = 0.060 \frac{Pl^2}{EI}$$

This represents the necessary discontinuity in the slope of the elastic curve shown in Fig. 12.16f to restore the beam to zero deflection at the right support. The beam must be capable of developing at least that amount of plastic rotation if the modified moment diagram assumed in Fig. 12.16c is to be valid.

d. Rotation Capacity

The capacity of concrete structures to absorb inelastic rotations at plastic-hinge locations is not unlimited. The designer adopting full limit analysis in concrete must calculate not only the amount of rotation required at critical sections to achieve the assumed degree of moment redistribution but also the rotation capacity of the members at those sections to ensure that it is adequate.

Curvature at initiation of yielding is easily calculated from the elastic strain distribution shown in Fig. 12.13b.

$$\psi_y = \frac{\epsilon_y}{d(1 - k)} \quad (12.3)$$

in which the ratio k establishing the depth of the elastic neutral axis is found from Eq. (3.12). The curvature corresponding to the nominal moment can be obtained from the geometry of Fig. 12.13c:

$$\psi_u = \frac{\epsilon_{cu}}{c} \quad (12.4)$$

Although it is customary in flexural strength analysis to adopt $\epsilon_{cu} = 0.003$, for purposes of limit analysis a more refined value is needed. Extensive experimental studies (Refs. 12.7 and 12.8) indicate that the ultimate strain capacity of concrete is strongly influenced by the beam width b , by the moment gradient, and by the presence of additional reinforcement in the form of compression steel and confining steel (i.e., web reinforcement). The last parameter is conveniently introduced by means of a reinforcement ratio ρ'' , defined as the ratio of the volume of one stirrup plus its tributary compressive steel volume to the concrete volume tributary to one stirrup. On the basis of empirical studies, the ultimate flexural strain at a plastic hinge is

$$\epsilon_{cu} = 0.003 + 0.02 \frac{b}{z} + \left(\frac{\rho'' f_y}{14.5} \right)^2 \quad (12.5)$$

where z is the distance between points of maximum and zero moment. Based on Eqs. (12.3) to (12.5), the inelastic curvature for the idealized relation shown in Fig. 12.13a is

$$\psi_p = \psi_u - \psi_y \frac{M_n}{M_y} \quad (12.6)$$

This plastic rotation is not confined to one cross section but is distributed over a finite length referred to as the *hinging length*. The experimental studies upon which Eq. (12.5) is based measured strains and rotations in a length equal to the effective depth d of the test members. Consequently, ϵ_{cu} is an *average* value of ultimate strain over a finite length, and ψ_p , given by Eq. (12.6), is an *average* value of curvature. The total inelastic rotation θ_p can be found by multiplying the average curvature by the hinging length:

$$\theta_p = \left(\psi_u - \psi_y \frac{M_n}{M_y} \right) l_p \quad (12.7)$$

On the basis of current evidence, it appears that the hinging length l_p in support regions, on either side of the support, can be approximated by the expression

$$l_p = 0.5d + 0.05z \quad (12.8)$$

in which z is the distance from the point of maximum moment to the nearest point of zero moment.

e. Moment Redistribution under the ACI Code

Full use of the plastic capacity of reinforced concrete beams and frames requires an extensive analysis of all possible mechanisms and an investigation of rotation requirements and capacities at all proposed hinge locations. The increase in design time may not be justified by the gains obtained. On the other hand, a restricted amount of redistribution of elastic moments can safely be made without complete analysis, yet may be sufficient to obtain most of the advantages of limit analysis.

A limited amount of redistribution is permitted by ACI Code 8.4, depending upon a rough measure of available ductility, without explicit calculation of rotation requirements and capacities. The net tensile strain in the extreme tension steel at nominal strength ϵ_t , given in Eq. (3.29), is used as an indicator of rotation capacity. Accordingly, ACI Code 8.4 provides as follows:

Except where approximate values for moments are used, it shall be permitted to decrease factored moments calculated by elastic theory at sections of maximum negative or maximum positive moment in any span of continuous flexural members for any assumed loading arrangement by not more than $1000\epsilon_t$ percent, with a maximum of 20 percent. Redistribution of moments shall be made only when ϵ_t is equal to or greater than 0.0075 at the section at which moment is reduced. The reduced moment shall be used for calculating redistributed moments at all other sections within the spans. Static equilibrium shall be maintained after redistribution of moments for each loading arrangement.

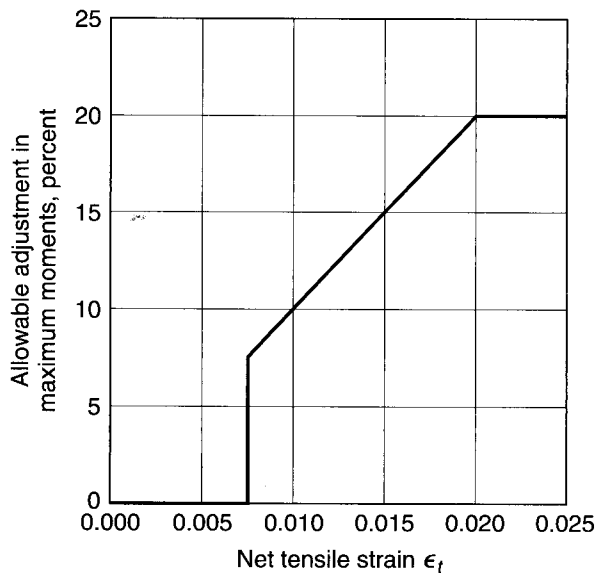
Redistribution for values of $\epsilon_t < 0.0075$ is conservatively prohibited. The ACI Code provisions are shown graphically in Fig. 12.17. The value of ρ corresponding to a given value of ϵ_t , and thus a given percentage change in moment, can be calculated using Eq. (3.30a) from Section 3.4d.

To demonstrate the advantage of moment redistribution when alternative loadings are involved, consider the concrete beam of Fig. 12.18. A three-span continuous beam is shown, with dead load of 1 kip/ft and live load of 2 kips/ft. To obtain maximum moments at all critical design sections, it is necessary to consider three alternative loadings. Case *a*, with live and dead load over exterior spans and dead load only over the interior span, will produce the maximum positive moment in the exterior spans. Case *b*, with dead load on exterior spans and dead and live load on the interior span, will produce the maximum positive moment in the interior span. The maximum negative moment over the interior support is obtained by placing dead and live load on the two adjacent spans and dead load only on the far exterior span, as shown in case *c*.

It will be assumed for simplicity that a 10 percent adjustment of maximum negative and positive moments is permitted throughout, provided that other span moments are modified accordingly. An overall reduction in design moments through the entire three-span beam may be possible. Case *a*, for example, produces an elastic

FIGURE 12.17

Allowable moment redistribution under the ACI Code.



maximum span moment in the exterior spans of 109 ft-kips. Corresponding to this is an elastic negative moment of 82 ft-kips at the interior support. Adjusting the maximum positive moment downward by 10 percent, one obtains a positive moment of 98 ft-kips, which results in an upward adjustment of the support moment to 104 ft-kips.

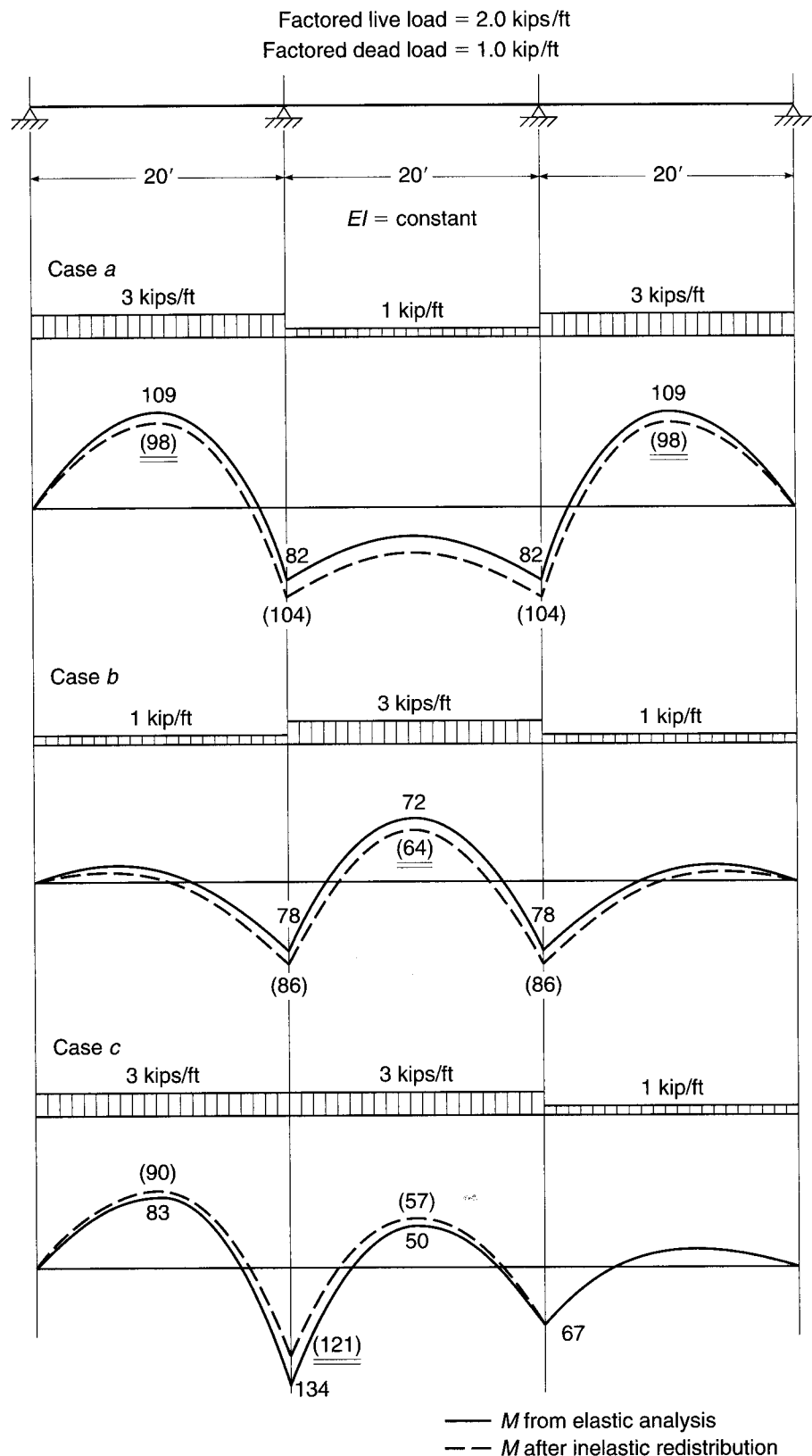
Now consider case *b*. By a similar redistribution of moments, a reduced middle-span moment of 64 ft-kips is accompanied by an increase in the support moment from 78 to 86 ft-kips.

The moment obtained at the first interior support for loading case *c* can be decreased by 10 percent to 121 ft-kips. To limit the increase in the controlling span moment of the interior span, the right interior support moment is not decreased. The positive moments in the left exterior span and in the interior span corresponding to the modified moment at the left interior support are 90 and 57 ft-kips, respectively.

It will be observed that the reduction obtained for the span moments in cases *a* and *b* was achieved at the expense of increasing the moment at the first interior support. However, the increased support moment in each case was less than the moment for which that support would have to be designed based on the loading *c*, which produced the maximum support moment. Similarly, the reduction in support moment in case *c* was taken at the expense of an increase in span moments in the two adjacent spans. However, in each case the increased span moments were less than the maximum span moments obtained for other loading conditions. The final design moments at all critical sections are underlined in Fig. 12.18. It can be seen, then, that the net result is a reduction in design moments over the entire beam. This modification of moments does not mean a reduction in safety factor below that implied in code safety provisions; rather, it means a reduction of the *excess* strength that would otherwise be present in the structure because of the actual redistribution of moments that would occur before failure. It reflects the fact that the maximum design moments are obtained from alternative load patterns, which could not exist concurrently. The end result is a more realistic appraisal of the actual collapse load of the indeterminate structure.

FIGURE 12.18

Redistribution of moments in a three-span continuous beam. The final design moments are underlined.



12.10 CONCLUSION

The problems associated with analysis of reinforced concrete structures are many. The engineer not only must accept the uncertainties of load placement, magnitude, and duration typical of any structural analysis, but also must cope with other complications that are unique to reinforced concrete. These are mainly associated with estimation of moment of inertia of the reinforced concrete sections and with the influence of concrete creep. They may be summarized briefly as follows: (1) effective moments of inertia change depending on the sign of the bending moment; (2) moments of inertia depend not only on the effective concrete section, but also on the steel, a part of which may be discontinuous; (3) moments of inertia depend on cracking, which is both location-dependent and load-dependent; and (4) the concrete is subject to creep under sustained loads, reducing its effective modulus. In addition, joint restraints and conditions of support for complex structures are seldom completely in accordance with the idealization. The student may well despair of accurate calculation of the internal forces for which the members of a reinforced concrete frame must be designed.

It may be reassuring to know that reinforced concrete has a remarkable capacity to adapt to the assumptions of the designer. This has been pointed out by a number of outstanding engineers. *Luigi Nervi*, the renowned Italian architect-engineer, has stated it eloquently as follows:

Mainly because of plastic flow, a concrete structure tries with admirable docility to adapt itself to our calculations—which do not always represent the most logical and spontaneous answer to the request of the forces at play—and even tries to correct our deficiencies and errors. Sections and regions too highly stressed yield and channel some of their loads to other sections or regions, which accept this additional task with commendable spirit of collaboration, within the limits of their own strength.[†]

Hardy Cross, best known for his development of the moment distribution method of analysis (see Section 12.4), noted the beneficial effects of concrete creep, by which a structure can adapt to support settlements, which, on the basis of elastic analysis, cause forces and movements sufficient to fail the structure. *Halvard Birkeland*, one of the pioneers in the development of prestressed concrete in the United States, referred to the “wisdom of the structure,” noting that “. . . the structure, in many instances, will accept our rash assumptions and our imperfect mathematical models . . . the structure will exhaust all means of standing before it decides to fall.”[‡]

Thus it may be of some comfort to know that *a reinforced concrete structure will tend to act as the engineer has assumed it will act*. Reasonable assumptions in the analysis may safely be made. But corollary to this important principle is the acceptance of its limits: *the general pattern of forces and moments must be recognized, and at least one reasonable load path provided*. Too great a deviation from the actual distribution of internal forces can result in serviceability problems associated with cracking and deflection, and can even result in premature failure. It is for this reason that methods of limit analysis for reinforced concrete include restrictions on the amount of redistribution of elastic moments (see Section 12.9). But it is reassuring to know that if good judgment is used in assigning internal forces to critical sections, the *wisdom of the structure* will prevail.

[†] P. L. Nervi, *Structures*, F. W. Dodge Corp., New York, 1956.

[‡] H. L. Birkeland, “The Wisdom of the Structure,” *J. ACI*, April 1978, pp. 105–111.

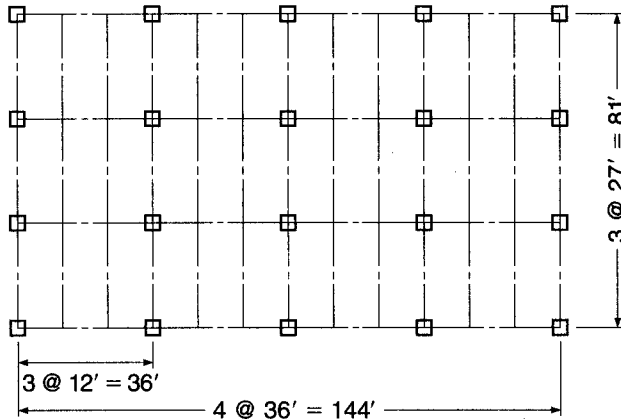
REFERENCES

- 12.1. J. C. McCormac, *Structural Analysis Using Classical and Matrix Methods*, 4th ed., Wiley, Hoboken, New Jersey, 2007.
- 12.2. W. McGuire, R. H. Gallagher, and R. D. Ziemian, *Matrix Structural Analysis, with MASTAN2*, 2nd ed., McGraw-Hill, New York, 1999.
- 12.3. M. Paz and W. Leigh, *Integrated Matrix Structural Analysis for Structures*, Kluwer, Boston, 2001.
- 12.4. K. M. Leet, C.-M. Uang, and A. Gilbert, *Fundamentals of Structural Analysis*, 3rd ed., McGraw-Hill, New York, 2008.
- 12.5. *Continuity in Concrete Building Frames*, 4th ed., Portland Cement Association, Skokie, IL, 1959.
- 12.6. G. C. Ernst, "A Brief for Limit Design," *Trans. ASCE*, vol. 121, 1956, pp. 605–632.
- 12.7. A. H. Mattock, "Rotation Capacity of Hinging Regions in Reinforced Concrete Frames," *Proc. Int. Symp. Flexural Mech. Reinforced Concrete*, ACI Publication SP-12, 1964.
- 12.8. J. S. Ford, D. C. Chang, and J. E. Breen, "Design Implications from Tests of Unbraced Multi-panel Concrete Frames," *Concr. Intl.*, vol. 3, no. 3, 1981, pp. 37–47.

PROBLEMS

- 12.1.** Complete the preliminary design of the four-story heavy storage facility shown in Fig. P12.1. The floor live load is 250 psf, the roof live load is 12 psf, and the dead load on all floors and the roof consists of the structure self-weight plus 10 psf for utilities. The building is enclosed in a self-supporting curtain wall that also carries the lateral load on the structure. Beams are spaced at 12 ft; girders are spaced at 27 ft. The minimum clear space between floors is 11 ft, and the floor depth should not exceed 30 in. The column cross sections should be maintained from floor to floor. Use $f_y = 60,000$ psi and $f'_c = 4000$ psi for the floors. Concrete with f'_c up to 8000 psi is available for the columns. The preliminary design should include the initial dimensions of the structural slab, beams, girders, and columns for a typical floor.

FIGURE P12.1



- 12.2.** A concrete beam with $b = 12$ in., $h = 26.5$ in., and $d = 24$ in., having a span of 24 ft, can be considered fully fixed at the left support and supported vertically but with no rotational restraint (e.g., roller) at the right end. It is reinforced for positive bending with a combination of bars giving $A_s = 2.45$ in 2 , and for negative bending at the left support with $A_s = 2.88$ in 2 . Positive bars are carried 6 in. into the face of the left support, according to the ACI Code requirements, but lack the embedded length to be considered effective as compression steel. No. 3 (No. 10) closed hoop stirrups are provided at 9 in. spacing over the

full span. The factored load consists of a single concentrated force of 63.3 kips at midspan. Self-weight of the beam may be neglected in the calculations. Calculate the rotation requirement at the first plastic hinge to form (a) if the beam is reinforced according to the description above; (b) if, to reduce bar congestion at the left support, that steel area is reduced by 12.5 percent, with an appropriate increase in the positive steel area; and (c) if the steel area at the left-support is reduced by 25 percent, compared with the original description, with an appropriate increase in the positive steel area. Also calculate the rotation capacity of the critical section, for comparison with the requirements of (a), (b), and (c). Comment on your results and compare with the approach to moment redistribution presented in the ACI Code. Material strengths are $f_y = 60$ ksi and $f'_c = 4$ ksi.

- 12.3.** A 12-span continuous reinforced concrete T beam is to carry a calculated dead load of 900 lb/ft including self-weight, plus a service live load of 1400 lb/ft on uniform spans measuring 26.5 ft between centers of supporting columns (25 ft clear spans). The slab thickness is 6 in., and the effective flange width is 75 in. Web proportions are $b_w = 0.6d$, and the maximum reinforcement ratio will be set at 0.011. All columns will be 18 in. square. Material strengths are $f'_c = 4000$ psi and $f_y = 60,000$ psi.

- Find the factored moments for the exterior and first interior span based on the ACI Code moment coefficients of Table 12.1.
- Find the factored moments in the exterior and first interior span by elastic frame analysis, assuming the floor-to-floor height to be 10 ft. Note that alternative live loadings should be considered (see Section 12.2a) and that moments can be reduced to account for the support width (see Section 12.5a). Compare your results with those obtained using the ACI moment coefficients.
- Adjust the factored negative and positive moments, taking advantage of the redistribution provisions of the ACI Code. Assume that a 10 percent minimum redistribution is possible.
- Design the exterior and first interior spans for flexure and shear, finding concrete dimensions and bar requirements, basing your design on the assumptions and modified moments in part (c).

- 12.4.** A continuous reinforced concrete frame consists of a two-span rectangular beam ABC , with center-to-center spans AB and BC of 24 ft. Columns measuring 14 in. square are provided at A , B , and C . The columns may be considered fully fixed at the floors above and below for purposes of analysis. The beam will carry a service live load of 1200 lb/ft and a calculated dead load of 1000 lb/ft, including self-weight. Floor-to-floor height is 12 ft. Material strengths are $f_y = 60,000$ psi and $f'_c = 4000$ psi.

- Carry out an elastic analysis of the two-span frame, considering alternate live loadings to maximize the bending moment at all critical sections. Design the beams, using a maximum reinforcement ratio of 0.012 and $d = 2b$. Find the required concrete section and required steel areas at positive and negative bending sections. Select the reinforcement. Cutoff points can be determined according to Fig. 5.20a. Note that negative design moments are at the face of supports, not support centerlines.
- Take maximum advantage of the redistribution provisions of ACI Code 8.4 (see Section 12.9e) to reduce design moments at all critical sections, and redesign the steel for the beams. Keep the concrete section unchanged. Select reinforcement and determine cutoff points.

- (c) Comment on your two designs with regard to the amount of steel required and the possible congestion of steel at the critical bending sections. You may assume that the shear reinforcement is unchanged in the redesigned beam.

- 12.5.** Complete the preliminary design of the four-story library building shown in Fig. P12.5, using a beam-girder (or joist-girder) floor system. The first floor (slab-on-grade) is supported on drilled piers and serves as the reading and library services area. The upper three floors serve as stack areas (see Table 1.1). The out-to-out building dimensions are 90×150 ft, exclusive of the exterior facade. Columns should be spaced at approximately 30 ft in each direction. The minimum clear space between floors is 12 ft, and the floor depth should not exceed 24 in. Assume a load of 70 psf on the roof for the mechanical penthouse and a snow load of 20 psf. The building is enclosed in a self-supporting curtain wall that also carries the lateral load on the structure. The column cross sections should be maintained from floor to floor. Use $f_y = 60,000$ psi and $f'_c = 4000$ psi for the floors. Concrete with f'_c up to 8000 psi is available for the columns. The preliminary design should include the initial dimensions of the structural slab, beams, girders, and columns for a typical floor.

FIGURE P12.5

